NASA Technical Memorandum 78118

(NASA-TM-78118) TERRESTRIAL ENVIRONMENT (CLIMATIC) CRITERIA GUIDELINES FOR USE IN AEROSPACE VEHICLE DEVELOPMENT, 1977 REVISION (NASA) 531 p HC A23/MF A01 CSCL 22B
N78-13108
Unclas
G3/15 55268

Terrestrial Environment (Climatic) Criteria Guidelines for Use in Aerospace Vehicle Development, 1977 Revision

Edited by John W. Kaufman

NOVEMBER 1977

NASA

ADDENDUM TO NASA TM 78118

"Terrestrial Environment (Climatic) Criteria Guidelines for Use in Space Vehicle Development, 1977 Revision"

Section VII PRECIPITATION, FOG, AND ICING
Paragraph 7.5 HAIL

prepared by

S. Clark Brown/Dale L. Johnson
Atmospheric Sciences Division
Space Sciences Laboratory

This Addendum Replaces Paragraph 7.5 Hail, 7.5.1 Hail at Surface, and 7.5.2 Distribution of Hail with Altitude.

APPROVAL:

William W. Vaughan
William W. Vaughan, Chief
Aerospace Environment Division

Oct 14/1980
Date

Charles A. Lundquist
Charles A. Lundquist, Director
Space Sciences Laboratory

Oct 16, 1980
Date

NASA Technical Memorandum 78118

Terrestrial Environment (Climatic) Criteria Guidelines for Use in Aerospace Vehicle Development, 1977 Revision

Edited by John W. Kaufman
George C. Marshall Space Flight Center
Marshall Space Flight Center, Alabama

NASA
National Aeronautics
and Space Administration

Scientific and Technical Information Office

1977

ACKNOWLEDGMENTS

A large number of aerospace engineers and personnel in varying scientific fields have contributed to the preparation of this document. The following MSFC personnel contributed extensively to sections identified as follows:

	SECTION	RESPONSIBLE PERSONS
I.	Summary and Introduction	William W. Vaughan and John W. Kaufman
II.	Atmospheric Composition	John W. Kaufman
III.	Thermal and Radiation	Dale L. Johnson and O. E. Smith
IV.	Atmospheric Density (Surface)	Dale L. Johnson and S. Clark Brown
V.	Atmospheric Pressure (Surface)	Dale L. Johnson and S. Clark Brown
VI.	Humidity	John W. Kaufman
VII.	Precipitation, Fog, and Icing	John W. Kaufman and Dale L. Johnson
VIII.	Wind	George H. Fichtl and O. E. Smith
IX.	Sea State	S. Clark Brown and George H. Fichtl
X.	Inflight Thermodynamic Properties	O. E. Smith and George H. Fichtl
XI.	Atmospheric Attenuation	S. Clark Brown and O. E. Smith
XII.	Cloud Phenomena	John W. Kaufman and Dale L. Johnson

XIII.	Atmospheric Electricity	John W. Kaufman and O. E. Smith
XIV.	Atmospheric Corrosion and Abrasion	John W. Kaufman
XV.	Atmospheric Oxidants	John W. Kaufman
XVI.	Fungi, Bacteria, and Other Microorganisms	John W. Kaufman
XVII.	Distribution of Surface Extremes in the United States	Lee W. Falls and Dale L. Johnson
XVIII.	Worldwide Surface Extremes	Lee W. Falls and Dale L. Johnson
XIX.	Information on Occurrences of Tornadoes and Hurricanes Plus Selected Climatological Data Source	Lee W. Falls and Dale L. Johnson
XX.	Geologic Hazards	William M. Greene, Coordinator
XXI.	Aerospace Vehicle Effluent Diffusion Modeling for Tropospheric Air Quality and Environment Assessments	J. Briscoe Stephens and C. Warren Campbell
XXII.	Conversion Units	John W. Kaufman

Other members of the Atmospheric Sciences Division, Space Sciences Laboratory, who contributed to the document were Joseph C. Sloan, Dennis W. Camp, Michael Susko, Robert E. Smith, C. Kelly Hill, O. H. Vaughan, Robert E. Turner, and Philip A. Hamilton.

Special acknowledgments are given to Mr. O. E. Smith, Atmospheric Sciences Division, and Dr. William W. Vaughan, Chief, Atmospheric Sciences Division (ES81), for their concerted guidance which led to the completion of the revision of this report.

FOREWORD

This document provides information relative to the natural environment for altitudes of 90 km to the surface of the earth. NASA Technical Memorandum TM-78119, entitled "Space and Planetary Environment Criteria Guidelines for Use in Space Vehicle Development, 1977 Revision," dated 1977, provides natural environment information for altitudes above 90 km.

There is no intent to automatically change any references to previous documents in contract scopes of work by the issuance of the 1977 revision of this document.

This document, which succeeds all editions of TM X-64757, entitled "Terrestrial Environment (Climatic) Criteria Guidelines for Use in Aerospace Vehicle Development, 1973 Revision," is recommended for use in the development of space vehicles and associated equipment.

The information presented in this document is based on data and models considered to be accurate. However, in those design applications which indicate a critical environment interface the user should consult an environmental specialist to insure application of the most current information and scientific engineering interpretation.

Various programs of NASA's Office of Space Flight, Office of Aeronautics and Space Technology, Office of Applications, and Office of Space Science provided resources required for the preparation of this document.

TABLE OF CONTENTS

TABLE OF CONTENTS (Continued)

TABLE OF CONTENTS (Concluded)

TECHNICAL MEMORANDUM TM-78118

TERRESTRIAL ENVIRONMENT (CLIMATIC) CRITERIA GUIDELINES FOR USE IN AEROSPACE VEHICLE DEVELOPMENT, 1977 REVISION

SUMMARY

Atmospheric phenomena play a significant role in the design and flight of aerospace vehicles and in the integrity of the associated aerospace systems and structures. Environmental design criteria guidelines in this report are based on statistics of atmospheric and climatic phenomena relative to various aerospace industrial, operational, and vehicle launch locations. This revision contains new and updated material in most sections. The section on sea state is new, as is the one on cloud phenomena; the geologic hazards section has been expanded, and the new vector wind model has been included.

Specifically, aerospace vehicle design guidelines are established for the following environmental phenomena and presented by sections: Atmospheric Composition; Thermal and Radiation; Atmospheric Density (Surface); Atmospheric Pressure; Humidity; Precipitation, Fog, and Icing; Wind; Sea State; Inflight Thermodynamic Properties; Atmospheric Attenuation; Cloud Phenomena; Atmospheric Electricity; Atmospheric Corrosion and Abrasion; Atmospheric Oxidants; Fungi, Bacteria and Other Microorganisms; Distribution of Surface Extremes in the United States; Worldwide Surface Extremes; Severe Weather and Selected Climatologies; Geologic Hazards; and Aerospace Engine Exhaust Cloud Physics, and other select data. The last section includes conversion constants.

Atmospheric data are presented and analyzed for application to aerospace vehicle design studies. The atmospheric parameters are scaled to show the probability of reaching or exceeding certain limits to assist in establishing design and operating criteria. Additional information on the different parameters may be found in the numerous references cited in the text following each section.

SECTION I. INTRODUCTION

1.1 General

For climatic extremes, there is no known physical upper or lower bound except for certain conditions; that is, for wind speed there does exist a strict physical lower bound of zero. Therefore, for any observed extreme condition, there is a finite probability of its being exceeded. Consequently, climatic extremes for design must be accepted with the knowledge that there is some risk of the values being exceeded. Also, the accuracy of measurement of many environmental parameters is not as precise as desired. In some cases, theoretical estimates of extreme values are believed to be more representative than those indicated by empirical distributions from short periods of record. Therefore, theoretical values are given considerable weight in selecting extreme values for some parameters, i.e., the peak surface winds.

Aerospace vehicles are not normally designed for launch and flight in severe weather conditions such as hurricanes, thunderstorms, and squalls. Atmospheric parameters associated with severe weather which may be hazardous to space vehicles are strong ground and inflight winds, strong wind shears, turbulence, icing conditions, and electrical activity. Criteria guidelines are presented for various percentiles based on available data samples. Caution should be exercised in the interpretation of these percentiles in vehicle studies to ensure consistency with physical reality and the specific design and operational problems of concern.

Environmental data in this report are primarily limited to information below 90 km. Specific space vehicle natural environmental design criteria are normally specified in the appropriate organizational space vehicle design ground rules and design criteria data documentation. The information in this document is recommended for use in the development of space vehicles and associated equipment design criteria unless otherwise stated in contract work specifications.

The data in all sections are based on conditions which have actually occurred, or are statistically probable in nature, over a longer reference period than the available data. When appropriate, cycles (diurnal or other) are given to provide information for environmental testing in the laboratory. In many cases, the natural test cycles may not agree with standard laboratory tests, frequently being less severe, although occasionally the natural cycle as given is more severe than the laboratory test. Such cycles need careful consideration to determine whether the laboratory tests need adjustment.

Assessment of the natural environment in the early stages of an aerospace vehicle development program will be advantageous in developing a vehicle with a minimum operational sensitivity to the environment. For those areas of the environment that need to be monitored prior to and during tests and operations, this early planning will permit development of the required measuring and communication systems for accurate and timely monitoring of the environment. Reference 1.4 is an example of this type of study.

A knowledge of the earth's atmospheric environmental parameters is necessary for the establishment of design requirements for space vehicles and associated equipment. Such data are required to define the design condition for fabrication, storage, transportation, test, preflight, and inflight design conditions and should be considered for both the whole system and the components which make up the system. The purpose of this document is to provide guideline data on natural environmental conditions for the various major geographic locations which are applicable to the design of space vehicle and associated equipment.

Good engineering judgment must be exercised in the application of the earth's atmospheric data to space vehicle design analysis. Consideration must be given to the overall vehicle mission and performance requirements. Knowledge still is lacking on the relationships between some of the atmospheric variates which are required as inputs to the design of space vehicles. Also, interrelationships between space vehicle parameters and atmospheric variables cannot always be clearly defined. Therefore, a close working relationship and team philosophy should exist between the design/operational engineer and the respective organization's aerospace meteorologists. Although, ideally, a space vehicle design should accommodate all expected operational atmospheric conditions, it is neither economically nor technically feasible to design space vehicles to withstand all atmospheric extremes. For this reason, consideration should be given to protection of space vehicles from some extremes by use of support equipment and by using specialized forecast personnel to advise on the expected occurrence of critical environmental conditions. The services of specialized forecast personnel may be very economical in comparison with more expensive designing which would be necessary to cope with all environmental possibilities.

In general this document does not specify how the designer should use the data in regard to a specific space vehicle design. Such specifications may be established only through analysis and study of a particular design problem. Although of operational significance, descriptions of some atmospheric conditions have been omitted since they are not of direct concern for structural and control system design. Induced environments (vehicle caused) may be more critical than natural environments for certain vehicle operational situations, and in some cases the combination of natural and induced environments will be more severe than either environment alone. Induced environments are considered in other space vehicle criteria documents, which should be consulted for such data.

The environment criteria data presented in this document were formulated based on discussions and requests from engineers involved in space vehicle development and operations; therefore, they represent responses to actual engineering problems and are not just a general compilation of environmental data. This report is used extensively by the Marshall Space Flight Center

(MSFC), other NASA centers, various other government agencies, and their associated contractors in design and operational studies. Considerably more information is available on topics covered in this report than is presented here. Users of this document who have questions or require further information on the data provided may direct their requests to the Atmospheric Sciences Division (ES81), Space Sciences Laboratory, Marshall Space Flight Center, Alabama 35812.

1.2 Main Geographical Areas Covered in Document

a. George C. Marshall Space Flight Center, Huntsville, Alabama.

b. John F. Kennedy Space Center and Air Force Eastern Test Range, Florida.

c. Space and Missile Test Center (SAMTEC), Vandenberg AFB, California.

d. Edwards Air Force Base, California.

e. Hickam Air Force Base, Hawaii.

f. Andersen Air Force Base, Guam.

g. Santa Susana, California.

h. Brigham, Utah.

i. Lyndon B. Johnson Space Center, Houston, Texas.

j. Wallops Flight Center, Wallops Island, Virginia.

k. White Sands Missile Range, New Mexico.

l. Sacramento, California.

m. Michoud Assembly Facility, New Orleans, Louisiana.

n. National Space Technology Laboratory (NSTL), Bay St. Louis, Mississippi.

SECTION II. ATMOSPHERIC COMPOSITION

2.1 Composition

Nitrogen, oxygen, argon, and carbon dioxide make up over 99.99 percent by volume of the atmosphere. Table 2.1 gives the composition of the atmosphere to an altitude of 90 km (Ref. 2.1). Excluding water vapor and the gases listed previously, the other gases make up less than 0.004 percent of the total. The gases shown in the table are considered to be proportionally invariant below 90 km. This is not exactly the case. Carbon dioxide varies slightly in amount over long periods of time. Also, ozone is mostly concentrated in a layer between 15 and 60 km above sea level, and water vapor is mostly contained is the lower 10 km of the Earth's atmosphere. At standard conditions, as defined in Reference 2.1, the molecular weight of air is 28.9. Table 2.1 depicts the percent by weight of the listed atmospheric constituents.

While there are a large variety of chemical elements and compounds in the Earth's atmosphere, the two abundant gases (nitrogen and oxygen), plus argon, carbon dioxide, ozone, and water vapor are of primary concern because of their more direct influence on natural processes and their contribution to the mandatory needs of life in general. Various constituents of the atmosphere provide selective absorption of solar radiation. Water vapor in the atmosphere may vary to as much as 0.3 percent by volume plus about 0.008 percent water droplets and ice crystals. Little is known about the effects of variations in the composition of the atmosphere. The space shuttle design criteria commits the space shuttle program, as all NASA programs, to maintain the quality of the atmosphere. Therefore, actual measurements, theoretical estimates, and research are required, beginning with the initial concepts to design, build, and operate aerospace vehicle systems to insure a proper frame of reference relative to atmospheric composition influences.

This section deals mainly with atmospheric composition from sea level to an altitude of 90 km. The vast complexities of atmospheric moisture, aerosols, rarefied gases, etc., are discussed in their respective sections.

2.2 Chemical and Physical Properties

Table 2.2 provides additional information on the chemical and physical properties of the atmospheric constituents commonly referred to and used in studies related to and associated with atmospheric and aerospace physics (Refs. 2.1 and 2.2). These parametric data are based on standard conditions (i.e., temperature, 15°C or 288.15°K; pressure, 1013.25 mb or 1.01325×10^{-5} newton m^{-2}, and density, 1.2250 kg m^{-3}). Reference 2.3 is a useful comprehensive and current source of information on atmospheric chemistry and composition.

TABLE 2.1 NORMAL ATMOSPHERIC COMPOSITION FOR CLEAN, DRY AIR AT ALL LOCATIONS (VALID TO 90 KILOMETERS GEOMETRIC ALTITUDE)

Gas	Percent by Volume	Percent by Weight*
Nitrogen (N_2)	78.084	75.520
Oxygen (O_2)	20.9476	23.142
Argon (Ar)	0.934	1.288
Carbon dioxide (CO_2)	0.0314	0.048
Neon (Ne)	1.818×10^{-3}	1.27×10^{-3}
Helium (He)	5.24×10^{-4}	7.24×10^{-5}
Krypton (Kr)	1.14×10^{-4}	3.30×10^{-4}
Xenon (Xe)	8.7×10^{-6}	3.9×10^{-5}
Hydrogen (H_2)	5×10^{-5}	3×10^{-6}
Methane (CH_4)	2×10^{-4}	1×10^{-4}
Nitrous Oxide (N_2O)	5×10^{-5}	8×10^{-5}
Ozone (O_3) summer	0 to 7×10^{-6}	0 to 1.1×10^{-5}
winter	0 to 2×10^{-6}	0 to 3×10^{-6}
Sulfur dioxide (SO_2)	0 to 1×10^{-4}	0 to 2×10^{-4}
Nitrogen dioxide (NO_2)	0 to 2×10^{-6}	0 to 3×10^{-6}
Ammonia (NH_3)	0 to trace	0 to trace
Carbon monoxide (CO)	0 to trace	0 to trace
Iodine (I_2)	0 to 1×10^{-6}	0 to 9×10^{-6}

*On basis of Carbon 12 isotope scale for which $C^{12} = 12.000$, as adopted by the International Union of Pure and Applied Chemistry meeting, Montreal, in 1961.

TABLE 2.2 COMPOSITION OF THE ATMOSPHERE (DRY) UP TO ABOUT 90 km

Constituent	Symbol	Molecular or Atomic Weight,	Molecular or Atomic Mass (g)	Melting Point (°C)	Boiling Point (°C)	Density (g/l, 0°C)	C_p (15.0°C) (cal/g)
Nitrogen	N_2	28.016	46.50880×10^{-24}	-209.8	-195.8	1.2506	0.2477
Oxygen	O_2	32.000	53.12256×10^{-24}	-218.4	-182.96	1.429	0.2178
Nitrogen (atomic)	N	14.008	23.25440×10^{-24}	—	—	—	—
Oxygen (atomic)	O	16.000	26.56128×10^{-24}	—	—	—	—
Argon	A	39.944	66.31024×10^{-24}	-189.2	-185.7	1.784	0.1253
Carbon Dioxide	CO_2	44.011	73.06168×10^{-24}	- 56.6 5.2 atm***	- 7.85 subl****	1.977	0.1989
Neon	Ne	20.183	33.50539×10^{-24}	-248.67	-245.9	0.9002	0.247
Krypton	Kr	83.800	$139.11470 \times 10^{-24}$	-156.6	-152.9	3.708	0.0603*
Xenon	Xe	131.3	217.9685×10^{-24}	-112	-107.1	5.851	0.0384*
Helium	He	4.003	6.64530×10^{-24}	-272.2 26 atm***	-268.9	0.1785	1.24**
Hydrogen (atomic)	H	1.008	1.673361×10^{-24}	-259.14	-252.8	0.0899	3.389
Nitrous Oxide	N_2O	44.016	73.07008×10^{-24}	-102.4	- 89.49	1.977	0.2004
Ozone	O_3	48.000	79.68384×10^{-24}	-192.5	-111.9	2.144	0.1959

*At 19°C
**At -180°C
***Must be pressurized to solidify.
****Goes from solid to gaseous phase by sublimation process.

REFERENCES

2.1 "U.S. Standard Atmosphere, 1976." United States Government Printing Office, Washington, D.C., October 1976.

2.2 "Handbook of Geophysics and Space Environments." United States Air Force, Air Force Cambridge Research Laboratories, 1965.

2.3 Heicklen, Julian: "Atmospheric Chemistry." Academic Press, New York, 1976.

SECTION III. THERMAL AND RADIATION

3.1 Introduction

One of the more important environmental influences on a vehicle is the thermal environment. Combinations of air temperature, solar radiation, and sky radiation can cause various structural problems. Some examples of potential problems are: (1) Heating of one side of the vehicle by the sun while the other side is cooled by a clear sky causes stresses since the vehicle sides will be of different length; (2) the temperature of the fuel influences the volume/mass relationship; and (3) too high a temperature may destroy the usefulness of a lubricant. The heating or cooling of a surface by air temperature and radiation is a function of the heat transfers taking place; therefore, methods of determining these relationships are presented in this section.

3.2 Definitions

The following terms are used in this section.

Absorption bands are those portions of the solar (or other continuous) spectrum which have lesser intensity because of absorption by gaseous elements or molecules. In general, elements give sharp lines, but molecules such as water vapor or carbon dioxide in the infrared give broad diffuse bands.

Air mass is the amount of atmosphere that the solar radiation passes through, considering the vertical path at sea level as unity (i.e., when the sun is at the zenith, directly overhead).

Air temperature (surface) is the free or ambient air temperature measured under standard conditions of height, ventilation, and radiation shielding. The air temperature is normally measured with liquid-in-glass thermometers in a louvered wooden shelter, painted white inside and outside, with the base of the shelter normally 1.22 meters (4 ft) above a close-cropped grass surface (Ref. 3.1). Unless an exception is stated, surface air temperatures given in this report are temperatures measured under these standard conditions.

Astronomical unit is a unit of length defined as equal to the mean distance between the earth and sun. The current accepted value is 1.495978930 x 10^8 kilometers.

Atmospheric transmittance is the ratio between the intensity of the extraterrestrial solar radiation and intensity of the solar radiation after passing through the atmosphere.

Black body is an ideal emitter which radiates energy at the maximum possible rate per unit area at each wavelength for any given temperature and which absorbs all incident radiation at all wavelengths.

Diffuse sky radiation is the solar radiation reaching the earth's surface after having been scattered from the direct solar beam by molecules or suspensoids in the atmosphere. It is measured on a surface after the direct solar radiation is subtracted from the total horizontal radiation.

Direct solar radiation is the solar radiation received on a surface directly from the Sun and does not include diffuse sky radiation, sometimes called "Beam Radiation".

Emittance is the ratio of the energy emitted by a body to the energy which would be emitted by a black body at the same temperature. All real bodies will emit energy in different amounts from a black body at various wavelengths; i.e., colored bodies are colored because of higher emittance at specific wavelengths. In this document, the assumption is made that the absorptivity of an object is numerically equal to the emittance of the object at the same wavelengths. Therefore, the value of the emittance can be used to determine the portion of the energy received by the object which heats (or energy lost which cools) the object.

Extraterrestrial solar radiation is that solar radiation received outside the earth's atmosphere at one astronomical unit from the sun. The term "solar spectral irradiance" is used when the extraterrestrial solar radiation at small wavelength intervals is considered.

Fraunhofer lines are the dark absorption bands in the solar spectrum caused by gases in the outer portions of the sun and earth's atmosphere.

Horizontal solar radiation is the solar radiation measured on a horizontal surface. This is frequently referred to as "global radiation" or "total horizontal radiation" when solar and diffuse sky radiation are included.

Irradiation is often used to mean solar radiation received by a surface.

Normal incident solar radiation is the radiation received on a surface, normal to the direction of the sun, direct from the sun, and does not include diffuse sky radiation.

Radiation temperature is the absolute temperature of a radiating black body determined by Wien's displacement law, expressed as

$$T_R = \frac{w}{\lambda \max} \quad , \tag{3.1}$$

where T_R is the absolute temperature of the radiating body (°K), w is the Wein's displacement constant (0.2880 cm °K), and λ max is the wavelength of the maximum radiation intensity for the black body.

Sky radiation temperature is the average radiation temperature of the sky when it is assumed to be a black body. Sky radiation is the radiation to and through the atmosphere from outer space. While this radiation is normally termed nocturnal radiation, it takes place under clear skies even during daylight hours.

Solar constant is the rate at which solar radiation is received outside the earth's atmosphere on a surface normal to the incident radiation and at the earth's mean distance from the sun. The solar constant equals 1.940 cal cm^{-2} min^{-1} (0.1353 W cm^{-2}) (Ref. 3.2).

Solar radiation in this document will be defined as the radiant energy from the sun between 0.22 and 20.0 μm (subsection 3.3.2).

Surface (skin) temperature is the temperature which a given surface will have when exposed to air temperature and radiation within the approximate wavelength interval of 0.22 to 20.0 μm.

3.3 Spectral Distribution of Radiation

3.3.1 Introduction

All objects radiate energy in the electromagnetic spectrum. The amount and frequency of the radiation distribution is a function of temperature. The higher the temperature, the greater the amount of total energy emitted and the higher the frequency (shorter the wavelength) of the peak energy emission.

3.3.2 Solar Radiation

The sun emits energy in the electromagnetic spectrum from 10^{-7} to greater than 10^5 μm. This radiation ranges from cosmic rays through the very long wave radio waves. The total amount of radiation from the sun is nearly constant in intensity with time.

Of the total electromagnetic spectrum of the sun, only the radiant energy from that portion of the spectrum between 0.22 and 20.0 μm (the light spectrum) will be considered in this document since it contains 99.8 percent of the total electromagnetic energy. The spectral distribution of this region closely resembles the emission of a gray body radiating at 6000°K. This is the spectral region which causes nearly all of the heating or cooling of an object.

Solar radiation outside the earth's atmosphere is distributed in a continuous spectrum with many narrow absorption bands caused by the elements and molecules in the colder solar atmosphere. These absorption bands are the Fraunhofer lines, whose widths are usually very small ($< 10^{-4}$ μm in most cases).

The earth's atmosphere also absorbs a part of the solar radiation such that the major portion of the solar radiation reaching the earth's surface is between about 0.35 and 4.00 μm. The distribution of the solar energy outside the earth's atmosphere[2] (extraterrestrial) is as follows:

Region (μm)	Distribution (%)	Solar Intensity[2] g-cal cm^{-2} (min^{-1})
Ultraviolet below 0.38	7.003	0.136
0.38 to 0.75	44.688	0.867
Infrared above 0.75	48.309	0.937

The first detailed information published for use by engineers on the distribution of solar radiation energy (solar irradiation) wavelength was that by Parry Moon in 1940 (Ref. 3.3). These data were generally based on theoretical curves but are still used as the basic solar radiation in design by many engineers.

---

2. At one astronomical unit on a surface normal to the sun.

3.3.3 Intensity Distribution

Table 3.1 presents data on the distribution with wavelength of solar radiation outside the earth's atmosphere and at the earth's surface after 1.0 atmosphere absorption. The solar radiation distribution data outside the earth's atmosphere (solar spectral irradiance) are based on recent extraterrestrial data obtained by high-flying aircraft and published by Thekaekara (Ref. 3.4). The values of solar radiation for 1.0 atmosphere absorption are representative of a very clear atmosphere which provides a minimum of atmospheric absorption. This gives a total normal solar radiation value (area under the spectral curve) equal to the highest values measured at the earth's surface in mid-latitudes. These data are for use in solar radiation design studies when extreme solar radiation effects are desired at the earth's surface. The same data are shown in graphical form in Figure 3.1.

3.3.4 Atmospheric Transmittance of Solar Radiation

The atmosphere of the earth is composed of a mixture of gases, aerosols, and dust which absorb radiation in different amounts at various wavelengths. If the ratio is taken of the solar spectral irradiance I_o to that of the solar radiation after absorption through one air mass $I_{1.00}$, an atmospheric transmittance factor M can be found [equation (3.2)]:

$$M = \frac{I_o}{I_{1.00}} \tag{3.2}$$

The atmospheric transmittance constant can be used in the following equation for computations of intensities for any other number of air masses:

$$I_N = I_o (M^N) \quad , \tag{3.3}$$

where

I_N = intensity of solar radiation for N air mass thickness

N = number of air masses.

Equation (3.3) can also be used to obtain solar radiation intensities versus wavelengths for other total normal incident solar radiation intensities

TABLE 3.1 SOLAR SPECTRAL IRRADIANCE (outside atmosphere) AND SOLAR RADIATION AFTER ABSORPTION BY CLEAR ATMOSPHERE

Wavelength (microns) λ	Solar Spectral Irradiance (watts $cm^{-2}\ \mu^{-1}$)	Area Under Solar Spectral Irradiance Curve (watts cm^{-2})	Solar Radiation After One Atmosphere Absorption (watts $cm^{-2}\ \mu^{-1}$)	Area Under One Atmosphere Solar Radiation Curve (watts cm^{-2})	Percentage of Solar Radiation After One Atmosphere Absorption for Wavelengths Shorter than λ (%)
0.120	0.000010	0.00000060	0.000000	0.000000	0.00
0.140	0.000003	0.00000073	0.000000	0.000000	0.00
0.150	0.000007	0.00000078	0.000000	0.000000	0.00
0.160	0.000023	0.00000093	0.000000	0.000000	0.00
0.170	0.000063	0.00000136	0.000000	0.000000	0.00
0.180	0.000125	0.00000230	0.000000	0.000000	0.00
0.190	0.000271	0.00000428	0.000000	0.000000	0.00
0.200	0.00107	0.000010	0.000001	0.000000	0.00
0.210	0.00229	0.000027	0.000003	0.000000	0.00
0.220	0.00575	0.000067	0.000007	0.000000	0.00
0.225	0.00649	0.000098	0.000007	0.000000	0.00
0.230	0.00667	0.000131	0.000008	0.000000	0.00
0.235	0.00593	0.000162	0.000007	0.000000	0.00
0.240	0.00630	0.000193	0.000007	0.000000	0.00
0.245	0.00723	0.000227	0.000008	0.000000	0.00
0.250	0.00704	0.000263	0.000008	0.000000	0.00
0.255	0.0104	0.000306	0.000012	0.000000	0.00
0.260	0.0130	0.000365	0.000015	0.000000	0.00
0.265	0.0185	0.000443	0.000021	0.000000	0.00
0.270	0.0232	0.000548	0.000026	0.000000	0.00
0.275	0.0204	0.000657	0.000023	0.000000	0.00
0.280	0.0222	0.000763	0.000025	0.000000	0.00
0.285	0.0315	0.000897	0.000036	0.000001	0.00
0.290	0.0482	0.001097	0.000055	0.000001	0.00
0.295	0.0584	0.001363	0.000066	0.000001	0.00
0.300	0.0514	0.001638	0.006677	0.000035	0.03
0.305	0.0603	0.001917	0.019830	0.000134	0.12
0.310	0.0689	0.002240	0.029084	0.000279	0.25
0.315	0.0764	0.002603	0.038941	0.000474	0.42
0.320	0.0830	0.003002	0.047684	0.000712	0.64
0.325	0.0975	0.003453	0.062018	0.001022	0.92
0.330	0.1059	0.003961	0.073829	0.001392	1.25
0.335	0.1081	0.004496	0.080896	0.001796	1.61
0.340	0.1074	0.005035	0.084636	0.002219	1.99
0.345	0.1069	0.005571	0.087080	0.002655	2.39
0.350	0.1093	0.006111	0.091327	0.003111	2.80
0.355	0.1083	0.006655	0.092186	0.003572	3.40
0.360	0.1068	0.007193	0.092857	0.004036	3.63
0.365	0.1132	0.007743	0.099873	0.004536	4.08
0.370	0.1181	0.008321	0.105507	0.005063	4.55
0.375	0.1157	0.008906	0.104596	0.005586	5.03
0.380	0.1120	0.009475	0.102971	0.006101	5.49
0.385	0.1098	0.010030	0.102273	0.006613	5.95
0.390	0.1098	0.010579	0.103977	0.007132	6.42
0.395	0.1189	0.011150	0.114309	0.007704	6.93
0.400	0.1429	0.011805	0.137403	0.008391	7.55
0.405	0.1644	0.012573	0.158076	0.009181	8.26
0.410	0.1751	0.013422	0.168365	0.010023	9.02
0.415	0.1774	0.014303	0.170576	0.010876	9.79
0.420	0.1747	0.015183	0.167980	0.011716	10.54
0.425	0.1693	0.016043	0.162788	0.012530	11.28
0.430	0.1639	0.016876	0.157596	0.013318	11.99
0.435	0.1663	0.017702	0.159903	0.014117	12.71
0.440	0.1810	0.018570	0.174038	0.014988	13.40
0.445	0.1922	0.019503	0.184807	0.015912	14.30
0.450	0.2006	0.020485	0.192884	0.016876	15.19
0.455	0.2057	0.021501	0.195904	0.017656	16.07
0.460	0.2066	0.022532	0.196761	0.018839	16.96
0.465	0.2048	0.023560	0.196923	0.019824	17.84
0.470	0.2033	0.024580	0.195480	0.020801	18.72

TABLE 3.1 (Continued)

Wavelength (microns) λ	Solar Spectral Irradiance (watts $cm^{-2}\mu^{-1}$)	Area Under Solar Spectral Irradiance Curve (watts cm^{-2})	Solar Radiation After One Atmosphere Absorption (watts $cm^{-2}\mu^{-1}$)	Area Under One Atmosphere Solar Radiation Curve (watts cm^{-2})	Percentage of Solar Radiation After One Atmosphere Absorption for Wavelengths Shorter than λ (%)
0.475	0.2044	0.025600	0.196538	0.021784	19.61
0.480	0.2074	0.026629	0.197523	0.022772	20.50
0.485	0.1976	0.027642	0.186415	0.023704	21.34
0.490	0.1950	0.028623	0.183962	0.024624	22.17
0.495	0.1960	0.029601	0.183177	0.025539	22.99
0.500	0.1942	0.030576	0.179814	0.026439	23.80
0.505	0.1920	0.031542	0.176146	0.027319	24.60
0.510	0.1882	0.032492	0.172660	0.028183	25.37
0.515	0.1833	0.033421	0.168165	0.029023	26.13
0.520	0.1833	0.034337	0.168165	0.029864	26.88
0.525	0.1852	0.035259	0.169908	0.030714	27.65
0.530	0.1842	0.036182	0.168990	0.031559	28.41
0.535	0.1818	0.037097	0.166788	0.032393	29.16
0.540	0.1783	0.037997	0.163977	0.033211	29.90
0.545	0.1754	0.038882	0.160917	0.034015	30.62
0.550	0.1725	0.039751	0.158256	0.034806	31.33
0.555	0.1720	0.040613	0.157798	0.035595	32.05
0.560	0.1695	0.041466	0.155504	0.036373	32.75
0.565	0.1705	0.042316	0.156422	0.037155	33.45
0.570	0.1712	0.043171	0.157064	0.037940	34.16
0.575	0.1719	0.044028	0.157726	0.038729	34.87
0.580	0.1715	0.044887	0.157339	0.039516	35.57
0.585	0.1712	0.045744	0.157064	0.040301	36.28
0.590	0.1700	0.046597	0.155963	0.041081	36.98
0.595	0.1682	0.047442	0.154311	0.041852	37.68
0.600	0.1666	0.048279	0.152844	0.042616	38.37
0.605	0.1647	0.049107	0.151100	0.043372	39.05
0.610	0.1635	0.049928	0.150000	0.044122	39.72
0.620	0.1602	0.051546	0.146972	0.045592	41.05
0.630	0.1570	0.053132	0.145370	0.047045	42.30
0.640	0.1544	0.054689	0.144299	0.048488	43.66
0.650	0.1511	0.056217	0.142547	0.049914	44.94
0.660	0.1486	0.057715	0.141523	0.051329	46.22
0.670	0.1456	0.059186	0.140000	0.052729	47.48
0.680	0.1427	0.060628	0.137211	0.054101	48.71
0.690	0.1402	0.062042	0.134807	0.055449	49.93
0.700	0.1369	0.063428	0.131634	0.056766	51.11
0.710	0.1344	0.064784	0.129230	0.058058	52.27
0.720	0.1314	0.066113	0.126346	0.059321	53.41
0.730	0.1290	0.067415	0.124038	0.060562	54.53
0.740	0.1260	0.068690	0.121153	0.061773	55.62
0.750	0.1235	0.069938	0.118750	0.062961	56.69
0.800	0.1107	0.075793	0.106442	0.068283	61.48
0.850	0.0988	0.081030	0.095000	0.073033	65.76
0.900	0.0889	0.085723	0.080090	0.077037	69.36
0.950	0.0835	0.090033	0.077314	0.080903	72.84
1.000	0.0746	0.093985	0.071730	0.084490	76.07
1.100	0.0592	0.100675	0.056923	0.090182	81.20
1.200	0.0484	0.106055	0.046538	0.094836	85.39
1.300	0.0396	0.110455	0.036000	0.098436	88.63
1.400	0.0336	0.114115	0.002240	0.098660	88.83
1.500	0.0287	0.117230	0.027333	0.101393	91.29
1.600	0.0244	0.119885	0.023461	0.103739	93.40
1.700	0.0202	0.122115	0.019423	0.105681	95.15
1.800	0.0159	0.123920	0.013826	0.107064	96.40
1.900	0.0126	0.125345	0.000126	0.107077	96.41
2.000	0.0103	0.126490	0.009809	0.108057	97.29
2.100	0.0090	0.127455	0.008653	0.108923	98.07
2.200	0.0079	0.128300	0.007596	0.109682	98.76
2.300	0.0068	0.129035	0.006538	0.110336	99.34

TABLE 3.1 (Concluded)

Wavelength (microns) λ	Solar Spectral Irradiance (watts cm^{-2} μ^{-1})	Area Under Solar Spectral Irradiance Curve (watts cm^{-2})	Solar Radiation After One Atmosphere Absorption (watts cm^{-2} μ^{-1})	Area Under One Atmosphere Solar Radiation Curve (watts cm^{-2})	Percentage of Solar Radiation After One Atmosphere Absorption for Wavelengths Shorter than λ (%)
2.4	0.0064	0.129695	0.006153	0.110951	99.90
2.5	0.0054	0.130285	0.001080	0.111059	100.00
2.6	0.0048	0.130795	0.000005	0.111060	100.00
2.7	0.0043	0.131250	0.000004	0.111060	100.00
2.8	0.00390	0.131660	0.000004	0.111061	100.00
2.9	0.00350	0.132030	0.000004	0.111061	100.00
3.0	0.00310	0.132360	0.000003	0.111061	100.00
3.1	0.00260	0.132645	0.000002	0.111062	100.00
3.2	0.00226	0.132888	0.000002	0.111062	100.00
3.3	0.00192	0.133097	0.000002	0.111062	100.00
3.4	0.00166	0.133276	0.000001	0.111062	100.00
3.5	0.00146	0.133432	0.000001	0.111062	100.00
3.6	0.00135	0.133573	0.000001	0.111062	100.00
3.7	0.00123	0.133702	0.000001	0.111062	100.00
3.8	0.00111	0.133819	0.000001	0.111063	100.00
3.9	0.00103	0.133926	0.000001	0.111063	100.00
4.0	0.00095	0.134025	0.000001	0.111063	100.00
4.1	0.00087	0.134116	0.000001	0.111063	100.00
4.2	0.00078	0.134198	0.000000	0.111063	100.00
4.3	0.00071	0.134273	0.000000	0.111063	100.00
4.4	0.00065	0.134341	0.000000	0.111063	100.00
4.5	0.00059	0.134403	0.000000	0.111063	100.00
4.6	0.00053	0.134459	0.000000	0.111063	100.00
4.7	0.00048	0.134509	0.000000	0.111063	100.00
4.8	0.00045	0.134556	0.000000	0.111063	100.00
4.9	0.00041	0.134599	0.000000	0.111063	100.00
5.0	0.0003830	0.13463906	0.000000	0.111063	100.00
6.0	0.0001750	0.13491806	0.000000	0.111063	100.00
7.0	0.0000990	0.13505506	0.000000	0.111063	100.00
8.0	0.0000600	0.13513456	0.000000	0.111063	100.00
9.0	0.0000380	0.13518356	0.000000	0.111063	100.00
10.0	0.0000250	0.13521506	0.000000	0.111063	100.00
11.0	0.0000170	0.13523606	0.000000	0.111063	100.00
12.0	0.0000120	0.13525056	0.000000	0.111063	100.00
13.0	0.0000087	0.13526091	0.000000	0.111063	100.00
14.0	0.0000055	0.13526801	0.000000	0.111063	100.00
15.0	0.0000049	0.13527321	0.000000	0.111063	100.00
16.0	0.0000038	0.13527756	0.000000	0.111063	100.00
17.0	0.0000031	0.13528101	0.000000	0.111063	100.00
18.0	0.0000024	0.13528376	0.000000	0.111063	100.00
19.0	0.0000020	0.13528596	0.000000	0.111063	100.00
20.0	0.0000016	0.13528776	0.000000	0.111063	100.00
25.0	0.000000610	0.13529328	0.000000	0.111063	100.00
30.0	0.000000300	0.13529556	0.000000	0.111063	100.00
35.0	0.000000160	0.13529671	0.000000	0.111063	100.00
40.0	0.000000094	0.13529734	0.000000	0.111063	100.00
50.0	0.000000038	0.13529800	0.000000	0.111063	100.00
60.0	0.000000019	0.13529829	0.000000	0.111063	100.00
80.0	0.000000007	0.13529855	0.000000	0.111063	100.00
100.0	0.000000003	0.13529865	0.000000	0.111063	100.00
1000.0	0.000000000	0.13530000	0.000000	0.111063	100.00

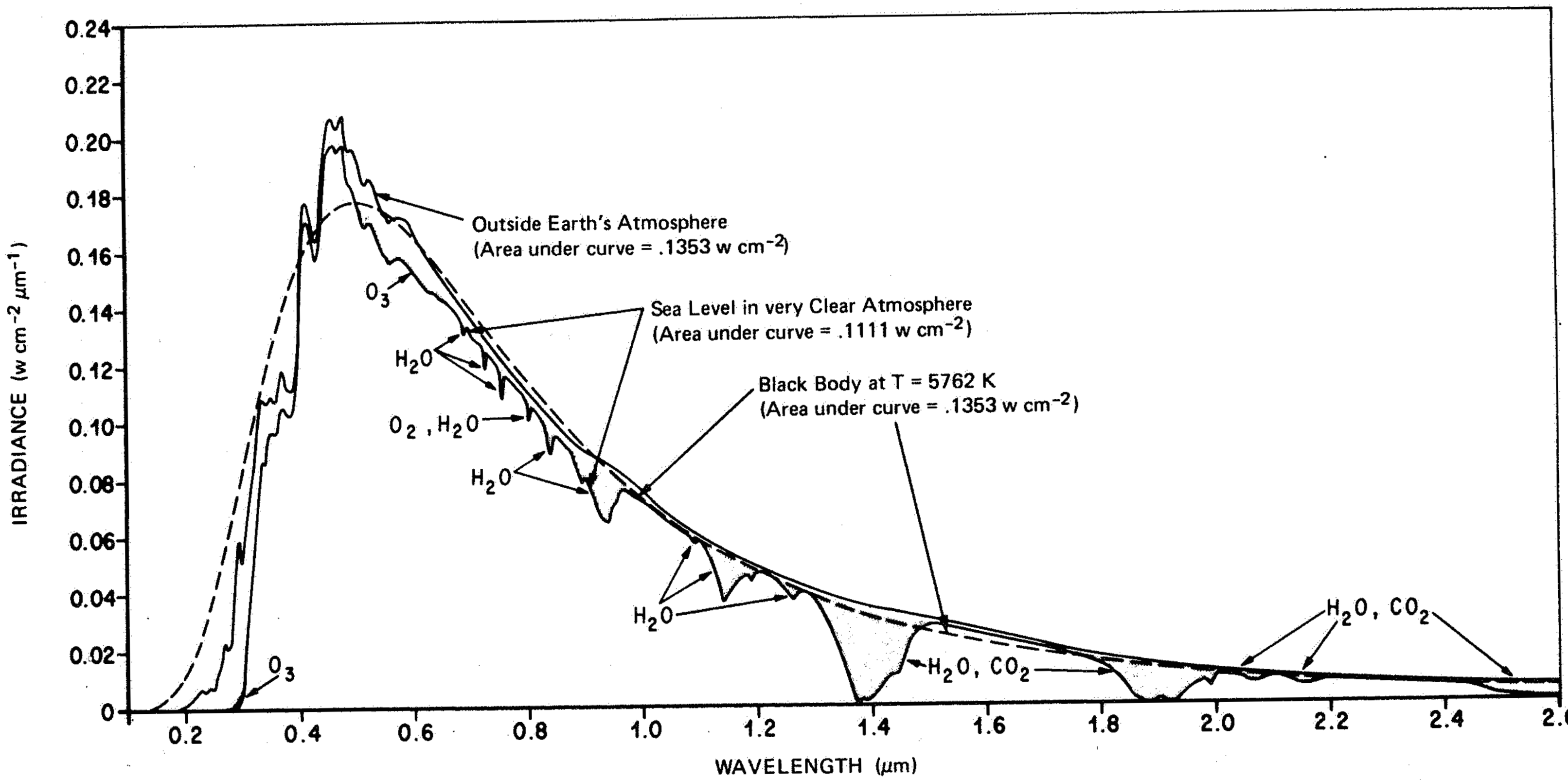

FIGURE 3.1. NORMAL INCIDENT SOLAR RADIATION AT SEA LEVEL ON VERY CLEAR DAYS, SOLAR SPECTRAL IRRADIANCE OUTSIDE THE EARTH'S ATMOSPHERE AT 1 AU (REF. 3.3), AND BLACK BODY SPECTRAL IRRADIANCE CURVE AT T = 5762°K (NORMALIZED TO 1 AU)

(area under curve) by computation of new values of atmospheric transmittance as follows:

$$M_N = M \frac{I_{TN}}{0.1111} \quad , \qquad (3.4)$$

where

I_{TN} = new value of total normal incident solar radiation intensity in $W\,cm^{-2}$

M = value for atmospheric transmittance given in Table 3.1

M_N = new value of atmospheric transmittance.

Equations (3.3) and (3.4) are valid only for locations relatively near the earth's surface (below 5 km altitude). For higher altitudes, corrections would be needed for the change of the amount of ozone and water vapor in the atmosphere. Also, equation (3.4) should be used only for values of I_{TN} greater than 0.0767 $W\,cm^{-2}$ (1.10 g-cal cm^{-2} min^{-1}) since values lower than this would indicate a considerably higher ratio of water vapor to ozone in the atmosphere and require that the curve be adjusted to give more absorption in the infrared water vapor bands at long wavelengths (infrared) and a smaller increase for the ozone at shorter wavelengths.

3.3.5 Sky (Diffuse) Radiation

When solar radiation, which is a nearly parallel beam of light, enters the atmosphere of the earth, molecules of air, dust particles, and aerosols such as water vapor droplets either diffuse or absorb a part of the radiation. The diffuse radiation then reaches the earth as nonparallel light from all directions.

3.3.5.1 Scattered Radiation

The scattered radiation gives the sky its brightness and color. The color is a result of selective scattering at certain wavelengths as a function of the size of the molecules and particles.

On a clear day the amount of scattering is very low because there are few particles and water droplets. The clear sky can be as little as 10^{-6} as bright as the surface of the sun. This sky radiation is called "diffuse radiation"

TABLE 3.2 SURFACE AIR AND SKY RADIATION TEMPERATURE EXTREMES

Area		Surface Air Temperature Extremes[a]				Sky Radiation	
		Maximum		Minimum		Extreme Minimum Equivalent Temperature	Equivalent Radiation (g-cal cm^{-2}min^{-1})
		Extreme	95%[b]	Extreme	95%[b]		
Huntsville, Ala.	°C	40.0	36.7	-23.9	-12.8	-30.0	0.28
	°F	104	98	-11	9	-22	
Kennedy Space Center, Fla.	°C	37.2	33.3	-3.9	1.7	-15.0	0.36
	°F	99	92	25	35	5	
Space and Missile Test Center Vandenberg AFB, Calif.	°C	37.8	29.4	-3.3	1.1	-15.0	0.36
	°F	100	85	26	34	5	
Edwards AFB, Calif.	°C	45.0	41.7	-15.6	-7.8	-30.0	0.28
	°F	113	107	4	18	-22	
Honolulu, Oahu — Hickam Field	°C	33.9	32.8	11.1	15.6	-15.0	0.36
	°F	93	91	52	60	5	
Guam — Andersen AFB	°C	34.4	31.1	18.9	22.2	-15.0	0.36
	°F	94	88	66	72	5	
Santa Susana, Calif.	°C	42.2	36.1	-2.2	1.7	-15.0	0.36
	°F	108	97	28	35	5	
Thiokol Wasatch Division, Utah	°C	38.3	35.6	-27.8	-16.1	-30.0	0.28
	°F	101	96	-18	3	-22	
New Orleans, La.	°C	37.8	35.0	-10.0	-3.3	-17.8	0.35
	°F	100	95	14	26	0	
National Space Tech. Lab., Miss.	°C	37.8	35.6	-13.9	-2.2	-17.8	0.35
	°F	100	96	7	28	0	
Continent Transportation (rail, truck, river barge)	°C	47.2	—	-34.4	—	-30.0	0.28
	°F	117	—	-30	—	-22	
Ship Transportation (West Coast, Panama Canal, Gulf of Mexico)	°C	37.8	—	-12.2	—	-15.0	0.36
	°F	100	—	10	—	5	
Johnson Space Center, Tex.	°C	40.0	36.7	-9.4	-2.2	-17.8	0.35
	°F	104	98	15	28	0	
Wallops Flight Center, Va.	°C	37.2	33.3	-20.0	-5.6	-17.8	0.35
	°F	99	92	-4	22	0	
White Sands Missile Range, N.M.	°C	41.7	38.9	-23.9	-10.0	-30.0	0.28
	°F	107	102	-11	14	-22	

a. The extreme maximum and minimum temperatures will be encountered during periods of wind speeds less than about 1 meter per second.

b. Based on daily extreme (maximum or minimum) observations for worst month.

in this document. On a clear day the total energy contribution from the diffuse radiation from the entire sky hemisphere to a horizontal surface is between 0.0007 and 0.014 W cm^{-2} (0.01 and 0.20 g-cal cm^{-2} min^{-1}).

As a black body radiator, the clear sky is considered equivalent to a cold surface (Table 3.2). The temperature of the clear sky is the same during the daytime as at nighttime. Values of sky radiation for several localities are given in Table 3.3. It is the clear sky at night acting as a cold sink, without the solar radiation heating the surface of the earth, that causes air temperatures to be lower than the daytime values.

With clouds the amount of diffuse radiation is greater. The total hemisphere during an overcast day may contribute as much as 0.069 W cm^{-2} (1.0 g-cal cm^{-2} min^{-1}) of radiation to a horizontal surface.

The greater scattering by clouds makes the effective temperature of the clouds warmer than the clear air. At night the clouds act as a barrier to the outgoing radiation. Since they are warmer than the clear sky, the air near the ground will not cool to as low a temperature.

3.3.5.2 Absorbed Radiation

The various gases in the atmosphere selectively absorb some of the incoming radiation. Absorption changes some of the radiation into heat or radiation at wavelengths different from that received. Absorption by gases is observed in the solar spectrum as bands of various widths. The major gases in the earth's atmosphere, which show as absorption bands in the solar spectrum, are water vapor, carbon dioxide, ozone, and molecular oxygen.

3.4 Average Emittance of Colored Objects

In thermal engineering studies, the color of a painted surface is not important when one considers low-temperature radiation, i.e., from 10° to 68°C, since most painted surfaces have the same absorptivity at these low temperatures. Colored surfaces may differ in absorptivity. A list of values of emissivity and absorptivity for various surfaces and different colors of paint exposed to solar radiation are presented in Reference 3.5. Similar data are given in other publications that give either a range of values or mean values for the type of surface. The change of temperature (above or below the air temperature), which is the amount of heating or cooling, is proportional to the emissivity or absorptivity; therefore, the accuracy of determining the temperature of a surface is related to the accuracy of the emissivity and absorptivity. Spectral distribution curves of emittance are available for many surfaces. The average emittance of any surface can be computed by the following method:

a. Divide the spectral emittance curve (i.e., Figure 3.1) into small intervals that have little or no change of emittance within the interval.

b. Using the same intervals from the spectral distribution of radiation (i.e., from Table 3.1), multiply each value of emittance over the selected interval by the percentage of radiation over the interval.

c. Sum the resultant products to give the average emittance.

Table 3.4 and Figure 3.2 give an example of such computations with data from Figure 3.1 and Table 3.1 being used. Similar computations can be accomplished for other sources of radiation such as the night sky or from cloudy skies.

3.5 Computation of Surface Temperature for Several Simultaneous Radiation Sources

The extreme value of temperature which a surface may reach when exposed to daytime (solar) or nighttime (night sky) radiation with no wind (calm), assuming it has no mass or heat transfer within the object, is

$$T_S = T_A + E\,(\Delta T_{BS}) \quad , \tag{3.5}$$

where

T_S = surface temperature (°K)

T_A = air temperature (°K)

E = emittance of surface

ΔT_{BS} = increase in black body temperature (°K) from daytime solar radiation (plus) or decrease in black body temperature (°K) from nighttime sky radiation (minus), calculated from

TABLE 3.3 SOLAR RADIATION MAXIMUM VALUES ASSOCIATED WITH EXTREME WIND VALUES

Maximum Solar Radiation (Normal Incident)						
Steady-State Ground Wind Speed at 18 m Height	Huntsville, New Orleans, NSTL, JSC Gulf Transportation, Eastern Test Range, Western Test Range, West Coast Transportation and Wallops Test Range			White Sands Missile Range		
($m\ sec^{-1}$)	($kJm^{-2}\ sec^{-1}$)	($g\text{-}cal\ cm^{-2}\ min^{-1}$)	($BTU\ ft^{-2}\ hr^{-1}$)	($kJm^{-2}\ sec^{-1}$)	($g\text{-}cal\ cm^{-2}\ min^{-1}$)	($BTU\ ft^{-2}\ hr^{-1}$)
10	0.84	1.20	265	1.05	1.50	332
15	0.56	0.80	177	0.70	1.00	221
≥20	0.35	0.50	111	0.56	0.80	177

TABLE 3.4 COMPUTATION OF EMITTANCE OF WHITE PAINT EXPOSED TO DIRECT SOLAR RADIATION AT THE EARTH'S SURFACE

Wavelength (μ)	Emittance	Average Emittance	Solar Radiation, 1 Atmosphere (%)	Solar Radiation over Interval (%)	Product of Average Emittance and Percent Solar Radiation over Interval Divided by 100
0.300	0.73		0.03		
		0.590		1.22	0.0072
0.330	0.45		1.25		
		0.410		1.55	0.0063
0.350	0.37		2.80		
		0.365		21.00	0.0766
0.500	0.36		23.80		
		0.325		11.77	0.0382
0.580	0.29		35.57		
		0.260		15.54	0.0404
0.700	0.23		51.11		
		0.225		10.37	0.0233
0.800	0.22		61.48		
		0.260		7.88	0.0205
0.900	0.30		69.36		
		0.370		6.71	0.0248
1.000	0.44		76.07		
		0.520		9.32	0.0485
1.200	0.60		85.39		
		0.650		3.44	0.0224
1.400	0.70		88.83		
		0.745		4.57	0.0340
1.600	0.79		93.40		
		0.810		3.01	0.0244
1.900	0.83		96.41		
		0.830		3.59	0.0298
50.000	0.83		100.00		
			Sum = average emittance = 0.396		

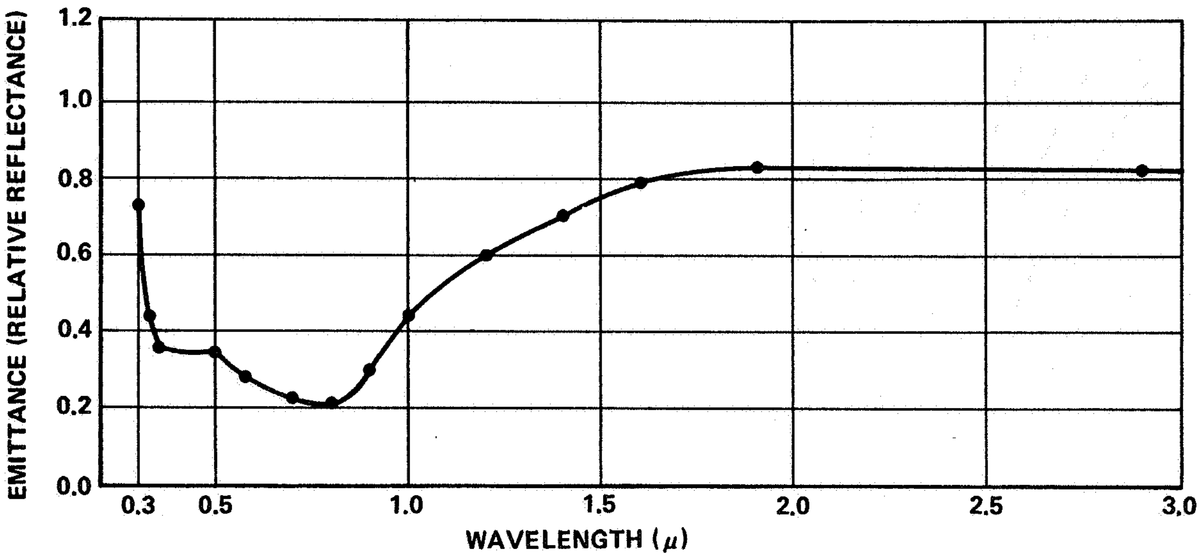

FIGURE 3.2 EMITTANCE OF BARIUM SULPHATE AND MAGNESIUM OXIDE VERSUS WAVELENGTH

$$\Delta T_{BS} = \left(\frac{I_{TS}}{\sigma}\right)^{1/4} - T_A \quad . \tag{3.6}$$

Extreme values of ΔT_{BS} can be obtained from Figure 3.3A or Table 3.5, where

I_{TS} = total radiation (solar by day) (sky for night) received at surface. These values can be extremes from Tables 3.6, 3.7 or 3.2 from this report.

σ = Stefan-Boltzmann constant

= 8.1296×10^{-11} g-cal cm^{-2} K^{-4}

= 5.6692×10^{-12} W cm^{-2} K^{-4}

The term $\left(\frac{I_{TS}}{\sigma}\right)^{1/4}$ is equal to the extreme black body surface temperature.

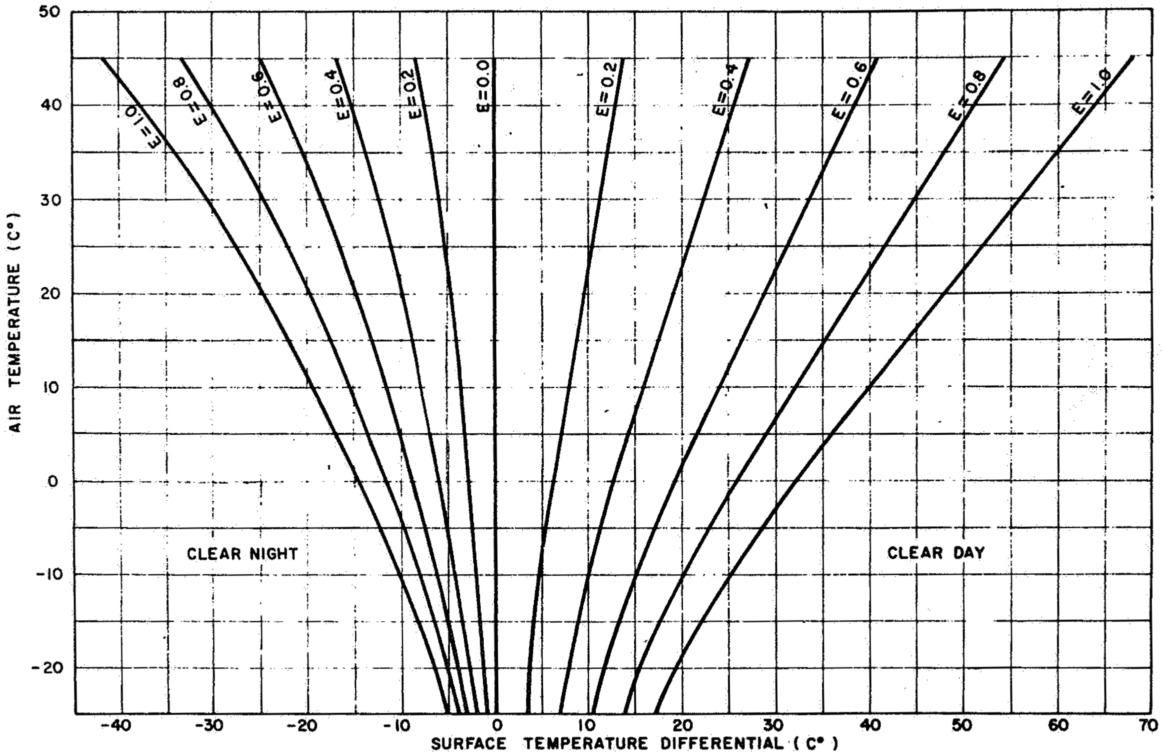

A. Surface temperature differentials with respect to air temperature for surface of emittance from 0.0 to 1.0 for calm wind conditions. Temperature difference after correction for wind is to be added or subtracted to the air temperature to give surface (skin) temperature.

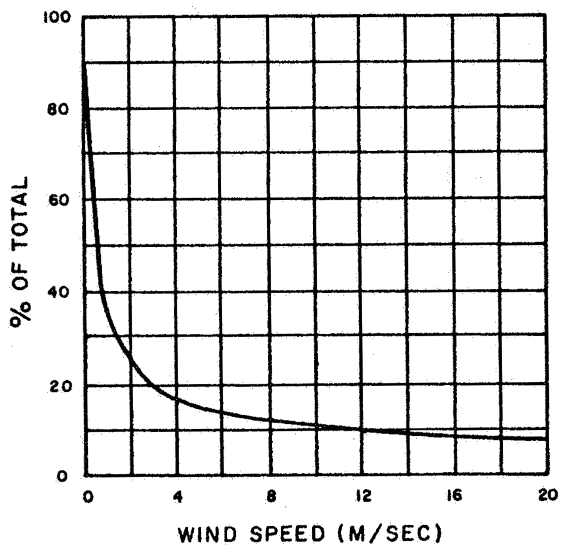

B. Correction for wind speed obtained from Graph A. Valid only for a pressure of one atmosphere.

FIGURE 3.3. EXTREME SURFACE (skin) TEMPERATURE OF AN OBJECT NEAR THE EARTH'S SURFACE (0 to 300m) FOR CLEAR SKY

TABLE 3.5 EXTREME SURFACE (skin) TEMPERATURE ABOVE OR BELOW AIR TEMPERATURE OF AN OBJECT NEAR THE EARTH'S SURFACE

Air Temperature	Surface Temperature Differential (°C)									
	Clear Night					Clear Day				
	Wind Speed (m sec^{-1})					Wind Speed (m sec^{-1})				
	0	2	4	10	20	0	2	4	10	20
	Correction Factor					Correction Factor				
(°C)	1.00	0.25	0.17	0.11	0.08	1.00	0.25	0.17	0.11	0.08
-25	-5.0	-1.2	-0.8	-0.6	-0.4	16.9	4.2	2.9	1.9	1.4
-20	-6.5	-1.6	-1.1	-0.7	-0.5	19.2	4.8	3.3	2.1	1.5
-15	-8.2	-2.0	-1.4	-0.9	-0.6	22.0	5.5	3.7	2.4	1.8
-10	-10.2	-2.6	-1.7	-1.1	-0.8	25.1	6.3	4.3	2.8	2.0
- 5	-12.2	-3.0	-2.1	-1.3	-1.0	28.5	7.1	4.8	3.1	2.3
0	-14.5	-3.6	-2.5	-1.6	-1.2	32.0	8.0	5.4	3.5	2.6
5	-16.9	-4.2	-2.9	-1.9	-1.4	36.0	9.0	6.1	4.0	2.9
10	-19.4	-4.8	-3.3	-2.1	-1.6	40.0	10.0	6.8	4.4	3.2
15	-21.9	-5.5	-3.7	-2.4	-1.8	44.0	11.0	7.5	4.8	3.5
20	-24.6	-6.2	-4.2	-2.7	-2.0	48.0	12.0	8.2	5.3	3.8
25	-27.4	-6.8	-4.6	-3.0	-2.2	52.0	13.0	8.8	5.7	4.2
30	-30.5	-7.6	-5.2	-3.4	-2.4	56.0	14.0	9.5	6.2	4.5
35	-34.0	-8.5	-5.8	-3.7	-2.7	60.0	15.0	10.2	6.6	4.8
40	-37.7	-9.4	-6.4	-4.1	-3.0	64.0	16.0	10.9	7.0	5.1
45	-41.7	-10.4	-7.1	-4.6	-3.3	68.0	17.0	11.6	7.5	5.4

NOTE: Values are given for an emittance value of 1.0. Temperature differences for other emittance can be determined by multiplying tabular value by the appropriate emittance.

TABLE 3.6 EXTREME VALUES OF SOLAR RADIATION FOR THE SPACE AND MISSILE TEST CENTER, WEST COAST TRANSPORTATION, SANTA SUSANA, WHITE SANDS MISSILE RANGE, BRIGHAM CITY, AND EDWARDS AFB

TIME OF DAY (Local Standard Time)	Total Horizontal Solar Radiation g-cal cm^{-2} min^{-1}		Diffuse Radiation Associated with Total Horizontal Solar Radiation Extremes g-cal cm^{-2} min^{-1}		Total Normal Incident Solar Radiation g-cal cm^{-2} min^{-1}		Total 45° Surface Solar Radiation g-cal cm^{-2} min^{-1}	
	JUNE							
	EXTREME	95 Percentile	EXTREME	95 Percentile	EXTREME	95 Percentile	EXTREME	95 Percentile
0500	0	0	0	0	0	0	0	0
0600	0.16	0.11	.02	.04	1.14	0.78	0.04	0
0700	0.46	0.40	.05	.08	1.34	1.08	0.19	0.16
0800	0.82	0.76	.06	.09	1.54	1.38	0.34	0.31
0900	1.16	1.11	.04	.08	1.74	1.62	0.84	0.77
1000	1.45	1.42	0	.03	1.79	1.71	1.19	1.12
1100	1.64	1.56	0	.10	1.79	1.69	1.39	1.31
1200	1.69	1.63	0	.08	1.74	1.68	1.49	1.38
1300	1.69	1.64	0	.07	1.74	1.68	1.49	1.40
1400	1.59	1.54	.06	.12	1.74	1.68	1.34	1.29
1500	1.45	1.39	0	.06	1.79	1.70	1.14	1.09
1600	1.21	1.19	0	.02	1.79	1.71	0.89	0.78
1700	0.87	0.83	.03	.05	1.69	1.60	0.34	0.18
1800	0.46	0.42	.05	.08	1.39	1.23	0.19	0.13
1900	0.14	0.12	.02	.04	1.19	0.93	0.04	0
2000	0	0	0	0	0	0	0	0
	DECEMBER							
	EXTREME	95 Percentile	EXTREME	95 Percentile	EXTREME	95 Percentile	EXTREME	95 Percentile
0800	0	0	0	0	0	0	0	0
0900	0.35	0.32	0.04	0.05	1.59	1.39	0.99	0.85
1000	0.65	0.60	0.03	0.05	1.64	1.53	1.29	1.21
1100	0.86	0.80	0	0.04	1.84	1.64	1.64	1.49
1200	0.96	0.89	0.02	0.06	1.79	1.69	1.74	1.63
1300	0.99	0.89	0	0.06	1.84	1.70	1.79	1.64
1400	0.85	0.80	0.01	0.04	1.79	1.64	1.59	1.49
1500	0.66	0.60	0.02	0.05	1.69	1.54	1.34	1.21
1600	0.38	0.31	0.02	0.05	1.64	1.38	1.04	0.87
1700	0	0	0	0	0	0	0	0

ORIGINAL PAGE IS OF POOR QUALITY

TABLE 3.7 EXTREME VALUES OF SOLAR RADIATION FOR EASTERN TEST RANGE, NSTL, JSC, NEW ORLEANS, GULF TRANSPORTATION, AND HUNTSVILLE

TIME OF DAY (Local Standard Time)	Total Horizontal Solar Radiation g-cal cm^{-2} min^{-1}		Diffuse Radiation Associated with Total Horizontal Solar Radiation Extremes g-cal cm^{-2} min^{-1}		Total Normal Incident Solar Radiation g-cal cm^{-2} min^{-1}		Total 45° Surface Solar Radiation g-cal cm^{-2} min^{-1}	
	JUNE							
	EXTREME	95 Percentile	EXTREME	95 Percentile	EXTREME	95 Percentile	EXTREME	95 Percentile
0500	0	0	0	0	0	0	0	0
0600	0.12	0.07	0	0	1.09	1.00	0	0
0700	0.42	0.36	0.05	0.07	1.29	1.04	0.19	0.16
0800	0.82	0.71	0.04	0.10	1.59	1.30	0.34	0.27
0900	1.23	1.02	0	0.10	1.59	1.48	0.49	0.41
1000	1.35	1.30	0.02	0.06	1.59	1.54	0.99	0.95
1100	1.52	1.45	0.03	0.09	1.59	1.54	1.19	1.14
1200	1.58	1.53	0.10	0.16	1.64	1.55	1.29	1.24
1300	1.58	1.50	0.10	0.20	1.64	1.53	1.29	1.24
1400	1.50	1.44	0.05	0.12	1.59	1.52	1.19	1.09
1500	1.35	1.30	0.02	0.06	1.59	1.52	1.04	0.95
1600	1.10	1.01	0.05	0.12	1.54	1.44	0.54	0.44
1700	0.77	0.72	0.05	0.09	1.49	1.33	0.34	0.30
1800	0.48	0.40	0.03	0.06	1.44	1.14	0.19	0.18
1900	0.11	0.08	0	0	1.14	1.00	0.14	0.03
2000	0	0	0	0	0	0	0	0
	DECEMBER							
	EXTREME	95 Percentile	EXTREME	95 Percentile	EXTREME	95 Percentile	EXTREME	95 Percentile
0700	0	0	0	0	0	0	0	0
0800	0.16	0.10	0	0	1.34	1.12	0.64	0.50
0900	0.46	0.42	0.04	0.06	1.44	1.36	0.94	0.89
1000	0.79	0.71	0.01	0.07	1.69	1.60	1.39	1.29
1100	0.95	0.92	0.02	0.04	1.79	1.68	1.64	1.56
1200	1.09	1.02	0	0.03	1.79	1.70	1.74	1.66
1300	1.05	1.02	0	0.03	1.79	1.78	1.74	1.66
1400	0.94	0.89	0.02	0.05	1.74	1.67	1.59	1.63
1500	0.79	0.70	0	0.03	1.74	1.57	1.39	1.27
1600	0.46	0.41	0.04	0.06	1.54	1.40	0.99	0.91
1700	0.16	0.10	0	0	1.34	1.12	0.64	0.50
1800	0	0	0	0	0	0	0	0

If a correction for wind speed is desired, equation (3.5) can be used as follows:

$$T_S = T_A + E(\Delta T_{BS}) \frac{Wc}{100} \quad , \qquad (3.5A)$$

where Wc is the correction for wind speed in percent from Figure 3.3B. Equations (3.5), (3.6), and (3.5A) are only for computing the effect of one source of radiation on a surface. When more than one radiation source is received by an object, then a more complex method must be used, as given in the following discussion.

If we have a black body with several radiation sources and no convection, then

$$\sigma T^4 = \sum_1^n I_i \quad i = 1, 2, 3 \ldots n \quad . \qquad (3.7)$$

Then

$$T - T_A = \Delta T = \left(\frac{\sum_1^n I_i}{\sigma} \right)^{1/4} - T_A \quad , \qquad (3.8)$$

where T_A is the air temperature.

For any object exposed to radiation in the earth's atmosphere

$$\Delta T = f_w \left(\frac{\sum_1^n E_i I_i}{\sigma} \right)^{1/4} - T_A \quad , \qquad (3.9)$$

where

E_i = emittance of object for corresponding radiation source I_i

$$\Delta T = T - T_A \tag{3.10}$$

f_w = wind effect (convection)

$$f_w = \frac{0.325}{\sqrt{w}} \tag{3.11}$$

w = wind speed (m/sec) .

3.6 Total Solar Radiation

3.6.1 Introduction

The standard solar radiation sensors measure the intensity of direct solar radiation from the sun falling on a horizontal surface plus the diffuse (sky) radiation from the total sky hemisphere. Diffuse radiation is lowest with dry clear air; it increases with increasing dust and moisture in the air. With extremely dense clouds or fog, the measured horizontal solar radiation will be nearly all diffuse radiation. The higher (≥ 95 percentile) values of measured horizontal solar radiation occur under clear skies or under conditions of scattered fair weather cumulus clouds which reflect additional solar radiation onto the measuring sensor.

In this document all solar radiation values given are intensities. Solar radiation intensities are measured in gram calories per square centimeter (same as langleys per square centimeter) by stations of the National Oceanic and Atmospheric Administration, National Weather Service; therefore, these units are used in this section.

3.6.2 Use of Solar Radiation in Design

When radiation data are used in design studies, the direct solar radiation should be applied from one direction as parallel rays, and at the same time, the diffuse radiation should be applied as rays from all directions of a hemisphere (Fig. 3.4).

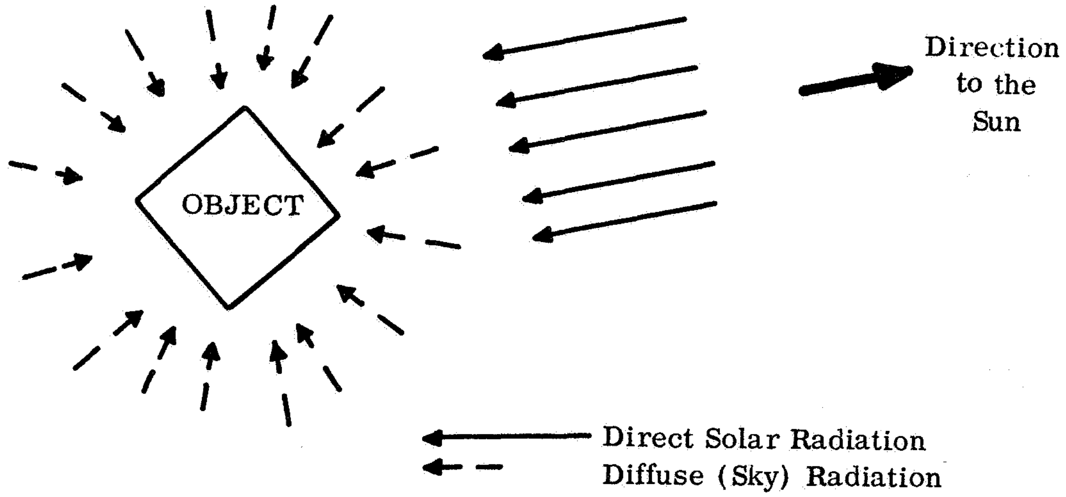

FIGURE 3.4. METHOD OF APPLYING RADIATION FOR DESIGN

Because the sun provides heat (from radiation) from a specific direction, differential heating of an object occurs; i.e., one part is heated more than another, resulting in stress and deformation. As an example, the sun heats the side of the Space Shuttle vehicle facing the sun, while the sky cools the opposite side. This differential heating causes the vehicle to bend away from the sun sufficiently at the top to require consideration in design of platforms surrounding the vehicle. These platforms are used to ready the vehicle on the launch pad and must be designed so as to prevent damage to the vehicle skin as the vehicle bends away from the sun.

3.6.3 Total Solar Radiation Extremes

Ten years of total horizontal solar and sky radiation data at two stations were selected for analysis to determine the frequency distribution of solar radiation for use in design. The data analysis was made by The National Oceanic and Atmospheric Administration, National Climatic Center, under contract to NASA-Marshall Space Flight Center.

3.6.3.1 Basic Data Computations

The basic data used were hourly totals of horizontal solar and sky radiation (I_{TH}) for each hour of the day for 10-year periods at each of two stations: Apalachicola, Florida, and Santa Maria, California. The hourly totals were divided by 60 to obtain the average solar radiation values per minute for each hour. The average values per minute are numerically equal to intensity, and these values were used in the computations of frequency distributions. The diffuse sky radiation intensities I_{dH} were empirically estimated for each value based on the amount of total horizontal solar and sky radiation and solar altitude, similar to the method used in Reference 3.6. After the diffuse sky radiation is subtracted from the total horizontal solar and sky radiation, the resultant horizontal solar radiation I can be used to compute the direct normal incident solar radiation I_{DN} by using the following equation (Refs. 3.7 and 3.8):

$$I_{DN} = \frac{I}{\sin b} \quad , \tag{3.12}$$

where

I_{DN} = direct normal incident solar radiation

I = horizontal solar radiation = $I_{TH} - I_{dH}$

b = sun's altitude[3] (Ref. 3.9).

The total normal incident solar radiation I_{TN} values were found by adding the direct normal incident solar radiation I_{DN} and the diffuse sky radiation I_{dH} previously estimated. This method of finding the total normal incident solar radiation may result in a slight overestimate of the value for low solar altitudes because the sky hemisphere is intercepted by the ground surface. This error is insignificant, however, when extreme values are used and would be small for values equal to or greater than the mean plus one standard deviation.

Total solar radiation intensities on a south-facing surface,[3] with the normal to the surface at 45 degrees to the horizontal, are calculated as follows:

$$I_D 45 = I(\sin 45\ \text{deg} + \cot b \cos a \cos 45\ \text{deg}) \quad , \tag{3.13}$$

---

3. Duffie, John A. and William A. Beckman, "Solar Energy Thermal Processes", John Wiley & Sons, N.Y., 1974.

where

I_{D45} = intensity of direct solar radiation on a south-facing surface, with normal 45 degrees to the horizontal

I = horizontal solar radiation = $I_{TH} - I_{dH}$

a = sun's azimuth measured from the south direction

b = sun's altitude.

3.6.3.2 Solar Radiation Extreme and 95 Percentile

To present the solar radiation data in a simplified form, the month of June was selected to represent the summer and the longest period of daylight and December for the winter and shortest period of daylight. The June data for normal incident solar radiation from Santa Maria, California, were increased for the period from 1100 to 1900 hours to reflect the higher values which occur early in July (first week) during the afternoon. Tables 3.6 and 3.7 give the frequency distributions for the extreme[4] values and the 95 percentile values of solar radiation for hours of the day. The values given for diffuse radiation are the values which occurred associated with the other extreme and 95 percentile values of the other solar radiations given. Since the diffuse radiation decreases with increasing horizontal radiation, the values given in Tables 3.6 and 3.7 are considerably lower than the highest values of diffuse radiation occurring during the period of record. Solar radiation data recommended for use in design are given in Table 3.8 and Figure 3.5, valid for all areas.

3.6.3.3 Variation with Altitude

Solar radiation intensity on a surface will increase with altitude above the earth's surface, with clear skies, according to the following equation:

$$I_H = I_{DN} + (1.94 - I_{DN})\left(1 - \frac{\rho_H}{\rho_S}\right) , \qquad (3.14)$$

4. Extreme as used in this section is the highest measured value of record.

TABLE 3.8 RECOMMENDED DESIGN OF SOLAR RADIATION DATA

Time of Day	Design High Solar Radiation		Design Low Solar Radiation	
Hour	BTU/ft^2/hr	gm-cal/cm^2/min	BTU/ft^2/hr	gm-cal/cm^2/min
0500	0	0.00	0	0.00
1100	363	1.64	70	0.32
1300			80	0.36
1400	363	1.64		
2000	0	0.00	0	0.00

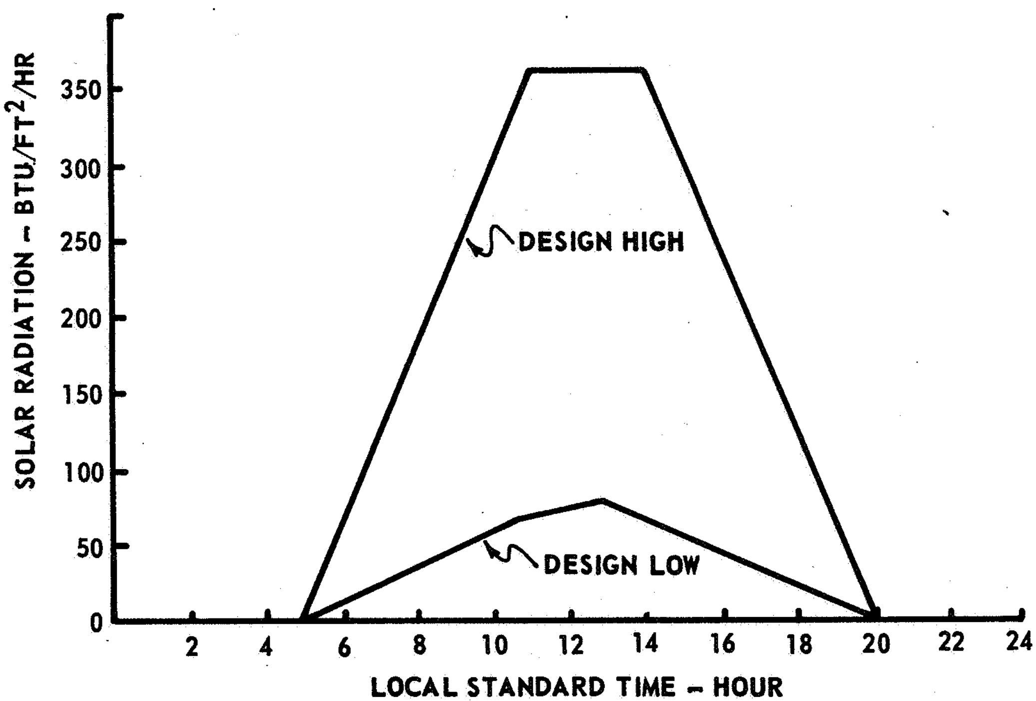

FIGURE 3.5 RECOMMENDED DESIGN SOLAR RADIATION DESIGN

where

I_H = intensity of solar radiation normal to surface at required height

I_{DN} = intensity of solar radiation normal to surface at the earth's surface assuming clear skies ($I_{DN} = I_{TN} - I_{dH}$)

ρ_H = atmospheric density at required height (from U. S. Standard, U. S. Supplemental Atmospheres, or this document) (kg m^{-3})

ρ_S = atmospheric density at sea level (from U. S. Standard, U. S. Supplemental Atmospheres, or this document) (kg m^{-3})

1.94 = solar constant (g-cal cm^{-2}).

The diffuse radiation I_{dH} decreases with altitude above the earth's surface, with clear skies. A good estimate of the value can be obtained from the following equation[5]:

$$I_{dH} = 0.7500 - 0.4076\, I_H \quad , \tag{3.15}$$

where

I_{dH} = intensity of diffuse radiation

I_H = intensity of solar radiation normal to surface.

Equation (3.15) is valid for values of I_H from equation (3.14) up to 1.84 g-cal cm^{-2}. For values of I_H greater than 1.84 g-cal cm^{-2}, I_{dH} = 0.

3.6.3.4 Solar Radiation During Extreme Conditions

When ground winds occur exceeding the 95, 99, or 99.9 percentile design winds given in this document in Section VIII, the associated weather normally is such that clouds, rain, or dust are generally present; therefore,

5. Equation (3.15) is based on a cloudless and dust-free atmosphere.

the intensity of the incoming solar radiation will be less than the maximum values given in Tables 3.6 and 3.7. Maximum values of solar radiation intensity to use with corresponding wind speeds are given in Table 3.3.

3.7 Temperature

Several types of temperatures at the earth's boundary layer must be considered in design. These are as follows:

a. Air temperature[normally measured at 1.22 meters (4 ft) above a grass surface.]

b. Changes of air temperature (usually the rapid changes which occur in less than 24 hours are considered.)

c. Surface or skin temperature measured of a surface exposed to radiation.

d. Temperatures within a closed compartment.

All of the above will be discussed in the following subsections.

3.7.1 Air Temperature Near the Surface

Surface air temperature extremes (maximum, minimum, and the 95 percentile values) and the extreme minimum sky radiation (equal to the outgoing radiation) are given in Table 3.2 for various geographical areas. Maximum and minimum temperature values should be expected to last only a few hours during a daily period.[6] Generally, the maximum temperature is reached after 12 noon and before 5 p.m., while the minimum temperature is reached just before sunrise. Table 3.9A shows the maximum and minimum air temperatures which have occurred on each hour at Kennedy Space Center, but not necessarily on the same day, although these curves represent a cold and hot extreme day. The method of sampling the day (frequency of occurrence of observations) will result in the same extreme values if the same period of time for the data is used, but the 95 percentile values will be different for hourly, daily, and monthly data reference periods. Selection of the reference period depends on engineering application. Table 3.9B gives monthly mean temperatures, standard deviations and 2.5 and 97.5 percentiles of values of temperature for Kennedy Space Center, Florida, and Vandenberg AFB, California. United States temperature extremes are given in Section XVII. Worldwide extremes are given in Section XVIII.

---

6. The equivalent radiation values given here were computed from the equivalent temperature minimum extremes by using the Stefan-Boltzmann Law (σT^4).

TABLE 3.9A MAXIMUM AND MINIMUM SURFACE AIR TEMPERATURES AT EACH HOUR FOR EASTERN TEST RANGE[a]

Time	Annual Maximum		Annual Minimum	
	°C	°F	°C	°F
1 a.m.	28.9	84	1.1	34
2	28.9	84	0.6	33
3	29.4	85	-1.1	30
4	28.3	83	-0.6	29
5	28.3	83	-1.1	28
6	29.4	85	-1.1	27
7	30.6	87	-1.7	26
8	30.6	87	-2.2	25
9	31.7	89	-0.6	28
10	33.9	93	1.1	30
11	35.0	95	2.2	35
12 noon	35.6	96	5.0	41
1 p.m.	37.2	99	5.6	42
2	35.6	97	5.0	41
3	35.6	97	5.6	42
4	35.6	97	5.6	42
5	35.6	97	5.6	42
6	35.0	95	3.9	39
7	33.3	92	2.2	36
8	31.7	89	2.2	36
9	30.0	86	1.7	35
10	30.0	86	1.7	35
11	30.0	86	1.1	34
12 mid	30.0	86	1.1	34

a. Based on 10 years of record for Patrick Air Force Base and Kennedy Space Center.

TABLE 3.9B MONTHLY MEAN, STANDARD DEVIATIONS (STD), AND 2.5 and 97.5 PERCENTILE VALUES OF TEMPERATURE FOR KENNEDY SPACE CENTER AND VANDENBERG AFB, CALIFORNIA

	Kennedy Space Center				Vandenberg AFB			
			Percentiles				Percentiles	
Month	Monthly Mean or 50 Percentile (°F)	Standard Deviation 30-day avg.	30-Day 2.5%[a] (°F)	Average 97.5%[a] (°F)	Monthly Mean or 50 Percentile (°F)	Standard Deviation 30-day avg.	30-Day 2.5%[a] (°F)	Average 97.5%[a] (°F)
Jan.	60.3	2.9	54.6	66.0	52.2	2.0	48.3	56.1
Feb.	61.7	4.0	53.9	69.4	52.6	1.9	48.9	56.3
Mar.	65.3	3.3	58.8	71.8	52.3	1.8	48.8	55.8
Apr.	70.0	2.6	64.9	75.1	54.2	1.7	50.9	57.5
May	74.8	2.2	70.5	79.1	53.9	1.5	51.0	56.8
June	79.2	1.6	76.1	82.3	56.8	1.5	53.9	59.7
July	80.7	0.5	79.7	81.7	58.4	1.4	55.7	61.1
Aug.	80.9	0.8	79.3	82.5	59.8	1.5	56.9	62.7
Sept.	80.0	1.2	77.7	82.4	60.2	1.8	56.7	63.7
Oct.	75.2	2.3	70.7	79.7	60.1	1.9	56.4	63.8
Nov.	68.0	3.5	61.1	74.9	55.8	2.0	51.9	59.7
Dec.	61.7	4.0	53.9	69.5	53.1	2.5	48.2	58.0

a. Recommended for use in Solid Rocket Motor Propellant bulk temperature preditions for design analyses.

NOTE: See Office memorandum S & E-AERO-YT-15-73, subject " Ambient Temperature for Space Shuttle SRB Propellant Temperature Predictions", Atmospheric Sciences Division, Marshall Space Flight Center, Alabama 35812, for additional information.

3.7.2 Extreme Air Temperature Change

a. For all areas the design values of extreme air temperature changes (thermal shock) are:

(1) An increase of air temperature of 10°C (18°F) with a simultaneous increase of solar radiation (measured on a normal surface) from 0.50 g-cal cm^{-2} min^{-1} (110 Btu ft^{-2} hr^{-1}) to 1.85 g-cal cm^{-2} min^{-1} (410 Btu ft^{-2} hr^{-1}) may occur in a 1-hour period. Likewise, the reverse change of the same magnitude may occur for decreasing air temperature and solar radiation.

(2) A 24-hour change may occur with an increase of 27.7°C (50°F) in air temperature in a 5-hour period, followed by 4 hours of constant air temperature, then a decrease of 27.7°C (50°F) in a 5-hour period, followed by 10 hours of constant air temperature.

b. For Eastern Test Range (Kennedy Space Center), the 99.9 percentile air temperature changes are as follows:

(1) An increase of air temperature of 5.6°C (11°F) with a simultaneous increase of solar radiation (measured on a normal surface) from 0.50 g-cal cm^{-2} min^{-1} (110 Btu ft^{-2} hr^{-1}) to 1.60 g-cal cm^{-2} min^{-1} (354 Btu ft^{-2} hr^{-1}), or a decrease of air temperature of 9.4°C (17°F) with a simultaneous decrease of solar radiation from 1.60 g-cal cm^{-2} min^{-1} (354 Btu ft^{-2} hr^{-1}) to 0.50 g-cal cm^{-2} min^{-1} (110 Btu ft^{-2} hr^{-1}) may occur in a 1-hour period.

(2) A 24-hour temperature change may occur as follows: An increase of 16.1°C (29°F) in air temperature (wind speed under 5 m/sec) in an 8-hour period, followed by 2 hours of constant air temperature (wind speed under 5 m/sec), then a decrease of 21.7°C (39°F) in air temperature (wind speed between 7 and 10 m/sec) in a 14-hour period.

3.7.3 Surface (Skin) Temperature

The temperature of the surface of an object exposed to solar, day sky, or night sky radiation is usually different from the air temperature (Refs. 3.10 and 3.11). The amount of the extreme difference in temperature between the object and the surrounding air temperature is given in Table 3.5 and Figure 3.3, Part A, for exposure to a clear night (or day)[7] sky or to the sun on a clear day. Since the flow of air across an object changes the balance between the heat transfers from radiation and convection-conduction between the air and

7. Without the sun's rays striking, the daytime sky is about as cold as the nighttime sky.

the object, the difference in the temperature between the air and the object will decrease with increasing wind speed (Ref. 3.9). Part B of Figure 3.3 provides information for making the corrections for wind speed. Values are tabulated in Table 3.5 for various wind speeds.

3.7.4 Compartment Temperature

3.7.4.1 Introduction

A cover of this material enclosing an air space will conduct heat to (or remove heat from) the inside air when the cover is heated by solar radiation (or cooled by the night sky). This results in the compartment air space being frequently considerably hotter or cooler than the surrounding air. The temperature reached in a compartment is dependent on the location of the air space with respect to the heated surface, the type and thickness of the surface material, the type of construction, and the insulation; i.e., an addition of a layer of insulation on the inside surface of the compartment will greatly reduce the heating or cooling of the air in the compartment space (Refs. 3.12 and 3.13).

3.7.4.2 Compartment Extreme High Temperature

A compartment probable extreme average high temperature of 87.8°C (190°F) for a period of 1 hour and an average high temperature of 65.6°C (150°F) for a period of 6 hours must be considered at all geographic locations while aircraft or other transportation equipment are stationary on the ground without air conditioning in the compartment. These extremes will be found at the top and center of the compartment.

3.8 Data on Air Temperature Distribution with Altitude

Data on air temperature distribution with altitude are given in Section X.

REFERENCES

3.1 Middleton, W. E. K.; and Spilhaus, A. F.: "Meteorological Instruments." University of Toronto Press, 3rd Edition, revised 1960.

3.2 "Solar Electromagnetic Radiation," NASA SP-8005, Rev. April 1971. National Aeronautics and Space Administration, Washington, D. C.

3.3 Moon, Parry: "Proposed Standard Solar Radiation Curves for Engineering Use." Journal of the Franklin Institute, vol. 230, Nov. 1940, pp. 583-617.

3.4 Thekaekara, Mathew P., Editor, "The Solar Constant and the Solar Spectrum Measured from a Research Aircraft." NASA TR R-351, National Aeronautics and Space Administration, Washington, D. C., Oct. 1970.

3.5 ASHRAE Handbook of Fundamentals. American Society of Heating, Refrigerating and Air Conditioning Engineers, New York, 1967.

3.6 Parmalee, G. V.: "Irradiation of Vertical and Horizontal Surfaces by Diffuse Solar Radiation from Cloudless Skies." Heating, Piping and Air Conditioning, vol. 26, Aug. 1954, pp. 129-136.

3.7 Becker, C. F.; and Boyd, J. S.: "Solar Radiation Availability on Surfaces in the United States as Affected by Season, Orientation, Latitude, Altitude, and Cloudiness." Journal of Solar Engineering, Science and Engineering, vol. 1, Jan. 1957, pp. 13-21.

3.8 Ornstein, M. P.: "Solar Radiation." Journal of Environmental Sciences, vol. 5, Apr. 1962, pp. 24-27.

3.9 "Tables of Computed Altitude and Azimuth," Publication H. O. No. 214, United States Hydrographic Office, United States Government Printing Office, 1940.

3.10 Fishenden, Margaret; and Saunders, Owen A.: "The Calculation of Heat Transmission." His Majesty's Stationary Office, London, 1932.

3.11 Daniels, Glenn E.: "Measurement of Gas Temperature and the Radiation Compensating Thermocouple." Journal of Applied Meteorology, vol. 7, 1968, pp. 1026-1035.

REFERENCES (Concluded)

3.12 Porter, William L.: "Occurrence of High Temperatures in Standing Boxcars." Technical Report EP-27, Headquarters Quartermaster Research and Development Center, United States Army, Natick, Massachusetts, Feb. 1956.

3.13 Cavell, W. W.; and Box, R. H.: "Temperature Data on Standard and Experimental Cartridges in Pilot Ejection Devices in a B47E Aircraft Stationed at Yuma, Arizona." Memo Report No. M60-16-1, Frankford Arsenal, Pitman-Dunn Laboratories Group, Philadelphia, Pennsylvania, 1960.

SECTION IV. ATMOSPHERIC DENSITY (SURFACE)

4.1 Definition

Density is the ratio of the mass of a substance to its volume. (It also is defined as the reciprocal of specific volume.) Density is usually expressed in grams per cubic centimeter or kilograms per cubic meter.

4.2 Atmospheric Density

The variation of the density of the atmosphere at the surface from the average for any one station, and between the areas of interest, is small and should have no important effect on preflight operations. Table 4.1 gives the median density at the surface for the five test ranges.

TABLE 4.1 MEDIAN SURFACE DENSITIES

Area	Surface Altitude	Source of Data	Density	
	m*		kg m^{-3}	lb ft^{-3}
Eastern Test Range (Kennedy Space Center)	5	(Ref. 4.1)	1.1830	7.385×10^{-2}
Vandenberg AFB (SAMTEC)	113	(Ref. 4.2)	1.2190	7.610×10^{-2}
White Sands Missile Range	1292	(Ref. 4.3)	1.0418	6.504×10^{-2}
Wallops Flight Center	2	(Ref. 4.4)	1.2317	7.689×10^{-2}
Edwards AFB	706	(Ref. **)	1.1361	7.092×10^{-2}

* Station elevation above mean sea level.

** Edwards surface density value from Section X, Table 10.10.

However, atmospheric density, especially low density, is important to aircraft takeoff and landing operations and should therefore be considered when planning Space Shuttle orbiter ferry flights. Table 4.2 gives low density values that are equaled or exceeded approximately 5 percent of the time during the hottest part of the day in summer. Typical associated temperatures needed for engine power calculations are also listed. Since low density is found at high elevation and high temperatures, only the highest enroute airfield and the ferry flight terminals were considered. Since Kennedy Space Center and Vandenberg AFB extremes are given in Section X, only Edwards AFB and Biggs AFB are listed here.

TABLE 4.2 LOW DENSITY (5 PERCENTILE WORST) AND ACCOMPANYING TEMPERATURES FOR ORBITER FERRY OPERATIONS

Location	Low Density		Temperature	
	$kg\ m^{-3}$	% Departure from US 62	°C	°F
Edwards AFB California	1.0246	-10.5	39.4	103
Biggs AFB Texas	0.97555	-10.5	38	100

4.3 Surface Variability and Altitude Variations

Data on the variation of surface density and density aloft about its median annual values can be found in Section X. The Global Reference Atmosphere (Ref. 4.5) will also provide density values versus altitude together with variability, by month, for any point on the globe.

REFERENCES

4.1 Smith, O. E.; and Weidner, Don K.: "A Reference Atmosphere for Patrick AFB, Florida, Annual (1963 Revision)." NASA TM X-53139, 1964. NASA-Marshall Space Flight Center, Huntsville, Alabama.

4.2 Carter, E. A.; and Brown, S. C.: "A Reference Atmosphere for Vandenberg AFB, California, Annual (1971 Version)." NASA TM X-64590, NASA-Marshall Space Flight Center, Alabama, 1971.

4.3 "White Sands Missile Range Reference Atmosphere (Part I)," 1964. IRIG Document No. 104-63, Secretariat, Range Commander's Council, White Sands Missile Range, New Mexico.

4.4 "Wallops Island Test Range Reference Atmosphere (Part I)", 1965. IRIG Document No. 104-63, Secretariat, Range Commander's Council, White Sands Missile Range, New Mexico.

4.5 Justus, C. G., et al.: "Four-D Global Reference Atmosphere Technical Description, Part I." NASA TM X-64871, September 1974, NASA-Marshall Space Flight Center, Huntsville, Alabama.

SECTION V. ATMOSPHERIC PRESSURE (SURFACE)

5.1 Definition

Atmospheric pressure (also called barometric pressure) is the force exerted as a consequence of gravitational attraction, by the mass of the column of air of unit cross section lying directly above the area in question.

5.2 Pressure

The total variation of pressure from day to day is relatively small. Rapid but slightly greater variations occur as the result of the passage of frontal systems, while the passage of a hurricane can cause somewhat larger, but still not significant changes for pressure environment design of space vehicles. Surface pressure extremes for various locations and their extreme ranges are given in Table 5.1. These data use the results of a study of pressure extremes. See Section XVII for extreme pressures across the United States. The pressure drop in a tornado can exceed 20 percent of ambient during the few seconds of its passage.

5.3 Pressure Change

a. A gradual rise or fall in pressure of 3 mb (0.04 lb in.$^{-2}$) and then a return to original pressure can be expected over a 24-hour period.

b. A maximum pressure change (frontal passage change) of 6 mb (0.09 lb in.$^{-2}$) (rise or fall) can be expected within a 1-hour period at all localities.

5.4 Pressure Decrease with Altitude

a. Pressure decrease is approximately logarithmic with height. Materials transported in mountainous terrain or in cargo compartments of aircraft must be packaged to stand the pressure differential without damage. Near sea level (i.e., < 3 km) the pressure will vary about 1 mb for each 10-m change in altitude. Figure 5.1 shows the standard atmospheric pressure decrease with altitude.

b. More detailed data on pressure distribution with altitude are given in Section X.

TABLE 5.1 SURFACE PRESSURE EXTREMES (values apply to station altitude above MSL) [Ref. 5.1]

Location	Units	Pressure Maximum	Pressure Mean	Pressure Minimum**	Station Elevation ft	Station Elevation m
Huntsville	N m^{-2} mb lb in.$^{-2}$	102 080 1 020.8 14.8	99 540 995.4 14.4	97 210 972.1 14.1	644	196
Kennedy Space Center		103 600 1 036.0 15.0	101 670 1 016.7 * 14.7	99 970 999.7 14.5	16 9***	5 2.7***
SAMTEC/Vandenberg AFB		102 000 1 020.0 14.8	100 250 1 002.5 * 14.5	99 010 990.1 14.4	371 368***	113 112.2***
Edwards AFB		95 560 955.6 13.9	93 410 934.1 * 13.5	92 030 920.3 13.3	2 316 2302***	706 701.7***
Honolulu/Hickam Field		102 660 1 026.6 14.9	101 560 1 015.6 14.7	100 190 1 001.9 14.5	17 13***	5 4.0***
Guam/Andersen AFB		99 900 999.0 14.5	98 960 989.6 14.4	97 870 978.7 14.2	634 624***	193 190.2***
Santa Susana		96 440 964.4 14.0	94 820 948.2 13.8	93 330 933.3 13.5	1 965	599
Thiokol Wasatch Div., Utah		88 900 889.0 12.9	86 300 863.0 12.5	84 300 843.0 12.2	4 469	1 362
New Orleans		104 160 1 041.6 15.1	101 780 1 017.8 14.8	99 900 999.0 14.5	6	2
NSTL/Bay St. Louis		104 410 1 044.1 15.1	101 640 1 016.4 14.7	99 150 991.5 14.4	31	9
Johnson Space Center		103 960 1 039.6 15.1	101 530 1 015.3 14.7	99 530 995.3 14.4	50	15
Wallops Flight Center		104 750 1 047.5 15.2	101 700 1 017.0 * 14.8	98 770 987.7 14.3	7	2
White Sands Missile Range	↓	89 010 890.1 12.9	87 130 871.3 * 12.6	85 200 852.0 12.4	4 239	1 292

* The mean values given here will differ from the median surface values as given in Tables 10.8, 10.9, 10.10, and Ref. 10.3 of Section X.

** Hurricane-influenced low pressures are not given here.

*** Runway elevations above MSL.

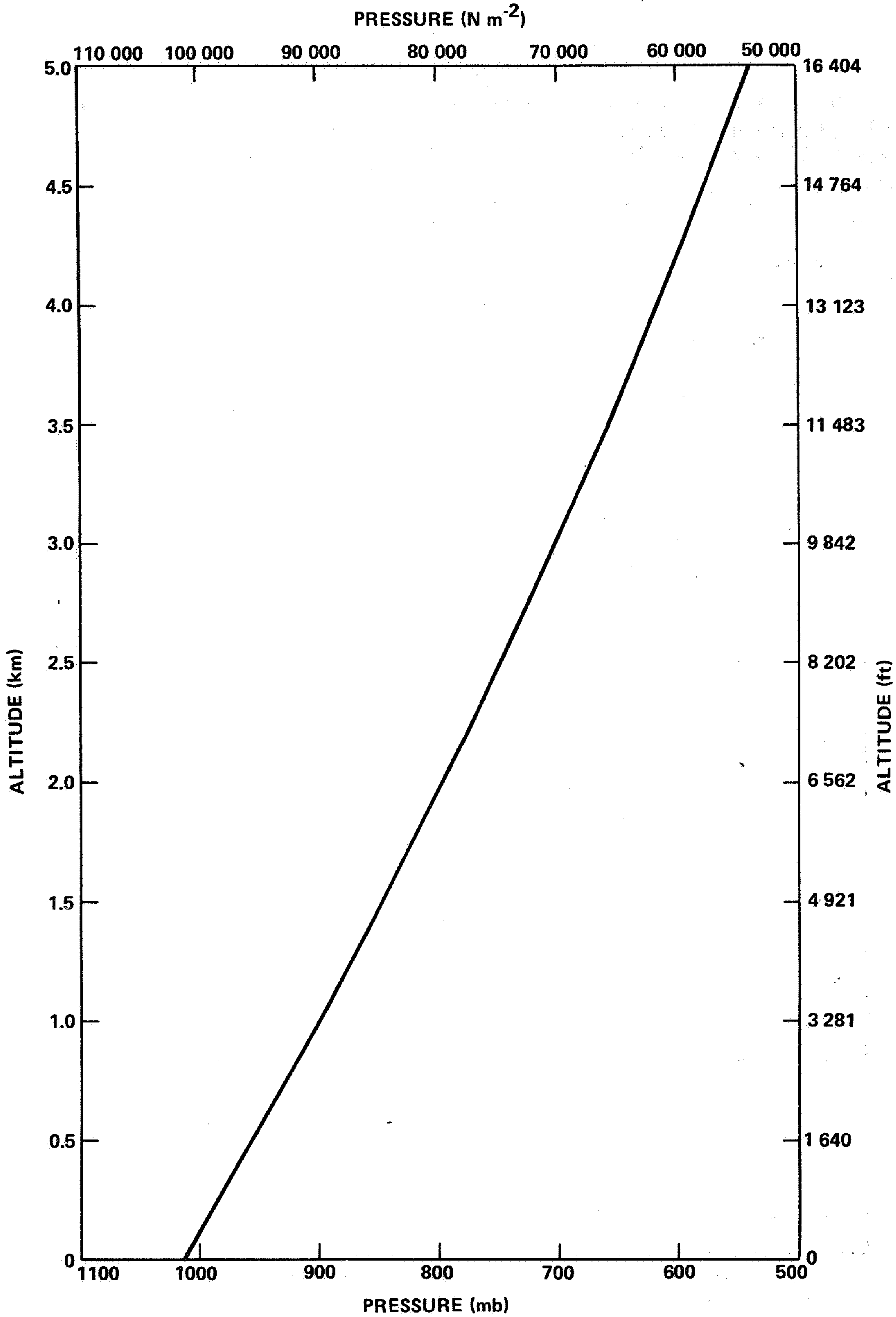

FIGURE 5.1 PRESSURE CHANGE WITH ALTITUDE FOR PACKAGING MATERIALS

REFERENCE

5.1 "Revised Uniform Summary of Surface Weather Observations – Edwards AFB, California." Part F, USAF-ETAC, Data Processing Division, Air Weather Service (MAC), Federal Building, Asheville, North Carolina, March 20, 1974.

SECTION VI. HUMIDITY

6.1 Definitions (Ref. 6.1)

Absolute Humidity: In a system of moist air, the ratio of the mass of water vapor present to the volume occupied by the mixture; that is, the density of the water vapor component.

Condensation: The physical process by which a vapor becomes a liquid or solid; the opposite of evaporation.

Dew-Point Temperature: The temperature to which a given parcel of air must be cooled at constant pressure and constant water-vapor content in order for saturation to occur. When this temperature is below 0°C, it is sometimes called the frost point.

Dry-Bulb Temperature: The temperature of the air. The temperature registered by the dry-bulb thermometer of a psychrometer (sometimes referred to as ambient temperature).

Evaporation: The physical process by which a liquid or solid is transformed to the gaseous state; the opposite of condensation.

Frost Point: The highest temperature at which atmospheric moisture will sublimate in the form of hoar frost on a cooled polished surface. It is analogous to the dew point, applying when the moisture in the atmosphere will not condense above 0°C.

Humidity: Generally, some measure of the water-vapor content in air. (See: absolute humidity, relative humidity, specific humidity, mixing ratio or dew point.)

Hydrology: That branch of physical geography which deals with the waters of the earth exclusive of the oceans. The moisture (vapor, liquid, and solid) in the atmosphere is one phase of the "hydrologic cycle".

Hygrometer: An instrument which measures the water vapor content of the atmosphere.

Hygrometry: The study which treats the measurements of the humidity of the atmosphere and other gases.

Latent Heat of Condensation: The heat released per unit mass as water vapor condenses to form water droplets or ice crystals.

Latent Heat of Vaporization: The heat absorbed per unit mass as water or ice is vaporized into the gaseous state.

Mixing Ratio: In a system of moist air, the dimensionless ratio of the water vapor to the mass of dry air.

Moisture: A term usually referring to the water vapor content of the atmosphere, or to the total water substance (gaseous, liquid, and solid) present in a given volume of air.

Moisture Inversion: An increase with height of the moisture content of the air; specifically, the layer through which this increase occurs, or the altitude at which the increase begins.

Relative Humidity: The dimensionless ratio of the actual vapor pressure of the air to the saturation vapor pressure.

Saturation: The condition in which the partial pressure of any fluid constituent is equal to its maximum possible partial pressure under the existing environmental conditions, such that any increase in the amount of that constituent will initiate within it a change to a more condensed state.

Specific Humidity: In a system of moist air, the dimensionless ratio of the mass of water vapor to the total mass of the system.

Sublimation: The transition of a substance from the solid phase directly to the vapor phase, or vice versa, without passing through an intermediate liquid phase.

Supersaturation: The condition existing in a given portion of the atmosphere (or other space) when the relative humidity is greater than 100 percent, that is, when it contains more water vapor than is needed to produce saturation with respect to a plane surface of pure water or pure ice.

Vapor: Any substance existing in the gaseous state at a temperature lower than that of its critical point; that is, a gas cool enough to be liquefied if sufficient pressure were applied to it.

Vapor Concentration: [previously called absolute humidity (Ref. 6.2)] is the ratio of the mass of water vapor present to the volume occupied by the mixture, i.e., the density of the water content. This is expressed in grams of water vapor per cubic meter of air.

Vapor Pressure: The pressure exerted by the molecules of a given vapor. For a pure, confined vapor, it is that vapor's pressure on the walls of its containing vessel, and for a vapor mixed with other vapors or gases, it is that vapor's contribution to the total pressure (i.e., its partial pressure).

Water Vapor: Water substance in vapor form; one of the most important of all constituents of the atmosphere.

Wet-Bulb Temperature: The temperature an air parcel would have if cooled adiabatically to saturation at constant pressure by evaporation of water into it, all latent heat being supplied by the parcel.

6.2 Vapor Concentration

The physical state of water may exist in the gaseous, liquid, and solid phases in the atmosphere. The earth's atmosphere contains a significant amount of moisture because of the ample supply of the substance. The equatorial region of the earth is the main source from which moisture is supplied to the atmosphere. This is due to the vast oceanic area and moist land regions from which broad-scale evaporation of water takes place and is introduced into the air.

Water in vapor form is invisible. Since the partial pressure of water vapor is less than the partial pressure of the dry air it displaces, moist air is less dense than dry (dryer) air. This contributes to the lower atmospheric pressure as is common to warm, moist air masses. Atmospheric pressure differentials are extremely significant between moist (warm) and dry (cold) air. This is the main driving factor which causes the dynamic variations of the global atmospheric circulation.

Humidity plays a significant role in the design, fabrication, operations, and flight of aerospace vehicles. In some cases moisture plays the main role especially where long-term on-pad stay times must be encountered. Moisture is also of primary concern when satellites and any space probe, as well as delicate test equipment, must undergo exposure to the ambient air.

The following statements contain the reasons why detriments due to moist, humid air must be considered by researchers during the development of space vehicles and space probes in general.

a. Minute particulate material suspended in the air, especially at the lower altitudes, tends to settle on any surface. When combined with moisture, such debris can become very corrosive and react with many things on which it is deposited. Water, by itself, is a dissolving agent and associates with almost everything it comes into contact with. In general, water is the most important single agent affecting the surface of the earth and all materials exposed to the substance commonly undergo some chemical or physical change. Degradation of surfaces where dissimilar metals are in contact can take place at a rapid rate in the presence of moisture. The rate of corrosion of materials increases proportionally with humidity (Ref. 6.3). See Section XIV of this report for additional details on atmospheric corrosion and abrasion.

b. Atmospheric humidity can impair or alter the performance of electronic equipment. Some of the primary problems are (1) dielectric constants of capacitors in tuned networks can change with variations of humidity, (2) electronic components may deteriorate as a result of metallic corrosion and electrode chemical reactions with components can take place with the presence of moisture; examples of these are corrosive buildup on inductors, memory cores, etc., and parametric changes of components due to the formation of condensing vapor across contacts, and (3) the increase of humidity tends to decrease the breakdown voltage between potentials. These are a few problems that are identifiable when working with electronic components in a humid environment.

c. Organic growth, bacteria and fungi, multiply rampantly under conditions of high humidity and warm air temperature. Special emphasis must be placed on controlling the growth of these undesirable organisms where they may degrade the performance of aerospace systems and sensors. Stringent moisture controls must be placed within and around such systems.

d. A decrease in the temperature of the air to the dew point will result in the condensation of water vapor from the atmosphere into the liquid or frozen state. Considerable difficulty may result from ice forming on space vehicles when moist air is cooled by the low temperature of the fuel. Damage may result if pieces of this ice should drop onto vehicle or ground-support equipment before or during launch. Optical surfaces, such as lenses of optical equipment, may become coated with water droplets or ice crystals and become inoperative. Various other factors can result because of the condensation of water or ice at, or near, the vehicle launch site, causing many problems.

Controlled chamber tests are conducted where humidity is closely regulated. This is referred to as humidity cycling (Ref. 6.4). Relative humidity and temperature are gradually raised and lowered to simulate environmental conditions. The chamber shall be constructed and function, and accessories shall be arranged in the chamber, according to the specifications provided in Reference 6.4. This reference describes five different humidity test procedures that can be applied, depending upon the requirements needed. Procedure I under method 507 on Humidity Testing is stated by the following steps:

Step 1. Place the test item in the test chamber in accordance with section 3, paragraph 3.2.2, of Reference 6.4. Prior to starting the test, the internal chamber temperature shall be at standard ambient with uncontrolled humidity.

Step 2. Gradually raise internal chamber temperature to 71°C (160°F) and the relative humidity to 95 percent over a period of 2 hours.

Step 3. Maintain condition of step 2 for not less than 6 hours.

Step 4. Maintain 85 percent, or greater, relative humidity and reduce internal chamber temperature in 16 hours to 28° ± 10°C (82° ± 18°F).

Step 5. Repeat steps 2, 3, and 4 for 10 cycles (not less than 240 hours).

Step 6. Remove the test item from chamber and allow the test item to return to 28° ± 10°C (82° ± 18°F)

Step 7. Operate the test item and compare results with the data obtained in accordance with section 3, paragraph 3.2.1, of Reference 6.4. Prior to measurements excess moisture may be removed from the exterior surfaces of the test item by turning the test item upside down or by wiping external surfaces only.

Step 8. Inspect the test item in accordance with section 3, paragraph 3.2.4, within 1 hour as stated in Reference 6.4.

A temperature of 71°C (160°F) and 95 percent relative humidity represents a dew point temperature of 69°C (156°F) that is much higher than any natural extreme in the world. Dew points above 32°C (90°F) are extremely unlikely in nature (Ref. 6.5), since the dew-point temperature is limited by the source of the water vapor, i.e., the surface temperature of the water body from which the water evaporates (Ref. 6.6).

Reference 6.4 includes humidity test Procedures II through V. Certain tests are not as rigorous as described by Procedure I above, although others are more stringent.

For many equipment qualification tests the procedures presented herein may be too lenient or too rigid. A less stringent quality-control test used to test select electronic-mechanical components to be used in the Apollo Telescope Mount (ATM) reads as follows (Ref. 6.7).

The humidity test is conducted to determine the resistance of components to exposure to a warm, highly humid atmosphere, such as may be encountered in the southeastern and south central United States. The use of temperature cycling in the test procedures provides alternate periods of condensation and drying essential to the development of corrosion processes and produces a "breathing" action which tends to force moisture into partially sealed components and containers. (The test chamber, chamber hardware, and accessories are not included in this discussion.)

The ATM components shall be placed in the test chamber and subjected to the following humidity-temperature cycling:

a. Maintain chamber for 6 hours at 37.2°C (99°F) and 50 percent relative humidity.

b. Over a 5-hour period, gradually reduce air temperature to 24.4°C (76°F) with relative humidity increasing to 100 percent.

c. Over an 8-hour period, gradually reduce air temperature to 21.1°C (70°F) with a release of water as condensate and with the relative humidity of the chamber remaining at 100 percent.

d. Over a 4-hour period, increase air temperature to 37.2°C (99°F) with a resultant decrease in relative humidity to 41 percent.

e. Over a 1-hour period, with temperature at 37.2°C (99°F), increase relative humidity to 50 percent.

f. The preceding steps constitute one humidity cycle. This cycle shall be repeated a minimum of five times. At the completion of the test the component shall be removed from the chamber and returned to room ambient conditions. Functional tests, as specified in the individual component specification or procedure, shall be performed within 1 hour after removal from the chamber.

The External Tank Verification Plan (Ref. 6.8) lists the following general statements under Test Controls and Test Methods. The statements are (1) the item is sealed or potted and subjected to a seal test, (2) the item is located in a controlled-humidity or air-conditioned environment during operation and is protected from humidity when nonoperating, (3) the item is subjected to propellant compatibility testing which is considered to be a more severe environment, and (4) the item is fabricated from materials which preclude corrosion by humidity. This, again, requires additional and different quality control standards than those discussed previously.

The Space Shuttle Program, Shuttle Master Verification Plan document, also states that the humidity and other environmental parameter tests will use the procedures given in "Military Standards 810B" (Ref. 6.4).

Some information and test procedures have been provided on humidity-temperature chamber test criteria for various systems and their associated electrical-mechanical components. A wide variety of such tests are identified in the various system requirements documents. However, this document has been prepared to emphasize actual environmental criteria, including extreme values, which must be considered in conducting any such tests of components to promote realism about the actual environment.

6.2.1 High Vapor Concentration at Surface

a. Huntsville, River Transportation, New Orleans, Gulf Transportation, Eastern Test Range, and Wallops Flight Center:

(1) The following extreme humidity cycle of 24 hours with a wind of less than 5 m sec^{-1} (9.7 knots) should be considered in design: Three hours of 37.2°C (99°F) air temperature at 50 percent relative humidity and a vapor concentration of 22.2 g m^{-3} (9.7 gr ft^{-3}); six hours of decreasing air temperature to 24.4°C (76°F) with relative humidity increasing to 100 percent (saturation); eight hours of decreasing air temperature to 21.1°C (70°F), with a release of 3.8 grams of water as liquid per cubic meter of air (1.7 grains of water per cubic foot of air),[1] humidity remaining at 100 percent; and seven hours of increasing air temperature to 37.2°C (99°F) and a decrease to 50 percent relative himidity (Fig. 6.1).

(2) An extreme relative humidity between 75 and 100 percent and air temperature between 22.8°C (73°F) and 27.8°C (82°F), which would result in corrosion and bacterial and fungal growths, can be expected for a period of 15 days. A humidity of 100 percent occurs one-fourth of the time at the lower temperature in cycles not exceeding 24 hours. Any loss of water vapor from the air by condensation is replaced from outside sources to maintain at least 75 percent relative humidity at the higher temperature.

---

1. The release of water as a liquid onthe test object may be delayed for several hours after the start of this part of the test because of thermal lag in a large test object. If the lag is too large, the test should be extended in time for each cycle to allow condensation.

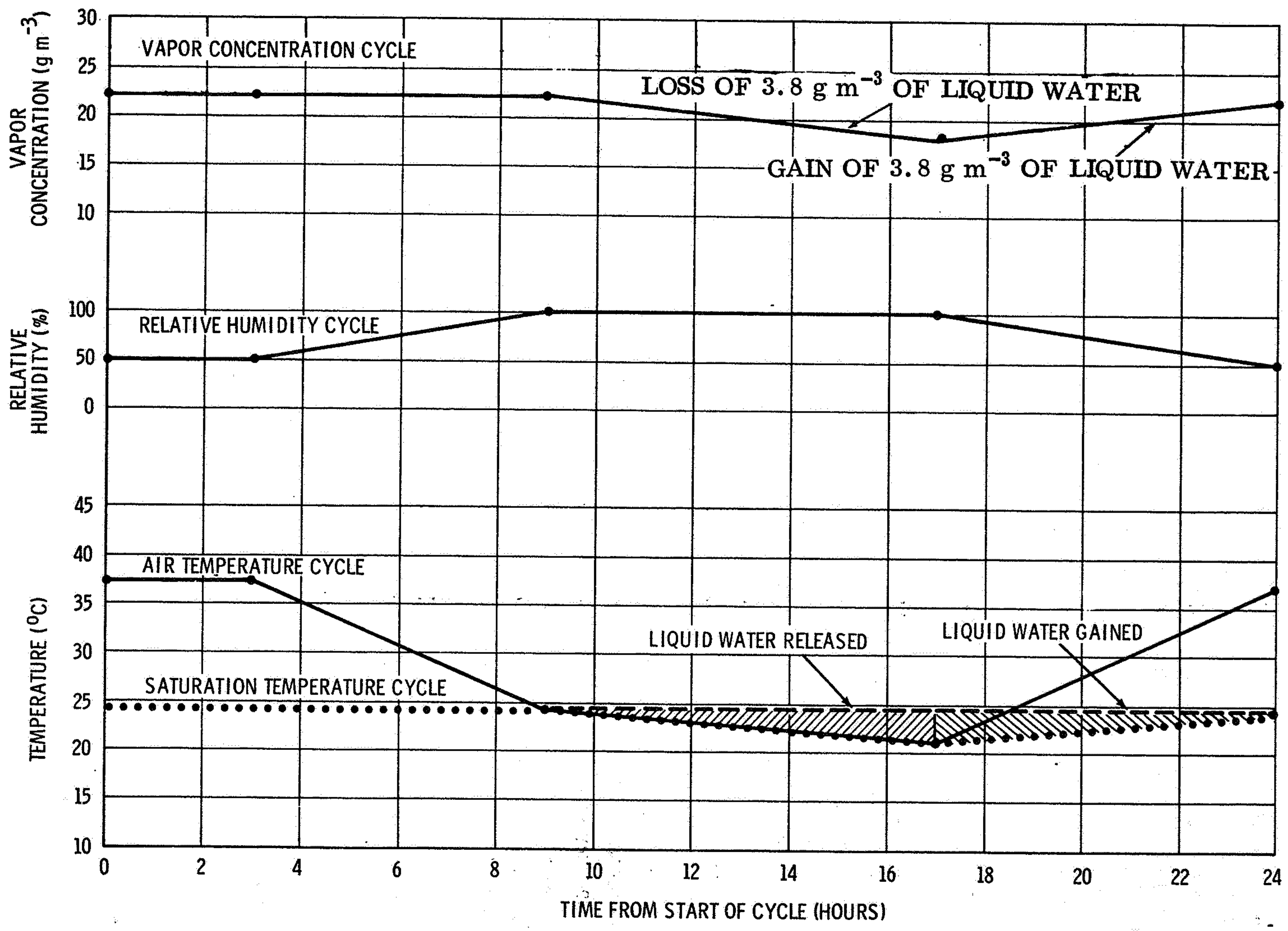

FIGURE 6.1. EXTREME HIGH VAPOR CONCENTRATION CYCLE FOR HUNTSVILLE, RIVER TRANSPORTATION, NEW ORLEANS, GULF TRANSPORTATION, EASTERN TEST RANGE, AND WALLOPS FLIGHT CENTER

b. Panama Canal Transportation:

(1) The following extreme humidity cycle of 24 hours with a wind of less than 5 m sec^{-1} (9.7 knots) should be considered in design: Three hours of 32.2°C (90°F) air temperature at 75 percent relative humidity, and a vapor concentration of 25.4 g m^{-3} (11.1 gr ft^{-3}); six hours of decreasing air temperature to 26.7°C (80°F) with relative humidity increasing to 100 percent; eight hours of decreasing air temperature to 21.7°C (71°F) with a release of 6.3 grams of water as liquid per cubic meter of air (2.8 grains of water per cubic foot of air),[2] humidity remaining at 100 percent; four hours of increasing air temperature to 26.7°C (80°F) and a decrease to 75 percent relative humidity; and three hours of increasing air temperature to 32.2°C (90°F) with the relative humidity remaining at 75 percent (moisture added to air by evaporation, mixing, or replacement with air of higher vapor concentration). See Figure 6.2.

(2) An extreme relative humidity between 85 and 100 percent and air temperature between 23.9°C (75°F) and 26.1°C (79°F), which would result in corrosion and bacterial and fungal growth, can be expected for a period of 30 days. The humidity should be 100 percent during one-fourth of the time at the lower temperature in cycles not exceeding 24 hours. Any loss of water vapor from the air by condensation is replaced from outside sources to maintain at least 85 percent relative humidity at the higher temperature.

(3) Equipment shipped from the West Coast through the Panama Canal may accumulate moisture (condensation) while in the ship's hold because of the increasing moisture content of the air while traveling south to the Panama Canal and the slower increase of temperature of the equipment being transported. This condensation may result in corrosion, rusting, or other deterioration of the equipment (Ref. 6.9). Extreme values of condensation are

(a) Maximum condensation conditions occur during the period between December and March, but condensation conditions may occur during all months.

(b) The maximum dew point expected is 30.0°C (86°F), with dew points over 21.1°C (70°F) for ship travel of 6 days prior to arrival at the Panama Canal from the West Coast and for the remainder of the trip to Cape Kennedy.

2. Ibid.

ORIGINAL PAGE IS OF POOR QUALITY

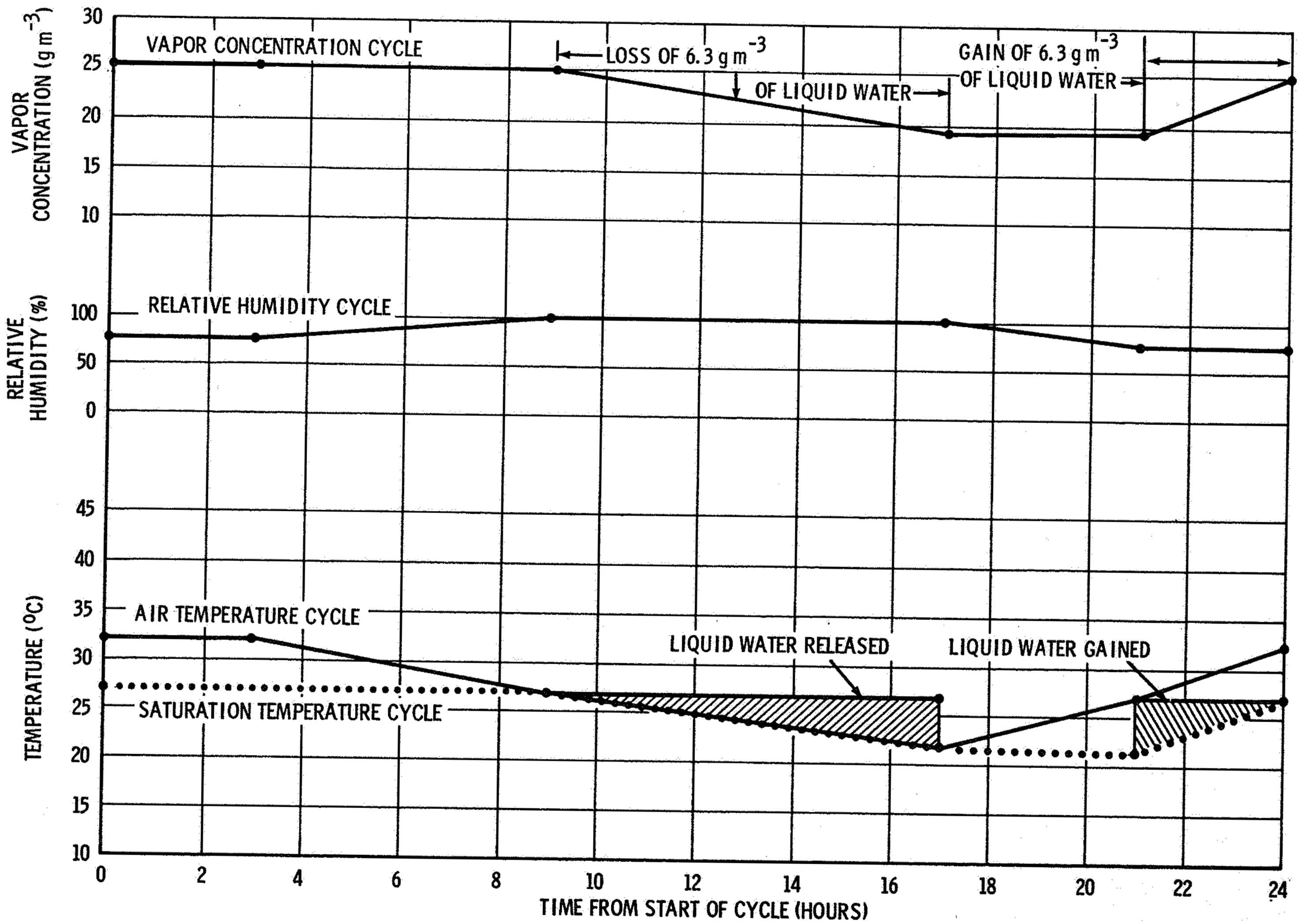

FIGURE 6.2. EXTREME HIGH VAPOR CONCENTRATION CYCLE FOR PANAMA CANAL TRANSPORTATION

c. The Space and Missile Test Center, West Coast Transportation, and Sacramento:

(1) The following extreme humidity cycle of 24 hours with a wind of less than 5 m sec^{-1} (9.7 knots) should be considered in design: Three hours of 23.9°C (75°F) air temperature at 75 percent relative humidity and a vapor concentration of 16.2 g m^{-3} (7.1 gr ft^{-3}); six hours of decreasing air temperature to 18.9°C (66°F) with relative humidity increasing to 100 percent; eight hours of decreasing air temperature to 12.8°C (55°F) with a release of 5.0 grams of water as liquid per cubic meter of air (2.2 gr of water per cubic foot of air),[3] humidity at 100 percent; and seven hours of increasing air temperature to 23.9°C (75°F) and the relative humidity decreasing to 75 percent (Fig. 6.3).

(2) Bacterial and fungal growth should present no problem because of the lower temperatures in this area. For corrosion, an extreme humidity of between 75 and 100 percent relative humidity and air temperature between 18.3°C (65°F) and 23.3°C (74°F) can be expected for a period of 15 days. The humidity should be 100 percent during one-fourth of the time at the lower temperature in cycles not exceeding 24 hours. Any loss of water vapor from the air condensation is replaced from outside sources to maintain at least 75 percent relative humidity at the higher temperature.

d. White Sands Missile Range: This area is located at 1216 m (4000 ft) above sea level and is on the eastern side of higher mountains. The mean annual rainfall of 250 cm (10 in.) is rapidly absorbed in the sandy soil. Fog rarely occurs. Therefore, at this location, a high-vapor concentration over periods longer than a few hours need not be considered.

6.2.2 Low Vapor Concentration at Surface

6.2.2.1 Introduction

Low water-vapor concentration can occur at very low or at high temperatures when the air is very dry. In both cases, the dew points are very low. However, in the case of low dew points and high temperatures, the relative humidity is low. When any storage area or compartment of a vehicle is heated to temperatures well above the ambient air temperature (such as the high temperatures of the storage area in an aircraft standing on the ground in the sun), the relative humidity will be even lower than the relative humidity of the

3. The release of water as a liquid on the test object may be delayed for several hours after the start of this part of the test because of thermal lag in a large test object. If the lag is too large, the test should be extended in time for each cycle to allow condensation.

ORIGINAL PAGE IS
OF POOR QUALITY

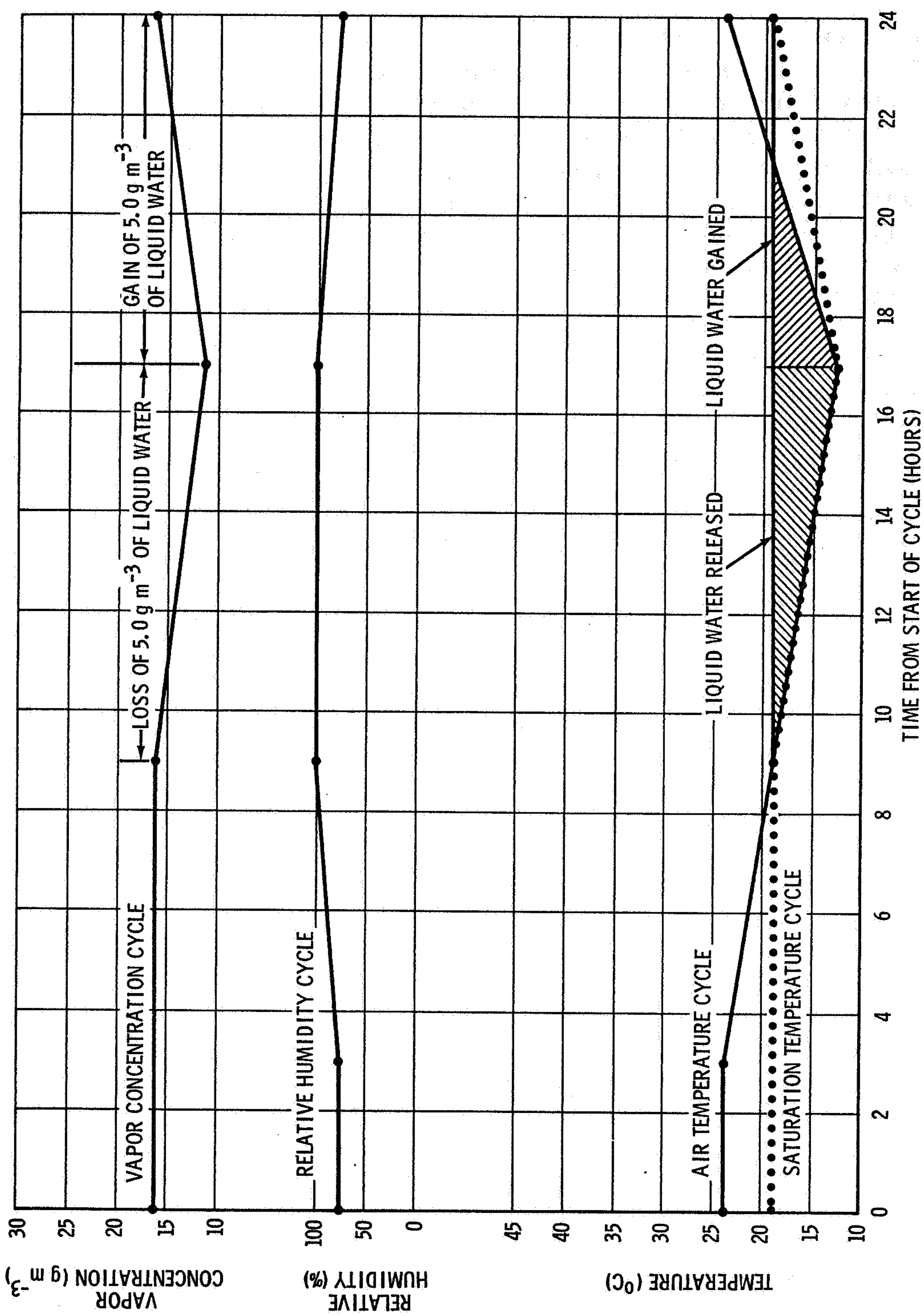

FIGURE 6.3. EXTREME HIGH VAPOR CONCENTRATION CYCLE FOR SAMTEC, WEST COAST TRANSPORTATION, AND SACRAMENTO

ambient air. These two types of low water-vapor concentrations have entirely different environment effects. In the case of low air temperatures, ice or condensation may form on equipment while in the high temperature-low humidity condition; organic materials may dry and split or otherwise deteriorate. When a storage area (or aircraft) is considerably warmer than the ambient air (even when the air is cold), the drying increases even more. Low relative humidities may also result in another problem — that of static electricity. Static electrical charges on equipment may ignite fuel or result in shocks to personnel when discharged. Because of this danger, two types of low water-vapor concentrations (dry extremes) are given for the surface.

6.2.2.2 Surface Extremes of Low Vapor Concentration.

a. Huntsville, River Transportation, Wallops Flight Center, and White Sands Missile Range:

(1) A vapor concentration of 2.1 g m^{-3} (0.9 gr ft^{-3}), with an air temperature of -11.7°C (+11°F) and a relative humidity between 98 and 100 percent for a duration of 24 hours, must be considered.

(2) A vapor concentration of 4.5 g m^{-3} (2.0 gr ft^{-3}), corresponding to a dew point of -1.1°C (30°F) at an air temperature of 28.9°C (84°F) and a relative humidity of 15 percent occurring for 6 hours each 24 hours, and a maximum relative humidity of 34 percent at an air temperature of 15.6°C (60°F) for the remaining 18 hours of each 24 hours for a 10-day period, must be considered.

b. New Orleans, Gulf Transportation, Panama Canal Transportation, and Eastern Test Range:

(1) A vapor concentration of 4.2 g m^{-3} (1.8 gr ft^{-3}), with an air temperature of -2.2°C (28°F) and a relative humidity of 98 to 100 percent for a duration of 24 hours, must be considered.

(2) A vapor concentration of 5.6 g m^{-3} (2.4 gr ft^{-3}) corresponding to a dew point of 2.2°C (36°F) at an air temperature of 22.2°C (72°F) and a relative humidity of 29 percent occurring for 8 hours, and a maximum relative humidity of 42 percent at an air temperature of 15.6°C (60°F) for the remaining 16 hours of each 24 hours for 10 days, must be considered.

c. Space and Missile Test Center:

(1) A vapor concentration of 4.2 g m^{-3} (1.8 gr ft^{-3}), with an air temperature of -2.2°C (28°F) and a relative humidity of 98 to 100 percent for a duration of 24 hours, must be considered.

(2) A vapor concentration of 4.8 g m^{-3} (2.1 gr ft^{-3}), corresponding to a dew point of 0.0°C (32°F) at an air temperature of 37.8°C (100°F) and a relative humidity of 11 percent occurring for 4 hours each 24 hours, and a maximum relative humidity of 26 percent at an air temperature of 21.1°C (70°F) for the remaining 20 hours of each 24 hours for 10 days, must be considered.

d. West Coast Transportation and Sacramento:

(1) A vapor concentration of 3.1 g m^{-3} (1.4 gr ft^{-3}), with an air temperature of -6.1°C (21°F) and a relative humidity of 98 to 100 percent for a duration of 24 hours, must be considered.

(2) A vapor concentration of 10.1 g m^{-3} (4.4 gr ft^{-3}), corresponding to a dew point of 11.1°C (52°F) at an air temperature of 37.8°C (100°F) and a relative humidity of 22 percent occurring for 4 hours each 24 hours, and a maximum relative humidity of 55 percent at an air temperature of 21.1°C (70°F) for the remaining 20 hours of each 24 hours for 10 days, must be considered.

6.2.3 Compartment Vapor Concentration at Surface

A low water-vapor concentration extreme of 10.1 g m^{-3} (4.4 gr ft^{-3}), corresponding to a dew point of 11.1°C (52°F) at a temperature of 87.8°C (190°F) and a relative humidity of two percent occurring for one hour, a linear change over a four-hour period to an air temperature of 37.8°C (100°F) and a relative humidity of 22 percent occurring for 15 hours, then a linear change over a four-hour period to the initial conditions, must be considered at all locations.

6.3 Vapor Concentration at Altitude

In general, the vapor concentration decreases with altitude in the troposphere because of the decrease of temperature with altitude. The data given in this section on vapor concentration are appropriate for design purposes.

6.3.1 High Vapor Concentration at Altitude

The following tables present the relationship between maximum vapor concentration and the associated temperature normally expected as a function of altitude (Ref. 6.10).

a. Maximum Vapor Concentrations for Eastern Test Range, Table 6.1.

b. Maximum Vapor Concentrations for Wallops Flight Center, Table 6.2.

c. Maximum Vapor Concentrations for White Sands Missile Range, Table 6.3.

d. Maximum Vapor Concentrations for SAMTEC/Vandenberg AFB, Table 6.4.

6.3.2 Low Vapor Concentration at Altitude

The values presented as low extreme vapor concentrations in the following tables are based on data measured by standard radiosonde equipment.

a. Minimum Vapor Concentrations for Eastern Test Range, Table 6.5.

b. Minimum Vapor Concentrations for Wallops Flight Center, Table 6.6.

c. Minimum Vapor Concentrations for White Sands Missile Range, Table 6.7.

d. Minimum Vapor Concentrations for SAMTEC/Vandenberg AFB, Table 6.8.

TABLE 6.1. MAXIMUM VAPOR CONCENTRATION FOR EASTERN TEST RANGE

Geometric Altitude		Vapor Concentration		Temperature Associated with Maximum Vapor Concentration	
(km)	(ft)	($g\ m^{-3}$)	($gr\ ft^{-3}$)	(°C)	(°F)
SFC (0.005 MSL)	(16)	27.0	11.8	30.5	87
1	3,300	19.0	8.3	24.5	76
2	6,600	13.3	5.8	18.0	64
3	9,800	9.3	4.1	12.0	54
4	13,100	6.3	2.8	5.5	42
5	16,400	4.5	2.0	-0.5	31
6	19,700	2.9	1.3	-6.8	20
7	23,000	2.0	0.9	-13.0	9
8	26,200	1.2	0.5	-20.0	-4
9	29,500	0.6	0.3	-27.0	-17
10	32,800	0.3	0.1	-34.5	-30
16.2	53,100	0.025	0.01	-57.8	-72
20	65,600	0.08	0.03	-47.8	-54

TABLE 6.2. MAXIMUM VAPOR CONCENTRATION FOR WALLOPS FLIGHT CENTER

Geometric Altitude		Vapor Concentration		Temperature Associated with Maximum Vapor Concentration	
(km)	(ft)	(g m^{-3})	(gr ft^{-3})	(°C)	(°F)
SFC (0.002 MSL)	(8)	22.5	9.8	27.5	82
1	3,300	20.0	8.7	26.1	79
2	6,600	13.9	6.1	17.2	63
3	9,800	10.3	4.5	12.8	55
4	13,100	7.4	3.2	7.8	46
5	16,400	6.0	2.6	2.8	37
6	19,700	3.9	1.7	-1.1	30
7	23,000	2.6	1.1	-5.0	23
8	26,200	1.7	0.7	-11.1	12
9	29,500	0.9	0.4	-17.8	0
10	32,800	0.4	0.2	-27.8	-18
16.5	54,100	0.08	0.03	-47.2	-55
20	65,600	0.09	0.04	-46.2	-51

TABLE 6.3. MAXIMUM VAPOR CONCENTRATION FOR WHITE SANDS MISSILE RANGE

Geometric Altitude		Vapor Concentration		Temperature Associated with Maximum Vapor Concentration	
(km)	(ft)	(g m^{-3})	(gr ft^{-3})	(° C)	(°F)
SFC (1.2 MSL)	(3,989)	16.0	7.0	21.5	71
2	6,600	13.2	5.8	18.9	66
3	9,800	9.0	3.9	12.8	55
4	13,100	6.8	3.0	7.8	46
5	16,400	4.9	2.1	2.2	36
6	19,700	3.4	1.5	-2.2	28
7	23,000	2.2	1.0	-10.0	14
8	26,200	1.3	0.6	-16.1	3
9	29,500	0.6	0.3	-22.8	-9
10	32,800	0.2	0.1	-30.0	-22
16.5	54,100	0.08	0.03	-47.8	-54
20	65,600	0.05	0.02	-52.2	-62

TABLE 6.4 MAXIMUM VAPOR CONCENTRATIONS FOR SAMTEC/VANDENBERG AFB

Geometric Altitude		Vapor Concentration		Temperature Associated with Maximum Vapor Concentration	
(km)	(ft)	(g m^{-3})	(gr ft^{-3})	(°C)	(°F)
SFC (0.113 MSL)	371	17.5	7.6	30.5	86.9
1	3,300	14.8	6.5	24.2	75.6
2	6,600	10.0	4.4	20.6	69.1
3	9,800	7.5	3.3	11.0	51.8
4	13,100	5.0	2.2	4.7	40.5
5	16,400	3.7	1.6	- 1.4	29.5
6	19,700	2.3	1.0	- 8.1	17.4
7	23,000	1.6	0.7	-12.5	9.5
8	26,200	0.8	0.3	-20.2	- 4.4
9	29,500	0.4	0.2	-28.2	-18.8
10	32,800	0.2	0.1	-34.3	-29.7

TABLE 6.5 MINIMUM VAPOR CONCENTRATIONS FOR EASTERN TEST RANGE

Geometric Altitude		Vapor Concentration		Temperature Associated with Minimum Vapor Concentration	
(km)	(ft)	(g m^{-3})	(gr ft^{-3})	(°C)	(°F)
SFC (0.005 MSL)	(16)	4.0	1.7	29	84.2
1	3,300	0.5	0.2	6	42.8
2	6,600	0.2	0.1	0	32.0
3	9,800	0.1	0.04	-11	12.2
4	13,100	0.1	0.04	-14	6.8

TABLE 6.6 MINIMUM VAPOR CONCENTRATION FOR WALLOPS FLIGHT CENTER

Geometric Altitude		Vapor Concentration		Temperature Associated with Minimum Vapor Concentration	
(km)	(ft)	(g m^{-3})	(gr ft^{-3})	(°C)	(°F)
SFC (0.002 MSL)	(8)	0.5	0.2	-4	24.8
1	3,300	0.3	0.1	-11	12.2
2	6,600	0.2	0.1	-17	1.4
3	9,800	0.2	0.1	-23	-9.4
4	13,100	0.2	0.1	-31	-23.8
5	16,400	0.1	0.04	-39	-38.2
7.5	24,600	0.08	0.03	-47	-43.9
10	32,800	0.017	0.007	-61	-51.7

TABLE 6.7 MINIMUM VAPOR CONCENTRATION FOR WHITE SANDS MISSILE RANGE

Geometric Altitude		Vapor Concentration		Temperature Associated with Minimum Vapor Concentration	
(km)	(ft)	(g m^{-3})	(gr ft^{-3})	(°C)	(°F)
SFC (1.2 MSL)	(3,989)	1.2	0.5	-1	30.2
2	6,600	0.9	0.4	-5	23.0
3	9,800	0.6	0.3	-12	10.4
4	13,100	0.4	0.2	-20	-4.0
5	16,400	0.2	0.1	-26	-14.8
6	19,700	0.1	0.04	-36	-32.8
7	23,000	0.09	0.03	-42	-43.6
8	26,200	0.07	0.03	-49	-56.2
9	29,500	0.03	0.01	-55	-67.0
10	32,800	0.02	0.01	-60	-76.0

TABLE 6.8 MINIMUM VAPOR CONCENTRATIONS FOR SAMTEC/VANDENBERG AFB

Geometric Altitude		Vapor Concentration		Temperature Associated with Maximum Vapor Concentration	
(km)	(ft)	(g m^{-3})	(gr ft^{-3})	(°C)	(°F)
SFC (0.113 MSL)	371	1.6	0.7	4.5	40.1
1	3,300	0.7	0.3	- 1.4	29.5
2	6,600	0.4	0.2	- 7.5	18.5
3	9,800	0.3	0.1	-12.6	9.3
4	13,100	0.1	0.04	-19.4	- 2.9
5	16,400	0.07	0.03	-27.3	-17.1
6	19,700	0.03	0.01	-35.1	-31.2
7	23,000	0.02	0.009	-39.5	-39.1

REFERENCES

6.1 "Glossary of Meteorology." American Meteorological Society, Boston, Mass., 1959.

6.2 Sheppard, P.A.: "The Physical Properties of Air With Reference to Meteorological Practice and the Air-Conditioning Engineer." ASME, Vol. 71, 1949, pp. 915-919.

6.3 "Climatic and Environmental Criteria for Aircraft Design." ANC-22 Munitions Board Aircraft Committee, 1952.

6.4 "Military Standard, Environmental Test Methods." MIL-STD-810C, March 10, 1975.

6.5 Sissenwine, Norman; and Court, Arnold: "Climatic Extremes for Military Equipment." Report No. 146, Environmental Protection Branch, Research and Development Division, Office of the Quartermaster General, Washington, D.C., 1951.

6.6 Sverdrup, H.V.: "Oceanography for Meteorologists." Prentice-Hall, Inc., New York, 1942.

6.7 "Environmental Design and Qualification Test Criteria for Apollo Telescope Mount Components." 50M02408, Revision D, final report by Program Management (PM/SE-ATM), Marshall Space Flight Center, Huntsville, Ala., Jan. 15, 1970.

6.8 "External Tank Verification Plan." MMC-ET-TM01-B, Contract No. NAS8-30300, WBS No. 1.6.2.2, DR. NO. TM01, Martin Marietta, Michoud Assembly Facility, New Orleans, La., Sept. 9, 1974.

6.9 Cohen, Raymond K.; and Nelson, Michael: "Evaluation and Control of Sweat Damage." Final Report SR 1, Project No. S-2179, Stanford Research Institute, Menlo Park, Calif., July 1, 1959.

6.10 Sissenwine, Norman; Grantham, D.D.; and Salmela, H. A.: "Mid-Latitude Humidity to 32 Km." Journal of the Atmosphere Sciences, Vol. 25, 1968, pp. 1129-1140.

SECTION VII. PRECIPITATION, FOG, AND ICING

7.1 Introduction

Precipitation, fog, and icing are special atmospheric phenomena of interest to the design, fabrication, and flight of aerospace vehicles. In some arid areas of the world, however, precipitation does not occur for several years. Likewise, in areas of moderate to heavy rainfall, there are periods of time without rain. Because precipitation does occur in discrete events, statistical representation may be misleading; therefore, caution must be taken to ensure that data relative to the desired location are used. Definitions used in this section are given in the following paragraphs.

7.2 Definitions

Precipitation is usually defined as all forms of hydrometeors, liquid or solid, which are free in the atmosphere and reach the ground. In this report the definition is extended to those hydrometeors which do not reach the ground but impinge on a flying surface, such as space vehicles. Accumulation is reported in depth over a horizontal surface, i.e., millimeters or inches for the liquid phase, and in depth or depth-of-water equivalent for the frozen phase.

Snow is defined as all forms of frozen precipitation except large hail. It encompasses snow pellets, snow grains, ice crystals, ice pellets, and small hail.

Hail is precipitation in the form of balls or irregular lumps of ice and is always produced by convective clouds. Through established convention, to be classified as hail the diameter of the ice must be 5 mm or more and the specific gravity between 0.60 and 0.92.

Freezing rain is rain that falls in liquid form but freezes upon impact to form a coating of glaze upon the ground or exposed objects.

Small hail is precipitation in the form of semitransparent round or conical grains of frozen water under 5 mm in diameter. Each grain consists of a nucleus of soft hail (ball of snow) surrounded by a very thin ice layer. The grains are not crisp and do not usually rebound when striking a hard surface.

Drizzle: Drizzle consists of droplets which are so small that they make no precipitable impact on surfaces. If individual droplets make a distinct splash on striking the ground or a water surface, they should be recorded as rain (Ref. 7.1).

Mist: Mist is composed of a suspension of very small water droplets in the air. Mist reduces the horizontal visibility at the earth's surface, as does fog, rain, snow, and other hydrospheric and lithospheric substances.

The previously described precipitation forms are sufficiently different that each must be considered separately in design problems.

7.3 Rainfall

There are four major rainfall-producing atmospheric conditions: (1) the monsoon, which produces the heaviest precipitation over long periods (most world records of rainfall rates for periods greater than 12 hours are a result of monsoons), (2) thunderstorms, which generate high rates of precipitation for short periods, (3) cold and warm frontal systems, frequently accompanied by bands of steady light rain. Frontal-produced rain can persist for several days, depending upon the movement of synoptic scale weather systems(thunderstorms may occur with frontal systems to give heavier rain), and (4) hurricanes, which produce heavy rain associated with winds. These four rainfall types are defined in the following paragraphs.

Monsoon: The monsoon is a seasonal wind which blows for long periods of time, usually several months from one direction. When these winds blow from the water to land with increasing elevation from the water, the orographic lifting of the moisture-laden air releases precipitation in heavy amounts. In Cherraponji, India, 9144 mm (360 in.) of rain has fallen in a one-month period from monsoon rains. The amount of rain from monsoons at low elevations is considerably less than at higher elevations.

Thunderstorm: In general, the thunderstorm (local storm) is produced either by lifting of unstable moist air, heating of the land mass, lifting by frontal systems, or a combination of these conditions. Cumulonimbus clouds, which are produced by these storms, are always accompanied by lightning and thunder. The thunderstorm is a consequence of atmospheric instability and is defined loosely as an overturning of air layers in order to achieve a stable condition. Strong wind gusts, heavy rain, severe electrical discharges, and sometimes hail occur with the thunderstorm, with the most frequent and severe occurrences in the late afternoons and evenings.

Cold and warm front precipitation: When two masses of air meet — one more dense than the other — the lighter air mass (warm) will slide up over the more dense air mass (cold). If sufficient moisture is in the air mass being lifted, then the moisture will be condensed out and fall as precipitation, either rain or snow, depending on the temperature of air masses.

Hurricanes: A hurricane is a severe "tropical storm" which forms over the various oceans and seas, nearly always in tropical latitudes. At maturity the tropical cyclone (storm) is one of the most intense and feared storms in the world: Winds exceeding 90 m/s (175 knots) have been measured, and its rainfall can be torrential. The wind speed must exceed 33 m/s (64 knots) for the storm to be classified as a hurricane.

Orographic effects should not be overlooked in a discussion of rainfall. Islands located in persistent moist air flow receive extreme rainfall as a result of the moist air being lifted to the condensation level (frequently only 2000 to 5000 ft altitude) with resulting persistent rain. This phenomena accounts for wide variations in precipitation amounts between locations in close proximity in mountainous areas.

7.3.1 Record Rainfall

In design analysis, the maximum amounts of rainfall for various periods need to be considered. These extreme values vary consideraby in different areas of the world, but in areas of similar climatic conditions the extreme values are similar.

7.3.1.1 World Record Rainfall

To best study the maximum amounts of rainfall that have occurred worldwide for different periods, log-log graph paper is used. Figure 7.1 shows these worldwide values and the envelope of these values as a straight line with the equation

$$R = 363.0\sqrt{D_h}\ (\text{mm}) \quad \text{or} \quad R = 14.3\sqrt{D_h}\ (\text{in.}) \tag{7.1}$$

where R is the depth of rainfall in millimeters for period D, and D is the duration of rainfall in hours.

7.3.1.2 Design Rainfall Rates

For design and testing, the rate of rainfall per unit time is more useful than the total depth of rainfall. The normal rates used are shown in millimeters per hour or inches per hour. Figure 7.2 shows the envelope of world record values plotted as the rate per hour (inches and millimeters) versus duration. The Eastern Test Range (Kennedy Space Center) and Vandenberg AFB (SAMTEC) design rainfall rate curves are also shown in Figure 7.2 with the 5-year and 100-year return periods for a few select stations. The 5-year and

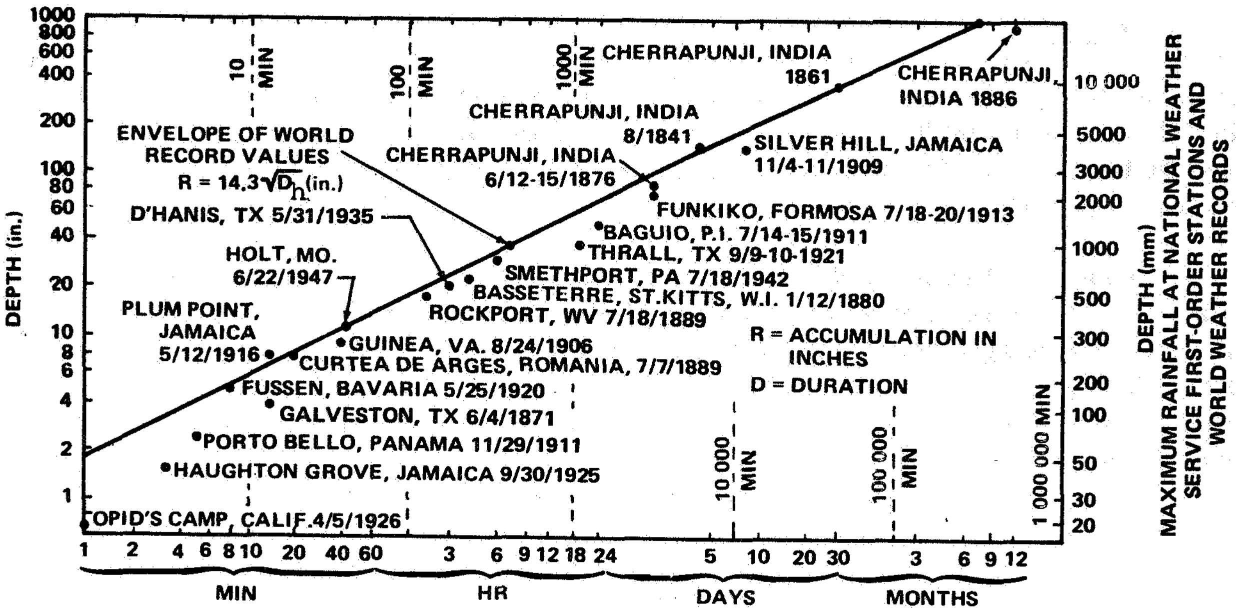

FIGURE 7.1. WORLD RECORD RAINFALLS AND AN ENVELOPE OF WORLD RECORD VALUES (After R. D. Fletchter and D. Sartos, Air Weather Service Tech. Rept. No. 105-81, 1951.)

100-year return period data were taken from Rainfall Intensity-Duration-Frequency curves published by the U. S. Department of Commerce, Weather Bureau (Ref. 7.2). These data were analyzed by the Extreme Value Method of Gumble (Ref. 7.3).

The term "return period" is a measure of the average time interval between occurrences of a specific event. For example, the 99th percentile rainfall rate for Tampa, Florida, is approximately 10 in./hr for a duration of 6 minutes (from Fig. 7.2 and Table 7.1). On the average this rainfall rate can be expected to return in 100 years at Tampa. Return periods can be expressed as probabilities, as shown in Table 7.1.

Values of design rainfall for various locations and worldwide extremes of rainfall are given in Tables 7.2, 7.3, 7.4, and 7.5 with values of the corresponding drop size. For design purposes, use the values of wind speed and temperature given in Table 7.6.[1] The worldwide extremes would not normally be used for design of space vehicles but may be needed for facility design, tracking stations, etc. The values of rainfall rates are represented with the following equation:

---

[1] Environmental Test Methods. Military Standard MIL-STD-810C, Department of Defense, 10 March 1975.

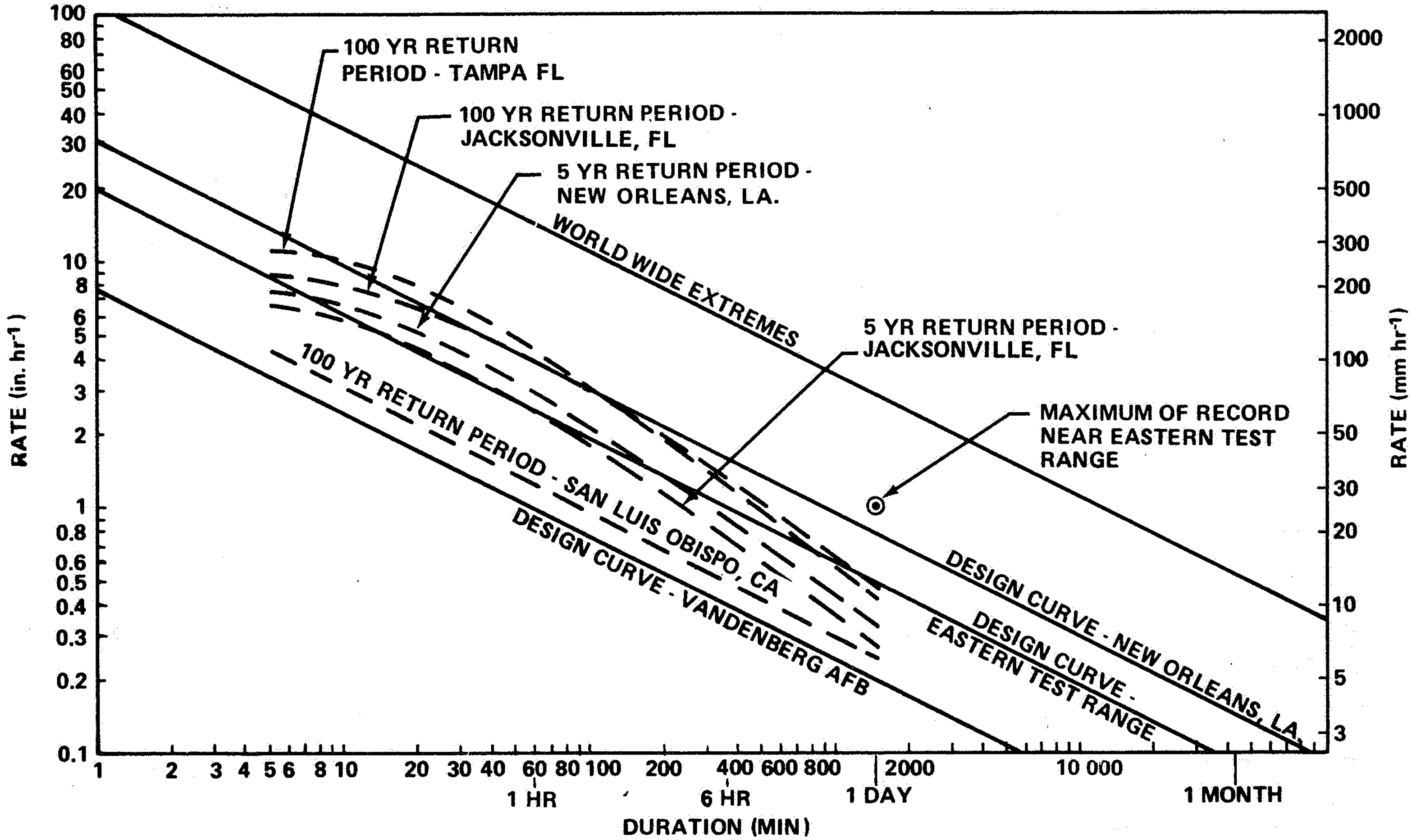

FIGURE 7.2 DESIGN RAINFALL RATES

TABLE 7.1 RELATIONSHIP OF RETURN PERIODS TO PROBABILITIES

Return Period (yr)	Percentile (%)	Return Period (yr)	Percentile (%)
2	50	50	98
5	80	100	99
10	90	1000	99.9

$$r = \frac{C\sqrt{D_m}}{D_m} = \frac{C}{\sqrt{D_m}} \tag{7.2}$$

where

r = rate per hour

D_m = time in minutes

C = constant for location as given in Table 7.7.

7.3.2 Raindrop Size

A knowledge of raindrop sizes is required to (1) simulate rainfall tests in the laboratory, (2) know the rate of fall of the raindrops and impact energy, and (3) use in erosion tests of materials.

At the surface, the size of the raindrops varies with the rate of rainfall per unit time; the heavier the rainfall, the larger the drops. Any one rainstorm will contain a variety of sizes of raindrops ranging in size from less than 0.5 mm (the lower limit of size measurement) to greater than 4.0 mm. The more intense the storm (the higher the rate of fall), the larger some of the drops will be. Reference 7.4 shows data on probability of occurrence of various raindrop sizes with relation to types of rain-producing storms: (1) thunderstorms, (2) rain showers, and (3) continuous rain. Thunderstorms have the greatest occurrence of the larger drops (over 2 mm). Rain showers have the next greatest occurrence, while the continuous rain produces the lowest occurrence of the larger drops. Raindrop sizes below 2 mm in diameter occur with

TABLE 7.2 DESIGN RAINFALL, KENNEDY SPACE CENTER, FL.; HUNTSVILLE, AL.; AND WALLOPS FLIGHT CENTER, VA.; BASED ON YEARLY LARGEST RATE FOR STATED DURATIONS

Time Period	Rainfall Rate		Rainfall Total Accumulation		Raindrop Size Average	Raindrop Size Largest	Average Rate of Fall
	mm hr^{-1}	in. hr^{-1}	mm	in.	mm	mm	m sec^{-1}
1 min	492	19.4	8	0.3	2.0	6.0	6.5
5 min	220	8.7	18	0.7	2.0	5.8	6.5
15 min	127	5.0	32	1.25	2.0	5.7	6.5
1 hr	64	2.5	64	2.5	2.0	5.0	6.5
6 hr	26	1.0	156	6.1	1.8	5.0	6.5
12 hr	18	0.7	220	8.7	1.6	4.5	6.5
24 hr	13	0.5	311	12.2	1.5	4.5	6.5

TABLE 7.3 DESIGN RAINFALL, NEW ORLEANS, LA.; BASED ON YEARLY LARGEST RATE FOR STATED DURATIONS

Time Period	Rainfall Rate		Rainfall Total Accumulation		Raindrop Size Average	Raindrop Size Largest	Average Rate of Fall
	mm hr^{-1}	in. hr^{-1}	mm	in.	mm	mm	m sec^{-1}
1 min	787	31.0	13	0.5	2.1	6.0	6.5
5 min	352	13.9	29	1.2	2.0	6.0	6.5
15 min	203	8.0	51	2.0	2.0	5.7	6.5
1 hr	102	4.0	102	4.0	2.0	5.5	6.5
6 hr	41	1.6	249	9.8	1.9	5.0	6.5
12 hr	29	1.2	352	13.9	1.8	5.0	6.5
24 hr	21	0.8	498	19.6	1.6	5.0	6.5

TABLE 7.4 DESIGN RAINFALL, VANDENBERG AFB (SAMTEC), CA.; EDWARDS AFB, CA; AND WHITE SANDS MISSLE RANGE, NM; BASED ON YEARLY LARGEST RATE FOR STATED DURATIONS

Time Period	Rainfall Rate		Rainfall Total Accumulation		Raindrop Size Average	Raindrop Size Largest	Average Rate of Fall
	mm hr^{-1}	in. hr^{-1}	mm	in.	mm	mm	m sec^{-1}
1 min	197	7.7	3	0.1	2.0	5.6	6 5
5 min	88	3.5	7	0.3	2.0	5.3	6.5
15 min	51	2.0	13	0.5	2.0	5.0	6.5
1 hr	25	1.0	25	1.0	1.8	5.0	6.5
6 hr	10	0.4	62	2.4	1.5	4.6	6.0
12 hr	7	0.3	88	3.5	1.3	4.3	5.8
24 hr	5	0.2	124	4.9	1.3	4.0	5.5

TABLE 7.5 DESIGN RAINFALL, WORLDWIDE EXTREMES, BASED ON YEARLY LARGEST RATE FOR STATED DURATIONS

Time Period	Rainfall Rate		Rainfall Total Accumulation		Raindrop Size Average	Raindrop Size Largest	Average Rate of Fall
	mm hr^{-1}	in. hr^{-1}	mm	in.	mm	mm	m sec^{-1}
1 min	2813	110.8	47	1.8	2.5	6.0	6.5
5 min	1258	49.5	105	4.1	2.2	6.0	6.5
15 min	726	28.6	182	7.1	2.1	6.0	6.5
1 hr	363	14.3	363	14.3	2.0	6.0	6.5
6 hr	148	5.8	890	35.3	2.0	5.8	6.5
12 hr	105	4.1	1258	49.5	2.0	5.5	6.5
24 hr	74	2.9	1779	70.1	2.0	5.2	6.5

TABLE 7.6 IDEALIZED RAIN CYCLE, KENNEDY SPACE CENTER, FL.; BASED ON HIGHEST RAIN MONTH

Cycle	Rainfall Rate		Wind Speed		Raindrop Size		Temperature			
							Summer		Winter	
min	mm hr^{-1}	in. hr^{-1}	m sec^{-1}	knots	largest mm	average mm	°F	°C	°F	°C
0	0	0	5.1	10	0	0	90	32	55	13
30	30.0	1.17	5.1	10	5.0	2	90	32	55	13
32	30.0	1.17	5.1	10	5.0	2	75	24	50	10
33.5	30.0	1.17	15.4	30	5.0	2	75	24	50	10
34	30.0	1.17	5.1	10	5.0	2	75	24	50	10
48.5	30.0	1.17	15.4	30	5.0	2	75	24	50	10
49	30.0	1.17	5.1	10	5.0	2	75	24	50	10
63.5	30.0	1.17	15.4	30	5.0	2	75	24	50	10
64	30.0	1.17	5.1	10	5.0	2	75	24	50	10
78.5	30.0	1.17	15.4	30	5.0	2	75	24	50	10
79	30.0	1.17	5.1	10	5.0	2	75	24	50	10
90	220.0	8.7	5.1	10	5.9	2	75	24	50	10
93.5	220.0	8.7	15.4	30	5.9	2	75	24	50	10
94	220.0	8.7	5.1	10	5.9	2	75	24	50	10
95	89.0	3.5	5.1	10	5.8	2	75	24	50	10
108.5	89.0	3.5	15.4	30	5.8	2	75	24	50	10
109	89.0	3.5	5.1	10	5.8	2	75	24	50	10
110	30.0	1.17	5.1	10	5.0	2	75	24	50	10
123.5	30.0	1.17	15.4	30	5.0	2	75	24	50	10
124	30.0	1.17	5.1	10	5.0	2	75	24	50	10
138.5	30.0	1.17	15.4	30	5.0	2	75	24	50	10
139	30.0	1.17	5.1	10	5.0	2	75	24	50	10
153.5	30.0	1.17	15.4	30	5.0	2	75	24	50	10
154	30.0	1.17	5.1	10	5.0	2	75	24	50	10
168.5	30.0	1.17	15.4	30	5.0	2	75	24	50	10
169	30.0	1.17	5.1	10	5.0	2	75	24	50	10
170	0	0	5.1	10	0	0	75	24	50	10
180	0	0	5.1	10	0	0	90	32	50	10

TABLE 7.7 CONSTANTS TO USE WITH EQUATION (7.2) FOR RAINFALL RATES

	Eastern Test Range Huntsville, Wallops Flight Center	New Orleans	Vandenberg AFB (SAMTEC) Edwards AFB, White Sands Missile Range	World-wide Extremes
in. hr^{-1} mm hr^{-1}	19.365 491.87	30.984 786.99	7.746 196.75	110.767 2813.48
Values given in Table No.	2	3	4	5

near equal probability from all types of storms. In comparing drop sizes with various rainfall rates, the larger drops occurred with the highest probability from the highest rainfall rates. Raindrops over 6 mm in diameter are not expected to occur frequently because the rate of fall breaks these large drops into smaller ones.

7.3.3 Statistics of Rainfall Occurrences

One set of statistical data on precipitation will not be satisfactory for all needs in design; therefore, several sets of statistical data are presented in this section as follows.

7.3.3.1 Design Rainfall Rates

The design rainfall rates in Figure 7.2 and Tables 7.2, 7.3, 7.4 and 7.5 are based on precipitation occurrences; i.e., if precipitation is occurring, what is the probability of exceeding a rate? These data are based on occurrences over a year and would be used in design of items continuously exposed, such as launch facilities.

7.3.3.2 Probability that Precipitation Will Not Exceed a Specific Amount in Any One Day

Values for each month with the probability that precipitation will not exceed a specified amount in any one day are given for several selected sites of aerospace vehicle design interest — Cape Kennedy, FL; Edwards Air Force Base and Vandenberg Air Force Base, CA; New Orleans, LA; and Wallops Flight Center, VA, in Tables 7.8 through 7.12, respectively. The values in the tables should not be interpreted to mean that the amount of precipitation occurs uniformly over the 24-hour period, since it is more likely that most or all of the amounts occurred in a short period of the day.

7.3.3.3 Rainfall Rates Versus Duration for 50th, 95th, and 99th Percentile, Given a Day with Rain for the Highest Rain Month, Kennedy Space Center, FL

Rainfall rates for various durations for the 50th, 95th, and 99th percentile, given a day with rain in the highest rain month, are given in Table 7.13 for the Kennedy Space Center, Florida. The precipitation amounts should not be interpreted to mean that the rain fell uniformly for a brief period for the referenced time periods with no rain the remainder of the time period. As an example, the 99th percentile total of 49 mm (1.93 in.) (i.e., left column, 99th percentile, 1-hour duration as shown on Table 7.13) could have occurred as follows: 25 mm (1.0 in.) could have fallen during a 5-minute period within a particular hour, with an additional 24 mm (1.0 in.) of rainfall for another 5-minute period, making a total of 49 mm (1.93 in.) for a total of about 10 minutes. Subsequently, no rain would have fallen for 50 minutes of the hypothetical 1-hour period. The 99th percentile rainfall data are referenced in that such extremes are important to consider in vehicle and facility design studies. Table 7.2 has rainfall rates listed as well as total accumulation, raindrop size, etc., for various periods for Kennedy Space Center, Huntsville, and Wallops Flight Center, which are also valuable data to use as vehicle criteria.

7.3.4 Distribution of Rainfall Rates with Altitude

Rainfall rates normally decrease with altitude when rain is striking the ground. The rainfall rates at various altitudes in percent of the surface rates are given in Table 7.14 for all areas (Ref. 7.5).

TABLE 7.8 PROBABILITY THAT PRECIPITATION WILL NOT EXCEED A SPECIFIC AMOUNT IN ANY ONE DAY, CAPE KENNEDY, FL.

Amount		Jan	Feb	March	Apr	May	June
(in.)	(mm)	%	%	%	%	%	%
0.00	0.00	68.1	60.8	62.2	70.6	64.2	54.7
Trace	Trace	77.1	71.4	71.3	80.0	76.2	65.7
0.01	0.25	79.0	74.3	72.5	82.7	79.4	68.4
0.05	1.27	84.8	79.4	77.5	86.6	84.7	74.1
0.10	2.54	87.1	82.3	81.6	89.3	89.4	75.8
0.25	6.35	90.0	85.8	87.8	93.5	92.9	82.8
0.50	12.70	93.9	91.6	91.6	95.9	96.4	90.8
1.00	25.40	97.1	96.1	96.3	98.0	99.3	97.1
2.50	63.50	99.4	100.0	99.5	99.5	100.0	99.8
5.00	127.00	100.0	100.0	99.8	99.8	100.0	100.0
Amount		July	Aug.	Sept	Oct	Nov	Dec
(in.)	(mm)	%	%	%	%	%	%
0.00	0.00	56.8	52.6	40.0	47.4	62.1	64.2
Trace	Trace	65.8	63.9	53.9	61.6	74.2	78.1
0.01	0.25	68.4	66.2	57.5	63.9	77.2	81.0
0.05	1.27	73.2	69.4	62.7	72.0	83.9	86.8
0.10	2.54	75.8	74.9	67.9	76.8	86.9	89.4
0.25	6.35	83.5	80.7	75.8	85.5	90.8	93.3
0.50	12.70	88.3	88.4	83.7	91.3	92.6	96.5
1.00	25.40	93.8	93.6	92.2	95.5	96.2	99.1
2.50	63.50	99.6	99.7	97.4	99.4	99.2	100.0
5.00	127.00	99.6	100.0	99.8	99.7	99.5	100.0

The 100% values in the table indicate no chance of exceeding certain amounts of precipitation during most of the months, however, it should be realized that the length of available data records is not long and that there is always a chance of any meteorological extreme of record being exceeded.

TABLE 7.9 PROBABILITY THAT PRECIPITATION WILL NOT EXCEED A SPECIFIC AMOUNT IN ANY ONE DAY, EDWARDS AFB, CA.

Amount (in.)	Amount (mm)	Jan %	Feb %	March %	Apr %	May %	June %
0.00	0.00	81.7	81.8	82.6	86.7	95.1	98.8
Trace	Trace	88.0	88.9	89.6	93.8	98.6	99.5
0.01	0.25	88.9	89.5	91.3	94.8	99.0	99.5
0.05	1.27	91.7	92.1	93.8	96.4	99.1	99.5
0.10	2.54	93.5	93.5	95.5	97.6	99.4	99.5
0.25	6.35	96.9	95.6	98.0	99.0	100.0	99.9
0.50	12.70	98.8	98.3	99.1	99.6	100.0	100.0
1.00	25.40	99.8	99.6	99.8	100.0	100.0	100.0
2.50	63.50	100.0	100.0	99.9	100.0	100.0	100.0
5.00	127.00	100.0	100.0	100.0	100.0	100.0	100.0
Amount (in.)	**Amount (mm)**	**July %**	**Aug %**	**Sept %**	**Oct %**	**Nov %**	**Dec %**
0.00	0.00	94.7	95.2	94.6	93.0	89.8	85.2
Trace	Trace	99.0	98.1	97.8	95.8	94.2	90.8
0.01	0.25	99.3	98.1	98.2	96.1	94.4	91.4
0.05	1.27	99.7	98.9	98.9	97.2	96.4	93.7
0.10	2.54	99.7	99.3	98.9	98.2	97.0	94.9
0.25	6.35	100.0	99.6	99.2	99.2	98.4	96.7
0.50	12.70	100.0	99.9	99.8	99.6	99.3	99.0
1.00	25.40	100.0	100.0	99.9	99.7	100.0	99.9
2.50	63.50	100.0	100.0	100.0	100.0	100.0	100.0
5.00	127.00	100.0	100.0	100.0	100.0	100.0	100.0

The 100% values in the table indicate no chance of exceeding certain amounts of precipitation during most of the months, however, it should be realized that the length of available data records is not long and that there is always a chance of any meteorological extreme of record being exceeded.

TABLE 7.10 PROBABILITY THAT PRECIPITATION WILL NOT EXCEED A SPECIFIC AMOUNT IN ANY ONE DAY, VANDENBERG AFB, CA.

Amount		Jan	Feb	March	Apr	May	June
(in.)	(mm)	%	%	%	%	%	%
0.00	0.00	69.4	70.4	61.7	70.4	71.8	70.0
Trace	Trace	79.1	75.9	72.2	80.4	94.0	94.8
0.01	0.25	81.1	76.9	74.6	82.5	96.8	97.7
0.05	1.27	83.5	81.4	83.9	87.9	98.0	100.0
0.10	2.54	88.3	84.4	85.9	90.8	98.8	100.0
0.25	6.35	91.5	90.4	91.5	95.4	99.6	100.0
0.50	12.70	95.1	94.4	96.3	97.5	100.0	100.0
1.00	25.40	98.3	96.9	98.7	99.2	100.0	100.0
2.50	63.50	99.9	99.9	99.5	100.0	100.0	100.0
5.00	127.00	100.0	100.0	99.9	100.0	100.0	100.0
Amount		**July**	**Aug**	**Sept**	**Oct**	**Nov**	**Dec**
(in.)	(mm)	%	%	%	%	%	%
0.00	0.00	62.4	63.4	77.9	79.4	73.3	73.8
Trace	Trace	98.2	94.9	95.4	95.1	82.6	80.6
0.01	0.25	98.9	98.1	95.8	95.5	83.3	83.1
0.05	1.27	100.0	98.8	97.5	95.9	85.9	87.4
0.10	2.54	100.0	99.5	97.9	96.7	87.4	89.2
0.25	6.35	100.0	99.9	98.7	97.5	90.0	93.5
0.50	12.70	100.0	100.0	99.9	98.7	94.4	97.1
1.00	25.40	100.0	100.0	100.0	99.5	98.8	99.6
2.50	63.50	100.0	100.0	100.0	99.9	99.9	100.0
5.00	127.00	100.0	100.0	100.0	100.0	100.0	100.0

The 100% values in the table indicate no chance of exceeding certain amounts of precipitation during most of the months, however, it should be realized that the length of available data records is not long and that there is always a chance of any meteorological extreme of record being exceeded.

TABLE 7.11 PROBABILITY THAT PRECIPITATION WILL NOT EXCEED A SPECIFIC AMOUNT IN ANY ONE DAY, NEW ORLEANS, LA.

Amount		Jan	Feb	March	Apr	May	June
(in.)	(mm)	%	%	%	%	%	%
0.00	0.00	77.1	70.2	73.6	79.7	75.9	72.2
0.01	0.25	77.7	71.1	74.1	79.9	76.4	72.6
0.05	1.27	80.9	74.5	78.1	81.9	78.0	77.7
0.10	2.54	85.7	76.4	81.0	83.6	82.9	82.3
0.20	5.08	89.1	80.4	82.8	87.0	86.5	85.3
0.50	12.70	94.0	88.8	88.6	91.2	92.2	90.3
1.00	25.40	97.4	93.8	92.9	95.3	95.6	93.8
2.00	50.8	98.9	97.8	97.9	97.8	99.0	98.8
5.00	127.00	99.7	99.7	99.7	100.0	100.0	100.0
10.00	254.00	100.0	100.0	100.0	100.0	100.0	100.0
Amount		July	Aug	Sept	Oct	Nov	Dec
(in.)	(mm)	%	%	%	%	%	%
0.00	0.00	54.5	70.1	69.2	84.4	83.4	77.6
0.01	0.25	55.8	71.3	71.1	85.6	84.7	78.2
0.05	1.27	61.4	74.4	76.3	88.2	85.7	80.7
0.10	2.54	67.4	79.3	79.2	90.5	87.4	83.2
0.20	5.08	73.3	83.5	84.4	93.4	89.4	85.2
0.50	12.70	81.5	92.4	90.3	96.0	94.0	91.9
1.00	25.40	91.5	95.7	94.5	98.0	97.3	95.2
2.00	50.80	96.7	98.2	98.0	99.7	98.3	99.4
5.00	127.00	100.0	100.0	99.0	100.0	99.7	99.7
10.00	254.00	100.0	100.0	100.0	100.0	100.0	100.0

The 100% values in the table indicate no chance of exceeding certain amounts of precipitation during most of the months, however, it should be realized that the length of available data records is not long and that there is always a chance of any meteorological extreme of record being exceeded.

TABLE 7.12 PROBABILITY THAT PRECIPITATION WILL NOT EXCEED A SPECIFIC AMOUNT IN ANY ONE DAY, WALLOPS FLIGHT CENTER, VA. (BASED ON LANGLEY AFB DATA)

Amount		Jan	Feb	March	Apr	May	June
(in.)	(mm)	%	%	%	%	%	%
0.00	0.00	54.2	51.4	50.0	51.7	54.2	54.0
Trace	Trace	68.8	66.8	65.5	70.1	69.3	70.0
0.01	0.25	71.2	69.0	68.7	72.4	71.4	71.2
0.05	1.27	75.9	74.3	74.2	78.8	76.1	76.0
0.10	2.54	80.5	78.0	78.9	82.4	79.4	79.5
0.25	6.35	87.7	84.3	86.3	89.2	86.6	87.2
0.50	12.70	93.3	90.2	92.5	94.5	92.8	92.9
1.00	25.40	98.0	97.7	97.7	97.7	97.5	97.4
2.50	63.50	99.0	100.0	99.8	100.0	99.5	99.5
5.00	127.00	100.0	100.0	100.0	100.0	100.0	99.8
10.00	254.00	100.0	100.0	100.0	100.0	100.0	99.9
Amount		**July**	**Aug**	**Sept**	**Oct**	**Nov**	**Dec**
(in.)	(mm)	%	%	%	%	%	%
0.00	0.00	52.6	55.2	62.8	64.0	58.1	59.4
Trace	Trace	68.0	69.0	75.4	76.5	71.0	72.6
0.01	0.25	70.1	72.5	77.8	78.0	73.2	74.5
0.05	1.27	74.2	77.7	81.5	81.8	78.7	79.1
0.10	2.54	78.2	79.8	84.7	85.6	82.8	83.2
0.25	6.35	84.0	85.3	88.0	90.2	88.3	88.2
0.50	12.70	90.6	90.5	91.6	93.4	93.2	93.1
1.00	25.40	94.9	94.8	96.3	96.9	97.6	98.6
2.50	63.50	99.2	98.8	99.2	99.6	99.8	99.9
5.00	127.00	100.0	99.9	99.8	99.8	100.0	100.0

The 100% values in the table indicate no chance of exceeding certain amounts of precipitation during most of the months, however, it should be realized that the length of available data records is not long and that there is always a chance of any meteorological extreme of record being exceeded.

TABLE 7.13 HIGHEST RAINFALL RATE VERSUS DURATION FOR VARIOUS PROBABILITIES, GIVEN A DAY WITH RAIN FOR THE HIGHEST RAIN MONTH, KENNEDY SPACE CENTER, FL

Duration	PERCENTILE											
	50				95				99			
	(in.)	(mm)	in. hr^{-1}	mm hr^{-1}	(in.)	(mm)	in. hr^{-1}	mm hr^{-1}	(in.)	(mm)	in. hr^{-1}	mm hr^{-1}
5 min	0.22	5.6	2.6	66.0	0.72	18.0	8.7	221.0	1.00	25.0	12.0	305.0
15 min	0.23	5.8	0.93	24.0	0.88	22.0	3.5	89.0	1.30	33.0	5.2	132.0
1 hr	0.25	6.4	0.25	6.4	1.17	30.0	1.17	30.0	1.93	49.0	1.93	49.0
6 hr	0.28	7.1	0.05	1.3	1.55	39.0	0.26	6.6	3.18	81.0	0.53	13.0
24 hr	0.43	10.9	0.02	0.5	2.62	67.0	0.11	2.8	5.00	127.0	0.21	5.3

TABLE 7.14 DISTRIBUTION OF RAINFALL RATES WITH HEIGHT FOR ALL LOCATIONS [7.5]

Height (Geometric) Above Surface (km)	% Surface Rate
SFC	100
1	90
2	75
3	57
4	34
5	15
6	7
7	2
8	1
9	0.1
10 and over	< 0.1

Precipitation above the ground is generally colder than at the ground and frequently occurs as supercooled drops which may cause icing on objects moving through the drops. Such icing can be expected to occur when the air temperature is about -2.2°C (28°F). The major factors that influence the rate of ice formation are (1) the amount of liquid water, (2) the droplet size, (3) airspeed, and (4) the size and shape of the airfoil (Ref. 7.6).

7.3.5 Types of Ice Formation

The type of ice which will form on the outside exposed surfaces of cyrogenic tanks is related to the temperature of the tank surface, the precipitation rate, drop size, and wind velocity (or tank velocity). In general, the larger the drop size and the higher the temperature, precipitation rate, and wind speed, the denser the ice will form until a condition is reached where surface temperatures are too high for ice formation. If the precipitation is at too high a temperature at relatively high precipitation rates and wind speed, it may warm the tank sufficiently to melt ice which formed previously.

Table 7.15 summarizes ice types for various tank wall temperatures with moderate precipitation (over 10 mm hr^{-1}).

TABLE 7.15 ICE TYPES AS A FUNCTION OF TANK WALL TEMPERATURES [7.6]

Temperature of Tank Wall			Density Range		
°F	°C	Type of Ice	lb ft^{-3}	g cm^{-3}	Remarks
23 to 32	-5 to 0	Clear ice	60	0.69	hard dense ice
15 to 23	-9 to -5	milky ice or clear ice with air bubbles	43-53	0.69-0.85	
below 15	below -9	Rime ice	18-25	0.29-0.40	crumbly

7.3.6 Hydrometeor Characteristics with Altitude

Raindrops falling on the surface may originate at a higher altitude as some other form of hydrometeor, such as ice or snow. The liquid water content of these hydrometeors per unit volume would have a distribution similar to that given in Table 7.10 for rainfall. A summary of the hydrometeor characteristics from Reference 7.7 is given in Table 7.16.

7.4 Snow

The accumulation of snow on a surface produces stress. For a flat horizontal surface, the stress is proportional to the weight of the snow directly above the surface. For long narrow objects, such as pipes or wires lying horizontally above a flat surface (which can accumulate the snow), the stress can be figured as approximately equal to the weight of the wedge of snow with the sharp edge along the object and extending above the object in both directions at about 45 deg to the vertical. (In such cases, the snow load would be computed for the weight of the snow wedge above the object and not the total snow depth on the ground). The weight of new-fallen snow on a surface varies between 0.5 kg m^{-2} per cm of depth (0.25 lb $ft^{-2}in.^{-1}$) and 2.0 kg m^{-2} per cm of depth (1.04 lb $ft^{-2}in.^{-1}$), depending on the atmospheric conditions at the time of the snowfall.

TABLE 7.16 SUMMARY OF HYDROMETEOR CHARACTERISTICS [7.7]

Type of Hydrometeor	Altitude (km)	Drop Diameter (μm)		Concentration per Unit Volume (cm^3)		Liquid Water Content Per Unit Volume ($g\ m^{-3}$)		Ambient Temperature (°C)
	Range	Range	Rep.	Range	Rep.	Range	Rep.	Range ≈
Layer Clouds	sfc-1.5	<1-40	11	<10-10 000	500	<0.1-1	0.2	+30 to -15
Layer Clouds	2.5-7.5	<1-50	12	<20-1000	100	<0.1-1	0.2	+20 to -25
Layer Clouds (ice crystals)	7.5-15.0	<10-10 000	100	<0.1-10	0.2	<0.01-0.1	0.02	-10 to -55
Convective Clouds								
Fair Weather Cumulus	0.5-8.0	<1-75	12	<10-10 000	300	<0.1-1	0.5	+20 to -30
Cumulus Congestus	0.5-13.0	<1-200	25	<10-10 000	150	<1-10	4.0	+20 to -55
Continuous Type Rain	sfc-6.0	<500-3000	1000	<50-3000*	500*	<0.05-0.7	0.1	+30 to -15
Shower Type Rain	sfc-13.0	<500-7000	2000	<10-3000*	500*	<0.1-30	1.0	+30 to -55
Coalescence (Warm) Rain	sfc-5.0	<100-1000	500	<500-50 000*	3000*	<0.05-0.1	0.1	+30 to 0
Hail	sfc-13.0	<0.01-13cm	0.8cm	<0.5-1000*	50*	<0.1-0.9**	0.8**	+15 to -55
Ice and Snow Crystals	sfc-13.0	<100-20 000	5000	<1-1000*	100*	<0.001-0.7***	0.07***	+5 to -55

1. Rep.: Representative value or value most frequently encountered
* Per m^3
** Density of particles ($g\ cm^{-3}$)
*** Mass of crystals (mg)

7.4.1 Snow Loads at Surface

Maximum snow loads for the following areas are:

a. Huntsville, Wallops Flight Center, and Edwards Air Force Base. For horizontal surfaces a snow load of 25 kg m^{-2} (5.1 lb ft^{-2}) per 24-hour period (equivalent to a 10-in. snowfall) to a maximum of 50 kg m^{-2} (10.2 lb ft^{-2}) in a 72-hr period, provided none of the snow is removed from the surface during that time, should be considered for design purposes.

b. Vandenberg Air Force Base, White Sands Missile Range, and Sacramento areas. For horizontal surfaces, a maximum snow load of 10 kg m^{-2} (2.0 lb ft^{-2}) per one 24-hr period should be considered for design purposes.

c. Kennedy Space Center and New Orleans area snow loads need not be considered.

7.4.2 Snow Particle Size

Snow particles may penetrate openings (often openings of minute size) in equipment and cause a malfunction of mechanical or electrical components, either before or after melting. Particle size, associated wind speed, and air temperature to be considered are as follows:

a. Huntsville, Wallops Flight Center, and Edwards Air Force Base. Snow particles 0.1-mm (0.0039-in.) to 5-mm (0.20-in.) diameter; wind speed 10 m sec^{-1} (19 knots); air temperature -17.8°C (0°F).

b. Vandenberg Air Force Base, White Sands Missile Range, and Sacramento areas. Snow particles 0.5-mm (0.020-in.) to 5-mm (0.20-in.) diameter; wind speed 10 m sec^{-1} (19 knots); air temperature -5.0°C (23°F).

7.5 Hail[1]

Hail is precipitation in the form of balls or irregular lumps of ice and is always produced by convective clouds. By definition, hail has a diameter of 5 mm (0.2 inch) or more. Hail falls are small-scale areal phenomena, with a relatively infrequent occurrence rate at any given geographical point. The resulting time and space variability of hail is its prime characteristic.

There are two areas of confusion regarding hail: (1) definition of it and (2) assessment of damage due to hail. First is the question of whether snow or ice pellets (often called "small hail") are hailstones. Sleet has also been confused with small hail, but convective cloud origin and size of stone are two factors which separate hail from any other form of frozen hydrometeors. The second area of confusion associated with hail concerns delineating crop loss due to hail. This type of loss often includes damage by wind, either that with the hail or that before or after the hail. The wind-induced damage can easily be mistaken as damage due to hail.

While North American hail data and information are generally sparse, there is much more information available than for any other location. In North America, very extensive hail data information are available for Alberta, Canada, and Illinois and Colorado in the United States. Hail phenomena studies have generally centered on hailstones, point hailfalls, hailstreaks, hailstorms, hailswaths, and hail days over areas of various sizes.

The principal hail area on the North American continent is located on the lee side of the Rocky Mountains where frequent and intense hail causes great damage over the Great Plains region. Another high-frequency hail area, related to spring storms, extends from Michigan to Texas. However, less crop damage is observed here because hail activity largely precedes the crop season.

The worldwide hail occurrence pattern is characterized by a greater hail frequency in continental interiors of mid-latitudes, with decreasing frequencies seaward, poleward and equatorward. Most all hail is either orographically or frontally induced, although the Great Lakes affect the frequency close to that region. There are very few local-type hailstorms away from the mountains. The United States hail-days pattern is shown in Figure A1.

Four key hail characteristics (1. average frequency, 2. primary cause of hail, 3. peak hail season, and 4. hail intensity) were analyzed in order to delineate hail regions within the United States. Figure A2 indicates that 14 hail regions exist across the United States, with a marine-effect influence on the west coast and in the lee of the Great Lakes.

---

[1]Paragraph 7.5 contains figures and information from, "The Scales of Hail", by Stanley A. Changnon, Jr., _JAM_, Vol. 16, June 1977 (7.8).

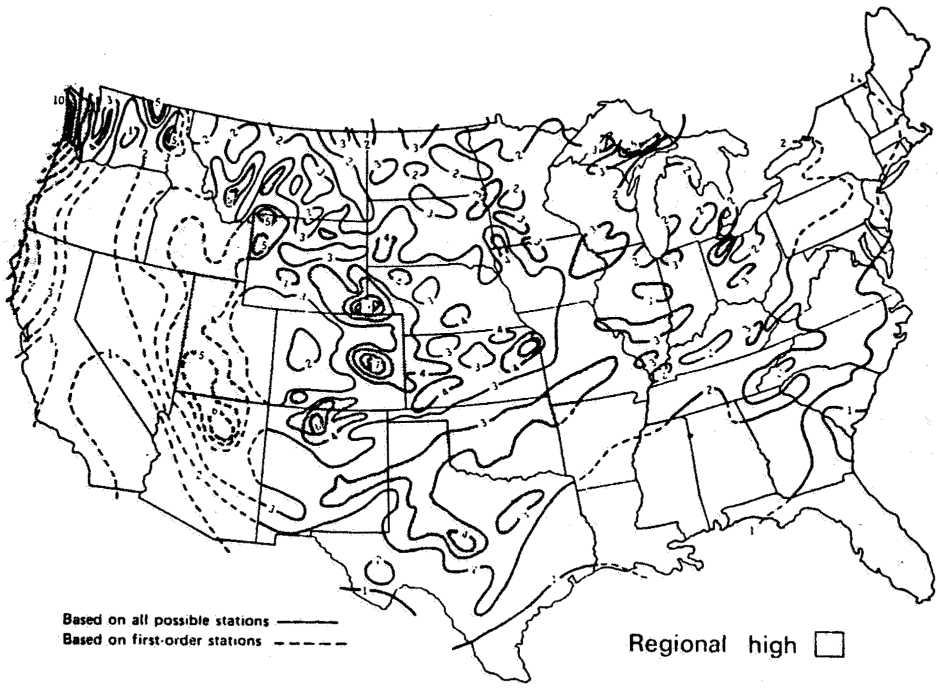

FIGURE A1. AVERAGE NUMBER OF HAIL DAYS BASED ON POINT FREQUENCIES

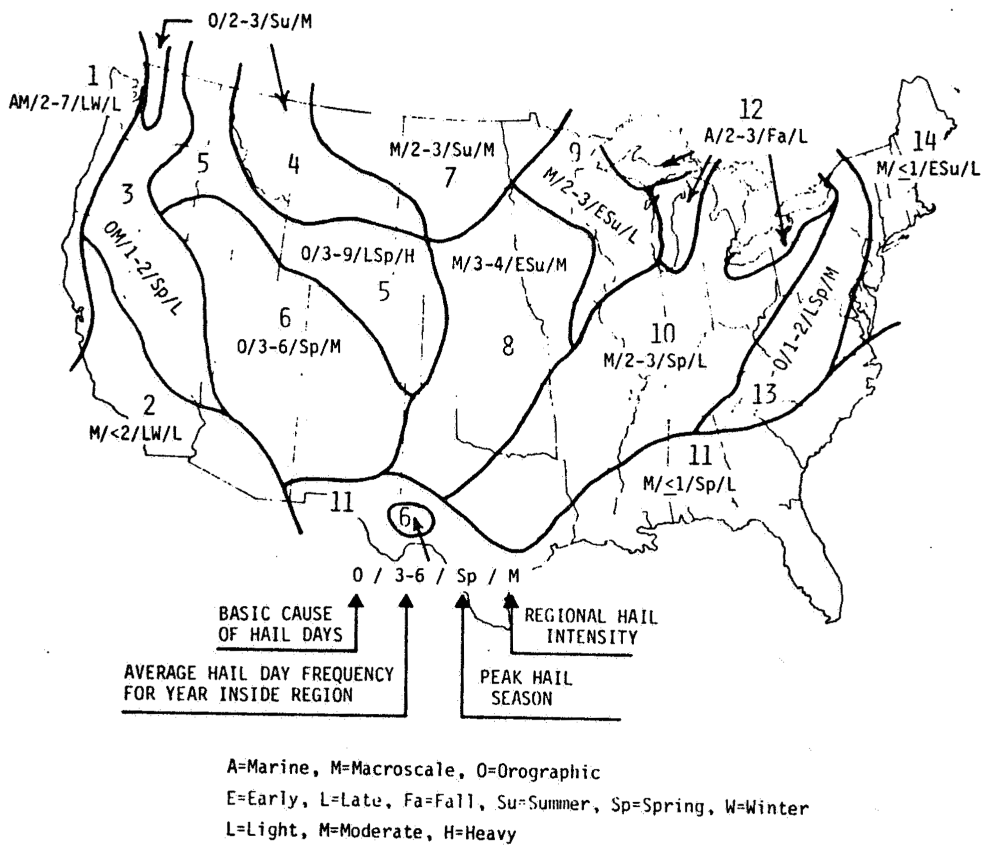

FIGURE A2. HAIL REGIONS OF THE UNITED STATES

Although most all hail is produced by thunderstorms, the special climatologies of these two phenomena differ in some respects. The main difference is that thunderstorms generally exhibit a latitudinal distribution across North America, whereas hail has an inner-continental maxima with frequency decreasing outward in all directions, as mentioned previously.

The "intensity" of hail produces the damage. Intensity is a direct function of the number of stones, their size, and the wind. A hail intensity pattern has been developed specifically for potential property loss. The development of this pattern incorporated insurance data, stone size data, and extreme wind frequency data. The hail intensity pattern is shown in Figure A3, which indicates a north-south oriented maximum located in the Great Plains region. This is the region of the continental United States in which large hailstones, (the major factor in property loss) are most frequent and high winds occur most often.

Since hailstone sizes as well as the number of stones are important to intensity, size distributions help account for regional differences. Hailstone sizes have not been systematically measured throughout the United States, but small-area studies have provided some information. Figure A4 indicates that the greatest frequency of large stones is found in the lee of mountain localities like Colorado. Small hailstones dominate in Illinois, New England, and mountain-top areas of Arizona. An Illinois hailfall averages 24 stones per hailpad (930 cm^2), and only approximately 2 percent of these are more than 1.3 cm in diameter. In northeast Colorado, a hailfall averages 202 stones/ft^2, and more than half (51 percent) of these are larger than 1.3 cm.

The season of high hail activity varies across the country. East of the Great Plains, maximum hail activity occurs in the spring months, starting in March in the far south and in May in the northern states. In the lee-of-the-mountain states, maximum hail activity occurs in the summer months. The Great Lakes area is the only place in North America where maximum hail occurs in fall months. Along the West Coast, certain areas have maximum hail in late winter or spring.

The duration of hailstorms is also variable. The average duration of hail near the mountains is 10 to 15 minutes, while in the Midwest it is 3 to 6 minutes. Hailstreaks, which have a median size of 20.7 km^2 (8 square miles), last an average of 10 minutes. A hailstreak is an area hit by a single volume of hail produced in a storm. A single storm may produce one or many hailstreaks.

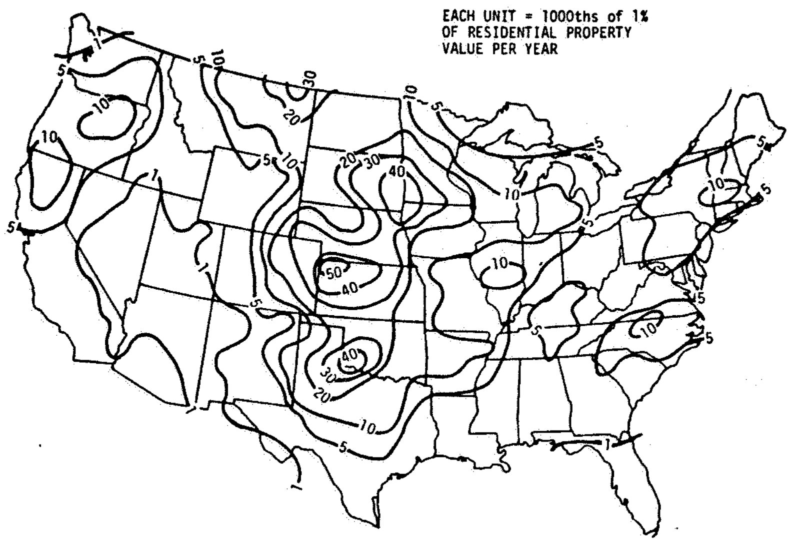

FIGURE A3. INDEX OF POTENTIAL HAIL DAMAGE TO PROPERTY

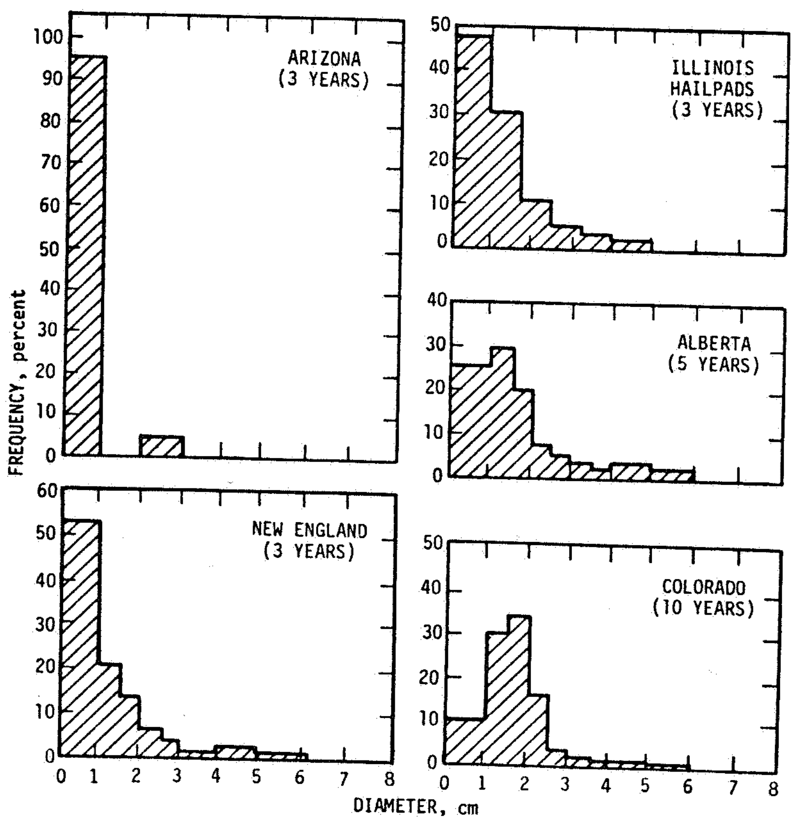

FIGURE A4. FREQUENCY DISTRIBUTIONS OF MAXIMUM HAILSTONE SIZES REPORTED FROM MANY HAILFALLS AT DIFFERENT LOCALES

In large areas, such as Iowa, Illinois, or Colorado, hail occurs on approximately 70 percent of all days with thunderstorms. In the Midwest, 50 percent of all thunderstorms connected with warm fronts and low pressure centers produce hail, but 75 percent of the thunderstorm days associated with cold fronts or stationary fronts are hail days.

Hail may also be accompanied by moderate to heavy rainfall, tornadoes, or wind. Crop-damaging hailstorms in Nebraska, Colorado, and Kansas are generally associated with moderate rains of 0.2 to 1.0 inch, and 25 percent of the rain through the entire crop season falls with damaging hail. Hail days in Illinois typically have rainfall so heavy it averages nearly half (48 percent) of the monthly average. There have been cases where hailstones, falling at the same time or immediately before heavy rains, have blocked drains and downspouts, preventing much of the rain runoff from flat roofs and thereby causing roof collapse from the weight of the rainfall (7.9).

A study of tornadoes in Illinois shows that major large tornadoes--those having tracks longer than 40 km (>25 miles)--always have hailfalls somewhere near their track. During 1951-1960, nearly 96 percent of the 103 tornado days in Illinois were also hail days, and 12 percent of all hail days in Illinois were tornado days as well.

Wind with hail is another critical factor in crop loss, and the Illinois studies show that windblown stones occurred in 60 percent of all hailfalls. Whenever this happens, an average of 66 percent of the stones at any one point are windblown.

7.5.1 Hail at Surface

An estimate has been made of hail characteristics at selected space vehicle development and test locations. Figures A5, A6, A7, and Table A1 give estimated hail characteristics for KSC, VAFB, EAFB, White Sands, MSFC, and NSTL. Since no direct measurements, except for the number of hail days, exist for these locations, all other items were estimated from Illinois hailpad measurements reported by Changnon (7.8). Hail characteristics estimated for use in evaluating hail protection needs and requirements are:

1. Hailstone Size. Figure A5 gives the risk in percent of a point hailfall producing stones larger than indicated sizes. For example, only 33 percent of the hailfalls at KSC will produce stones larger than 2.5 cm, while 50 percent will produce some stones larger than 0.9 cm.

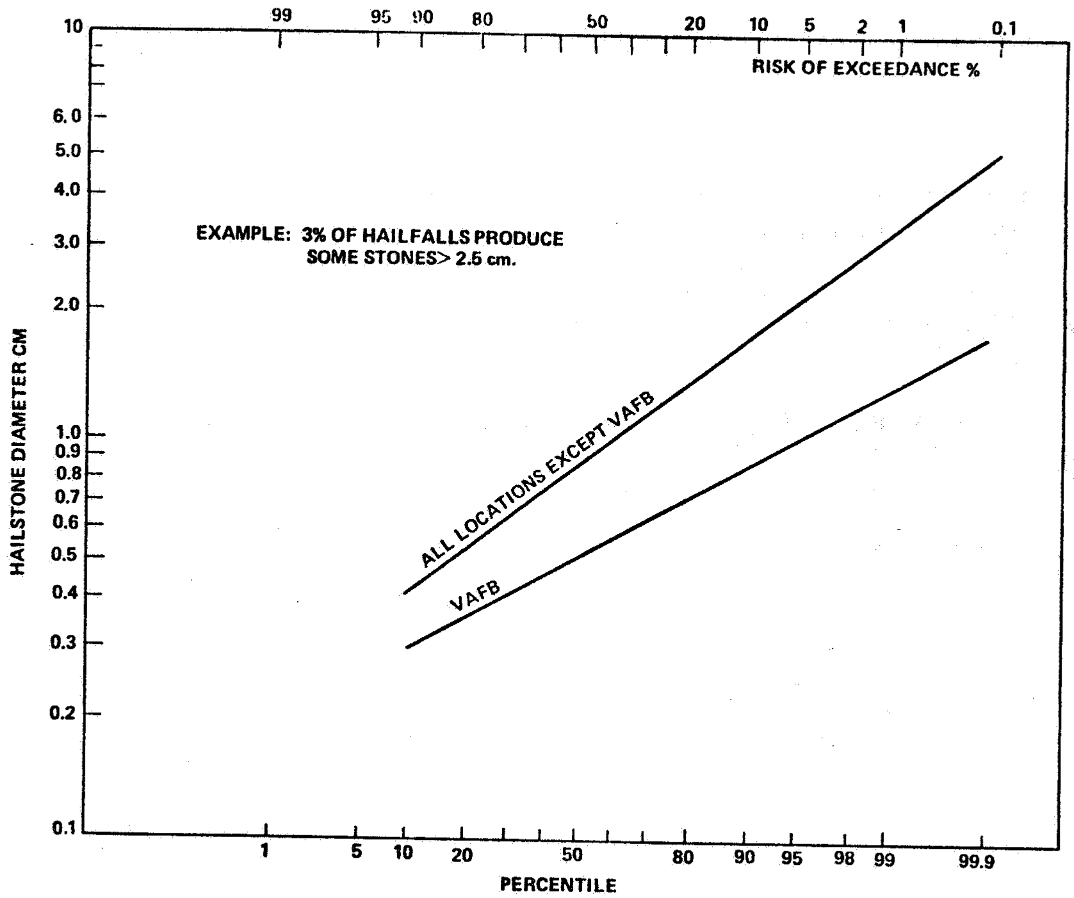

FIGURE A5. MAXIMUM HAILSTONE SIZE PER POINT HAILFALL

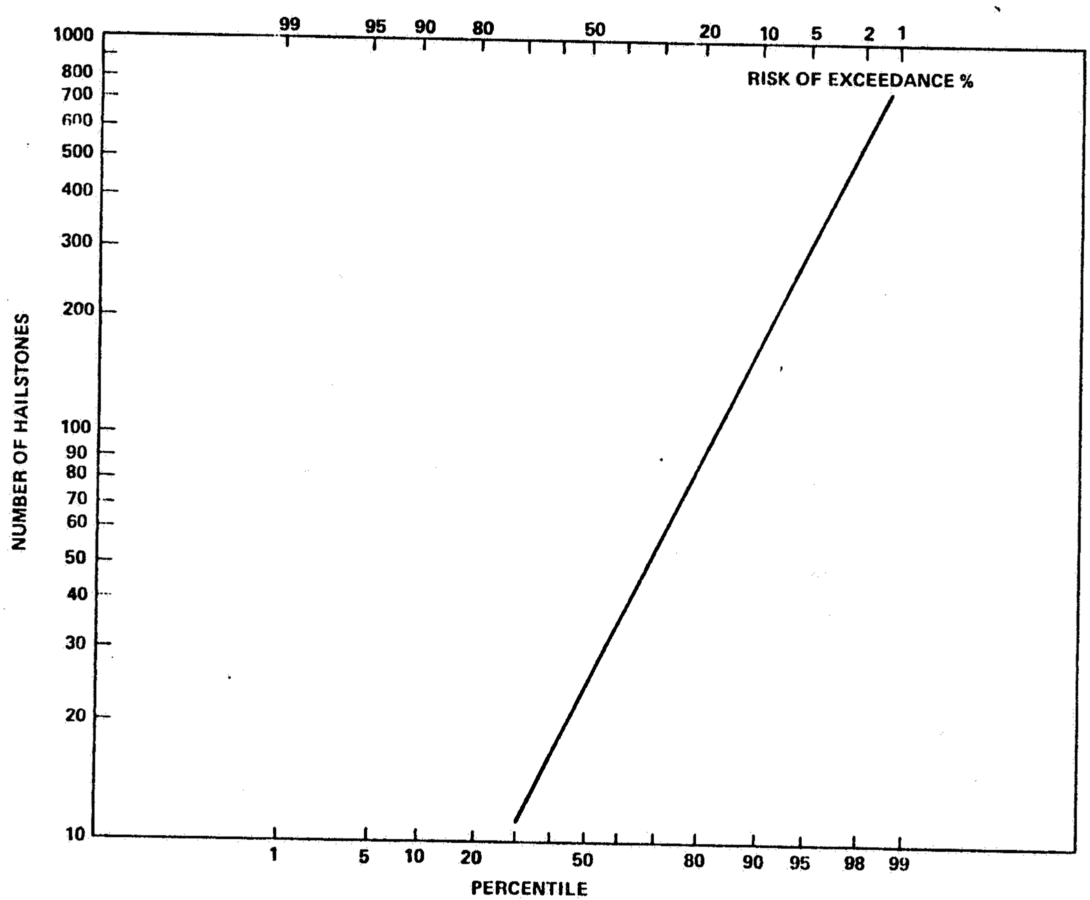

FIGURE A6. PROBABILITY (%) OF NUMBER OF STONES PER HAILFALL ON HAILPAD OF 930 CM^2 (1 FT^2)

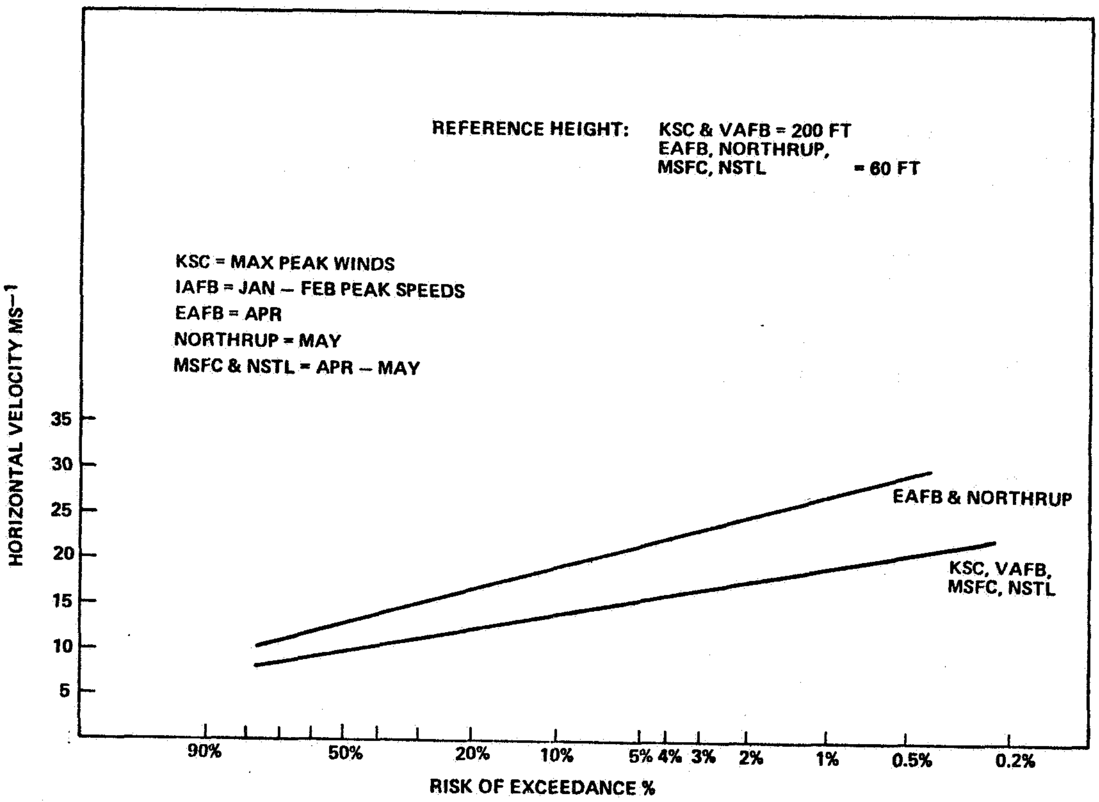

FIGURE A7. HORIZONTAL HAILSTONE VELOCITY

TABLE A1. ESTIMATED HAIL CHARACTERISTICS AT SELECTED SPACE VEHICLE LOCATIONS

ESTIMATED HAIL CHARACTERISTICS	KSC	VAFB	EAFB	NORTHRUP	MSFC	NSTL
EXPOSURE TIME RISK (%) - WORST MONTH	1	8	5	12	17	3
- WORST 6 MONTHS	7	41	25	53	67	18
MEAN NO. OF HAILSTORM DAYS PER YEAR	0.1	1.1	0.6	1.5	2.2	0.4
AVERAGE POINT DURATION OF HAILFALL (MIN.)	5	5	5	5	5	5
AVERAGE NO. OF HAILSTONES PER 930 CM^2 (1 FT^2)	24	24	24	24	24	24
DENSITY OF HAILSTONES (G/CM^3)	0.9	0.9	0.9	0.9	0.9	0.9
SIZE-DIAMETER (CM) & TERMINAL VELOCITY (M/S)						
REPRESENTATIVE SIZE (50% RISK)	0.9	0.5	0.9	0.9	0.9	0.9
TERMINAL VELOCITY	11	8	11	11	11	11
LARGE SIZE (5% RISK)	2.2	1.0	2.2	2.2	2.2	2.2
TERMINAL VELOCITY	17	11.5	17	17	17	17
HORIZONTAL VELOCITY (M/S) - ALL DIRECTIONS[1]						
MEAN SPEED	9	9	13	13	9	9
5% RISK SPEED	15	15	22	22	15	15
MONTHS OF MAX FREQUENCY	MAY	JAN-FEB	FEB-APR	MAY-JUL	APRIL	APR-MAY
PERIOD OF RECORD - YEARS	22	20	28	30	9	28

[1]KSC & VAFB REFERENCE HEIGHT = 61 M (200 FT). ALL OTHERS = 18 M (60 FT)

2. Terminal Velocity. The best estimate of hailstone terminal velocity, as reported by several investigators, is given by the expression:

$$W = K\sqrt{D}$$

where: W = terminal velocity in ms^{-1}

D = hailstone diameter in cm

K = 11.5

3. Number of Hailstones Per Hailfall. Values used for space vehicle locations were taken from Illinois measurements which showed that point hailfalls averaged 24 stones and that only 5 percent of the storms produced more than 300 stones per hailpad of 930 cm^2 (1 ft^2). These numbers were used to prepare Figure A6.

4. Horizontal Velocity of Hailstones. These values (Figure A7) were derived from peak wind speed distributions for each space vehicle location. These wind speeds may be different from other Shuttle design values because only hail season winds were used rather than the windiest period concept.

The reference height at KSC and VAFB is 61 m (200 ft). At all other locations it is 18.3 m (60 ft).

5. Density of Hailstones. A generally accepted value for the density of hail at all locations is 0.89 g cm^{-3} (56 lbs ft^{-3}).

6. Recommended Procedures for Evaluating Protection Requirements.

1. Use 50 percent values for stone size and number of stones.
2. Use 5 percent risk horizontal wind speeds.
3. Calculate risk of experiencing a hailfall during a specified continuous exposure period from:

$$\text{Risk} = 1 - e^{-\lambda t}$$

where λ = mean number of independent hailstorm days per year

t = exposure time in year

7.5.2 Distribution of Hail with Altitude.

Although it is not the current practice to design space vehicles for flight in thunderstorms, data on distribution with altitude are presented as an item of importance. The probability of hail increases with altitude from the surface to 5 km and then decreases rapidly with increasing height. Data on Florida thunderstorms, giving the number of times hail was encountered at various altitudes during aircraft flights (7.10), are given in Table A2[2] for areas specified in Paragraph 7.5.1. It should be noted that the results presented in Table A2 are based on a very limited amount of available data.

TABLE A2. DISTRIBUTION OF HAIL WITH HEIGHT FOR ALL LOCATIONS (7.10)

Height (Geometric) Above Surface (km)	Occurrence of Hail % of Flights Through Thunderstorms
2	0
3	3.5
5	10
6	4
8	3

[2] Table A2 is a repeat of Table 7.17 in TM 78118.

REFERENCES

7.8 Changnon, Stanley A., Jr.: The Scales of Hail. Journal of Applied Meteorology, Vol. 16, No. 6, July 1977, pp. 626-648.

7.9 Changnon, Stanley A., Jr.: Heavy Falls of Hail and Rain Leading to Roof Collapse. Journal of the Structural Division, ASCE, Vol. 104, No. ST1, Technical Notes, January 1978, pp. 198-200.

7.10 Byers, Horace R. and Braham, Roscoe, R., Jr.: The Thunderstorm. United States Government Printing Office, Washington, D. C., 1949.

☆ U.S. GOVERNMENT PRINTING OFFICE 1980—740-066/190 REGION NO. 4

7.6 Laboratory Test Simulation

In the laboratory, simulated rain droplets are usually produced by use of a single orifice, mounted above the equipment being tested. Such a test will not necessarily duplicate the natural occurrence of precipitation and may or may not reflect the true effect of natural precipitation on the equipment since a single orifice produces drops all nearly the same size.

Each test should be evaluated to determine if the following factors which occur in natural precipitation are important in the test.

TABLE 7.17 DISTRIBUTION OF HAIL WITH HEIGHT FOR ALL LOCATIONS [7.9]

Height (Geometric) Above Surface (km)	Occurrence of Hail % of Flights Through Thunderstorms
2	0
3	3.5
5	10
6	4
8	3

7.6.1 Rate of Fall of Raindroplets

Natural raindroplets will have usually fallen a sufficient distance to reach their terminal velocity (maximum rates of fall). Simulation of such rates of fall in the laboratory requires the droplets to fall a suitable distance. Large droplets (4-mm diam. and greater) will require about 12 m (39 ft) to reach terminal velocity.

Values of terminal velocities of water droplets were measured by Gunn and Kinzer (Ref. 7.11). Their results gave the values in Table 7.18. Reference 7.11 should be obtained for more detailed information.

Gunn and Kinzer (Ref. 7.11) found that water droplets greater than 5.8 mm would usually break up before the terminal velocity was reached.

7.6.2 Raindrop Size and Distribution

Normal rainfall has a variety of drop sizes with a distribution as shown in Figure 7.3, which illustrates the wider distribution of droplet sizes in the heavier rain which has the larger droplets. The maximum drop diameter distribution could be adequately simulated by a number of orifices, all at the same water pressure, to produce droplets of about 1-, 2-, 3-, and 4- and 5-mm diameter. For the median drop diameter, the use of a single orifice to produce 1-mm droplets would be suitable.

TABLE 7.18 VALUES OF TERMINAL VELOCITIES OF WATER DROPLETS [7.11]

Drop Diameter (mm)	Terminal Velocity ($m\ sec^{-1}$)
1	4.0
2	6.5
3	8.1
4	8.8
5	9.1
5.8	9.2

7.6.3 Wind Speed

In most cases of natural rain there will be wind blowing near horizontal. This wind will modify the droplet paths from a vertical path to a path at some angle to the vertical, thus causing the rain droplets to strike at an angle. In addition, unless the equipment is streamlined in the direction of the wind, small vortices may develop at the surface of the equipment. These vortices may cause a considerable amount of the precipitation to flow in a variety of directions, including upward against the bottom of the equipment.

Studies of thunderstorms with rainfall rates from 12.7 to 76.2 mm hr^{-1} (0.5 to 3.0 in. hr^{-1}) with relationship to wind speeds occurring at the same time have shown an average mean wind speed of 5 m sec^{-1} for all storms combined. Peak winds were as high as 16 m sec^{-1}. All storms, except one with rates exceeding 25 mm hr^{-1}, had peak winds at least 5 m sec^{-1} greater than the mean wind for the same storm.

7.6.4 Temperatures

The air temperature at the ground usually decreases several degrees at the start of rainfall. The amount of the temperature decrease is greatest in the summer, about 8°C (14°F), when the temperature is high [greater than 32°C (90°F)], with the final temperature approximately 24°C (75°F). In the winter the temperature decrease is usually about 2.8°C (5°F). At the end of the rainfall the summer temperature will increase again to nearly the same values as before the storm, but in the winter there is no general pattern of warming. This decrease in temperature is caused by the water droplets being colder than the surface air temperature.

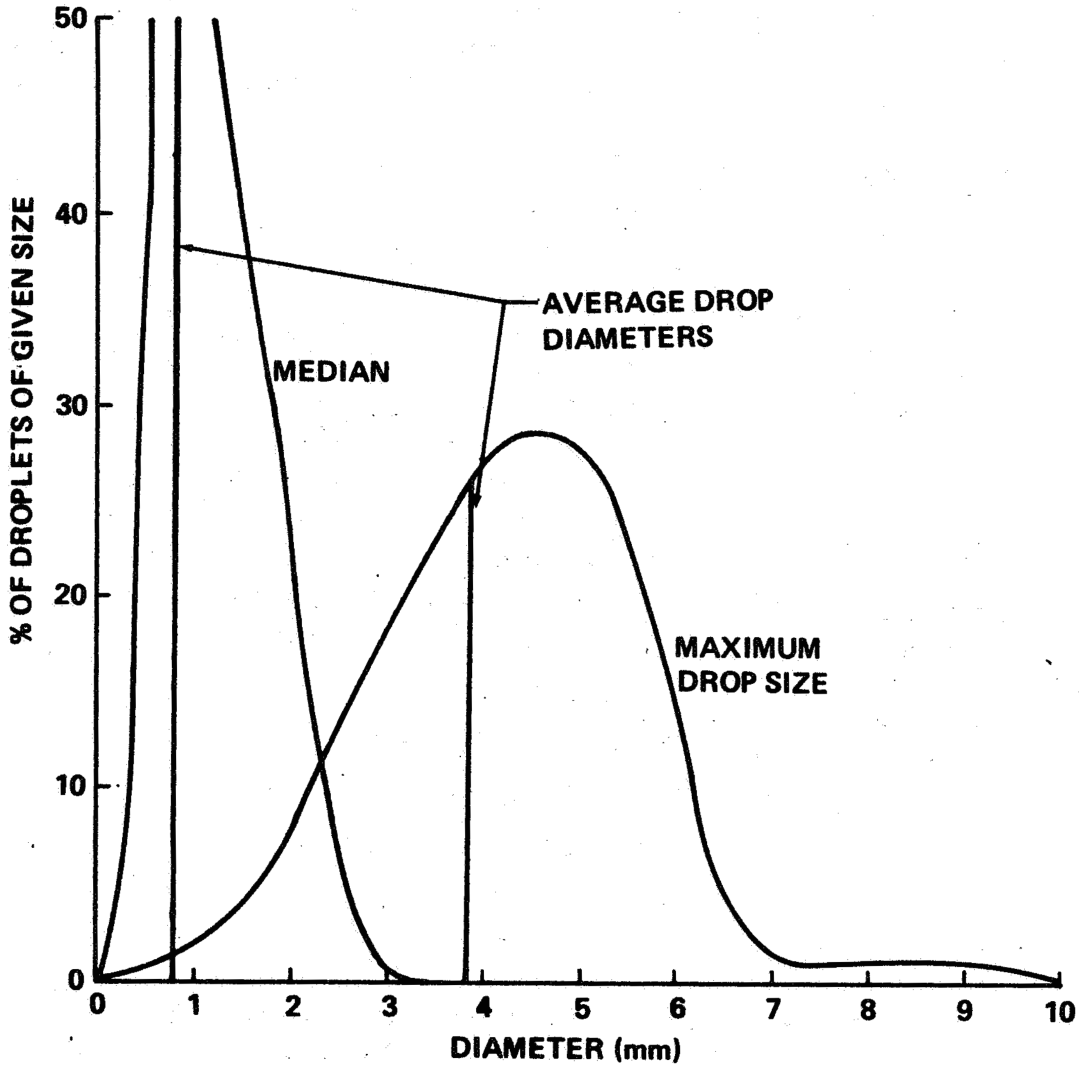

FIGURE 7.3 DISTRIBUTION OF DROP SIZES OF RAIN

7.6.5 Recommended Items to Include in Laboratory Rainfall Tests

The following items need to be considered in rainfall tests in the laboratory:

a. Raindrop size distribution.
Rates less than 25 mm hr^{-1} — drop size of 1 mm.
Rates greater than 25 mm hr^{-1} — drop size from 1 to 5 mm.

b. Rate of fall of drops. Drops should fall at least 12 m to obtain terminal velocity.

c. Wind Speed. A mean wind of 5 m sec^{-1} with gusts of 15 m sec^{-1} of 30-sec duration at least once in each 15-min period.

d. Temperature. The temperature in the chamber should decrease from 32°C (90°F) to 24°C (75°F) at the start of rainfall for representative summer tests and should be maintained at 10°C (50°F) for winter tests. The decrease in air temperature may be obtained by using water at, or slightly below 24°C for the summer tests.

7.6.5.1 Idealized Rain Cycle, Kennedy Space Center, FL

For design studies and laboratory tests, the idealized rain cycle shown in Figure 7.4 and Table 7.6 should be used. The rainfall in the cycle is representative of the 95th percentile Cape Kennedy rainfall on any day with rain during the worst rain month and the associated wind speeds, temperatures, and drop sizes expected with the rain.

7.7 <u>Rain Erosion</u>

7.7.1 Introduction

With the advent of high-speed aircraft a new phenomenon was encountered in the erosion of paint coatings, structural plastic components, and even metallic parts by the impingement of raindrops on surfaces. This was first observed soon after World War II on fighter aircraft capable of speeds over 178 m sec^{-1} (400 mph) (Ref. 7.12). This initiated rain erosion research at the Air Force Materials Laboratory, Wright-Patterson Air Force Base, and at the Royal Aircraft Establishment, Farmborough, England. Tests conducted

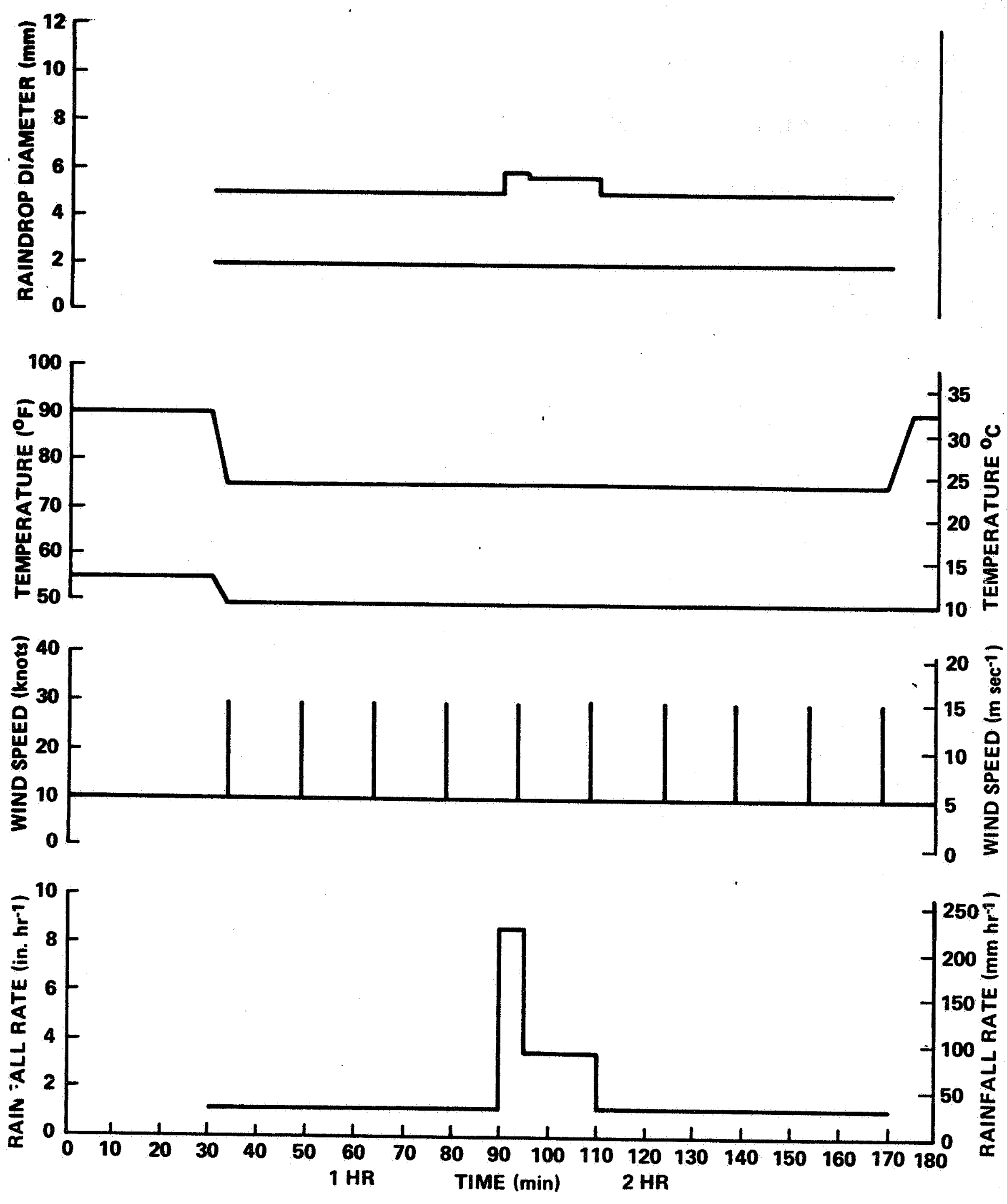

FIGURE 7.4 IDEALIZED RAIN CYCLE, KENNEDY SPACE CENTER, FL; BASED ON HIGHEST RAIN MONTH.

by the British Ministry of Aviation at the Royal Aircraft Establishment (Ref. 7.13) have resulted in a table of rates of erosion for various materials and coatings. These materials and coatings were tested at speeds of 220 m sec^{-1} (428 knots). At the Air Force Materials Laboratory, a number of rotating (whirling) arm apparatuses have been used. The current rotating arm apparatus will permit testing of samples of materials at speeds up to 403 m sec^{-1} (900 mph) (Mach 1.2) with simulated rainfall variable through a wide variety of rates. Normally the tests are made at 224 m sec^{-1} (500 mph) and at 25.4 mm hr^{-1} (1 in. hr^{-1}) or 50.8 mm hr^{-1} (2 in. hr^{-1}) of rainfall (Ref. 7.14). A number of flight tests using F-80 aircraft in rain were made and compared with the rotating arm tests. The ranking of the test materials for rain erosion was similar for the variety of materials tested, but the time to erode materials varied because of differences in the intensities of the various environments. The natural erosion conditions included hail, ice crystal, and liquid water impingement (Ref. 7.15).

7.7.2 Rain Erosion Criteria

Rain erosion may be severe enough to affect the performance of a space vehicle. Sufficient data are not available to present specific extreme values of exposure for various materials used in design. Experience and results of the various tests indicate that materials should be carefully considered. Any materials in which failure in rain erosion would have an effect on the mission should be subjected to tests for rain erosion.

Tests by A. A. Fyall at the Royal Aircraft Establishment (Ref. 7.16) on single rain droplets have shown that the rain erosion rate may increase considerably with lower air pressure (higher altitude) because of the lower cushioning effect of the air on the droplets at impact.

7.8 Fogs

Fogs are classified as either warm or supercooled fog, depending upon whether the ambient temperature is above or below 0°C. In either case, fog consists of a considerable number of minute water drops suspended in the atmosphere near the earth's surface and which reduce visibility to less than 1 km (Glossary of Meteorology — Definitions). The definition, in terms of visibility, distinguishes a fog from a mist. The mist does not restrict visibility as a fog does and is considered to be intermediate between a fog and a haze. In terms of waterdrop sizes, the mist has larger-size drops and usually occurs at lower relative humidity.

The conditions most favorable for the formation of fog are high relative humidity, light surface winds, no overcast so that radiative cooling is most effective, and an abundance of condensation nuclei. Fog occurs more frequently in coastal areas than in inland areas since there is an abundance of water vapor.

Fogs are formed either by cooling the air until the water vapor condenses or by the evaporation of additional water vapor into the air. Common types are (1) radiation fogs, (2) advection fogs, (3) up-slope fogs, (4) frontal fogs, and (5) steam fogs. A brief description of each fog type follows.

Radiation Fog forms on clear nights when the earth loses heat very rapidly to the atmosphere. When humidity is high and cooling takes place rapidly, condensation occurs. If there are no winds, the fog will be very shallow or will be reduced to a dew or frost deposit. If winds are present (about 5 knots), then the fog will thicken and deepen. These fogs do not occur at sea since the sea surface does not cool as the land does.

Advection Fog forms as warm, moist air moves over a colder surface. These fogs occur in coastal areas because the moist air moves inland by breezes over the colder land in the winter. In summer the warm, moist air is carried out to sea, where it forms a fog over the cool water and then the sea breezes advect the fog inland. These fogs are common along the coast of California in the summer.

Up-Slope Fog forms when stable, moist air moves up sloping terrain and is cooled by expansion. This cooling produces the condensation and fog forms. An up-slope wind is necessary for the formation and maintenance of this type of fog. Usually these fogs produce low stratus-type clouds.

Frontal Fog forms in the cold air mass of the frontal system. The precipitation from the warm air mass, overrunning the cold air mass, evaporates as it falls through and saturates the cold air, thus producing the frontal-type fog. These fogs form rapidly, cover large areas, occur frequently in winter, and are associated with slow-moving or stationary fronts.

Steam Fog forms by the movement of cold air over a warmer water surface. Steam fog rises from the surface of lakes, rivers, and oceans.

Although not classified as a common-type fog, there is a fog type called the ice (crystal) fog which is of interest. This fog occurs when the air temperature is approximately -34°C, and as water vapor from the exhaust of aircraft engines, automobiles, etc., is produced, the vapor changes directly to ice crystals instead of condensing directly to liquid drops. The suspension of the ice crystals in the atmosphere produces the ice fog. These fogs can persist from a few minutes to several days and are quite a problem in arctic or polar regions.

Some typical microphysical characteristics of both radiation and advection types of fogs are as follows:

a. Radiation Fog (Inland)

(1) Diameter of drops (av) — 10 μm

(2) Typical drop size — 5 — 35 μm

(3) Liquid water content — 110 mg/m^3

(4) Droplet concentration — 200 cm^{-3}

(5) Vertical depth

(a) Typical — 100 m

(b) Severe — 300 m

(6) Horizontal visibility — 100 m

b. Advection Fog (Coastal)

(1) Diameter of drops (av) — 20 μm

(2) Typical drop size — 7 — 65 μm

(3) Liquid water content — 170 mg/m^3

(4) Droplet concentration — 40 cm^{-3}

(5) Vertical depth

(a) Typical — 200 m

(b) Severe — 600 m

(6) Horizontal visibility — 300 m

7.9 Precipitation or Fog (VAFB and KSC)

Figures 7.5 and 7.6, showing the percentage frequency of precipitation or fog with visibility $\leq$ 0.8 km (0.5 mi.) at Vandenberg AFB and Kennedy Space Center, were developed from historical records of hourly observations. Certain Vandenberg and KSC climatic characteristics that may be of significance to aerospace mission planning and operations are immediately apparent. That is, potentially unfavorable climatic conditions occur mainly during summer night and early morning hours at VAFB but during summer afternoons at KSC. This, of course, is due to the high frequency of fog at VAFB and summer afternoon showers in central Florida.

For climatological studies useful in operational and design data for spacecraft and aircraft operations, the Department of Transportation-Federal Aviation Administration has produced a tabulation of ceilings, visibilities, wind, and weather data by various periods of the day and by various temperature and wind categories for 41 airports (Ref. 7.17).

Some precipitation criteria presented in this section are found in Ref. 7.18 together with additional criteria.

ORIGINAL PAGE IS
OF POOR QUALITY

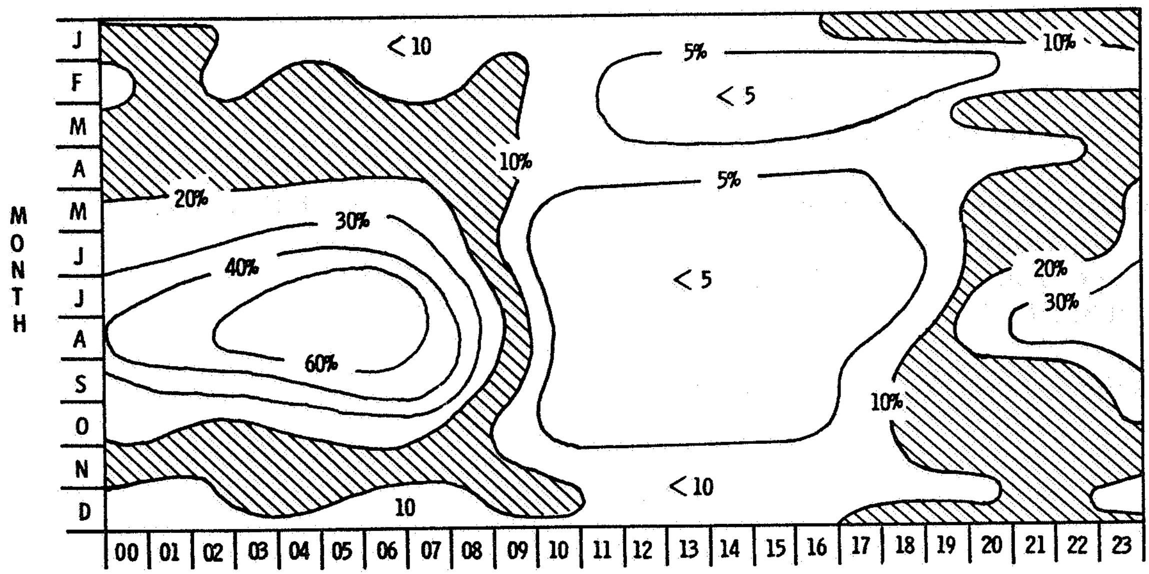

HOUR (LST)

VANDENBERG AFB

FIGURE 7.5. PROBABILITY OF PRECIPITATION OR FOG WITH VISIBILITY ≤ 0.8 KM (0.5 MI.).

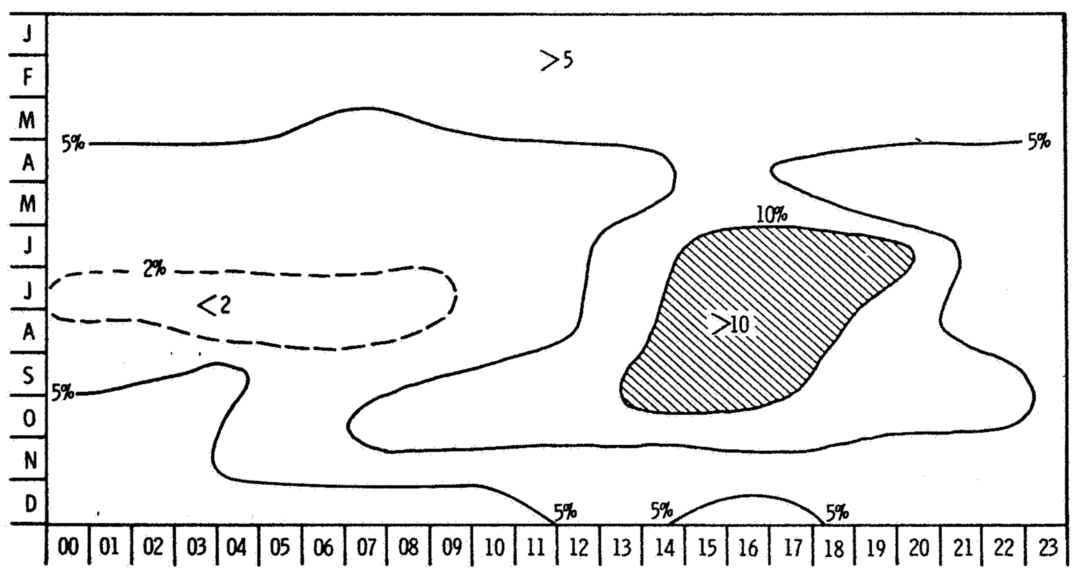

HOUR (LST)

KENNEDY SPACE CENTER (KSC)

FIGURE 7.6. PROBABILITY OF PRECIPITATION OR FOG WITH VISIBILITY ≤ 0.8 KM (0.5 MI.).

REFERENCES

7.1 "Handbook of Aviation Meteorology, Second Edition." Her Majesty's Stationery Office, London, 1971.

7.2 "Rainfall Intensity-Duration-Frequency Curves for Selected Stations in the United States, Alaska, Hawaiian Islands, and Puerto Rico." Technical Paper No. 25, U. S. Department of Commerce, Washington, D.C., December 1955.

7.3 Gumble, E. J.: "Statistics of Extremes." Columbia University Press, 1958.

7.4 Billions, Novella S.: "A Study of Raindrop Size Distributions and Probability of Occurrence." Report No. RR-TR-65-1, U.S. Army Missile Command, Redstone Arsenal, Ala., 1965.

7.5 "Handbook of Geophysics," Revised Edition. The MacMillan Company, New York, 1960.

7.6 "Aviation Weather for Pilots and Flight Operations Personnel." Federal Aviation Agency, Department of Commerce, Weather Bureau, Washington, D. C., 1975.

7.7 Vaughan, William W.: "Distribution of Hydrometeors with Altitude for Missile Design and Performance Studies." ABMA DA-TM-138-59, Army Missile Command, Huntsville, Ala., 1959.

7.8 "1941 Yearbook of Agriculture, Climate and Man." United States Department of Agriculture, United States Government Printing Office, Washington, D.C., 1941.

7.9 "National Summary, Annual 1960, Climatological Data." United States Department of Commerce, Weather Bureau, 1960.

7.10 Byers, Horace R.; and Braham, Roscoe R., Jr.: "The Thunderstorm." United States Government Printing Office, Washington, D.C., 1949.

7.11 Gunn, Ross; and Kinzer, Gilbert D.: "The Terminal Velocity of Fall for Water Droplets in Stagnant Air." Journal of Meteorology, Vol. 6, August 1949.

REFERENCES (Concluded)

7.12 Wahl, Norman E.: "Investigation of the Phenomena of Rain Erosion at Subsonic and Supersonic Speeds." Technical Report AFML-TR-65-330, Air Force Materials Laboratory, Research and Technical Division, Air Force Systems Command, Wright-Patterson Air Force Base, Ohio, October 1965.

7.13 Fyall, A. A.; King, R. B.; and Strain, R. N. C.: "Rain Erosion Aspects of Aircraft and Guided Missiles." Journal of the Royal Aeronautical Society, Vol. 66, July 1962.

7.14 Hurley, Charles J.; and Schmitt, George F. Jr.: "Development and Calibration of a Mach 1.2 Rain Erosion Test Apparatus." AFML-TR-70-240, Air Force Material Laboratory, Air Force Systems Command, Wright-Patterson Air Force Base, Ohio, October 1970.

7.15 Schmitt, George F., Jr.: "Flight Test-Whirling Army Correlation of Rain Erosion Resistance of Materials." AFML-TR-67-420, Air Force Materials Laboratory, Air Force Systems Command, Wright-Patterson Air Force Base, Ohio, September 1968.

7.16 Fyall, A. A.: "Single Impact Studies of Rain Erosion." Technical Air, Vol. 26, October 1970, pp. 4-11.

7.17 Climatological Summaries — Visibilities below 1/2 Mile and Ceilings Below 200 Feet. FAA-RD-69-22, FA-67-WAI-12, National Weather Record Center, Asheville, N.C., June 1969.

7.18 Daniels, Glenn E.: "Precipitation Criteria Guidelines for Use in Aerospace Vehicle Development." NASA TM X-64650, March 22, 1972.

SECTION VIII. WIND

8.1 Introduction

An aerospace vehicle's response to atmospheric disturbances, and especially wind, must be carefully evaluated to insure an acceptable design relative to operational requirements. The choice of criteria depends upon the specific launch location(s), vehicle configuration, and mission. Vehicle design, operation and flight procedures must be separated into particular phases for proper assessment of environmental influences and impacts upon the life history of each vehicle and all associated systems. These phases include such things as, (1) initial purpose and concept of the vehicle, (2) preliminary engineering and design for flight, (3) structural design, (4) vehicle guidance and flight control design (preliminary and final), (5) optimizations of design limits regarding the various environmental factors, and (6) final assessment of environmental capability for launch and flight operations. The proper selection, analyses, and interpretation of wind information is an essential requirement of atmospheric scientists responsible for establishing environmental wind criteria to support all aerospace programs and missions.

Winds are characterized by three-dimensional motions of the air, composed of very large to very small scale spatial and temporal variations. The variability of wind is caused and governed by the rotation of the earth, geographic characteristics, and the available solar energy reaching the earth's atmosphere and surface. This energy drives the large scale global circulation in which massive wave patterns form and significant imbalances are established among major atmospheric pressure regimes. Due to the earth-sun orbital behavior, seasonal wind variations occur and may be seen in synoptic weather changes that affect all locations. Other dominating factors cause the winds to vary so drastically are land-sea influences, geographic locations, terrain type, elevation, available water, vegetation, and a vast assortment of other natural and manmade constituents.

Since the wind environment affects the design of aerospace vehicles and their operations, it is necessary to use good technical judgement and to apply sound engineering principles in preparing wind criteria that are descriptive and concise. Although wind criteria contained in this report were especially prepared for application in aerospace vehicle programs it is important to note that much of this information is directly applicable in other programs such as aeronautical engineering, architecture, atmospheric diffusion, wind and solar energy conversion research, atmospheric sound propagation, and many others.

The synthetic ground and inflight wind criteria concept has its major value and contribution to the design during the initial and intermediate phases of the development cycles of aerospace vehicles. Although a certain overall vehicle performance capability in terms of probability may be stated as a guideline, it is not realistic to expect a design to be developed that will precisely meet this specified performance capability because of the many unknowns in the vehicle characteristics and design criteria. Many advancements have been achieved regarding aerospace vehicle design, operations, and flight but it is still not possible to make exact statements on the overall design risks or operational capabilities of a vehicle. Therefore, it makes good engineering sense to establish a set of idealized or synthetic ground and inflight wind models which characterize such features as wind magnitude versus height, gust factors, turbulence spectra, wind shear phenomena, and vector properties of winds. These models may then be referenced and used in a consistent manner to establish preliminary and intermediate design criteria necessary to ensure completion of the expected missions of vehicles through application of proper wind criteria in the vehicle development. Furthermore, representative wind models aid in isolating those features of the winds (ground and inflight) that are critical to vehicle ground and inflight operations.

It is an accepted practice to use the synthetic wind criteria approach described herein for NASA space vehicle developments during the preliminary and intermediate design phases. These criteria should be carefully formulated to ensure that the appropriate models are used in the vehicle design studies and to be consistent in applying wind criteria from one vehicle to another in structural/control system simulation models. The synthetic wind profile features may readily be employed to isolate critical design problems without resorting to lengthy and elaborate computer routines which are unjustified with respect to other design input parameters which also require special attention. In some cases, for example, the designer may use close approximations of steady-state wind limits for design and operational assessments. Other features of the wind forcing function may be accomplished by using combinations of steady-state winds, wind shears, and gusts. For steady-state wind limits, a multitude of mission and vehicle performance analyses can rapidly be accomplished relative to launch windows, etc., using representative historical records of the steady-state inflight wind data (rawinsonde) and available ground wind data sets. Such records, described in this section, are available for all major launch sites. These statistical records and the synthetic profile concept are also adequate for bias of pitch and yaw programs, range safety studies, preliminary and final abort analyses, water entry of space vehicle components (Space Shuttle solid rocket motor water entry, for example) and related space vehicle operational problems.

When adequately documented and referenced, the synthetic wind criteria concept provides a powerful tool for ensuring consistent design inputs for all users, and it essentially avoids the problem of any oversight errors which may be costly to correct in later vehicle development phases. Furthermore, they enable design engineers at various locations to simultaneously conduct studies and compare their results on a standard basis.

During the latter stages of a vehicle development program, when adequate vehicle response data are available, it is highly desirable, if not mandatory, to simulate the vehicle ascent flight and response to actual wind velocity profiles. However, these wind profiles should contain an adequate frequency content (gusts, turbulence, embedded jets, extreme shears, etc.) to encompass the significant frequencies of response of the vehicle to winds (control mode frequencies, first bending mode frequency, liquid propellant slosh modes, etc.). Anything short of this suggested approach would correspond to the use of only another preliminary design approximation of the natural environment. The current acceptable practice is to use a selection of detailed inflight wind profiles (resolution to at least one cycle per 100 meters) obtained by the FPS-16 Radar/Jimsphere technique for the launch sites of concern. These data and their availability are discussed at pertinent subsections in this document. The number of flight performance simulations and detailed wind profiles selected will depend upon the particular vehicle and the design problems involved and how well the vehicle performance characteristics were identified during the preliminary and intermediate design phase. The vehicle simulation to detailed inflight wind profiles should constitute a verification of the design. It should provide the necessary information to ensure a design optimization with added routines to isolate any critical areas requiring further analysis to refine vehicle control and structural responses to wind. The profiles used should constitute a selection of representative data from the available detailed wind profile records. The selection must portray adequate statistical confidence of wind velocity variability required for vehicle design and development and especially to meet mission objectives. Such goals can only be reached through thorough collaboration among vehicle design groups and the cognizant organization concerned with preparing and interpreting environmental wind criteria.

Special attention is placed on techniques for developing synthetic vector wind profiles for aerospace vehicle applications — this information is presented within this section and illustrates how several statistical wind models can be derived. More specifically, synthetic vector wind and vector wind shear criteria models can now be generated for use in vehicle design and flight studies using analytical techniques where statistical probabilities and distributions of vector winds are more ideally presented and understood.

For the preflight simulation and flight evaluation of a space vehicle related to the wind environment, it is recommended that established ground wind reference height anenometers and detailed inflight wind profiles measured by the FPS-16 Radar/Jimsphere system be used to obtain reliable data. A rapid reduction scheme to ensure a prompt input into prelaunch flight simulation programs is required. During the prelaunch phase, accurate and near real-time wind data are mandatory, especially if critical, or near critical, launch wind conditions exist. Furthermore, adequate flight simulations cannot be made without timely and accurate launch wind profile data.

The information given in this section constitutes wind models and criteria guidelines applicable to various design problems. The selected risk levels employed are characterized by ground and inflight winds required for the design and depend upon the design philosophy used by management for the development efforts. To maximize vehicle performance flexibility, it is considered best to utilize those wind data associated with the minimum acceptable risk levels. In addition, the critical mission related parameters such as exposure time of a vehicle being affected by natural environment quantities, launch windows, reentry periods, launch turnaround periods, etc., should carefully be considered. Initial design work using unbiased (wind) trajectories on the basis of nondirectional ground or inflight winds may be used unless the vehicle and its mission are well known and the exact launch azimuth and time(s) are established and adhered to throughout the program. In designs that use wind-biased trajectories and directional (vector) wind criteria, rather severe wind constraints can result if the vehicle is used for other missions, different flight azimuths, or in another vehicle configuration. Therefore, caution must be exercised in using wind criteria models to ensure consistency with the physical interpretation of each specific vehicle design problem. Several references are cited throughout this section which discuss special and specific problems related to the development and specification of wind environments for aerospace vehicle programs.

8.2 Definitions

The following terms are used in this section with the meanings specified here.

8.2.1 Ground Winds

Ground Winds are winds which affect space vehicles during ground operations and immediately on launch and for purposes of this document, can be considered to be winds below a height of about 150 meters above the natural grade.

Average wind speed — See steady-state wind speed.

Gust is a sudden increase in the ground wind speed. It is frequently stated with respect to a mean wind speed. A sudden decrease in the wind speed is sometimes also referred to as a gust (negative).

Free-standing winds are the ground winds that are applied to the vehicle when it is standing on the launch pad (with or without fuel) after any service structure, support, or shelter has been removed.

Gust factor is the ratio of peak ground wind speed to the average or mean ground wind speed over a finite time period.

Launch design winds are the peak ground winds for which the vehicle can be launched, normally involving a stated design wind at a reference height plus the associated peak wind profile ($\sim$99.9%) shape.

On-pad winds are the ground winds that are applied when the vehicle is on the launch pad with protective measures in place, i.e., service structures, support, or shelter.

Peak wind speed is the maximum (essentially, instantaneous) wind speed measured during a specified reference period, such as hour, day, or month.

Steady-state or average wind speed is the mean over a period of about 10 minutes or longer, of the wind speed measured at a fixed height. It is usually assumed constant as, for example, in spectral calculations. Thus, the steady-state or average wind should be the mean which filters out, over a sufficient duration, the effects that would very definitely contribute to the random responses of aerospace vehicles and structures. The average wind speed is sometimes referred to as quasi-steady-state winds.

Reference height (ground winds) is the height above the ground surface (natural grade) to which wind speeds are referred for the establishment of climatological conditions, reference for construction of design wind profiles, and statements of an operational wind constraint. Normally during the design and development phase, a reference height near the base of the vehicle (usually given as the 10- or 18.3-m level) is used. After completion of vehicle development, the operational constraints are stated with respect to a reference height near the top of the vehicle.

Causes of high ground winds are summarized as follows:

a. Tornadoes: Upper limit unknown; estimated about 103 m/sec (200 knots).

b. Hurricanes: By definition, a storm of tropical origin with winds greater than 33 m/sec (64 knots), upper limit unknown; estimated about 82 m/sec (160 knots).

c. Tropical Storms: By definition, a storm with winds less than 33 m/sec (64 knots) and greater than 17 m/sec (33 knots).

d. Thunderstorms: Upper limit not defined; typical values about 23 m/sec (45 knots); severe thunderstorm by definition greater than 26 m/sec (50 knots) (Ref. 8.1).

e. Frontal Passages: Without thunderstorms; winds less than 18 m/sec (35 knots), with squalls same as for thunderstorms.

f. Pressure Gradients: Long duration gusty winds; winds less than 31 m/sec (60 knots).

8.2.2 Inflight Winds

Inflight winds are those winds above a height of about 150 meters.

Design verification data tapes are a selection of detail wind profile data compiled from FPS-16 Radar/Jimsphere data records for use in vehicle final design verification analysis. They consist of a representative monthly selection of wind profiles from which the integrated response of a vehicle to the combined effect of speed, direction, shear, and turbulence (gusts) may be derived. It has application to computation of absolute values of launch probability for a given vehicle.

Design wind speed profile envelopes are envelopes of scalar or vector component or resultant wind speeds representing the extreme steady-state inflight wind value for any selected altitude that will not be exceeded by the probability selected for a given reference period.

Detail wind profile is a wind profile measured by the FPS-16 Radar/Jimsphere or equivalent technique and having a resolution to at least one cycle per 100 meters. Application intended for final design verification purposes and launch delay risk calculations.

Steady-state inflight wind, in this document, refers to the mean wind speed as measured with the rawinsonde system and averaged over approximately 1000 meters in the vertical direction. The assigned height of this wind measurement will be the middle of the 1000 meter layer.

Reference height (inflight winds) is that referred to in constructing a synthetic wind profile.

Scale-of-distance is the vertical distance (thickness of layer) between two wind measurements used in computing wind shears.

Serial complete data represent the completion of a sample of rawinsonde data (selected period) by filling in (inserting) missing data by interpolation, by extrapolation, or by use of data from nearby stations. This operation is performed by professional meteorological personnel familiar with the data.

Shear build-up envelope is the curve determined by combining the reference height wind speed from the wind speed profile envelope with the shears (wind speed change) below the selected altitude (reference height). The shear build-up envelope curve usually starts at zero altitude difference (scale-of-distance) and zero wind speed and ends at the design wind speed value at the referenced altitude for inflight wind response studies.

Synthetic wind speed profile is a design wind profile representing the combination of a reference height design wind with associated envelope shears (wind speed change) and gusts for engineering design and mission analysis purposes.

Wind speed change envelopes (wind shear) represent the values of the change in wind speed over various increments of altitude (100 to 5000 m), computed for a given probability level and associated reference height or related wind speed value at the reference height. These values are combined, and an envelope of the wind speed change is found useful in constructing synthetic wind profiles. Usually the 99 percentile probability level is used for design purposes.

8.2.3 General

Calm winds are those winds with a speed less than 0.5 m/sec (1 knot).

Component wind speed is the equivalent wind speed that any selected wind vector would have if resolved to a specific direction, that is, a wind from the northeast (45-deg azimuth) of 60 m/sec would have a component from the east (90-deg azimuth) of 42.4 m/sec. This northeast wind would be equivalent to a 42.4 m/sec head wind on the vehicle, if the vehicle is launched on an east (90-deg) azimuth.

Percentile — The P percentile is that value of a variable at or below which lies the lowest P percent of a set of data. The following relationships exist between probabilities (P) and percentiles in a NORMAL or GAUSSIAN DISTRIBUTION function:

Percentiles	Probability P(%) for normal distribution
Minimum	0.000
Mean - 3σ (standard deviation)	0.135
Mean - 2σ (standard deviation)	2.275
Mean - 1σ (standard deviation)	15.866
Mean ± 0σ (standard deviation)	50.000
Mean + 1σ (standard deviation)	84.134
Mean + 2σ (standard deviation)	97.725
Mean + 3σ (standard deviation)	99.865
Maximum	100.000

Scalar wind speed is the magnitude of the wind vector without regard to direction.

Vector wind includes both magnitude and direction of winds.

Wind direction is the direction from which the wind is blowing, measured clockwise from true North.

Windiest monthly reference period is the month that has the highest tropospheric wind speeds at a given probability level.

Wind shear is equal to the difference between wind speeds measured at two specific positions divided by the distance between the two positions.

8.3 Ground Winds (1-150m)

8.3.1 Introduction

Ground winds for aerospace vehicle applications are defined in this document to be those winds in the lowest 150 meters of the atmosphere. A vehicle positioned vertically on-pad may penetrate this entire region. The winds in this layer of the atmosphere are characterized by very complicated three-dimensional flow patterns with rapid variations in magnitude and direction in space and time. An engineering requirement exists for models which define the structure of wind in this layer because of the complicated and possible critical manner in which a vehicle might respond to certain aspects of the flow in this layer, both while the vehicle is stationary on the launch pad and while in the first few seconds of launch. Some examples of wind effects on space vehicles are von Karman vortex shedding forces resulting in lateral displacements of the vehicle while on pad, and steady-state and time dependent aerodynamic drag forces resulting in base bending moments (steady and time-dependent) in the case of vehicles on pad and vehicle drift and pitch and yaw-plane angular accelerations during vehicle lift-off. Other equally important examples can be cited. The basic treatment of the ground wind problem relative to vertically erect vehicles on-pad and during lift-off has been to statistically define the steady-state and time-dependent aspects of the wind profile along the vertical in such a manner that a particular aspect of the wind environment crucial to space vehicle operations can be specified upon specifying the risk of encountering that particular aspect of the wind environment. It should be noted that in addition to the engineering requirements for on-pad and launch winds for vertically ascending vehicles, a requirement for ground wind models also exists for horizontally flying vehicles for take-off and landing. In a space vehicle context this is especially true for the return flight of the Space Shuttle orbiter vehicle. In this case, there exists in addition to the vertical definition of winds a requirement for models to define the horizontal structure or rather the structure of wind along the landing flight path of the vehicle. This aspect of the natural wind environment will be discussed in Sections 8.4.13 through 8.4.15.

Until recently, several years of average wind speed data measured at the 10-meter level above ground were the only available records with which to develop design and launch ground wind profile criteria. With the evolution of larger and more sophisticated space vehicles, the requirements for more adequate wind profile information have increased. For example, to fulfill the need to provide improved ground wind data, a 150-meter ground wind tower facility was constructed on Merritt Island, Kennedy Space Center, Florida, in close proximity to the Apollo/Saturn launch complex 39. Wind and temperature profile data from this facility have been used in many new studies that have contributed to a significant portion of the information in this chapter on wind profile shaping, gusts, and turbulence spectra. Similar towers are in operation at the various national ranges.

Since ground wind data are applied by space vehicle engineers in various ways and degrees, dependent upon the specific problem, various viewpoints and kinds of analytical techniques were used to obtain the environmental models presented here. Program planning, for instance, requires considerable climatological insight to determine the frequency and persistence distributions for wind speeds and wind directions. However, for design purposes the space vehicle must withstand certain unique predetermined structural loads that are generated from exposure to known peak ground wind conditions. Ground wind profiles and the ground wind turbulence spectra contribute to the development of the design ground wind models. Surface roughness, thermal environment, and various transient local and large-scale meteorological systems influence the ground wind environment for each launch site.

8.3.2 Considerations in Ground Wind Design Criteria

To establish the ground wind design criteria for aerospace vehicles, several important factors must be considered.

a. Where is the vehicle to operate?

b. What is the launch location?

c. What are the proposed vehicle missions?

d. How many hours, days, or months will the vehicle be exposed to ground winds?

e. What are the consequences of operational constraints that may be imposed upon the vehicle because of wind constraints?

f. What are the consequences if the vehicle is destroyed or damaged by ground winds?

g. What are the cost and engineering practicalities for designing a functional vehicle to meet the desired mission requirements?

h. What is the risk that the vehicle will be destroyed or damaged by excessive wind loading?

In view of this list of questions or any similar list that a design group may enumerate, it becomes obvious that in establishing the ground wind environment design criteria for a space vehicle an interdisciplinary approach between the several engineering and scientific disciplines is required.

Furthermore, the process is an iterative one. To begin the iterative process, specific information on ground winds is required.

8.3.3 Introduction to Exposure Period Analysis

Valid, quantitative answers to such questions as the following are of primary concern in the design, mission planning, and operations of space vehicles.

a. How probable is it that the peak surface wind at some specified reference height will exceed (or not exceed) a given magnitude in some specified time period?

b. Given a design wind profile in terms of peak wind speed versus height from 10 to 150 meters, how probable is it that the design wind profile will be exceeded in some specified time period?

Given a statistical sample of peak wind measurements for a specific location, the first question can be answered in as much detail as a statistical analyst finds necessary and sufficient. This first question has been thoroughly analyzed for Kennedy Space Center and partially for Vandenberg AFB, and to a lesser degree for other locations of interest.

The analysis becomes considerably more complex in answering the second question. A wind profile model is required, and, to develop the model, measurements of the wind profiles by properly instrumented ground wind towers are required as well as a program for scheduling the measurements and data reduction. Every instantaneous wind profile is unique; similarity is a matter of degree. Given the peak wind speed at one height, there is a whole family of possible profiles extending from the specified wind at that height. Thus for each specified wind speed at a given height, there is a statistical distribution of wind profiles. Recommended profile shapes for Kennedy Space Center and other locations are given in this report. The analysis needed to answer the second question is not complete, but we can assume that, given a period of time, the design wind profile shape will occur for a specified wind speed at a given height. In the event that a thunderstorm passes over the vehicle, it is logical to assume that the design wind profile shape ($\sim$99.9 shape) will occur and that the chance of the design wind profile being exceeded is the same as the probability that the peak wind during the passage of the thunderstorm will strike the vehicle or point of interest.

8.3.4 Development of Extreme Value Concept

It has been estimated from wind tunnel tests that only a few seconds are required for the wind to produce near steady-state drag loads on a vehicle such as the Space Shuttle in an exposed condition on the launch pad. For this and other reasons (subsection 8.3.5), we have adopted the peak wind speed as our fundamental measurement of wind. Equally important, when the engineering applications of winds can be made in terms of peak wind speeds, it is possible to obtain an appropriate statistical sample that conforms to the fundamental principles of extreme value theory. One hour is a convenient and physically meaningful minimum time interval from which to select the peak wind. The reader is referred to Section 8.3.5.5.1 for details concerning averaging times in the context of structural response. An hourly peak wind speed sample has been established for Kennedy Space Center from wind information on continuous recording charts. Peak wind samples for Vandenberg AFB have been derived from hourly steady-state wind measurements using statistical and physical principles.

8.3.4.1 Envelope of Distributions

In the development of the statistics for peak winds, it was recognized that the probability of hourly, daily, and monthly peak winds exceeding (or not exceeding) specified values varied with time of day and from month to month. In other words, the distributions of like variables were different for the various reference periods. Even so, the Gumbel distribution was an excellent fit to the samples of all hourly, daily, monthly, bimonthly (in two combinations), and trimonthly (in three combinations) periods taken over the complete period of record, justifying the use of these distributions. However, in establishing vehicle wind design criteria for the peak winds versus exposure time, it is desired to present a simple set of wind statistics in such a manner that every reference period and exposure time would not have to be examined to determine the probability that the largest peak wind during the exposure time would exceed some specified magnitude. To accomplish this objective, envelopes of the distributions of the largest peak winds for various time increments from which the extremes were taken for the various reference periods were constructed. For example to obtain the envelope distribution of hourly peak winds for the month of March, the largest peak wind was selected at each percentage point from the twenty-four peak wind distributions (one for each hour). The annual envelope distribution is the envelope of the twelve hourly envelopes (one for each month).

Selected envelopes of distributions are given in subsection 8.3.5. It is recommended that these envelopes of distributions be used for vehicle wind design considerations. This recommendation is made under the assumption that it is not known what time of day or season of year critical vehicle operations are to be conducted; furthermore, it is not desirable to design a vehicle to operate only during selected hours or months. Should all other design alternatives fail to lead to a functionally engineered vehicle with an acceptable risk of not being compromised by wind loads, then distributions for peak winds by time of day for monthly reference periods may be considered for limited missions. For vehicle operations, detailed statistics of peak winds for specific missions are meaningful for management decisions, in planning missions, and in establishing mission rules and alternatives to the operational procedures. To present the wind statistics for these purposes is beyond the scope of this document. Each space mission has many facets that make it difficult to generalize and to present the statistics in brief form. Specific data for these applications are available upon request.

8.3.5 Design Wind Profiles (Vehicles)

Specific information about the wind profile is required to calculate ground wind loads on space vehicles. The earth's surface is a rigid boundary that exerts a frictional force on the lower layers of the atmosphere, causing the wind to vanish at the ground. In addition, the characteristic length and velocity scales of the mean (steady-state) flow in the first 150 meters (boundary layer) of the atmosphere combine to yield extremely high Reynolds numbers with values that range between approximately 10^6 and 10^8, so that for most conditions (wind speeds > 1 m/sec) the flow is fully turbulent. The lower boundary condition, the thermal and dynamic stability properties of the boundary layer, the distributions of the large scale pressure, the Coriolis forces, and the structure of the turbulence combine to yield an infinity of wind profiles.

Data on basic wind speed profiles given in this section are to be used for vehicle design. With respect to design practices, the application of peak winds and the associated turbulence spectra and discrete gusts should be considered. The maximum response obtained for the selected risk levels for each physically realistic combination of conditions should be employed in the design. Care should be exercised so that wind inputs are not taken into account more than once. For example, the discrete gust and spectrum of turbulence are representations of the same thing, namely atmospheric turbulence. Thus, one should not calculate the responses of a vehicle due to the discrete gust and spectrum and then combine the results by addition, root-sum-square or any other procedure since these inputs represent the same thing. Rather the responses should be calculated with each input and then enveloped.

8.3.5.1 Philosophy

An example of a peak wind speed is given in Figure 8.3.1. Peak wind statistics have three advantages over mean wind statistics. First, peak wind statistics do not depend upon an averaging operation as do mean wind statistics. Second, to construct a mean wind sample, a chart reader or weather observer must perform an "eyeball" average of the wind data, causing the averaging process to vary from day to day according to the mood of the observer, and from observer to observer. Hourly peak wind speed readings avoid this subjective averaging process. Third, to monitor winds during the countdown phase of a space vehicle launch, it is easier to monitor the peak wind speed than the mean wind speed.

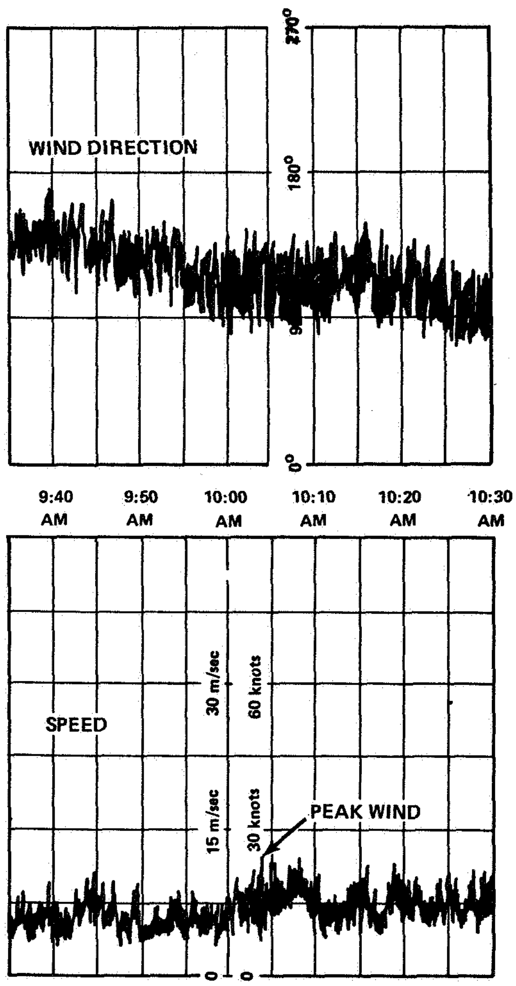

FIGURE 8.3.1 EXAMPLE OF PEAK WIND SPEED RECORDS

O. E. Smith, et al. (Ref. 8.2) have performed extensive statistical analyses with peak wind speed samples measured at the 10-meter level. In the course of the work, he and his collaborators introduced the concept of exposure period probabilities into the design and operation of space vehicles. By determining the distribution functions of peak wind speeds for various periods of exposure (hour, day, month, year, etc.), it is possible to determine the probability of occurrence of a certain peak wind speed magnitude occurring during a prescribed period of exposure of a space vehicle to the natural environment. Thus, if an operation requires, for example, 1 hour to complete, and if the critical wind loads on the space vehicle can be defined in terms of the peak wind speed, then it is the probability of occurrence of the peak wind speed during a 1-hour period that gives a measure of the risk of the occurrence of structural failure. Similarly, if an operation requires 1 day to complete, then it is the probability of occurrence of the peak wind speed during a 1-day period that gives a measure of the risk of structural failure.

All probability statements concerning the capabilities of the space vehicles that are launched at NASA's Kennedy Space Center are prescribed in terms of Smith's peak wind speed exposure statistics. These peak wind statistics are usually transformed to the 18.3-meter (60-foot) reference level for design purposes (or higher levels for operational applications). However, to perform loading and response calculations resulting from steady-state and random turbulence drag loads and von Karman vortex shedding loads, the engineer requires information about the vertical variation of the mean wind and the structure of turbulence in the atmospheric boundary layer. The philosophy is to extrapolate the peak wind statistics up into the atmosphere via a peak wind profile, and the associated steady-state or mean wind profile is obtained by applying a gust factor that is a function of wind speed and height.

8.3.5.2 Peak Wind Profile Shapes

To develope a peak wind profile model, approximately 6000 hourly peak wind speed profiles measured at NASA's ground wind tower facility at Kennedy Space Center have been analyzed. The sample, comprised of profiles of hourly peak wind speeds measured at the 18-, 30-, 60-, 90-, 120-, and 150-meter levels, showed that the variation of the peak wind speed in the vertical, below 150 meters, for engineering purposes, could be described with a power law relationship given by

$$u(z) = u_{18.3}\left(\frac{z}{18.3}\right)^{k} \quad , \qquad (8.1)$$

where $u(z)$ is the peak wind speed at height z in meters above natural grade and $u_{18.3}$ is a known peak wind speed at $z = 18.3$ meters. The peak wind is referenced to the 18.3-meter level because this level has been selected as the standard reference for the Kennedy Space Center launch area. A reference level should always be stated when discussing ground winds to avoid confusion in interpretation of risk statements and structural load calculations.

A statistical analysis of the peak wind speed profile data revealed that, for engineering purposes, k is distributed normally for any particular value of the peak wind speed at the 18.3-meter level. Thus, for a given percentile level of occurrence, k is approximately equal to a constant for $u_{18.3} \leq 2$ m/sec. For $u_{18.3} > 2$ m/sec,

$$k = c\,(u_{18.3})^{-3/4}, \tag{8.2}$$

where $u_{18.3}$ has the units of meter per second. The parameter, c, for engineering purposes, is distributed normally with mean value 0.52 and standard deviation 0.36 and has units of $m^{3/4}\,sec^{-3/4}$. The distribution of k as a function $u_{18.3}$ is depicted in Figure 8.3.2. The $\bar{k} + 3\sigma$ values are used in design studies.

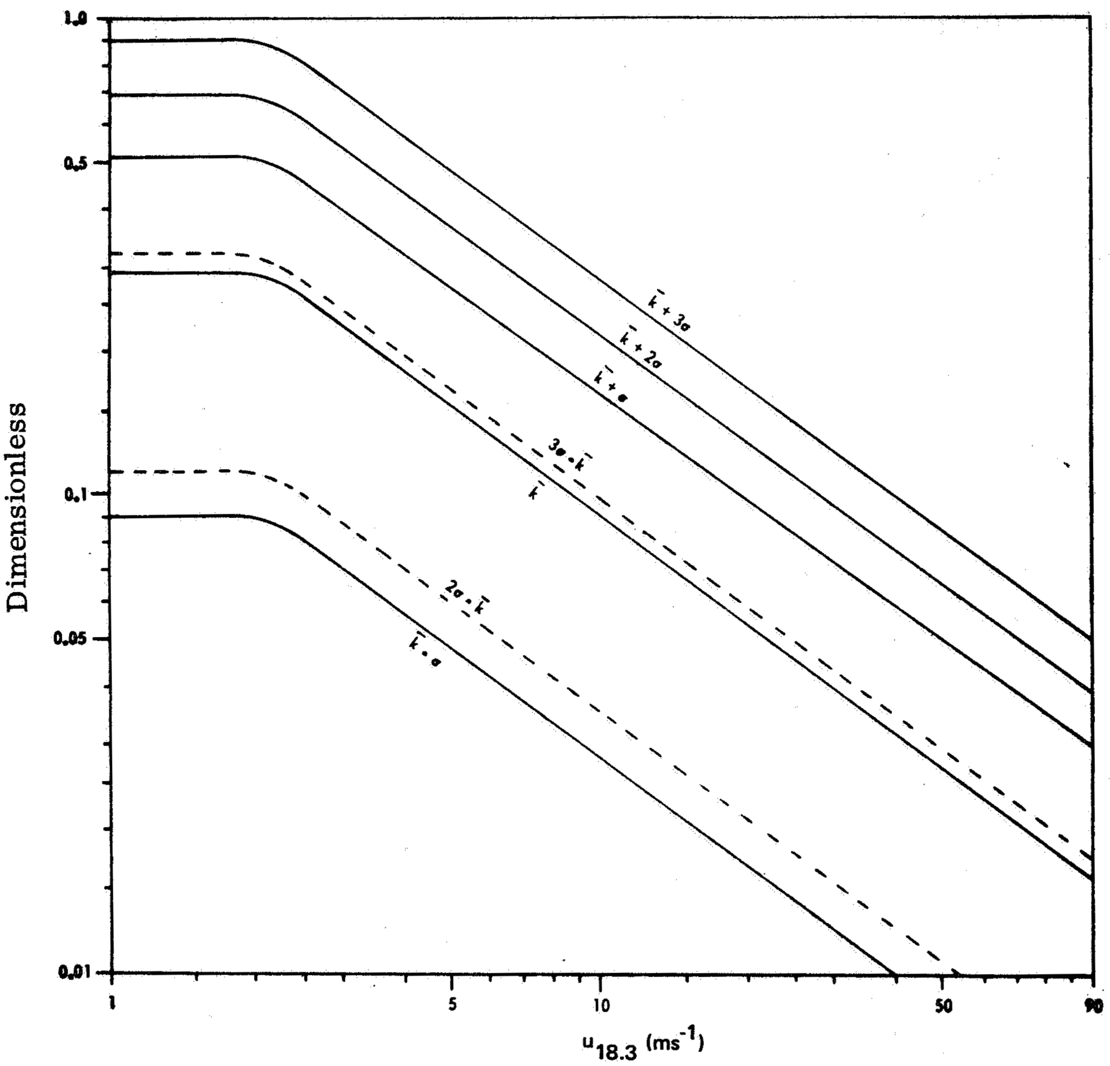

FIGURE 8.3.2 DISTRIBUTION OF THE PEAK WIND PROFILE PARAMETER k FOR VARIOUS WIND SPEEDS AT THE 18.3-m LEVEL FOR THE EASTERN TEST RANGE

8.3.5.3 Instantaneous Extreme Wind Profiles

The probability that the hourly peak wind speeds at all levels occur simultaneously is small. Accordingly, the practice of using peak wind profiles introduces some conservatism into the design criteria; however, the probability is relatively large that when the hourly peak wind occurs at the 18.3-meter level, the winds at the other levels almost take on the hourly peak values.

To gain some insight into this question, approximately 35 hours of digitized magnetic tape data were analyzed. The data were digitized at 0.1-second intervals in real time and partitioned into 0.5-, 2-, 5-, and 10-minute samples. The vertical average peak wind speed $\bar{u}_P$ and the 18-meter mean wind $\bar{u}_{18}$ were calculated for each sample. In addition, the instantaneous vertical average wind speed time history at 0.1-second intervals was calculated for each sample, and the peak instantaneous vertical average wind speed $\bar{u}_I$ was selected from each sample. The quantity $\bar{u}_I/\bar{u}_P$ was then interpreted to be a measure of how well the peak wind profile approximates the instantaneous extreme wind profile. Figure 8.3.3 is a plot of $\bar{u}_I/\bar{u}_P$ as a function of $\bar{u}_{18}$. The data points tend to scatter about a mean value of $\bar{u}_I/\bar{u}_P \simeq 0.93$; however, some of the data points have values equal to 0.98. These results justify the use of peak wind profiles for engineering purposes.

8.3.5.4 Peak Wind Profile Shapes for Other Test Ranges and Sites

Detailed analyses of wind profile statistics are not available for other test ranges and sites. The exponent k in equation (8.1) is a function of wind speed, surface roughness, etc. For moderate surface roughness conditions, the extreme value of k is usually equal to 0.2 or less during high winds ($\gtrsim$ 15 m/sec). For design and planning purposes for test ranges and sites other than the Eastern Test Range, it is recommended that the values of k given in Table 8.3.1 be used. These values of k are the only values used in this report for sites other than the Eastern Test Range and represent estimates for 99.87 percentile-mean + 3σ (0.13 percent risk) values for the peak wind speed profile shape.

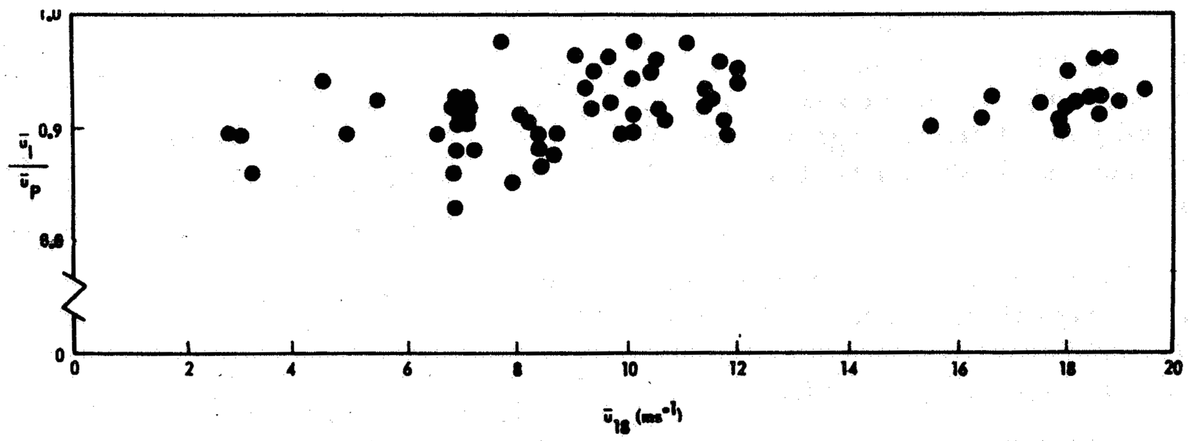

FIGURE 8.3.3 THE RATIO $\bar{u}_I/\bar{u}_P$ AS A FUNCTION OF THE 18.3-m MEAN WIND SPEED ($\bar{u}_{18}$) FOR A 10-min SAMPLING PERIOD

TABLE 8.3.1 VALUES OF k TO USE FOR TEST RANGES OTHER THAN THE EASTERN TEST RANGE

k Value	18.3-Meter Level Peak Wind Speed (ms^{-1})
k = 0.2	$7 \leq u_{18.3} < 22$
k = 0.14	$22 \leq u_{18.3}$

8.3.5.5 Aerospace Vehicle Design Wind Profiles

The data presented in this section provide basic peak wind speed profile (envelope) information for use in studies to determine load factors for test, free-standing, launch, and lift-off conditions to ensure satisfactory performance of the space vehicle. To establish vehicle response requirements, the peak design surface winds are assumed to act normal to the longitudinal axis of the vehicle on the launch pad and to be from the most critical direction.

8.3.5.5.1 Design Wind Profiles for the Eastern Test Range

Peak wind profiles are characterized by two parameters, the peak wind speed at the 18.3-meter level and the shape parameter k. Once these two quantities are defined, the peak wind speed profile envelope is completely specified. Accordingly, to construct a peak wind profile envelope for the Eastern Test Range, in the context of launch vehicle loading and response calculations, two pieces of information are required. First, the risk of exceeding the design wind peak speed at the reference level for a given period must be specified. Once this quantity is given, the design peak wind speed at the reference level is automatically specified (Figure 8.3.4). Second, the risk associated with compromising the structural integrity of the vehicle, once the reference level design wind occurs, must be specified. This second quantity and the reference level peak wind speed will determine the value of k that is to be used in equation (8.1).

It is recommended that the $\bar{k} + 3\sigma$ value of k be used for the design of space vehicles. Thus, if a space vehicle designed to withstand a particular value of peak wind speed at the 18.3-meter reference level is exposed to that peak wind speed, the vehicle has at least a 99.865-percent chance of withstanding possible peak wind profile conditions.

Operational ground wind constraints for established vehicles should be determined for a reference level (above natural grade) near the top of the vehicle while on the launch pad. The profile may be calculated using equations (8.1) and (8.2) with a value of $k = \bar{k} - 3\sigma$. This will produce a peak wind profile envelope associated with an upper reference level ground wind constraint. Tables for these calculations and those associated with the design reference level are available for various wind speeds and k values applicable to Kennedy Space Center upon request to the Atmospheric Sciences Division, Space Sciences Laboratory, NASA, Marshall Space Flight Center, Alabama 35812.

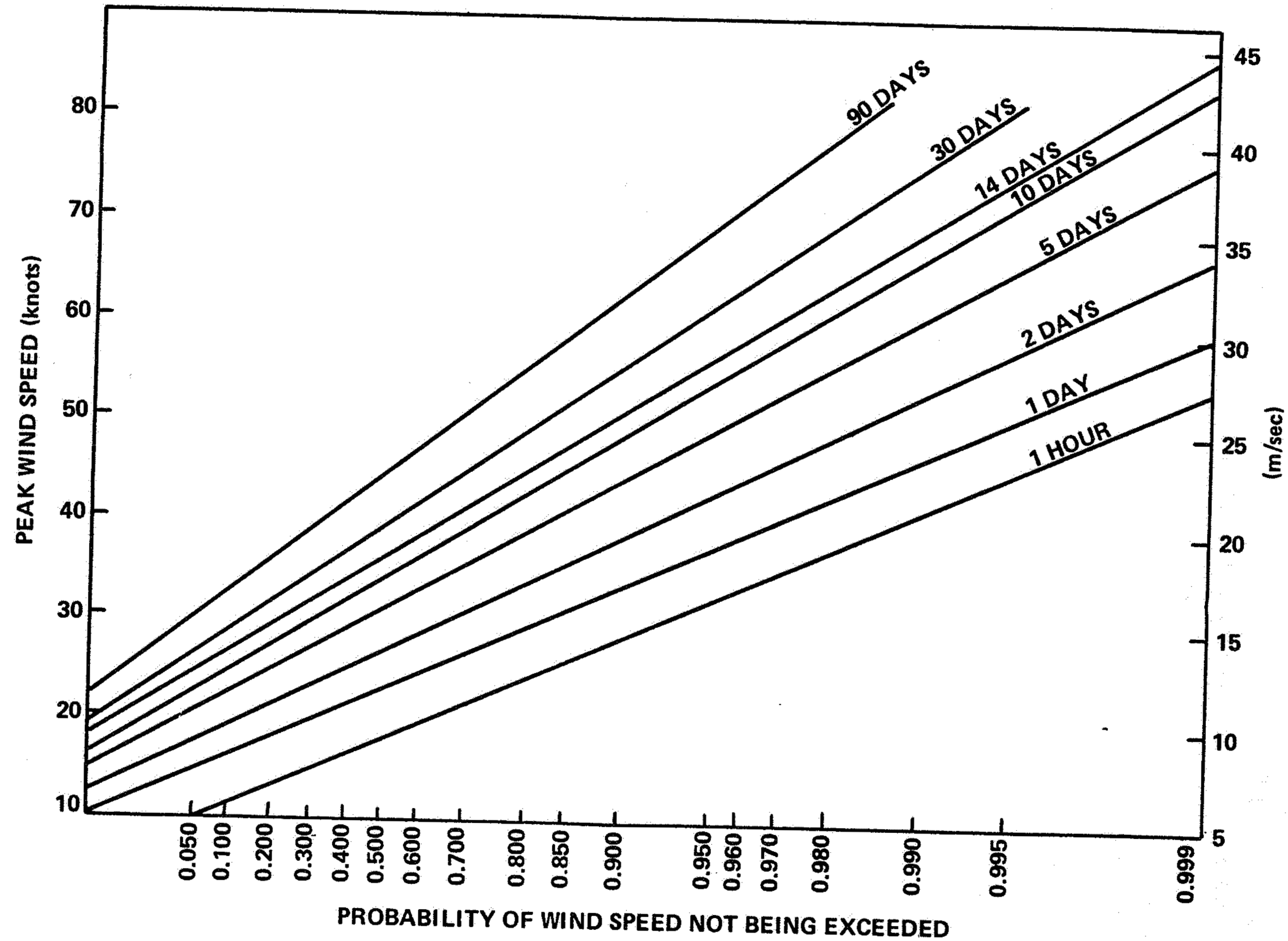

FIGURE 8.3.4. 18.3-m REFERENCE LEVEL; KENNEDY SPACE CENTER PEAK WIND SPEED FOR WINDIEST REFERENCE PERIOD VERSUS PROBABILITY FOR SEVERAL EXPOSURE PERIODS APPLICABLE TO VEHICLE DESIGN CRITERIA DEVELOPMENT

Table 8.3.2 contains peak wind speed profiles for various envelope values of peak wind speed at the 10-meter level for fixed values of risk for the worst monthly-hourly reference periods of the year for a 1-hour exposure. To construct these profiles, the 1-hour exposure period statistics for each hour in each month were constructed. This exercise yielded 288 distribution functions (12 months times 24 hours), which were enveloped to yield the largest or "worst" 10-meter level peak wind speed associated with a given level of risk for all monthly-hourly reference periods. Thus, for example, according to Table 8.3.2 there is at most a 10-percent risk that the peak wind speed will exceed 13.9 m/sec (27.0 knots) during any particular hour in any particular month at the 10-meter level, and if a peak wind speed equal to 13.9 m/sec (27.0 knots) should occur at the 10-meter level, then there is only a 0.135-percent chance that the peak wind speed will exceed 24.1 m/sec (46.8 knots) at the 152.4-meter level or the corresponding values given at the other heights.

Tables 8.3.3 through 8.3.5 contain peak wind profile envelopes for various values of peak wind speed at the 10-meter level and fixed values of risk for various exposure periods. The 1-day exposure values of peak wind speed were obtained by constructing the daily peak wind statistics for each month and then enveloping these distributions to yield the worst 1-day exposure, 10-meter level peak wind speed for a specified value of risk (daily-monthly reference period). The 30-day exposure envelope peak wind speeds were obtained by constructing the monthly peak wind statistics for each month and then constructing the envelope of the distributions (monthly-annual reference period). The 10-day exposure statistics were obtained by interpolating between the 1- and 30-day exposure period results. The envelopes of the 90-day exposure period statistics are the 90-day exposure statistics associated with the 12 trimonthly periods (January-February-March, February-March-April, March-April-May, and so forth) (90-day-annual reference period). Finally, the 365-day exposure period statistics were calculated with the annual peak wind sample (17 data points) to yield one distribution. Tables 8.3.3 through 8.3.5 contain the largest or "worst" 10-meter level peak wind speed associated with a given level of risk for the stated exposure periods.

It is recommended that the data in Tables 8.3.2 through 8.3.5 be used as the basis for space vehicle design for Kennedy Space Center operations. Wind profile statistics for the design of permanent ground support equipment are discussed in subsection 8.3.10.

TABLE 8.3.2 PEAK WIND SPEED PROFILE ENVELOPES FOR VARIOUS VALUES OF RISK OF EXCEEDING THE 10-m LEVEL PEAK WIND SPEED FOR 1-hr EXPOSURE (hourly-monthly reference period) FOR KENNEDY SPACE CENTER[1]

Height		Risk (%)									
		20		10		5		1		0.1	
(m)	(ft)	knots	ms^{-1}	knots	ms^{-1}	knots	ms^{-1}	knots	ms^{-1}	knots	ms^{-1}
10.0	33	22.9	11.8	27.0	13.9	30.8	15.8	39.5	20.3	51.9	26.7
18.3	60	26.3	13.5	30.5	15.7	34.4	17.7	43.4	22.3	56.0	28.8
30.5	100	29.5	15.2	33.8	17.4	37.9	19.5	47.0	24.2	59.8	30.8
61.0	200	34.5	17.8	38.9	20.0	43.0	22.1	52.3	26.9	65.4	33.6
91.4	300	37.8	19.5	42.2	21.7	46.4	23.9	55.7	28.7	68.9	35.4
121.9	400	40.4	20.8	44.7	23.0	48.9	25.2	58.3	30.0	71.5	36.8
152.4	500	42.5	21.9	46.8	24.1	51.0	26.2	60.3	31.0	73.6	37.8

TABLE 8.3.3 PEAK WIND SPEED PROFILE ENVELOPES FOR A 10-PERCENT RISK VALUE OF EXCEEDING THE 10-m LEVEL PEAK WIND SPEED FOR VARIOUS REFERENCE PERIODS OF EXPOSURE FOR KENNEDY SPACE CENTER[1]

Height		Exposure (days)									
		1		10		30		90		365	
(m)	(ft)	knots	ms^{-1}	knots	ms^{-1}	knots	ms^{-1}	knots	ms^{-1}	knots	ms^{-1}
10.0	33	32.1	16.5	46.9	24.1	53.9	27.7	61.0	31.4	70.0	36.0
18.3	60	35.8	18.4	51.0	26.2	58.2	29.9	65.3	33.6	74.5	38.3
30.5	100	39.2	20.2	54.7	28.1	62.0	31.9	69.3	35.7	78.5	40.4
61.0	200	44.4	22.8	60.2	31.0	67.6	34.8	75.0	38.6	84.4	43.4
91.4	300	47.8	24.6	63.6	32.7	71.1	36.6	78.5	40.4	88.0	45.3
121.9	400	50.3	25.9	66.2	34.1	73.7	37.9	81.1	41.7	90.6	46.6
152.4	500	52.4	27.0	68.3	35.1	75.8	39.0	83.2	42.8	92.8	47.7

1. Recommended for design criteria development

TABLE 8.3.4 PEAK WIND SPEED PROFILE ENVELOPES FOR A 5-PERCENT RISK VALUE OF EXCEEDING THE 10-m LEVEL PEAK WIND SPEED FOR VARIOUS REFERENCE PERIODS OF EXPOSURE FOR KENNEDY SPACE CENTER[2]

Height		Exposure (days)									
		1		10		30		90		365	
(m)	(ft)	knots	ms^{-1}	knots	ms^{-1}	knots	ms^{-1}	knots	ms^{-1}	knots	ms^{-1}
10.0	33	36.1	18.5	52.3	26.9	60.1	30.9	67.9	34.9	77.7	40.0
18.3	60	39.8	20.5	56.5	29.1	64.4	33.1	72.4	37.3	82.4	42.4
30.5	100	43.3	22.3	60.3	31.0	68.3	35.1	76.4	39.3	86.5	44.5
61.0	200	48.6	25.0	65.9	33.9	74.0	38.1	82.2	42.3	92.5	47.6
91.4	300	52.0	26.8	69.4	35.7	77.6	40.0	85.8	44.2	96.1	49.4
121.9	400	54.5	28.0	72.0	37.0	80.2	41.3	88.5	45.5	98.8	50.8
152.4	500	56.6	29.1	74.1	38.1	82.3	42.3	90.6	46.6	101.0	52.0

TABLE 8.3.5 PEAK WIND SPEED PROFILE ENVELOPES FOR A 1-PERCENT RISK VALUE OF EXCEEDING THE 10-m LEVEL PEAK WIND SPEED FOR VARIOUS REFERENCE PERIODS OF EXPOSURE FOR KENNEDY SPACE CENTER[2]

Height		Exposure (days)									
		1		10		30		90		365	
(m)	(ft)	knots	ms^{-1}	knots	ms^{-1}	knots	ms^{-1}	knots	ms^{-1}	knots	ms^{-1}
10.0	33	45.0	23.1	64.7	33.3	74.0	38.1	83.4	42.9	95.4	49.1
18.3	60	49.0	25.2	69.1	35.6	78.6	40.4	88.2	45.4	100.3	51.6
30.5	100	52.6	27.1	73.1	37.6	82.8	42.6	92.4	47.5	104.7	53.9
61.0	200	58.1	30.0	78.8	40.6	88.6	45.6	98.4	50.6	110.9	57.1
91.4	300	61.5	31.6	82.4	42.4	92.3	47.5	102.1	52.5	114.6	59.0
121.9	400	64.1	33.0	85.1	44.8	95.0	48.9	104.8	53.9	117.4	60.4
152.4	500	66.1	34.0	87.2	44.9	97.1	50.0	107.0	55.0	119.6	61.5

2. Recommended for design criteria development.

Mean wind profiles or steady-state wind profiles can be obtained from the peak wind profiles by dividing the peak wind by the appropriate gust factor (subsection 8.3.7). It is recommended that the 10-minute gust factors be used for structural design purposes. Application of the 10-minute gust factors to the peak wind profile corresponds to averaging the wind speed over a 10-minute period. This averaging period appears to result in a stable mean value of the wind speed. Within the range of variation of the data, the 1-hour and 10-minute gust factors are approximately equal for sufficiently high wind speed. This occurs because the spectrum of the horizontal wind speed near the ground is characterized by a broad energy gap centered at a frequency approximately equal to 0.000278 hertz (1 cycle/hr) and typically extends over the frequency domain 0.000139 hertz (0.5 cycles/hr) $< \omega <$ 0.0014 hertz (5 cycles/hr). The Fourier spectral components associated with frequencies less than 0.000278 hertz (1 cycle/hr) correspond to the meso- and synoptic-scale motions, while the remaining high-frequency spectral components correspond to mechanically and thermally produced turbulence. Thus, a statistically stable estimate of the mean or steady-state wind speed can be obtained by averaging over a period in the range from 10 minutes to an hour. Since this period is far longer than any natural period of structural vibration, it assures that effects caused by the mean wind properly represent steady-state, nontransient effects. The steady-state wind profiles, calculated with the 10-minute gust factors, that correspond to those in Tables 8.3.2 through 8.3.5 are given in Tables 8.3.6 through 8.3.9.

8.3.5.5.2 Design Ground Wind Profiles for Other Locations

Tables 8.3.10 through 8.3.21 contain recommended design ground wind profiles for several different risks of exceeding the 10-meter level peak wind speed and 10-minute mean wind speed for a 1-hour exposure period. These tables are based on the same philosophy as Table 8.3.2 and Table 8.3.6 for the Eastern Test Range. The locations for which data are provided include Wallops Flight Center, Virginia; White Sands Missile Range, New Mexico; Air Force Flight Center, Edwards AFB, California; Space and Missile Test Center, Vandenberg AFB, California; Huntsville, Alabama; New Orleans, Louisiana; and National Space Technology Laboratory, Mississippi.

TABLE 8.3.6 10-min MEAN WIND SPEED PROFILE ENVELOPES FOR VARIOUS VALUES OF RISK OF EXCEEDING THE 10-m LEVEL MEAN WIND SPEED FOR A 1-hr EXPOSURE (hourly-monthly reference period) FOR KENNEDY SPACE CENTER

Height		Risk (%)									
		20		10		5		1		0.1	
(m)	(ft)	knots	ms^{-1}	knots	ms^{-1}	knots	ms^{-1}	knots	ms^{-1}	knots	ms^{-1}
10.0	33	14.1	7.2	16.6	8.6	19.1	9.8	24.6	12.7	32.4	16.7
18.3	60	17.1	8.8	19.9	10.3	22.6	11.7	28.7	14.8	37.2	19.1
30.5	100	20.0	10.3	23.1	11.9	26.0	13.4	32.6	16.8	41.6	21.4
61.0	200	24.7	12.7	28.1	14.5	31.3	16.1	38.3	19.7	48.1	24.7
91.4	300	27.8	14.3	31.3	16.1	34.7	17.9	42.0	21.6	52.1	26.8
121.9	400	30.3	15.6	33.9	17.4	37.3	19.2	44.8	23.0	55.1	28.3
152.4	500	32.3	16.6	35.9	18.5	39.4	20.3	47.0	24.2	57.5	29.6

TABLE 8.3.7 10-min MEAN WIND SPEED PROFILE ENVELOPES FOR A 10-PERCENT RISK VALUE OF EXCEEDING THE 10-m LEVEL MEAN WIND SPEED FOR VARIOUS REFERENCE PERIODS OF EXPOSURE FOR KENNEDY SPACE CENTER

Height		Exposure (days)									
		1		10		30		90		365	
(m)	(ft)	knots	ms^{-1}	knots	ms^{-1}	knots	ms^{-1}	knots	ms^{-1}	knots	ms^{-1}
10.0	33	20.0	10.3	29.3	15.1	33.7	17.3	38.1	19.6	43.8	22.5
18.3	60	23.6	12.1	33.8	17.4	38.7	19.9	43.3	22.3	49.5	25.5
30.5	100	27.1	13.9	38.0	19.5	43.1	22.2	48.2	24.8	54.6	28.1
61.0	200	32.4	16.7	44.2	22.7	49.6	25.5	55.1	28.3	62.1	31.9
91.4	300	35.8	18.4	48.1	24.7	53.8	27.7	59.4	30.6	66.6	34.3
121.9	400	38.5	19.8	51.0	26.2	56.8	29.2	62.6	32.2	69.9	36.0
152.4	500	40.6	20.9	53.3	27.4	59.2	30.5	65.1	33.5	72.6	37.3

TABLE 8.3.8 10-min MEAN WIND SPEED PROFILE ENVELOPES FOR A 5-PERCENT RISK VALUE OF EXCEEDING THE 10-m LEVEL MEAN WIND SPEED FOR VARIOUS REFERENCE PERIODS OF EXPOSURE FOR KENNEDY SPACE CENTER

Height		Exposure (days)									
		1		10		30		90		365	
(m)	(ft)	knots	ms^{-1}	knots	ms^{-1}	knots	ms^{-1}	knots	ms^{-1}	knots	ms^{-1}
10.0	33	22.5	11.6	32.7	16.8	37.6	19.3	42.5	21.9	48.6	25.0
18.3	60	26.3	13.5	37.5	19.3	42.8	22.0	48.1	24.7	54.8	28.2
30.5	100	30.0	15.4	41.9	21.6	47.5	24.4	53.2	27.4	60.2	31.0
61.0	200	35.5	18.3	48.4	24.9	54.5	28.0	60.4	31.1	68.1	35.0
91.4	300	39.2	20.2	52.5	27.0	58.7	30.2	64.9	33.4	72.9	37.5
121.9	400	41.9	21.6	55.5	28.6	61.9	31.8	68.2	35.1	76.3	39.3
152.4	500	44.0	22.6	57.9	29.8	64.4	33.1	70.9	36.4	79.1	40.7

TABLE 8.3.9 10-min MEAN WIND SPEED PROFILE ENVELOPES FOR A 1-PERCENT RISK VALUE OF EXCEEDING THE 10-m LEVEL MEAN WIND SPEED FOR VARIOUS REFERENCE PERIODS OF EXPOSURE FOR KENNEDY SPACE CENTER

Height		Exposure (days)									
		1		10		30		90		365	
(m)	(ft)	knots	ms^{-1}	knots	ms^{-1}	knots	ms^{-1}	knots	ms^{-1}	knots	ms^{-1}
10.0	33	28.1	14.5	40.9	21.0	46.3	23.8	52.2	26.9	59.7	30.7
18.3	60	32.5	16.7	46.5	23.9	52.2	26.9	58.6	30.1	66.7	34.3
30.5	100	36.6	18.8	51.4	26.4	57.6	29.6	64.3	33.1	72.9	37.5
61.0	200	42.6	21.9	58.6	30.1	65.2	33.5	72.5	37.3	81.6	42.0
91.4	300	47.2	24.3	63.0	32.4	69.9	36.0	77.4	39.8	86.9	44.7
121.9	400	49.4	25.4	66.3	34.1	73.4	37.8	81.0	41.7	90.7	46.7
152.4	500	51.7	26.6	68.9	35.4	76.1	39.1	83.8	43.1	93.7	48.2

TABLE 8.3.10 PEAK WIND SPEED PROFILE ENVELOPES FOR VARIOUS VALUES OF RISK OF EXCEEDING THE 10-m LEVEL PEAK WIND SPEED FOR 1-hr EXPOSURE (hourly-monthly reference period) FOR HUNTSVILLE, ALABAMA

Height		Risk (%)									
		20		10		5		1		0.1	
(m)	(ft)	knots	ms^{-1}	knots	ms^{-1}	knots	ms^{-1}	knots	ms^{-1}	knots	ms^{-1}
10.0	33	19.1	9.8	21.6	11.1	24.0	12.4	31.5	16.2	47.5	24.5
18.3	60	21.5	11.1	24.4	12.5	27.1	14.0	35.6	18.3	51.7	26.7
30.5	100	23.9	12.3	27.0	13.9	30.0	15.5	39.4	20.3	55.5	28.6
61.0	200	27.4	14.1	31.0	15.9	34.5	17.8	45.2	23.3	61.0	31.5
91.4	300	29.7	15.3	33.6	17.3	37.4	19.3	49.1	25.2	64.7	33.4
121.9	400	31.5	16.2	35.6	18.3	39.6	20.5	52.0	26.7	67.4	34.7
152.4	500	33.0	16.9	37.3	19.2	41.5	21.4	54.4	28.0	69.5	35.8

TABLE 8.3.11 10-min MEAN WIND SPEED PROFILE ENVELOPES FOR VARIOUS VALUES OF RISK OF EXCEEDING THE 10-m LEVEL MEAN SPEED FOR 1-hr EXPOSURE (hourly-monthly reference period) FOR HUNTSVILLE, ALABAMA

Height		Risk (%)									
		20		10		5		1		0.1	
(m)	(ft)	knots	ms^{-1}	knots	ms^{-1}	knots	ms^{-1}	knots	ms^{-1}	knots	ms^{-1}
10.0	33	13.6	7.0	15.4	7.9	17.1	8.8	22.5	11.6	33.9	17.5
18.3	60	15.4	7.9	17.4	9.0	19.4	10.0	25.4	13.1	36.9	19.0
30.5	100	17.1	8.8	19.3	9.9	21.4	11.1	28.1	14.5	39.6	20.4
61.0	200	19.6	10.1	22.2	11.4	24.6	12.7	32.3	16.6	43.6	22.5
91.4	300	21.3	10.9	24.0	12.4	26.7	13.8	35.0	18.0	46.2	23.8
121.9	400	22.5	11.6	25.5	13.1	28.3	14.6	37.1	19.1	48.1	24.8
152.4	500	23.6	12.1	26.7	13.7	29.6	15.3	38.9	20.0	49.6	25.6

TABLE 8.3.12 SURFACE PEAK WIND SPEED PROFILE ENVELOPES FOR VARIOUS VALUES OF RISK OF EXCEEDING THE 10-m LEVEL PEAK WIND SPEED FOR 1-hr EXPOSURE (hourly-monthly reference period) FOR NEW ORLEANS AND NATIONAL SPACE TECHNOLOGY LABORATORY AREA

Height		Risk (%)									
		20		10		5		1		0.1	
(m)	(ft)	knots	ms^{-1}	knots	ms^{-1}	knots	ms^{-1}	knots	ms^{-1}	knots	ms^{-1}
10.0	33	19.8	10.2	23.9	12.3	27.6	14.2	37.2	19.1	53.0	27.3
18.3	60	22.4	11.5	27.0	13.9	31.2	16.0	42.0	21.5	57.7	29.7
30.5	100	24.8	12.8	29.9	15.4	34.5	17.8	46.5	23.9	61.9	31.8
61.0	200	28.4	14.6	34.3	17.7	39.6	20.4	53.4	27.4	68.1	35.1
91.4	300	30.8	15.9	37.2	19.2	43.0	22.1	57.9	29.8	72.2	37.2
121.9	400	32.7	16.8	39.4	20.3	45.5	23.4	61.4	31.5	75.2	38.7
152.4	500	34.2	17.6	41.3	21.3	47.7	24.5	64.3	33.0	77.5	39.9

TABLE 8.3.13 SURFACE MEAN WIND SPEED PROFILE ENVELOPES FOR VARIOUS VALUES OF RISK OF EXCEEDING THE 10-m LEVEL 10-min MEAN WIND SPEED FOR 1-hr EXPOSURE (hourly-monthly reference period) FOR NEW ORLEANS AND NATIONAL SPACE TECHNOLOGY LABORATORY AREA

Height		Risk (%)									
		20		10		5		1		0.1	
(m)	(ft)	knots	ms^{-1}	knots	ms^{-1}	knots	ms^{-1}	knots	ms^{-1}	knots	ms^{-1}
10.0	33	14.1	7.3	17.1	8.8	19.7	10.1	26.6	13.7	37.9	19.5
18.3	60	16.0	8.2	19.3	9.9	22.3	11.4	30.0	15.4	41.2	21.2
30.5	100	17.7	9.1	21.4	11.0	24.7	12.7	33.2	17.1	44.2	22.8
61.0	200	20.3	10.5	24.5	12.6	28.3	14.6	38.2	19.6	48.6	25.0
91.4	300	22.0	11.3	26.6	13.7	30.7	15.8	41.4	21.3	51.6	26.6
121.9	400	23.3	12.0	28.2	14.5	32.5	16.7	43.8	22.5	53.7	27.7
152.4	500	24.4	12.6	29.5	15.2	34.1	17.5	45.9	23.6	55.4	28.5

TABLE 8.3.14 SURFACE PEAK WIND SPEED PROFILE ENVELOPES FOR VARIOUS VALUES OF RISK OF EXCEEDING THE 10-m LEVEL PEAK WIND SPEED FOR 1-hr EXPOSURE (hourly-monthly reference period) FOR THE SPACE AND MISSILE TEST CENTER,[3] VANDENBERG AFB, CALIFORNIA

Height		Risk (%)									
		20		10		5		1		0.1	
(m)	(ft)	knots	ms^{-1}	knots	ms^{-1}	knots	ms^{-1}	knots	ms^{-1}	knots	ms^{-1}
10.0	33	20.0	10.3	23.8	12.3	27.5	14.2	35.8	18.4	47.3	24.3
18.3	60	22.5	11.6	26.8	13.8	31.0	16.0	40.3	20.8	51.4	26.5
30.5	100	25.0	12.9	29.7	15.3	34.3	17.7	44.7	23.0	55.2	28.5
61.0	200	28.7	14.8	34.1	17.6	39.4	20.3	51.3	26.4	60.9	31.3
91.4	300	31.1	16.0	37.0	19.0	42.8	22.0	55.7	28.7	64.4	33.2
121.9	400	32.9	16.9	39.2	20.2	45.3	23.3	59.0	30.4	67.1	34.5
152.4	500	34.4	17.7	41.0	21.1	47.4	24.4	61.7	31.7	69.2	35.6

TABLE 8.3.15 SURFACE MEAN WIND SPEED PROFILE ENVELOPES FOR VARIOUS VALUES OF RISK OF EXCEEDING THE 10-m LEVEL 10-min MEAN WIND SPEED FOR 1-hr EXPOSURE (hourly-monthly reference period) FOR THE SPACE AND MISSILE TEST CENTER, VANDENBERG AFB, CALIFORNIA[3]

Height		Risk (%)									
		20		10		5		1		0.1	
(m)	(ft)	knots	ms^{-1}	knots	ms^{-1}	knots	ms^{-1}	knots	ms^{-1}	knots	ms^{-1}
10.0	33	14.3	7.4	17.0	8.9	19.6	10.1	25.6	13.1	33.8	17.4
18.3	60	16.1	8.3	19.2	9.9	22.1	11.4	28.8	14.8	36.7	18.9
30.5	100	17.8	9.2	21.2	10.9	24.5	12.6	31.9	16.4	39.5	20.3
61.0	200	20.5	10.5	24.4	12.6	28.1	14.5	36.7	18.9	43.5	22.4
91.4	300	22.2	11.4	26.4	13.6	30.5	15.7	39.8	20.5	46.0	23.7
121.9	400	23.5	12.1	28.0	14.4	32.3	16.7	42.1	21.7	47.9	24.7
152.4	500	24.6	12.7	29.3	15.1	33.8	17.4	44.0	22.7	49.4	25.5

3. Formerly Western Test Range.

TABLE 8.3.16 SURFACE PEAK WIND SPEED PROFILE ENVELOPES FOR VARIOUS VALUES OF RISK OF EXCEEDING THE 10-m LEVEL PEAK WIND SPEED FOR 1-hr EXPOSURE (hourly-monthly reference period) FOR WALLOPS FLIGHT CENTER

Height		Risk (%)									
		20		10		5		1		0.1	
(m)	(ft)	knots	ms^{-1}	knots	ms^{-1}	knots	ms^{-1}	knots	ms^{-1}	knots	ms^{-1}
10.0	33	22.9	11.8	27.1	13.9	31.2	16.1	38.6	19.9	55.0	28.3
18.3	60	25.9	13.3	30.6	15.7	35.2	18.2	43.6	22.5	59.8	30.8
30.5	100	28.6	14.8	33.9	17.4	39.0	20.1	48.3	24.9	64.3	33.1
61.0	200	32.9	16.9	38.9	20.0	44.8	23.1	55.4	28.6	70.6	36.3
91.4	300	35.7	18.4	42.2	21.7	48.6	25.1	60.1	31.0	74.9	38.6
121.9	400	37.8	19.5	44.7	22.9	51.5	26.6	63.7	32.8	78.0	40.1
152.4	500	39.6	20.4	46.8	24.0	53.9	27.8	66.7	34.4	80.5	41.4

TABLE 8.3.17 SURFACE MEAN WIND SPEED PROFILE ENVELOPES FOR VARIOUS VALUES OF RISK OF EXCEEDING THE 10-m LEVEL 10-min MEAN WIND SPEED FOR 1-hr EXPOSURE (hourly-monthly reference period) FOR WALLOPS FLIGHT CENTER

Height		Risk (%)									
		20		10		5		1		0.1	
(m)	(ft)	knots	ms^{-1}	knots	ms^{-1}	knots	ms^{-1}	knots	ms^{-1}	knots	ms^{-1}
10.0	33	16.4	8.4	19.3	9.9	22.3	11.5	27.6	14.2	39.3	20.2
18.3	60	18.5	9.5	21.9	11.2	25.2	13.0	31.1	16.1	42.7	22.0
30.5	100	20.5	10.5	24.2	12.4	27.9	14.4	34.5	17.8	45.9	23.6
61.0	200	23.5	12.1	27.8	14.3	32.0	16.5	39.6	20.4	50.4	26.0
91.4	300	25.5	13.1	30.2	15.5	34.7	17.9	42.9	22.1	53.5	27.5
121.9	400	27.0	13.9	31.9	16.4	36.8	19.0	45.5	23.5	55.7	28.7
152.4	500	28.3	14.6	33.5	17.2	38.5	19.9	47.7	24.6	57.5	29.6

TABLE 8.3.18 SURFACE PEAK WIND SPEED PROFILE ENVELOPES FOR VARIOUS VALUES OF RISK OF EXCEEDING THE 10-m LEVEL PEAK WIND SPEED FOR 1-hr EXPOSURE (hourly-monthly reference period) FOR WHITE SANDS MISSILE RANGE

Height		Risk (%)									
		20		10		5		1		0.1	
(m)	(ft)	knots	ms^{-1}	knots	ms^{-1}	knots	ms^{-1}	knots	ms^{-1}	knots	ms^{-1}
10.0	33	15.3	7.9	20.9	10.7	24.7	12.7	34.3	17.7	52.1	26.8
18.3	60	17.3	8.9	23.6	12.1	27.9	14.3	38.7	20.0	56.7	29.2
30.5	100	19.1	9.9	26.1	13.4	30.9	15.9	42.9	22.1	60.9	31.3
61.0	200	22.0	11.3	30.0	15.4	35.5	18.2	49.3	25.4	66.9	34.4
91.4	300	23.8	12.3	32.6	16.7	38.5	19.8	53.4	27.6	71.0	36.5
121.9	400	25.2	13.0	34.5	17.7	40.8	21.0	56.6	29.2	73.9	38.0
152.4	500	26.4	13.7	36.1	18.5	42.7	22.0	59.3	30.6	76.2	39.2

TABLE 8.3.19 SURFACE MEAN WIND SPEED PROFILE ENVELOPES FOR VARIOUS VALUES OF RISK OF EXCEEDING THE 10-m LEVEL 10-min MEAN WIND SPEED FOR 1-hr EXPOSURE (hourly-monthly reference period) FOR WHITE SANDS MISSILE RANGE

Height		Risk (%)									
		20		10		5		1		0.1	
(m)	(ft)	knots	ms^{-1}	knots	ms^{-1}	knots	ms^{-1}	knots	ms^{-1}	knots	ms^{-1}
10.0	33	10.9	5.6	14.9	7.7	17.6	9.1	24.5	12.6	37.2	19.2
18.3	60	12.3	6.4	16.9	8.6	19.9	10.2	27.7	14.3	40.5	20.8
30.5	100	13.7	7.1	18.7	9.6	22.1	11.3	30.7	15.8	43.4	22.4
61.0	200	15.7	8.1	21.4	11.0	25.3	13.0	35.2	18.2	47.8	24.6
91.4	300	17.0	8.8	23.3	11.9	27.5	14.1	38.2	19.7	50.7	26.1
121.9	400	18.0	9.3	24.6	12.6	29.1	15.0	40.4	20.9	52.8	27.1
152.4	500	18.9	9.8	25.8	13.2	30.5	15.7	42.3	21.9	54.4	28.0

TABLE 8.3.20 SURFACE PEAK WIND SPEED PROFILE ENVELOPES FOR VARIOUS VALUES OF RISK OF EXCEEDING THE 10-m LEVEL PEAK WIND SPEED FOR 1-hr EXPOSURE (hourly-monthly reference period) FOR EDWARDS AIR FORCE BASE

Height		Risk (%)									
		20		10		5		1		0.1	
(m)	(ft)	knots	ms^{-1}	knots	ms^{-1}	knots	ms^{-1}	knots	ms^{-1}	knots	ms^{-1}
10.0	33	24.4	12.6	28.3	14.6	31.5	16.2	38.4	19.8	47.0	24.2
18.3	60	27.6	14.2	32.0	16.5	35.6	18.3	43.4	22.4	51.1	26.3
30.5	100	30.5	15.8	35.4	18.3	39.4	20.3	48.0	24.8	54.9	28.3
61.0	200	35.0	18.1	40.6	21.0	45.2	23.3	55.1	28.4	60.3	31.1
91.4	300	38.0	19.6	44.1	22.7	49.1	25.2	59.8	30.8	64.0	33.0
121.9	400	40.3	20.8	46.7	24.1	52.0	26.7	63.4	32.7	66.6	34.3
152.4	500	42.2	21.8	48.9	25.2	54.4	28.0	66.4	34.2	68.8	35.4

TABLE 8.3.21 SURFACE MEAN WIND SPEED PROFILE ENVELOPES FOR VARIOUS VALUES OF RISK OF EXCEEDING THE 10-m LEVEL 10-min MEAN WIND SPEED FOR 1-hr EXPOSURE (hourly-monthly reference period) FOR EDWARDS AIR FORCE BASE

Height		Risk (%)									
		20		10		5		1		0.1	
(m)	(ft)	knots	ms^{-1}	knots	ms^{-1}	knots	ms^{-1}	knots	ms^{-1}	knots	ms^{-1}
10.0	33	17.4	9.0	20.2	10.4	22.5	11.6	27.4	14.1	33.6	17.3
18.3	60	19.7	10.2	22.8	11.8	25.4	13.1	31.0	16.0	36.5	18.8
30.5	100	21.8	11.3	25.3	13.0	28.1	14.5	34.4	17.7	39.2	20.2
61.0	200	25.0	12.9	29.0	15.0	32.3	16.6	39.4	20.3	43.1	22.2
91.4	300	27.1	14.0	31.5	16.2	35.0	18.0	42.7	22.0	45.7	23.5
121.9	400	28.8	14.9	33.4	17.2	37.1	19.1	45.3	23.3	47.6	24.5
152.4	500	30.1	15.6	34.9	18.0	38.9	20.0	47.4	24.4	49.1	25.3

The peak/mean wind profiles were constructed with a 1.4 gust factor and mean + 3σ value of k, as given in subsection 8.3.5.4. Some additional general ground wind data are given in References 8.3 and 8.4 for several other locations. See Section IX for a discussion of low level profiles over water for Space Shuttle Solid Rocket Booster (SRB) water entry studies.

8.3.5.5.3 Frequency of Calm Winds

Generally, design criteria wind problems are concerned with high wind speeds, but a condition of calm or very low speeds may also be important. For example, with no wind to disperse venting vapors such as LOX, a poor visibility situation could develop around the vehicle. Calm wind conditions can also have significant implications relative to the atmospheric diffusion of vehicle exhaust clouds. In addition calm wind in conjunction with high solar heating can result in significantly high vehicle compartment temperatures. Table 8.3.22 shows the frequency of calm winds at the 10-meter for Cape Kennedy as a function of time of day and month. The maximum percentage of calms appears in the summer and during the early morning hours, with the minimum percentage appearing throughout the year during the afternoon. Similar tables for other locations are available upon request.

8.3.6 Spectral Ground Wind Turbulence Model

Under most conditions ground winds are fully developed turbulent flows. This is particularly true when the wind speed is greater than a few meters per second, the atmosphere is unstable, or when both conditions exist. During nighttime conditions when the wind speed is typically low and the stratification is stable, the intensity of turbulence is small if not nil. Spectral methods are a particularly useful way of representing the turbulent portion of the ground wind environment for launch vehicle design purposes, as well as for use in diffusion calculations of toxic fuels and atmospheric pollutants.

8.3.6.1 Introduction

At a fixed point in the atmospheric boundary layer, the instantaneous wind vector fluctuates in time about the horizontal steady-state wind vector. The vector departure of the horizontal component of the instantaneous wind vector from the quasi-steady wind vector is the horizontal vector component of turbulence. This vector departure can be represented by two components, the longitudinal and the lateral components of turbulence which are parallel and perpendicular to the steady-state wind vector in the horizontal plane (Figure 8.3.5). The model contained herein is a spectral representation

TABLE 8.3.22 FREQUENCY (%) OF CALM WIND AT THE 10-m LEVEL, KENNEDY SPACE CENTER

Hour EST	Month												Annual
	Jan	Feb	Mar	Apr	May	June	July	Aug	Sept	Oct	Nov	Dec	
00	4.8	4.0	3.6	1.3	7.3	9.2	11.7	13.7	6.3	6.9	6.3	6.0	6.8
01	2.8	1.3	2.4	1.7	8.9	8.3	10.9	14.1	7.1	4.8	6.3	6.5	6.3
02	4.8	2.2	3.6	2.9	7.7	10.0	11.7	13.7	10.4	7.3	5.4	4.0	7.0
03	5.2	3.1	2.0	3.8	8.5	12.1	11.3	17.3	12.1	5.2	2.9	3.2	7.3
04	2.8	4.4	2.4	3.8	5.2	13.8	14.5	13.7	10.8	5.2	4.6	2.8	7.0
05	4.4	4.0	3.2	2.9	9.7	16.3	15.3	18.5	13.3	3.6	4.6	4.4	8.4
06	4.4	4.0	4.4	2.9	8.9	16.3	19.8	19.0	13.3	3.2	5.0	5.2	8.9
07	3.6	4.4	4.8	6.3	10.5	16.7	18.1	19.4	15.8	4.4	5.4	5.6	9.6
08	3.6	6.6	6.5	2.9	2.4	5.4	6.0	6.9	4.6	4.0	8.8	4.4	5.2
09	3.6	1.8	2.0	2.1	2.8	3.8	4.8	1.6	4.2	0.8	4.6	5.6	3.1
10	0.4	1.8	1.6	1.7	0.4	3.8	4.0	2.8	2.1	*	1.3	2.4	1.8
11	0.4	1.3	1.2	1.7	0.8	1.3	2.4	0.8	2.9	0.8	1.7	0.8	1.3
12	1.6	0.4	*	*	*	0.8	0.8	0.4	1.3	0.4	2.1	1.2	0.8
13	2.0	0.4	*	*	0.4	1.3	0.4	1.6	0.8	0.4	1.7	0.4	0.8
14	0.8	4.0	0.8	0.4	0.4	0.8	1.2	1.6	1.3	0.8	*	0.4	0.7
15	0.4	1.3	*	*	*	0.8	0.4	1.6	2.5	0.4	0.4	0.4	0.7
16	0.4	0.4	0.4	*	0.8	0.4	0.8	0.4	1.3	0.8	*	0.8	0.5
17	1.6	0.4	*	0.4	0.4	2.1	0.8	3.2	2.1	1.6	1.7	2.0	1.4
18	4.0	1.8	0.8	0.4	1.6	2.5	3.2	4.0	2.9	1.2	5.0	7.7	2.9
19	2.8	3.5	2.0	*	1.6	5.0	2.8	5.2	4.6	1.2	7.1	6.5	3.5
20	4.4	3.5	2.8	1.7	3.2	6.7	5.6	8.5	7.5	1.6	6.3	6.0	4.8
21	5.2	4.0	3.2	1.3	4.8	7.5	10.5	8.9	8.3	4.4	5.0	6.0	5.8
22	3.6	2.2	2.4	1.7	6.0	7.5	7.7	12.9	7.9	4.8	6.3	5.2	5.7
23	5.6	3.5	4.8	0.8	6.5	8.3	10.5	15.3	10.0	5.6	4.6	5.2	6.8
All Hours	3.1	2.5	2.3	1.7	4.1	6.7	7.3	8.6	6.4	2.9	4.0	3.9	4.5

* values < 0.4 percent

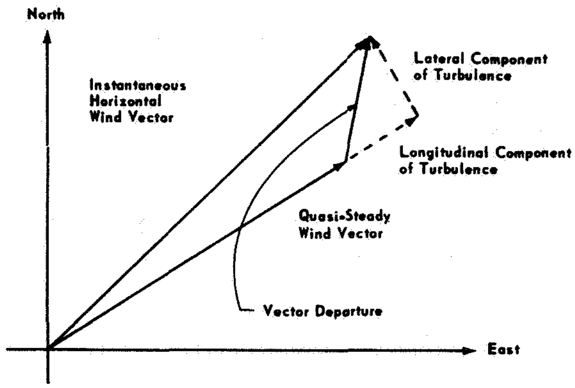

FIGURE 8.3.5 THE RELATIONSHIP BETWEEN THE QUASI-STEADY AND THE HORIZONTAL INSTANTANEOUS WIND VECTORS AND THE LONGITUDINAL AND LATERAL COMPONENTS OF TURBULENCE

of the characteristics of the longitudinal and lateral components of turbulence. The model analytically defines the spectra of these components of turbulence for the first 200 meters of the boundary layer. In addition, it defines the longitudinal and lateral cospectra, quadrature spectra, and the corresponding coherence functions associated with any pair of levels in the boundary layer. Details concerning the model herein can be found in References 8.5, 8.6, and 8.7.

8.3.6.2 Turbulence Spectra

The longitudinal and lateral spectra of turbulence at frequency ω and height z can be represented by a dimensionless function of the form

$$\frac{\omega\, S(\omega)}{\beta u_*^{\,2}} = \frac{c_1\, f/f_m}{\left[1 + 1.5\,(f/f_m)^{c_2}\right]^{(5/3)c_2}} , \qquad (8.3)$$

where

$$f = \frac{\omega z}{u(z)} \qquad (8.4)$$

$$f_m = c_3 \left(\frac{z}{z_r}\right)^{c_4} \qquad (8.5)$$

$$\beta = \left(\frac{z}{z_r}\right)^{c_5} \qquad (8.6)$$

$$u_* = c_6\, u(z_r) \qquad (8.7)$$

In these equations z_r is a reference height equal to 18.3 meters (60 ft); $\bar{u}(z)$ is the quasi-steady wind speed at height z; and the quantities c_i $(i = 1, 2, 3, 4, 5)$ are dimensionless constants that depend upon the site and

TABLE 8.3.23 DIMENSIONLESS CONSTANTS FOR THE LONGITUDINAL SPECTRUM OF TURBULENCE FOR THE EASTERN TEST RANGE

Condition	c_1	c_2	c_3	c_4	c_5
Light Wind Daytime Conditions	2.905	1.235	0.04	0.87	-0.14
Strong Winds	6.198	0.845	0.03	1.00	-0.63

TABLE 8.3.24 DIMENSIONLESS CONSTANTS FOR THE LATERAL SPECTRUM OF TURBULENCE FOR THE EASTERN TEST RANGE

Condition	c_1	c_2	c_3	c_4	c_5
Light Wind Daytime Conditions	4.599	1.144	0.033	0.72	-0.04
Strong Winds	3.954	0.781	0.1	0.58	-0.35

the stability. The frequency ω is defined with respect to a structure or vehicle at rest relative to the earth. The reader is referred to Sections 8.4.13 and 8.4.14 for the definition of turbulence spectral inputs for application to the take-off and landing of conventional aeronautical systems and the landing of the Shuttle Orbiter Vehicle. The spectrum $S(\omega)$ is defined so that integration over the domain $0 \leq \omega \leq \infty$ yields the variance of the turbulence. Engineering values of c_i are given in Table 8.3.23 for the longitudinal spectrum and Table 8.3.24 for the lateral spectrum. The constant c_6 can be estimated with the equation

$$c_6 = \frac{0.4}{\ln\left(\frac{z_r}{z_0}\right) - \Psi} , \qquad (8.8)$$

where z_0 is the surface roughness length of the site and Ψ is a parameter that depends upon the stability. If z_0 is not available for a particular site, then an estimate of z_0 can be obtained by taking 10 percent of the typical height of the surface obstructions (grass, shrubs, trees, rocks, etc.) over

TABLE 8.3.25 TYPICAL VALUES OF SURFACE ROUGHNESS LENGTH (z_0) FOR VARIOUS TYPES OF SURFACES

Type of Surface	z_0 (m)	z_0 (ft)
Mud flats, ice	10^{-5} - $3\cdot 10^{-5}$	$3\cdot 10^{-5}$ - 10^{-4}
Smooth sea	$2\cdot 10^{-4}$ - $3\cdot 10^{-4}$	$7\cdot 10^{4}$ - 10^{-3}
Sand	10^{-4} - 10^{-3}	$3\cdot 10^{-4}$ - $3\cdot 10^{-3}$
Snow surface	10^{-3} - $6\cdot 10^{-3}$	$3\cdot 10^{-4}$ - $2\cdot 10^{-2}$
Mown grass $(\sim 0.01$ m$)$	10^{-3} - 10^{-2}	$3\cdot 10^{-3}$ - $3\cdot 10^{-2}$
Low grass, steppe	10^{-2} - $4\cdot 10^{-2}$	$3\cdot 10^{-2}$ - 10^{-1}
Fallow field	$2\cdot 10^{-2}$ - $3\cdot 10^{-2}$	$6\cdot 10^{-2}$ - 10^{-1}
High grass	$4\cdot 10^{-2}$ - 10^{-1}	10^{-1} - $3\cdot 10^{-1}$
Palmetto	10^{-1} - $3\cdot 10^{-1}$	$3\cdot 10^{-1}$ - 1
Suburbia	1 - 2	3 - 6
City	1 - 4	3 - 13

a fetch from the site with length equal to approximately 1500 meters. The parameter Ψ vanishes for strong wind conditions and is of order unity for light wind unstable daytime conditions at the Kennedy Space Center. Typical values of z_0 for various surfaces are given in Table 8.3.25.

The function given by equation (8.3) is depicted in Figures 8.3.6 and 8.3.7. Upon prescribing the steady-state wind profile $u(z)$ and the site (z_0), the longitudinal and lateral spectra are completely specified functions of height z and frequency ω. A discussion of the units of the various parameters mentioned above is given in subsection 8.3.6.4.

8.3.6.3 The Cospectrum and Quadrature Spectrum

The cospectrum and the quadrature spectrum associated with either the longitudinal or lateral components of turbulence at levels z_1 and z_2 can be represented by the following:

$$C(\omega, z_1, z_2) = \sqrt{S_1 S_2}\ \exp\left(-0.3465 \frac{\Delta f}{\Delta f_{0.5}}\right) \cos(2\pi\gamma\Delta f) \qquad (8.9)$$

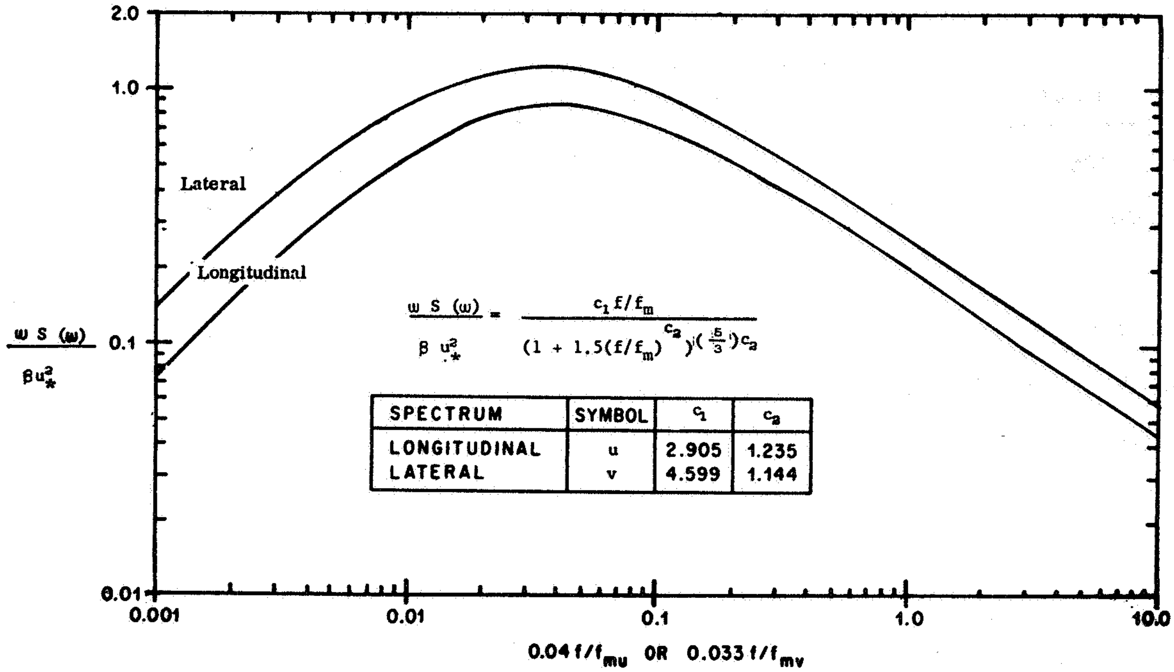

SPECTRUM	SYMBOL	c_1	c_2
LONGITUDINAL	u	2.905	1.235
LATERAL	v	4.599	1.144

FIGURE 8.3.6 $\frac{\omega S(\omega)}{\beta u_*^2}$ VERSUS $\frac{0.04f}{f_m}$ (longitudinal) AND $\frac{0.033f}{f_m}$ (lateral) FOR LIGHT WIND DAYTIME CONDITIONS

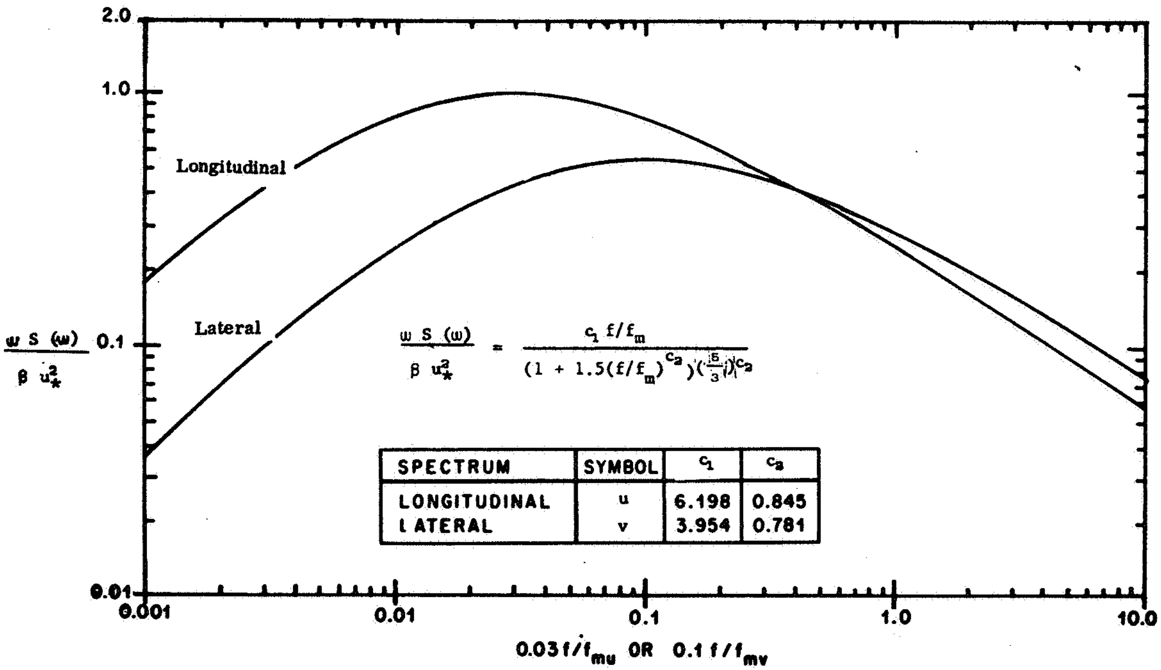

SPECTRUM	SYMBOL	c_1	c_2
LONGITUDINAL	u	6.198	0.845
LATERAL	v	3.954	0.781

FIGURE 8.3.7 $\frac{\omega S(\omega)}{\beta u_*^2}$ VERSUS $\frac{0.03f}{f_m}$ (longitudinal) AND $\frac{0.1f}{f_m}$ (lateral) FOR STRONG WIND CONDITIONS

$$Q(\omega, z_1, z_2) = \sqrt{S_1 S_2} \exp\left(-0.3465 \frac{\Delta f}{\Delta f_{0.5}}\right) \sin(2\pi\gamma\Delta f) \quad , \qquad (8.10)$$

where

$$\Delta f = \frac{\omega z_2}{\bar{u}(z_2)} - \frac{\omega z_1}{\bar{u}(z_1)} \quad . \qquad (8.11)$$

TABLE 8.3.26 VALUES OF $\Delta f_{0.5}$ FOR THE EASTERN TEST RANGE

Turbulence Component	Light Wind Daytime Conditions	Strong Winds
Longitudinal	0.04	0.036
Lateral	0.06	0.045

TABLE 8.3.27 VALUES OF γ FOR THE EASTERN TEST RANGE

Turbulence Component	$(z_1 + z_2)/2 \leq 100$m	$(z_1 + z_2)/2 > 100$m
Longitudinal	0.7	0.3
Lateral	1.4	0.5

The quantities S_1 and S_2 are the longitudinal or lateral spectra at levels z_1 and z_2, respectively, and $\bar{u}(z_1)$ and $\bar{u}(z_2)$ are the steady-state wind speeds at levels z_1 and z_2. The quantity $\Delta f_{0.5}$ is a nondimensional function of stability, and values of this parameter for the Eastern Test Range are given in Table 8.3.26. The nondimensional quantity γ should depend upon height and stability. However, it has only been possible to detect a dependence on height at the Eastern Test Range. Based upon analysis of turbulence data measured at the NASA 150 ground wind facility at the Kennedy Space Center, the values of γ in Table 8.3.27 are suggested for the Eastern Test Range. The quantity $\Delta f_{0.5}$ can be interpreted by constructing the coherence function, which is defined to be

$$\text{coh}(\omega, z_1, z_2) = \frac{C^2 + Q^2}{S_1 S_2} \quad . \qquad (8.12)$$

Substituting equations (8.9) and (8.10) into equation (8.12) yields

$$\text{coh}(\omega, z_1, z_2) = \exp\left(-0.693 \frac{\Delta f}{\Delta f_{0.5}}\right) \qquad (8.13)$$

It is clear from this relationship that $\Delta f_{0.5}$ is that value of Δf for which the coherence (coh) is equal to 0.5.

8.3.6.4 Units

The spectral model of turbulence presented in subsections 8.3.6.2 and 8.3.6.3 is a dimensionless model. Accordingly, the user is free to select the system of units he desires, except that ω must have the units of cycles per unit time. Table 8.3.28 gives the appropriate metric and U. S. customary units for the various quantities in the model.

TABLE 8.3.28 METRIC AND U. S. CUSTOMARY UNITS OF VARIOUS QUANTITIES IN THE TURBULENCE MODEL

Quantity	Metric Units	U. S. Customary Units
ω	Hz	Hz
$S(\omega)$, $Q(\omega)$, $C(\omega)$	$m^2\, s^{-2}/Hz$	$ft^2\, s^{-2}/Hz$
f, f_m, Δf, $\Delta f_{0.5}$	Dimensionless	Dimensionless
z, z_r, z_0	m	ft
u, u_*	ms^{-1}	$ft\, s^{-1}$
β	Dimensionless	Dimensionless
Coh	Dimensionless	Dimensionless
γ	Dimensionless	Dimensionless
Ψ	Dimensionless	Dimensionless

8.3.7 Ground Wind Gust Factors

The gust factor G is defined to be

$$G = \frac{u}{\bar{u}} \tag{8.14}$$

where

u = maximum wind speed at height z within an averaging period of length τ in time

$\bar{u}$ = mean wind speed associated with the averaging period τ, given by

$$\bar{u} = \frac{1}{\tau} \int_0^{\tau} u_i (t)\, dt \tag{8.15}$$

$u_i(t)$ = instantaneous wind speed at time t

t = time reckoned from the beginning of the averaging period.

If $\tau = 0$, then $\bar{u} = u$ according to equation (8.15) and it follows from equation (8.14) that G = 1.0. As τ increases, $\bar{u}$ departs from u, and $\bar{u} \leq u$ and G > 1.0. Also, as τ increases, the probability of finding a maximum wind of a given magnitude increases. In other words, the maximum wind speed increases as τ increases. In the case of $\bar{u} \to 0$ and $u \geq 0$ ($\bar{u} = 0$ might correspond to windless free convection), $G \to \infty$. As $\bar{u}$ or u increases, G tends to decrease for fixed $\tau > 0$; while for very high wind speeds, G tends to approach a constant value for given values of z and τ. Finally, as z increases, G decreases. Thus, the gust factor is a function of the averaging time τ over which the mean wind speed is calculated, the height z, and the wind speed (mean or maximum).

8.3.7.1 Gust Factor as a Function of Peak Wind Speed ($u_{18.3}$) at Reference Height for Cape Kennedy

Investigations (Ref. 8.8) of gust factor data have revealed that the vertical variation of the gust factor can be described with the following relationship:

$$G = 1 + \frac{1}{g_0} \left(\frac{18.3}{z} \right)^p , \tag{8.16}$$

where z is the height in meters above natural grade. The parameter p, a function of the 18.3-meter peak wind speed in meters per second, is given by

$$p = 0.283 - 0.435\, e^{-0.2\, u_{18.3}} . \tag{8.17}$$

The parameter g_0, depends on the averaging time and the 18.3-meter peak wind speed and is given by

$$g_0 = 0.085 \left(\ln \frac{\tau}{10}\right)^2 - 0.329 \left(\ln \frac{\tau}{10}\right) + 1.98 - 1.887\, e^{-0.2\, u_{18.3}} \quad , \qquad (8.18)$$

where τ is given in minutes and, $u_{18.3}$ in meters per second.

These relationships are valid for $u_{18.3} \geq 4$ m/sec and $\tau \leq 10$ min. In the interval 10 min $\leq \tau \leq$ 60 min, G is a slowly increasing monotonic function of τ, and for all engineering purposes the 10-minute gust factor (τ = 10 min) can be used as estimates of the gust factors associated with averaging times greater than 10 minutes and less than 60 minutes (10 min $\leq$ $\tau \leq$ 60 min).

The dependence of the gust factor upon the averaging time and the peak wind speed is shown in Figure 8.3.8. Figure 8.3.9 illustrates the dependence of the 10-minute gust factors upon the peak wind speed and height.

The calculated mean gust factors for 10 minutes for values of $u_{18.3}$ in the interval 4.63 m/sec $\leq u_{18.3} \leq \infty$ are presented in Table 8.3.29 in both the U. S. Customary and Metric units for $u_{18.3}$ and z. As an example, the gust factor profile for τ = 10 minutes and $u_{18.3}$ = 9.27 m/sec (18 knots) is given in Table 8.3.30.

Since the basic wind statistics are given in terms of hourly peak winds, use the τ = 10 minute gust factors to convert the peak winds to mean winds by dividing by G. All gust factors in these sections are expected values for any particular set of values for u, τ, and z.

8.3.7.2 Gust Factors for Other Locations

For design purposes, the gust factor value of 1.4 will be used over all altitudes of the ground wind profile at other test ranges. This gust factor should correspond to approximately a 10-minute averaging period.

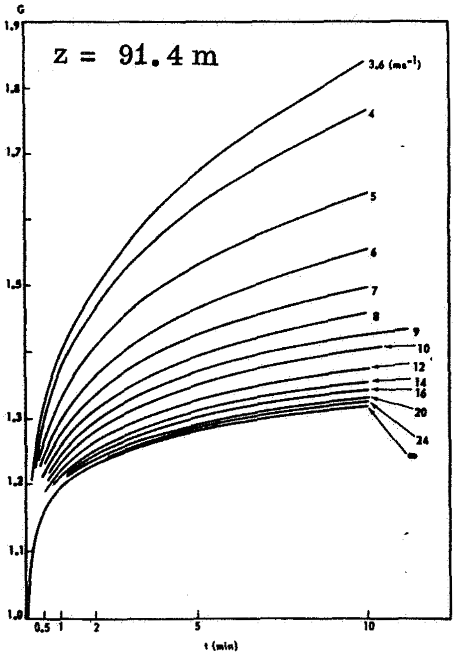

FIGURE 8.3.8 GUST FACTOR AS A FUNCTION OF TIME FOR VARIOUS VALUES OF $u_{18.3}$ IN THE INTERVAL

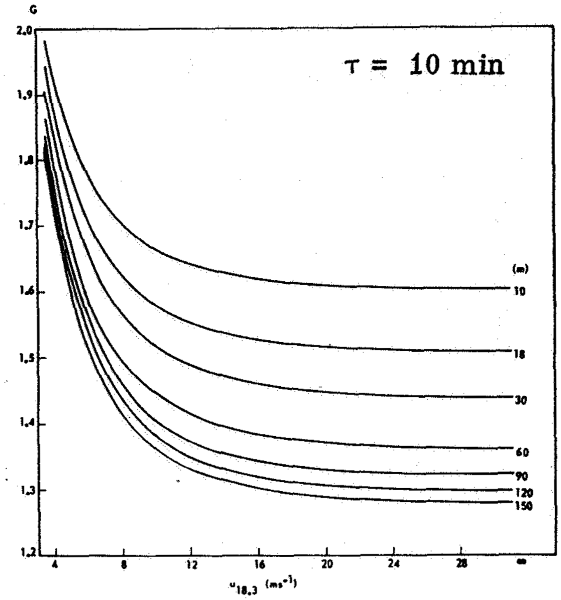

FIGURE 8.3.9 GUST FACTOR AS A FUNCTION OF PEAK WIND (u) FOR VARIOUS HEIGHTS

8.3.8 Ground Wind Shear

Wind shear near the surface, for design purposes, is a shear that acts upon a space vehicle, free-standing on the pad, or at time of lift-off. For overturning moment calculations the wind shear shall be computed by first subtracting the ten-minute mean wind speed at the height corresponding to the base of the vehicle from the peak wind speed at the height corresponding to the top of the vehicle (See Section 8.3.5.5 for mean and peak wind profiles) and then dividing the difference by the distance between the two profiles. The reader should consult References 8.9 through 8.17 for a detailed discussion of the statistical properties of wind shear near the ground for engineering applications.

TABLE 8.3.29 10-min GUST FACTORS FOR KENNEDY SPACE CENTER

60-ft (18.3-m) peak wind kts (ms^{-1})	Height Above Natural Grade in Feet (meters)						
	33 (10.0)	60 (18.3)	100 (30.5)	200 (61.0)	300 (91.4)	400 (121.9)	500 (152.4)
9.0 (4.63)	1.868	1.812	1.767	1.710	1.679	1.658	1.642
10.0 (5.15)	1.828	1.766	1.718	1.657	1.624	1.602	1.585
11.0 (5.66)	1.795	1.729	1.678	1.614	1.580	1.556	1.539
12.0 (6.18)	1.768	1.699	1.645	1.579	1.544	1.520	1.502
13.0 (6.69)	1.746	1.674	1.618	1.550	1.514	1.489	1.471
14.0 (7.21)	1.727	1.652	1.595	1.525	1.488	1.464	1.446
15.0 (7.72)	1.712	1.634	1.576	1.505	1.467	1.442	1.424
16.0 (8.24)	1.698	1.619	1.559	1.487	1.449	1.424	1.406
17.0 (8.75)	1.686	1.606	1.545	1.472	1.434	1.409	1.390
18.0 (9.27)	1.676	1.594	1.532	1.459	1.421	1.395	1.377
19.0 (9.78)	1.668	1.584	1.522	1.447	1.409	1.384	1.365
20.0 (10.30)	1.660	1.575	1.512	1.437	1.399	1.374	1.355
25.0 (12.87)	1.634	1.545	1.480	1.403	1.365	1.339	1.321
30.0 (15.44)	1.619	1.528	1.462	1.385	1.346	1.321	1.302
∞ (∞)	1.599	1.505	1.437	1.359	1.320	1.295	1.277

TABLE 8.3.30 GUST FACTOR PROFILE FOR τ = 10 min AND $u_{18.3}$ = 9.27 m/sec (18 knots)

Height		Gust Factor (G)
(ft)	(m)	
33	10.0	1.676
60	18.3	1.594
100	30.5	1.532
200	61.0	1.459
300	91.4	1.421
400	121.9	1.395
500	152.4	1.377

8.3.9 Ground Wind Direction Characteristics

Figure 8.3.1 (Subsection 8.3.5) shows a time trace of wind direction (section of a wind direction recording chart). This wind direction trace may be visualized as being composed of a mean wind direction plus fluctuations about the mean. An accurate measure of ambient wind direction near the ground is difficult to obtain sometimes because of the interference of the structure that supports the instrumentation and other obstacles in the vicinity of the measurement location (Ref. 8.18). This is particularly true for launch pads, so that care must be exercised in locating wind sensors in order to obtain representative measurements of wind direction.

General information such as that which follows is available and may be used to specify conditions for particular studies. For instance, the variation of wind direction as a function of mean wind speed and height from analysis of NASA's 150 m ground wind tower data at KSC is discussed in Reference 8.2. A graph is shown in Reference 8.2 that gives values of the standard deviation of the wind direction σ_θ as a function of height for a sampling time of about 5 minutes.

8.3.10 Design Winds for Facilities and Ground Support Equipment

8.3.10.1 Introduction

In this section, the important relationships between desired lifetime N, calculated risk U, design return period T_D, and design wind W_D will be described for use in facilities design for several locations.

a. The desired lifetime N is expressed in years, and preliminary estimates must be made as to how many years the proposed facility is to be used.

b. The calculated risk U is a probability expressed either as a percentage or as a decimal fraction. Calculated risk, sometimes referred to as design risk, is a probability measure of the risk the designer is willing to accept that the facility will be destroyed by wind loading in less time than the desired lifetime.

c. The design return period T_D is expressed in years and is a function of desired lifetime and calculated risk.

d. The design wind W_D is a function of the desired lifetime and calculated risk and is derived from the design return period and a probability distribution function of yearly peak winds.

8.3.10.2 Development of Relationships

From the theory of repeated trial probability we can derive the following expression:

$$N = \frac{\ln(1 - U)}{\ln\left(1 - \frac{1}{T_D}\right)} \quad . \tag{8.19}$$

Equation (8.19) gives the important relationships for the three variables, calculated risk U, design return period T_D, and desired lifetime N. If estimates for any two variables are available, the third can be determined from this equation.

Design return period T_D, calculated with equation (8.19), for various values of desired lifetime N and design risk are given in Table 8.3.31. In Table 8.3.31, the exact and adopted values for design return period versus desired lifetime for various design risk are presented. The adopted values for T_D are in some cases greatly oversized to facilitate a convenient use of the tabulated probabilities for the distributions of yearly peak winds.

TABLE 8.3.31 EXACT AND ADOPTED VALUES FOR DESIGN RETURN PERIOD (T_D, years) VERSUS DESIRED LIFETIME (N, years) FOR VARIOUS DESIGN RISKS (U)

N (years)	Design Return Period (years)									
	U = 50%		U = 20%		U = 10%		U = 5%		U = 1%	
	Exact	Adopted	Exact	Adopted	Exact	Adopted	Exact	Adopted	Exact	Adopted
1	2	2	15	5	10	10	20	20	100	100
10	15	15	45	50	95	100	196	200	996	1000
20	29	30	90	100	190	200	390	400	1991	2000
25	37	40	113	125	238	250	488	500		
30	44	50	135	150	285	300	585	600		
50	73	100	225	250	475	500	975	1000		
100	145	150	449	500	950	1000	1950	2000		

8.3.10.3 Design Winds for Facilities at Kennedy Space Center

To obtain the design wind, it is required that the wind speed corresponding to the design return period be determined. Since the design return period is a function of risk, either of two procedures can be used to determine the design wind: One is through a graphical or numerical interpolation procedure; the second is based on an analytical function. A knowledge of the distribution of yearly peak winds is required for both procedures. For the greatest statistical efficiency in arriving at a knowledge of the probability that peak winds will be less than or equal to some specified value of yearly peak winds, the choice of an appropriate probability distribution function is made, and the parameters for the function are estimated from the sample of yearly peak winds. From an investigation leading to the distribution of hourly, daily, monthly, and yearly peaks it was learned that the Gumbel distribution was an excellent fit for the 17 years of yearly peak ground winds at the 10-meter level for Kennedy Space Center. The distribution of yearly peak wind (10-meter level), as obtained by the Gumbel distribution, is tabulated for various percentiles along with the corresponding return periods in Table 8.3.32. The values for the parameters α and μ for this distribution are also given in this table.

The design wind can now be determined by making a choice for desired lifetime and design risk and by taking the design return period from Table 8.3.31 and looking up the wind speed corresponding to the return period given in Table 8.3.32. For combinations not tabulated in Tables 8.3.31 and 8.3.32, the design return period can be interpolated.

8.3.10.4 Procedure to Determine Design Winds for Facilities

The design wind, W_D as a function of desired lifetime, N and calculated risk, U for the Gumbel distribution of peak winds at the 10-meter reference level, can be derived as

$$W_D = \frac{1}{\alpha}\{-\ell n[-\ell n(1-U)] + \ell n\ N\} + \mu \quad , \tag{8.20}$$

where α and μ are estimated from the sample of yearly peak winds.

TABLE 8.3.32 GUMBEL DISTRIBUTION FOR YEARLY PEAK WIND SPEED, 10-m REFERENCE LEVEL, INCLUDING HURRICANE WINDS, KENNEDY SPACE CENTER

Return Period (years)	Probability	y	m/sec	Knots
2	0.50	0.36651	25.45	49.47
5	0.80	1.49994	31.79	61.79
10	0.90	2.25037	35.98	69.95
15	0.933	2.66859	38.33	74.50
20	0.95	2.97020	40.01	77.77
30	0.967	3.39452	42.38	82.39
45	0.978	3.80561	44.68	86.86
50	0.98	3.90191	45.22	87.90
90	0.9889	4.49523	48.54	94.35
100	0.99	4.60015	49.12	95.49
150	0.9933	5.00229	51.37	99.86
200	0.995	5.29581	53.01	103.05
250	0.996	5.51946	54.26	105.48
300	0.9967	5.71218	55.34	107.58
400	0.9975	5.99021	56.90	110.60
500	0.9980	6.21361	58.14	113.02
600	0.9983	6.37628	58.75	114.20
1 000	0.9990	6.90726	62.02	120.56
10 000	0.9999	9.21029	74.90	145.60

$\alpha^{-1} = 5.5917$ m/sec (10.8695 knots) $\quad \mu = 23.4$ m/sec (45.49 knots)

$$\Phi = e^{-e^{-y}}, \quad \text{where} \quad y = \alpha[x-\mu]$$

Taking the values for $\alpha^{-1} = 5.5917$ m/sec (10.8695 knots) and for $\mu = 23.4$ m/sec (45.49 knots) from Table 8.3.32 and evaluation equation (8.20) for selected values of N and U, yields the data in Table 8.3.33.

ORIGINAL PAGE IS
OF POOR QUALITY

TABLE 8.3.33 FACILITY DESIGN WIND $W_{D_{10}}$ WITH RESPECT TO THE 10-m REFERENCE LEVEL PEAK WIND SPEED FOR VARIOUS LIFETIMES (N), KENNEDY SPACE CENTER

U	1 - U	-ln [-ln(1 - U)]	Design Wind ($W_{D_{10}}$) for Various Lifetimes (N) *							
			N = 1		N = 10		N = 30		N = 100	
			(m/sec)	(knots)	(m/sec)	(knots)	(m/sec)	(knots)	(m/sec)	(knots)
0.63212	0.36788	0	23.40	45.49	36.28	70.52	42.42	82.46	49.15	95.55
0.50	0.50	0.36651	25.45	49.47	38.33	74.50	44.47	86.44	51.20	99.53
0.4296	0.5704	0.57722	26.62	51.76	39.50	76.79	45.65	88.73	52.38	101.82
0.40	0.60	0.67173	27.16	52.79	40.03	77.82	46.18	89.76	52.92	102.85
0.30	0.70	1.03093	29.17	56.70	42.04	81.72	48.19	93.67	54.92	106.75
0.20	0.80	1.49994	31.79	61.79	44.66	86.82	50.81	98.76	57.54	111.85
0.10	0.90	2.25037	35.99	69.95	48.86	94.98	55.00	106.92	61.74	120.01
0.05	0.95	2.97020	40.01	77.77	52.88	102.80	59.03	114.74	65.76	127.83
0.01	0.99	4.60016	49.12	95.49	62.00	120.52	68.14	132.46	74.88	145.55

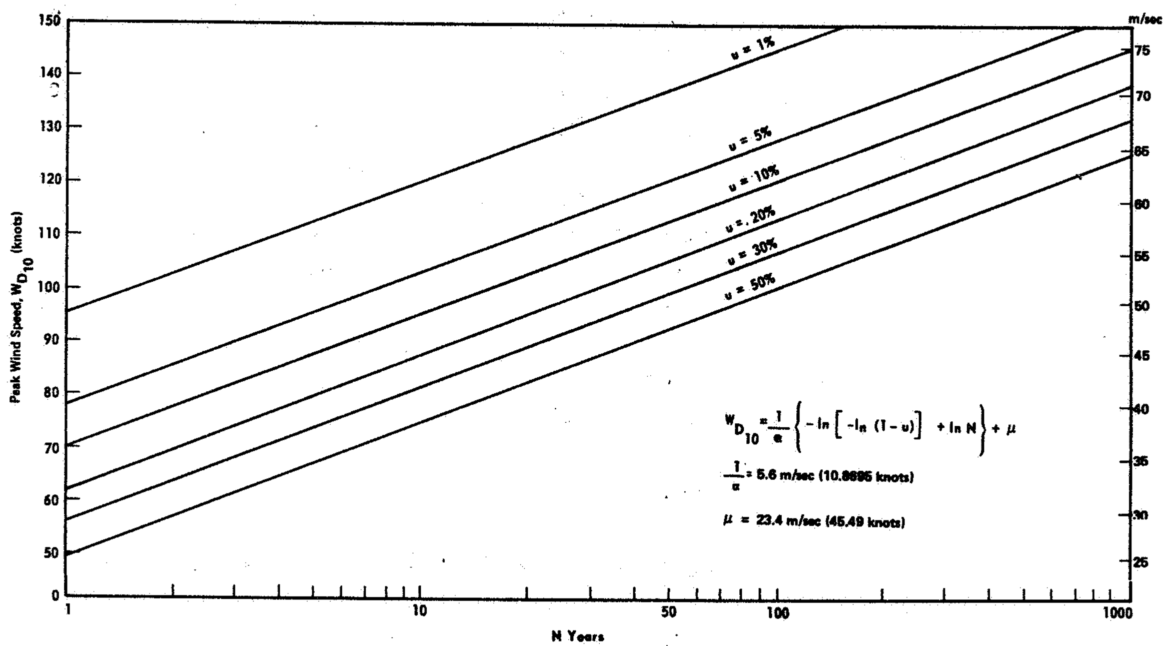

FIGURE 8.3.10 FACILITY DESIGN WIND $W_{D_{10}}$ WITH RESPECT TO THE 10-m REFERENCE LEVEL PEAK WIND SPEED FOR VARIOUS LIFETIMES (N), KENNEDY SPACE CENTER

* Values of N are given in years.

A convenient plot for design wind versus desired lifetime is illustrated in Figure 8.3.10. The slopes of the lines in Figure 8.3.10 are equal.

8.3.10.5 Requirements for Wind Load Calculations

The design wind for a structure cannot be determined solely by wind statistics at a particular height. The design engineer is most interested in designing a structure which satisfies the user's requirements for utility, which will have a small risk of failure within the desired lifetime of the structure, and which can carry a sufficiently large wind load and be constructed at a sufficiently low cost. The total wind loading on a structure is composed of two interrelated components, steady-state drag wind loads and dynamic wind loads (time dependent drag loads, vortex shedding, forces, etc.). The time required for a structure to respond to the drag wind loads dictates the averaging time for the wind profile. In general, the structure response time depends upon the shape and size of the structure. The natural frequency of the structure and the size and shape of the structure and its components are important in estimating the dynamic wind load. It is conceivable that a structure could be designed to withstand very high wind speeds without structural failure and still oscillate in moderate wind speeds. If such a structure, for example, is to be used to support a precision tracking radar, then there may be little danger of overloading the structure by high winds; but the structure might be useless for its intended purpose if it were to oscillate in a moderate wind. Also, a building may have panels or small members that could respond to dynamic loading in such a way that long-term vibrations could cause failure, without any structural failure of the main supporting members. Since dynamic wind loading requires an intricate knowledge of the particular facility and its components, no attempt is made here to state generalized design criteria for dynamic wind loading. The emphasis in this section is upon winds for estimating drag wind loads in establishing design wind criteria for structures. Reference is made to subsection 8.3.5 for information appropriate to dynamic wind loads.

8.3.10.6 Wind Profile Construction

Given the peak wind at the 10-meter level, the peak wind profile can be constructed with the peak wind profile law from subsection 8.3.5. Steady-state wind profiles can be obtained by using appropriate gust factors which are discussed in subsection 8.3.7.

To illustrate the procedures and operations in deriving the wind profile and the application of the gust factor, three examples are worked out for Kennedy Space Center. The peak wind speed at the 10-meter level of 36, 49, and 62 m/sec (70, 95, and 120 knots) have been selected for these examples. These three wind speeds were selected because they correspond to a return period of 10, 100, and 1000 years for a peak wind at the 10-meter level at Kennedy Space Center (see Table 8.3.32). Table 8.3.34 contains the risks of exceeding these peak winds for various values of desired lifetime.

TABLE 8.3.34 CALCULATED RISK (U) VERSUS DESIRED LIFETIME (N, years) FOR ASSIGNED DESIGN WINDS RELATED TO PEAK WINDS AT THE 10-m REFERENCE LEVEL, KENNEDY SPACE CENTER

N (years)	$W_{D_{10}}$ = 36 m/sec (70 knots) T_D = 10 years U%	$W_{D_{10}}$ = 49 m/sec (95 knots) T_D = 100 years U%	$W_{D_{10}}$ = 62 m/sec (120 knots) T_D = 1000 years U%
1	10	1.0	0.1
10	65	10	1
20	88	18	2
25	93	22	2.5
30	95.8	26	3
50	99.5	39.5	5
100	99.997	63.397	10

T_D = Design return period

Table 8.3.35 gives the peak design wind profiles corresponding to the desired lifetimes and calculated risks presented in Table 8.3.34. These profiles were calculated with equation (8.1).

8.3.10.7 Use of Gust Factors Versus Height

In estimating the drag load on a particular structure, it may be determined that wind force of a given magnitude must act on the structure for some period (for example, 1 min) to produce a critical drag load. To obtain the wind profile corresponding to a time averaged wind, the peak wind profile values are divided by the required gust factors. The gust factors for winds greater than 15 m/sec (29 knots) versus height given in Table 8.3.36 are taken from subsection 8.3.7. This operation may seem strange to someone who is accustomed to multiplying the given wind by a gust factor in establishing the design wind. This is because most literature on this subject gives the reference wind as averaged over some time increment (for example, 1, 2, or 5 min) or in terms of the "fastest mile" of wind that has a variable averaging time depending upon the wind speed. The design wind profiles for the three examples, that is, in terms of the peak winds of 36, 49, and 62 m/sec (70, 95, and 120 knots) at the 10-meter level, for various averaging times τ, given in minutes, are illustrated in Tables 8.3.37, 8.3.38, and 8.3.39. Following the procedures presented by this example, the design engineer can objectively derive several important design parameters that can be used in meeting the objective of designing a facility that will (1) meet the requirements for utility and desired lifetime, (2) withstand a sufficiently large wind loading with a known calculated risk of failure, caused by wind loads, and (3) allow him to proceed with trade-off studies between the design parameters and to estimate the cost of building a structure to best meet these design objectives.

8.3.10.8 Recommended Design Risk Versus Desired Lifetime

Unfortunately, there is not a clear-cut precedent from building codes to follow in recommending design risk for a given desired lifetime of a structure. This could be because the consequences of total loss of a structure due to wind forces differ according to the purpose of the structure. Conceivably, a value analysis in terms of original investment cost, replacement cost, safety of property and human life, loss of national prestige, and many other factors could be made to give a measure of the consequences for the loss of a particular structure in arriving at a decision as to what risk management is willing to accept for the loss within the desired lifetime of the structure. If the structure

TABLE 8.3.35 DESIGN[4] PEAK WIND PROFILES FOR DESIGN WIND RELATIVE TO THE 10-m REFERENCE LEVEL, KENNEDY SPACE CENTER

Height		$W_{D_{10}}$ = 36 m/sec (70 knots)		$W_{D_{10}}$ = 49 m/sec (95 knots)		$W_{D_{10}}$ = 62 m/sec (120 knots)	
(ft)	(m)	(knots)	(ms^{-1})	(knots)	(ms^{-1})	(knots)	(ms^{-1})
33	10	70.0	36.0	95.0	48.9	120.0	61.8
60	18.3	74.5	38.4	99.9	51.4	125.2	64.5
100	30.5	78.6	40.4	104.2	53.7	129.8	66.8
200	61.0	84.4	43.4	110.4	56.8	136.2	70.1
300	91.4	88.0	45.3	114.2	58.8	140.2	72.2
400	121.9	90.7	46.7	117.0	60.2	143.0	73.62
500	152.4	92.8	47.8	119.1	61.3	145.3	74.8

TABLE 8.3.36 GUST FACTORS FOR VARIOUS AVERAGING TIMES (τ) FOR PEAK WINDS > 15 m/sec (30 knots) AT THE 10-m REFERENCE LEVEL VERSUS HEIGHT, KENNEDY SPACE CENTER

Height		Various Averaging Times (τ, min)				
(ft)	(m)	τ=0.5	τ=1	τ=2	τ=5	τ=10
33	10	1.318	1.372	1.435	1.528	1.599
60	18.3	1.268	1.314	1.366	1.445	1.505
100	30.5	1.232	1.271	1.317	1.385	1.437
200	61.0	1.191	1.223	1.261	1.316	1.359
300	91.4	1.170	1.199	1.232	1.282	1.320
400	121.9	1.157	1.183	1.214	1.260	1.295
500	152.4	1.147	1.172	1.201	1.244	1.277

4. See Table 8.3.34 for calculated risk values versus desired lifetime for these design winds.

TABLE 8.3.37 DESIGN[5] WIND PROFILES FOR VARIOUS AVERAGING TIMES (τ) FOR PEAK DESIGN WIND OF 36.0 m/sec (70 knots) RELATIVE TO THE 10-m REFERENCE LEVEL, KENNEDY SPACE CENTER

Height		Design Wind Profiles for Various Averaging Times (τ) in minutes											
(ft)	(m)	τ=0		τ=0.5		τ=1		τ=2		τ=5		τ=10	
		(m/sec)	(knots)	(m/sec)	(knots)	(m/sec)	(knots)	(m/sec)	(knots)	(m/sec)	(knots)	(m/sec)	(knots)
33	10	36.0	70.0	27.3	53.1	26.2	51.0	25.1	48.8	23.6	45.8	22.5	43.8
60	18.3	38.3	74.5	30.2	58.8	29.2	56.7	28.0	54.5	26.5	51.6	25.5	49.5
100	30.5	40.4	78.6	32.8	63.8	31.8	61.8	30.7	59.7	29.2	56.8	28.1	54.7
200	61.0	43.4	84.4	36.5	70.9	35.5	69.0	34.4	66.9	33.0	64.1	31.9	62.1
300	91.4	45.3	88.0	38.7	75.2	37.8	73.4	36.7	71.4	35.3	68.6	34.3	66.7
400	121.9	46.7	90.7	40.3	78.4	39.5	76.7	38.4	74.7	37.0	72.0	36.0	70.0
500	152.4	47.7	92.8	41.6	80.9	40.7	79.2	39.8	77.3	38.4	74.6	37.4	72.7

TABLE 8.3.38 DESIGN[5] WIND PROFILES FOR VARIOUS AVERAGING TIMES (τ) FOR PEAK DESIGN WIND OF 49.0 m/sec (95 knots) RELATIVE TO THE 10-m REFERENCE LEVEL, KENNEDY SPACE CENTER

Height		Design Wind Profiles for Various Averaging Times (τ) in minutes											
(ft)	(m)	τ=0		τ=0.5		τ=1		τ=2		τ=5		τ=10	
		(m/sec)	(knots)	(m/sec)	(knots)	(m/sec)	(knots)	(m/sec)	(knots)	(m/sec)	(knots)	(m/sec)	(knots)
33	10	48.9	95.0	37.1	72.1	35.6	69.2	34.1	66.2	32.0	62.2	30.6	59.4
60	18.3	51.4	99.9	40.5	78.8	39.1	76.0	37.6	73.1	35.5	69.1	34.2	66.4
100	30.5	53.6	104.2	43.5	84.6	42.2	82.0	40.7	79.1	38.7	75.2	37.3	72.5
200	61.0	56.8	110.4	47.7	92.7	46.5	90.3	45.0	87.5	43.2	83.9	41.8	81.2
300	91.4	58.7	114.2	50.2	97.6	49.0	95.2	47.7	92.7	45.8	89.1	44.5	86.5
400	121.9	60.2	117.0	52.0	101.1	50.9	98.9	49.6	96.4	47.8	92.9	46.5	90.3
500	152.4	61.3	119.1	53.4	103.8	52.3	101.6	51.0	99.2	49.2	95.7	48.0	93.3

5. See Table 8.3.34 for calculated risk values versus desired lifetime for these design winds.

TABLE 8.3.39 DESIGN WIND[6] PROFILES FOR VARIOUS AVERAGING TIMES (τ) FOR PEAK DESIGN WIND OF 62.0 m/sec (120 knots) RELATIVE TO THE 10-m REFERENCE LEVEL, KENNEDY SPACE CENTER

Height		Design Wind Profiles for Various Averaging Times (τ) in minutes											
(ft)	(m)	τ=0		τ=0.5		τ=1		τ=2		τ=5		τ=10	
		(m/sec)	(knots)	(m/sec)	(knots)	(m/sec)	(knots)	(m/sec)	(knots)	(m/sec)	(knots)	(m/sec)	(knots)
33	10	61.7	120.0	46.8	91.0	45.0	87.5	43.0	83.6	40.4	78.5	38.6	75.0
60	18.3	64.4	125.2	50.8	98.7	49.0	95.3	47.2	91.7	44.6	86.6	42.8	83.2
100	30.5	66.8	129.8	54.2	105.4	52.5	102.1	50.7	98.6	48.2	93.7	46.5	90.3
200	61.0	70.1	136.2	58.9	114.4	57.3	111.4	55.6	108.0	53.2	103.5	51.5	100.2
300	91.4	72.1	140.2	61.6	119.8	60.1	116.9	58.5	113.8	56.3	109.4	54.6	106.2
400	121.9	73.6	143.0	63.6	123.6	62.2	120.9	60.6	117.8	58.4	113.5	56.8	110.4
500	152.4	74.7	145.3	65.2	126.7	63.8	124.0	62.2	121.0	60.1	116.8	58.5	113.8

is an isolated shed then obviously its loss is not as great as a structure that would house many people or a structure that is critical to the mission of a large organization; nor is it as potentially unsafe as the loss of a nuclear power plant or storage facility for explosives or highly radioactive materials. To give a starting point for design studies aimed at meeting the design objectives, it is recommended that a design risk of 10 percent for the desired lifetime be used in determining the wind loading on structures that have a high replacement cost. Should the loss of the structure be extremely hazardous to life or property, or critical to the mission of a large organization, then a design risk of five percent or less for the desired lifetime is recommended. These are subjective recommendations involving arbitrary assumptions about the design objectives. Note that the larger the desired lifetime, the greater the design risk is for a given wind speed (or wind loading). Therefore, realistic appraisals should be made for desired lifetimes.

8.3.10.9 Design Winds for Facilities at The Space and Missile Test Center, (Vandenberg AFB), Wallops Flight Center, White Sands Missile Range, Edwards Air Force Base, New Orleans,[7] and Huntsville

8.3.10.9.1 The Wind Statistics

The basic wind statistics for these five locations are taken from Reference 8.19, which presents isotach maps for the United States for the

6. See Table 8.3.34 for calculated risk values versus desired lifetime for these design winds.

7. Includes National Space Technology Laboratory, Bay St. Louis, Mississippi.

50, 98, and 99 percentile values for the yearly maximum "fastest mile" of wind at the 30-foot (~ 10-m) reference height above natural grade. By definition, the fastest mile is the fastest wind speed in miles per hour of any mile of wind during a specified period (usually taken as the 24-hour observational day), and the largest of these in a year for the period of record constitutes the statistical sample of yearly fastest mile. From this definition, it is noted that the fastest mile as a measure of wind speed has a variable averaging time; for example, if the wind speed is 60 miles per hour, the averaging time for the fastest mile of wind is 1 minute. For a wind speed of 120 miles per hour, the averaging time for the fastest mile of wind is 0.5 minute. Thom reports that the Fréchet probability distribution function fits his samples of fastest mile very well. The Fréchet distribution function is given as

$$F(x) = e^{-\left(\frac{x}{\beta}\right)^{-\gamma}} \tag{8.21}$$

where the two parameters β and γ are estimated from the sample by the maximum likelihood method. From Thom's maps of the 50, 98, and 99 percentiles of fastest mile of wind for yearly extremals, we have estimated (interpolated) for these percentiles for the five locations and calculated the values for the parameters β and γ for the Fréchet distribution function and computed several additional percentiles, as shown in Table 8.3.40. To have units consistent with the other sections of this document, the percentiles and the parameters β and γ have been converted from miles per hour to knots and m/sec. Thus, Table 8.3.40 gives the Fréchet distribution for the fastest mile of winds at the 30-foot (~10-m) level for the five locations with the units in knots and m/sec.

The discussion in subsection 8.3.10.2.4, devoted to desired lifetime, calculated risk, and design winds with respect to the wind statistics at a particular height (10-m level) is applicable here, except that the reference statistics are with respect to the fastest mile converted to knots and m/sec.*

8.3.10.9.2 Conversion of Fastest Mile to Peak Winds

It was mentioned in subsection 8.3.10.3 that the Fréchet distribution for the 17-year sample of yearly peak winds for Kennedy Space Center was an acceptable fit to this sample. The Fréchet distributions for the fastest mile were obtained from Thom's analysis for Kennedy Space Center. From these two distributions (the Fréchet for the peak winds as well as for the fastest mile), the ratio of the percentiles of the fastest mile to the peak winds were taken. This ratio varied from 1.12 to 1.09, over the range of probabilities from 30 to 99 percent. Thus we adopted 1.10 as a factor to multiply the statistics of the

* Also see paper by H. C. S. Thom, "Distributions of Extreme Winds over Oceans." J. Waterways, Harbors and Coastal Engr. Div., Proc. Am. Soc. Civ. Engr., February 1973, pp. 1-17.

TABLE 8.3.40 FRECHET DISTRIBUTION OF FASTEST MILE WIND AT THE 10-m HEIGHT OF YEARLY EXTREMES FOR THE INDICATED STATIONS

P Probability	T_D Return Period (years)	Fastest Mile Wind									
		Huntsville		New Orleans		Space and Missile Test Center *		Wallops Flight Center		Edwards AFB	
		(m/sec)	(knots)	(m/sec)	(knots)	(m/sec)	(knots)	(m/sec)	(knots)	(m/sec)	(knots)
0.50	2	20.1	39.0	22.1	42.9	18.0	34.9	24.6	47.9	11.3	22.0
0.80	5	23.9	46.4	26.6	51.8	21.6	42.0	29.6	57.6	15.0	29.1
0.90	10	26.8	52.0	30.1	58.6	24.4	47.4	33.4	65.0	18.1	35.2
0.95	20	29.8	58.0	33.9	65.9	27.4	53.3	37.6	73.0	21.6	42.0
0.98	50	34.5	67.0	39.6	76.9	31.8	61.9	43.7	84.9	27.3	53.0
0.99	100	38.3	74.4	44.4	86.4	35.7	69.4	48.9	95.0	32.4	63.1
0.9933	150	40.7	79.2	47.4	92.2	38.0	73.9	52.2	101.4	35.1	68.3
0.995	200	42.3	82.2	49.7	96.7	39.9	77.6	54.7	106.3	38.6	75.0
0.996	250	44.1	85.7	51.6	100.4	41.4	80.4	56.7	110.2	40.8	79.3
0.99667	300	45.4	88.2	53.2	103.5	42.6	82.9	58.4	113.6	42.7	83.1
0.9975	400	47.4	92.1	55.8	108.4	44.6	86.7	61.2	118.9	45.8	89.1
0.998	500	49.0	95.3	57.9	112.5	46.2	89.9	63.4	123.2	48.5	94.2
0.99833	600	50.2	97.6	59.4	115.5	47.5	92.3	65.1	126.6	50.5	98.1
0.99875	800	52.7	102.4	62.6	121.6	50.3	97.7	68.4	133.0	54.0	105.0
0.999	1000	54.5	106.0	64.9	126.1	51.8	100.6	70.9	137.8	57.6	111.9
γ	Unitless	6.54686		6.08075		6.19591		6.19949		4.02093	
$1/\gamma$	Unitless	0.15274		0.16445		0.16140		0.16130		0.24870	
$\ln \beta$	Unitless	3.60758		3.70093		3.49620		3.81208		2.99989	
β	m/sec (knots)	18.979 (36.892)		20.829 (40.488)		16.968 (32.983)		23.274 (45.241)		10.322 (20.065)	

* Vandenberg AFB, California.

fastest mile of wind to obtain peak (instantaneous) wind statistics. This procedure is based on the evidence of only one station. A gust factor of 1.10 is often applied to the fastest mile statistics in facility design work to account for gust loads.

8.3.10.9.3 The Peak Wind Profile

The peak wind profile law adopted for the five locations for peak winds at the 10-meter level greater than 22.6 m/sec (44 knots) is

$$u = u_{10}\left(\frac{z}{10}\right)^{1/7} \tag{8.22}$$

where u_{10} is the peak wind at the 10-meter height and u is the peak wind at height z in meters.

8.3.10.9.4 The Mean Wind Profile

To obtain the mean wind profile for various averaging times, the gust factors given in subsection 8.3.7, are applied to the peak wind profile as determined by equation (8.22).

8.3.10.9.5 Design Wind Profiles for Six Station Locations

The design peak wind profiles for the peak winds in Table 8.3.41 are obtained from the adopted peak wind power law given by equation (8.22), and the mean wind profile for various averaging times are obtained by dividing by the gust factors for the various averaging times. (The gust factors versus height and averaging times are presented in Table 8.3.36.) The resulting selected design wind profiles for design return periods of 10, 100, and 1000 years for the five stations are given in Tables 8.3.42 through 8.3.56, in which values of τ are given in minutes. The design risk versus desired lifetime for the design return periods of 10, 100, and 1000 years is presented in Table 8.3.34.

8.3.11 Runway Orientation Optimization

Runway orientation is influenced by a number of factors; for example winds, terrain features, population interference, etc. In some cases the frequency of occurrence of crosswind components of some significant speed have received insufficient consideration. Aligning the runway with the prevailing wind will not insure that crosswinds will be minimized. In fact, two common synoptic situations (one producing light easterly winds, and the other causing strong northerly winds)

TABLE 8.3.41 PEAK WINDS (fastest mile values times 1.10) FOR THE 10-m REFERENCE LEVEL FOR 10-, 100-, and 1000-YEAR RETURN PERIODS

T_D (years)	Peak Winds									
	Huntsville		New Orleans		SAMTEC * and White Sands		Wallops Flight Center		Edwards AFB	
	(m/sec)	(knots)	(m/sec)	(knots)	(m/sec)	(knots)	(m/sec)	(knots)	(m/sec)	(knots)
10	29.4	57.2	33.2	64.5	26.8	52.1	36.8	71.5	19.9	38.7
100	42.1	81.8	48.9	95.0	39.3	76.3	53.8	104.5	35.7	69.4
1000	60.0	116.6	71.4	138.7	56.9	110.7	78.0	151.6	63.4	123.2

TABLE 8.3.42 FACILITIES DESIGN WIND AS A FUNCTION OF AVERAGING TIME (τ) FOR A PEAK WIND OF 29.4 m/sec (57.2 knots) (10-year return period) FOR HUNTSVILLE, ALABAMA

Height		Facilities Design Wind as a Function of Averaging Time (τ) in minutes											
(ft)	(m)	τ=0 (peak)		τ=0.5		τ=1		τ=2		τ=5		τ=10	
		(m/sec)	(knots)	(m/sec)	(knots)	(m/sec)	(knots)	(m/sec)	(knots)	(m/sec)	(knots)	(m/sec)	(knots)
33	10	29.4	57.2	22.3	43.4	21.5	41.7	20.5	39.9	19.2	37.4	18.4	35.8
60	18.3	32.1	62.4	25.3	49.2	24.4	47.5	23.5	45.7	22.2	43.2	21.3	41.5
100	30.5	34.5	67.1	28.0	54.5	27.2	52.8	26.2	50.9	24.9	48.4	24.0	46.7
200	61.0	38.1	74.1	32.0	62.2	31.2	60.6	30.2	58.8	29.0	56.3	28.0	54.5
300	91.4	40.4	78.5	34.5	67.1	33.7	65.5	32.8	63.7	31.5	61.2	30.6	59.5
400	121.9	42.1	81.8	36.4	70.7	31.2	60.7	34.7	67.4	33.4	64.9	32.5	63.2
500	152.4	43.0	83.6	37.5	72.9	36.7	71.3	35.8	69.6	34.6	67.2	33.7	65.5

* Vandenberg AFB, California.

TABLE 8.3.43 FACILITIES DESIGN WIND AS A FUNCTION OF AVERAGING TIME (τ) FOR A PEAK WIND OF 42.1 m/sec (81.8 knots) (100-year return period) FOR HUNTSVILLE, ALABAMA

Height		Facilities Design Wind as a Function of Averaging Time (τ) in minutes											
(ft)	(m)	τ=0 (peak)		τ=0.5		τ=1		τ=2		τ=5		τ=10	
		(m/sec)	(knots)	(m/sec)	(knots)	(m/sec)	(knots)	(m/sec)	(knots)	(m/sec)	(knots)	(m/sec)	(knots)
33	10	42.1	81.8	31.9	62.1	30.7	59.6	29.3	57.0	27.5	53.5	26.3	51.2
60	18.3	45.9	89.2	36.2	70.3	34.9	67.9	33.6	65.3	31.7	61.7	30.5	59.3
100	30.5	49.3	95.9	40.0	77.8	38.8	75.5	37.5	72.8	35.6	69.2	34.3	66.7
200	61.0	54.5	105.9	45.7	88.9	44.6	86.6	43.2	84.0	41.4	80.5	40.1	77.9
300	91.4	57.7	112.2	49.3	95.9	48.2	93.6	46.9	91.1	45.0	87.5	43.7	85.0
400	121.9	59.9	116.5	51.8	100.7	50.7	98.5	49.4	96.0	47.6	92.5	46.3	90.0
500	152.4	61.5	119.5	53.6	104.2	52.5	102.0	51.2	99.5	49.4	96.1	48.2	93.6

TABLE 8.3.44 FACILITIES DESIGN WIND AS A FUNCTION OF AVERAGING TIME (τ) FOR A PEAK WIND OF 60.0 m/sec (116.6 knots) (1000-year return period) FOR HUNTSVILLE, ALABAMA

Height		Facilities Design Wind as a Function of Averaging Time (τ) in minutes											
(ft)	(m)	τ=0 (peak)		τ=0.5		τ=1		τ=2		τ=5		τ=10	
		(m/sec)	(knots)	(m/sec)	(knots)	(m/sec)	(knots)	(m/sec)	(knots)	(m/sec)	(knots)	(m/sec)	(knots)
33	10	60.0	116.6	45.5	88.5	43.7	85.0	41.8	81.3	39.2	76.3	37.5	72.9
60	18.3	65.3	127.0	51.5	100.2	49.7	96.7	47.8	93.0	45.2	87.9	43.[illegible]	84.4
100	30.5	70.3	136.6	57.1	110.9	55.3	107.5	53.3	103.7	50.7	98.6	48.9	95.1
200	61.0	77.6	150.8	65.1	126.6	63.4	123.3	61.5	119.6	59.0	114.6	57.1	111.0
300	91.4	82.2	159.8	70.3	136.6	68.6	133.3	66.7	129.7	64.1	124.6	62.3	121.1
400	121.9	85.7	166.5	74.0	143.9	72.4	140.7	70.5	137.1	68.0	132.1	66.2	128.6
500	152.4	88.4	171.9	77.1	149.9	75.5	146.7	73.6	143.1	71.1	138.2	69.2	134.6

TABLE 8.3.45 FACILITIES DESIGN WIND AS A FUNCTION OF AVERAGING TIME (τ) FOR A PEAK WIND OF 33.2 m/sec (64.5 knots) (10-year return period) FOR NEW ORLEANS

Height		Facilities Design Wind as a Function of Averaging Time (τ) in minutes											
(ft)	(m)	τ=0 (peak)		τ=0.5		τ=1		τ=2		τ=5		τ=10	
		(m/sec)	(knots)	(m/sec)	(knots)	(m/sec)	(knots)	(m/sec)	(knots)	(m/sec)	(knots)	(m/sec)	(knots)
33	10	33.2	64.5	25.2	48.9	24.2	47.0	23.1	44.9	21.7	42.2	20.7	40.3
60	18.3	36.2	70.3	28.5	55.4	27.5	53.5	26.5	51.5	25.1	48.7	24.0	46.7
100	30.5	38.9	75.6	31.6	61.4	30.6	59.5	29.5	57.4	28.1	54.6	27.1	52.6
200	61.0	43.0	83.5	36.1	70.1	35.1	68.3	34.1	66.2	32.6	63.4	31.6	61.4
300	91.4	45.5	88.5	38.9	75.6	38.0	73.8	36.9	71.8	35.5	69.0	34.5	67.0
400	121.9	47.4	92.2	41.0	79.7	40.1	77.9	39.0	75.9	37.7	73.2	36.6	71.2
500	152.4	48.5	94.3	42.3	82.2	41.4	80.5	40.4	78.5	39.0	75.8	38.0	73.8

TABLE 8.3.46 FACILITIES DESIGN WIND AS A FUNCTION OF AVERAGING TIME (τ) FOR A PEAK WIND OF 48.9 m/sec (95.0 knots) (100-year return period) FOR NEW ORLEANS

Height		Facilities Design Wind as a Function of Averaging Time (τ) in minutes											
(ft)	(m)	τ=0 (peak)		τ=0.5		τ=1		τ=2		τ=5		τ=10	
		(m/sec)	(knots)	(m/sec)	(knots)	(m/sec)	(knots)	(m/sec)	(knots)	(m/sec)	(knots)	(m/sec)	(knots)
33	10	48.9	95.0	37.1	72.1	35.6	69.2	34.1	66.2	32.0	62.2	30.6	59.4
60	18.3	53.3	103.6	42.0	81.7	40.5	78.8	39.0	75.8	36.9	71.7	35.4	68.8
100	30.5	57.3	111.4	46.5	90.4	45.1	87.6	43.5	84.6	41.4	80.4	40.8	79.3
200	61.0	63.3	123.0	53.1	103.3	51.8	100.6	50.2	97.5	48.1	93.5	46.6	90.5
300	91.4	67.0	130.3	57.3	111.4	55.9	108.7	54.4	105.8	52.3	101.6	50.8	98.7
400	121.9	69.9	135.8	60.4	117.4	59.1	114.8	57.6	111.9	55.5	107.8	54.0	104.9
500	152.4	71.4	138.8	62.2	121.0	60.9	118.4	59.5	115.6	57.4	111.6	55.9	108.7

TABLE 8.3.47 FACILITIES DESIGN WIND AS A FUNCTION OF AVERAGING TIME (τ) FOR A PEAK WIND OF 71.4 m/sec (138.7 knots) (1000-year return period) FOR NEW ORLEANS

Height		Facilities Design Wind as a Function of Averaging Time (τ) in minutes											
(ft)	(m)	τ=0 (peak)		τ=0.5		τ=1		τ=2		τ=5		τ=10	
		(m/sec)	(knots)	(m/sec)	(knots)	(m/sec)	(knots)	(m/sec)	(knots)	(m/sec)	(knots)	(m/sec)	(knots)
33	10	71.4	138.7	54.1	105.2	52.0	101.1	49.7	96.7	46.7	90.8	44.6	86.7
60	18.3	77.8	151.2	61.3	119.2	59.2	115.1	56.9	110.7	53.8	104.6	51.7	100.5
100	30.5	83.7	162.7	68.0	132.1	65.8	128.0	63.5	123.5	60.4	117.5	58.2	113.2
200	61.0	92.4	179.6	77.6	150.8	75.6	146.9	73.3	142.4	70.2	136.5	68.0	132.2
300	91.4	97.9	190.3	83.6	162.6	81.6	158.7	79.5	154.5	76.3	148.4	74.2	144.2
400	121.9	102.0	198.2	88.1	171.3	86.2	167.5	84.0	163.3	80.9	157.3	78.8	153.1
500	152.4	104.3	202.7	90.9	176.7	89.0	173.0	86.8	168.8	83.8	162.9	81.6	158.7

TABLE 8.3.48 FACILITIES DESIGN WIND AS A FUNCTION OF AVERAGING TIME (τ) FOR A PEAK WIND OF 26.8 m/sec (52.1 knots) (10-year return period) FOR THE SPACE AND MISSILE TEST CENTER AND WHITE SANDS MISSILE RANGE

Height		Facilities Design Wind as a Function of Averaging Time (τ) in minutes											
(ft)	(m)	τ=0 (peak)		τ=0.5		τ=1		τ=2		τ=5		τ=10	
		(m/sec)	(knots)	(m/sec)	(knots)	(m/sec)	(knots)	(m/sec)	(knots)	(m/sec)	(knots)	(m/sec)	(knots)
33	10	26.8	52.1	20.3	39.5	19.5	38.0	18.7	36.3	17.5	34.1	16.8	32.6
60	18.3	29.2	56.8	23.0	44.8	22.2	43.2	21.4	41.6	20.2	39.3	19.4	37.7
100	30.5	31.4	61.1	25.5	49.6	24.7	48.1	23.9	46.4	22.7	44.1	21.9	42.5
200	61.0	34.7	67.5	29.2	56.7	28.4	55.2	27.5	53.5	26.4	51.3	25.6	49.7
300	91.4	36.8	71.5	31.4	61.1	30.7	59.6	29.8	58.0	28.7	55.8	27.9	54.2
400	121.9	38.3	74.5	33.1	64.4	32.4	63.0	31.6	61.4	30.4	59.1	29.6	57.5
500	152.4	39.1	76.1	34.1	66.3	33.4	64.9	32.6	63.3	31.5	61.2	30.7	59.6

ORIGINAL PAGE IS OF POOR QUALITY

TABLE 8.3.49 FACILITIES DESIGN WIND AS A FUNCTION OF AVERAGING TIME (τ) FOR A PEAK WIND OF 39.3 m sec (76.3 knots) (100-year return period) FOR THE SPACE AND MISSILE TEST CENTER AND WHITE SANDS MISSILE RANGE

Height		Facilities Design Wind as a Function of Averaging Time (τ) in minutes											
(ft)	(m)	τ=0 (peak)		τ=0.5		τ=1		τ=2		τ=5		τ=10	
		(m/sec)	(knots)	(m/sec)	(knots)	(m/sec)	(knots)	(m/sec)	(knots)	(m/sec)	(knots)	(m/sec)	(knots)
33	10	39.3	76.3	29.8	57.9	28.6	55.6	27.4	53.2	25.7	49.9	24.5	47.7
60	18.3	42.8	83.2	33.7	65.6	32.6	63.3	31.3	60.9	29.6	57.6	28.4	55.3
100	30.5	46.0	89.5	37.3	72.6	36.2	70.4	35.0	68.0	33.2	64.6	32.0	62.3
200	61.0	50.8	98.8	42.7	83.0	41.6	80.8	40.3	78.4	38.6	75.1	37.4	72.7
300	91.4	53.9	104.7	46.0	89.5	44.9	87.3	43.7	85.0	42.0	81.7	40.8	79.3
400	121.9	56.1	109.1	48.5	94.3	47.4	92.2	46.2	89.9	44.6	86.6	43.3	84.2
500	152.4	57.4	111.5	50.0	97.2	48.9	95.1	47.7	92.8	46.1	89.6	44.9	87.3

TABLE 8.3.50 FACILITIES DESIGN WIND AS A FUNCTION OF AVERAGING TIME (τ) FOR A PEAK WIND OF 56.9 m/sec (110.7 knots) (1000-year return period) FOR THE SPACE AND MISSILE TEST CENTER AND WHITE SANDS MISSILE RANGE

Height		Facilities Design Wind as a Function of Averaging Time (τ) in minutes											
(ft)	(m)	τ=0 (peak)		τ=0.5		τ=1		τ=2		τ=5		τ=10	
		(m/sec)	(knots)	(m/sec)	(knots)	(m/sec)	(knots)	(m/sec)	(knots)	(m/sec)	(knots)	(m/sec)	(knots)
33	10	56.9	110.7	43.2	84.0	41.5	80.7	39.7	77.1	37.2	72.4	35.6	69.2
60	18.3	62.1	120.7	49.0	95.2	47.3	91.9	45.5	88.4	43.0	83.5	41.3	80.2
100	30.5	66.8	129.8	54.2	105.4	52.5	102.1	50.7	98.6	48.2	93.7	46.5	90.3
200	61.0	73.7	143.3	61.9	120.3	60.3	117.2	58.4	113.6	56.0	108.9	54.2	105.4
300	91.4	78.1	151.9	66.8	129.8	65.2	126.7	63.4	123.3	61.0	118.5	59.2	115.1
400	121.9	81.4	158.2	70.3	136.7	68.8	133.7	67.0	130.3	64.6	125.6	62.9	122.2
500	152.4	83.2	161.8	72.6	141.1	71.0	138.1	69.3	134.7	66.9	130.1	65.2	126.7

TABLE 8.3.51 FACILITIES DESIGN WIND AS A FUNCTION OF AVERAGING TIME (τ) FOR A PEAK WIND OF 36.8 m/sec (71.5 knots) (10-year return period) FOR WALLOPS FLIGHT CENTER

Height		Facilities Design Wind as a Function of Averaging Time (τ) in minutes											
(ft)	(m)	τ=0 (peak)		τ=0.5		τ=1		τ=2		τ=5		τ=10	
		(m/sec)	(knots)	(m/sec)	(knots)	(m/sec)	(knots)	(m/sec)	(knots)	(m/sec)	(knots)	(m/sec)	(knots)
33	10	36.8	71.5	27.9	54.2	26.8	52.1	25.6	49.8	24.1	46.8	23.0	44.7
60	18.3	40.1	77.9	31.6	61.4	30.5	59.3	29.3	57.0	27.7	53.9	26.6	51.8
100	30.5	43.1	83.8	35.0	68.0	33.9	65.9	32.7	63.6	31.1	60.5	30.0	58.3
200	61.0	47.6	92.6	40.0	77.7	38.9	75.7	37.8	73.4	36.2	70.4	35.0	68.1
300	91.4	50.5	98.1	43.1	83.8	42.1	81.8	40.9	79.6	39.4	76.5	38.2	74.3
400	121.9	52.6	102.2	45.4	88.3	44.4	86.4	43.3	84.2	41.7	81.1	40.6	78.9
500	152.4	53.8	104.5	46.9	91.1	45.9	89.2	44.8	87.0	43.2	84.0	42.1	81.8

TABLE 8.3.52 FACILITIES DESIGN WIND AS A FUNCTION OF AVERAGING TIME (τ) FOR A PEAK WIND OF 53.8 m/sec (104.5 knots) (100-year return period) FOR WALLOPS FLIGHT CENTER

Height		Facilities Design Wind as a Function of Averaging Time (τ) in minutes											
(ft)	(m)	τ=0 (peak)		τ=0.5		τ=1		τ=2		τ=5		τ=10	
		(m/sec)	(knots)	(m/sec)	(knots)	(m/sec)	(knots)	(m/sec)	(knots)	(m/sec)	(knots)	(m/sec)	(knots)
33	10	53.8	104.5	40.8	79.3	39.2	76.2	37.5	72.8	35.2	68.4	33.6	65.4
60	18.3	58.6	113.9	46.2	89.8	44.6	86.7	42.9	83.4	40.5	78.8	38.9	75.7
100	30.5	63.0	122.5	51.1	99.4	49.6	96.4	47.8	93.0	45.5	88.4	43.8	85.2
200	61.0	69.6	135.3	58.4	113.6	56.9	110.6	55.2	107.3	52.9	102.8	51.2	99.6
300	91.4	73.8	143.4	63.1	122.6	61.5	119.6	59.9	116.4	57.6	111.9	55.9	108.6
400	121.9	76.9	149.4	66.4	129.1	65.0	126.3	63.3	123.1	61.0	118.6	59.4	115.4
500	152.4	78.6	152.7	68.5	133.1	67.0	130.3	65.4	127.1	63.1	122.7	61.5	119.6

TABLE 8.3.53 FACILITIES DESIGN WIND AS A FUNCTION OF AVERAGING TIME (τ) FOR A PEAK WIND OF 78.0 m/sec (151.6 knots) (1000-year return period) FOR WALLOPS FLIGHT CENTER

Height		Facilities Design Wind as a Function of Averaging Time (τ) in minutes											
(ft)	(m)	τ=0 (peak)		τ=0.5		τ=1		τ=2		τ=5		τ=10	
		(m/sec)	(knots)	(m/sec)	(knots)	(m/sec)	(knots)	(m/sec)	(knots)	(m/sec)	(knots)	(m/sec)	(knots)
33	10	78.0	151.6	59.2	115.0	56.8	110.5	54.3	105.6	51.0	99.2	48.8	94.8
60	18.3	85.0	165.3	67.1	130.4	64.7	125.8	62.2	121.0	58.9	114.4	56.5	109.8
100	30.5	91.5	177.8	74.2	144.3	72.0	139.9	69.4	135.0	66.1	128.4	63.6	123.7
200	61.0	101.0	196.3	84.8	164.8	82.6	160.5	80.1	155.7	76.8	149.2	74.3	144.4
300	91.4	107.0	208.0	91.5	177.8	89.3	173.5	86.9	168.9	83.4	162.2	81.1	157.6
400	121.9	111.5	216.7	96.4	187.3	94.2	183.2	91.8	178.5	88.5	172.0	86.1	167.3
500	152.4	113.9	221.5	99.3	193.1	97.2	189.0	94.9	184.4	91.6	178.1	89.3	173.5

TABLE 8.3.54 FACILITIES DESIGN WIND AS A FUNCTION OF AVERAGING TIME (τ) FOR A PEAK WIND OF 19.9 m/sec (38.7 knots) (10-year return period) FOR EDWARDS AFB

Height		Facilities Design Wind as a Function of Averaging Time (τ) in minutes											
(ft)	(m)	τ=0 (peak)		τ=0.5		τ=1		τ=2		τ=5		τ=10	
		(knots)	(m/sec)	(knots)	(m/sec)	(knots)	(m/sec)	(knots)	(m/sec)	(knots)	(m/sec)	(knots)	(m/sec)
33	10	38.7	19.9	29.4	15.1	28.2	14.5	27.0	13.9	25.3	13.0	24.2	12.4
60	18.3	42.1	21.7	33.2	17.1	32.0	16.5	30.8	15.8	29.1	15.0	28.0	14.4
100	30.5	45.1	23.2	36.6	18.8	35.5	18.3	34.2	17.6	32.6	16.8	31.4	16.2
200	61.0	50.1	25.8	42.1	21.7	41.0	21.1	39.7	20.4	38.1	19.6	36.9	19.0
300	91.4	53.1	27.3	45.4	23.4	44.3	22.8	43.1	22.2	41.4	21.3	40.2	20.7
400	121.9	55.3	28.4	47.8	24.6	46.7	24.0	45.6	23.5	43.9	22.6	42.7	22.0
500	152.4	57.1	29.4	49.8	25.6	48.7	25.1	47.5	24.4	45.9	23.6	44.7	23.0

TABLE 8.3.55 FACILITIES DESIGN WIND AS A FUNCTION OF AVERAGING TIME (τ) FOR A PEAK WIND OF 35.7 m/sec (69.4 knots) (100-year return period) FOR EDWARDS AFB

Height		Facilities Design Wind as a Function of Averaging Time (τ) in minutes											
(ft)	(m)	τ=0 (peak)		τ=0.5		τ=1		τ=2		τ=5		τ=10	
		(knots)	(m/sec)	(knots)	(m/sec)	(knots)	(m/sec)	(knots)	(m/sec)	(knots)	(m/sec)	(knots)	(m/sec)
33	10	69.4	35.7	52.7	27.1	50.6	26.0	48.4	24.9	45.4	23.4	43.4	22.3
60	18.3	75.5	38.8	59.5	30.6	57.5	29.6	55.3	28.4	52.2	26.9	50.2	25.8
100	30.5	80.9	41.6	65.7	33.8	63.7	32.8	61.4	31.6	58.4	30.0	56.3	29.0
200	61.0	89.9	46.2	75.5	38.8	73.5	37.8	71.3	36.7	68.3	35.1	66.2	34.1
300	91.4	95.2	49.0	81.4	41.9	79.4	40.8	77.3	39.8	74.3	38.2	72.1	37.1
400	121.9	99.2	51.0	85.7	44.1	83.9	43.2	81.7	42.0	78.7	40.5	76.6	39.4
500	152.4	102.4	52.7	89.3	45.9	87.4	45.0	85.3	43.9	82.3	42.3	80.2	41.3

TABLE 8.3.56 FACILITIES DESIGN WIND AS A FUNCTION OF AVERAGING TIME (τ) FOR A PEAK WIND OF 63.3 m/sec (123.0 knots) (1000-year return period) FOR EDWARDS AFB

Height		Facilities Design Wind as a Function of Averaging Time (τ) in minutes											
(ft)	(m)	τ=0 (peak)		τ=0.5		τ=1		τ=2		τ=5		τ=10	
		(knots)	(m/sec)	(knots)	(m/sec)	(knots)	(m/sec)	(knots)	(m/sec)	(knots)	(m/sec)	(knots)	(m/sec)
33	10	123.0	63.3	93.3	48.0	89.7	46.1	85.7	44.1	80.5	41.4	76.9	39.6
60	18.3	133.8	68.8	105.5	54.3	101.8	52.4	98.0	50.4	92.6	47.6	88.9	45.7
100	30.5	143.2	73.7	116.2	59.8	112.7	58.0	108.7	55.9	103.4	53.2	99.7	51.3
200	61.0	159.3	82.0	133.8	68.8	130.3	67.0	126.3	65.0	121.0	62.2	117.2	60.3
300	91.4	168.7	86.8	144.2	74.2	140.7	72.4	136.9	70.4	131.6	67.7	127.8	65.7
400	121.9	175.8	90.4	151.9	78.1	148.6	76.4	144.8	74.5	139.5	71.8	135.8	69.9
500	152.4	181.5	93.4	158.2	81.4	154.9	79.7	151.1	77.7	145.9	75.1	142.1	73.1

might exist in such a relationship that a runway oriented with the prevailing wind might be the least useful to an aircraft constrained by crosswind components. Two methods, one empirical, the other theoretical, of determining the optimum runway orientation to minimize critical crosswind component speeds are available (Ref. 8.20).

In the empirical method the runway crosswind components are computed for all azimuth and wind speed categories in the wind rose (Ref. 8.20). From these values the optimum runway orientation can be selected that will minimize the risk of occurrence of any specified crosswind speed.

The theoretical method requires that the wind components are bivariate normally distributed; i.e., a vector wind data sample is resolved into wind components in a rectangular coordinate system and the bivariate normal elliptical distribution is applied to the data sample of component winds. For example, let x_1 and x_2 be normally distributed variables with parameters (ξ_1, σ_1) and (ξ_2, σ_2). ξ_1 and ξ_2 are the respective means, while σ_1 and σ_2 are the respective standard deviations. Let ρ be the correlation coefficient, which is a measure of the dependence between x_1 and x_2. Now, the bivariate normal density function is

$$p(x_1, x_2) = \left[2\pi\sigma_1\sigma_2(1-\rho^2)^{1/2}\right]^{-1} \exp\left\{-[2(1-\rho^2)]^{-1}\left[\left(\frac{x_1-\xi_1}{\sigma_1}\right)^2 - 2\rho\left(\frac{x_1-\xi_1}{\sigma_1}\right)\left(\frac{x_2-\xi_2}{\sigma_2}\right) + \left(\frac{x_2-\xi_2}{\sigma_2}\right)^2\right]\right\} . \tag{8.23}$$

Let α be any arbitrary angle in the rectangular coordinate system. From the statistics in the (x_1, x_2) space, the statistics for any rotation of the axes of the bivariate normal distribution through any arbitrary angle α may be computed (Ref. 8.21). Let $\Delta\alpha$ denote the desired increments for which runway orientation accuracy is required; e.g., one may wish to minimize the probability of crosswinds with a runway orientation accuracy down to $\Delta\alpha = 10$ deg. This means we must rotate the bivariate normal axes through every 10 degrees. It is only necessary to rotate the bivariate normal surface through 180 degrees since the distribution is symmetric in the other two quadrants. Let (y_1, y_2) denote the bivariate normal space after rotation. This rotation process will result in 18 sets of statistics in the (y_1, y_2) space. The quantity y_1 is the head wind component while y_2 is the crosswind component. Since we are concerned with minimizing the probability of cross winds (y_2) only, we now examine the marginal distributions $p(y_2)$ for the 18 orientations (α). Since $p(y_1, y_2)$ is bivariate normal, the 18 marginal distributions $p(y_2)$ must be univariate normal:

$$p(y_2) = \left[\sigma_2 (2\pi)^{1/2}\right]^{-1} \exp \left\{-\tfrac{1}{2}\left[(y_2 - \xi_2)/\sigma_2\right]^2\right\} \quad . \tag{8.24}$$

ξ_2 and σ_2 are replaced by their sample estimates $\overline{Y}_2$ and S_{y_2}. Now, let

$$z = \frac{Y_2 - \overline{Y}_2}{S_{y_2}} \quad , \tag{8.25}$$

where y_2 is the critical crosswind of interest. The quantity z is a standard normal variable and the probability of its exceedance is easily calculated from the tables of the standard normal integral. Since a right or left crosswind (y_2) is a constraint to an aircraft, the critical region (exceedance region) for the normal distribution is two-tailed; i.e., we are interested in twice the probability of exceeding $|y_2|$. Let this probability of exceedance or risk equal R. Now, the orientation for which R is a minimum is the desired optimum runway orientation. The procedure described may be used for any station. Only parameters estimated from the data are required as input. Consequently, many runways and locations may be examined rapidly.

Either the empirical or theoretical method may be used to determine an aircraft runway orientation that minimizes the probability of critical crosswinds. Again, it is emphasized that the wind components must be bivariate normally distributed to use the theoretical method. In practical applications, the following steps are suggested:

1. Test the component wind samples for bivariate normality if these samples are available.

2. If the component winds are available and cannot be rejected as bivariate normal using the bivariate normal goodness-of-fit test, use the theoretical method since it is more expedient and easily programmed.

3. If the component wind data samples are not available and there is doubt concerning the assumption of bivariate normality of the wind components, use the empirical method.

8.4 Inflight Winds

8.4.1 Introduction

Inflight wind speed profiles are used in vehicle design studies primarily to establish structural and control system capabilities and compute performance requirements. The inflight wind speeds selected for vehicle design may not represent the same percentile value as the design surface wind speed. The selected wind speeds (inflight and surface) are determined by the desired vehicle launch capability and can differ in the percentile level since the inflight and surface wind speeds differ in degree of persistance for a given reference time period and can be treated as being statistically independent for engineering purposes.

Wind information for inflight design studies is presented in two basic forms: discrete or synthetic profiles and measured profile samples. There are certain limitations to each of these wind input forms, and their utility in design studies depends upon a number of considerations such as, (1) accuracy of basic measurements, (2) complexi of input to vehicle design, (3) economy and practicality for design use, (4) ability to represent significant features of the wind profile, (5) statistical assumption versus physical representation of the wind profile, (6) ability of input to ensure control system and structural integrity of the vehicle, and (7) flexibility of use in design trade-off studies.

An accurate and adequate number of measured wind profiles are necessary for developing a valid statistical description of the wind profile. Fortunately, current records of data from some locations (Kennedy Space Center in particular) fulfill these requirements, although a continuing program of data acquisition is vital to further enhance the confidence of the statistical information generated. Various methods and sensors for obtaining inflight profiles include the rawinsonde, the FPS-16 Radar/Jimsphere, and the rocketsonde. The statistical analyses performed on the inflight wind profiles provide detailed descriptions of the upper winds and an understanding of the profile characteristics such as temporal and height variations, as well as indications of the frequency and the persistence of transient meteorological systems.

The synthetic type of wind profile is the oldest method used to present inflight design wind data. The synthetic wind profile data are presented in this document since this method of presentation provides a reasonable approach for most design studies when properly used, especially during the early design periods. Also, the concept of synthetic wind profiles is generally understood and employed in most aerospace organizations for design computations. It should be understood that the synthetic wind profile includes the wind speed, wind speed change, maximum wind layer thickness, and gusts that are required to establish vehicle design values.

C-3

Generally, launch vehicles for use at various launch sites and in comprehensive space research mission and payload configurations are designed by use of synthetic wind profiles based upon scalar wind speeds without regard to specific wind directions. However, if a vehicle is restricted to a given launch site, rather narrow flight azimuths, and a specific configuration and mission, wind components (head, tail, left cross or right cross) are used. For a given percentile, the magnitudes of component winds are equal to or less than those of the scalar winds. Component or directional dependent winds should not be employed in initial design studies unless specifically authorized by the cognizant design organization. Vector wind and vector wind shear models may be more applicable.*

Selection of a set of detailed wind profiles for final design verification and launch delay risk calculations requires the matching of vehicle simulation resolution and technique to frequency or information content of the profile. A detailed wind profile data set is available for KSC. Data acquisition programs are currently underway to acquire data to develop corresponding sets for other test ranges. Detailed wind profile data sets for design verification use are for Kennedy Space Center, Florida, and Vandenberg AFB, California (see Section 8.4.12.1). Selected samples of detail wind profiles are available for other locations.

The synthetic wind profile provides a conditionalized wind shear/gust state with respect to the given design wind speed. Therefore, in concept, the synthetic wind profile should produce a vehicle design which has a launch delay risk not greater than a specified value which is generally the value associated with the design wind speed. This statement, although generally correct, depends on the control system response characteristics, the vehicle structural integrity, etc. In using the design verification selection of detailed wind profiles a joint condition of wind shear, gust, and speeds is given. Therefore, the resulting launch delay risk for a given vehicle design is the specified value of risk computed from the vehicle responses associated with the various profiles. For the synthetic profile a vehicle inflight wind speed capability and maximum launch delay risk may be stated which is <u>conditional</u> upon the wind/gust design values. However, for the selection of detailed wind profiles only a vehicle launch risk value may be given, since the wind characteristics are treated as a <u>joint</u> condition. These two differences in philosophy should be understood to avoid misinterpretation of vehicle response calculation comparisons. In both cases allowance for dispersions in vehicle characteristics should be made prior to flight simulation through the wind profiles and establishment of vehicle design response or operational launch delay risk values. The objective is to insure that a space vehicle will accommodate the desired percentage of wind profiles or conditions in its non-nominal flight mode.

---

* Considerable effort has been expended recently to formulate a vector wind and vector wind shear model for use in the Space Shuttle design and operational analysis studies. Reference should be made to Section 8.4.11 for more details on this subject.

8.4.2 Wind Aloft Climatology

The development of design wind speed profiles and associated shears and gusts requires use of the measured wind speed and wind direction data collected at the area of interest for some reasonably long period of time, i.e., five years or longer. The subject of wind climatology for an area, if treated in detail, would make up a voluminous document. The intent here is to give a brief treatment of selected topics that are frequently considered in space vehicle development and operations problems and provide references to more extensive information.

Considerable data summaries (monthly and seasonal) exist on wind aloft statistics for the world. However, it is necessary to interpret these data in terms of the engineering design problem and design philosophy. For example, wind requirements for performance calculations relative to aircraft fuel consumption requirements must be derived for the specific routes and design reference period. Such data are available on request.

8.4.3 Wind Component Statistics

Wind component statistics are used in mission planning to provide information on the probability of exceeding a given wind speed in the pitch or yaw planes and to bias the tilt program at a selected launch time.

Computations of the wind component statistics is made for various launch azimuths (15-degree intervals were selected at MSFC) for each month for the pitch plane (range) and yaw plane (cross range) at the Eastern Test Range and the Space and Missile Test Center (Vandenberg AFB, California). References 8.22 through 8.24 contain information on the statistical distributions of wind speeds and vector wind components for the various vehicle flight centers and test ranges.

8.4.3.1 Upper Wind Correlations

Coefficients of correlations of wind components between altitude levels with means and standard deviations at altitude levels may be used in a statistical model to derive representative wind profiles. A method of preparing synthetic wind profiles by use of correlation coefficients between wind components is described in Reference 8.25. In addition, these correlation data are applicable to certain statistical studies of vehicle responses (Ref. 8.26).

Data on correlations of wind between altitude levels for various geographical locations are presented in References 8.27, 8.28, and 8.29. The reports give values of the interlevel and intralevel coefficients of linear correlations between wind components. Because of the occurrence of the regular increase of winds with altitude below and the decrease of winds above the 10- to 14-kilometer level, the correlation coefficients decrease with greater altitude separation of the levels being correlated. Likewise, the highest correlation coefficients between components occur in the 10- to 14-kilometer level.

Correlations between wind components separated by a horizontal distance are now becoming available. The reader is referenced to the work of Buell (Refs. 8.30 and 8.31) for a detailed discussion of the subject.

8.4.3.2 Thickness of Strong Wind Layers

Wind speeds in the middle latitudes generally increase with altitude to a maximum between 10- and 14-kilometers. Above 14 kilometers, the wind speeds decrease with altitude, then increase at higher altitude, depending upon season and location. Frequently, these winds exceed 50 m/sec in the jet stream, a core of maximum winds over the midlatitudes in the 10- to 14-kilometer altitudes. The vertical extent of the core of maximum winds, or the sharpness of the extent of peak winds on the wind profile is important in some vehicle design studies. For information concerning the thickness of strong wind layers the reader is referred to Reference 8.32.

Table 8.4.1 shows design values of vertical thickness (based on maximum thickness) of the wind layers for wind speeds for the Eastern Test Range. Similar data for the Space and Missile Test Center are given in Table 8.4.2. At both ranges, the thickness of the layer decreases with increase of wind speed; that is, the sharpness of the wind profile in the vicinity of the jet core becomes more pronounced as wind speed increases.

TABLE 8.4.1 DESIGN THICKNESS FOR STRONG WIND LAYERS AT THE EASTERN TEST RANGE

Quasi-Steady-State Wind Speed ($\pm 5\ ms^{-1}$)	Maximum Thickness (km)	Altitude Range (km)
50	4	8.5 to 16.5
75	2	10.5 to 15.5
92	1	10.0 to 14.0

TABLE 8.4.2 DESIGN THICKNESS FOR STRONG WIND LAYERS AT THE SPACE AND MISSILE TEST CENTER (Vandenberg AFB, California)

Quasi-Steady-State Wind Speed ($\pm 5\ ms^{-1}$)	Maximum Thickness (km)	Altitude Range (km)
50	4	8.0 to 16
75	2	9.5 to 14

8.4.3.3 Exceedance Probabilities

The probability of inflight winds exceeding or not exceeding some critical wind speed for a specified time duration may be of considerable importance in mission planning, and in many cases, more information than just the occurrence of critical winds is desired. If a dual launch, with the second vehicle being launched 1 to 3 days after the first, is planned, and if the launch opportunity extends over a 10-day period, what is the probability that winds below (or above) critical levels will last for the entire 10 days? What is the probability of 2 or 3 consecutive days of favorable winds in the 10-day period? Suppose the winds are favorable on the scheduled launch day, but the mission is delayed for other reasons. Now, what is the probability that the winds will remain favorable for 3 or 4 more days? Answers to these questions could also be used for certain design considerations involving specific vehicles prepared for a given mission and launch window. A body of statistics is available from the Atmospheric Sciences Division, which can be used to answer these and possibly other related questions. An example of the kind of wind persistence statistics that are available is given in Fig. 8.4.1.

This figure gives the probability of the maximum wind speed in the 10 to 15 km region being less than, equal to, or greater than 50 and 75 $m s^{-1}$ as the case may be for various multiples of 12 hours for the month of January. Thus, for example, there is approximately an 18% chance that the wind speed will be greater than or equal to 50 m/sec for ten consecutive 12-hour periods in January.

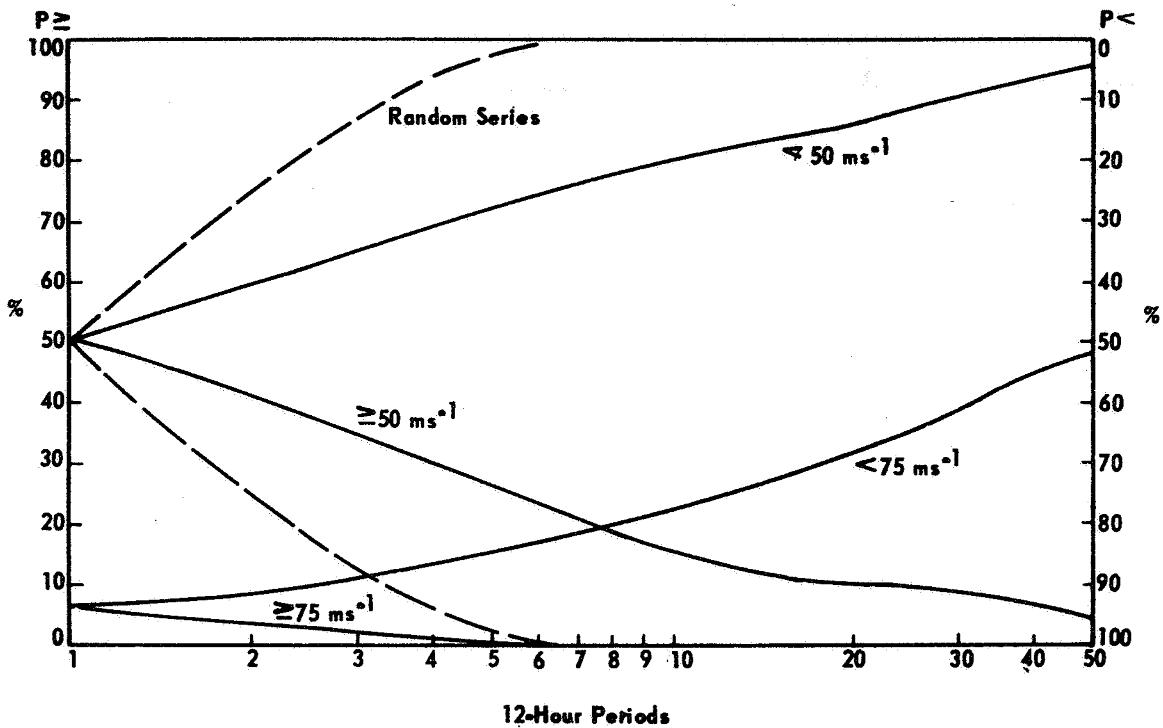

FIGURE 8.4.1 PROBABILITY OF THE MAXIMUM WIND SPEED IN THE 10- TO 15-km LAYER BEING LESS THAN, EQUAL TO, OR GREATER THAN SPECIFIED VALUES FOR k-CONSECUTIVE 12-hr PERIODS DURING JANUARY AT KENNEDY SPACE CENTER

8.4.3.4 Design Scalar Wind Speeds (10-15 km Altitude Layer)

The distributions of design scalar wind speed in the 10- to 15-kilometer altitude layer over the United States are shown in Figure 8.4.2 for the 95 percentile and Figure 8.4.3 for the 99 percentile values. The line of local maximum in the isopleths (maximum wind speeds) is shown by heavy lines with arrows. These winds occur at approximately the level of maximum dynamic pressure for most space vehicles.

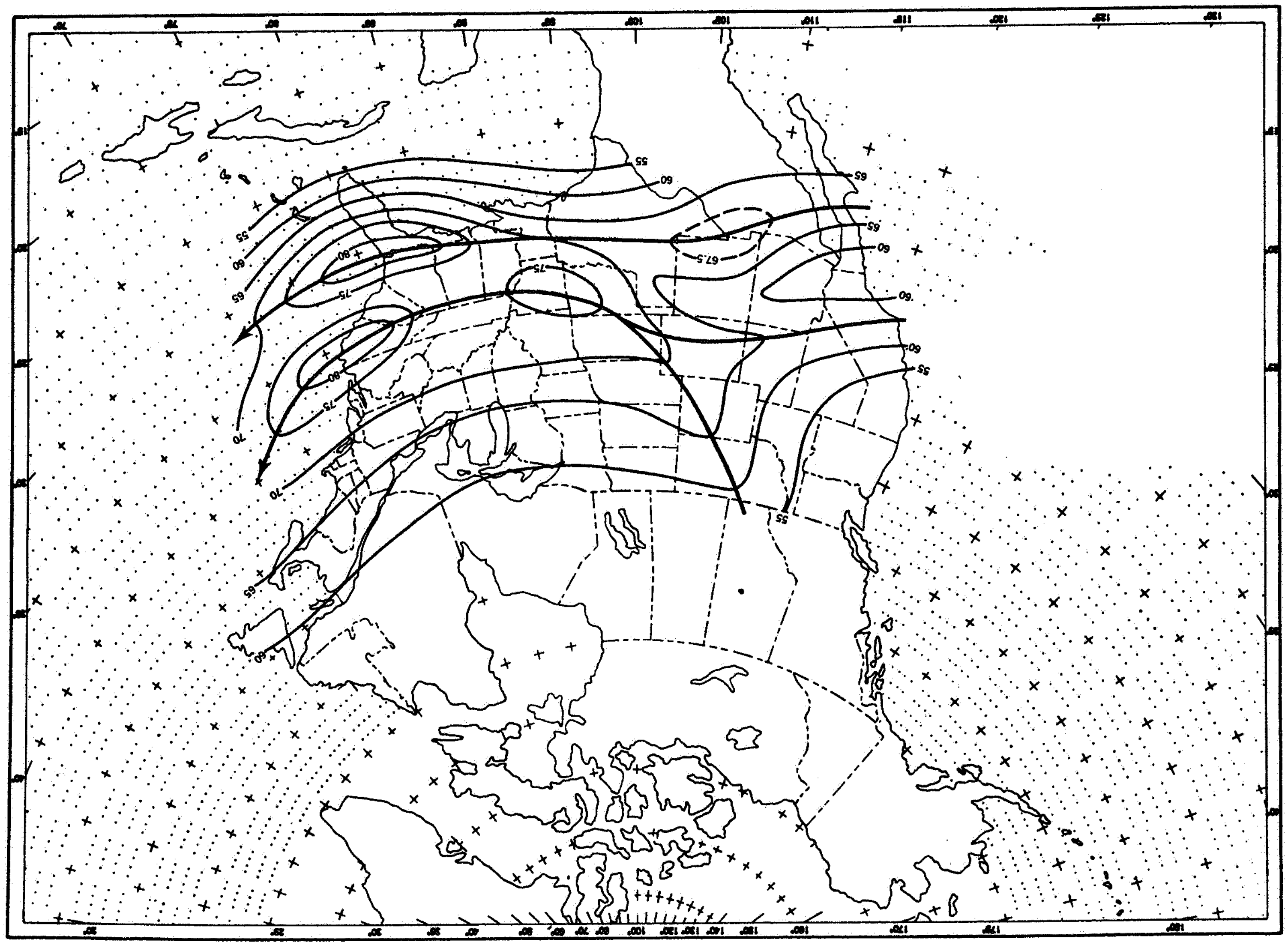

FIGURE 8.4.2 DESIGN SCALAR WIND SPEEDS (m/sec) 95 PERCENTILE ENVELOPE ANALYSIS PREPARED FROM WINDIEST MONTH AND MAXIMUM WINDS IN THE 10- TO 15-km LAYER

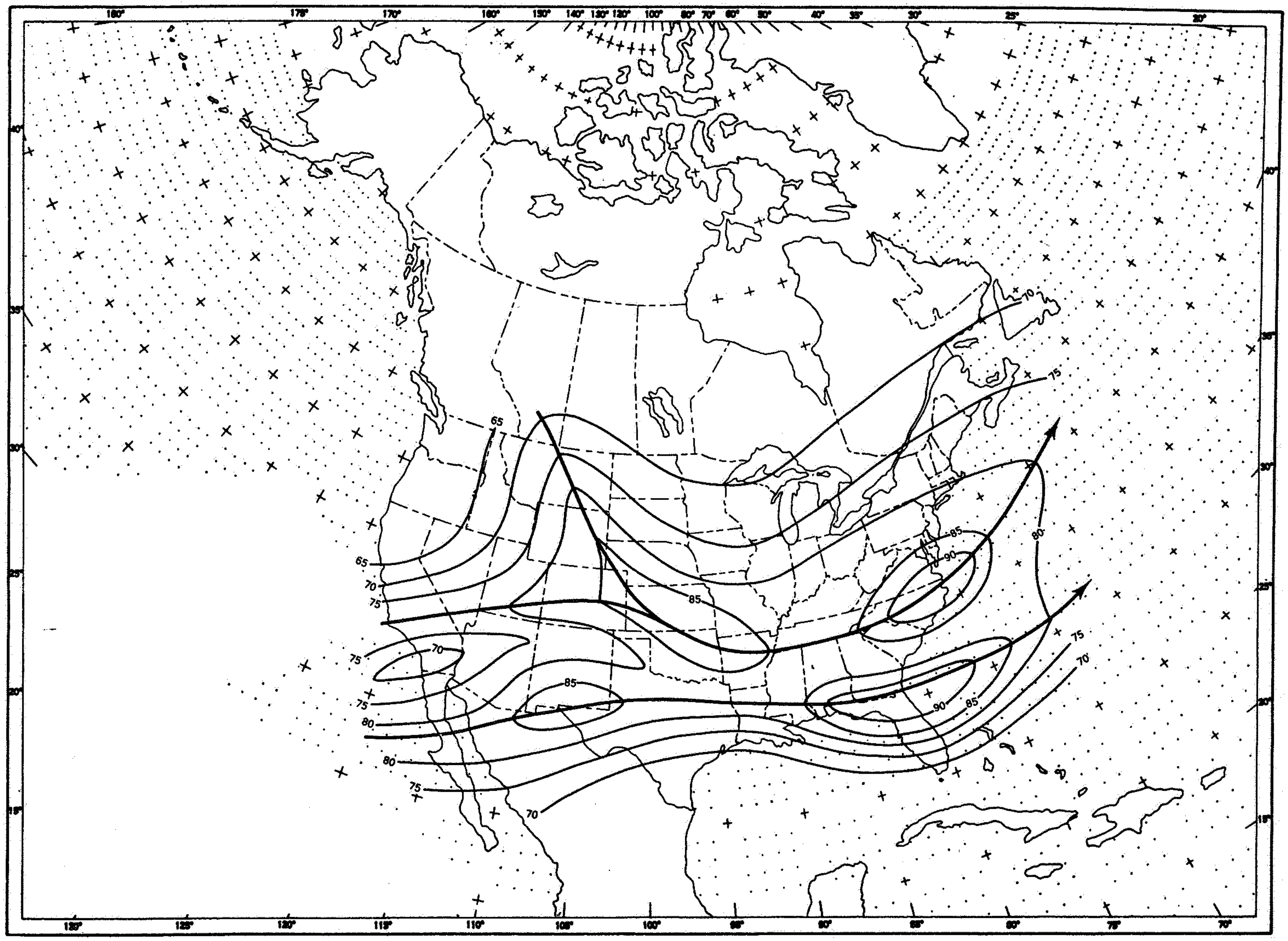

FIGURE 8.4.3 DESIGN SCALAR WIND SPEEDS (m/sec) 99 PERCENTILE ENVELOPE ANALYSIS PREPARED FROM WINDIEST MONTH AND MAXIMUM WINDS IN THE 10- TO 15-km LAYER

8.4.3.5 Temporal Wind Changes

Atmosphere flows at a point change in time. Wind direction and speed change can occur over time scales as short as a few minutes. There is no upper bound limit on the time scale over which the wind field can change. In order to develop wind biasing programs for space vehicle control purposes, which involve the use of wind profiles observed a number of hours prior to launch, it is necessary that consideration be given to the changes in wind speed and direction that can occur during the time elapsed from entering the biasing profile into the vehicle control system logic to the time of launch. Thus, for example, if the observed wind profile eight hours prior to launch is to be used as a wind biasing profile, then consideration should be given to the dispersions in wind direction and speed that could occur over this period of time. Wind speed and direction change data are also useful for mission operation purposes. Results of studies conducted by the Atmospheric Sciences Division to define these dispersions in a statistical context are presented herein.

In order to account for the differences between the dynamics of the flow in the atmospheric boundary layer and the free atmosphere, the atmosphere is usually partitioned at the 2-kilometer level in studies of the temporal changes of the wind field. Below the 2-kilometer level the flow is significantly influenced by the surface of the earth and the flow is predominantly a turbulent one. In the free atmosphere above the 2-kilometer level the flow is for all practical purposes free of the effects of the surface of the earth.

Figures 8.4.4 and 8.4.5 contain idealized 99% wind direction and speed changes as a function of elapsed time and observed or reference wind speed for altitudes between 3 m and 2 km for ETR. The wind speed may increase or decrease from the reference profile value; thus, envelopes of each category are presented in Figure 8.4.5. Figures 8.4.6 and 8.4.7 are the idealized 99% wind direction and speed changes as a function of elapsed time and observed or reference wind speed for altitudes between 2 to 16 km.

A few cautionary statements regarding the data given above are in order. They are applicable only to the Eastern Test Range, Kennedy Space Center launch area because differences are known to exist in the data with the geographical sites. Conclusions should not be drawn relative to frequency content and phase relationships of the wind profile since the data given herein provides only envelope conditions for ranges of speed and direction changes. Direction correlations have not been developed between the changes of wind direction and wind speed.

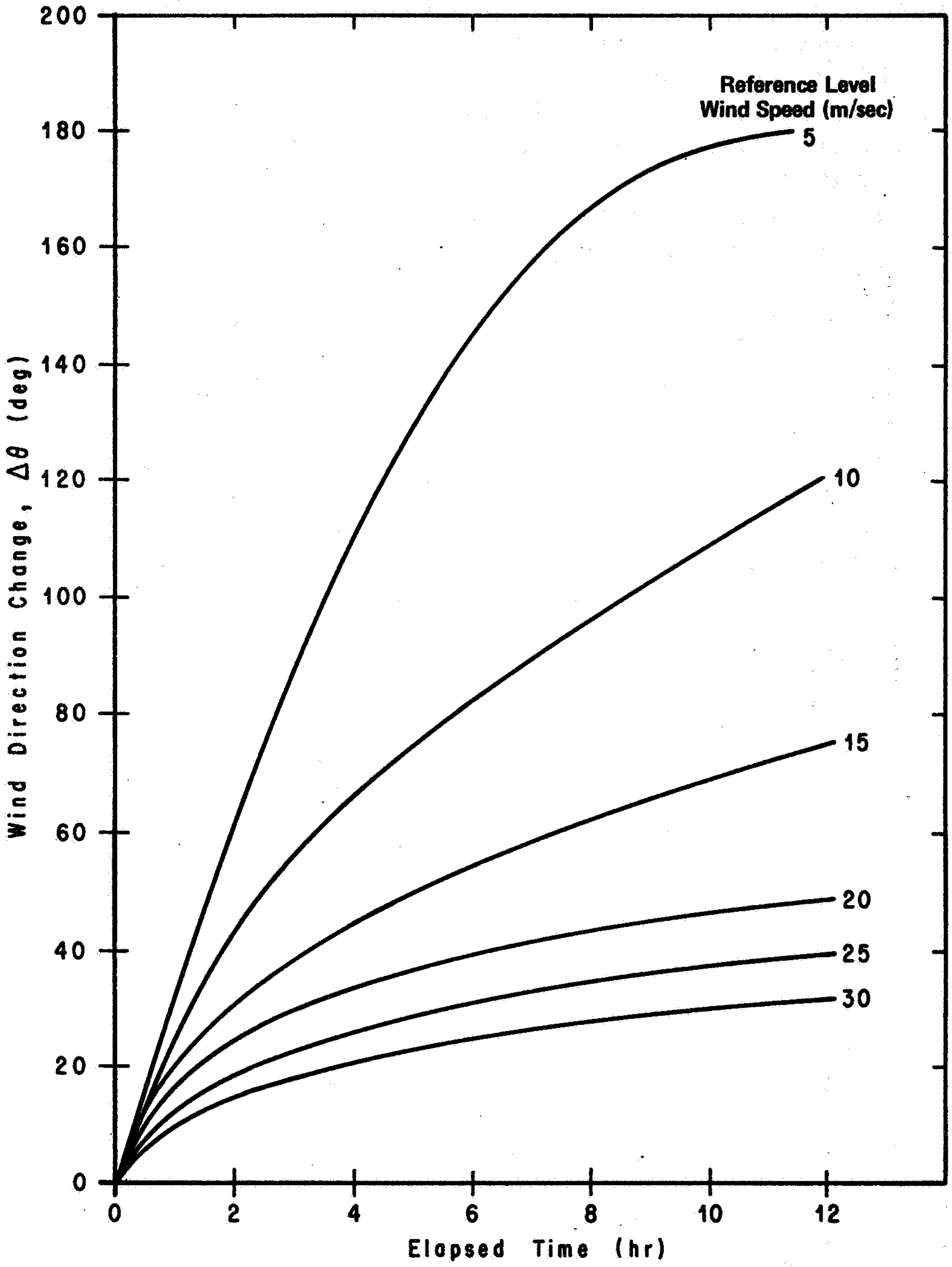

FIGURE 8.4.4 IDEALIZED 99% WIND DIRECTION CHANGE AS A FUNCTION OF TIME AND WIND SPEED IN THE 3-m TO 2-km ALTITUDE REGION OF THE EASTERN TEST RANGE

C-3

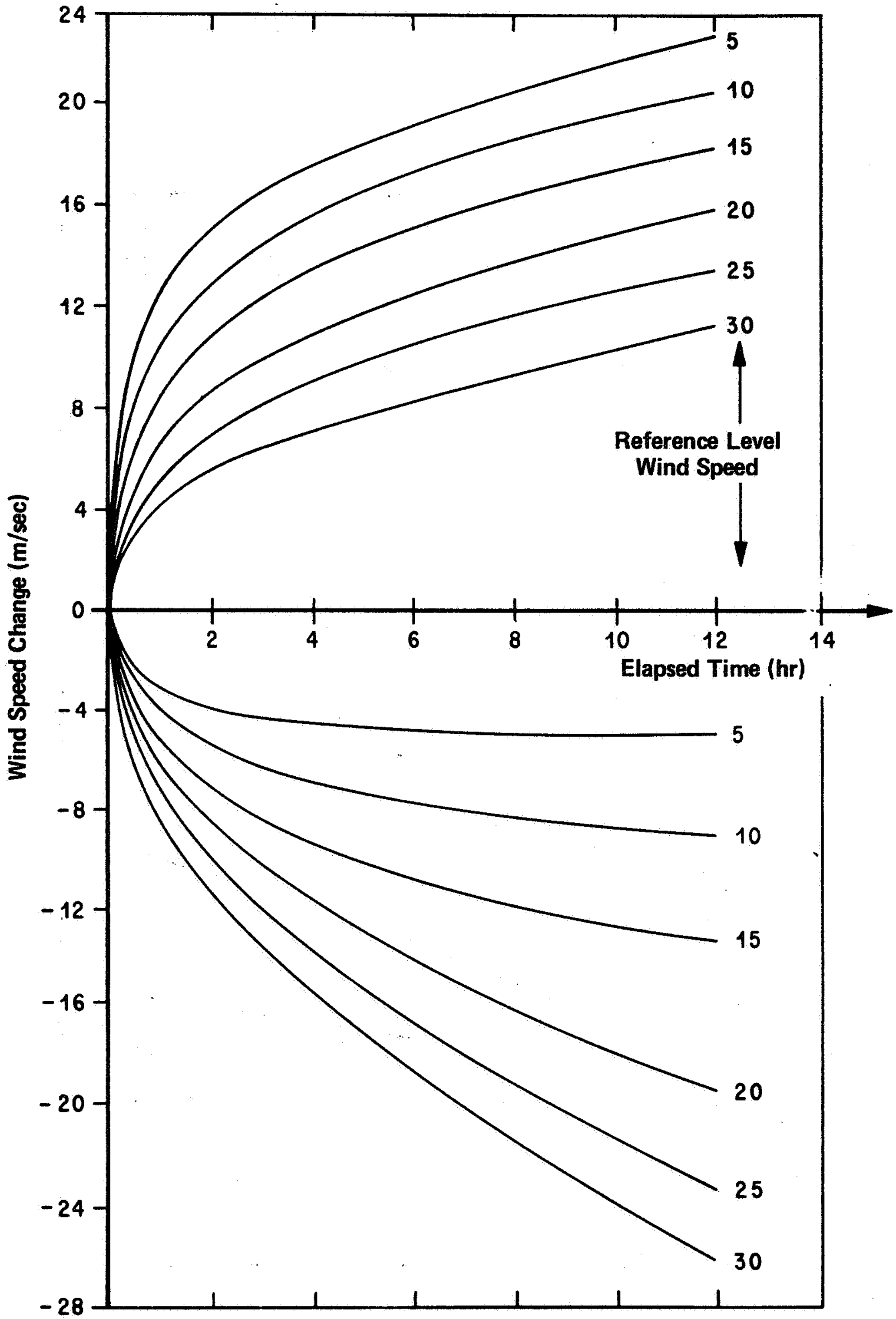

FIGURE 8.4.5 IDEALIZED 99% WIND SPEED CHANGE AS A FUNCTION OF TIME AND WIND SPEED IN THE 3-m TO 2-km ALTITUDE REGION OF THE EASTERN TEST RANGE

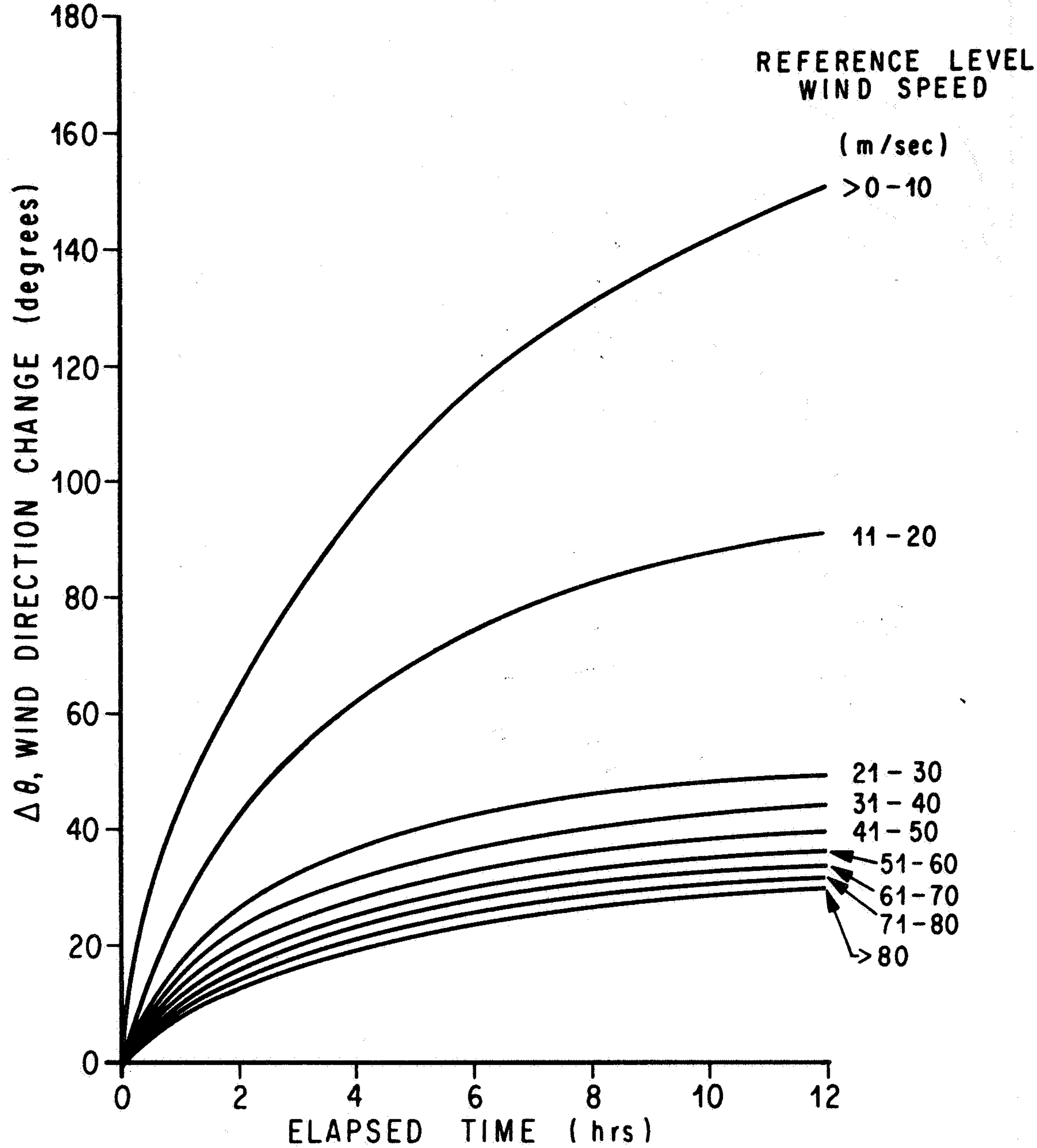

FIGURE 8.4.6 IDEALIZED 99% WIND DIRECTION CHANGE AS A FUNCTION OF TIME AND WIND SPEED IN THE 2- TO 16-km REGION OF THE EASTERN TEST RANGE

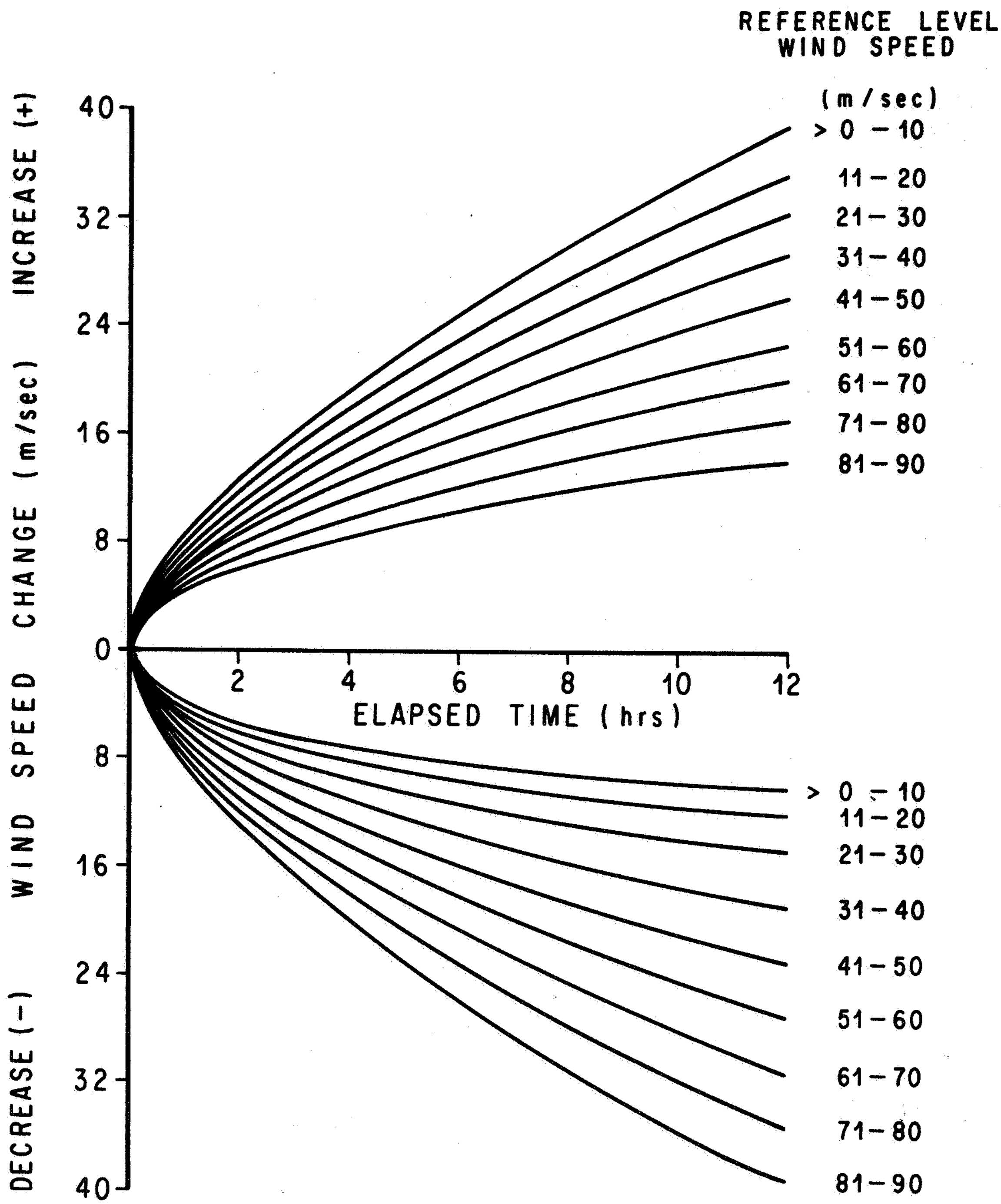

FIGURE 8.4.7 IDEALIZED 99% WIND SPEED CHANGE AS A FUNCTION OF TIME AND WIND SPEED IN THE 2- TO 16-km REGION OF THE EASTERN TEST RANGE

Additional information concerning wind speed and direction changes can be found in reports by Camp and Susko (Ref. 8.33), and Camp and Fox for Santa Monica (Ref. 8.34). Studies are now under way on temporal vector wind changes, and results may be obtained upon request to Atmospheric Sciences Division, Space Sciences Laboratory, MSFC.

8.4.4 Wind Speed Profiles for Biasing Tilt Program

In attempting to maintain a desired flight path for a space vehicle through a strong wind region, the vehicle control system could introduce excessive bending moments and orbit anomalies. To reduce this problem, it is sometimes desirable to wind bias the pitch program, that is, to tilt the vehicle sufficiently to produce the desired flight path and minimize maximum dynamic pressure level loads with the expected wind profile. Since most inflight strong winds over Kennedy Space Center are winter westerlies, it is sometimes expedient to use the monthly or seasonal pitch plane median wind speed profile for bias analyses.

Head and tail wind components and right and left cross wind components from 0- to 70-kilometer altitudes were computed for every 15 degrees of flight azimuth for the Eastern Test Range launch area and were published by NASA (Refs. 8.23 and 8.24). Similar calculations are available upon request for other ranges.

It is not usually necessary to bias the vehicle in the yaw plane because of the flight azimuths normally used at Kennedy Space Center. For applications where both pitch and yaw biasing are used at Kennedy Space Center, monthly vector mean winds may be more efficient for wind biasing. Such statistics will be made available upon request or see Reference 8.37.

8.4.5 Design Wind Speed Profile Envelopes

The wind data given are not expected to be exceeded by the given percentage of time (time as related to the observational interval of the data sample) based upon the windiest monthly reference period. To obtain the profiles, monthly frequency distributions are combined for each percentile level to give the envelope over all months. The profiles represent horizontal wind flow referenced to the earth's surface. Vertical wind flow is negligible except for that associated with gusts or turbulence. The scalar wind speed envelopes are normally applied without regard to flight directions to establish the initial design requirements. Directional wind criteria for use with the synthetic wind profile techniques should be applied with care and specific knowledge of the vehicle mission and flight path, since severe wind constraints could result for other flight paths and missions.

8.4.5.1 Scalar Wind Speed Envelopes*

Scalar wind speed profile envelopes are presented in Tables 8.4.3 through 8.4.7 and Figure 8.4.8 through 8.4.12. These are idealized steady-state scalar wind speed profile envelopes for five active or potential operational space vehicle launch or landing sites, i.e., Eastern Test Range, Florida; The Space and Missile Test Center (Vandenberg AFB), California; Wallops Flight Center, Virginia; White Sands Missile Range, New Mexico; and Edwards Air Force Base, California. Table 8.4.8 and Figure 8.4.13 envelope the 95 and 99 percentile steady-state scalar wind speed profile envelopes from the same five locations. They are applicable for design criteria when initial design or operational capability has not been restricted to a specific launch site or may involve several geographical locations. However, if the specific geographical location for application has been determined as being near one of the five referenced sites then the relevant data should be applied.

This section provides design nondirectional wind data for various percentiles; therefore, the specific percentile wind speed envelope applicable to design should be specified in the appropriate space vehicle specification documentation. For engineering convenience the design wind speed profile envelopes are given as linear segments between altitude levels; therefore, the tabular values are connected, when graphed, by straight lines between the points.

---

* This section and several others that follow present data and instructions relative to the development and use of <u>scalar</u> synthetic wind profiles in aerospace vehicle design analyses and related studies. In many cases these will prove adequate for preliminary design investigations. However, a <u>vector</u> synthetic wind profile design input may prove more adequate when a more realistic synthetic wind profile input is desirable. The reader should consult Section 8.4.11 for more details on vector wind and vector wind shear models. In either case, the most realistic test of an aerospace vehicle performance is by flight simulation through detailed wind profile data sets (see Section 8.4.12.1).

TABLE 8.4.3 SCALAR WIND SPEED V(m/sec) STEADY-STATE ENVELOPES AS FUNCTIONS OF ALTITUDE H (km) FOR VARIOUS PROBABILITIES P (%) FOR THE EASTERN TEST RANGE

Altitude	Percentile				
(km)	50	75	90	95	99
1	8	13	16	19	24
6	23	31	39	44	52
11	43	55	66	73	88
12	45	57	68	75	92
13	43	56	67	74	86
20	7	12	17	20	25
23	7	12	17	20	25
40	43	57	70	78	88
50	75	83	91	95	104
58	85	96	106	112	123
60	85	96	106	112	123
75	15	22	28	30	37
80	15	22	28	30	37

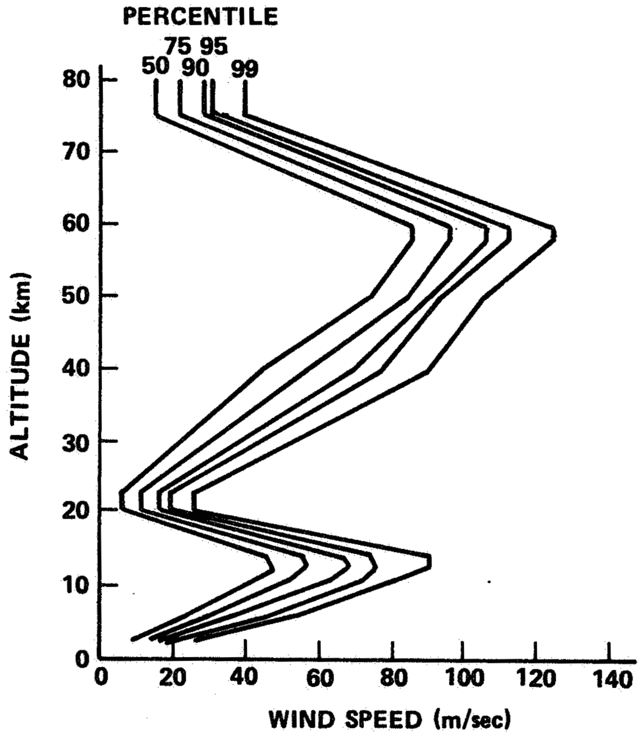

FIGURE 8.4.8 SCALAR WIND SPEED PROFILE ENVELOPES STEADY-STATE, FOR THE EASTERN TEST RANGE

TABLE 8.4.4 SCALAR WIND SPEED V(m/sec) STEADY-STATE ENVELOPES AS FUNCTIONS OF ALTITUDE H (km) FOR VARIOUS PROBABILITIES P (%) FOR THE SPACE AND MISSILE TEST CENTER
Vandenberg AFB, California

Altitude (km)	Percentile				
	50	75	90	95	99
1	7	10	13	15	19
6	20	29	36	41	50
10	31	43	53	60	73
11	32	44	55	62	79
12	32	44	55	62	79
20	6	10	14	17	26
23	6	10	14	17	26
40	55	67	82	90	105
50	79	96	111	120	132
58	83	107	128	140	164
60	83	107	128	140	164
75	50	65	87	98	118
80	50	65	87	98	118

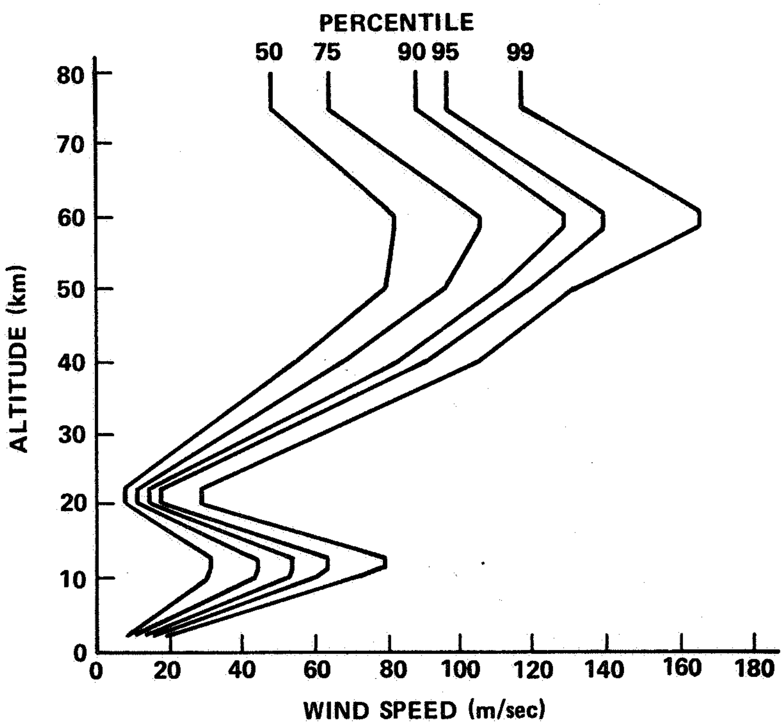

FIGURE 8.4.9 SCALAR WIND SPEED PROFILE ENVELOPES, STEADY-STATE FOR THE SPACE AND MISSILE TEST CENTER, Vandenberg AFB, California

TABLE 8.4.5 SCALAR WIND SPEED V (m/sec) STEADY-STATE ENVELOPES AS FUNCTIONS OF ALTITUDE H (km) FOR VARIOUS PROBABILITIES P (%) FOR WALLOPS FLIGHT CENTER

P = 50		P = 75		P = 90		P = 95		P = 99	
H	V	H	V	H	V	H	V	H	V
1	11	1	15	1	19	1	22	1	28
		3	24	3	28	3	31	3	38
7	36	7	46	7	55	6	54		
9	47	10	60	10	69	10	75	9	82
11	51							11	88
12	50	12	60	12	69	12	75		
17	25	17	33	17	39	15	54		
20	15	20	21	20	26	20	29	20	38
23	15	23	21	23	26	23	29	23	38
50	102	50	120	50	140	50	150	50	170
60	102	60	120	60	140	60	150	60	170
75	85	75	100	75	113	75	120	75	135
80	85	80	100	80	113	80	120	80	135

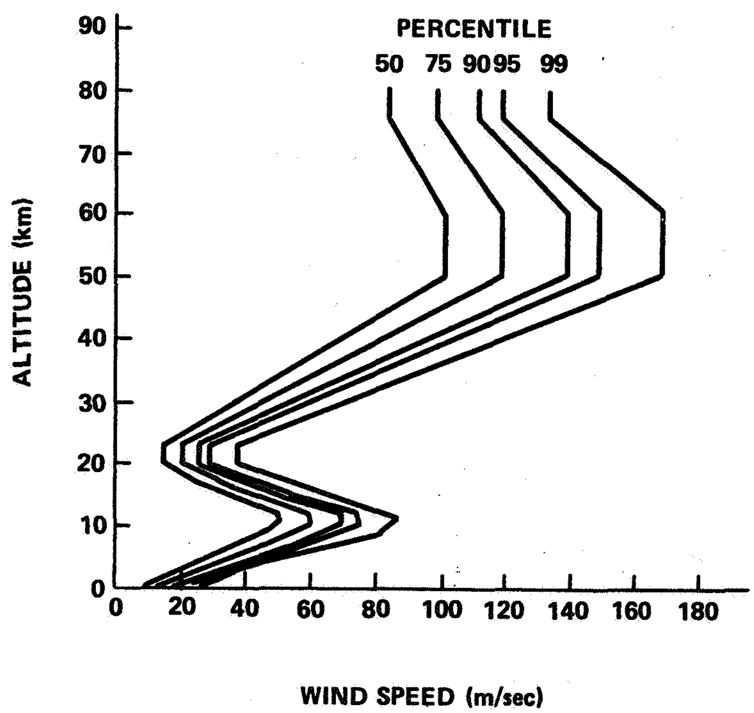

FIGURE 8.4.10 SCALAR WIND SPEED PROFILE ENVELOPES, STEADY-STATE FOR WALLOPS FLIGHT CENTER

TABLE 8.4.6 SCALAR WIND SPEED V (m/sec) STEADY-STATE ENVELOPES AS FUNCTIONS OF ALTITUDE H (km) FOR VARIOUS PROBABILITIES P (%) FOR WHITE SANDS MISSILE RANGE

P = 50		P = 75		P = 90		P = 95		P = 99	
H	V	H	V	H	V	H	V	H	V
1	4	1	7	1	11	1	13	1	22
2	5	2	8	2	12	2	15	2	22
						7	50	7	68
		9	45	8	49	9	67	9	88
11	42	10	53	11	71	11	76		
13	42	12	55	13	63	12	78	14	88
				15	45	15	52	15	69
20	10	20	14	20	20	20	24	20	41
23	10	23	14	23	20	23	24	23	41
50	85	50	104	50	120	50	130	50	150
60	85	60	104	60	120	60	130	60	150
75	60	75	77	75	93	75	102	75	120
80	60	80	77	80	93	80	102	80	120

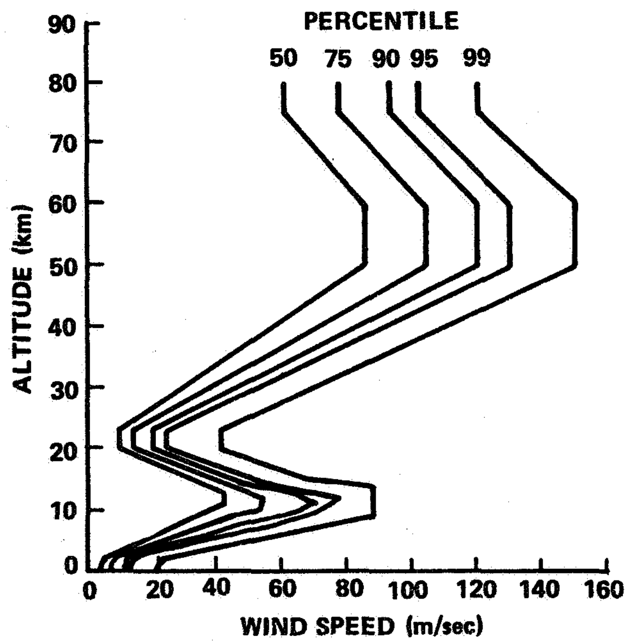

FIGURE 8.4.11 SCALAR WIND SPEED PROFILE ENVELOPES, STEADY-STATE, FOR WHITE SANDS MISSILE RANGE

TABLE 8.4.7 SCALAR WIND SPEED V (m/sec) STEADY-STATE ENVELOPES AS FUNCTIONS OF ALTITUDE H (km) FOR VARIOUS PROBABILITIES P (%) FOR EDWARDS AIR FORCE BASE

P = 50		P = 75		P = 90		P = 95		P = 99	
H	V	H	V	H	V	H	V	H	V
1	8	1	11	1	16	1	17	1	25
2	8	2	12	2	16	2	18	2	28
				5	30	5	36	5	56
10	29			10	51	10	61	10	77
12	32	11	44	11	56			12	77
15	25	13	39	12	56	12	61	14	65
18	13	17	21	17	28	16	38	16	43
20	9	20	13	20	19	20	23	20	30
23	9	23	13	23	19	23	23	23	30
50	85	50	104	50	120	50	130	50	150
60	85	60	104	60	120	60	130	60	150
75	60	75	77	75	93	75	102	75	120
80	60	80	77	80	93	80	102	80	120

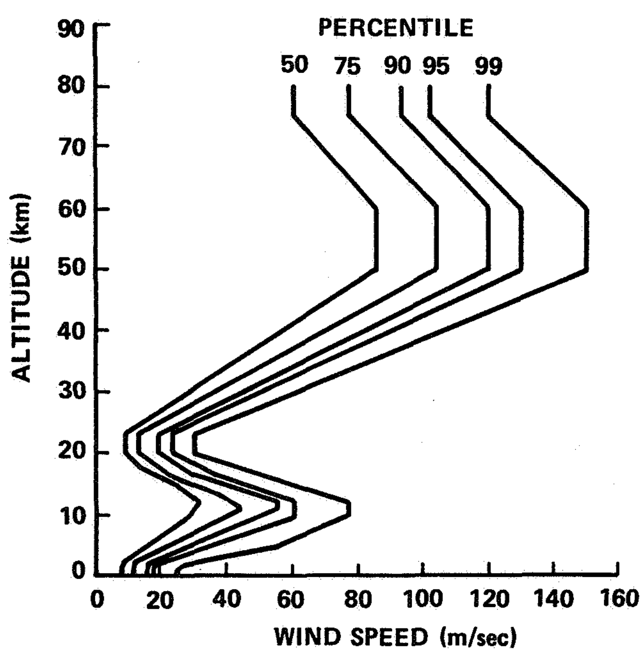

FIGURE 8.4.12 SCALAR WIND SPEED PROFILE ENVLOPES, STEADY - STATE, FOR EDWARDS AIR FORCE BASE

TABLE 8.4.8 SCALAR WIND SPEED V (m/sec) STEADY-STATE ENVELOPES AS FUNCTIONS OF ALTITUDE H (km) FOR TWO PROBABILITIES P (%) ENCOMPASSING ALL FIVE LOCATIONS

P = 95				P = 99			
H	V	H	V	H	V	H	V
1	22	17	44	1	28	15	70
3	31	20	29	3	38	20	41
		23	29	5	56	23	41
6	54	50	150	6	60	50	170
		60	150	7	68	60	170
10	75	75	120	9	88	75	135
11	76	80	120	11	88	80	135
12	78			12	92		
13	74			13	88		
				14	88		

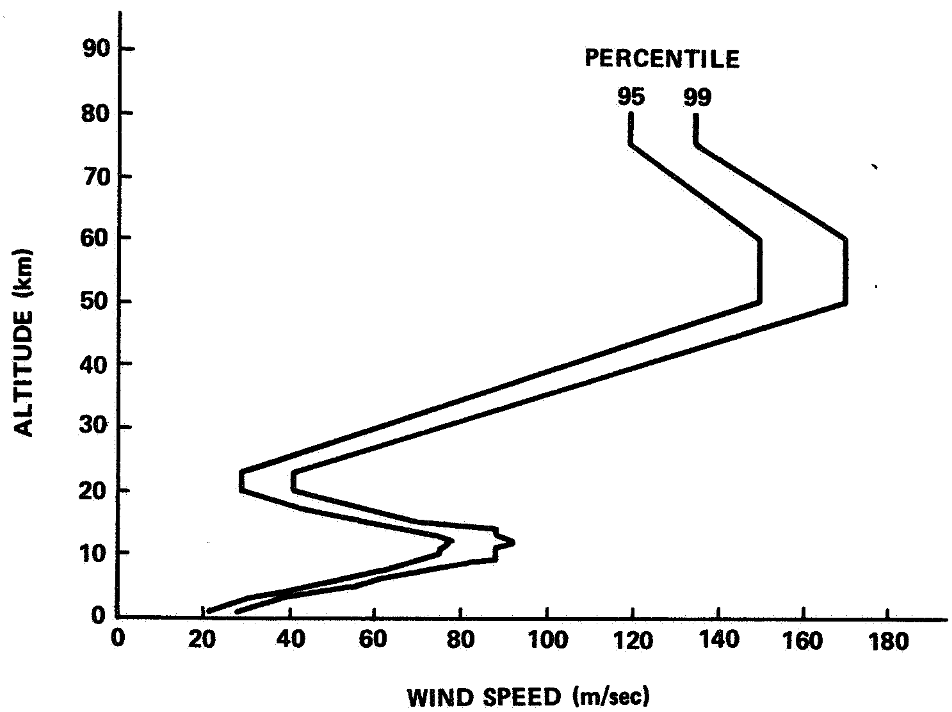

FIGURE 8.4.13 SCALAR WIND SPEED PROFILE ENVELOPES, STEADY-STATE FOR ALL FIVE LOCATIONS

This page intentionally blank.

8.4.6 Wind Speed Change Envelopes

This section provides representative information on wind speed change (shear) for scales of distance $\Delta H \leq 500$ meters. Wind speed change is defined as the total magnitude (speed) change between the wind vectors at the top and bottom of a specified layer, regardless of wind direction. Wind shear is the wind speed change divided by the altitude interval. When applied to space vehicle synthetic wind profile criteria, it is frequently referred to as a wind build-up or back-off rate depending upon whether it occurs below (build-up) or above (back-off) the reference height of concern. Thus, a build-up wind value is the change in wind speed which a vehicle may experience while ascending vertically through a specified layer to the known altitude. Back-off magnitudes describe the speed change which may be experienced above the chosen level. Both build-up and back-off wind speed change data are presented in this section as a function of reference level wind vector magnitude and geographic location. Wind build-up or back-off may be determined for a vehicle with other than a vertical flight path by multiplying the wind speed change by the cosine of the angle between the vertical axis and the vehicle trajectory. Wind shears for scales of distance $\Delta H \geq 1000$ meters thickness are computed from rawinsonde and rocketsonde observations, while the small scale shears associated with scales of distance $\Delta H < 1000$ meters are computed from a relationship developed by Fichtl (Ref. 8.35) based on experimental results from FPS-16 radar/Jimsphere balloon wind sensor measurements of the detail wind profile structure. This relationship states that the back-off or build-up wind shear Δu for $\Delta H < 1000$ meters for a given risk of exceedance is related to the $\Delta H = 1000$ meter shear, $(\Delta u)_{1000}$, at the same risk of exceedance, through the expression

$$\Delta u = (\Delta u)_{1000} \left(\frac{\Delta H}{1000} \right)^{0.7} \tag{8.26}$$

where ΔH has units of meters.

PRECEDING PAGE BLANK NOT FILMED

An envelope of the 99 percentile wind speed build-up is used currently in constructing synthetic wind profiles. For most design studies, the use of this 99 percentile scalar build-up wind shear data is warranted. The envelopes for back-off shears have application to certain design studies and should be considered where appropriate. These envelopes are not meant to imply perfect correlation between shears for the various scales of distance; however, certain correlations do exist, depending upon the scale of distance and the wind speed magnitude considered. This method of describing the wind shear for vehicle design has proven to be especially acceptable in preliminary design studies since the dynamic response of the structure or control system of a vehicle is essentially influenced by specific wavelengths as represented by a given wind shear. Construction of synthetic profiles for vehicle design applications is described in subsection 8.4.9.

Wind speed change (shear) statistics for various locations differ primarily because of prevailing meteorological conditions, orographic features, and data sample size. Significant differences, especially from an engineering standpoint, are known to exist in the shear profiles for different locations. Therefore, consistent vehicle design shear data representing five active or potentially operational space vehicle launch or landing sites are presented in Tables 8.4.9 through 8.4.18; i.e., for Eastern Test Range, Space and Missile Test Center, Wallops Island, White Sands Missile Range, and Edwards Air Force Base. Tables 8.4.19 and 8.4.20 envelope the 99 percentile shears from these five locations. They are applicable for design criteria when initial design or operational capability has not been restricted to a specific launch site or may involve several geographical locations. However, if the specific geographic location for application has been determined as being near one of the five referenced sites, then the relevant data should be applied. Equation (8.26) was used to construct Tables 8.4.9 through 8.4.20 for scales of distance.

8.4.7 Wind Direction Change Envelopes

This section provides representative information on wind direction change $\Delta\theta$ for scales of distance $\Delta H \leq 4000$ meters. Wind direction change is defined as the total change in direction of wind vectors at the top and bottom of a specified layer. Wind direction changes can occur above or below

ORIGINAL PAGE IS OF POOR QUALITY

TABLE 8.4.9 BUILD-UP DESIGN ENVELOPES OF 99 PERCENTILE WIND SPEED CHANGE, 1- TO 80-km ALTITUDE REGION, EASTERN TEST RANGE

Wind Speed at Reference Altitude (m/sec)	Scales of Distance (m)									
	5000	4000	3000	2000	1000	800	600	400	200	100
$\geq$ 90	65.6	59.5	52.3	43.5	34.0	29.0	23.8	17.9	11.2	6.8
= 80	60.4	55.5	49.7	42.0	32.7	27.7	22.7	17.0	10.6	6.5
= 70	56.0	51.7	47.0	40.4	31.2	26.6	21.8	16.4	10.1	6.2
= 60	51.3	48.5	44.5	38.6	30.0	25.6	21.1	15.8	9.8	6.0
= 50	46.5	45.0	41.2	36.5	28.5	24.4	20.0	15.0	9.2	5.7
= 40	38.5	37.7	36.8	34.9	26.5	22.6	18.5	13.8	8.6	5.3
= 30	28.0	27.5	26.5	24.5	20.8	17.8	14.5	10.8	6.7	4.1
= 20	17.6	17.3	16.6	15.8	14.6	12.5	10.2	7.2	4.7	2.9

TABLE 8.4.10 BACK-OFF DESIGN ENVELOPES OF 99 PERCENTILE WIND SPEED CHANGE, 1- TO 80-km ALTITUDE REGION, EASTERN TEST RANGE

Wind Speed at Reference Altitude (m/sec)	Scales of Distance (m)									
	5000	4000	3000	2000	1000	800	600	400	200	100
$\geq$ 90	77.5	74.4	68.0	59.3	42.6	36.4	29.7	22.4	13.8	8.5
= 80	71.0	68.0	63.8	56.0	40.5	34.7	28.5	21.4	13.2	8.1
= 70	63.5	61.0	57.9	52.0	38.8	33.1	27.0	20.3	12.5	7.7
= 60	56.0	54.7	52.3	47.4	36.0	31.0	25.3	18.9	11.7	7.2
= 50	47.5	47.0	46.2	43.8	33.0	28.3	23.2	17.5	10.7	6.6
= 40	39.0	38.0	37.0	35.3	29.5	25.3	20.6	15.5	9.6	5.9
= 30	30.0	30.0	29.4	26.9	22.6	19.4	15.8	11.9	7.3	4.5
= 20	18.0	17.5	16.7	15.7	14.2	12.2	9.9	7.5	4.6	2.8

TABLE 8.4.11 BUILD-UP DESIGN ENVELOPES OF 99 PERCENTILE WIND SPEED CHANGE, 1- TO 80-km ALTITUDE REGION, SPACE AND MISSILE TEST CENTER (Vandenberg AFB)

Wind Speed at Reference Altitude (m/sec)	Scales of Distance (m)									
	5000	4000	3000	2000	1000	800	600	400	200	100
$\geq$ 90	62.1	59.9	57.8	51.5	35.2	30.1	24.6	18.4	11.5	7.0
= 80	58.7	57.7	55.6	48.8	33.5	29.0	23.6	17.8	11.0	6.7
= 70	55.0	54.5	53.4	48.1	33.0	28.8	23.0	16.8	10.5	6.5
= 60	50.4	49.9	49.0	44.0	32.7	27.9	22.8	16.2	9.7	5.3
= 50	45.4	44.8	43.7	40.0	29.9	25.4	21.8	15.6	9.2	5.0
= 40	38.9	38.7	37.2	34.9	25.1	22.4	19.1	14.9	8.8	4.7
= 30	30.0	29.4	28.3	25.4	19.9	17.8	14.8	11.5	7.1	4.2
= 20	20.0	19.8	19.5	18.4	15.0	13.1	10.9	8.0	4.7	2.6

TABLE 8.4.12 BACK-OFF DESIGN ENVELOPES OF 99 PERCENTILE WIND SPEED CHANGE, 1- TO 80-km ALTITUDE REGION, SPACE AND MISSILE TEST CENTER (Vandenberg AFB)

Wind Speed at Reference Altitude (m/sec)	Scales of Distance (m)									
	5000	4000	3000	2000	1000	800	600	400	200	100
$\geq$ 90	66.9	62.5	57.7	49.9	37.5	32.1	26.1	19.7	12.0	7.4
= 80	64.1	60.8	56.6	48.3	36.9	31.5	25.6	19.1	11.6	6.8
= 70	62.0	59.2	54.8	47.1	36.0	31.0	25.0	18.6	11.2	6.5
= 60	57.1	54.5	51.3	45.4	32.6	28.5	23.0	17.1	10.2	5.3
= 50	49.6	47.8	45.7	42.1	30.1	25.9	20.8	15.5	9.2	5.0
= 40	39.4	38.8	37.9	35.5	25.9	23.5	19.6	14.0	8.2	4.8
= 30	29.9	29.3	28.3	26.3	20.5	18.6	15.8	12.2	8.0	4.6
= 20	19.8	19.5	19.0	17.7	13.4	12.2	10.7	9.0	6.3	4.3

TABLE 8.4.13 BUILD-UP DESIGN ENVELOPES OF 99 PERCENTILE WIND SPEED CHANGE, 1- TO 80-km ALTITUDE REGION, WHITE SANDS MISSILE RANGE

Wind Speed at Reference Altitude (m/sec)	Scales of Distances (m)									
	5000	4000	3000	2000	1000	800	600	400	200	100
$\geq$ 90	70.7	67.0	61.2	52.4	42.0	36.0	29.4	22.1	13.6	8.4
= 80	66.0	63.0	57.7	50.0	40.2	34.5	28.1	21.2	13.0	8.0
= 70	60.2	57.0	53.0	46.5	38.0	32.6	26.6	20.0	12.3	7.6
= 60	52.4	50.0	46.5	42.3	35.5	30.5	24.9	18.7	11.5	7.1
= 50	44.8	43.0	40.2	36.5	32.0	28.3	23.1	17.4	10.7	6.6
= 40	36.4	35.3	33.8	31.0	27.5	23.6	19.3	14.5	8.9	5.5
= 30	27.4	26.5	25.6	24.3	20.6	17.7	14.4	10.8	6.7	4.1
= 20	18.4	17.7	17.3	16.5	15.0	12.9	10.5	7.9	4.9	3.0

TABLE 8.4.14 BACK-OFF DESIGN ENVELOPES OF 99 PERCENTILE WIND SPEED CHANGE, 1- TO 80-km ALTITUDE REGION, WHITE SANDS MISSILE RANGE

Wind Speed at Reference Altitude (m/sec)	Scales of Distance (m)									
	5000	4000	3000	2000	1000	800	600	400	200	100
$\geq$ 90	66.2	62.0	57.0	50.0	37.0	31.7	25.9	19.5	12.0	7.4
= 80	62.0	58.5	54.0	48.0	35.8	30.7	25.1	18.9	11.6	7.1
= 70	57.5	54.5	50.7	44.3	34.2	29.3	23.9	18.0	11.1	6.8
= 60	52.6	49.2	45.5	40.5	32.8	28.1	23.0	17.3	10.6	6.5
= 50	45.0	42.8	40.1	37.0	31.0	26.6	21.7	16.3	10.0	6.2
= 40	36.5	35.5	34.8	33.5	29.3	25.1	20.5	15.4	9.5	5.8
= 30	27.4	27.0	26.4	24.8	22.0	19.3	15.8	11.8	7.3	4.5
= 20	17.7	17.3	16.7	15.8	14.1	12.1	9.9	7.4	4.6	2.8

TABLE 8.4.15 BUILD-UP DESIGN ENVELOPES OF 99 PERCENTILE WIND SPEED CHANGE, 1- TO 80-km ALTITUDE REGION, WALLOPS FLIGHT CENTER

Wind Speed at Reference Altitude (m/sec)	Scales of Distance (m)									
	5000	4000	3000	2000	1000	800	600	400	200	100
≥ 90	71.0	66.2	60.2	50.5	37.6	32.3	26.3	19.8	12.2	7.5
= 80	66.5	62.5	57.5	48.8	37.0	31.7	25.9	19.5	12.0	7.4
= 70	61.2	58.5	53.8	46.5	35.8	30.7	25.1	18.9	11.6	7.1
= 60	54.4	52.5	50.0	44.2	34.5	29.6	24.2	18.2	11.2	6.9
= 50	45.2	43.4	42.3	38.8	33.0	28.3	23.2	17.4	10.7	6.6
= 40	36.1	35.6	34.5	32.3	27.6	23.7	19.3	14.5	8.9	5.5
= 30	27.0	26.3	25.3	24.2	20.6	17.7	14.4	10.8	6.7	4.1
= 20	17.7	17.3	16.8	16.4	15.2	13.0	10.6	8.0	4.9	3.0

TABLE 8.4.16 BACK-OFF DESIGN ENVELOPES OF 99 PERCENTILE WIND SPEED CHANGE, 1- TO 80-km ALTITUDE REGION, WALLOPS FLIGHT CENTER

Wind Speed at Reference Altitude (m/sec)	Scales of Distance (m)									
	5000	4000	3000	2000	1000	800	600	400	200	100
≥ 90	72.5	67.0	59.2	49.0	31.5	27.0	22.1	16.6	10.2	6.3
= 80	66.3	62.0	56.0	46.0	30.0	25.7	21.0	15.8	9.7	6.0
= 70	60.0	56.5	51.5	43.6	28.5	24.5	20.0	15.0	9.2	5.7
= 60	53.5	50.7	46.8	40.4	27.0	23.2	18.9	14.2	8.7	5.4
= 50	46.2	44.2	41.0	35.8	25.2	21.6	17.6	13.3	8.2	5.0
= 40	36.7	35.2	32.7	28.7	21.5	18.4	15.1	11.3	7.0	4.3
= 30	27.2	26.1	24.8	22.5	18.2	15.6	12.7	9.6	5.9	3.6
= 20	17.8	17.3	16.4	15.2	13.0	11.1	9.0	6.8	4.2	2.6

TABLE 8.4.17 BUILD-UP DESIGN ENVELOPES OF 99 PERCENTILE WIND SPEED CHANGE, 1- TO 80-km ALTITUDE REGION, EDWARDS AIR FORCE BASE

	Scales of Distance (m)									
Wind Speed at Reference Altitude (m/sec)	5000	4000	3000	2000	1000	800	600	400	200	100
≥ 90	69.0	65.0	59.5	52.0	39.5	33.9	27.7	20.8	12.8	7.9
= 80	64.9	61.8	56.9	50.0	38.2	32.8	26.7	20.1	12.4	7.6
= 70	59.0	57.0	53.0	46.8	37.0	31.7	25.9	19.5	12.0	7.4
= 60	51.8	50.4	47.8	43.6	35.5	30.5	24.9	18.7	11.5	7.1
= 50	44.8	43.6	41.3	38.2	31.8	27.5	22.4	16.9	10.4	6.4
= 40	36.5	35.5	34.3	32.0	26.5	23.0	18.8	14.1	8.7	5.3
= 30	28.0	27.3	26.3	24.5	20.8	17.8	14.6	11.0	6.7	4.2
= 20	18.0	17.7	17.4	16.7	15.2	13.0	10.6	8.0	4.9	3.0

TABLE 8.4.18 BACK-OFF DESIGN ENVELOPES OF 99 PERCENTILE WIND SPEED CHANGE, 1- TO 80-km ALTITUDE REGION, EDWARDS AIR FORCE BASE

	Scales of Distance (m)									
Wind Speed at Reference Altitude (m/sec)	5000	4000	3000	2000	1000	800	600	400	200	100
≥ 90	75.2	72.0	67.3	59.0	42.8	36.7	30.2	22.5	13.9	8.5
= 80	68.0	66.3	62.5	55.5	40.8	35.0	28.6	21.5	13.2	8.1
= 70	60.4	59.0	56.8	51.4	38.7	33.2	27.0	20.4	12.5	7.7
= 60	53.0	51.8	49.3	45.0	36.0	30.9	25.2	19.0	11.7	7.2
= 50	44.5	43.3	41.5	38.4	32.0	27.5	22.4	16.9	10.4	6.4
= 40	35.7	35.3	34.5	33.0	27.0	23.2	18.9	14.2	8.8	5.4
= 30	27.1	27.0	26.9	26.3	21.4	18.4	15.0	11.3	6.9	4.3
= 20	18.0	17.0	16.6	15.7	14.2	12.2	9.9	7.5	4.6	2.8

TABLE 8.4.19 BUILD-UP DESIGN ENVELOPES OF 99 PERCENTILE WIND SPEED CHANGE, 1- TO 80-km ALTITUDE REGION, FOR ALL FIVE LOCATIONS

	Scales of Distance (m)									
Wind Speed at Reference Altitude (m/sec)	5000	4000	3000	2000	1000	800	600	400	200	100
$\geq$ 90	71.0	67.0	61.2	52.4	42.0	36.0	29.4	22.1	13.6	8.4
= 80	66.5	63.0	57.7	50.0	40.2	34.5	28.1	21.2	13.0	8.0
= 70	61.2	58.5	53.8	48.1	38.0	32.6	26.6	20.0	12.3	7.6
= 60	54.4	52.5	50.0	44.2	35.5	30.5	24.9	18.7	11.5	7.1
= 50	46.5	45.0	43.7	40.0	33.0	28.3	23.2	17.4	10.7	6.6
= 40	38.9	38.7	37.2	34.9	27.6	23.7	19.3	14.9	8.9	5.5
= 30	30.0	29.4	28.3	25.4	20.8	17.8	14.8	11.5	7.1	4.2
= 20	20.0	19.8	19.5	18.4	15.2	13.1	10.9	8.0	4.9	3.0

TABLE 8.4.20 BACK-OFF DESIGN ENVELOPES OF 99 PERCENTILE WIND SPEED CHANGE, 1- TO 80-km ALTITUDE REGION, FOR ALL FIVE LOCATIONS

	Scales of Distance (m)									
Wind Speed at Reference Altitude (m/sec)	5000	4000	3000	2000	1000	800	600	400	200	100
$\geq$ 90	77.5	74.4	68.0	59.3	42.8	36.7	30.2	22.5	13.9	8.5
= 80	71.0	68.0	63.8	56.0	40.8	35.0	28.6	21.5	13.2	8.1
= 70	63.5	61.0	57.9	52.0	38.8	33.2	27.0	20.4	12.5	7.7
= 60	57.1	54.7	52.3	47.4	36.0	31.0	25.3	19.0	11.7	7.2
= 50	49.6	47.8	46.2	43.8	33.0	28.3	23.2	17.5	10.7	6.6
= 40	39.4	38.8	37.9	35.5	29.5	25.3	20.6	15.5	9.6	5.9
= 30	30.0	30.0	29.4	26.9	22.6	19.4	15.8	12.2	7.3	4.6
= 20	19.8	19.5	19.0	17.7	14.2	12.2	10.7	9.0	6.3	4.3

a reference point in the atmosphere. As in the case of the wind speed changes in subsection 8.4.6, we will call changes below the reference level build-up wind changes and those above the reference level back-off wind direction changes. These changes can be significantly different. For example if the reference point is at the 4 km level, the build-up changes between the 1- and 4-kilometer levels will be distinctly different from the back-off changes between the 5- and 7-kilometer levels. This results from the fact that variations of wind direction tend to be larger in the atmospheric boundary layer (0-2 km) than in the free atmosphere above the atmospheric boundary layer. In this light the following model is recommended as an integrated wind direction change criteria for design studies. The model consists of the 8-16 km 99% direction changes in Figure 8.4.14 and a set of functions $R(\Delta H, H_r, u_r)$ to transfer these changes to any reference level H_r above the 1-kilometer level, where $\overline{u}_r$ is the reference level wind speed. The quantity R is defined such that multiplication of the 8-16 km wind direction changes by $R(\Delta H, H_r, \overline{u}_r)$ will yield the changes in wind direction over a layer of thickness ΔH with top or bottom of the reference level located at height H_r above sea level and reference level wind speed equal to $\overline{u}_r$. The functions $R(\Delta H, H_r, \overline{u}_r)$ for back-off and build-up wind direction changes are defined as

Back-off:

$$R = R^*, \qquad 1 \leq H_r < 1.5 \text{ km}$$

$$R = 2(1-R^*)(H_r - 1.5) + R^*, \qquad 1.5 \leq H_r < 2 \text{ km}$$

$$R = 1 \qquad 2 \text{ km} \leq H_r$$

Build-up:

$$R = R^*, \qquad 0 < H_r \leq 2 \text{ km}$$

$$\left.\begin{aligned} R &= \left[\frac{R^* - 1}{2}\right]\left[1 - \cos\pi(\Delta H - H_r + 3)\right] + 1, \quad 1 < \Delta H \leq H_r - 2 \\ R &= R^*, \quad H_r - 2 < \Delta H \leq H_r \end{aligned}\right\}, \quad 2 < H_r \leq 3 \text{ km}$$

$$
\left.
\begin{array}{l}
R = 1, \quad 0 < \Delta H \leq H_r - 3 \text{ km} \\[2ex]
R = \left[\dfrac{R^* - 1}{2}\right]\left[1 - \cos\pi(\Delta H - H_r + 3)\right] + 1, \quad H_r - 3 < \Delta H \leq H_r - 2 \\[2ex]
R = R^*, \quad H_r - 2 < \Delta H \leq 4 \text{km}
\end{array}
\right\}, \quad 3 < H_r \leq 6 \text{km}
$$

$$
R = 1, \qquad\qquad 6\text{km} \leq H_r,
$$

where ΔH, and H_r have units of kilometers and R is a nondimensional quantity. The quantity R^* is a function ΔH and $\bar{u}_r$ and is given in Figure 8.4.15.

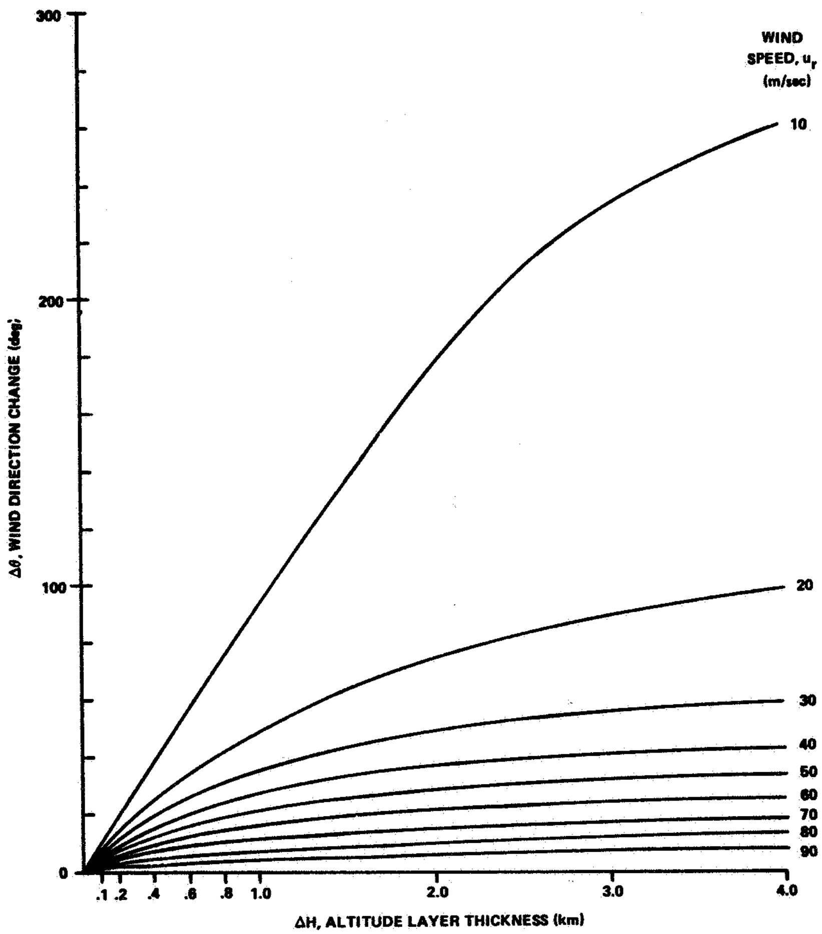

Figure 8.4.14 IDEALIZED 99% WIND DIRECTION CHANGE AS A FUNCTION OF WIND SPEED FOR VARYING LAYERS IN THE 8-16 KM ALTITUDE REGION OF THE EASTERN TEST RANGE

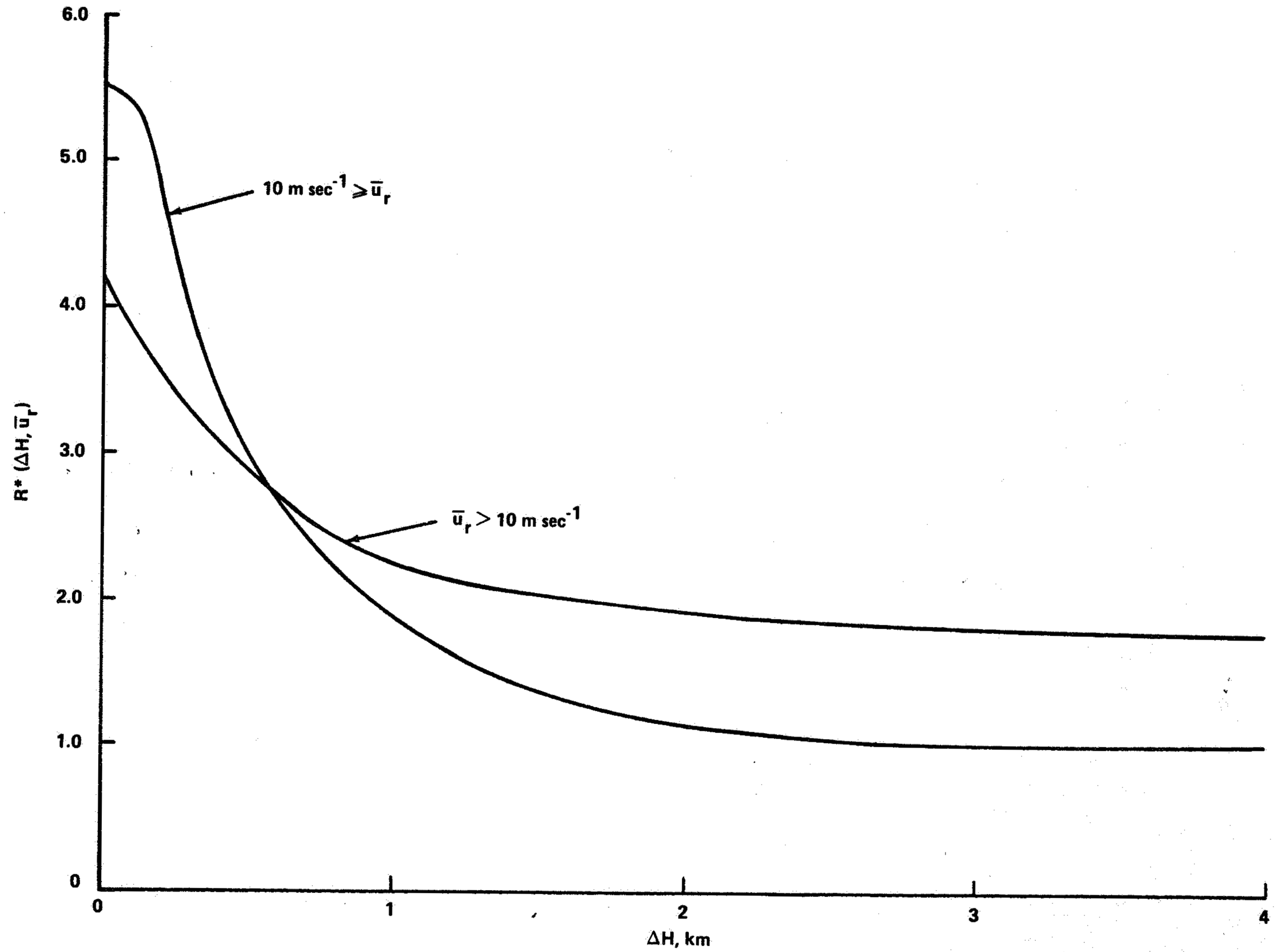

Figure 8.4.15 THE FUNCTION R* VERSUS H FOR VARIOUS CATEGORIES OF WIND SPEED $\bar{u}_r$ AT THE REFERENCE LEVEL

To apply these wind direction change data, one first constructs a synthetic wind profile (see Section 8.4.9) wind profile envelopes and wind shear envelopes, with or without gust (see Section 8.4.8) as the case may be. A point (reference point) at height H_r above sea level of potential concern on this synthetic wind profile is selected for analysis. One then turns the wind direction above or below this point according to the schedule of wind direction changes given by the above model. Thus, for example, if the 12-kilometer reference point wind speed and direction are 20 m sec^{-1} and 90^{o} (east wind i.e., a wind blowing from the east) then according to the wind direction change model discussed above the wind directions at 0.2, 0.6, 1.0, 2.0, 3.0, and 4.0 km below or above the 12-kilometer reference point, as the case may be, are 107^{o}, 123^{o}, 140^{o}, 165^{o}, 180^{o}, and 190^{o} for clockwise turning of the wind vector starting with the reference point wind vector at 12 km and looking toward the earth. Counterclockwise turning is also permissible. The direction of rotation of the wind vector should be selected to produce the most adverse wind situation from a vehicle response point of view.

In view of the unavailability of wind direction change statistics above the 16-kilometer level, at this time, it is recommended that the above procedure be used for $H_r > 16$ km.[8]

8.4.8 Gusts – Vertically Flying Vehicles

The steady-state inflight wind speed envelopes presented in subsection 8.4.5 do not contain the gust (high frequency content) portion of the wind profile. The steady-state wind profile measurements have been defined as those obtained by the rawinsonde system. These measurements represent wind speeds averaged over approximately 1000 meters in the vertical and, therefore, eliminate features with smaller scales. These smaller scale features are contained in the detailed profiles measured by the FPS-16 Radar/Jimsphere system.

A number of attempts have been made to represent the high frequency content of vertical wind profiles in a suitable form for use in vehicle design studies. Most of the attempts resulted in gust information that could be used for specific applications, but, to date, no universal gust representation has been formulated. Information on discrete and continuous gust representations is given below relative to vertically ascending space vehicles.

---

8. See subsection 8.4.14.2 for wind direction change statistics valid below the 1-kilometer level for take-off and landing design studies.

8.4.8.1 Discrete Gusts

Discrete gusts are specified in an attempt to represent, in a physically reasonable manner, characteristics of small scale motions associated with vertical wind velocity profiles. Gust structure usually is quite complex and it is not always understood. For vehicle design studies, discrete gusts are usually idealized because of their complexity and to enhance their utilization.

Well defined, sharp edged, and repeated sinusoidal gusts are important types in terms of their influence upon space vehicles. Quasi-square-wave gusts with amplitudes of approximately 9 m/sec have been measured. These gusts are frequently referred to as embedded jets or singularities in the vertical wind profile. By definition, a gust is a wind speed in excess of the defined steady-state value; therefore, these gusts are employed on top of the steady-state wind profile values.

If a design wind speed profile envelope without a wind shear envelope is to be used in a design study it is recommended that the associated discrete gust vary in length from 60 to 300 meters. The leading and trailing edge[9] should conform to a 1-cosine build-up of 30 meters and a corresponding decay also over 30 meters as shown in Figure 8.4.16. The plateau region of the gust can vary in thickness from zero to 240 m. An analytical expression for the value of this gust of height H above natural grade is given by

$$\left.\begin{aligned} u_g &= \frac{A}{2}\left\{1 - \cos\left[\frac{\pi}{30}(H-H_b)\right]\right\}, \quad H_b \le H \le H_b + 30\mathrm{m} \\ u_g &= A, \quad H_b + 30\ \mathrm{m} \le H \le H_b + \lambda - 30\mathrm{m} \\ u_g &= \frac{A}{2}\left\{1 - \cos\left[\frac{\pi}{30}(H - H_b - \lambda)\right]\right\}, \quad H_b + \lambda - 30\mathrm{m} \le H \le H_b + \lambda \end{aligned}\right\} \quad (8.27)$$

where H_b is the height of the base of the gust above natural grade, λ is the gust thickness ($60 \le \lambda \le 300$m), A is the gust amplitude, and MKS units are understood.

The gust amplitude is a function of H_b and for design purposes the 1% risk gust amplitude is given by

9. Leading and trailing edges are used here in the sense that as height H increases one first encounters the gust leading edge and then the trailing edge.

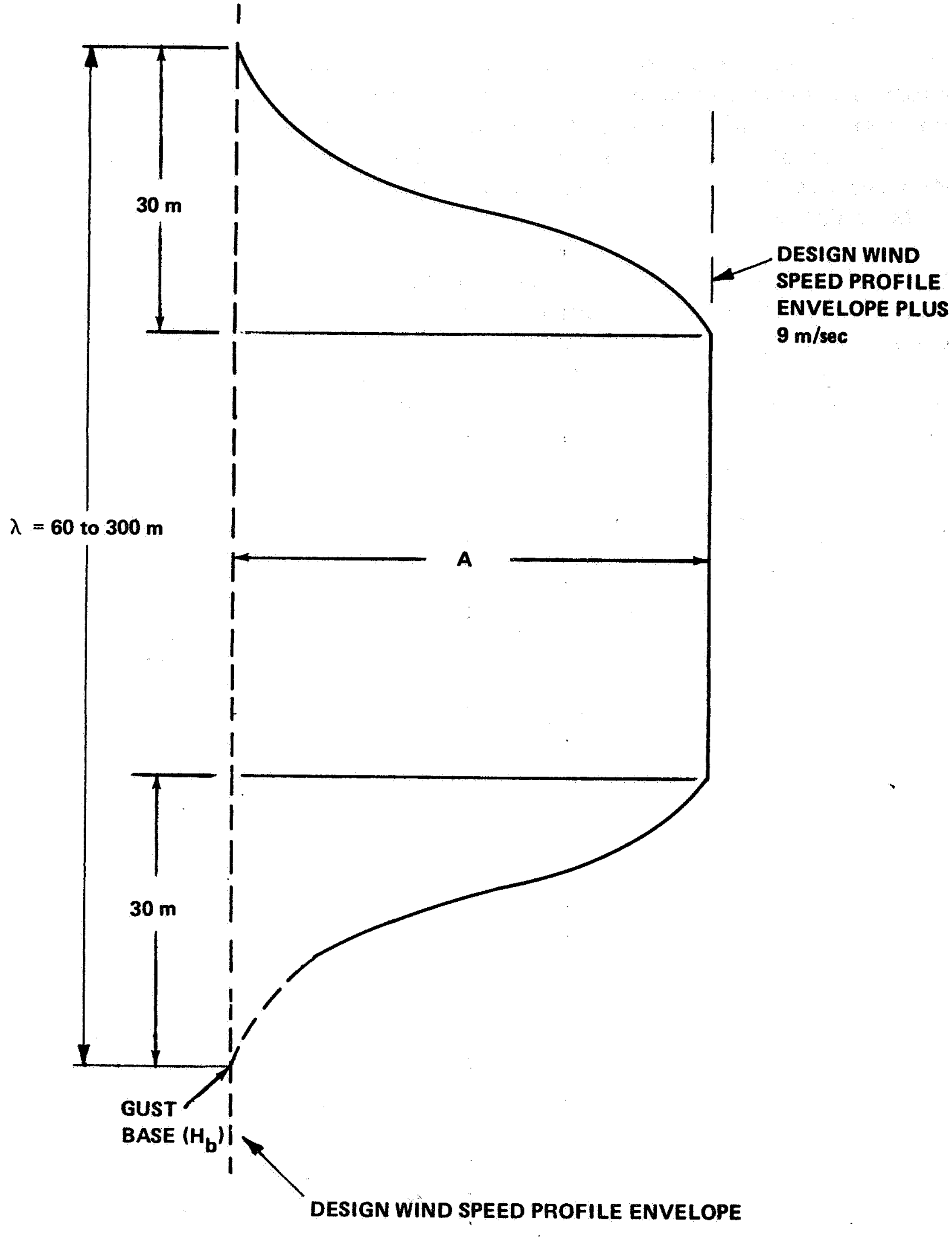

Figure 8.4.16 RELATIONSHIP BETWEEN DISCRETE GUST AND/OR EMBEDDED JET CHARACTERISTICS (quasi-square-wave shape) AND THE DESIGN WIND SPEED PROFILE ENVELOPE

$$\left.\begin{array}{l} A = 6\ \text{m/sec},\ H_b < 300\,\text{m} \\[2ex] A = \dfrac{3}{700}\,(H_b - 300) + 6,\ 300\ \text{m} \le H_b \le 1000\ \text{m} \\[2ex] A = 9\ \text{m/sec}^{-1} \quad 1000\ \text{m} < H_b . \end{array}\right\} \tag{8.28}$$

If a wind speed profile envelope with a build-up wind shear envelope (Section 8.4.6) is to be used in a design study it is recommended that the above mentioned discrete gust be modified by replacing the leading edge 1 - cosine shape with the following formula

$$u_g = 10A\left\{\left(\frac{H-H_b}{30}\right)^{0.9} - 0.9\left(\frac{H-H_b}{30}\right)\right\},\ H_b \le H \le H_b + 30\,\text{m} \tag{8.29}$$

The height of the gust base H_b corresponds to the point where the design wind speed profile envelope intersects the design build-up shear envelope. If a discrete gust is to be used with a back-off wind shear envelope then the 1-cosine trailing edge shall be given by

$$u_g = 10A\left\{\left(\frac{H_b+\lambda-H}{30}\right)^{0.9} - 0.9\left(\frac{H_b+\lambda-H}{30}\right)\right\},\ H_b + \lambda - 30\text{m} \le H \le H_b + \lambda \tag{8.30}$$

and the leading edge shall conform to a 1-cosine shape. In this case the height, $H_b + \lambda$, of the end of the gust corresponds to the point where the design wind speed profile envelope intersects the design back-off shear envelope. This modification of the 1-cosine shape at the leading and trailing edges as the case may be results in a continuous merger of the shear envelope and the discrete gust. See subsection 8.4.9 for further details. When applying the discrete gust with wind shears the discrete gust and shears should be reduced by a factor of 0.85 to account for the non-perfect correlation between wind shears and gusts (see subsection 8.4.9.2 for details).

Another form of discrete gust that has been observed is approximately sinusoidal in nature, where gusts occur in succession. Figure 8.4.17 illustrates the estimated number of consecutive sinusoidal type gusts that may occur and their respective amplitudes for design purposes. It is extremely important when applying these gusts in vehicle studies to realize that these are pure sinusoidal representations that have never been observed in nature. The degree of purity of these sinusoidal features on the vertical wind profiles has not been established. These gusts should be superimposed symmetrically upon the steady-state profile. The data presented here on sinusoidal discrete gusts are at best preliminary and should be treated as such in design studies.

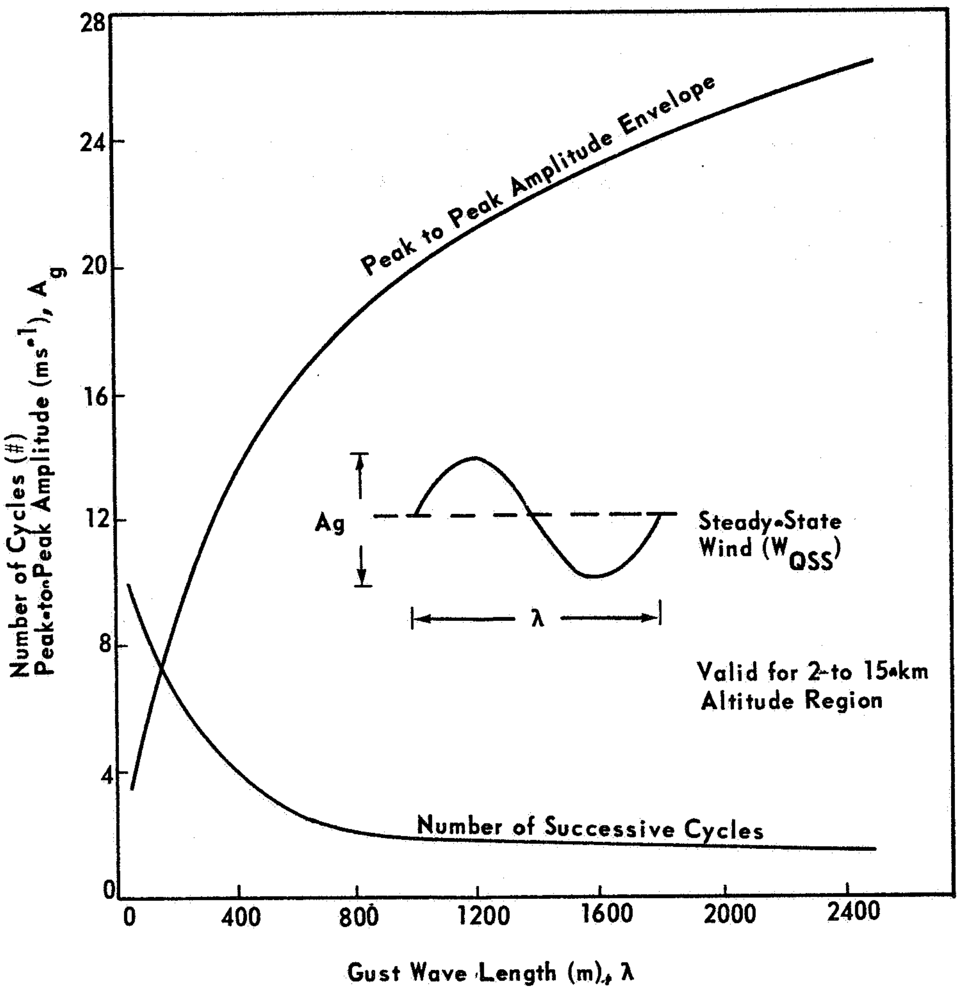

FIGURE 8.4.17 BEST ESTIMATE OF EXPECTED (≧ 99 percentile) GUST AMPLITUDE AND NUMBER OF CYCLES AS A FUNCTION OF GUST WAVELENGTHS

8.4.8.2 Spectra

In general, the small scale motions associated with vertical detailed wind profiles are characterized by a superposition of discrete gusts and many random frequency components. Spectral methods have been employed to specify the characteristics of this superposition of small scale motions.

A digital filter was developed to separate small scale motions from the steady-state wind profile. The steady-state wind profile defined by the separation process approximates those obtained by the rawinsonde system.[10] Thus, a spectrum of small scale motions is representative of the motions included in the FPS-16 radar/Jimsphere measurements, which are not included in the rawinsonde measurements. Therefore, a spectrum of those motions should be considered in addition to the steady-state wind profiles to obtain an equivalent representation of the detailed wind profile. Spectra of the small scale motions for various probability levels have been determined and are presented in Figure 8.4.18. The spectra were computed from approximately 1200 detailed wind profile measurements by computing the spectra associated with each profile, then determining the probabilities of occurrence of spectral density as a function of wave numbers (cycles/4000 m). Thus the spectra represent envelopes of spectral density for the given probability levels. Spectra associated with each profile were computed over the altitude range between approximately 4 and 16 kilometers. It has been shown that energy (variance) of the small scale motions is not vertically homogeneous; that is, it is not constant with altitude. The energy content over limited altitude intervals and for limited frequency bands may be much larger than that represented by the spectra in Figure 8.4.18. This should be kept in mind when interpreting the significance of vehicle responses when employing the spectra of small scale motions. Additional details on this subject are available upon request. Envelopes of spectra for detailed profiles without filtering (solid lines) are also shown in Figure 8.4.18. These spectra are well represented for wave numbers ≥ 5 cycles per 4000 meters by the equation

$$E(k) = E_0 k^{-p}, \tag{8.31A}$$

where E is the spectral density at any wave number k (cycles/4000 m) between 1 and 20, $E_0 = E(1)$, and p is a constant for any particular percentile level of occurrence of the power spectrum.

---

10. This definition was selected to enable use of the much larger rawinsonde data sample in association with a continuous type gust representation.

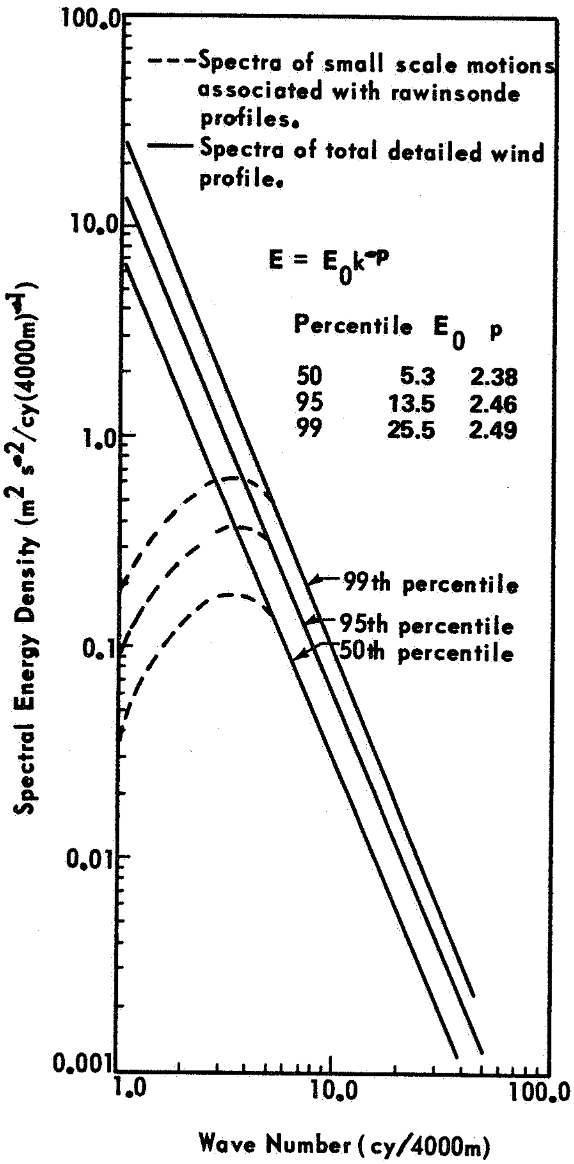

FIGURE 8.4.18 SPECTRA OF DETAILED WIND PROFILES

Spectra of the total wind speed profiles may be useful in control systems and other slow response parametric studies for which the spectra of small scale motions may not be adequate.

The power spectrum recommended for use in elastic body studies is given by the following expression:

$$E(\kappa) = \frac{683.4\ (4000\,\kappa)^{1.62}}{1 + 0.0067\ (4000\,\kappa)^{4.05}}, \tag{8.31B}$$

where the spectrum $E(\kappa)$ is defined so that integration over the domain $0 \leq \kappa \leq \infty$ yields the variance of the turbulence. In this equation $E(\kappa)$ is now the power spectral density [$m^2\ sec^{-2}$/(cycles per meter)] at wave number κ (cycles per meter). This function represents the 99 percentile scalar wind spectra for small-scale motions given by the dashed curve and its solid line extension into the high wave number region in Figure 8.4.18. The associated design turbulence loads are obtained by multiplying the load standard deviations by a factor of three. (Spectra for meridional and zonal components are available upon request).

Vehicle responses obtained from application of this turbulence spectra should be added to rigid vehicle responses resulting from use of the synthetic wind speed and wind shear profile (with the 0.85 factor on shears) but without a discrete gust.

8.4.9 Synthetic Wind Speed Profiles

Methods of constructing synthetic wind speed profiles are described herein. One method uses design wind speed profile envelopes (subsection 8.4.5), and discrete gusts or spectra (subsection 8.4.8) without consideration of any lack of correlation between the shears and gusts. Another method takes into account the relationships between the wind shear and gust characteristics.

8.4.9.1 Synthetic Wind Speed Profiles for Vertical Flight Path Considering Only Speeds and Shears

In the method that follows, correlation between the design wind speed profile envelope and wind shear envelope is considered. The method is illustrated with the 95 percentile design nondirectional (scalar) wind speed profile and the 99 percentile scalar wind speed build-up envelope for the Eastern Test Range (Figure 8.4.19) and is stated as follows:

a. Start with a speed on the design wind speed profile envelope at a selected (reference) altitude.

b. Subtract the amount of the shear (wind speed change) for each required altitude layer from the value of the wind speed profile envelope at the selected altitude. Figure 8.4.19 presents an example of a 99 percentile shear build-up envelope starting from a reference altitude of 11 km on the ETR 95 percentile wind speed profile envelope (Fig. 8.4.8). The 10 km wind speed of 41.3 m/sec is determined by subtracting 31.7 m/sec—a linearly interpolated shear value for 73 m/sec from the 1000 m column of Table 8.4.10—from 73 m/sec.

c. Plot values obtained for each altitude layer at the corresponding altitudes. (The value of 41.3 m/sec, obtained in the example in b, would be plotted at 10 km.) Continue plotting values until a 5000-meter layer is reached (5000 meters below the selected altitude).

d. Draw a smooth curve through the plotted points starting at the selected altitude on the wind speed profile envelope. The lowest point is extended from the origin with a straight line tangent to the plotted shear build-up curve. This curve then becomes the shear build-up envelope.

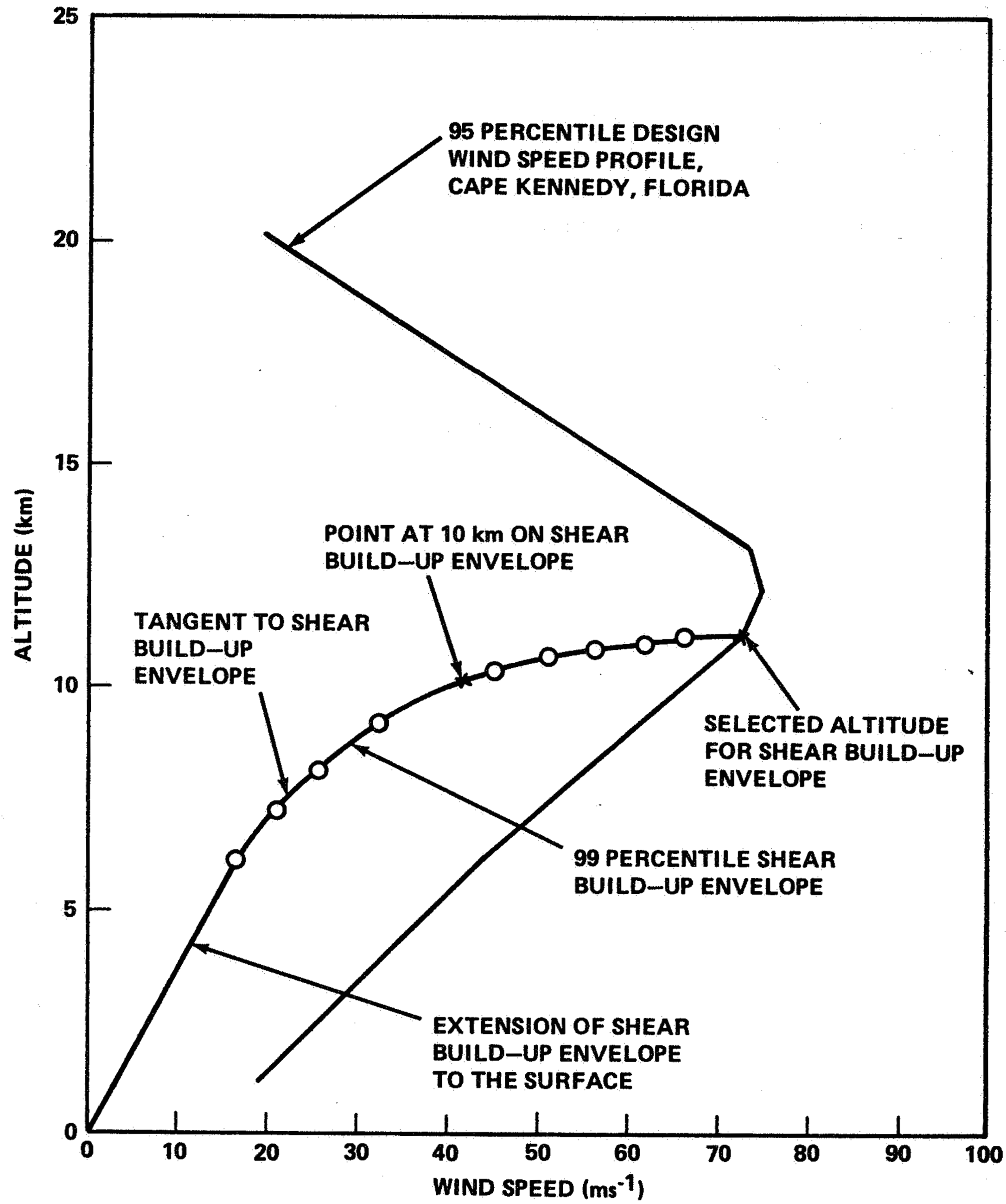

FIGURE 8.4.19 EXAMPLE OF SYNTHETIC WIND PROFILE CONSTRUCTION, WITHOUT ADDITION OF GUST

8.4.9.2 Synthetic Wind Speed Profiles For Vertical Flight Path Considering Relationships Between Speeds, Shears, and Gusts

In the construction of a synthetic wind speed profile, the lack of perfect correlation between the wind shear and gust can be taken into account by multiplying the shears (wind speed changes) (subsection 8.4.6) and the recommended design discrete gusts (subsection 8.4.8) by a factor of 0.85 before constructing the synthetic wind profile. This is equivalent, as an engineering approximation, to taking the combined 99 percentile values for the gusts and shears in a perfectly correlated manner. This approach was used successfully in the Apollo/Saturn vehicle development program.

Thus, to construct the synthetic wind speed profiles (considering relationships between shears, speeds, and gusts, using the design wind speed envelopes given in subsection 8.4.5), the procedure that follows is used. Figures 8.4.20 and 8.4.21 show an example using the 95 percentile design wind speed profile envelope, the 99 percentile wind speed build-up envelope, and the modified one-minus-cosine discrete gust shape.

a. Construct the shear build-up envelope in the way described in subsection 8.4.9.1, except multiply the values of wind speed change used for each scale-of-distance by 0.85. (In the example for the selected altitude of 11 km, the point at 10 km will be found by using the wind speed change of 31.2 x 0.85, or 26.5 m/sec.) This value subtracted from 73 m/sec then gives a value of 46.5 m/sec for the point plotted at 10 kilometers instead of the value of 41.8 m/sec used when shear and gust relationships were not considered.

b. The discrete gust is superimposed on the build-up wind shear envelope/wind speed profile envelope by adding the gust given by equation (8.27) with leading edge in the region $H_b \leq H \leq H_b + 30$ m replaced with equation (8.29). The base of the discrete gust is located at the intersection of the build-up wind shear envelope and the wind speed profile envelope (see Figure 8.4.20). The gust amplitude, A, shall be decreased by a factor of 0.85, in order to account for the nonperfect correlation between shears and gusts. Figure 8.4.21 gives an example of a synthetic profile with shears and gust in combination.

c. When the gust ends at the design wind envelope, the synthetic wind profile may follow the design wind speed envelope or shear back-off profile. If the synthetic wind profile follows the design wind speed envelope then the trailing edge of the discrete gust will be a 1-cosine shape as given by equation (8.27). If the synthetic wind profile follows the shear back-off profile then the trailing edge of the discrete gust will be that given by equation (8.30). This

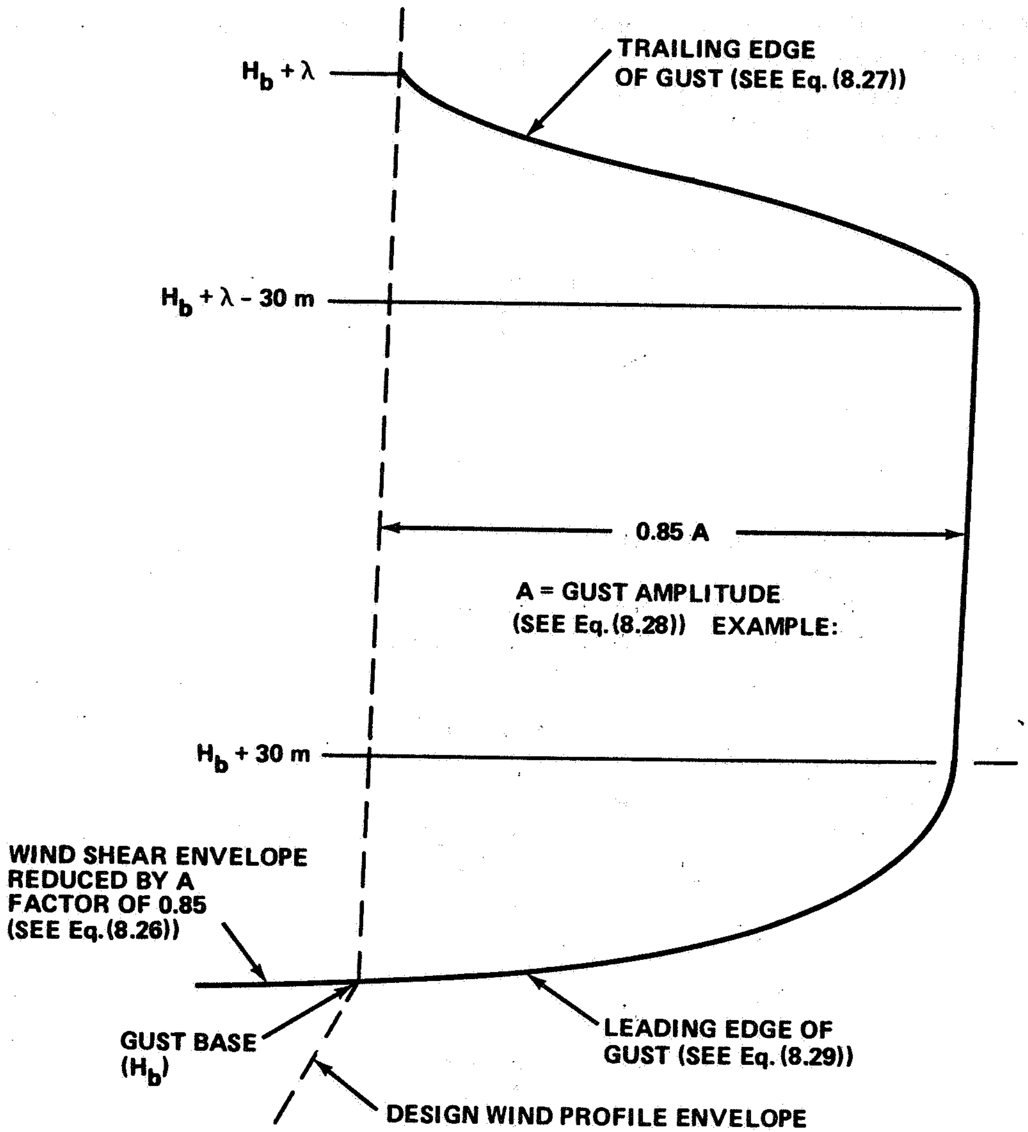

FIGURE 8.4.20 RELATIONSHIP BETWEEN REVISED GUST SHAPE, DESIGN WIND PROFILE ENVELOPE, AND SPEED BUILD-UP (SHEAR) ENVELOPE

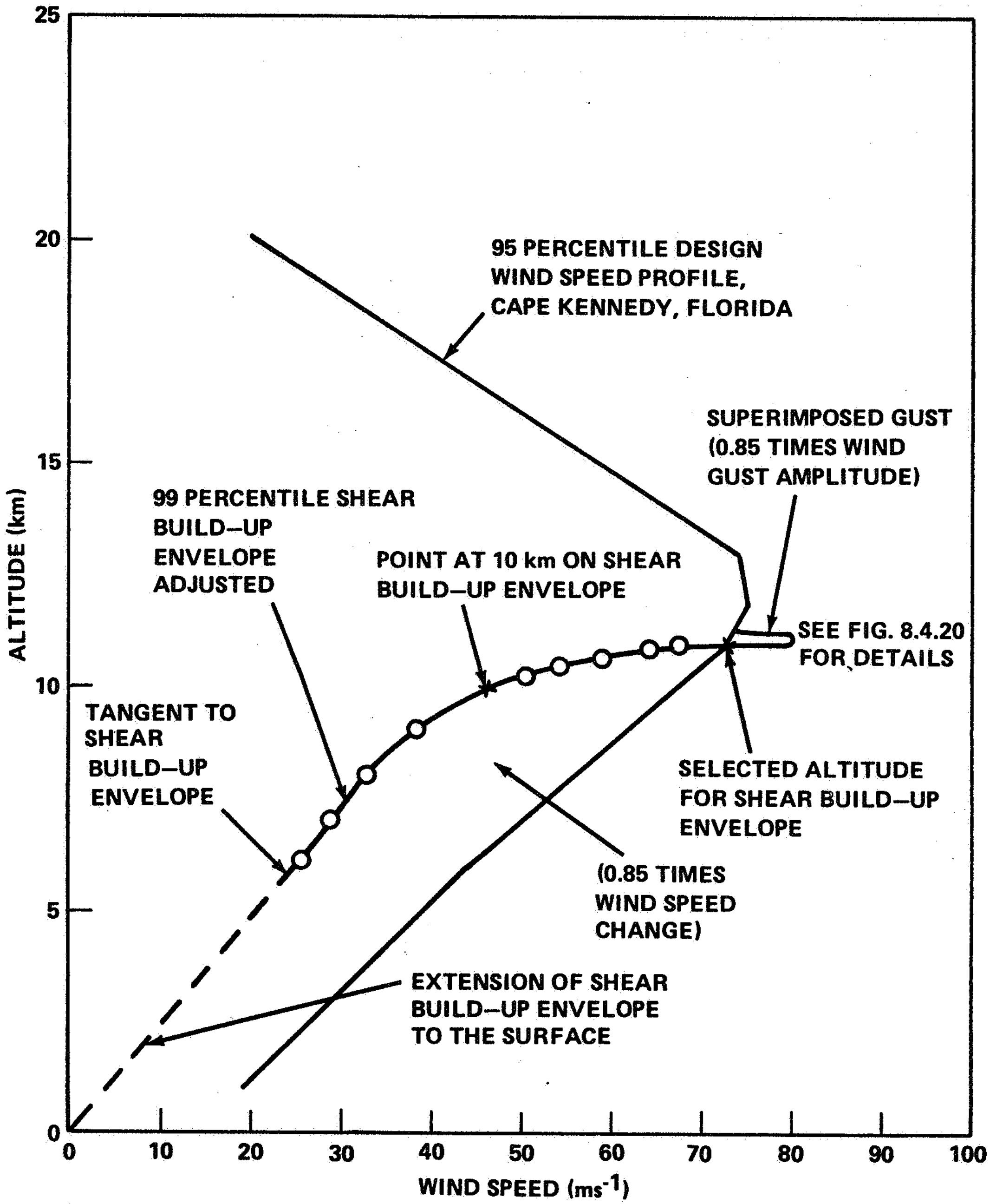

FIGURE 8.4.21 EXAMPLE OF SYNTHETIC WIND PROFILE CONSTRUCTION, WITH RELATIONSHIP OF WIND SHEARS AND GUSTS ASSUMED

modified gust shape will guarantee a continuous transition from the gust to the back-off shear envelope. Vehicle response through both the wind profile envelope with gusts and the synthetic wind profile with shears and gusts in combination should be examined.

d. If a power spectrum representation (see subsection 8.4.8.2) is used, then disregard all references to discrete gusts in the above. Use the 0.85 factor on shears and apply the spectrum as given in subsection 8.4.8.2.

8.4.9.3 Synthetic Wind Profile Merged to the Ground Wind Profile

Up to this point we have considered only those wind shear envelopes which are linearly extrapolated to a zero wind condition at the ground. This procedure does not allow for the possibility of the vehicle (Space Shuttle) to enter a wind shear envelope/gust above the H = 1000 m in a perturbed state resulting from excitations of the control system by the ground wind profile and the associated ground wind shears and gusts. To allow for these possibilities, it is recommended that the wind shear envelopes which begin above the 3000-meter level be combined with the wind profile envelope and discrete gust as stated in Section 8.4.9.2; however, a linear extrapolation shall be used to merge the wind defined by the shear envelope at the 3000-meter level with the 1000-meter wind on the wind profile envelope.

The steady-state ground wind profile up to the 150-meter level is defined by the peak wind profile (see Section 8.3.5.2) reduced to a steady-state wind profile by division with a 10-minute average gust factor profile (see Section 8.3.7.1). To merge this steady-state wind profile into the 1000-meter level steady-state wind speed envelope the steady-state wind speed in the layer between 150 to 300 meters shall take on a constant value equal to the steady-state wind at the 150-meter level defined by the peak wind profile and gust factor profile between the surface of the earth and the 150-meter level. The flow between the 300-meter level and the 1000-meter level shall be obtained by linear interpolation. If the discontinuities in slope of the wind profile at the 150-, 300- and 1000-meter levels resulting from this merging procedure introduce significant false vehicle responses it is recommended that this interpolation procedure be replaced with a procedure involving a smooth continuous function which closely approximates the piece-wise linear segment interpolation function between the 150- and 1000-meter levels with continuous values of wind speed and slope at the 150- and 1000-meter levels.

8.4.9.4 Synthetic Wind Speed Profiles For Non-Vertical Flight Path

To apply the synthetic wind profile for other than vertical flight, multiply the wind shear build-up and back-off values by the cosine of the angle between the vertical axis (earth fixed coordinate system) and the vehicle's flight path. The gust (or turbulence spectra) is applied directly to the vehicle without respect to the flight path angle. The synthetic wind profile is otherwise developed according to procedures given in Section 8.4.9.2.

8.4.10 Characteristic Wind Profiles to a Height of 18 Kilometers

8.4.10.1 Features of Wind Profiles

A significant problem in space vehicle design is to provide assurance of an adequate design for flight through wind profiles of various configurations. During the major design phase of a space vehicle, the descriptions of various characteristics of the wind profile are employed in determining the applicable vehicle response requirement. Since much of the vehicle is in a preliminary status of design and the desired detail data on structural dynamic modes and other characteristics are not known at this time, the use of statistical and synthetic representations of the wind profile are desirable. However, after the vehicle design has been finalized and tests have been conducted to establish certain dynamic capabilities and parameters, it is desirable to evaluate the total system by simulated dynamic flight through wind profiles containing adequate frequency resolution (Ref. 8.36). The profiles shown in Figures 8.4.22 through 8.4.27 are profiles of scalar wind measured by the FPS-16 Radar/Jimsphere wind measuring system, and they illustrate the following: (1) jet stream winds, (2) sinusoidal variation in wind with height, (3) high winds over a broad altitude band, (4) light wind speeds, and (5) discrete gusts.

These profiles show only a few of the possible wind profiles that can occur. Jet stream winds (Fig. 8.4.22) are quite common to the various test ranges during the winter months and can reach magnitudes in excess of 100 m/sec. These winds occur over a limited altitude range, making the wind shears very large. Figure 8.4.23 depicts winds having sinusoidal behavior in the 10- to 14-kilometer region. These types of winds can create excessive loads upon a vertically rising vehicle, particularly if the reduced forcing frequencies couple with the vehicle control frequencies and result in additive loads. It is not uncommon to see periodic variations occur in the vertical winds. Some variations are of more concern than others, depending upon wavelength and, of course, amplitude. Figure 8.4.24 is an interesting

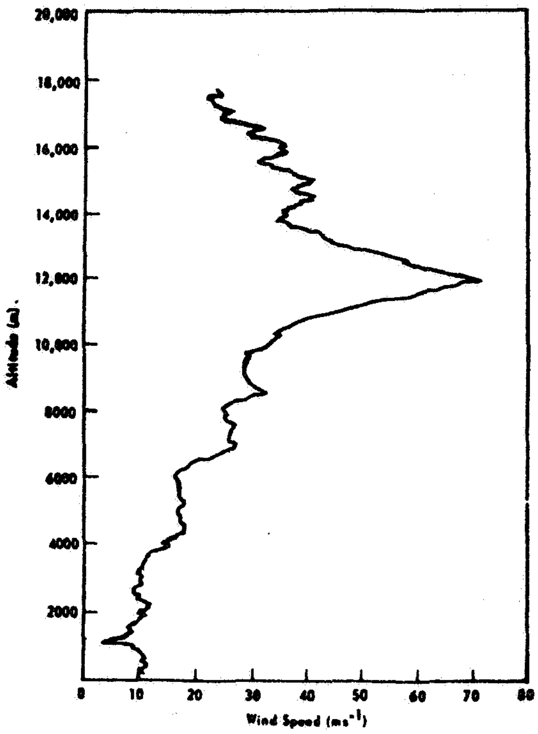

FIGURE 8.4.22 EXAMPLE OF JET STREAM WINDS

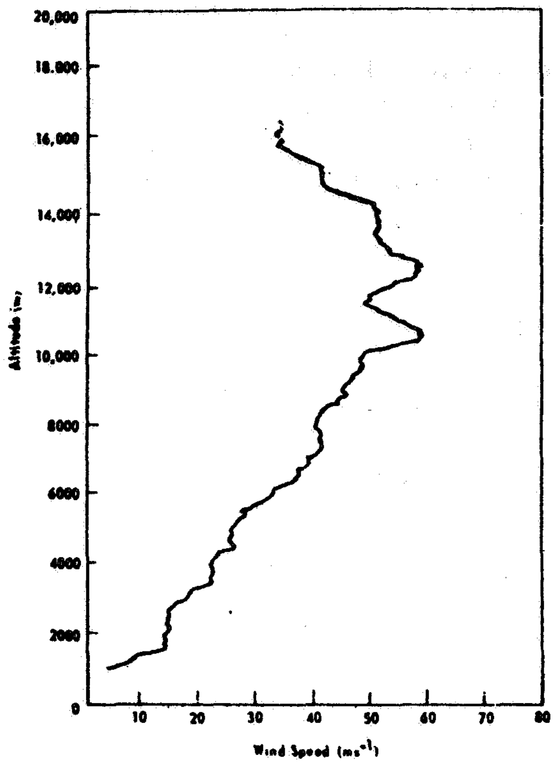

FIGURE 8.4.23 EXAMPLE OF SINE WAVE FLOW IN THE 10- TO 14-km ALTITUDE REGION

example of high wind speeds that occurred over 6 kilometers in depth. Such flow is not uncommon for the winter months. Figure 8.4.25 shows scalar winds of very low values. These winds were generally associated with easterly flow over the entire altitude interval (surface to 16 km) at Kennedy Space Center, Florida. The last examples (Figures 8.4.26 and 8.4.27) illustrate two samples of discrete gusts.

8.4.11 Vector Wind and Vector Wind Shear Models

8.4.11.1 Vector Wind Profile Models

This subsection presents the concepts for a vector wind profile model, an outline of procedures to compute synthetic vector wind profiles (SVWP) followed by examples, and some suggestions for alternate approaches. Applications of the theoretical relationships between the variables and the parameters of the multivariate probability distribution function presented in Section II are made. The vector wind profile models presented in this section have potential applications for aerospace vehicle ascent and reentry analysis for the altitude range from 1 to 27 km for Cape Kennedy, Florida, and Vandenberg AFB, California (Ref. 8.37).

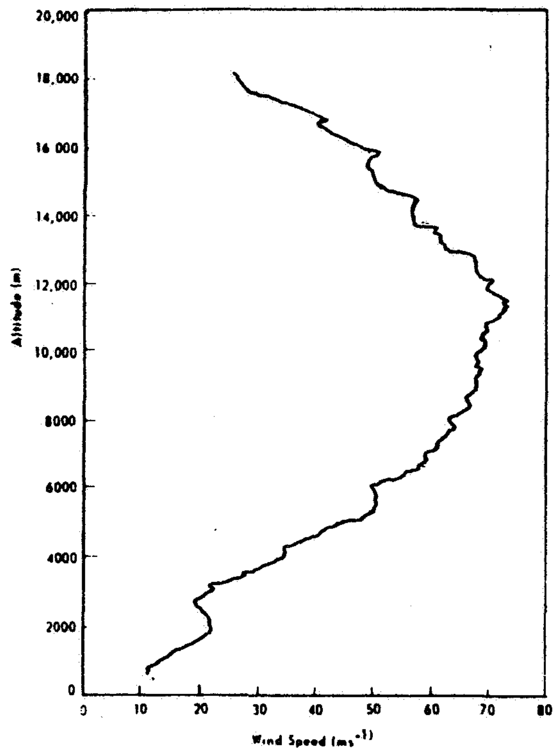

FIGURE 8.4.24 EXAMPLE OF HIGH WIND SPEEDS OVER A DEEP ALTITUDE LAYER

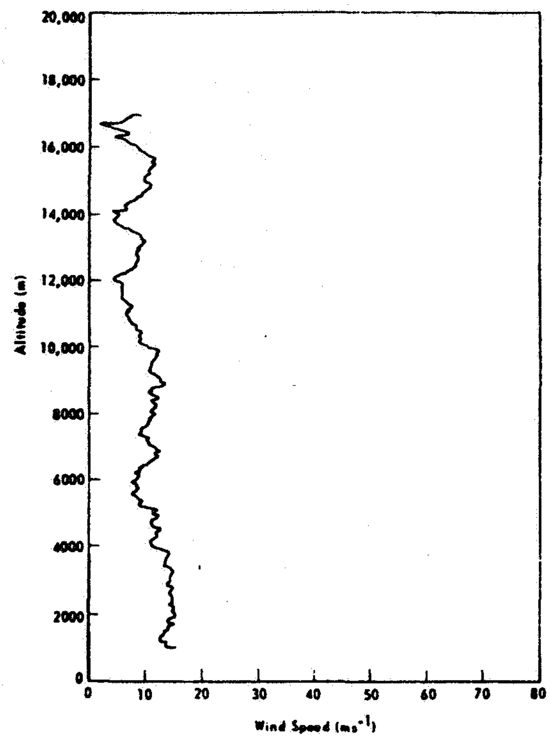

FIGURE 8.4.25 EXAMPLE OF LOW WIND SPEEDS

8.4.11.2 Vector Wind Profile Model Concepts

Purpose of a Model. What is a model? One definition is that a model is a representation of one or more attributes of a thing or concept. Hence, our objective in modeling the atmospheric winds is to simplify the complexity of the real wind profiles by a few attributes or characteristics to make the real wind profiles more understandable and less complicated for certain engineering applications. The modeling tools are those of mathematical probability theory and statistical analysis of wind data samples. Hopefully, through these methods, a wind model can be derived that will be a cost saving device for use in aerospace vehicle programs and still be sufficiently representative of the real wind profiles to answer engineering questions that arise in the aerospace vehicle analysis. However, the most realistic test of aerospace vehicle performance is an evaluation by flight simulations through detailed wind profiles. A sample of 150 detailed wind profiles (Jimsphere wind profiles) for each month for Cape Kennedy has been made available. A sample of 150 detailed wind

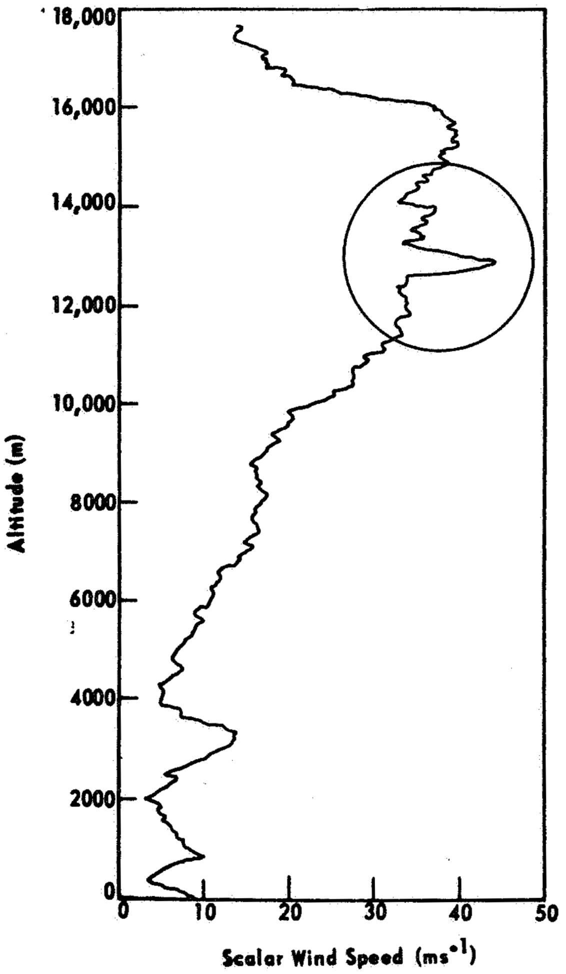

FIGURE 8.4.26 EXAMPLE OF A DISCRETE GUST OBSERVED AT 1300Z ON JANUARY 21, 1968, AT THE EASTERN TEST RANGE

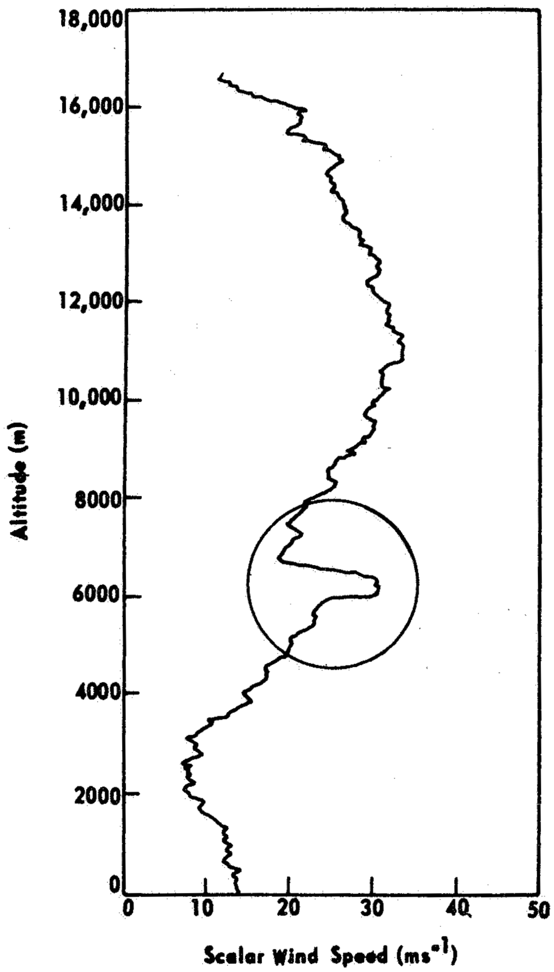

FIGURE 8.4.27 EXAMPLE OF A DISCRETE GUST OBSERVED BY A JIMSPHERE RELEASED AT 2103Z ON NOVEMBER 8, 1967, AT THE EASTERN TEST RANGE

profiles for each month which have all the power spectra characteristics that measured Jimsphere profiles have for Vandenberg Air Force Base has been made available for flight simulations for aerospace vehicle flights from Vandenberg Air Force Base. These two detailed wind profile data samples have the same moment statistical parameters at 1 km intervals (within statistical confidences) as the 14 parameters presented in the referenced report (Ref. 8.37). This was the basis for the selection of the 150 detailed wind profiles for each month.

<u>Synthetic Vector Wind Model</u>. In this discussion it is assumed that the reader is familiar with the synthetic scalar wind profile model presented in this report. By definition, the synthetic scalar wind profile model is the locus of wind speeds versus altitude obtained from conditional wind shears given a specified wind speed at a reference altitude. The profile is constructed by subtracting the conditional wind shears from the specified wind speed. The scalar wind shears are a function of wind speed only. The SVWP* extends this concept to the vector wind representation. For the SVWP the vector wind shears are a function of: (a) the reference altitude; (b) the given wind vector at the reference altitude, which makes the conditional vector wind shears wind-azimuth dependent; (c) the conditional wind shears; and (d) the monthly reference period.

For a given wind vector, the SVWP has three dimensions, whereas the synthetic scalar wind profile has two dimensions. A wind vector is selected at the reference altitude H_o, and the conditional vector wind shears are computed for altitudes H below and above H_o. The conditional vector shears are then subtracted from the given wind vector at H_o. For two-point separation in altitude $(H_o - H)$, the cone formed by this procedure contains a specified percentage of the wind vectors at altitude H for the given wind vector at H_o. The base is an ellipse in which a specified percentage (usually taken as 99 percent) of the wind vectors will lie given the wind vector at H_o. The interest in modeling the wind profile is to make some logical or orderly choice to arrive at the conditional wind vectors versus altitude. It is illustrated in Reference 8.37 that there are an infinite number of paths along the surface of the conditional cone from the reference altitude H_o down to the level H. Hence, a choice of an orderly path along the surface of the conditional cone of wind vectors should be dictated by the desired scientific or engineering application. A step-by-step procedure is given to compute the SVWP that is in-plane with the given wind vector. This in-plane profile has two branches: one is the smallest conditional vector wind and has the largest shears, and the other is the outer branch, which has the largest in-plane conditional wind vector but not necessarily the largest conditional shear. Also presented is the SVWP derived from the tangent intercepts to the conditional vector winds. These out-of-plane synthetic vector wind profiles have two branches: a right-turning wind direction and a left-turning wind direction with respect to altitude. The two-part in-plane SVWP and the two-part out-of-plane SVWP give a total of four synthetic vector wind profiles.

---

* Synthetic vector wind profile

Actual examples of the conditional vector winds is shown in Reference 8.37. The examples were derived from the December wind parameters for Vandenberg Air Force Base. The reference altitude H_o is 10 km; the given wind vector at H_o is from 330 degrees at 57.8 m/s or, in terms of the components, $u^* = 28$ m/s and $v^* = -50$ m/s. Instead of conditional ellipses, 99 percent conditional circles have been computed for each altitude at 1 km intervals from 0 to 27 km altitude. As presented, the dashed line connecting the center of the conditional circles versus altitude is the conditional mean vector. The smooth curve connecting the intercepts of the conditional circles is the in-plane SVWP that has the largest conditional shears.

8.4.11.3 Computation of the Synthetic Vector Wind Profile

Discussion in Reference 8.37 is in sufficient detail for a computer program development to code the procedures to compute the SVWP. Digressions are made in the procedures to clarify some points. The primary objectives, however, are to illustrate some applications of the probability theory of vector winds and to show the use of the tabulated wind statistical parameters to compute synthetic vector wind profiles.

8.4.12 Wind Profile Data Availability

8.4.12.1 Kennedy Space Center, Florida, and Vandenberg AFB, California, Jimsphere Wind Design Assessment and Verification Data Tape

The Jimsphere wind design assessment and verification data tapes serve as a very special data set for wind aloft vehicle response and other analytical studies. When properly integrated into a flight-simulation program (Space Shuttle, for example), vehicle operational risks can be more accurately assessed relative to the true representation of wind velocity profile characteristics. The wind velocity profiles contain wind vectors for each 25 m in altitude from near surface to an altitude of approximately 18 km. The high frequency resolution is one cycle per 100 m with an rms error of approximately 0.5 m/sec for velocities averaged over a 50-m height interval. Launch probability statements may be specified from flight simulations and related analyses. Through in-depth mathematical and statistical interpretations of these data very specific criteria can be generated on details of vector winds, gusts, shears, and the wind flow field interrelationships.

There are currently two special Jimsphere data sets prepared for Kennedy Space Center and Vandenberg AFB. They consist of 150 Jimsphere profiles per month. They were selected based on an extensive statistical and physical analysis of the vector wind profile characteristics and their representativeness. These data sets have been specified for use in the Space Shuttle program for assessment and verification of the system design. These data sets are available on magnetic computer tapes upon request to the Atmospheric Sciences Division, Space Sciences Laboratory, NASA/George C. Marshall Space Flight Center, Marshall Space Flight Center, Alabama 35812. There are also a large number of Jimsphere wind velocity profile data available for Kennedy Space Center, Point Mugu, White Sands Missile Range, Green River, Wallops Island, and Vandenberg AFB, California.

8.4.12.2 Availability of Serial Completed Rawinsonde Wind Velocity Profiles

Serially complete, edited, and corrected rawinsonde wind profile data are available for 19 years (two observations per day) for Kennedy Space Center (Eastern Test Range), for 9 years (four observations per day) for Santa Monica, and for 10 years (two observations per day) for Vandenberg Air Force Base (SAMTEC). A representative serial complete rawinsonde wind profile data set is now available for the Wallops Flight Center (12 years, two observations per day). Qualified requestors in aerospace, scientific, and engineering organizations may obtain these data, which are also on magnetic tapes, upon request to the Chief, Atmospheric Sciences Division, Space Sciences Laboratory, NASA/George C. Marshall Space Flight Center, Marshall Space Flight Center, Alabama 35812. They are also available as card deck 600 from the National Climatic Center, NOAA, Asheville, North Carolina 28801.

8.4.12.3 Availability of Rocketsonde Wind Velocity Profiles

Rocketsonde wind profile data have been collected for over 10 years from various launch sites around the world. These data can be obtained from the World Data Center A, Asheville, North Carolina 28801.

8.4.12.4 Availability of Smoke Trail Wind Velocity Profiles

A limited amount of wind velocity data has been obtained by the use of smoke trail techniques to determine the small scale variations of wind velocity with altitude. (Data are available from the Atmospheric Sciences Division, Space Sciences Laboratory, Marshall Space Flight Center.)

8.4.12.5 Utility of Data

All wind profile data records should be checked carefully by the user before employing them in any vehicle response calculations. Where-ever practical, the user should become familiar with the representativeness of the data and frequency content of the profile used, as well as the measuring system and reduction schemes employed in handling the data. For those organizations that have aerospace meteorology oriented groups or individuals on their staffs, consultations should be held with them. Otherwise, various government groups concerned with aerospace vehicle design and operation can be of assistance. Such action by the user can prevent expensive misuse and error in interpretation of the data relative to the intended application.

8.4.13 Atmospheric Turbulence Criteria for Horizontally Flying Vehicles

In this section is presented the continuous turbulence random model for the design of aerospace vehicles capable of flying horizontally, or nearly so, through the atmosphere. In general both the continuous random model (Sections 8.4.13 and 8.4.14) and the discrete model (Section 8.4.15) are used to calculate vehicle responses with the procedure producing the larger response being used for design.

To a reasonable degree of approximation, inflight atmospheric turbulence experienced by horizontally flying vehicles can be assumed to be homogeneous, stationary, Gaussian, and isotropic. Under some conditions, these assumptions might appear to be drastic, but for engineering purposes they seem to be appropriate, except for low level flight in approximately the first 300 meters of the atmosphere. It has been found that the spectrum of turbulence first suggested by von Karman appears to be a good analytical representation of atmospheric turbulence. The longitudinal spectrum is given by

$$\Phi_u(\Omega, L) = \sigma^2 \frac{2L}{\pi} \frac{1}{[1 + (1.339\, L\Omega)^2]^{5/6}} , \qquad (8.32)$$

where σ^2 is the variance of the turbulence, L is the scale of turbulence, and Ω is the wave number in units of radians per unit length. The spectrum is defined so that

$$\sigma^2 = \int_0^\infty \Phi_u(\Omega, L)\, d\Omega \quad . \tag{8.33}$$

The theory of isotropic turbulence predicts that the spectrum Φ_w of the lateral and vertical components of turbulence are related to the longitudinal spectrum through the differential equation

$$\Phi_w = \frac{1}{2}\left(\Phi_u - \Omega \frac{d\Phi_u}{d\Omega}\right) \quad . \tag{8.34}$$

Substitution of equation (8.32) into equation (8.34) yields

$$\Phi_w = \sigma^2 \frac{L}{\pi} \frac{1 + \frac{8}{3}(1.339\, L\Omega)^2}{[1 + (1.339\, L\Omega)^2]^{11/6}} \quad . \tag{8.35}$$

The nondimensional spectra $2\pi\Phi_u/\sigma^2 L$ and $2\pi\Phi_w/\sigma^2 L$ are depicted in Figure 8.4.28 as function of ΩL. As $L\Omega \rightarrow \infty$, Φ_u and Φ_w asymptotically behave like

$$\Phi_u \sim \sigma^2 \frac{2L}{\pi} \frac{(L\Omega)^{-5/3}}{(1.339)^{5/3}} \quad (L\Omega \rightarrow \infty) \tag{8.36}$$

$$\Phi_w \sim \sigma^2 \frac{2L}{\pi} \frac{(L\Omega)^{-5/3}}{(1.339)^{5/3}} \quad (L\Omega \rightarrow \infty) \quad , \tag{8.37}$$

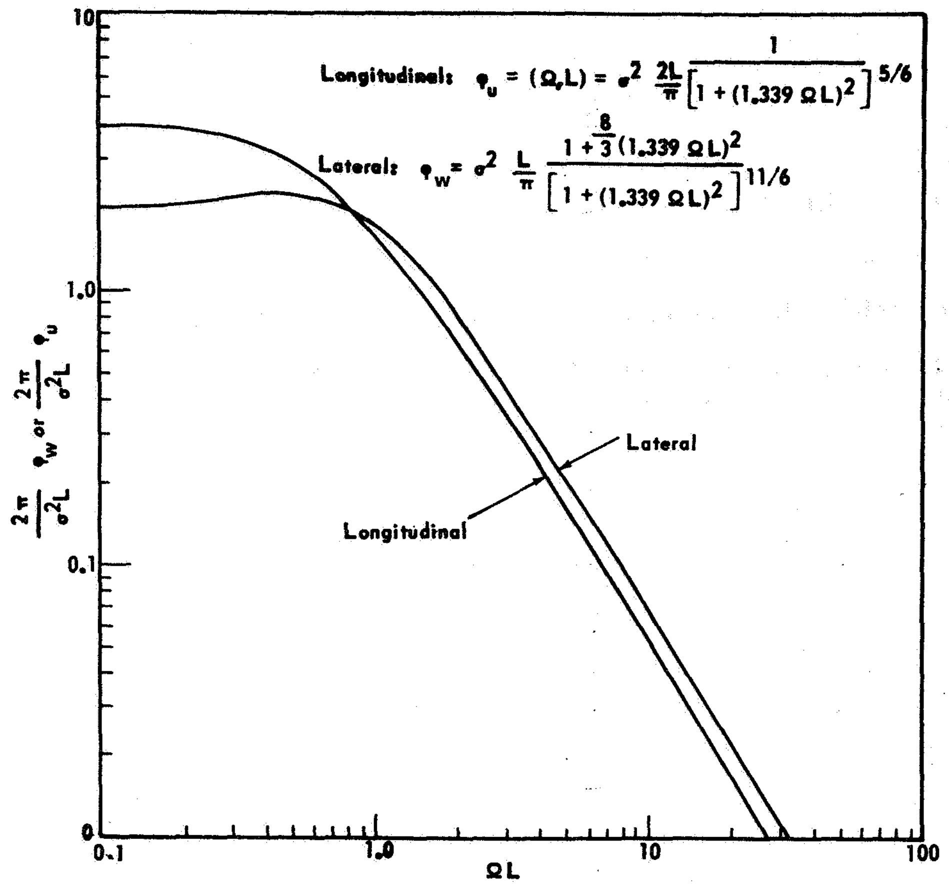

FIGURE 8.4.28 THE DIMENSIONLESS LONGITUDINAL AND LATERAL $\frac{2\pi\Phi_u}{\sigma^2 L}$ AND $\frac{2\pi\Phi_w}{\sigma^2 L}$ SPECTRA AS FUNCTIONS OF THE DIMENSIONLESS FREQUENCY $L\Omega$

consistent with the concept of the Kolmogorov inertial subrange. In addition, $\Phi_w/\Phi_u \rightarrow 4/3$ as $\Omega L \rightarrow \infty$. Design values of the scale of turbulence L are given in Table 8.4.21. Experience indicates that the scale of turbulence increases as height increases in the first 762 meters (2500 ft)[12] of the atmosphere, and typical values of L range from 10 meters (~ 30 ft) near the surface to 610 meters (2000 ft) at approximately a 762-meter (2500-ft) altitude. Above

12. U. S. customary units are used in the section in parentheses to maintain continuity with source of data – Air Force Flight Dynamics Laboratory and other documentation.

TABLE 8.4.21 PARAMETERS FOR THE TURBULENCE MODEL FOR HORIZONTALLY FLYING VEHICLES

Altitude (m)	Altitude (ft)	Mission Segment*	Turbulence Component**	P_1 (unitless)	b_1 (m/sec)	b_1 (ft/sec)	P_2 (unitless)	b_2 (m/sec)	b_2 (ft/sec)	L (m)	L (ft)
0 - 304.8	0 - 1 000	Low Level Contour (rough terrain)	V	1.00	0.82	2.7	10^{-5}	3.25	10.65	152.4	500
0 - 304.8	0 - 1 000	Low Level Contour (rough terrain)	L, L	1.00	0.94	3.1	10^{-5}	4.29	14.06	152.4	500
0 - 304.8	0 - 1 000	C, C, D	V, L, L	1.00	0.77	2.51	0.005	1.54	5.04	152.4	500
304.8 - 672	1 000 - 2 500	C, C, D	V, L, L	0.42	0.92	3.02	0.0033	1.81	5.94	533.4	1750
672 - 1 524	2 500 - 5 000	C, C, D	V, L, L	0.30	1.04	3.42	0.0020	2.49	8.17	762	2500
1 524 - 3 048	5 000 - 10 000	C, C, D	V, L, L	0.15	1.09	3.59	0.00095	2.81	9.22	762	2500
3 048 - 6 096	10 000 - 20 000	C, C, D	V, L, L	0.062	1.00	3.27	0.00028	3.21	10.52	762	2500
6 096 - 9 144	20 000 - 30 000	C, C, D	V, L, L	0.025	0.96	3.15	0.00011	3.62	11.88	762	2500
9 144 - 12 192	30 000 - 40 000	C, C, D	V, L, L	0.011	0.89	2.93	0.000095	3.00	9.84	762	2500
12 192 - 15 240	40 000 - 50 000	C, C, D	V, L, L	0.0046	1.00	3.28	0.000115	2.69	8.81	762	2500
15 240 - 18 288	50 000 - 60 000	C, C, D	V, L, L	0.0020	1.16	3.82	0.000078	2.15	7.04	762	2500
18 288 - 21 336	60 000 - 70 000	C, C, D	V, L, L	0.00088	0.89	2.93	0.000057	1.32	4.33	762	2500
21 336 - 24 384	70 000 - 80 000	C, C, D	V, L, L	0.00038	0.85	2.80	0.000044	0.55	1.80	762	2500
above 24 384	above 80 000	C, C, D	V, L, L	0.00025	0.76	2.50	0	0	0	762	2500

* Climb, cruise, and descent (C, C, D).
** Vertical, lateral, and longitudinal (V, L, L).

the 762-meter (2500-ft) level, typical values of L are in the order of 762 to 1829 meters (2500 to 6000 ft). The scales of turbulence in Table 8.4.21 above the 300-meter level are probably low, and they would be expected to give a somewhat conservative or high number of load or stress exceedances per unit length of flight. The scale of turbulence indicated for the first 304.8 meters of the atmosphere in Table 8.4.21 is a typical value. The use of this average scale of turbulence may be approximate for load studies; however, it is inappropriate for control system and flight simulation purposes in which event the vertical variation of the scale of turbulence in the first 300 meters of the atmosphere should be taken into account.

The power spectrum analysis approach is applicable only to stationary Gaussian continuous turbulence, but atmospheric turbulence is neither statistically stationary nor Gaussian over long distances. The statistical quantities used to describe turbulence vary with altitude, wind direction, terrain roughness, atmospheric stability, and a host of other variables. Nevertheless, it is valid to a sufficient degree of engineering approximation to recommend that atmospheric turbulence be considered locally Gaussian and stationary and that the total flight history of a horizontally flying vehicle be considered to be composed of an ensemble of exposures to turbulence of various intensities, all using the same power spectrum shape. Furthermore, it is recommended that the following statistical distribution of rms gust intensities be used:

$$p(\sigma) = \frac{P_1}{b_1}\sqrt{\frac{2}{\pi}}\,\exp\left(-\frac{\sigma^2}{2b_1^2}\right) + \frac{P_2}{b_2}\sqrt{\frac{2}{\pi}}\,\exp\left(-\frac{\sigma^2}{2b_2^2}\right) , \tag{8.38}$$

where b_1 and b_2 are the standard deviations of σ in nonstorm and storm turbulence. The quantities P_1 and P_2 denote the fractions of flight time or distance flown in nonstorm and storm turbulence. It should be noted that if P_0 is the fraction of flight time or distance in smooth air, then

$$P_0 + P_1 + P_2 = 1 \quad . \tag{8.39}$$

The recommended design values of P_1, P_2, b_1, and b_2 are given in Table 8.4.22. Note that over rough terrain b_2 can be extremely large in the first 304 meters (1000 ft) above the terrain and the b's for the vertical, the lateral, and the longitudinal standard deviations of the turbulence are not equal. Thus in the first 304 meters (1000 ft) of the atmosphere above rough terrain, turbulence is significantly anisotropic and this anisotropy must be taken into account in engineering calculations.

An exceedance model of gust loads and stresses can be developed with the above information. Let y denote any load quantity that is a dependent variable in a linear system of response equations (for example, bending moment at a particular wing station). This system is forced by the longitudinal, lateral, and vertical components of turbulence, and upon producing the Fourier transform of the system, it is possible to obtain the spectrum of y. This spectrum will be proportional to the input turbulence spectra, the function of proportionality being the system transfer function. Upon integrating the spectrum of y over the domain $0 < \Omega < \infty$, we obtain the relationship

$$\sigma_y = A\sigma \quad , \tag{8.40}$$

where A is a positive constant that depends upon the system parameters and the scale of turbulence, and where σ_y is the standard deviation of y.

If the output y is considered to be Gaussian for a particular value of σ, then the expected number of fluctuations of y that exceed y^* with positive slope per unit distance with reference to a zero mean is

$$N(y^*) = N_0 \exp\left(-\frac{{y^*}^2}{2\sigma_y^2}\right) \quad , \tag{8.41}$$

where N_0 is the expected number of zero crossings of y unit distance with h positive slope and is given by

$$N_0 = \frac{1}{2\pi\sigma_y}\left[\int_0^\infty \Omega^2 \, \Phi_y(\Omega)\, d\Omega\right]^{1/2} \quad . \tag{8.42}$$

In this equation, Φ_y is the spectrum of y and

$$\sigma_y = \left[\int_0^\infty \Phi_y(\Omega)\, d\Omega\right]^{1/2} \quad . \tag{8.43}$$

The standard deviation of σ_y is related to standard deviation of turbulence through equation (8.40), and σ is distributed according to equation (8.38). Accordingly, the number of fluctuations of y that exceed y* for standard deviations of turbulence in the interval σ to $\sigma + d\sigma$ is $N(y^*)\ p(\sigma)d\sigma$, so that integration over the domain $0 < \sigma < \infty$ yields

$$\frac{M(y^*)}{N_0} = P_1 \exp\left(-\frac{|y^*|}{b_1 A}\right) + P_2 \exp\left(-\frac{|y^*|}{b_2 A}\right) , \qquad (8.44)$$

where $M(y^*)$ is the overall expected number of fluctuations of y that exceed y* with positive slope. To apply this equation, the engineer needs only to calculate A and N_0 and specify the risk of failure he wishes to accept. The appropriate values of P_1, P_2, b_1, and b_2 are given in Table 8.4.21. Figures 8.4.29 and 8.4.30 give plots of $M(y^*)/N_0$ as a function of $|y^*|/A$ for the various altitudes for the design data given in Table 8.4.21. Table 8.4.22 provides a summary of the units of the various quantities in this model.

8.4.13.1 Application of Power Spectral Model

To apply equation (8.44), the engineer can either calculate A and N_0 and then calculate the load quantity y* for a specified value of $M(y^*)$, or calculate A and calculate the load quantity y* for a specified value of

TABLE 8.4.22 METRIC AND U.S. CUSTOMARY UNITS OF VARIOUS QUANTITIES IN THE TURBULENCE MODEL FOR HORIZONTALLY FLYING VEHICLES

Quantity	Metric Units	U. S. Customary Units
Ω	rad/m	rad/ft
Φ_u, Φ_w	$m^2/sec^2/rad/m$	$ft^2/sec^2/rad/ft$
σ^2	m^2/sec^2	ft^2/sec^2
L	m	ft
b_1, b_2	m/sec	ft/sec
P_1, P_2	dimensionless	dimensionless
σ_y/A	m/sec	ft/sec
$\lvert y^*\rvert/A$	m/sec	ft/sec
N_0, N, M	rad/sec	rad/sec

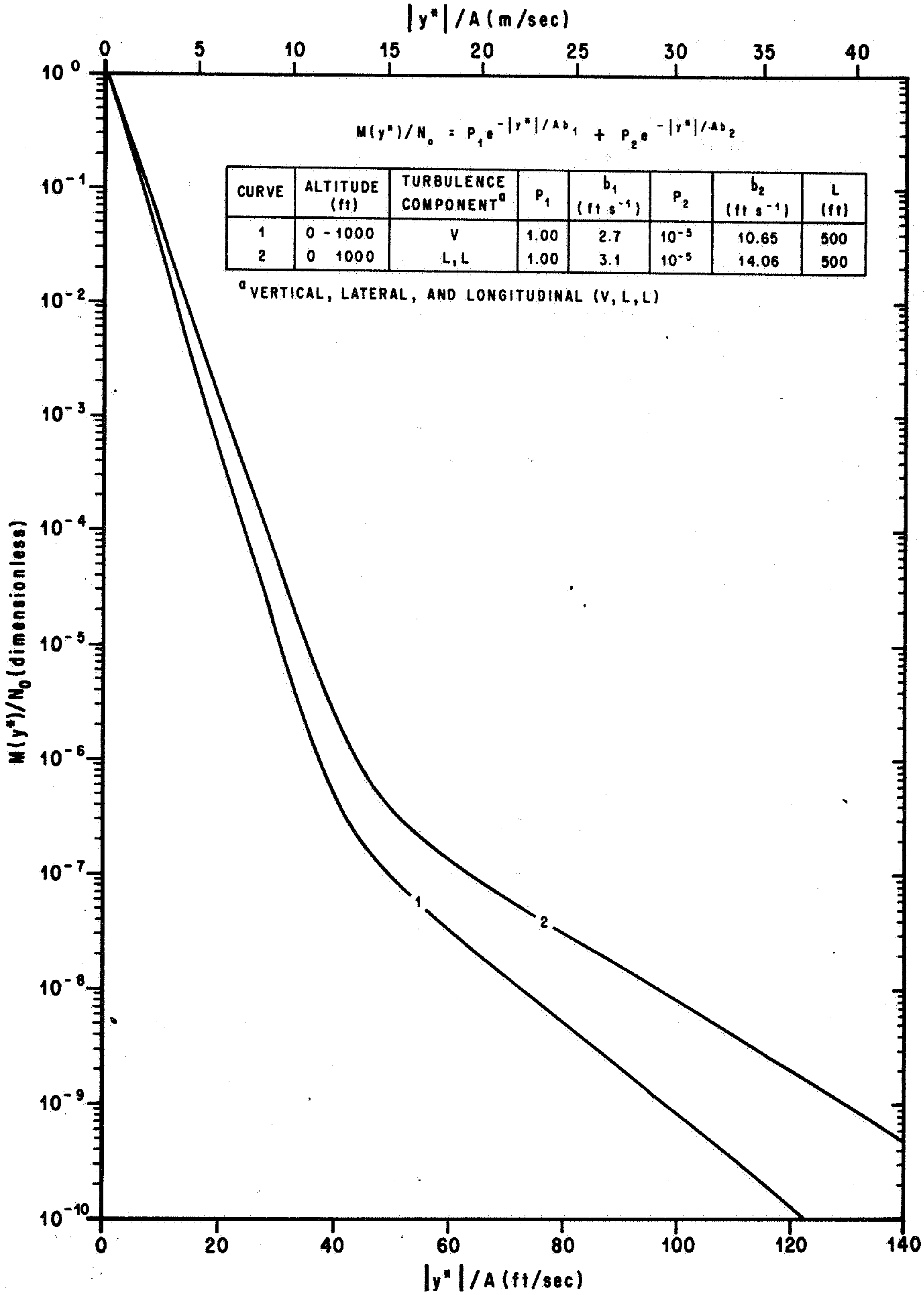

FIGURE 8.4.29 EXCEEDANCE CURVES FOR THE VERTICAL, LATERAL, AND LONGITUDINAL COMPONENTS OF TURBULENCE FOR THE 0- TO 1000-ft ALTITUDE RANGE

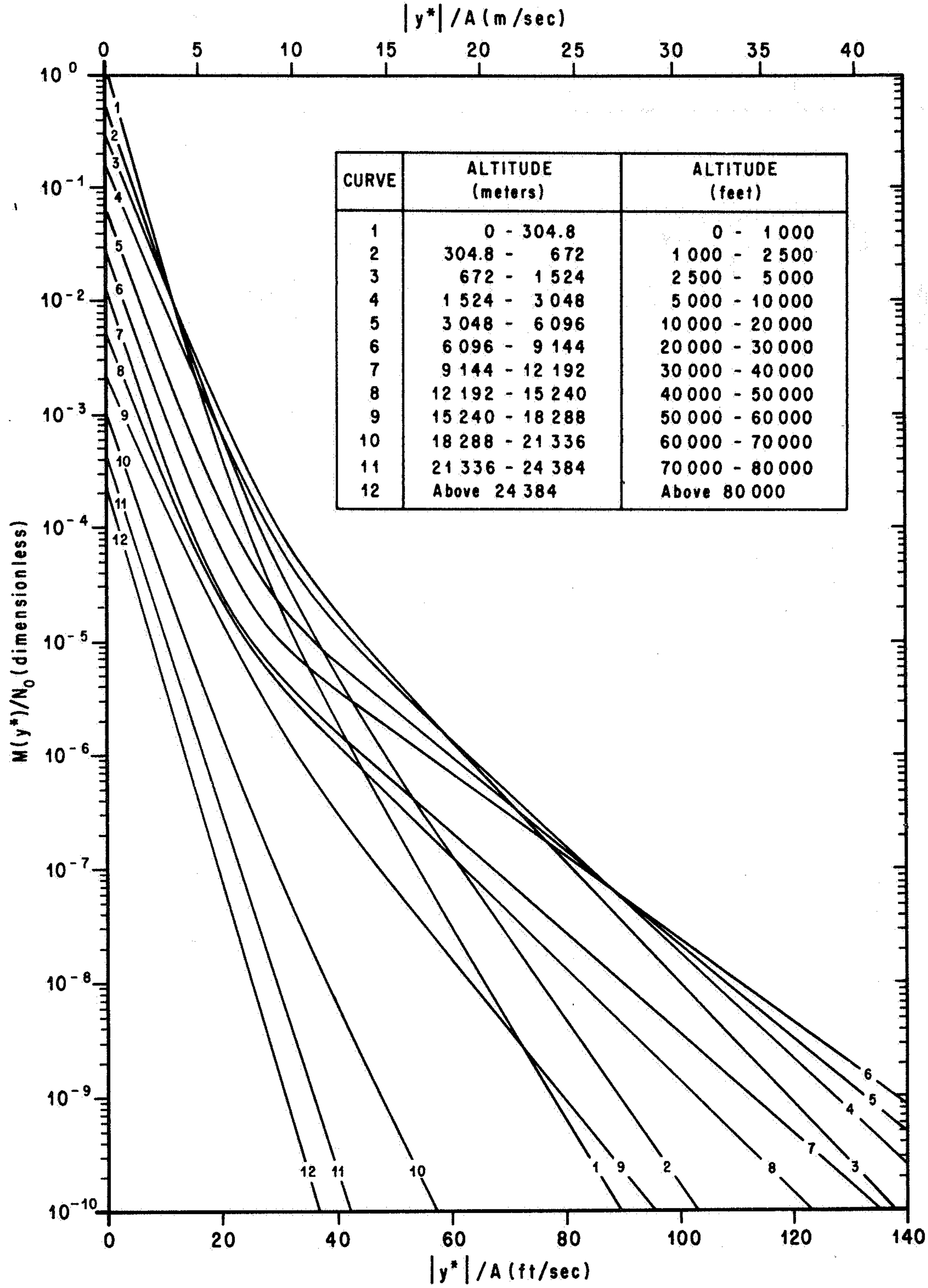

CURVE	ALTITUDE (meters)	ALTITUDE (feet)
1	0 - 304.8	0 - 1 000
2	304.8 - 672	1 000 - 2 500
3	672 - 1 524	2 500 - 5 000
4	1 524 - 3 048	5 000 - 10 000
5	3 048 - 6 096	10 000 - 20 000
6	6 096 - 9 144	20 000 - 30 000
7	9 144 - 12 192	30 000 - 40 000
8	12 192 - 15 240	40 000 - 50 000
9	15 240 - 18 288	50 000 - 60 000
10	18 288 - 21 336	60 000 - 70 000
11	21 336 - 24 384	70 000 - 80 000
12	Above 24 384	Above 80 000

FIGURE 8.4.30 EXCEEDANCE CURVES FOR THE VERTICAL, LATERAL, AND LONGITUDINAL COMPONENTS OF TURBULENCE FOR VARIOUS ALTITUDE RANGES

$M(y^*)/N_0$. These design criteria were consistent with the limit load capabilities of present day commercial aircraft. The criterion in which $M(y^*)$ is specified is suitable for a mission analysis approach to the design problem. The criterion in which $M(y^*)/N_0$ is specified is suitable for a design envelope approach to aircraft design.

In the design envelope approach, it is assumed that the airplane operates 100 percent of the time at its critical design envelope point. The philosophy is that if the vehicle can operate 100 percent of the time at any point on the envelope it can surely operate adequately in any combination of operating points on the envelope. A new vehicle is designed on a limit load basis for a specified value of M/N_0. Accordingly, $M/N_0 = 6 \times 10^{-9}$ is suitable for the design of commercial aircraft. To apply this criterion, all critical altitudes, weights, and weight distributions are specified and associated values of A are calculated. The limit loads are calculated for each of the specified configurations with equation (8.44) for $M/N_0 = 6 \times 10^{-9}$.

In the mission analysis approach, a new aircraft is designed on a limit load basis for $M = 2 \times 10^{-5}$ load exceedances per hour. To apply this criterion, the engineer must construct an ensemble of flight profiles which define the expected range of payloads and the variation with time of speed, altitude, gross weight, and center of gravity position. These profiles are divided into mission segments, or blocks, for analysis; and average or effective values of the pertinent parameters are defined for each segment. For each mission segment, values of A and N_0 are determined by dynamic analysis. A sufficient number of load and stress quantities are included in the dynamic analysis to assure that stress distributions throughout the structure are realistically or conservatively defined. Now the contribution of $M(y^*)$ from the ith flight segment is $t_i M_i (y^*/T)$ where t_i is the amount of time spent in the ith flight regime (mission segment, T is the total time flown by the vehicle over all mission segments, and $M_i(y^*)$ is the exceedance rate associated with the ith segment. The total exceedance rate for all mission segments, k say, is

$$M(y^*) = \sum_{i=1}^{k} \frac{t_i}{T} N_{0_i} \left(P_1 e^{-|y^*|/b_1 A} + P_2 e^{-|y^*|/b_2 A}\right) \quad , \quad (8.45)$$

where subscript i denotes the ith mission segment. The limit gust load quantity $|y^*|$ can be calculated with this formula upon setting $M(y^*) = 2 \times 10^{-5}$ exceedances per hour.

The above mentioned limit load design criteria were derived for commercial aircraft which are normally designed for 50,000-hour lifetimes. Therefore, to apply these criteria to horizontally flying aerospace vehicles which will have relatively short lifetimes would be too conservative. However, it is possible to modify these criteria so that they will reflect a shorter vehicle lifetime. The probability F_p that a load will be exceeded in a given number of flight hours T is

$$F_p = 1 - e^{-TM} \quad . \tag{8.46}$$

It it is assumed that the limit load criterion $M = 2 \times 10^{-5}$ exceedances per hour is associated with an aircraft with a lifetime T equal to 50,000 hours, this means that $F_p = 0.63$, i.e., there is a 63 percent chance that an aircraft designed for a 50,000-hour operating lifetime will exceed its limit load capability at least once during its operating lifetime. This high failure probability, based on limit loads, is not excessive in view of the fact that an aircraft will receive many inspections on a routine basis during its operating lifetime. In addition, after safety factors are applied to the design limit loads the ultimate load exceedance rate will be on the order of 10^{-8} exceedances per hour. Substitution of this load exceedance rate into equation (8.46) for $T = 50{,}000$ hours yields a failure probability, on an ultimate load basis, of $F_p = 0.0005$. This means that there will only be a 0.05 percent chance that an aircraft will exceed its ultimate load capability during its operating lifetime of 50,000 hours. Thus, a failure probability of $F_p = 0.63$ on a limit load basis is reasonable for design. Let us now assume that $F_p = 0.63$ is the limit load design failure probability so that equation (8.46) can be used to calculate design values of M associated with a specified vehicle lifetime. Thus, for example, if we expect a vehicle to fly only 100 hours, then according to equation (8.46), we have $M = 10^{-2}$ exceedances per hour. Similarly, if we expect a vehicle to be exposed to the atmosphere for 1000 hours of flight, then $M = 10^{-3}$ exceedances per hour.

The corresponding design envelope criterion can be obtained by dividing the above calculated values of M by an appropriate value of N_0. In the case of the 50,000 hours cirterion, we have $M/N_0 = 6 \times 10^{-9}$ and $M = 2 \times 10^{-5}$ exceedances per hour so that an estimate of N_0 for purposes of obtaining a design criterion is $N_0 = 0.333 \times 10^4 \text{ hr}^{-1}$. Thus, upon solving equation (8.46) for M and dividing by $N_0 = 0.333 \times 10^4 \text{ hr}^{-1}$, the design envelope criterion takes the form

$$\frac{M}{N_0} = \frac{3 \times 10^{-4}}{T} \tag{8.47}$$

where we have used $F_p = 0.63$. Thus, for a 100-hour aircraft, the design envelope criterion is $M/N_0 = 3 \times 10^{-6}$ and for a 1000-hour aircraft $M/N_0 = 3 \times 10^{-7}$.

It is recommended that the power spectral approach be used in place of the standard discrete gust methods. Reasonably discrete gusts undoubtedly occur in the atmosphere; however, there is accumulating evidence that the preponderance of gusts are better described in terms of continuous turbulence models. It has long been accepted that clear air turbulence at moderate intensity levels is generally continuous in nature. Thunderstorm gust velocity profiles are now available in considerable quantity, and they almost invariably display the characteristics of continuous turbulence. Also, low level turbulence is best described with power spectral methods. A power spectral method of load analysis is not necessarily more difficult to apply than a discrete gust method. The present static load "plunge-only discrete gust methods" can, in fact, be converted to a power spectral basis by making a few simple modifications in the definitions of the gust alleviation factor and the design discrete gust. To be sure, this simple rigid-airplane analysis does not exploit the full potentiality of the power spectral approach, but it does account more realistically for the actual mix of gust gradient distances in the atmosphere and the variation of gust intensity with gradient distance.

8.4.14 Turbulence Model for Flight Simulation*

For simulation of turbulence in either an analog or digital fashion, the turbulence realizations are to be generated by passing a white noise process through a passive filter. The model of turbulence as given in subsection 8.4.13 is not particularly suited for the simulation of turbulence with white noise. This results because the von Karman spectra given by equations (8.32) and (8.35) are irrational. Thus, for engineering purposes, the Dryden spectra may be used for simulation of continuous random turbulence. They are given by

$$\text{Longitudinal:} \quad \Phi_u(\Omega) = \sigma^2 \frac{2L}{\pi} \frac{1}{1 + (L\Omega)^2} \tag{8.48}$$

$$\text{Lateral and Vertical:} \quad \Phi_w(\Omega) = \sigma^2 \frac{L}{\pi} \frac{1 + 3(L\Omega)^2}{[1 + (L\Omega)^2]^2} . \tag{8.49}$$

* Details on simulations should be requested from Atmospheric Sciences Division, Space Sciences Laboratory, MSFC.

Since these spectra are rational, a passive filter may be generated. It should be noted that the Dryden spectra are somewhat similar to the von Karman spectra. As $\Omega L \rightarrow 0$ the Dryden spectra asymptotically approach the von Karman spectra. As $\Omega L \rightarrow \infty$ the Dryden spectra behave like $(\Omega L)^{-2}$, while the von Karman spectra behave like $(\Omega L)^{-5/3}$. Thus, the Dryden spectra depart from the von Karman spectra by a factor proportional to $(\Omega L)^{-1/3}$ as $\Omega L \rightarrow \infty$, so that at sufficiently large values of ΩL the Dryden spectra will fall below the von Karman spectra. However, this deficiency in spectral energy of the Dryden spectra with respect to the von Karman spectra is not serious from an engineering point of view. If the capability to use the von Karman spectra is already available, the user should use it in flight simulation rather than the Dryden spectra.

The spectra as given by equations (8.48) and (8.49) can be transformed from the wave number (Ω) domain to the frequency domain (ω, rad/sec) with a Jacobian transformation by noting that $\Omega = \omega / V$, so that

$$\Phi_u(\omega) = \frac{L}{V} \frac{2\sigma^2}{\pi} \frac{1}{1 + (L\omega/V)^2} \tag{8.50}$$

$$\Phi_w(\omega) = \frac{L}{V} \frac{\sigma^2}{\pi} \frac{1 + 3(L\omega/V)^2}{[1 + (L\omega/V)^2]^2} \quad . \tag{8.51}$$

The quantity V is the magnitude of the mean wind vector relative to the aerospace vehicle, $\vec{\bar{u}} - \vec{C}$. The quantities $\vec{\bar{u}}$ and $\vec{C}$ denote the velocity vectors of the mean flow of the atmosphere and the aerospace vehicle relative to the earth. In the region above the 300-meter level the longitudinal component of turbulence is defined to be the component of turbulence parallel to the mean wind vector relative to the aerospace vehicle $(\vec{\bar{u}} - \vec{C})$. The lateral and vertical components of turbulence are perpendicular to the relative mean wind vector and act in the lateral and vertical directions relative to the vehicle flight path.

8.4.14.1 Transfer Functions

Atmospheric turbulence can be simulated by passing white noise through filters with the following frequency response functions:

$$\text{Longitudinal:} \quad F_u(j\omega) = \frac{(2k)^{1/2}}{a + j\omega} \tag{8.52}$$

$$\text{Lateral and Vertical:} \quad F_w(j\omega) = \frac{(3k)^{1/2}\left(3^{-1/2}a + j\omega\right)}{(a + j\omega)^2} \quad , \tag{8.53}$$

where

$$a = \frac{V}{L} \tag{8.54}$$

$$k = \frac{a\sigma^2}{\pi} \quad . \tag{8.55}$$

To generate the three components of turbulence, three distinct uncorrelated Gaussian white noise sources should be used.

To define the rate of change of gust velocities about the pitch, yaw, and roll axes for simulation purposes, a procedure consistant with the above formulation can be found in Section 3.7.5, "Application of Turbulence Models and Analyses," of Reference 8.38. This should be checked for applicability.

8.4.14.2 Boundary Layer Turbulence Simulation

The turbulence in the atmospheric boundary layer, defined here for engineering purposes to be approximately the first 300 meters of the atmosphere, is inherently anisotropic. To simulate this turbulence realistically as possible, the differences between the various scales and intensities of turbulence should be taken into account. There are various problems associated with developing an engineering model of turbulence for simulation purposes. The most outstanding one concerns how one should combine the landing or take-off steady-state wind and turbulence conditions near the ground (18.3-meter level, for example) with the steady-state wind and turbulence conditions at approximately the 300-meter level. The wind conditions near the ground are controlled by local conditions and are usually derived from considerations of the risks associated with exceeding the design take-off or landing wind condition during any particular mission. The turbulence environments at and above the 300-meter level are controlled by relatively large scale conditions rather than local landing or take-off wind conditions, and these turbulence environments are usually derived from considerations of the risks associated with exceeding the design turbulence environment during the total life or total exposure time of the vehicle to the natural environment. The use of the risk associated with exceeding the design wind environment near the ground during a given mission rather than the use of the risk of exceeding the design turbulence environment during the total life of the vehicle is justified on the basis that, if the landing conditions are not acceptable, the pilot has the option to land at an alternate airfield and thus avoid the adverse landing wind conditions at the primary landing site. Similarly, in the take-off problem, the pilot can wait until the adverse low level wind and turbulence conditions have subsided before taking-off. The use of the risk associated with exceeding the design turbulence environment during the total life of the vehicle above the atmospheric boundary layer to develop design turbulence environments for vehicle design studies is justified because the pilot does not have the option of avoiding adverse inflight turbulence conditions directly ahead of the vehicle. In addition, the art of forecasting inflight turbulence has not progressed to the point where a flight plan can be established which avoids inflight turbulence with a reasonably small risk, such that design environments can be established on a per flight basis rather than on a total lifetime basis.

How does one then establish a set of values for L and σ for each component of turbulence which merges together these two distinctly different philosophies? It is recommended that design values for each component of turbulence be established at the 18.3-meter and at the 304.8-meter levels based on the above stated philosophies. Once these values of σ and L are established, the corresponding values between the 18.3- and 304.8-meter levels can be obtained with the following interpolation formulae

$$\sigma(H) = \sigma_{18.3}\left(\frac{H}{18.3}\right)^{p} \tag{8.56}$$

$$L(H) = L_{18.3}\left(\frac{H}{18.3}\right)^{q} \tag{8.57}$$

where σ (H) and L(H) are the values of σ and L at height H above natural grade, $\sigma_{18.3}$ and $L_{18.3}$ are the values of σ and L at the 18.3-meter level, p and q are constants selected such that the appropriate values of σ and L occur at the 304.8-meter level. Representative values of $L_{18.3}$ for the Dryden spectrum are given by

$$L_{u_{18.3}} = 31.5\text{m};\ L_{v_{18.3}} = 18.4\text{m};\ L_{w_{18.3}} = 10.0\text{m} \tag{8.58}$$

where subscript u, v, and w denote the longitudinal, lateral and vertical components of turbulence. The corresponding design values of $\sigma_{18.3}$ are given by

$$\sigma_{u_{18.3}} = 2.5\,u_{*o} \tag{8.59}$$

$$\sigma_{v_{18.3}} = 1.91 u_{*o} \tag{8.60}$$

$$\sigma_{w_{18.3}} = 1.41 u_{*o} \tag{8.61}$$

where u_{*o} is the surface friction velocity which is given by

$$u_{*o} = 0.4 \frac{\bar{u}_{18.3}}{\ln\left(\frac{18.3}{z_o}\right)} \tag{8.62}$$

The quantity $\bar{u}_{18.3}$ is the mean wind or steady-state wind at the 18.3-meter level, z_o is the surface roughness length (see subsection 8.3.6.2) and SI units are understood. The quantity $u_{18.3}$ is related to the 18.3-meter level peak wind speed $u_{18.3}$ (see Section 8.3.4) through the equation

$$\bar{u}_{18.3} = \frac{u_{18.3}}{G_{18.3}} \tag{8.63}$$

where $G_{18.3}$ is the 18.3-meter level gust factor (see subsection 8.3.7.1) associated with a one-hour average wind. This gust factor is a function of the 18.3-meter level peak wind speed so that upon specifying $u_{18.3}$ and the surface roughness length the quantity u_{*o} is defined by equation (8.62) and the standard deviations of turbulence are in turn defined by equations (8.59) through (8.61).

The values of L and σ must satisfy the Dryden isotropy conditions demanded by the equation of mass continuity for incompressible flow. These isotropy conditions are given by

$$\frac{\sigma_u^2}{L_u} = \frac{\sigma_v^2}{L_v} = \frac{\sigma_w^2}{L_w} \tag{8.64}$$

and must be satisfied at all altitudes. The length scales given by equation (8.58) and the standard deviations of turbulence given by equations (8.59) through (8.61) were selected such that they satisfy the isotropy condition given by equation (8.64), i.e.,

$$\frac{\sigma^2_{u_{18.3}}}{L_{u_{18.3}}} = \frac{\sigma^2_{u_{18.3}}}{L_{v_{18.3}}} = \frac{\sigma^2_{w_{18.3}}}{L_{w_{18.3}}} \tag{8.65}$$

At the 304.8-meter level, equation (8.64) is automatically satisfied because $\sigma_u = \sigma_v = \sigma_w$ and $L_u = L_v = L_w$ at the 304.8-meter level.

To calculate the value of $\sigma_{304.8}$ appropriate for performing a simulation, the following procedure is used to calculate the design instantaneous gust from which the design value of $\sigma_{304.8}$ shall be obtained. The procedure consists of specifying the vehicle lifetime T; calculating the limit load design value of M/N_o with equation (8.47); and then calculating the limit load instantaneous gust velocity, w*, say, with equation (8.44) for A = 1 with the values of P_1, P_2, b_1, and b_2 associated with the 0-304.8 meter height interval for climb, cruise, wind descent in Table 8.4.21. The instantaneous gust velocity w^* should be associated with the 99.98 percent value of gust velocity for a given realization of turbulence. In addition, the turbulence shall be assumed to be Gaussian, so that the value of $\sigma_{304.8}$ for performing a simulation shall be obtained by dividing w^* by 3.5. This value of $\sigma_{304.8}$ and the values of σ at the 18.3-meter level [see equations (8.59)-(8.61)] shall be used to determine the values of p for each component of turbulence with equation (8.56), i.e.,

$$p = 0.356 \ln \left(\frac{\sigma_{304.8}}{\sigma_{18.3}} \right) \tag{8.66}$$

The integral scale of turbulence at the 304.8-meter level appropriate for simulation of turbulence with the Dryden turbulence model is $L_{304.8} = 190$ m. This scale of turbulence and the 18.3-meter level scales of turbulence given by equation (8.58) yield the following values of q appropriate for the simulation of turbulence with the Dryden turbulence model in the atmospheric boundary layer:

$$q_u = 0.64; \; q_v = 0.83; \; q_w = 1.05. \tag{8.67}$$

The vertical distributions of σ and L given by equations (8.56) and (8.57) satisfy the isotropy condition given by equation (8.64).

Below the 18.3-meter level σ and L shall take on constant values equal to corresponding 18.3-meter level values.

The steady-state wind profile to be used with this model shall be obtained by the procedure given in Section 8.4.9.3 for merging ground winds and inflight wind profile envelopes.

To determine the steady-state wind direction $\Theta(z)$ at any level H between the surface and the 1000-meter level, use the following formula

$$\Theta(H) = \Theta_{1000} + \left[2\left(\frac{H - 1000}{1000}\right) + \left(\frac{H - 1000}{1000}\right)^2 \right] \Delta ,$$

where Θ_{1000} is the selected 1000-meter level wind direction and H is altitude above the surface of the earth in meters. The quantity Δ is the angle between the wind vectors at the 10- and 1000-meter levels. This quantity for engineering purposes is distributed according to a Gaussian distribtuion with mean value and standard deviation given by

$$\bar{\Delta} = 31°, \; \bar{u}_{1000} \leq 4 \text{ m sec}^{-1} ,$$

$$\bar{\Delta} = 31 - 2.183 \ln(\bar{u}_{1000}/4), \; \bar{u}_{1000} > 4 \text{ m sec}^{-1} ,$$

$$\sigma_{\Delta} = 64^{\circ}, \quad \bar{u}_{1000} \leq 4 \text{ m sec}^{-1},$$

$$\sigma_{\Delta} = 64 e^{-0.0531\left(\bar{u}_{1000} - 4\right)}, \quad \bar{u}_{1000} > 4 \text{ m sec}^{-1},$$

where $\bar{u}_{1000}$ is the 1000-meter level steady-state wind speed. To avoid unrealistic wind direction changes, Δ, between the surface and the 1000-meter level, only those values of Δ that occur in the interval $-180° \leq 0 \leq 180°$ should be used. It is recommended that ± 1% risk wind direction changes be used for vehicle design studies.

To apply this model, the longitudinal component of turbulence shall be assigned to be that component of turbulence parallel to the horizontal component of the relative wind vector. The lateral component of turbulence perpendicular to the longitudinal component and lies in the horizontal plane. The vertical component of turbulence is orthogonal to the horizontal plane.

The following procedure shall be used to calculate profiles of σ and L in the first 304.8 m of the atmosphere for simulation of turbulence with the Dryden turbulence model:

a. Specify the peak wind speed at the 18.3-meter level consistent with the accepted risks of exceeding the design 18.3-meter level peak wind speed.

b. Calculate the steady-state wind speed at the 18.3-meter level with equation (8.63).

c. Calculate the surface friction velocity with equation (8.62).

d. Calculate the 18.3-meter levels standard deviations of turbulence with equations (8.59) through (8.61).

e. Calculate the 304.8-meter level standard deviation of turbulence consistent with the accept risks of encountering the design instantaneous gust during the total exposure of the vehicle to the natural environments (remember $\sigma_u = \sigma_v = \sigma_w$ at the 304.8-meter level).

f. Calculate p_u, p_v, and p_w with equation (8.66).

g. Calculate the distribution of σ and L with equations (8.56) and (8.57) for the altitudes at and between the 18.3- and 304.8-meter levels.

h. Below the 18.3-meter level σ and L shall take on constant values equal to the 18.3-meter levels values of σ and L.

The reader should consult Reference 8.39 for a detailed discussion concerning the philosophy and problem associated with the simulation of turbulence for engineering purposes.

8.4.14.3 Turbulence Simulation in the Free Atmosphere (above 304.8 m)

To simulate turbulence in the free atmosphere (above 304.8 m) it is recommended that equations (8.44) and (8.47) and the supporting data in Table 8.4.21 be used to specify the appropriate values of σ. The turbulence at these altitudes can be considered to be isotropic for engineering purposes so that the integral scales and intensities of turbulence are independent of direction. Past studies have shown that when the Dryden turbulence model is being used the scales of turbulence L = 533.4 m in the 304.8 - 672 m altitude band and L = 762 m above the 672-meter level in Table 8.4.21 should be replaced with the values L = 300 m and L = 533 m respectively (Ref. 8.38). This reduction in scales tends to bring the Dryden spectra in line with the von Karman spectra over the band of wave numbers of the turbulence which are of primary importance in the design of aerospace vehicles. Accordingly, it is recommended that these reduced scales be used in the simulation of turbulence above the 304.8-meter level when the Dryden model is being used.

To calculate the values of σ above the 304.8-meter level appropriate for performing a simulation of turbulence, it is recommended that the procedure used to calculate the 304.8-meter level value of σ be used. The appropriate values of P_1, P_2, b_1, and b_2 for the various altitude bands above the 304.8-meter level are given in Table 8.4.21.

8.4.14.4 Design Floor on Gust Environments

If the design lifetime, T, is sufficiently small it is possible that the turbulence models described herein for horizontally and nearly horizontal flying vehicles will result in a vehicle design gust environment which is characterized by discrete gusts with amplitudes less that 9 m sec^{-1} for $dm/L > 10$ in Figure 8.4.31 above the 1-kilometer level. This is especially true for altitudes above the 18-kilometer level. In view of the wide spread acceptance of the 9 m sec^{-1} gust as a minimum gust amplitude for design studies in the aerospace community and in view of the increased uncertainty in gust data as altitude increases it is recommended that a floor be established on gust environments for altitudes above the 1-kilometer level such that the least permissible value of σ shall be 3.4 m sec^{-1} above the 1-kilometer level.

8.4.15 Discrete Gust Model - Horizontally Flying Vehicles

Often it is useful for the engineer to use discrete gusts in load and flight control system calculations of horizontally flying vehicles. The discrete gust is defined as follows:

$$V_d = 0, \quad x < 0$$

$$V_d = \frac{V_m}{2}\left(1 - \cos\frac{\pi x}{d_m}\right), \quad 0 \le x \le 2d_m$$

$$V_d = 0, \quad x > 2d_m,$$

where x is distance and V_m is maximum velocity of the gust which occurs at position $x = d_m$ in the gust. To apply the model, the engineer specifies several values of the gust half-width d_m, so as to cover the range of frequencies of the system to be analyzed. To calculate the gust parameter V_m one enters Figure 8.4.31 with d_m/L and reads out V_m/σ. Figure 8.4.31 is based on the Dryden spectrum of turbulence. Accordingly, the procedures outlined in subsections 8.4.14.2 and 8.4.14.3 can be used for the specification of the σ's and L's to determine the gust magnitude V_m from Figure 8.4.31. In the boundary layer, three values of V_m will occur at each altitude, one for each component of turbulence. In the free atmosphere the lateral and vertical values of V_m are equal at each altitude. In general both the continuous random gust model (Sections 8.4.13 and 8.4.14) and the discrete gust model are often used to calculate vehicle responses with the procedure producing the larger response being used for design.

8.4.16 Flight Regimes For Use of Horizontal and Vertical Turbulence Models (Spectra and Discrete Gusts)

Sections 8.4.8, 8.4.13, and 8.4.15 contain turbulence (spectra and discrete gusts) models for response calculations of vertically ascending and horizontally flying aerospace vehicles.

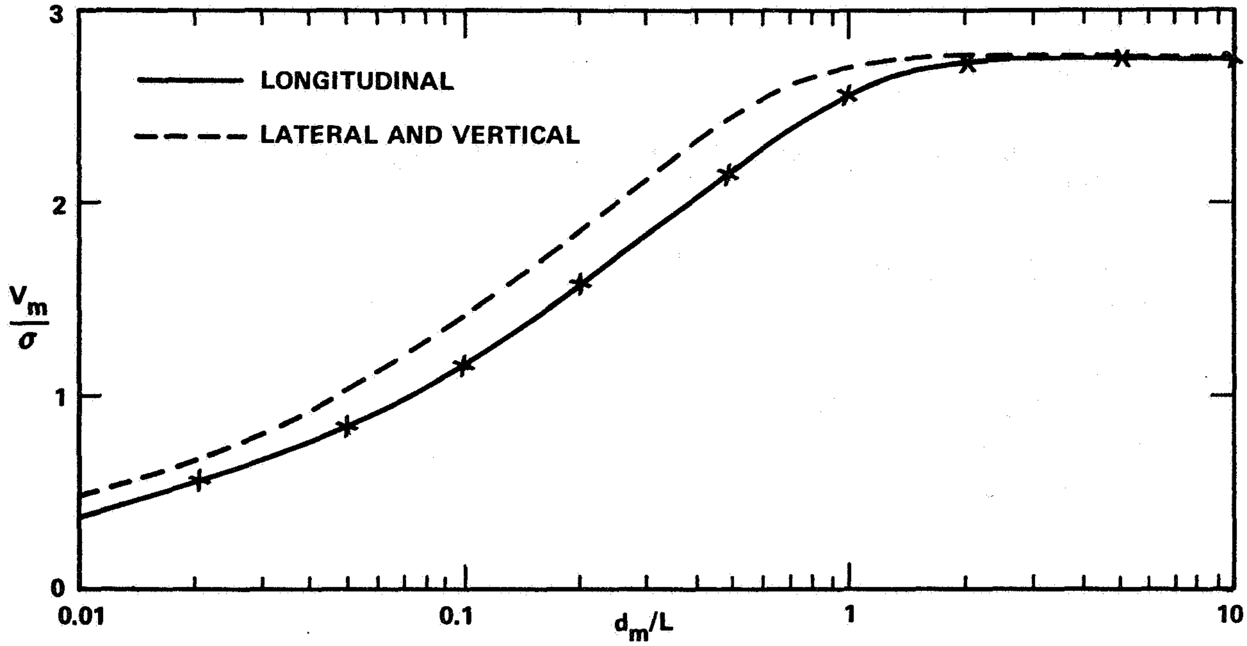

FIGURE 8.4.31. NONDIMENSIONAL DISCRETE GUST MAGNITUDE V_m/σ AS A FUNCTION OF NONDIMENSIONAL GUST HALF-WIDTH

The turbulence model for the horizontally flying vehicles was derived from turbulence data gathered with airplanes. The turbulence model for the vertically ascending or descending vehicles was derived from wind profile measurements made with vertically ascending Jimsphere ballons and smoke trails. In many instances aerospace vehicles neither fly in a pure horizontal flight mode nor ascend or descend in a strictly vertical flight path. At this time there does not appear to be a consistent way of combining the turbulence models for horizontal and vertical flight so as to be applicable to the design of aerospace vehicles with other than near horizontal or vertical flight paths without being unduly complicated or overly conservative. In addition, the unavailability of a sufficient large data sample of turbulence measurements in three dimensions precludes the development of such a combined model.

Accordingly, in lieu of the availability of a combined turbulence model and for the sake of engineering simplicity the turbulence model in Section 8.4.8 should be applied to ascending and descending aerospace vehicles when the angle between the flight path and the local vertical is less than or equal to 30 degrees. Similarly, the turbulence model in Sections 8.4.13 and and 8.4.15 should be applied to aerospace vehicles when the angle between the flight path and the local horizontal is less than or equal to 30 degrees. In the remaining flight path region between 30 degrees from the local vertical and 30 degrees from the local horizontal, both turbulence models should be independently applied and the most adverse responses used in the design.

8.5 Mission Analysis, Prelaunch Monitoring, and Flight Evaluation

Wind information is useful in the following three general cases of mission analysis:

a. Mission Planning. Since this activity will normally take place well in advance of the mission, the statistical attributes of the wind are used.

b. Prelaunch Operations. Although wind statistics are useful at the beginning of this period, the emphasis is placed upon forecasting and wind monitoring.

c. Postflight Evaluation. The effect of the observed winds on the flight is analyzed.

8.5.1 Mission Planning

From wind climatology, the optimum time (month and time of day) and place to conduct the operation can be identified. Missions with severe wind constraints may have such a low probability of success that the risk is unacceptable. Feasibility studies based upon wind statistics can identify these problem areas and answer questions such as: "Is the mission feasible as planned?" and "If the probable risk of mission delay or failure is unacceptably high, can it be reduced by rescheduling to a lighter wind period?"

The following examples are given to illustrate the use of some of the many wind statistics available to the mission planner.

If it is necessary to remove the wind loads damper from a large launch vehicle for a number of hours and this operation must be scheduled some days in advance, the well known diurnal ground wind variation should be considered for this problem. If, for example, 10.3 m/sec (20 knots) were the critical wind speed, there is a 1-percent risk at 0600 EST, but a 13-percent risk at 1500 EST in July. Obviously, the midday period in the summer should be avoided for this operation. Since these probability values apply to 1-hour exposure periods, it is important to recognize that the wind risk depends not only upon wind speed but also upon exposure time. From Figure 8.5.1, the risk in percentage associated with a 15.4 m/sec (30-knot) wind at 10 meters in February at Kennedy Space Center can be obtained for various exposure times. The upper curve shows the risk increasing from 1 percent for 1-hour exposure

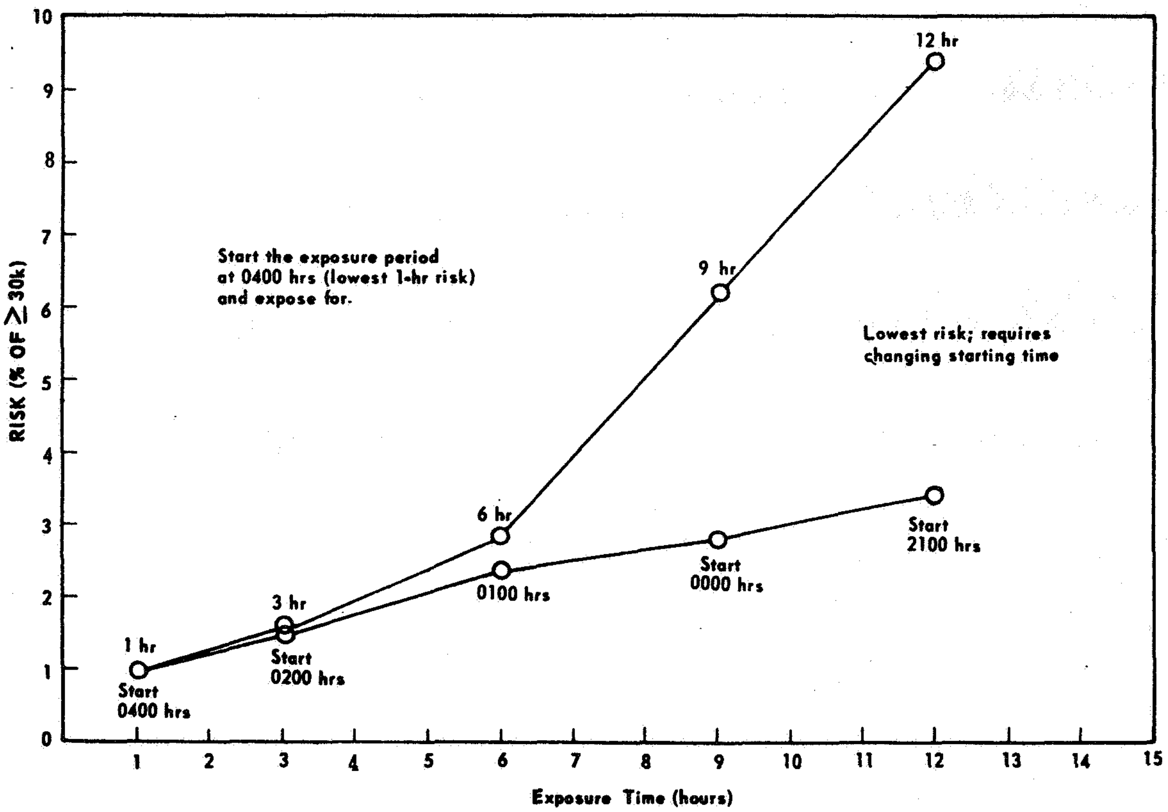

FIGURE 8.5.1 EXAMPLE OF WIND RISK FOR VARIOUS EXPOSURE TIMES

starting at 0400 EST to 9.3 percent for 12-hour exposure starting at 0400 EST. In this case the exposure period extends through the high risk part of the day. The lower curve illustrates the minimum risk associated with each exposure period. The lowest risk, of course, can be realized if the starting times are changed to avoid the windy portion of the day. Although there is no space here for the tabulation, wind risk probabilities by month and starting hour for exposure periods from 1 hour to 365 days are available upon request.

When winds aloft are considered for mission planning purposes, again the first step might be to acquire general climatological information on the area of concern. From Figures 8.5.2 and 8.5.3 it is readily apparent that for Kennedy Space Center most strong winds occur during winter in the 10- to 15-kilometer altitude region (this applies also to nearly all midlatitude locations). It is also true that these strong winds are usually westerly.

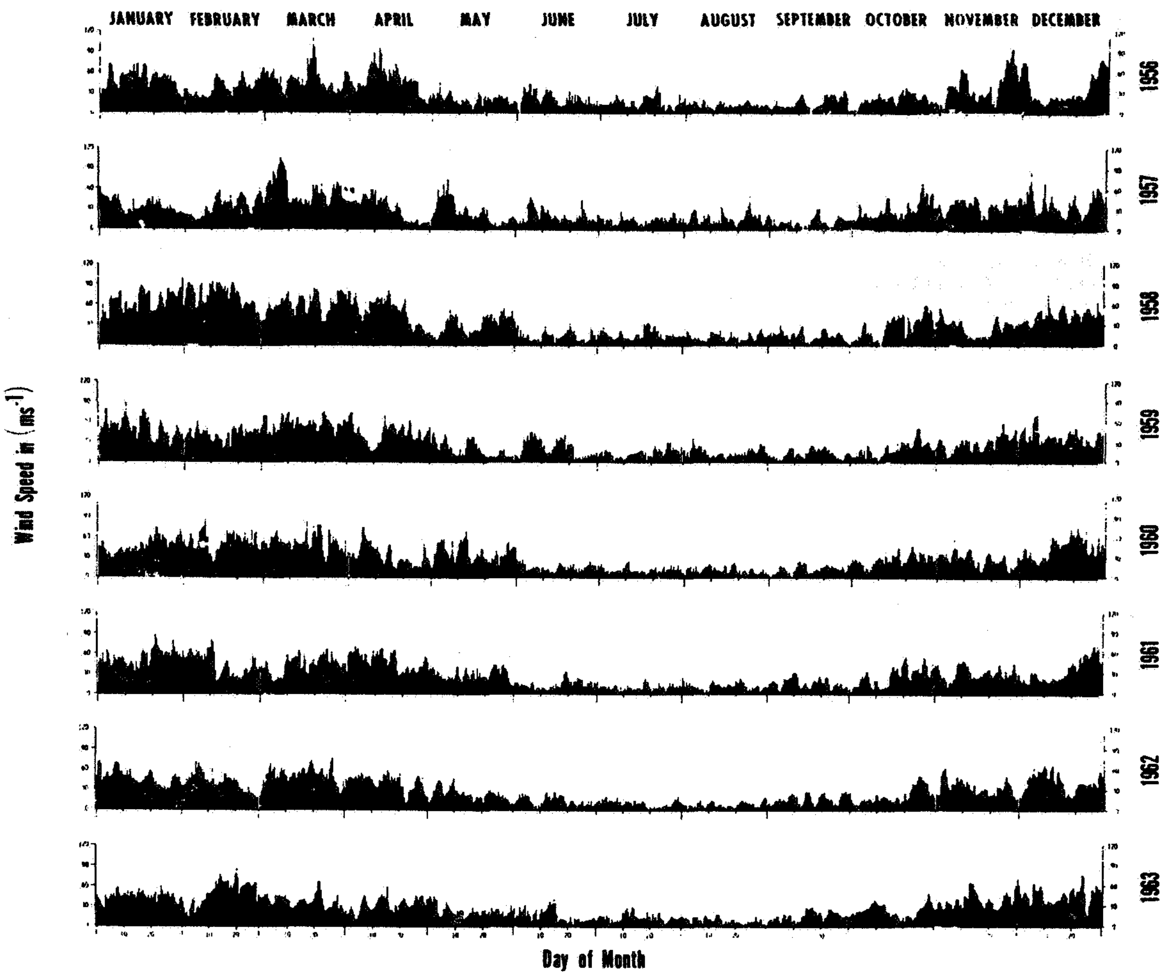

FIGURE 8.5.2 TWICE DAILY MAXIMUM WIND SPEED IN THE 10- TO 15-km LAYER AT CAPE KENNEDY

Next, the mission analyst might ask if a particular mission is feasible. If, for example, the flight is to take place in January and 10- to 15-kilometer altitude winds $\geqq 50$ m/sec are critical, the probability of favorable winds on any day in January is 0.496. With such a low probability of success, this mission may not be feasible. But, to continue the example, if it is necessary that continuously favorable winds exist for 3 days (perhaps for a dual launch) the probability of success will decrease to 0.256. Obviously an alternate mission schedule must be planned or else the scheduled space vehicle must be provided additional capability through redesign.

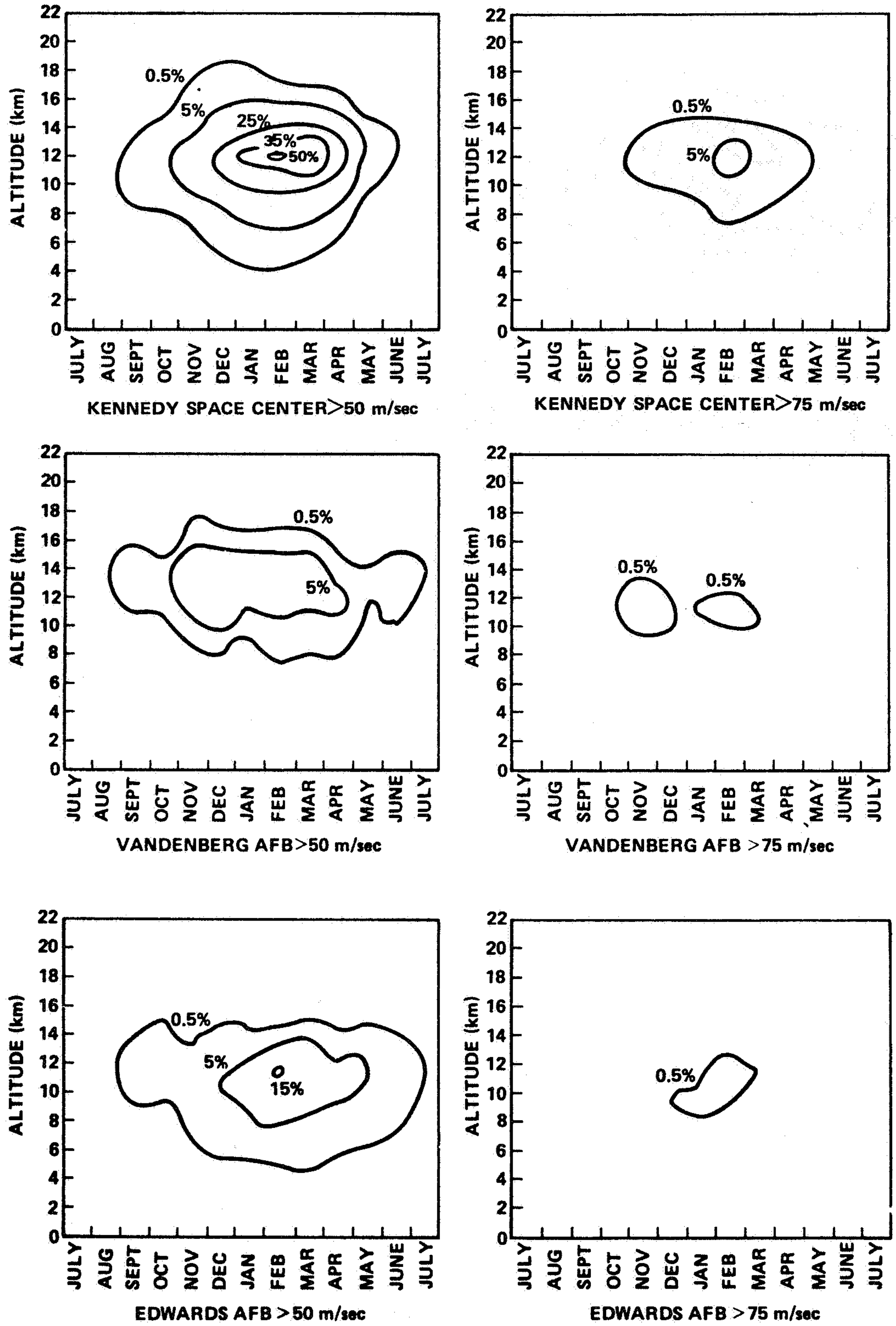

FIGURE 8.5.3 FREQUENCY OF SCALAR WIND SPEED EXCEEDING GIVEN WIND SPEED AS A FUNCTION OF ALTITUDE FOR STATIONS INDICATED

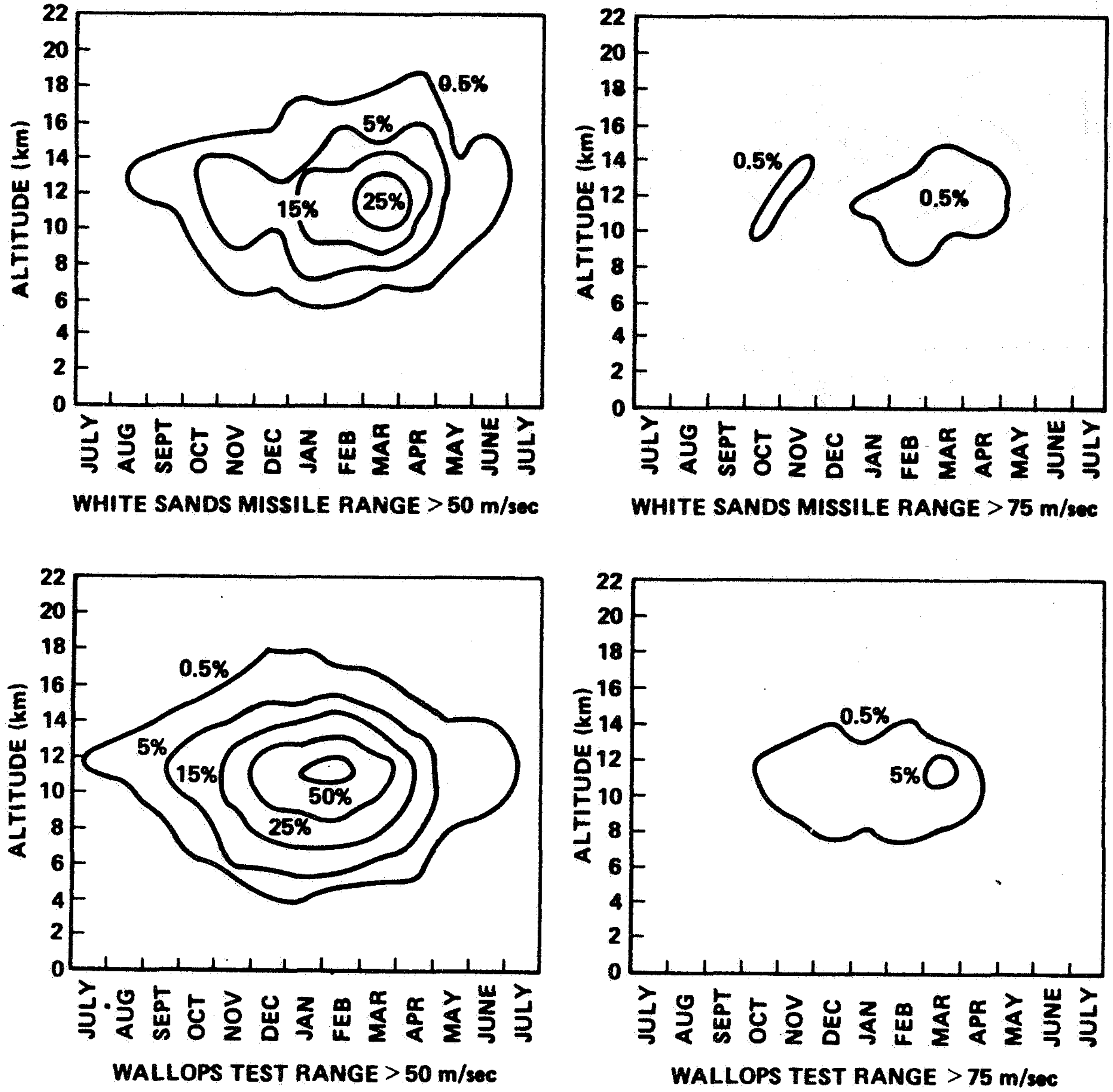

FIGURE 8.5.3 FREQUENCY OF SCALAR WIND SPEED EXCEEDING GIVEN WIND SPEED AS A FUNCTION OF ALTITUDE FOR STATIONS INDICATED (Concluded)

Perhaps the vehicle can remain on the pad in a state of near readiness awaiting launch for several days. In this case it would be desirable to know that the probability of occurrence of at least one favorable wind speed, for example, in a 4-day period is 0.813. If greater flexibility of operation is desired, one might require four favorable opportunities in 4 days. This probability is 0.550. Now, if consecutive favorable opportunities are required, for example, four consecutive successes in eight periods, the probability of success will be somewhat lower (0.431).

The mission planner might also gain some useful information from the persistence of the winds aloft. The probability of winds < 50 m/sec on any day in January is 0.496. But if a wind speed < 50 m/sec does occur, then the probability that the next observed wind 12 hours later would be < 50 m/sec is 0.82, a rather dramatic change. Furthermore, if the wind continues below 50 m/sec for five observations, the probability that it will remain there for one more 12-hour period is 0.92.

As the time of the operation approaches T-4 to T-1 days, the conditional probability statements assume a more significant role. At this point, as the winds will usually be monitored, the appropriate conditional probability value can be identified and used to greater advantage.

The above is intended to illustrate the type of analysis that can be accomplished to provide objective data for program decisions. This may best be accomplished by a close working relationship between the analyst and those concerned with the decision.

8.5.2 Prelaunch Wind Monitoring

Inflight winds constitute the major atmospheric forcing function in space vehicle and missile design and operations. A frequency content of the wind profile near the bending mode frequencies or wind shear with the characteristics of a step input may exceed the vehicle's structural capabilities (especially on forward stations for the small scale variations of the wind profiles). Wind profiles with high speeds and shears exert high structural loads at all stations on a large space vehicle, and when the influences of bending dynamics are high, even a profile with low speeds and high shears can create large loads (Ref. 8.40).

Because of the possibility of launch into unknown winds, operational missile systems must accept some inflight loss risk in exchange for a rapid-launch capability. But research and development missiles, and space vehicles in particular, cost so much that the overall success of a flight outweighs the consideration of launch delays caused by excessive inflight wind loads. If the exact wind profile could be known in advance, it would be a relatively simple task to decide upon the launch date and time. However, there is little hope of accurately forecasting the detailed wind profile very much into the future.

Over the years, these situations have increasingly put emphasis on prelaunch monitoring of inflight winds. Now, finally, prelaunch and profile determination techniques essentially preclude the risk of launching a space vehicle or research and development missile into an inflight wind condition that would cause it to fail.

Recent development and operational deployment of the FPS-16 Radar/Jimsphere system (Ref. 8.41) significantly minimizes vehicle failure risks when properly integrated into a flight simulation program. The Jimsphere sensor, when tracked with the FPS-16 or other radar with equal tracking capability, provides a very accurate "all weather" detailed wind profile measurement. FPS-16 radars are available at all national test ranges.

In general, the system provides a wind profile measurement from the surface to an altitude of 17 kilometers in slightly less than 1 hour, a vertical spatial frequency resolution of 1 cycle per 100 meters, and an rms error of about 0.5 m/sec or less for wind velocities averaged over 50-meter intervals. The resolution of these data permits calculating the structural loads associated with the first bending mode and generally the second mode of missiles and space vehicles during the critical, high dynamic pressure phase of flight. This provides better than an order-of-magnitude accuracy improvement over the conventional rawinsonde wind profile measuring system.

By employing the appropriate data transmission resources, a detailed wind profile from the FPS-16 radar can be ready for input to the vehicle's flight simulation program within a few minutes after tracking of the Jimsphere. The flight simulation program provides flexibility relative to vehicle dynamics and other parameters in order to make maximum use of the detailed wind profiles.

If very critical wind conditions exist and the mission requirement dictates a maximum effort to launch with provision for last minute termination of the operation, then a contingency plan that will provide essentially real-time wind profile and flight simulation data may be employed. This is done while the Jimsphere balloon is still in flight.

An example of the FPS-16 Radar/Jimsphere system data appears in Figure 8.5.4 — the November 8 and 9, 1967, sequence observed during prelaunch activities for the first Apollo/Saturn-V test flight, AS-501. References 8.42 and 8.43 contain additional sequential jimsphere wind profile sets for Cape Kennedy and the Pacific Missile Range (Point Mugu, California) respectively. The persistence over a period of 1 hour of some small scale features in the wind profile structure, as well as the rather distinct changes that developed in the profiles over a period of a few hours, is evident.

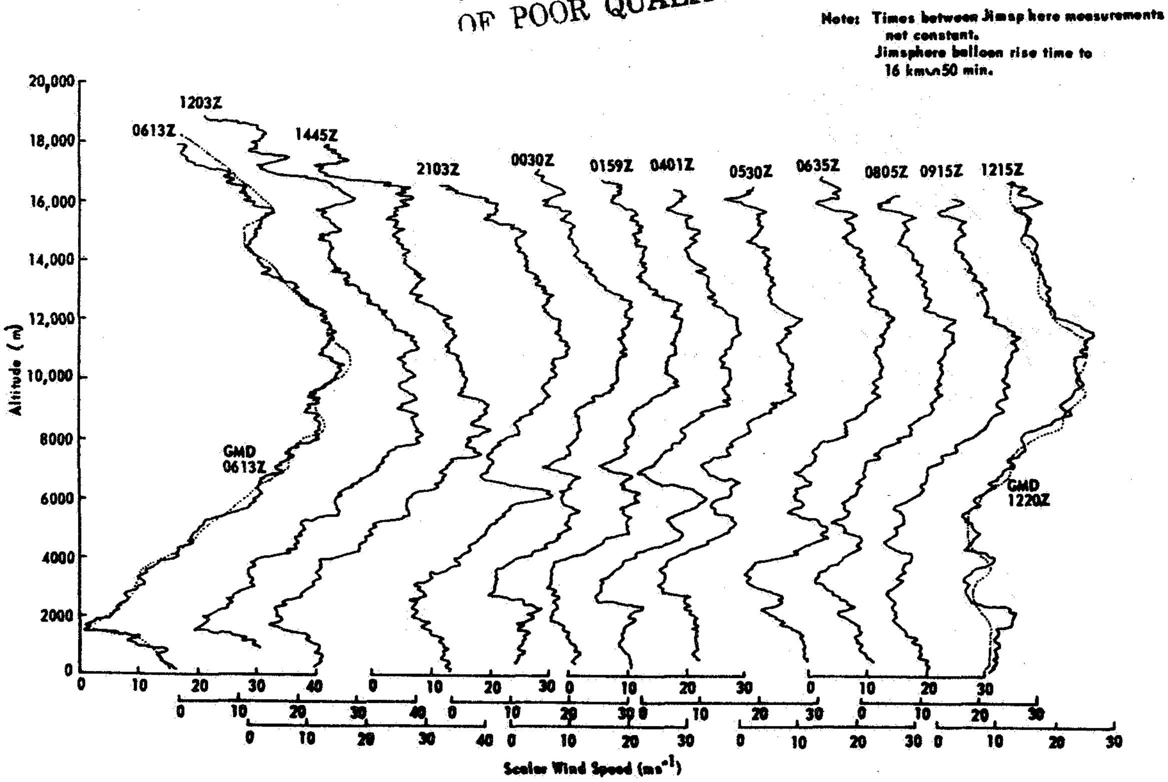

FIGURE 8.5.4 EXAMPLE OF THE FPS-16 RADAR/JIMSPHERE SYSTEM DATA, NOVEMBER 8-9, 1967

The FPS-16 Radar/Jimsphere system (Fig. 8.5.5) was routinely used in the prelaunch monitoring of NASA's Apollo/Saturn-IB and -V flights. The wind profile data were transmitted to the Johnson Space Center and Marshall Space Flight Center, and the flight simulation results were sent to the launch complex at Kennedy Space Center.

An FPS-16 Radar/Jimsphere operational measurement program capability exists at all the national test ranges to obtain detailed wind profile data for use in space vehicle and missile response studies, airplane turbulence analysis, atmospheric turbulence investigations, and mesometeorological studies. Sequential measurements similar to the Saturn-V data shown here — of eight to ten Jimsphere wind profiles approximately 1 hour apart — were made on at least 1 day per month for each location. Single profile measurements were also made daily at Eastern Test Range.

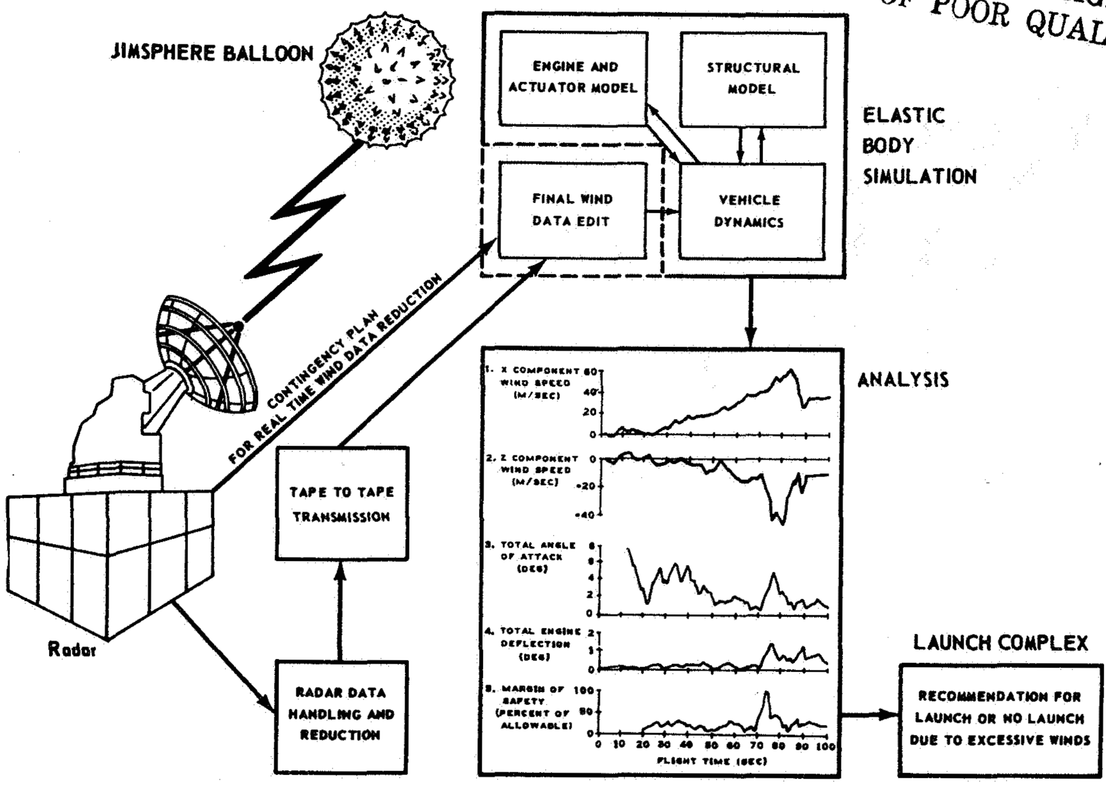

FIGURE 8.5.5 OPERATION OF THE FPS-16 RADAR/JIMSPHERE SYSTEM

8.5.3 Post-Flight Evaluation

8.5.3.1 Introduction

Because of the variable effects of the atmosphere upon a large space vehicle at launch and during flight, various meteorological parameters were measured at the time of each space vehicle launch, including wind and thermodynamic data at the earth's surface and up to an altitude of at least 50 kilometers. To make the data available, meteorological tapes were prepared, presentations were made at flight evaluation meetings, memoranda of data tabulations were prepared and distributed, and a summary was written for the final vehicle flight evaluation report. Reference 8.44 for Apollo/Saturn-503 is an example of one of the reports with an atmospheric section.

8.5.3.2 Meteorological Tapes

Shortly after the launch of each space vehicle, under the cognizance of the Marshall Space Flight Center, preliminary meteorological tape was prepared by combining the FPS-16 Radar/Jimsphere wind profile data and the rawinsonde wind profile and thermodynamic data (temperature, pressure, and humidity) observed as near the vehicle launch time as feasible. This was done under the supervision of the Marshall Space Flight Center's Atmospheric Sciences Division. The preliminary meteorological tape was normally available within 12 hours after launch time and provided data to about 35 kilometers. The final meteorological tape was prepared with the addition of rocketsonde wind and thermodynamic data extending the data to at least 50 kilometers and was available for use about 3 days after launch.

In the two meteorological data tapes (preliminary and final), thermodynamic data above the measured data are given by Patrick Reference Atmosphere values. To prevent unnatural jumps in the data when the two types are merged, the data were carefully examined to pick the best altitude for the merging.

The meteorological data tapes were made available to all government and contractor groups for their use in the space vehicle launch and flight evaluation. This provides a consistent set of data for all evaluation studies and ensures the best available information of the state of the atmosphere.

Twenty-one parameters of data were included in the meteorological data tape at 25-meter increments of altitude[13] in Table 8.5.1.

8.5.3.3 Presentations at Flight Evaluation Working Group Meetings

Unless the space vehicle performance was bad or the magnitude of some atmospheric parameters was near extremes at launch or during flight, only two presentations were made at the flight evaluation meetings on the atmospheric launch environment.

The first presentation was given at the "quick look" meeting normally held on the day following launch. At this meeting, preliminary values of the surface weather conditions (temperature, pressure, dew point or relative humidity, visibility, cloudiness, and launch pad wind speed and direction) were given, and plots of the upper wind speeds, direction, and components were shown up to the highest altitude of the available data. Any unusual features of the data were discussed in detail.

At the "first general" flight evaluation meeting, the final upper wind speeds and component graphs were shown for all the data used in the meteorological data tape.

---

13. Altitude increments of 25 meters were chosen to provide for maximum engineering value and for use of the available atmospheric data and do not necessarily represent the attainable frequency response of the measurements.

TABLE 8.5.1 FORMAT OF METEOROLOGICAL TAPE

First Record: Identification			
Word	Symbol	Parameter	Units
1	Y_S	Altitude (geometric) ($0=Y_S=700,000$) H=25	m
2	T	Temperature	°K
3	P	Pressure	mb
4	W	Wind Speed	m/sec
5	W_D	Wind Direction	deg
6	U/100	Relative Humidity (U is percent)	(10^{-2}) %
7	E	Water Vapor Pressure	mb
8	ρ	Density	kg/m^3
9	P'	Pressure	$newton/cm^2$
10	$V_S=C_S$	Velocity of Sound	m/sec
11	N_o	Optical Index of Refraction	unitless
12	N_e	Electomagnetic Index of Refraction	unitless
13	W_x	Pitch Component of Wind Velocity	m/sec
14	W_z	Yaw Component of Wind Velocity	m/sec
15	W_{w-e}	Zonal Component of Wind Velocity	m/sec
16	W_{s-n}	Meridional Component of Wind Velocity	m/sec
17	ρ	Density times Gravity	$newton/m^3$
18	μ	Coefficient of Viscosity	$newton\ sec/m^2$
19	T	Temperature	°C
20	$S_{x\,250}$	Pitch Component Wind Shear	sec^{-1}
21	$S_{z\,250}$	Yaw Component Wind Shear	sec^{-1}

Surface wind speeds and directions were measured and recorded at several locations and heights above the launch pad, starting several hours before launch time. Detailed tabulations were made from the various measuring locations and were distributed by memoranda for flight evaluation purposes. Reference 8.45 summarizes atmospheric data observations for 155 flights of NASA/MSFC related launches.

8.5.3.4 Atmospheric Data Section for Final Vehicle Launch Report

The results of the flight evaluation were presented in a final vehicle launch report. A section in this report gives the information on the atmospheric environment at launch time. Records were maintained on the atmospheric parameters for MSFC sponsored vehicle test flights conducted at Kennedy Space Center, Florida. Requests for summaries of these atmospheric data, or related questions on specific topics, should be directed to the Atmospheric Sciences Division, Space Sciences Laboratory, NASA-Marshall Space Flight Center, Alabama 35812.

REFERENCES

8.1 Carter, E. A. and Schuknecht, L. A., "Peak Wind Statistics Associated with Thunderstorms at Cape Kennedy, Florida." NASA CR-61304, NASA-George C. Marshall Space Flight Center, Marshall Space Flight Center, Alabama, August 1969.

8.2 Smith, O. E.; Falls, L. W.; and Brown, S. C., "Research Achievements Review," Vol. II, Report No. 10, "Terrestrial and Space Environment Research at MSFC," NASA TM X-53706, NASA-George C. Marshall Space Flight Center, Marshall Space Flight Center, Alabama, 1967.

8.3 Lee, Russel F.; Goodge, Grant W.; and Crutcher, H. L., "Surface Climatological Information for Twelve Selected Stations for Reentry Vehicles," NASA CR-61319, Marshall Space Flight Center, Alabama 1970.

8.4 Goodge, G. W., Bilton, T. H.; and Quinlin, F. T., "Surface Climatological Information for Twenty Selected Stations for Reentry Vehicles," NASA CR-61342, Marshall Space Flight Center, Alabama, 1971.

8.5 Fichtl, G. H. and McVehil, G. E., "Longitudinal and Lateral Spectra of Turbulence in the Atmospheric Boundary Layer at the Kennedy Space Center," Journal of Applied Meteorology, vol. 9, no. 1, Feb. 1970, pp. 51-63.

8.6 Blackadar, Alfred K., et al., "Investigation of the Turbulent Wind Field Below 150M Altitude at the Eastern Test Range," NASA CR-1410, NASA-George C. Marshall Space Flight Center, Marshall Space Flight Center, Alabama, Aug. 1969.

8.7 McVehil, G. E. and Camnitz, H. G., "Ground Wind Characteristics at Kennedy Space Center," NASA CR-1418, NASA-George C. Marshall Space Flight Center, Marshall Space Flight Center, Alabama, Sept. 1969.

8.8 Fichtl, G. H., Kaufman, J. W., and Vaughan, W. W., "Characteristics of Atmospheric Turbulence as Related to Wind Loads on Tall Structures." Journal of Spacecraft and Rockets, vol. 6, no. 12, Dec. 1969, pp. 1396-1403.

8.9 Fichtl, G. H., "Problems in the Simulation of Atmospheric Boundary Layer Flows." AGARD-CP-140 (1973) 2-1. (Paper presented AGARD Flight Mechanics Panel Symposium on "Flight in Turbulence," England, May 1973.)

REFERENCES (Continued)

8.10 Fichtl, G. H., "Wind Shear Near the Ground and Aircraft Operations." Journal of Spacecraft and Rockets, vol. 9, no. 11, November 1972, pp. 765-770.

8.11 Fichtl, G. H., "Probability Distribution of Vertical Longitudinal Shear Fluctuations." Journal of Applied Meteorology, vol. 11, no. 6, September 1972, pp. 918-925.

8.12 Fichtl, G. H., "Standard Deviation of Vertical Two-Point Longitudinal Velocity Differences in the Boundary Layer." Boundary-Layer Meteorology, vol. 2, 1971, pp. 137-151.

8.13 Luers, J. K. and Reese, J. B., "Effects of Shear and Aircraft Landing," NASA CR-2287, NASA-George C. Marshall Space Flight Center, Alabama, July 1973.

8.14 Luers, J. K., "A Model of Wind Shear and Turbulence in the Surface Boundary Layer," NASA CR-2288, NASA-George C. Marshall Space Flight Center, Alabama, July 1973.

8.15 Sowa, Danies, "Low-Level Wind Shear," D. C. Flight Approach, No. 20, Douglas Aircraft Co., Long Beach, CA, 1974.

8.16 Barr, Neal M.; Gangaas, D.; and Schaeffer, D. R., "Wind Models for Flight Simulator Certification of Landing and Approach Guidance and Control Systems," Report No. FAA-RD-74-206, U.S. Department of Transportation, Federal Aviation Administration, Washington, D.C. 20590, December 1974.

8.17 Lewell, W. S. and Williamson, Guy G., "Wind Shear and Turbulence Around Airports," NASA CR-2752, NASA-George C. Marshall Space Flight Center, Alabama, October 1976.

8.18 Camp, D. W. and Kaufman, J. W., "Comparison of Tower Influence on Wind Velocity for NASA's 150-meter Meteorological Tower and a Wind Tunnel Model of the Tower." Journal of Geophysical Research, vol. 75, no.6, February 20, 1970.

8.19. Thom, H. C. S., "New Distributions of Extreme Winds in the United States," Journal of the Structural Division Proceedings of the American Society of Civil Engineers, ST-7, July 1968, pp. 1787-1801.

REFERENCES (Continued)

8.20 Falls, L. W. and Brown, S. C., "Optimum Runway Orientation Relative to Crosswinds." NASA TN D-6930, September 1972.

8.21 Falls, L. W. and Crutcher, H. L., "Determination of Statistics for any Rotation of Axes of a Bivariate Normal Elliptical Distribution." NASA TM X-64595, May 1971.

8.22 IRIG Document No. 104-63, Range Reference Atmosphere Documents published by Secretariat, Range Commander's Council, White Sands Missile Range, New Mexico.

a. The following reference atmospheres have been published:

(1) Atlantic Missile Range Reference Atmosphere for Cape Kennedy, Florida (Part I), 1963.

(2) White Sands Missile Range Reference Atmosphere (Part I), 1964.

(3) Fort Churchill Missile Range Reference Atmosphere for Fort Churchill, Canada (Part I), 1964.

(4) Pacific Missile Range Reference Atmosphere for Eniwetok, Marshall Islands (Part I), 1964.

(5) Fort Greely Missile Range Reference Atmosphere (Part I), 1964.

(6) Eglin Gulf Test Range Reference Atmosphere for Eglin AFB, Florida (Part I), 1965.

(7) Pacific Missile Range Reference Atmosphere for Point Arguello, California (Part I), 1965.

(8) Wallops Island Test Range Reference Atmosphere (Part I), 1965.

(9) Eastern Test Range Reference Atmosphere for Ascension Island, South Atlantic (Part I), 1966.

REFERENCES (Continued)

(10) Lihue, Kauai, Hawaii Reference Atmosphere (Part I), 1970.

(11) Johnson Island Test Site Reference Atmosphere (Part I), 1970.

(12) Edwards Air Force Base Reference Atmosphere (Part I), 1972.

(13) Kwajalein Missile Range, Kwajalein, Marshall Islands, Reference Atmosphere (Part I), 1974.

(14) Cape Kennedy, Florida Reference Atmosphere (Part II), 1971.

(15) White Sands Missile Range Reference Atmosphere (Part II), 1971.

(16) Wallops Island Test Range Reference Atmosphere (Part II), 1971.

(17) Fort Greely Missile Range Reference Atmosphere (Part II), 1971.

(18) Pacific Missile Test Center Reference Atmosphere (Part II), November 1975.

8.23 Falls, L. W., "Normal Probabilities for Cape Kennedy Wind Components — Monthly Reference Periods for all Flight Azimuths — Altitudes 0 to 70 Kilometers," NASA TM X-64771, NASA-George C. Marshall Space Flight Center, Marshall Space Flight Center, Alabama, April 16, 1973.

8.24 Falls, L. W., "Normal Probabilities for Vandenberg AFB Wind Components — Monthly Reference Periods for all Flight Azimuths, 0- to 70-km Altitudes," NASA TM X-64897, NASA-George C. Marshall Space Flight Center, Marshall Space Flight Center, Alabama, January 1975.

8.25 Henry, Robert M., "A Statistical Model for Synthetic Wind Profiles for Aerospace Vehicle Design and Launching Criteria." NASA TN D-1813, 1963.

8.26 Bieber, Raymond E., "Missile Structural Loads by Non-Stationary Statistical Methods." Technical Report No. LMSD 49703, Lockheed Missile and Space Division, Huntsville, Alabama 35807, April 1959. (Also available as DDC AD220595 or NTIS PB157733.)

REFERENCES (Continued)

8.27 Vaughan, William W., "Interlevel and Intralevel Correlations of Wind Components for Six Geographical Locations." NASA TN D-561, Dec. 1960.

8.28 Daniels, Glenn, E.; and Smith, Orvel E., "Scalar and Component Wind Correlations Between Altitude Levels for Cape Kennedy, Florida, and Santa Monica, California," NASA TN D-3815, Apr. 1968.

8.29 Cochrane, James A.; Henry, Robert M.; and Weaver, William L., "Revised Upper Air Wind Data for Wallops Island Based on Serially Completed Data for the Years 1956 to 1964." NASA TN D-4570, NASA-Langley Research Center, Langley Station, Hampton, Virginia, May 1968.

8.30 Buell, C. E., "Correlation Functions for Wind and Geopotential on Isobaric Surfaces." Journal of Applied Meteorology, vol. II, no. 1, Feb. 1972, pp. 51-59.

8.31. Buell, C. E., "Variability of Wind with Distance and Time on an Isobaric Surface." Journal of Applied Meteorology, vol. II, no. 7, Oct. 1972, pp. 1085-1091.

8.32 Truppi, Lawrence E., "Probabilities of Zero Wind Shear Phenomena Based on Rawinsonde Data Records," NASA TM X-53452, NASA-George C. Marshall Space Flight Center, Marshall Space Flight Center, Alabama, Apr. 27, 1966.

8.33 Camp, Dennis W. and Susko, Michael, "Percentage Levels of Wind Speed Differences Computed by Using Rawinsonde Wind Profile Data from Cape Kennedy, Florida," NASA TM X-53461, NASA-George C. Marshall Space Flight Center, Marshall Space Flight Center, Alabama, May 12, 1966.

8.34 Camp, Dennis W. and Fox, Patricia A., "Percentage Levels of Wind Speed Differences Computed by Using Rawinsonde Wind Profile Data from Santa Monica, California." NASA TM X-53428, NASA-George C. Marshall Space Flight Center, Marshall Space Flight Center, Alabama, Oct. 21, 1966.

REFERENCES (Continued)

8.35 Fichtl, G. H., "Small-Scale Wind Shear Definition for Aerospace Vehicle Design." Journal of Spacecraft and Rockets, vol. 9, no. 2, Feb. 1972, pp. 79-83.

8.36 Fichtl, G. H.; Camp, D. W.; and Vaughan, W. W., "Detailed Wind and Temperature Profiles." Clear Air Turbulence and Its Detection, Edited by Yih-Hc Pao and Arnold Goldburg, Plenum Press, New York, 1969, pp. 308-333.

8.37 Smith, O. E.; "Vector Wind and Vector Wind Shear Models 0 to 27 km Altitude for Cape Kennedy, Florida, and Vandenberg AFB, California," NASA TM X-73319, NASA-George C. Marshall Space Flight Center, Marshall Space Flight Center, Alabama, July 1976.

8.38 Chalik, C. R., et al., "Background Information and User Guide for MIL-F-8758B ASG , 'Military Specification — Flying Qualities for Piloted Airplanes,'" AFFDL-TR-69-72, Air Force Flight Dynamics Laboratory, Air Force Systems Command, Wright-Patterson Air Force Base, Ohio, August 1969.

8.39 Dutton, J. A., "Broadening Horizons in Prediction of the Effects of Atmospheric Turbulence on Aeronautical Systems." AIAA Selected Reprints Series/Vol. XIII, The Earth's Atmosphere, W. W. Vaughan and L. L. DeVries, Editors, Published by the American Institute of Aeronautics and Astronautics, New York.

8.40 Ryan, Robert S.; Scoggins, James R.; and King, Alberta W., 'Use of Wind Shears in the Design of Aerospace Vehicles." Journal of Spacecraft and Rockets, vol. 4, no. 11, Nov. 1967, pp. 1526-1532.

8.41 Vaughan, William W., "New Wind Monitoring System Protects R and D Launches." Journal of Astronautics and Aeronautics, Dec. 1968, pp. 41-43.

8.42 Johnson, Dale and Alexander, Margaret, "70 Sequential Jimsphere Wind Profile Data Sets for Eastern Test Range Cape Kennedy, Florida December 1964-July 1970." NASA/MSFC-ES41, NASA-Marshall Space Flight Center, Alabama, August 1976.

REFERENCES (Concluded)

8.43 Johnson, Dale and Alexander, Margaret, "24 Sequential Jimsphere Wind Profile Data Sets for Pacific Missile Range Point Mugu, CA , January 1965-April 1970." NASA/MSFC-ES41, NASA-George C. Marshall Space Flight Center, Marshall Space Flight Center, Alabama, August 1976.

8.44 "Saturn V Launch Vehicle Flight Evaluation Report — AS-503, Apollo 8 Mission." MPR-SAT-FE-69-1, Saturn V Flight Evaluation Working Group, NASA-George C. Marshall Space Flight Center, Marshall Space Flight Center, Alabama, Feb. 20, 1969.

8.45 Johnson, D. L., "Summary of Atmospheric Data Observations for 155 Flights of MSFC/ABMA Related Aerospace Vehicles." NASA TM X-64796, NASA-George C. Marshall Space Flight Center, Marshall Space Flight Center, Alabama, December 5, 1973.

SECTION IX. SEA STATE *

9.1 Introduction

Natural environment design specifications for all applicable Space Shuttle activities are given in the appropriate Level II (Ref. 9.1) or Level III (Ref. 9.2) Space Shuttle documents. Since those documents are controlled by the program or project manager, it is not appropriate to repeat the design values here. Instead, this section contains the empirical distributions of several natural environment parameters that may be useful in other than Solid Rocket Booster (SRB) design studies and operational analyses.

In deep water the characteristics (sea states) are determined not only by the mean wind speed but also by the fetch (the distance over which it blows) and duration of the wind over the open water. A sea state is generally described by significant wave height, which is the average height of the one-third highest waves. Of course, higher waves exist in any given sea state. For example, from the relationship between wind speed and wave height for a fully arisen sea, as shown in Figure 9.1, it can be seen that in a code 3 sea state with significant wave heights about 1.2 m, 10 percent of the waves will average about 1.5 m. In other words, a wind speed of 8.2 m sec^{-1} (fetch and duration unlimited) will produce a sea with the highest one-third waves averaging about 1.2 m and the highest one-tenth waves about 1.5 m.

Figure 9.1 shows the distribution of wave heights versus wind speed at any given instant — information applicable to vehicle water entry. For all other operations (afloat, secure, towback recovery) where some considerable time interval is involved, the exposure period concept must be considered; that is, the longer the exposure period, the greater the probability of encountering a larger wave. Wave heights at the 5 percent risk level for exposure periods from 1 to 100 hours in a sea-state codes 3, 4, and 5 are shown in Figure 9.2. From Figure 9.2, for example, it can be seen that exposure for 1 hour in sea-state code 4 entails a 5 percent risk of encountering at least one wave greater than 5.3 m. If the exposure time is increased to 48 hours in the same sea-state code 4 condition, the wave height at the 5 percent risk level becomes 6.3 m.

The foregoing paragraphs dealt with general sea-state relationships valid in any deep-water area. This part will present empirical data applicable to the Cape Canaveral SRB recovery area (27 deg to 31 deg N; 77 deg to 80 deg W) or the Vandenberg Air Force Base SRB recovery area (31 deg to 33 deg N; 120 deg to 122 deg W).

* Further information and/or interpretation of these sea state criteria should be directed to the Atmospheric Sciences Division, Space Sciences Laboratory, Marshall Space Flight Center, Alabama 35812.

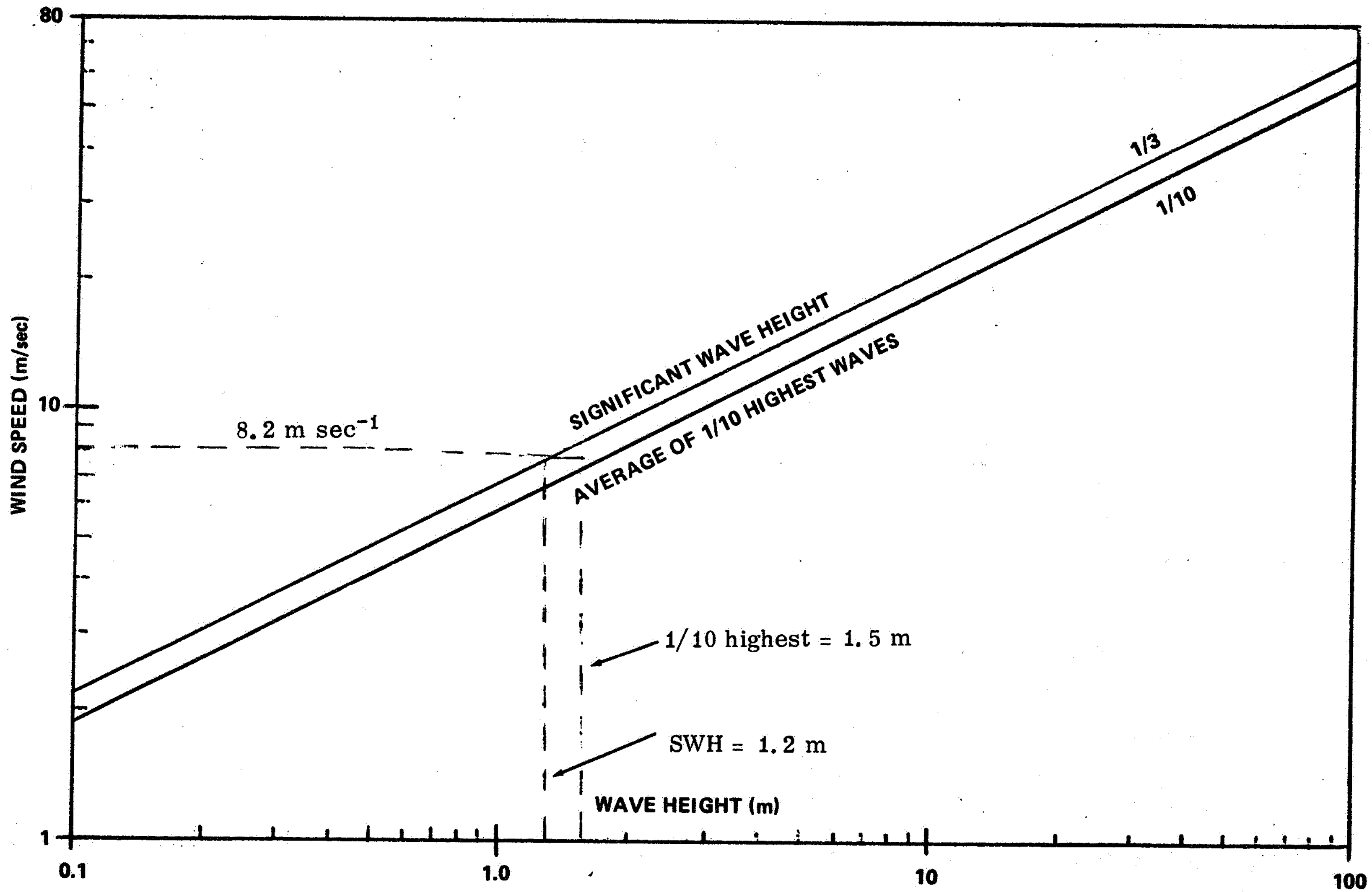

FIGURE 9.1 RELATIONSHIP BETWEEN WAVE HEIGHT AND WIND SPEED IN A FULLY ARISEN SEA

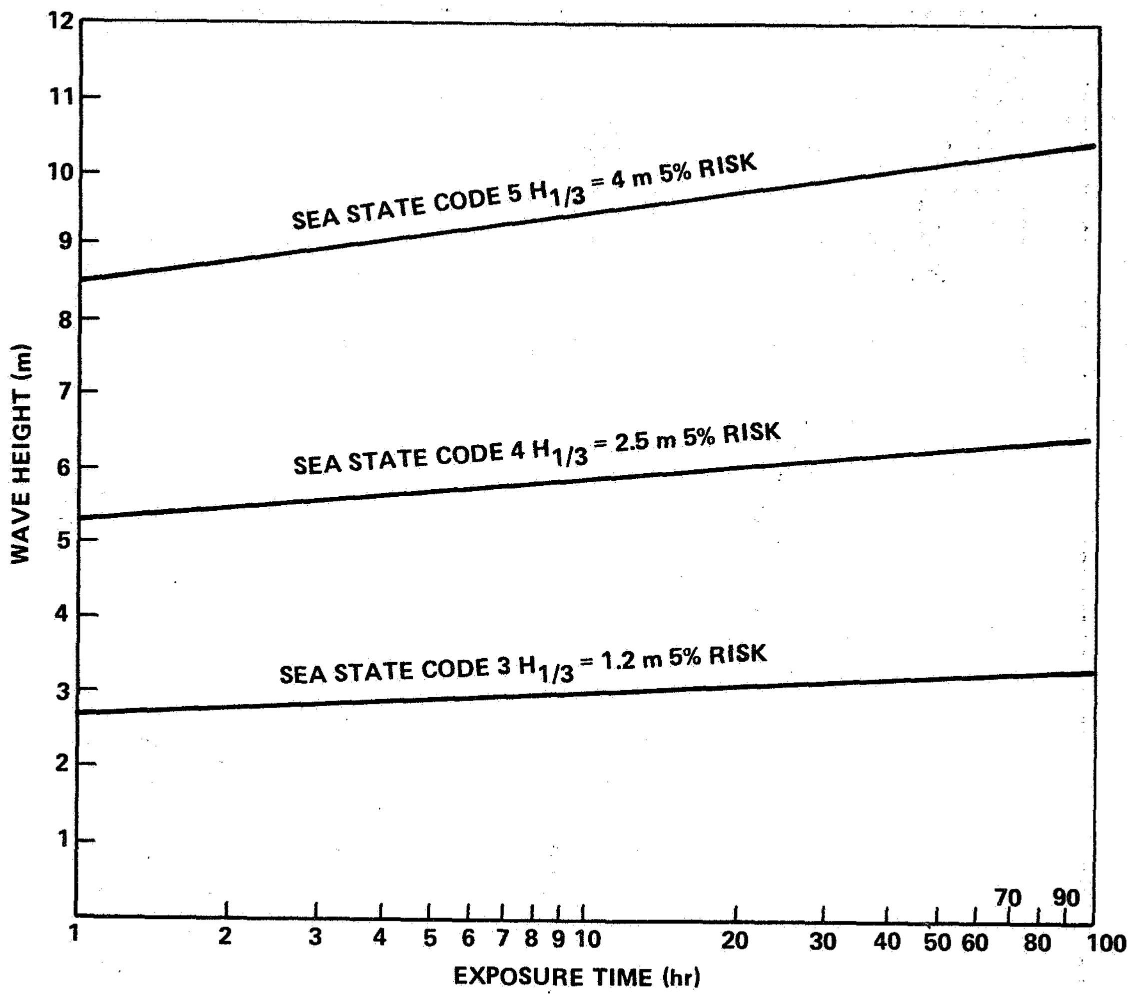

FIGURE 9.2 FIVE-PERCENT RISK WAVE HEIGHT VERSUS EXPOSURE TIME (assuming sea-state category remains unchanged for duration of exposure period)

It is emphasized that the following tables were generated from observations of significant waves ($H_{1/3}$ equals the average height of the one-third highest waves) without regard to fetch or duration (Ref. 9.3). In any given sea state there will always be waves higher than the significant heights. Also, exposure time increases the chances of higher waves occurring.

From Table 9.1, there is a 3 percent risk of exceeding sea-state code 5 and a 68 percent risk of exceeding sea-state code 3 in February. Also in February there is a 95 percent chance that the significant wave height will be

TABLE 9.1. CAPE CANAVERAL RECOVERY AREA SEA STATES
(27 to 31 deg north; 77 to 80 deg west)

Significant Wave Heights, Avg. of 1/3 Highest (m)	(ft)	Sea State Codes	Percent Probability of Exceeding Indicated Heights: J	F	M	A	M	J	J	A	S	O	N	D	Avg.
0.6	2	2	86	90	84	87	68	70	68	58	82	82	84	84	80
1.2	4	3	60	68	54	50	27	36	30	22	55	58	56	56	50
2.4	8	4	14	20	10	8	5	6	3	2	15	12	13	10	9
4.0	13	5	2	3	1	0.5	0.8	0.8	0.2	0.2	2	1.8	1.2	0.8	1
6.1	20	6	0.2	0.3	0.2	<0.1	0.2	0.2	<0.1	<0.1	0.2	0.3	<0.1	<0.1	0.1
Percentiles 50th (m)			1.4	1.6	1.4	1.2	0.8	0.9	0.8	0.7	1.3	1.4	1.4	1.4	1.2
95th (m)			3.3	3.7	2.8	2.7	2.4	2.6	2.2	2.1	3.3	3.2	3.0	2.8	2.9

≤3.7 m and, conversely, a 5 percent chance that it will exceed 3.7 m. On an annual basis the 95th percentile wave height is 2.9 m in the Cape Canaveral recovery area versus 2.8 m in the Vandenberg AFB recovery area (Table 9.2). While the annual $H_{1/3}$ values are very similar, some monthly distributions show considerable differences. In general, the Cape Canaveral area shows greater seasonal variation and consequently a more severe environment.

Table 9.3 presents the international meteorological codes for the state of the sea (Ref. 9.4).

TABLE 9.2. VANDENBERG AFB RECOVERY AREA SEA STATES
(31 to 33 deg north; 120 to 122 deg west)

Significant Wave Heights, Avg. of 1/3 Highest (m)	(ft)	Sea State Codes	Percent Probability of Exceeding Indicated Heights: J	F	M	A	M	J	J	A	S	O	N	D	Avg.
0.6	2	2	74	67	76	78	82	82	81	83	77	58	69	74	76
1.2	4	3	42	38	45	49	50	51	47	45	44	37	34	49	44
2.4	8	4	9	9	10	11	10	9	5	6	6	5	4	13	8
4.0	13	5	1.4	1	1.8	1.8	1.2	0.4	0.2	0.1	0.4	0.4	0.5	3	1
6.1	20	6	<0.1	<0.1	<0.1	<0.1	<0.1	<0.1	<0.1	<0.1	<0.1	<0.1	<0.1	<0.5	<0.1
Percentiles 50th (m)			1.0	0.9	1.1	1.2	1.2	1.2	1.1	1.1	1.1	0.7	0.9	1.2	1.1
95th (m)			2.9	3.2	3.2	3.0	3.2	2.8	2.4	2.5	2.6	2.4	2.4	3.5	2.8

TABLE 9.3. INTERNATIONAL METEOROLOGICAL CODES, CODE 3700, STATE OF SEA

Code Figure	Descriptive Terms	$H_{1/3}$ of Waves	
		m	ft
0	Calm (Glassy)	0	0
1	Calm (Rippled)	0-0.1	0-0.33
2	Smooth (Wavelets)	0.1-0.5	0.33-1.6
3	Slight	0.5-1.25	1.6-4.1
4	Moderate	1.25-2.5	4.1-8.2
5	Rough	2.5-4	8.2-13.1
6	Very Rough	4-6	13.1-19.7
7	High	6-9	19.7-29.5
8	Very High	9-14	29.5-45.9
9	Phenomenal	Over 14	Over 45.9

Note: Exact bounding height is assigned to lower code; e.g., a height of 4 m is coded 5.

9.2 Wave Slopes

The wave slopes shown in Tables 9.4 and 9.5 were calculated along the wind direction after assuming a Gaussian distribution in a fully aroused sea. The entire distribution of significant wave heights was used for the calculations.

TABLE 9.4. CAPE CANAVERAL RECOVERY AREA WAVE SLOPES (calculated from significant wave heights)

Risk of Exceeding	J	F	M	A	M	J	J	A	S	O	N	D	Avg.
5%	11°	12°	11°	10°	10°	10°	10°	9°	11°	11°	11°	11°	10°

TABLE 9.5 VANDENBERG AFB RECOVERY AREA WAVE SLOPES (calculated from significant wave heights)

Risk of Exceeding	J	F	M	A	M	J	J	A	S	O	N	D	A
5%	10°	10°	10°	10°	11°	11°	10°	10°	10°	10°	10°	11°	10°

9.3 Surface Currents

a. Cape Canaveral SRB Recovery Area. The dominant current, which is south to north, in the Cape Canaveral SRB recovery area is the Gulf Stream. Although the mean speed and position of the maximum current shows little change from season to season, daily synoptic changes may be rapid and intense (Ref. 9.5).

The means and standard deviations listed below may be applied to all seasons (Fig. 9.3).

Area	Mean	Standard Deviation
22	0.4 m sec^{-1} (0.8 knots)	0.6 m sec^{-1} (1.27 knots)
26	1.3 m sec^{-1} (2.5 knots)	0.6 m sec^{-1} (1.25 knots)

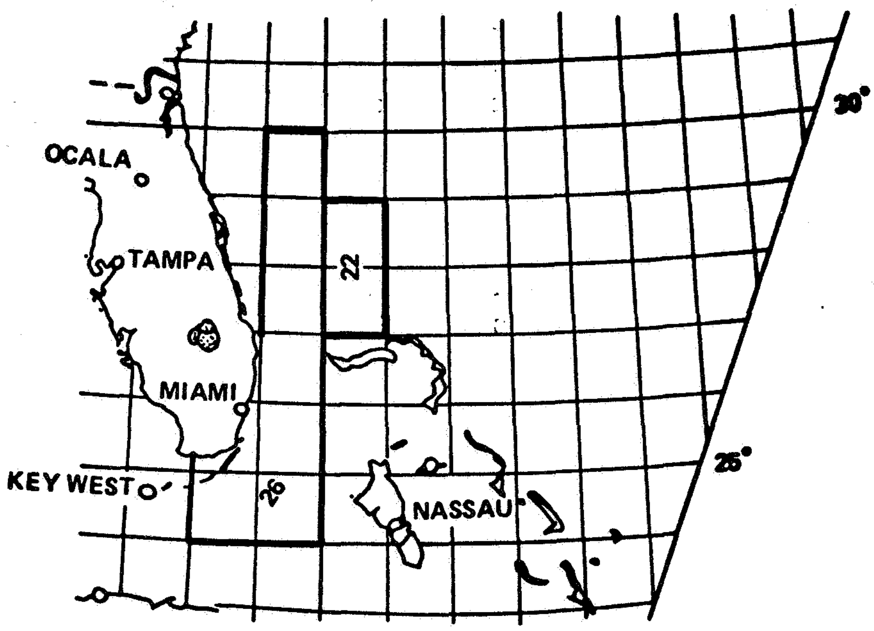

FIGURE 9.3. SURFACE CURRENT AREAS

b. Vandenberg AFB SRB Recovery Area. While the predominant direction is from north to south in all seasons, the currents are generally weak in the Vandenberg AFB SRB recovery area — less than 1 knot.

The mean and standard deviation listed below may be used for the entire recovery area for all seasons.

Mean	Standard Deviation
0.3 m sec^{-1} (0.54 knots)	0.3 m sec^{-1} (0.56 knots)

9.4 Sea-State Duration

The durations of rough seas (sea-state code 5 and greater) as shown in Figure 9.4 are deduced values based upon the usual consequences of prevailing synoptic meteorological situations. There are no direct observations of sea-state duration in the SRB recovery areas.

Figure 9.4 provides information only on the duration — not on the frequency of occurrence — of sea states greater than or equal to code 5. For example, in the Cape Canaveral recovery area there is a 5-percent risk that sea states greater than or equal to code 5 will last for 24 hours once they have developed. The risk of occurrence can be obtained from Table 9.1 (Ref. 9.3).

9.5 Ocean Temperatures

Maximum, mean, and minimum water temperatures for 3-month periods from the surface to depths of 50 m for KSC and VAFB SRB recovery areas are given in Table 9.6 (Ref. 9.6).

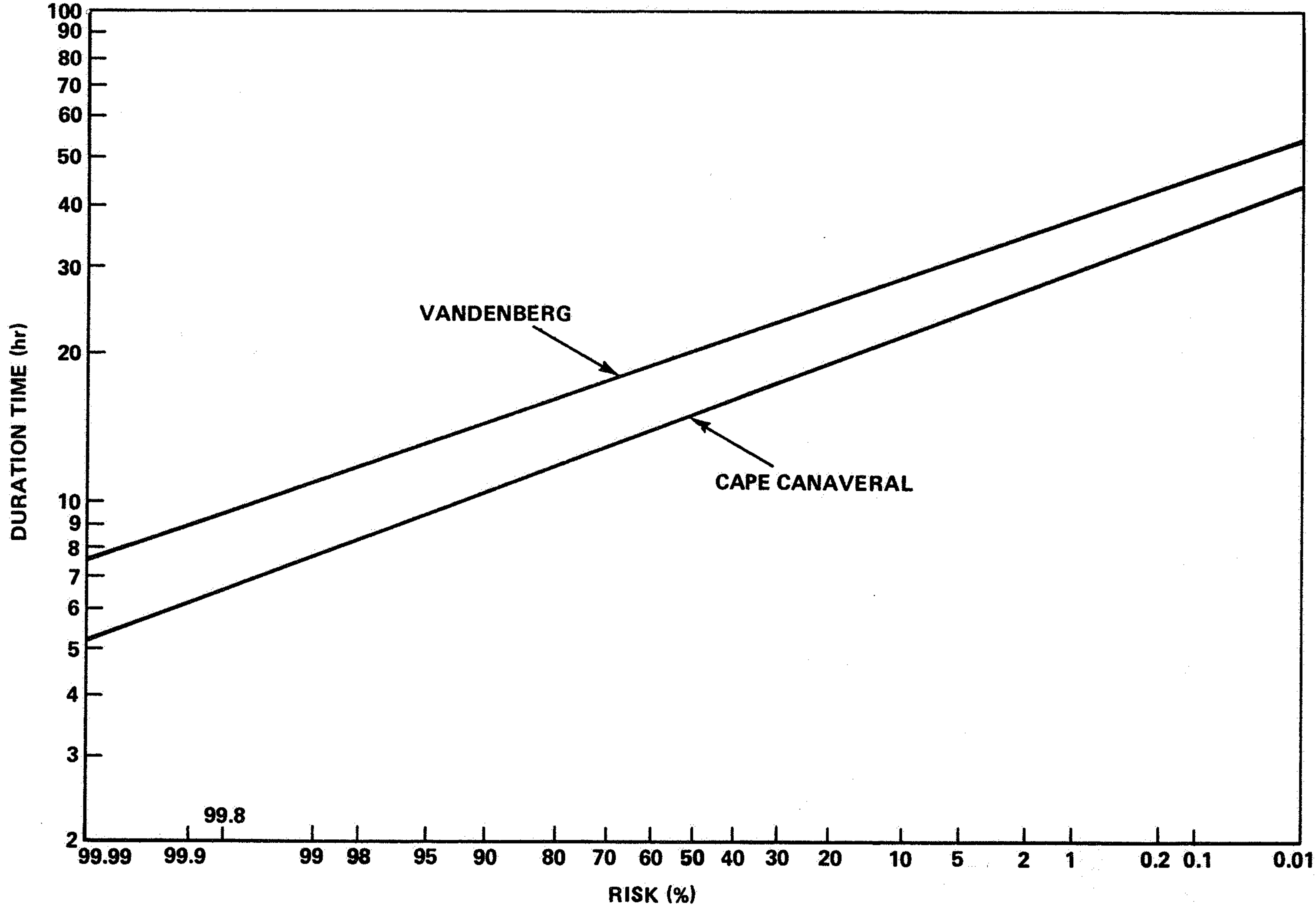

FIGURE 9.4. DISTRIBUTION OF DURATION TIMES FOR SEA STATES GREATER THAN OR EQUAL TO CODE 5 IN CAPE CANAVERAL AND VANDENBERG AFB SRB RECOVERY AREAS

TABLE 9.6. OCEAN TEMPERATURES IN THE SRB RECOVERY AREAS (°C)

Cape Canaveral SRB Recovery Area

Months / Depth (m)	Jan. — March			April — June			July — Sept.			Oct. — Dec.		
	Max.	Mean	Min.	Max.	Mean	Min.	Max.	Mean	Min.	Max.	Mean	Min.
0	26	23	16	29	26	21	31	29	27	29	26	19
10	26	23	16	29	26	20	30	29	26	29	26	19
20	26	23	17	29	26	19	30	28	23	29	26	20
30	26	23	16	28	26	17	29	28	21	29	26	21
50	26	23	17	28	25	17	29	27	19	28	26	22

VAFB SRB Recovery Area

Months / Depth (m)	Jan. — March			April — June			July — Sept.			Oct. — Dec.		
	Max.	Mean	Min.	Max.	Mean	Min.	Max.	Mean	Min.	Max.	Mean	Min.
0	17	14	12	19	14	11	21	17	13	20	17	13
10	17	14	11	18	14	11	21	17	11	20	17	13
20	17	14	11	17	14	11	20	16	10	20	16	12
30	17	14	11	17	14	10	20	16	10	20	16	11
50	17	14	10	17	13	9	19	14	9	20	14	10

REFERENCES

9.1 "Space Shuttle Flight and Ground System Specification." Vol. X, Appendix 10.10, Revision B, JSC 07700, NASA/Johnson Space Flight Center, Aug. 18, 1975.

9.2 "Natural Environment for the Space Shuttle Solid Rocket Booster." MSFC SE-019-043-2H, Marshall Space Flight Center, Huntsville, Alabama, May 20, 1975.

9.3 "Summary of Synoptic Meteorological Observations." North American Coast Marine Areas, Vol. 4, Vol. 7 and Vol. 8, Nos. AD707701, AD709055, and AD710771, respectively, U.S. Naval Weather Service Command, Washington, D.C., May 1970.

9.4 "International Meteorological Codes, 1972." Hydrographic Office Publication No. 118, Naval Weather Service Environmental Detachment, Federal Building, Asheville, N.C., (reproduced and distributed to Naval Weather Service Command Units by direction of the Commander, Naval Weather Service Command), March 1972.

9.5 "Environmental Conditions Within Specified Geographical Regions." U.S. Department of Commerce, National Oceanic and Atmospheric Administration, Environmental Data Service, a United States Department of Commerce Publication, National Data Buoy Center, April 1973.

9.6 Churgin, J.; and Halminski, S. J.: "Temperature, Salinity, Oxygen, and Phosphate in the Waters Off United States." Key to Oceanographic Records, Documentation No. 2, Vol. 2, "Gulf of Mexico," National Oceanographic Data Center, March 1974.

SECTION X. INFLIGHT THERMODYNAMIC PROPERTIES

10.1 Introduction

This section presents the inflight thermodynamic parameters (temperature, pressure, and density) of the atmosphere. Mean and extreme values of the thermodynamic parameters given here can be used in application of many aerospace problems, such as (1) research planning and engineering design of remote earth sensing systems; (2) vehicle design and development; and (3) vehicle trajectory analysis, dealing with vehicle thrust, dynamic pressure, aerodynamic drag, aerodynamic heating, vibration, structural and guidance limitations, and reentry analysis. Atmospheric density plays a very important role in most of the above problems. The first part of this section gives median and extreme values of these thermodynamic variables with respect to altitude. An approach is presented for temperature, pressure, and density as independent variables, with a method to obtain simultaneous values of these variables at discrete altitude levels. A subsection on reentry is presented, giving atmospheric models to be used for reentry heating, trajectory, etc., analyses.

Standard Sea Level Values used are (Ref. 10.1):

	Metric Units	U. S. Customary Units
Temperature	15.0°C or 288.15°K	59°F or 518.67°R
Pressure	1.013250×10^5 newton m^{-2} (Newton m^{-2} is equivalent to a pascal (Pa) in SI units)	2116.22 lb ft^{-2} or 14.696 lb in^{-2}
Density	1.2250 kg m^{-3}	0.076474 lb ft^{-3}

10.2 Atmospheric Temperature

10.2.1 Air Temperature at Altitude

Median and extreme air temperatures for the following list of test ranges were compiled from frequency distributions of radiosonde measured temperature data from 0 through 30 km altitude. Mean and extreme temperatures for the different test ranges above 30 km altitude were obtained from rocketsonde observations.

a. Eastern Test Range air temperature values with altitude are given in Table 10.1 (Ref. 10.2).

b. Space and Missile Test Center air temperature values with altitude are given in Table 10.2 (Ref. 10.5).

c. Wallops Test Range air temperature values with altitude are given in Table 10.3 (Ref. 10.3).

d. White Sands Missile Range air temperature values with altitude are given in Table 10.4 (Ref. 10.3).

e. Edwards Air Force Base air temperature values with altitude are given in Table 10.5 (Ref. 10.3).

A comprehensive listing of the extremes of surface temperature for different locations of interest can be obtained from Table 3.6.

10.2.2 Extreme Cold Temperature

Extreme cold temperatures during aircraft flight, when compartments are not heated, are given in Table 10.6. Hot compartment temperatures are given in Section III, paragraph 3.6.4.

10.3 Atmospheric Pressure

10.3.1 Definition

Atmospheric pressure (also called barometric pressure) is the force exerted, as a consequence of gravitational attraction, by the mass of the column of air of unit cross section lying directly above the area in question. It is expressed as force per unit area (newtons per square meter or newtons per square centimeter).

10.3.2 Pressure at Altitude

Atmospheric pressure extremes for all locations are given in Table 10.7. These values were taken from pressure frequency distributions of radiosonde observations from the five test ranges. Pressure means and extremes were used above 25 km altitude using rocketsonde observations.

Mean and extreme values of station pressure for different locations of interest are given in Table 5.1 of Section V, whereas median values aloft are given in Tables 10.8, 10.9, 10.10, and in Ref. 10.3.

TABLE 10.1 EASTERN TEST RANGE (Kennedy Space Center) AIR TEMPERATURES AT VARIOUS ALTITUDES

Geometric Altitude (km)	Minimum (°C)	Minimum (°F)	Median (°C)	Median (°F)	Maximum (°C)	Maximum (°F)
SFC (0.005 MSL)	-3.9	25	23.5	74	37.2	99
1	-8.9	16	17.4	63	27.8	82
2	-10.0	14	12.2	54	21.1	70
3	-11.1	12	7.1	45	16.1	61
4	-13.9	7	1.8	35	11.1	52
5	-20.0	-4	-4.1	25	5.0	41
6	-26.1	-15	-10.5	13	-1.1	30
7	-33.9	-29	-17.4	1	-7.2	19
8	-41.1	-42	-24.8	-13	-13.9	7
9	-50.0	-58	-32.4	-26	-21.1	-6
10	-56.1	-69	-40.0	-40	-30.0	-22
16.2	-80.0	-112	-70.3	-95	-57.8	-72
20	-76.1	-105	-62.8	-81	-47.8	-54
30	-58.9	-74	-42.4	-44	-30.0	-22
35	-47.4	-53	-30.6	-23	-14.6	6
40	-36.7	-34	-17.8	0	1.9	35
45	-23.0	-9	-6.3	21	12.8	55
50	-18.2	-1	-2.5	27	22.0	72
55	-34.4	-30	-12.4	10	18.9	66
60	-28.5	-19	-26.1	-15	17.0	63
*						

* For higher altitudes, see Refs. 10.2, 10.9, item 13 of Ref. 10.3, and Section 10.6 of this report.

10.4 Atmospheric Density

10.4.1 Definition

Density (ρ) is the ratio of the mass of a substance to its volume. (It is also defined as the reciprocal of specific volume.) Density is usually expressed in grams per cubic centimeter or kilograms per cubic meter.

TABLE 10.2 SPACE AND MISSILE TEST CENTER
(Vandenberg AFB, California)
AIR TEMPERATURES AT VARIOUS ALTITUDES

Geometric Altitude (km)	Minimum		Median		Maximum	
	(°C)	(°F)	(°C)	(°F)	(°C)	(°F)
SFC (0.1 MSL)	-3.3	26	13.0	55	37.8	100
1	-3.6	26	13.3	56	33.4	92
2	-7.0	19	10.1	50	28.0	82
3	-15.2	5	5.1	41	17.6	64
4	-22.6	-9	-1.0	30	12.1	54
5	-29.7	-22	-7.5	18	3.3	38
6	-35.6	-32	-14.4	6	-2.7	27
7	-43.3	-46	-21.8	-7	-9.9	14
8	-47.4	-53	-29.5	-21	-15.9	3
9	-51.3	-60	-37.3	-35	-26.8	-16
10	-57.0	-71	-44.6	-48	-31.2	-24
16.3	-76.0	-105	-64.0	-83	-51.0	-60
20	-74.9	-103	-59.8	-76	-49.0	-56
30	-63.7	-83	-42.7	-45	-29.4	-21
40	-42.2	-44	-19.3	-3	17.8	64
45	-30.5	-23	-5.8	21	27.6	82
50	-18.2	-1	-2.0	28	28.0	82
55	-21.8	-7	-6.8	20	31.6	89
60	-25.1	-13	-20.5	-5	35.7	96
*						

* For higher altitudes, see Refs. 10.1, 10.5 and 10.7, and item 18 of Ref. 10.3.

4-3

TABLE 10.3 WALLOPS TEST RANGE AIR TEMPERATURES AT VARIOUS ALTITUDES

Geometric Altitude (km)	Minimum (°C)	Minimum (°F)	Median (°C)	Median (°F)	Maximum (°C)	Maximum (°F)
SFC (0.002 MSL)	-20.0	-4	13.9	57	37.2	99
1	-21.1	-6	10.0	50	31.1	88
2	-26.1	-15	6.1	43	22.8	73
3	-30.0	-22	1.0	33	15.0	59
4	-33.9	-29	-4.1	25	7.8	46
5	-40.0	-40	-10.0	14	2.8	37
6	-43.9	-47	-16.8	2	-1.1	30
7	-47.8	-54	-24.0	-11	-7.8	18
8	-50.6	-59	-31.5	-25	-15.0	5
9	-56.1	-69	-38.7	-38	-21.1	-6
10	-61.1	-78	-45.9	-51	-27.2	-17
16.5	-77.8	-108	-62.2	-80	-47.2	-53
20	-71.1	-96	-58.3	-73	-46.1	-51
30	-65.0	-85	-43.9	-47	-27.2	-17
40	-35.7	-32	-19.3	-3	5.8	42
45	-27.7	-18	-5.7	22	14.8	59
50	-24.9	-13	-3.2	26	21.8	71
55	-22.6	-9	-5.6	22	35.0	95
*						

* For higher altitudes, see Ref. 10.1 and item 15 of Ref. 10.3.

TABLE 10.4 WHITE SANDS MISSILE RANGE AIR TEMPERATURES AT VARIOUS ALTITUDES

Geometric Altitude (km)	Minimum (°C)	Minimum (°F)	Median (°C)	Median (°F)	Maximum (°C)	Maximum (°F)
SFC (1.3 MSL)	-23.9	-11	18.1	65	41.7	107
2	-11.7	11	13.1	56	31.1	88
3	-18.9	-2	6.2	43	22.2	72
4	-23.9	-11	-0.2	32	12.8	55
5	-31.1	-24	-6.7	20	6.1	43
6	-36.1	-33	-13.6	7	0.0	32
7	-42.2	-44	-20.5	-5	-7.2	19
8	-48.9	-56	-29.8	-22	-13.9	7
9	-55.0	-67	-36.7	-34	-21.1	-6
10	-60.0	-76	-43.3	-46	-27.2	-17
16.5	-80.0	-112	-67.1	-89	-47.8	-54
20	-77.8	-108	-60.0	-76	-52.2	-62
30	-58.9	-74	-43.2	-46	-26.1	-15
35	-52.2	-62	-32.2	-26	-7.8	18
40	-41.8	-43	-18.7	-2	5.0	41
45	-30.5	-23	-4.7	24	19.6	67
50	-29.1	-20	-1.6	29	25.9	79
55	-28.7	-20	-4.6	24	30.2	86
60	-35.8	-32	-20.4	-5	28.0	82
65	-36.5	-34	-38.1	-37	31.3	88
*						

* For higher altitudes, see Ref. 10.1 and item 14 of Ref. 10.3.

TABLE 10.5 EDWARDS AFB TEMPERATURES AT VARIOUS ALTITUDES

Geometric Altitude (km)	Minimum (°C)	Minimum (°F)	Median (°C)	Median (°F)	Maximum (°C)	Maximum (°F)
SFC (0.7 MSL)	-15.6	4	17.3	63	45.0	113
1	-6.0	21	16.2	61	35.3	96
2	-12.9	9	11.4	53	26.2	79
3	-16.9	2	5.3	42	19.0	66
4	-23.4	-10	-1.3	30	10.7	51
5	-29.7	-21	-8.2	17	5.2	41
6	-35.2	-31	-15.3	4	-2.9	27
7	-42.0	-44	-22.8	-9	-12.1	10
8	-48.9	-56	-30.5	-23	-17.4	1
9	-55.0	-67	-38.3	-37	-24.2	-12
10	-58.8	-74	-45.7	-50	-30.8	-23
17.8	-78.0	-108	-63.3	-82	-53.0	-63
20	-73.5	-100	-60.2	-76	-49.6	-57
25	-73.2	-100	-52.3	-62	-40.4	-41
30	-66.1	-87	-45.1	-49	-29.1	-20
40	-42.2	-44	-19.3	-3	17.8	64
45	-30.5	-23	-5.8	21	27.6	82
50	-18.2	-1	-2.0	28	28.0	82
55	-21.8	-7	-6.8	20	31.6	89
60	-25.1	-13	-20.5	-5	35.7	96
*						

* For higher altitudes, see Refs. 10.1, 10.8, and item 18 of Ref. 10.3.

TABLE 10.6 LOW TEMPERATURE EXTREMES FOR ALL LOCATIONS

Maximum Flight Altitude (Geometric) of Aircraft Used for Transport		Compartment Cold Temperature Extreme	
(m)	(ft)	(°C)	(°F)
3 048	10 000	-25.0	-13
4 572	15 000	-35.0	-31
6 096	20 000	-45.0	-49
7 620	25 000	-50.0	-58
9 144	30 000	-57.0	-71
10 668	35 000	-65.0	-85
12 192	40 000	-70.0	-94
13 716	45 000	-75.0	-103

TABLE 10.7 ATMOSPHERIC PRESSURE-HEIGHT EXTREMES FOR ALL LOCATIONS

Geometric Altitude (above mean sea level)		Pressure			
		Maximum		Minimum	
(km)	(ft)	(mb)	(lb in.$^{-2}$)	(mb)	(lb in.$^{-2}$)
0	0	(Use values in Table 5.1 for surface pressure for each station)			
3	9 800	730	10.6	680	9.86
6	19 700	510	7.40	457	6.63
10	32 800	295	4.28	251	3.64
15	49 200	135	1.96	116	1.68
20	65 600	60	8.7×10^{-1}	51	7.4×10^{-1}
25	82 000	30	4.4×10^{-1}	22	3.2×10^{-1}
30	98 400	14.5	2.1×10^{-1}	10.4	1.5×10^{-1}
35	114 800	7.4	1.1×10^{-1}	4.9	7.1×10^{-2}
40	131 200	3.8	5.5×10^{-2}	2.4	3.5×10^{-2}
45	147 600	2.0	2.9×10^{-2}	1.2	1.7×10^{-2}
50	164 000	1.2	1.7×10^{-2}	6.1×10^{-1}	8.8×10^{-3}
55	180 400	6.0×10^{-1}	8.7×10^{-3}	3.1×10^{-1}	4.5×10^{-3}
60	196 800	3.2×10^{-1}	4.6×10^{-3}	1.6×10^{-1}	2.3×10^{-3}
65	213 300	1.7×10^{-1}	2.5×10^{-3}	8.3×10^{-2}	1.2×10^{-3}
70	229 700	8.5×10^{-2}	1.2×10^{-3}	4.1×10^{-2}	5.9×10^{-4}
75	246 100	3.1×10^{-2}	4.5×10^{-4}	2.1×10^{-2}	3.0×10^{-4}
80	262 500	1.4×10^{-2}	2.0×10^{-4}	8.9×10^{-3}	1.3×10^{-4}
85	278 900	5.9×10^{-3}	8.6×10^{-5}	3.7×10^{-3}	5.4×10^{-5}
90	295 300	2.6×10^{-3}	3.8×10^{-5}	1.4×10^{-3}	2.0×10^{-5}

TABLE 10.8 KENNEDY SPACE CENTER (PATRICK) REFERENCE ATMOSPHERE (PRA-63) (Ref. 10.2)

GEOMETRIC ALTITUDE	PRESSURE	KINETIC TEMPERATURE	VIRTUAL TEMPERATURE	DENSITY	KINEMATIC VISCOSITY	COEFFICIENT OF VISCOSITY	SPEED OF SOUND
meters	newtons cm^{-2}	degrees K	degrees K	kg m^{-3}	m^2 sec^{-1}	newton-sec m^{-2}	m sec^{-1}
0.	1.0170147+01	2.9967877+02	2.9937265+02	1.1835467+00	1.5464054-05	1.8302431-05	3.4685752+02
1000.	9.0603417+00	2.9059303+02	2.9244317+02	1.0793462+00	1.6687364-05	1.8011442-05	3.4281972+02
2000.	8.0521166+00	2.8533229+02	2.8653089+02	9.7902799-01	1.8137912-05	1.7757524-05	3.3933665+02
3000.	7.1335062+00	2.8025122+02	2.8097135+02	8.8525680-01	1.9779729-05	1.7510140-05	3.3602847+02
4000.	6.3151744+00	2.7491955+02	2.7530996+02	7.9915661-01	2.1583060-05	1.7248245-05	3.3262586+02
5000.	5.5714346+00	2.6909224+02	2.6927406+02	7.2084273-01	2.3526962-05	1.6959240-05	3.2895941+02
6000.	4.9008910+00	2.6267951+02	2.6274498+02	6.4983432-01	2.5603113-05	1.6637782-05	3.2494680+02
7000.	4.2967958+00	2.5571709+02	2.5573003+02	5.8535150-01	2.7820210-05	1.6284602-05	3.2057962+02
8000.	3.7532038+00	2.4833624+02	2.4833460+02	5.2651816-01	3.0208493-05	1.5905320-05	3.1591022+02
9000.	3.2649867+00	2.4073390+02	2.4073421+02	4.7249380-01	3.2824227-05	1.5509244-05	3.1103836+02
10000.	2.8277554+00	2.3314284+02	2.3314653+02	4.2255460-01	3.5754187-05	1.5108096-05	3.0609732+02
11000.	2.4373143+00	2.2567654+02	2.2567654+02	3.7638426-01	3.9076665-05	1.4707842-05	3.0115374+02
12000.	2.0909280+00	2.1882266+02	2.1882266+02	3.3302118-01	4.3046158-05	1.4335282-05	2.9654541+02
13000.	1.7861066+00	2.1289318+02	2.1289318+02	2.9232217-01	4.7922764-05	1.4008886-05	2.9250004+02
14000.	1.5199026+00	2.0815733+02	2.0815733+02	2.5432636-01	5.4046316-05	1.3745403-05	2.8922838+02
15000.	1.2392855+00	2.0482680+02	2.0482690+02	2.1920325-01	5.1853967-05	1.3558591-05	2.8690521+02
16000.	1.0911841+00	2.0304202+02	2.0304202+02	1.8717684-01	7.1899701-05	1.3457959-05	2.8565249+02
17000.	9.2252635-01	2.0285831+02	2.0285831+02	1.5845601-01	8.4866329-05	1.3447580-05	2.8552324+02
18000.	7.8097360-01	2.0530313+02	2.0530313+02	1.3239217-01	1.0261472-04	1.3585386-05	2.8723862+02
19000.	6.6260085-01	2.0778667+02	2.0778667+02	1.1096236-01	1.2368766-04	1.3724675-05	2.8897076+02
20000.	5.6315646-01	2.1035487+02	2.1035487+02	9.3193794-02	1.4880795-04	1.3867977-05	2.9075108+02
21000.	4.7949008-01	2.1291042+02	2.1291042+02	7.8447666-02	1.7858837-04	1.4009841-05	2.9251188+02
22000.	4.0899187-01	2.1537456+02	2.1537459+02	6.6193244-02	2.1370677-04	1.4145944-05	2.9419972+02
23000.	3.4949302-01	2.1768801+02	2.1768801+02	5.5991185-02	2.5491727-04	1.4273120-05	2.9577557+02
24000.	2.9918756-01	2.1981201+02	2.1981201+02	4.7478891-02	3.0306879-04	1.4389370-05	2.9721502+02
25000.	2.5656948-01	2.2172934+02	2.2172934+02	4.0357731-02	3.5913492-04	1.4493892-05	2.9850846+02
26000.	2.2038158-01	2.2344526+02	2.2344526+02	3.4382485-02	4.2425969-04	1.4587102-05	2.9966127+02
27000.	1.8957412-01	2.2498853+02	2.2498853+02	2.9351583-02	4.9982543-04	1.4670668-05	3.0069433+02
28000.	1.6327365-01	2.2643885+02	2.2643885+02	2.5119032-02	5.8716325-04	1.4748972-05	3.0166195+02
29000.	1.4071529-01	2.2860044+02	2.2860044+02	2.1943811-02	6.9321966-04	1.4865272-05	3.0309836+02
30000.	1.2146274-01	2.3079275+02	2.3079275+02	1.8334060-02	8.1720744-04	1.4982731-05	3.0454827+02
31000.	1.0500196-01	2.3302839+02	2.3302839+02	1.5697349-02	9.6207351-04	1.5102004-05	3.0601976+02
32000.	9.0905086-02	2.3531626+02	2.3531626+02	1.3457798-02	1.1312058-03	1.5223539-05	3.0751834+02
33000.	7.8914435-02	2.3766155+02	2.3766155+02	1.1552738-02	1.3284797-03	1.5347578-05	3.0904699+02
34000.	6.8429919-02	2.4006564+02	2.4006564+02	9.9301033-03	1.5583081-03	1.5474160-05	3.1060616+02
35000.	5.9498650-02	2.4252601+02	2.4252601+02	8.5464654-03	1.8256806-03	1.5603116-05	3.1219376+02
36000.	5.1807186-02	2.4507629+02	2.4507629+02	7.3654171-03	2.1362104-03	1.5734081-05	3.1380529+02
37000.	4.5174764-02	2.4758611+02	2.4758611+02	6.3563439-03	2.4961655-03	1.5866486-05	3.1543377+02
38000.	3.9447995-02	2.5016117+02	2.5016117+02	5.4934199-03	2.9124978-03	1.5999574-05	3.1706989+02
39000.	3.4436486-02	2.5274305+02	2.5274305+02	4.7548125-03	3.3928543-03	1.6132386-05	3.1870190+02
40000.	3.0209181-02	2.5530928+02	2.5530928+02	4.1220201-03	3.9455843-03	1.6263778-05	3.2031579+02
41000.	2.6491425-02	2.5783324+02	2.5783324+02	3.5793500-03	4.5797178-03	1.6392413-05	3.2189521+02
42000.	2.3262412-02	2.6028407+02	2.6028407+02	3.1134716-03	5.3049351-03	1.6516765-05	3.2342147+02
43000.	2.0453115-02	2.6262674+02	2.6262674+02	2.7130531-03	6.1315133-03	1.6635121-05	3.2487367+02
44000.	1.8004513-02	2.6482185+02	2.6482185+02	2.3684560-03	7.0702506-03	1.6745577-05	3.2622855+02
45000.	1.5865131-02	2.6682573+02	2.6682573+02	2.0714816-03	8.1323618-03	1.6846038-05	3.2746049+02
46000.	1.3994778-02	2.6859025+02	2.6859025+02	1.8151542-03	9.3293486-03	1.6934206-05	3.2854145+02
47000.	1.2353487-02	2.7006287+02	2.7006287+02	1.5935381-03	1.0672843-02	1.7007582-05	3.2944088+02
48000.	1.0910569-02	2.7118660+02	2.7118660+02	1.4015769-03	1.2174462-02	1.7063446-05	3.3012557+02
49000.	9.6365032-03	2.7187675+02	2.7187675+02	1.2347674-03	1.3846901-02	1.7097702-05	3.3054538+02
50000.	8.5180218-03	2.7061179+02	2.7061179+02	1.0965534-03	1.5534933-02	1.7034884-05	3.2977552+02
51000.	7.5234923-03	2.6909057+02	2.6909057+02	9.7403573-04	1.7410714-02	1.6958658-05	3.2884120+02
52000.	6.6393199-03	2.6730746+02	2.6730746+02	8.6526725-04	1.9497023-02	1.6870136-05	3.2775595+02
53000.	5.8534792-03	2.6531613+02	2.6531613+02	7.6857841-04	2.1820011-02	1.6770390-05	3.2653285+02
54000.	5.1553131-03	2.6312957+02	2.6312957+02	6.8253219-04	2.4409781-02	1.6660461-05	3.2518454+02
55000.	4.5353599-03	2.6077017+02	2.6077017+02	6.0588695-04	2.7301073-02	1.6541364-05	3.2372334+02
56000.	3.5852060-03	2.5825936+02	2.5825936+02	5.3756682-04	3.0534014-02	1.6414073-05	3.2216109+02
57000.	3.4973536-03	2.5561788+02	2.5561788+02	4.7663516-04	3.4155134-02	1.6279538-05	3.2050933+02
58000.	3.0651144-03	2.5286548+02	2.5286548+02	4.2227454-04	3.8218427-02	1.6138669-05	3.1877909+02
59000.	2.6825137-03	2.5002103+02	2.5002103+02	3.7376890-04	4.2786724-02	1.5992347-05	3.1699106+02
60000.	2.3442082-03	2.4710225+02	2.4710225+02	3.3048918-04	4.7933213-02	1.5841408-05	3.1512539+02
61000.	2.0454142-03	2.4412601+02	2.4412601+02	2.9188042-04	5.3743447-02	1.5686660-05	3.1322187+02
62000.	1.7818466-03	2.4110781+02	2.4110781+02	2.5745231-04	6.0317409-02	1.5528856-05	3.1127962+02
63000.	1.5496627-03	2.3806214+02	2.3806214+02	2.2676947-04	6.7772396-02	1.5368710-05	3.0930733+02
64000.	1.3454170-03	2.3500219+02	2.3500219+02	1.9944482-04	7.6246084-02	1.5206886-05	3.0731305+02
65000.	1.1660196-03	2.3193985+02	2.3193985+02	1.7513309-04	8.5900343-02	1.5043993-05	3.0530417+02
66000.	1.0086976-03	2.2888566+02	2.2888566+02	1.5352538-04	9.6925872-02	1.4880581-05	3.0328738+02
67000.	8.7096431-04	2.2584869+02	2.2584869+02	1.3434470-04	1.0954757-01	1.4717135-05	3.0126858+02
68000.	7.5059127-04	2.2283659+02	2.2283659+02	1.1734235-04	1.2403088-01	1.4554074-05	2.9925285+02
69000.	6.4558010-04	2.1985550+02	2.1985550+02	1.0229409-04	1.4068989-01	1.4391745-05	2.9724443+02
70000.	5.5414295-04	2.1690995+02	2.1690995+02	8.8997968-05	1.5989594-01	1.4230414-05	2.9524652+02
71000.	4.7467952-04	2.1400276+02	2.1400276+02	7.7271416-05	1.8208877-01	1.4070257-05	2.9326129+02
72000.	4.0576003-04	2.1113524+02	2.1113524+02	6.6949339-05	2.0778956-01	1.3911374-05	2.9128989+02
73000.	3.4610846-04	2.0830661+02	2.0830661+02	5.7882451-05	2.3761514-01	1.3753747-05	2.8933207+02
74000.	2.9458748-04	2.0551466+02	2.0551466+02	4.9935479-05	2.7229692-01	1.3597277-05	2.8738656+02
75000.	2.5018505-04	2.0275504+02	2.0275504+02	4.2986041-05	3.1270019-01	1.3441743-05	2.8545054+02
76000.	2.1200230-04	2.0002150+02	2.0002150+02	3.6923397-05	3.5984800-01	1.3286811-05	2.8351980+02
77000.	1.7924187-04	1.9730595+02	1.9730595+02	3.1647376-05	4.1494915-01	1.3132031-05	2.8158865+02
78000.	1.5119831-04	1.9459801+02	1.9459801+02	2.7067385-05	4.7942623-01	1.2976814-05	2.7964963+02
79000.	1.2724843-04	1.9188550+02	1.9199550+02	2.3101918-05	5.5495197-01	1.2820455-05	2.7769376+02
80000.	1.0684305-04	1.8915375+02	1.8915375+02	1.9677462-05	6.4348155-01	1.2662084-05	2.7571001+02
81000.	8.9499401-05	1.8638612+02	1.8638612+02	1.6728011-05	7.4729141-01	1.2500639-05	2.7368553+02
82000.	7.4793845-05	1.8356361+02	1.8356361+02	1.4194399-05	8.6901411-01	1.2335133-05	2.7160537+02
83000.	6.2355805-05	1.8066492+02	1.8066432+02	1.2023774-05	1.0116670+00	1.2164056-05	2.6945234+02
84000.	5.1878215-05	1.8065000+02	1.8065000+02	1.0004256-05	1.2157997+00	1.2163173-05	2.6944122+02
85000.	4.3163464-05	1.8065000+02	1.8065000+02	8.3236936-06	1.4612710+00	1.2163173-05	2.6944122+02
86000.	3.5914713-05	1.8065000+02	1.8065000+02	6.9258358-06	1.7562029+00	1.2163173-05	2.6944122+02
87000.	2.9885006-05	1.8065000+02	1.8065000+02	5.7630599-06	2.1105407+00	1.2163173-05	2.6944122+02
88000.	2.4869045-05	1.8065000+02	1.8065000+02	4.7957760-06	2.5362262+00	1.2163173-05	2.6944122+02
89000.	2.0696155-05	1.8065000+02	1.8065000+02	3.9910710-06	3.0475961+00	1.2163173-05	2.6944122+02
90000.	1.7224435-05	1.8065000+02	1.9065000+02	3.3215804-06		1.2163173-05	2.6944122+02

ORIGINAL PAGE IS
OF POOR QUALITY

TABLE 10.9 VANDENBERG AFB REFERENCE ATMOSPHERE (VRA-71) (Ref. 10.5)

GEOMETRIC ALTITUDE	PRESSURE	KINETIC TEMPERATURE	VIRTUAL TEMPERATURE	DENSITY	KINEMATIC VISCOSITY	COEFFICIENT OF VISCOSITY	SPEED OF SOUND
meters	newtons cm^{-2}	degrees K	degrees K	kg m^{-3}	m^2 sec^{-1}	newton-sec m^{-2}	m sec^{-1}
0.	1.0189904+01	2.8588177+02	2.8715277+02	1.2361775+00	1.4386405-05	1.7784150-05	3.3970470+02
1000.	9.0477941+00	2.8642662+02	2.8699761+02	1.0983266+00	1.6216058-05	1.7813528-05	3.3961291+02
2000.	8.0243502+00	2.8329711+02	2.8359425+02	9.8575564-01	1.7913862-05	1.7658691-05	3.3759326+02
3000.	7.1046558+00	2.7821440+02	2.7842334+02	8.8892961-01	1.9595771-05	1.7413372-05	3.3450165+02
4000.	6.2761809+00	2.7217236+02	2.7234509+02	8.0276189-01	2.1316859-05	1.7112362-05	3.3082996+02
5000.	5.5286658+00	2.6563136+02	2.6576157+02	7.2468088-01	2.3163579-05	1.6785203-05	3.2680685+02
6000.	4.8538800+00	2.5871198+02	2.5878904+02	6.5342553-01	2.5155218-05	1.6437062-05	3.2249129+02
7000.	4.2453086+00	2.5139878+02	2.5142269+02	5.8827869-01	2.7304746-05	1.6062801-05	3.1786835+02
8000.	3.6977986+00	2.4368403+02	2.4370449+02	5.2859970-01	2.9632266-05	1.5663607-05	3.1295134+02
9000.	3.2071987+00	2.3586146+02	2.3589045+02	4.7357411-01	3.2207045-05	1.5252423-05	3.0789330+02
10000.	2.7706815+00	2.2850072+02	2.2850072+02	4.2242641-01	3.5177528-05	1.4859917-05	3.0303224+02
11000.	2.3796741+00	2.2193979+02	2.2193979+02	3.7353754-01	3.8832351-05	1.4505341-05	2.9865008+02
12000.	2.0378622+00	2.1778813+02	2.1778813+02	3.2593435-01	4.3808243-05	1.4278611-05	2.9584359+02
13000.	1.7407523+00	2.1502290+02	2.1502290+02	2.8201088-01	5.0092260-05	1.4125562-05	2.9395944+02
14000.	1.4839231+00	2.1289493+02	2.1289493+02	2.4284485-01	5.7666966-05	1.4008983-05	2.9250124+02
15000.	1.2630643+00	2.1101876+02	2.1101876+02	2.0855008-01	6.6674156-05	1.3904901-05	2.9120953+02
16000.	1.0740324+00	2.0946258+02	2.0946258+02	1.7862758-01	7.7358000-05	1.3818273-05	2.9013377+02
17000.	9.1290847-01	2.0883855+02	2.0883855+02	1.5225517-01	9.0528671-05	1.3783459-05	2.8970126+02
18000.	7.7604645-01	2.1039268+02	2.1039268+02	1.2851184-01	1.0792843-04	1.3870081-05	2.9077721+02
19000.	6.6155133-01	2.1166882+02	2.1166882+02	1.0882416-01	1.2810581-04	1.3941003-05	2.9165773+02
20000.	5.6398303-01	2.1339162+02	2.1339162+02	9.2019110-02	1.5253866-04	1.4035472-05	2.9284225+02
21000.	4.8086911-01	2.1536418+02	2.1536418+02	7.7770908-02	1.8188514-04	1.4145373-05	2.9419263+02
22000.	4.1046343-01	2.1733892+02	2.1733892+02	6.5810409-02	2.1659138-04	1.4253967-05	2.9553832+02
23000.	3.5099534-01	2.1914086+02	2.1914086+02	5.5825416-02	2.5709956-04	1.4352690-05	2.9676094+02
24000.	3.0077469-01	2.2068008+02	2.2068008+02	4.7498948-02	3.0393812-04	1.4436741-05	2.9780132+02
25000.	2.5825416-01	2.2196423+02	2.2196423+02	4.0532336-02	3.5790363-04	1.4505670-05	2.9866653+02
26000.	2.2205890-01	2.2311148+02	2.2311148+02	3.4657364-02	4.2077229-04	1.4568995-05	2.9943738+02
27000.	1.9099714-01	2.2436256+02	2.2436256+02	2.9641456-02	4.9379501-04	1.4639803-05	3.0027575+02
28000.	1.6405777-01	2.2609358+02	2.2609358+02	2.5289117-02	5.8247786-04	1.4730351-05	3.0143187+02
29000.	1.4142399-01	2.2814065+02	2.2814065+02	2.1596011-02	6.8719054-04	1.4840574-05	3.0279339+02
30000.	1.2206691-01	2.3043426+02	2.3043426+02	1.8453921-02	8.1086060-04	1.4963557-05	3.0431165+02
31000.	1.0546830-01	2.3258450+02	2.3258450+02	1.5797158-02	9.5449946-04	1.5078353-05	3.0572815+02
32000.	9.1233502-02	2.3466267+02	2.3466267+02	1.3544035-02	1.1214437-03	1.5188873-05	3.0709098+02
33000.	7.9019569-02	2.3673119+02	2.3673119+02	1.1628319-02	1.3156191-03	1.5298438-05	3.0844149+02
34000.	6.8532667-02	2.3884268+02	2.3884268+02	9.9959356-03	1.5416105-03	1.5409839-05	3.0981399+02
35000.	5.9521749-02	2.4103908+02	2.4103908+02	8.6024678-03	1.8047440-03	1.5525252-05	3.1123525+02
36000.	5.1770654-02	2.4335058+02	2.4335058+02	7.4112084-03	2.1111540-03	1.5646202-05	3.1272402+02
37000.	4.5096980-02	2.4579478+02	2.4579478+02	6.3916438-03	2.4578365-03	1.5773532-05	3.1429059+02
38000.	3.9343655-02	2.4837562+02	2.4837562+02	5.5182770-03	2.8826674-03	1.5907357-05	3.1593631+02
39000.	3.4377026-02	2.5108266+02	2.5108266+02	4.7696810-03	3.3643858-03	1.6047047-05	3.1765333+02
40000.	3.0083150-02	2.5388979+02	2.5388979+02	4.1277733-03	3.9224962-03	1.6191175-05	3.1942409+02
41000.	2.6364320-02	2.5675467+02	2.5675467+02	3.5772217-03	4.5670959-03	1.6337515-05	3.2122122+02
42000.	2.3139577-02	2.5961737+02	2.5961737+02	3.1049844-03	5.3085585-03	1.6482981-05	3.2300700+02
43000.	2.0336609-02	2.6239986+02	2.6239986+02	2.6999312-03	6.1570753-03	1.6623680-05	3.2473332+02
44000.	1.7895922-02	2.6500471+02	2.6500471+02	2.3525465-03	7.1219673-03	1.6754759-05	3.2634116+02
45000.	1.5766305-02	2.6731429+02	2.6731429+02	2.0546863-03	8.2107314-03	1.6870477-05	3.2776014+02
46000.	1.3904100-02	2.6918990+02	2.6918990+02	1.7993759-03	9.4277728-03	1.6964107-05	3.2890799+02
47000.	1.2272031-02	2.7047061+02	2.7047061+02	1.5806507-03	1.0772633-02	1.7027864-05	3.2968948+02
48000.	1.0838504-02	2.7097250+02	2.7097250+02	1.3934194-03	1.2278103-02	1.7052811-05	3.2999523+02
49000.	9.5752799-03	2.7048761+02	2.7048761+02	1.2333525-03	1.3806948-02	1.7028710-05	3.2969984+02
50000.	8.4550115-03	2.7115662+02	2.7115662+02	1.0862549-03	1.5707140-02	1.7061957-05	3.3010733+02
51000.	7.4760636-03	2.7127369+02	2.7127369+02	9.6007037-04	1.7777625-02	1.7067771-05	3.3017857+02
52000.	6.6065708-03	2.7078585+02	2.7078585+02	8.4997924-04	2.0052652-02	1.7043536-05	3.2988156+02
53000.	5.8341419-03	2.6976022+02	2.6976022+02	7.5341944-04	2.2553960-02	1.6992517-05	3.2925623+02
54000.	5.1478915-03	2.6826166+02	2.6826166+02	6.6851096-04	2.5306703-02	1.6917808-05	3.2834042+02
55000.	4.5382458-03	2.6635233+02	2.6635233+02	5.9356636-04	2.8341122-02	1.6822337-05	3.2716987+02
56000.	3.9967607-03	2.6409158+02	2.6409158+02	5.2721934-04	3.1692461-02	1.6708879-05	3.2577843+02
57000.	3.5159756-03	2.6153592+02	2.6153592+02	4.6833031-04	3.5402517-02	1.6580072-05	3.2419829+02
58000.	3.0892362-03	2.5873822+02	2.5873822+02	4.1594443-04	3.9520649-02	1.6438394-05	3.2245963+02
59000.	2.7108367-03	2.5574828+02	2.5574828+02	3.6925677-04	4.4105342-02	1.6285194-05	3.2059106+02
60000.	2.3754195-03	2.5261192+02	2.5261192+02	3.2758510-04	4.9225845-02	1.6125656-05	3.1861922+02
61000.	2.0784015-03	2.4937169+02	2.4937169+02	2.9034881-04	5.4964365-02	1.5958838-05	3.1656918+02
62000.	1.8156504-03	2.4606511+02	2.4606511+02	2.5705139-04	6.1417989-02	1.5787579-05	3.1446338+02
63000.	1.5834767-03	2.4272632+02	2.4272632+02	2.2726500-04	6.8702127-02	1.5613583-05	3.1232265+02
64000.	1.3785800-03	2.3938440+02	2.3938440+02	2.0061984-04	7.6953251-02	1.5438349-05	3.1016513+02
65000.	1.1980055-03	2.3606390+02	2.3606390+02	1.7679378-04	8.6333018-02	1.5263141-05	3.0800647+02
66000.	1.0391056-03	2.3278436+02	2.3278436+02	1.5550474-04	9.7032473-02	1.5089010-05	3.0585949+02
67000.	8.9950478-04	2.2956021+02	2.2956021+02	1.3650376-04	1.0927724-01	1.4916755-05	3.0373397+02
68000.	7.7707160-04	2.2640073+02	2.2640073+02	1.1956965-04	1.2333327-01	1.4746916-05	3.0163655+02
69000.	6.6989220-04	2.2330920+02	2.2330920+02	1.0450475-04	1.3951253-01	1.4579723-05	2.9957003+02
70000.	5.7624817-04	2.2028366+02	2.2028366+02	9.1130767-05	1.5818059-01	1.4415118-05	2.9753372+02
71000.	4.9459703-04	2.1731552+02	2.1731552+02	7.9286366-05	1.7976209-01	1.4252583-05	2.9552241+02
72000.	4.2355436-04	2.1439084+02	2.1439084+02	6.8824123-05	2.0474928-01	1.4091690-05	2.9352707+02
73000.	3.6187395-04	2.1148819+02	2.1148819+02	5.9609427-05	2.3370430-01	1.3930980-05	2.9153326+02
74000.	3.0845853-04	2.0858051+02	2.0858051+02	5.1518217-05	2.6726563-01	1.3769049-05	2.8952223+02
75000.	2.6229794-04	2.0563354+02	2.0563354+02	4.4436379-05	3.0614461-01	1.3603953-05	2.8746957+02
76000.	2.2250776-04	2.0260577+02	2.0260577+02	3.8258777-05	3.5111696-01	1.3433306-05	2.8534546+02
77000.	1.8829458-04	1.9944855+02	1.9944855+02	3.2898548-05	4.0300428-01	1.3254226-05	2.8311344+02
78000.	1.5855186-04	1.9610583+02	1.9610583+02	2.8236629-05	4.6263842-01	1.3063349-05	2.8073096+02
79000.	1.3395155-04	1.9251422+02	1.9251422+02	2.4221368-05	5.3080305-01	1.2856776-05	2.7914833+02
80000.	1.1243729-04	1.8860150+02	1.8860150+02	2.0768398-05	6.0813347-01	1.2629957-05	2.7530724+02
81000.	9.4216307-05	1.8428839+02	1.8428839+02	1.7810079-05	6.9498529-01	1.2377743-05	2.7214104+02
82000.	7.8673815-05	1.8065000+02	1.8065000+02	1.5171552-05	8.0170920-01	1.2163173-05	2.6944122+02
83000.	6.5436167-05	1.8065000+02	1.8065000+02	1.2618788-05	9.6399390-01	1.2163173-05	2.6944122+02
84000.	5.4429003-05	1.8065000+02	1.8065000+02	1.0496153-05	1.1588219+00	1.2163173-05	2.6944122+02
85000.	4.5275370-05	1.8065000+02	1.8065000+02	8.7310716-06	1.3930905+00	1.2163173-05	2.6944122+02
86000.	3.7664308-05	1.8065000+02	1.8065000+02	7.2632298-06	1.6746231+00	1.2163173-05	2.6944122+02
87000.	3.1334090-05	1.8065000+02	1.8065000+02	6.0425029-06	2.0129361+00	1.2163173-05	2.6944122+02
88000.	2.6069278-05	1.8065000+02	1.8065000+02	5.0272304-06	2.4194579+00	1.2163173-05	2.6944122+02
89000.	2.1690308-05	1.8065000+02	1.8065000+02	4.1827847-06	2.9079126+00	1.2163173-05	2.6944122+02
90000.	1.8049200-05	1.8065000+02	1.8065000+02	3.4806292-06		1.2163173-05	2.6944122+02

TABLE 10.10 EDWARDS AFB REFERENCE ATMOSPHERE (ERA-75) (Ref. 10.8)

GEOMETRIC ALTITUDE	PRESSURE	KINETIC TEMPERATURE	VIRTUAL TEMPERATURE	DENSITY	KINEMATIC VISCOSITY	COEFFICIENT OF VISCOSITY	SPEED OF SOUND
meters	newtons cm^{-2}	degrees K	degrees K	kg m^{-3}	m^2 sec^{-1}	newton-sec m^{-2}	m sec^{-1}
706.	9.3407949+03	2.8927295+02	2.9026638+02	1.1210501+00	1.6009931-05	1.7947936-05	3.4154145+02
1000.	9.0176369+02	2.8935619+02	2.9008086+02	1.0829572+00	1.6576780-05	1.7951944-05	3.4143229+02
2000.	8.0072182+00	2.8435157+02	2.8469736+02	9.7979598-01	1.8075133-05	1.7709940-05	3.3824919+02
3000.	7.0923440+00	2.7821671+02	2.7841472+02	8.8743099-01	1.9618973-05	1.7410485-05	3.3449617+02
4000.	6.2741809+00	2.7217236+02	2.7234509+02	8.0276187-01	2.1316859-05	1.7112362-05	3.3082996+02
5000.	5.5286658+00	2.6563136+02	2.6576157+02	7.2468088-01	2.3163579-05	1.6786203-05	3.2680685+02
6000.	4.9538900+00	2.5871198+02	2.5878904+02	6.5342553-01	2.5155218-05	1.6437062-05	3.2249129+02
7000.	4.2453086+00	2.5138878+02	2.5142269+02	5.8827869-01	2.7304746-05	1.6062801-05	3.1786835+02
8000.	3.6977986+00	2.4368403+02	2.4370449+02	5.2859970-01	2.9632266-05	1.5663607-05	3.1295134+02
9000.	3.2071987+00	2.3586146+02	2.3589045+02	4.7357411-01	3.2207045-05	1.5252923-05	3.0789330+02
10000.	2.7706816+00	2.2850072+02	2.2850072+02	4.2242641-01	3.5177528-05	1.4859917-05	3.0303224+02
11000.	2.3796741+00	2.2193979+02	2.2193979+02	3.7353754-01	3.8832351-05	1.4505341-05	2.9865008+02
12000.	2.0378622+00	2.1778813+02	2.1778813+02	3.2593435-01	4.3808243-05	1.4278611-05	2.9584359+02
13000.	1.7407523+00	2.1502290+02	2.1502290+02	2.8201088-01	5.0092260-05	1.4126562-05	2.9395944+02
14000.	1.4839231+00	2.1289493+02	2.1289493+02	2.4284485-01	5.7684966-05	1.4008983-05	2.9250124+02
15000.	1.2630643+00	2.1101876+02	2.1101876+02	2.0855008-01	6.6674156-05	1.3904901-05	2.9120953+02
16000.	1.0740324+00	2.0946258+02	2.0946258+02	1.7862758-01	7.7358000-05	1.3818273-05	2.9013377+02
17000.	9.1290847-01	2.0883855+02	2.0883855+02	1.5225517-01	9.0528671-05	1.3783458-05	2.8970126+02
18000.	7.7604645-01	2.1039268+02	2.1039268+02	1.2851184-01	1.0792843-04	1.3870081-05	2.9077721+02
19000.	6.6155133-01	2.1166882+02	2.1166882+02	1.0882416-01	1.2810581-04	1.3941008-05	2.9165773+02
20000.	5.6398303-01	2.1339162+02	2.1339162+02	9.2019110-02	1.5253866-04	1.4036472-05	2.9284225+02
21000.	4.8086911-01	2.1536418+02	2.1536418+02	7.7770908-02	1.8188514-04	1.4145373-05	2.9419263+02
22000.	4.1046343-01	2.1733892+02	2.1733892+02	6.5810409-02	2.1659138-04	1.4253967-05	2.9553832+02
23000.	3.5099534-01	2.1914086+02	2.1914086+02	5.5825416-02	2.5709956-04	1.4352690-05	2.9676094+02
24000.	3.0077469-01	2.2068008+02	2.2068008+02	4.7498948-02	3.0393812-04	1.4436741-05	2.9780132+02
25000.	2.5825416-01	2.2196423+02	2.2196423+02	4.0532336-02	3.5790363-04	1.4506670-05	2.9866653+02
26000.	2.2205890-01	2.2311148+02	2.2311148+02	3.4657364-02	4.2037229-04	1.4568995-05	2.9943738+02
27000.	1.9099714-01	2.2436256+02	2.2436256+02	2.9641456-02	4.9379501-04	1.4636803-05	3.0027575+02
28000.	1.6405777-01	2.2609358+02	2.2609358+02	2.5289117-02	5.8247786-04	1.4730351-05	3.0143187+02
29000.	1.4142899-01	2.2814065+02	2.2814065+02	2.1596011-02	6.8719054-04	1.4840574-05	3.0279339+02
30000.	1.2206691-01	2.3043426+02	2.3043426+02	1.8453921-02	8.1086060-04	1.4963557-05	3.0431165+02
31000.	1.0546830-01	2.3258450+02	2.3258450+02	1.5797158-02	9.5449846-04	1.5078363-05	3.0572815+02
32000.	9.1233502-02	2.3466267+02	2.3466267+02	1.3544035-02	1.1214437-03	1.5188873-05	3.0709098+02
33000.	7.9019569-02	2.3673119+02	2.3673119+02	1.1628319-02	1.3156191-03	1.5298438-05	3.0844149+02
34000.	6.8532647-02	2.3884268+02	2.3884268+02	9.9959356-03	1.5416105-03	1.5409839-05	3.0981399+02
35000.	5.9521349-02	2.4103908+02	2.4103908+02	8.6024678-03	1.8047440-03	1.5525252-05	3.1123525+02
36000.	5.1770654-02	2.4335058+02	2.4335058+02	7.4112084-03	2.1111540-03	1.5646202-05	3.1272402+02
37000.	4.5096980-02	2.4579478+02	2.4579478+02	6.3916438-03	2.4678365-03	1.5773532-05	3.1429059+02
38000.	3.9343455-02	2.4837562+02	2.4837562+02	5.5182770-03	2.8826674-03	1.5907357-05	3.1593631+02
39000.	3.4377026-02	2.5108266+02	2.5108266+02	4.7696810-03	3.3643858-03	1.6047047-05	3.1765333+02
40000.	3.0083150-02	2.5388979+02	2.5388979+02	4.1277733-03	3.9224962-03	1.6191175-05	3.1942409+02
41000.	2.6364920-02	2.5675467+02	2.5675467+02	3.5772217-03	4.5670959-03	1.6337515-05	3.2122122+02
42000.	2.3139577-02	2.5961737+02	2.5961737+02	3.1049844-03	5.3085585-03	1.6482991-05	3.2300700+02
43000.	2.0336609-02	2.6239986+02	2.6239986+02	2.6999312-03	6.1570753-03	1.6623680-05	3.2473332+02
44000.	1.7895922-02	2.6500471+02	2.6500471+02	2.3525465-03	7.1219673-03	1.6754759-05	3.2634116+02
45000.	1.5766305-02	2.6731429+02	2.6731429+02	2.0546863-03	8.2107314-03	1.6870477-05	3.2776014+02
46000.	1.3984100-02	2.6918990+02	2.6918990+02	1.7993759-03	9.4277728-03	1.6964107-05	3.2890799+02
47000.	1.2272081-02	2.7047061+02	2.7047061+02	1.5806507-03	1.0772693-02	1.7027864-05	3.2968948+02
48000.	1.0838584-02	2.7097260+02	2.7097260+02	1.3934194-03	1.2238103-02	1.7052811-05	3.2999523+02
49000.	9.5762799-03	2.7048761+02	2.7048761+02	1.2333525-03	1.3804848-02	1.7028710-05	3.2969984+02
50000.	8.4550115-03	2.7115662+02	2.7115662+02	1.0862549-03	1.5707140-02	1.7061957-05	3.3010733+02
51000.	7.4760636-03	2.7127369+02	2.7127369+02	9.6007037-04	1.7777625-02	1.7067771-05	3.3017857+02
52000.	6.6046708-03	2.7074585+02	2.7074585+02	8.4983929-04	2.0052652-02	1.7043536-05	3.2988156+02
53000.	5.8341418-03	2.6976022+02	2.6976022+02	7.5341944-04	2.2553860-02	1.6992517-05	3.2925623+02
54000.	5.1478915-03	2.6826166+02	2.6826166+02	6.6851096-04	2.5306703-02	1.6917808-05	3.2834042+02
55000.	4.5382458-03	2.6635233+02	2.6635233+02	5.9356636-04	2.8341122-02	1.6822337-05	3.2716987+02
56000.	3.9967607-03	2.6409158+02	2.6409158+02	5.2721934-04	3.1692461-02	1.6708879-05	3.2577843+02
57000.	3.5159756-03	2.6153592+02	2.6153592+02	4.6833031-04	3.5402517-02	1.6580072-05	3.2419829+02
58000.	3.0892862-03	2.5873822+02	2.5873822+02	4.1594443-04	3.9520649-02	1.6438394-05	3.2245963+02
59000.	2.7108367-03	2.5574828+02	2.5574828+02	3.6925672-04	4.4105342-02	1.6286194-05	3.2059106+02
60000.	2.3754195-03	2.5261192+02	2.5261192+02	3.2758516-04	4.9225845-02	1.6125656-05	3.1861922+02
61000.	2.0784015-03	2.4937169+02	2.4937169+02	2.9034881-04	5.4964365-02	1.5958838-05	3.1656918+02
62000.	1.8156504-03	2.4606511+02	2.4606511+02	2.5705139-04	6.1417989-02	1.5787579-05	3.1446338+02
63000.	1.5834767-03	2.4272632+02	2.4272632+02	2.2726500-04	6.8702127-02	1.5613589-05	3.1232265+02
64000.	1.3785800-03	2.3938440+02	2.3938440+02	2.0061984-04	7.6953251-02	1.5438349-05	3.1016513+02
65000.	1.1980055-03	2.3606390+02	2.3606390+02	1.7679378-04	8.6333018-02	1.5263141-05	3.0800647+02
66000.	1.0391056-03	2.3278436+02	2.3278436+02	1.5550474-04	9.7032473-02	1.5089010-05	3.0585949+02
67000.	8.9950478-04	2.2956021+02	2.2956021+02	1.3650376-04	1.0927724-01	1.4916755-05	3.0373397+02
68000.	7.7707160-04	2.2640073+02	2.2640073+02	1.1956965-04	1.2333327-01	1.4746916-05	3.0163655+02
69000.	6.6989220-04	2.2330920+02	2.2330920+02	1.0450475-04	1.3951253-01	1.4579723-05	2.9957003+02
70000.	5.7624817-04	2.2028366+02	2.2028366+02	9.1130767-05	1.5818059-01	1.4415118-05	2.9753372+02
71000.	4.9459703-04	2.1731552+02	2.1731552+02	7.9286366-05	1.7976209-01	1.4252683-05	2.9552241+02
72000.	4.2355436-04	2.1439084+02	2.1439084+02	6.8824123-05	2.0474928-01	1.4091690-05	2.9352707+02
73000.	3.6187895-04	2.1148819+02	2.1148819+02	5.9609427-05	2.3370430-01	1.3930980-05	2.9153326+02
74000.	3.0845853-04	2.0858051+02	2.0858051+02	5.1518217-05	2.6726563-01	1.3769049-05	2.8952223+02
75000.	2.6229794-04	2.0563354+02	2.0563354+02	4.4436379-05	3.0614461-01	1.3603958-05	2.8746967+02
76000.	2.2250776-04	2.0260577+02	2.0260577+02	3.8258777-05	3.5111696-01	1.3433306-05	2.8534546+02
77000.	1.8829458-04	1.9944855+02	1.9944855+02	3.2888548-05	4.0300428-01	1.3254226-05	2.8311344+02
78000.	1.5895186-04	1.9610583+02	1.9610583+02	2.8236629-05	4.6263842-01	1.3063349-05	2.8073096+02
79000.	1.3385165-04	1.9251422+02	1.9251422+02	2.4221368-05	5.3080305-01	1.2856776-05	2.7814833+02
80000.	1.1243729-04	1.8860150+02	1.8860150+02	2.0768398-05	6.0813343-01	1.2629957-05	2.7530724+02
81000.	9.4216307-05	1.8428839+02	1.8428839+02	1.7810079-05	6.9498529-01	1.2377743-05	2.7214104+02
82000.	7.8673815-05	1.8065000+02	1.8065000+02	1.5171552-05	8.0170920-01	1.2163173-05	2.6944122+02
83000.	6.5436167-05	1.8065000+02	1.8065000+02	1.2618788-05	9.6389390-01	1.2163173-05	2.6944122+02
84000.	5.4429003-05	1.8065000+02	1.8065000+02	1.0496153-05	1.1588219+00	1.2163173-05	2.6944122+02
85000.	4.5275970-05	1.8065000+02	1.8065000+02	8.7310716-06	1.3930905+00	1.2163173-05	2.6944122+02
86000.	3.7664308-05	1.8065000+02	1.8065000+02	7.2632298-06	1.6746231+00	1.2163173-05	2.6944122+02
87000.	3.1334090-05	1.8065000+02	1.8065000+02	6.0425029-06	2.0129361+00	1.2163173-05	2.6944122+02
88000.	2.6069278-05	1.8065000+02	1.8065000+02	5.0272309-06	2.4194579+00	1.2163173-05	2.6944122+02
89000.	2.1690308-05	1.8065000+02	1.8065000+02	4.1827847-06	2.9079126+00	1.2163173-05	2.6944122+02
90000.	1.8049200-05	1.8065000+02		3.4806292-06		1.2163173-05	2.6944122+02

10.4.2 Atmospheric Density at Altitude

The density of the atmosphere decreases rapidly with height, decreasing to one-half of the surface at 7 km altitude. Density is also variable at a fixed altitude, with the greatest relative variability occurring at about 70 km altitude in the high northern latitudes (60°N). Other altitudes of maximum density variability occur around 16 km and 0 km. Altitudes of minimum variability (isopycnic levels) occur around 8, 24, and 90 km altitude.

Density varies with latitude in each hemisphere, with the mean annual density near the surface increasing toward the poles. In the region around 8 km in the northern hemisphere, for example, the density variation with latitude and season is small (isopycnic level). Above 8 km to about 28 km, the mean annual density decreases toward the north. Mean monthly densities between 30 and 90 km increase toward the north in July and toward the equator in January.

Considerable data are now available on the mean density and its variability below 30 km at the various test ranges from the data collected for preparation of the IRIG Range Reference Atmospheres (Ref. 10.3). Additional information on the seasonal variability of density below 30 km is presented in an article by J. W. Smith (Ref. 10.4). Above 30 km, the data are less plentiful and the accuracy of the temperature measurements (used to compute densities) decreases with altitude.

Extreme minimum and maximum values of density for the Eastern Test Range and Vandenberg AFB are given in Table 10.11. These extreme density values approach the $\pm 3\sigma$ (corresponding to the normal distribution) density values.

The relative density deviations for Kennedy Space Center and Vandenberg AFB, as given in Table 10.11, are respectively defined as percentage departures from the Patrick Reference Atmosphere (Ref. 10.2) and the Vandenberg Reference Atmosphere (Ref. 10.5).

Median values of surface density for different locations of interest are given in Table 4.1 of Section IV, with nominal values with altitude being given in Tables 10.8 through 10.10 and in Reference 10.3.

ORIGINAL PAGE IS OF POOR QUALITY

TABLE 10.11 DENSITY HEIGHT MAXIMUM (≈ +3 SIGMA), AND MINIMUM (≈ -3 SIGMA) FOR KENNEDY SPACE CENTER, FLORIDA (ETR) AND VANDENBERG AFB, CALIFORNIA (SAMTEC)

Altitude[a]		Kennedy Space Center Density				Vandenberg Density			
		Maximum		Minimum		Maximum		Minimum	
(km)	(ft)	(kg m^{-3})	% Deviation from PRA-63	(kg m^{-3})	% Deviation from PRA-63	(kg m^{-3})	% Deviation from VRA-71	(kg m^{-3})	% Deviation from VRA-71
0	0	1.326	12.0	1.141	-3.6	1.302	5.3	1.140	-7.8
2	6 600	1.047	6.1	9.497×10^{-1}	-3.0	1.046	6.1	9.518×10^{-1}	-3.5
4	13 100	8.287×10^{-1}	3.7	7.824×10^{-1}	-2.1	8.484×10^{-1}	5.7	7.766×10^{-1}	-3.3
6	19 700	6.706×10^{-1}	3.2	6.355×10^{-1}	-2.2	6.906×10^{-1}	5.7	6.299×10^{-1}	-3.6
8	26 200	5.428×10^{-1}	3.1	5.055×10^{-1}	-4.0	5.601×10^{-1}	6.0	4.971×10^{-1}	-6.0
10	32 800	4.352×10^{-1}	3.0	3.938×10^{-1}	-6.8	4.624×10^{-1}	9.5	3.835×10^{-1}	-9.2
15	49 200	2.345×10^{-1}	7.0	1.979×10^{-1}	-9.7	2.337×10^{-1}	12.0	1.851×10^{-1}	-11.3
20	65 600	1.002×10^{-1}	7.5	8.751×10^{-2}	-6.1	1.001×10^{-1}	8.8	8.420×10^{-2}	-8.5
25	82 000	4.274×10^{-2}	5.9	3.790×10^{-2}	-6.1	4.460×10^{-2}	10.0	3.634×10^{-2}	-10.4
30	98 400	1.976×10^{-2}	7.8	1.700×10^{-2}	-7.3	2.085×10^{-2}	13.0	1.634×10^{-2}	-11.5
35	114 800	9.427×10^{-3}	10.3	7.640×10^{-3}	-10.6	9.786×10^{-3}	13.8	7.505×10^{-3}	-12.8
40	131 200	4.637×10^{-3}	12.5	3.512×10^{-3}	-14.8	4.747×10^{-3}	15.0	3.424×10^{-3}	-17.0
50	164 000	1.275×10^{-3}	16.3	8.630×10^{-4}	-21.3	1.325×10^{-3}	22.0	8.473×10^{-4}	-22.0
60	196 800	3.946×10^{-4}	19.4	2.465×10^{-4}	-25.4	4.422×10^{-4}	35.0	2.359×10^{-4}	-28.0
70	229 700	1.100×10^{-4}	23.6	6.666×10^{-5}	-25.1	1.203×10^{-4}	32.0	6.197×10^{-5}	-32.0
80	262 500	2.342×10^{-5}	19.0	1.596×10^{-5}	-18.9	2.617×10^{-5}	26.0	1.433×10^{-5}	-31.0
90	295 300	3.684×10^{-6}	10.9	2.930×10^{-6}	-11.8	4.177×10^{-6}	20.0	2.785×10^{-6}	-20.0

a. Geometric altitude above mean sea level.

10.5 Simultaneous Values of Temperature, Pressure, and Density at Discrete Altitude Levels

10.5.1 Introduction

This subsection presents simultaneous values for temperature, pressure, and density as guidelines for aerospace vehicle design considerations. The necessary assumptions and the lack of sufficient statistical data sample restrict the precision by which these data can presently be presented; therefore, the analysis is limited to Kennedy Space Center.

10.5.2 Method of Determining Simultaneous Value

An aerospace vehicle design problem that often arises in considering natural environmental data is stated by way of the following question: "How should the extremes (maxima and minima) of temperature, pressure, and density be combined (a) at discrete altitude levels? (b) versus altitude?" As an example, suppose one desires to know what temperature and pressure should be used simultaneously with a maximum density at a discrete altitude. From statistical principles set forth by Dr. C. E. Buell in Reference 10.6, the solution results by allowing mean density plus three standard deviations to represent maximum density and using the coefficents of variation, correlations, and mean values as expressed in equation (10.1).

$$\text{maximum } \rho = (\bar{\rho} + 3\sigma_{\rho}) = \bar{\rho}\left(1 + 3\,\frac{\sigma_{\rho}}{\bar{\rho}}\right)$$

$$= \bar{\rho}\left\{1 + 3\left[\underbrace{\left(\frac{\sigma_{P}}{\bar{P}}\right) r(P\rho)}_{(A)} - \underbrace{\left(\frac{\sigma_{T}}{\bar{T}}\right) r(\rho T)}_{(B)}\right]\right\} \qquad (10.1)$$

TABLE 10.12 COEFFICIENTS OF VARIATION AND DISCRETE ALTITUDE LEVEL CORRELATION COEFFICIENTS BETWEEN PRESSURE - DENSITY r(Pρ); PRESSURE - TEMPERATURE r(PT); AND DENSITY - TEMPERATURE r(ρT), KENNEDY SPACE CENTER, ANNUAL

ALTI-TUDE	COEFFICIENTS OF VARIATION (CV)			CORRELATION COEFFICIENTS (r)		
(km)	$\sigma(\rho)/\bar{\rho}$ (percent)	$\sigma(P)/\bar{P}$ (percent)	$\sigma(T)/\bar{T}$ (percent)	r(Pρ) (unitless)	r(PT) (unitless)	r(ρT) (unitless)
0	1.8000	.6000	1.5000	.6250	-0.3500	-0.9500
1	1.7000	.5500	1.6000	.3382	-0.0156	-0.9462
2	1.5000	.8000	1.5900	.1508	.3609	-0.8675
3	1.1800	.9800	1.5700	-0.0485	.6606	-0.7818
4	.9700	.8500	1.4000	-0.1799	.7318	-0.8021
5	.8000	.8700	1.3400	-0.2864	.8203	-0.7830
6	.7400	.8400	1.2600	-0.2690	.8246	-0.7666
7	.8800	.9800	1.4200	-0.1633	.7913	-0.7324
8	.9000	1.1300	1.4700	-0.0364	.7910	-0.6402
9	1.1800	1.4700	1.6200	.2678	.7124	-0.4854
10	1.6300	1.7500	1.7200	.4840	.5588	-0.4553
11	1.8800	1.8000	1.7800	.5328	.4485	-0.5174
12	2.1500	1.8700	1.8500	.5841	.3320	-0.5717
13	2.3800	1.9000	1.8500	.6470	.1946	-0.6220
14	2.6200	1.9200	1.7700	.7373	-0.0066	-0.6804
15	2.7800	1.8800	1.6700	.8107	-0.2238	-0.7520
16	2.8800	1.8400	1.7100	.8262	-0.3154	-0.7953
17	2.8800	1.8000	1.7000	.8338	-0.3537	-0.8113
18	2.7500	1.7500	1.7000	.8036	-0.2706	-0.7904
19	2.5000	1.7800	1.6700	.7449	-0.0492	-0.7031
20	2.2700	1.8500	1.6500	.6969	.1625	-0.5944
21	2.0800	1.9500	1.6200	.6786	.3325	-0.4672
22	1.9800	2.1200	1.5700	.7087	.4565	-0.3041
23	1.9200	2.3200	1.4800	.7721	.5659	-0.0870
24	1.9500	2.4000	1.4300	.8032	.5831	-0.0157
25	2.000	2.4300	1.4200	.8116	.5682	-0.0196
26	2.0800	2.5000	1.5000	.8006	.5565	-0.0523
27	2.1500	2.6000	1.5800	.7948	.5640	-0.0528
28	2.2300	2.6700	1.7500	.7591	.5584	-0.1161
29	2.3700	2.6300	1.8700	.7249	.4877	-0.2479
30	2.5200	2.6300	1.9200	.7228	.4211	-0.3224
31	2.7000	2.7000	2.000	.7257	.3704	-0.3704
32	2.8800	2.7500	2.0800	.7279	.3142	-0.4222
33	3.0700	2.7300	2.1700	.7260	.2310	-0.5014
34	3.2700	2.6800	2.2300	.7361	.1223	-0.5817
35	3.4800	2.6000	2.3200	.7454	.0027	-0.6647
36	3.7000	2.5000	2.4300	.7587	-0.1263	-0.7421
37	3.9200	2.3700	2.5500	.7793	-0.2686	-0.8129
38	4.1200	2.4600	2.6300	.7947	-0.3096	-0.8232
39	4.3300	2.6400	2.6900	.8084	-0.3199	-0.8163
40	4.5500	2.7900	2.7680	.8220	-0.3442	-0.8176
41	4.7500	2.8600	3.0200	.7958	-0.3046	-0.8192
42	4.9300	2.9200	3.2600	.7712	-0.2706	-0.8215
43	5.1300	3.0000	3.3400	.7850	-0.3075	-0.8309
44	5.3200	3.1800	3.3500	.8037	-0.3270	-0.8252
45	5.5000	3.2400	3.6000	.7797	-0.2912	-0.8261
46	5.6700	3.3200	3.8300	.7571	-0.2539	-0.8242
47	5.8300	3.4100	3.9800	.7489	-0.2402	-0.8232
48	5.9800	3.4800	4.1900	.7284	-0.2090	-0.8223
49	6.1300	3.5900	4.1400	.7572	-0.2540	-0.8241
50	6.2700	3.6900	4.1900	.7644	-0.2633	-0.8232
51	6.4200	3.8200	4.0800	.7984	-0.3201	-0.8260
52	6.5500	3.9100	4.1800	.7950	-0.3103	-0.8234
53	6.7000	4.0100	4.2700	.7953	-0.3089	-0.8222
54	6.8000	4.0700	4.3100	.7990	-0.3164	-0.8232
55	6.9200	4.1400	4.3700	.8016	-0.3220	-0.8241
56	7.0300	4.2100	4.4200	.8043	-0.3267	-0.8244
57	7.1500	4.2800	4.4700	.8081	-0.3351	-0.8258
58	7.2700	4.3600	4.5100	.8127	-0.3434	-0.8263
59	7.3700	4.4200	4.5400	.8172	-0.3530	-0.8277
60	7.4700	4.4800	4.5900	.8188	-0.3565	-0.8283

TABLE 10.12 COEFFICIENTS OF VARIATION AND DISCRETE ALTITUDE LEVEL CORRELATION COEFFICIENTS BETWEEN PRESSURE - DENSITY r(Pρ); PRESSURE - TEMPERATURE r(PT); AND DENSITY - TEMPERATURE r(ρT), KENNEDY SPACE CENTER, ANNUAL (Concluded)

ALTITUDE	COEFFICIENTS OF VARIATION (CV)			CORRELATION COEFFICIENTS (r)		
(km)	$\sigma(\rho)/\rho$ (percent)	$\sigma(P)/P$ (percent)	$\sigma(T)/T$ (percent)	$r(P\rho)$ (unitless)	$r(PT)$ (unitless)	$r(\rho T)$ (unitless)
61	7.5700	4.5400	4.6300	.8217	-0.3629	-0.8293
62	7.6500	4.7000	4.8600	.7926	-0.2805	-0.8076
63	7.7500	4.9000	5.0000	.7778	-0.2256	-0.7878
64	7.8300	5.1500	5.1500	.7602	-0.1558	-0.7602
65	7.9000	5.3800	5.3800	.7342	-0.0781	-0.7342
66	7.9800	5.5700	5.4400	.7324	-0.0505	-0.7170
67	8.0300	5.6600	5.4700	.7326	-0.0408	-0.7099
68	8.0700	5.7700	5.4000	.7437	-0.0429	-0.6998
69	8.1000	5.8200	5.5100	.7331	-0.0215	-0.6957
70	8.1200	5.8700	5.4900	.7369	-0.0208	-0.6911
71	8.1200	5.8900	5.4700	.7392	-0.0205	-0.6885
72	8.0700	5.7900	5.3800	.7459	-0.0426	-0.6973
73	8.1200	5.6500	5.2900	.7615	-0.1008	-0.7216
74	8.0700	5.5000	5.1700	.7733	-0.1432	-0.7383
75	7.9000	5.2900	5.4100	.7313	-0.0901	-0.7452
76	7.6800	4.9900	5.6500	.6779	-0.0383	-0.7606
77	7.3800	5.0100	6.1600	.5628	.1390	-0.7403
78	7.0500	5.0400	6.5200	.4587	.2771	-0.7267
79	6.6800	5.1100	6.8400	.3508	.4045	-0.7145
80	6.3200	5.2700	6.7800	.3265	.4730	-0.6784
81	5.9500	5.3600	6.7200	.2975	.5342	-0.6482
82	5.5800	5.5200	6.6600	.2800	.5942	-0.6057
83	5.2500	5.1300	6.6100	.1891	.6259	-0.6475
84	4.9200	4.7800	6.5600	.0855	.6645	-0.6877
85	4.6300	4.4700	6.5100	-0.0232	.7032	-0.7272
86	4.4000	4.1900	6.4500	-0.1271	.7363	-0.7647
87	4.2000	3.9600	6.4000	-0.2296	.7694	-0.7983
88	4.0200	4.0500	6.3400	-0.2344	.7874	-0.7838
89	3.8800	4.1400	6.2800	-0.2255	.7986	-0.7665
90	3.7800	[illegible]	5.9600	-0.1608	.7706	-0.7432

The associated values for pressure and temperature are the last two terms of equation (10.1), (A) and (B), multiplied by $\overline{P}$ and $\overline{T}$, respectively, and then this result is added to $\overline{P}$ and $\overline{T}$, respectively. Appropriate values of r and CV are obtained from Table 10.12.

In general, the three extreme ρ, P, and T equations of interest are

$$\text{extreme } \rho = \left(\bar{\rho} \pm M\sigma_{\rho}\right) = \bar{\rho}\left[1 \pm M\left(\frac{\sigma_{\rho}}{\bar{\rho}}\right)\right]$$

$$= \bar{\rho}\left\{1 \pm M\left[\left(\frac{\sigma_P}{\overline{P}}\right) r(P\rho) - \left(\frac{\sigma_T}{\overline{T}}\right) r(\rho T)\right]\right\} \qquad (10.2)$$

ORIGINAL PAGE IS
OF POOR QUALITY

$$\text{extreme P} = \left(\bar{P} \pm M\sigma_P\right) = \bar{P}\left[1 \pm M\left(\frac{\sigma_P}{\bar{P}}\right)\right]$$

$$= \bar{P}\left\{1 \pm M\left[\left(\frac{\sigma_\rho}{\bar{\rho}}\right) r(P\rho) + \left(\frac{\sigma_T}{\bar{T}}\right) r(PT)\right]\right\} \tag{10.3}$$

$$\text{extreme T} = \left(\bar{T} \pm M\sigma_T\right) = \bar{T}\left[1 \pm M\left(\frac{\sigma_T}{\bar{T}}\right)\right]$$

$$= \bar{T}\left\{1 \pm M\left[\left(\frac{\sigma_P}{\bar{P}}\right) r(PT) - \left(\frac{\sigma_\rho}{\bar{\rho}}\right) r(\rho T)\right]\right\}, \tag{10.4}$$

where M denotes the multiplication factor to give the desired deviation. The values of M for the normal distribution and the associated percentile levels are as follows:

	M		Percentile
mean	-3	standard deviations	0.135
mean	-2	standard deviations	2.275
mean	-1	standard deviations	15.866
mean	±0	standard deviations = median	50.000
mean	+1	standard deviations	84.134
mean	+2	standard deviations	97.725
mean	+3	standard deviations	99.865

The two associated atmospheric parameters that deal with a third extreme parameter are listed, in more detail, in the following chart.

	For Extreme Density	For Extreme Temperature	For Extreme Pressure
$P_{assoc.} =$	$\bar{P}\left[1 \pm \left\{M\left(\frac{\sigma_P}{\bar{P}}\right) r(P\rho)\right\}\right]$	$\bar{P}\left[1 \pm \left\{M\left(\frac{\sigma_P}{\bar{P}}\right) r(PT)\right\}\right]$	
$T_{assoc.} =$	$\bar{T}\left[1 \pm \left\{M\left(\frac{\sigma_T}{\bar{T}}\right) r(\rho T)\right\}\right]$		$\bar{T}\left[1 \pm \left\{M\left(\frac{\sigma_T}{\bar{T}}\right) r(PT)\right\}\right]$
$\rho_{assoc.} =$		$\bar{\rho}\left[1 \pm \left\{M\left(\frac{\sigma_\rho}{\bar{\rho}}\right) r(\rho T)\right\}\right]$	$\bar{\rho}\left[1 \pm \left\{M\left(\frac{\sigma_\rho}{\bar{\rho}}\right) r(P\rho)\right\}\right]$

Use + sign when extreme parameter is maximum.
Use - sign when extreme parameter is minimum.

It must be emphasized that this procedure is to be used at discrete altitudes only. Whenever extreme profiles of pressure, temperature, and density are required for engineering application, the use of these correlated variables at discrete altitudes is not satisfactory. Subsection 10.6 deals directly with this problem, since a profile of extreme pressure, temperature, or density from 0 to 90 km altitude is unrealistic in the real atmosphere.

10.6 Extreme Atmospheric Profiles for Kennedy Space Center, Florida, Vandenberg AFB, California, and Edwards AFB, California

Given in this section are the two extreme density profiles that correspond to the summer (hot) and winter (cold) extreme atmospheres for Kennedy Space Center, Florida (Tables 10.13A and 10.13B); Vandenberg Air Force Base, California (Tables 10.14A and 10.14B); and Edwards AFB, California (Tables 10.15A and 10.15B) (see Ref. 10.7 and 10.8 for detailed information pertaining to the Vandenberg and Edwards extreme atmospheres, respectively). Associated values of extreme temperature and pressure vs. altitude are also tabulated. These extreme atmospheric profiles should be used in ascent design analyses at all altitudes. For re-entry studies they apply only from 30 km to the surface for vehicles to be used at Kennedy Space Center, Florida; Vandenberg AFB, California; or Edwards AFB, California. For those aerospace vehicles with ferrying capability, design calculations should use these extreme profiles in conjunction with the hot or cold day design ambient air temperatures over runways from paragraph 17.4.1 of Section XVII. The extreme atmosphere producing the maximum vehicle design requirement should be utilized to determine the design.

The envelopes of deviations of density in Table 10.11 imply that a typical individual extreme density profile may be represented by a similarly shaped profile, that is, deviations of density either all negative or all positive from sea level to 90 km altitude. However, examination of many individual density profiles shows that when large positive deviations of density occur at the surface, correspondingly large negative deviations will occur near 15 km altitude and above. Such a situation occurs during the winter season (cold atmosphere). The reverse is also true — density profiles with large negative deviations at lower levels will have correspondingly large positive deviations at higher levels. This situation occurs in the summer season (hot atmosphere) (Figs. 10.1, 10.2 and 10.3).

The two extreme Kennedy Space Center density profiles of Figure 10.1 are shown as percent deviations from the Patrick Reference Atmosphere, 1963 density profile (Ref. 10.2). The two profiles obey the hydrostatic equation and the ideal gas law. The extreme density profiles shown here to 30 km altitude were

TABLE 10.13A KENNEDY SPACE CENTER SUMMER (HOT) ATMOSPHERE (KHA-71)

Geometric Altitude	Geopotential Altitude	Virtual Temperature	Kinetic Temperature	Pressure	Density	Rel. Dev. (T*) with respect to PRA-63	Rel. Dev. (P) with respect to PRA-63	Rel. Dev. (D) with respect to PRA-63
Z(m)	H(m)	T* (°K)	T (°K)	P(N/cm²)	D(kg/m³)	RD(T*)%	RD(P)%	RD(D)%
0.	.0	3.0990000+02	3.0740000+02	1.0100000+01	1.1353705+00	3.52	-.69	-4.07
1000.	998.5	3.0313637+02	3.0105000+02	9.0346817+00	1.0382755+00	3.66	-.29	-3.81
2000.	1996.6	2.9637273+02	2.9470000+02	8.0614293+00	9.4757068-01	3.43	.17	-3.21
3000.	2994.5	2.8960909+02	2.8835000+02	7.1741153+00	8.6296655-01	3.07	.49	-2.52
4000.	3992.0	2.8284546+02	2.8200000+02	6.3668963+00	7.8418111-01	2.74	.62	-1.87
5000.	4989.2	2.7608182+02	2.7565001+02	5.6342022+00	7.1093916-01	2.53	1.13	-1.37
6000.	5986.1	2.6931818+02	2.6931818+02	4.9707288+00	6.4297218-01	2.50	1.43	-1.06
7000.	6982.7	2.6255455+02	2.6255455+02	4.3714321+00	5.8001870-01	2.67	1.74	-.91
8000.	7979.0	2.5579091+02	2.5579091+02	3.8315199+00	5.2182367-01	3.00	2.09	-.89
9000.	8975.0	2.4902728+02	2.4902728+02	3.3464479+00	4.6813915-01	3.44	2.49	-.92
10000.	9970.6	2.4226364+02	2.4226364+02	2.9119117+00	4.1872392-01	3.91	2.98	-.91
11000.	10965.9	2.3550000+02	2.3550000+02	2.5238402+00	3.7334363-01	4.35	3.55	-.81
12000.	11961.0	2.2820000+02	2.2820000+02	2.1780131+00	3.3249312-01	4.29	4.16	-.16
13000.	12955.7	2.2090000+02	2.2090000+02	1.8705877+00	2.9499874-01	3.76	4.73	.92
14000.	13950.1	2.1360000+02	2.1360000+02	1.5983606+00	2.6068215-01	2.61	5.16	2.60
15000.	14944.2	2.0630000+02	2.0630000+02	1.3583010+00	2.2936894-01	.72	5.35	4.64
16000.	15937.9	1.9900000+02	1.9900000+02	1.1475476+00	2.0088866-01	-1.99	5.17	7.33
17000.	16931.4	1.9816257+02	1.9816257+02	9.6617676-01	1.6985547-01	-2.39	4.72	7.27
18000.	17924.5	2.0000000+02	2.0000000+02	8.1369526-01	1.4173245-01	-2.58	4.19	7.05
19000.	18917.4	2.0416667+02	2.0416667+02	6.8712577-01	1.1724374-01	-1.74	3.70	5.66
20000.	19909.9	2.0833333+02	2.0833333+02	5.8222915-01	9.7358475-02	-.96	3.39	4.47
21000.	20902.1	2.1250000+02	2.1250000+02	4.9493667-01	8.1136631-02	-.19	3.23	3.44
22000.	21894.0	2.1566667+02	2.1566667+02	4.2201626-01	6.8172810-02	.14	3.17	2.97
23000.	22885.6	2.1883333+02	2.1883333+02	3.6056887-01	5.7401234-02	.53	3.16	2.51
24000.	23876.9	2.2200000+02	2.2200000+02	3.0875086-01	4.8447590-02	1.00	3.21	2.06
25000.	24867.8	2.2516667+02	2.2516667+02	2.6498604-01	4.0994491-02	1.55	3.30	1.60
26000.	25858.5	2.2833333+02	2.2833333+02	2.2793980-01	3.4775536-02	2.19	3.44	1.15
27000.	26848.8	2.3150000+02	2.3150000+02	1.9649475-01	2.9570541-02	2.89	3.64	.73
28000.	27838.9	2.3466667+02	2.3466667+02	1.6972565-01	2.5199219-02	3.63	3.93	.29
29000.	28828.6	2.3783333+02	2.3783333+02	1.4687393-01	2.1516243-02	4.04	4.35	.30
30000.	29818.0	2.4100000+02	2.4100000+02	1.2732124-01	1.8405121-02	4.42	4.82	.38
31000.	30807.1	2.4416667+02	2.4416667+02	1.1056625-01	1.5773346-02	4.78	5.32	.52
32000.	31795.9	2.4733333+02	2.4733333+02	9.6198730-02	1.3546524-02	5.11	5.86	.72
33000.	32784.4	2.5050000+02	2.5050000+02	8.3870697-02	1.1662445-02	5.40	6.44	.99
34000.	33772.6	2.5366667+02	2.5366667+02	7.3279037-02	1.0065735-02	5.67	7.06	1.32
35000.	34760.4	2.5683333+02	2.5683333+02	6.4129028-02	8.7031249-03	5.90	7.70	1.70
36000.	35748.0	2.6000000+02	2.6000000+02	5.6145477-02	7.5227375-03	6.11	8.37	2.14
37000.	36735.2	2.6288461+02	2.6288461+02	4.9269104-02	6.5290813-03	6.18	9.06	2.71
38000.	37722.1	2.6576923+02	2.6576923+02	4.3294535-02	5.6749344-03	6.24	9.75	3.31
39000.	38708.8	2.6865385+02	2.6865385+02	3.8097067-02	4.9400673-03	6.30	10.44	3.90
40000.	39695.1	2.7153846+02	2.7153846+02	3.3570537-02	4.3068771-03	6.36	11.13	4.49
41000.	40681.1	2.7442308+02	2.7442308+02	2.9622116-02	3.7603684-03	6.43	11.82	5.06
42000.	41666.8	2.7730769+02	2.7730769+02	2.6172104-02	3.2879410-03	6.54	12.51	5.60
43000.	42652.2	2.8019231+02	2.8019231+02	2.3153610-02	2.8787613-03	6.69	13.20	6.10
44000.	43637.3	2.8307692+02	2.8307692+02	2.0507717-02	2.5237846-03	6.89	13.90	6.56
45000.	44622.0	2.8596154+02	2.8596154+02	1.8186378-02	2.2154732-03	7.17	14.63	6.96
46000.	45606.5	2.8884615+02	2.8884615+02	1.6148109-02	1.9474564-03	7.54	15.39	7.30
47000.	46590.7	2.9173077+02	2.9173077+02	1.4355888-02	1.7142868-03	8.02	16.21	7.58
48000.	47574.5	2.9461538+02	2.9461538+02	1.2777672-02	1.5109100-03	8.64	17.10	7.79
49000.	48558.0	2.9750000+02	2.9750000+02	1.1384044-02	1.3330526-03	9.42	18.13	7.96
50000.	49541.3	2.9750000+02	2.9750000+02	1.0148231-02	1.1883979-03	9.94	19.15	9.38
51000.	50524.2	2.9325000+02	2.9325000+02	9.0407466-03	1.0739715-03	8.38	20.16	10.26
52000.	51506.8	2.8900000+02	2.8900000+02	8.0399930-03	9.6910328-04	8.12	21.09	12.00
53000.	52489.1	2.8475000+02	2.8475000+02	7.1372587-03	8.7313598-04	7.32	21.92	13.60
54000.	53471.1	2.8050000+02	2.8050000+02	6.3243675-03	7.8543025-04	6.60	22.67	15.07
55000.	54452.9	2.7625000+02	2.7625000+02	5.5935943-03	7.0539075-04	5.94	23.33	16.42
56000.	55434.2	2.7200000+02	2.7200000+02	4.9378836-03	6.3245458-04	5.32	23.91	17.65
57000.	56415.3	2.6775000+02	2.6775000+02	4.3505454-03	5.6608540-04	4.75	24.41	18.77
58000.	57396.1	2.6350000+02	2.6350000+02	3.8253748-03	5.0578808-04	4.21	24.82	19.78
59000.	58376.6	2.5925000+02	2.5925000+02	3.3566785-03	4.5108956-04	3.69	25.15	20.69
60000.	59356.7	2.5500000+02	2.5500000+02	2.9390943-03	4.0154946-04	3.20	25.39	21.50
61000.	60336.6	2.5075000+02	2.5075000+02	2.5678229-03	3.5675335-04	2.71	25.54	22.23
62000.	61316.1	2.4650000+02	2.4650000+02	2.2383559-03	3.1631672-04	2.24	25.61	22.86
63000.	62295.4	2.4225000+02	2.4225000+02	1.9464898-03	2.7987802-04	1.76	25.59	23.42
64000.	63274.3	2.3800000+02	2.3800000+02	1.6884637-03	2.4709821-04	1.28	25.47	23.89
65000.	64253.0	2.3375000+02	2.3375000+02	1.4609194-03	2.1766889-04	.78	25.25	24.28
66000.	65231.3	2.2950000+02	2.2950000+02	1.2605929-03	1.9129384-04	.27	24.93	24.59
67000.	66209.3	2.2525000+02	2.2525000+02	1.0846496-03	1.6770816-04	-.27	24.50	24.83
68000.	67187.0	2.2100000+02	2.2100000+02	9.3052387-04	1.4666247-04	-.82	23.95	24.98
69000.	68164.5	2.1675000+02	2.1675000+02	7.9586029-04	1.2791753-04	-1.41	23.29	25.05
70000.	69141.6	2.1250000+02	2.1250000+02	6.7856073-04	1.1126780-04	-2.03	22.49	25.04
71000.	70118.4	2.0825000+02	2.0825000+02	5.7664156-04	9.6510648-05	-2.69	21.56	24.92
72000.	71094.9	2.0400000+02	2.0400000+02	4.8844814-04	8.3469629-05	-3.38	20.49	24.70
73000.	72071.1	1.9975000+02	1.9975000+02	4.1236877-04	7.1975231-05	-4.11	19.26	24.37
74000.	73047.0	1.9550000+02	1.9550000+02	3.4700393-04	6.1864137-05	-4.87	17.87	23.91
75000.	74022.6	1.9125000+02	1.9125000+02	2.9097080-04	5.3004503-05	-5.67	16.32	23.31
76000.	74997.9	1.8700000+02	1.8700000+02	2.4319172-04	4.5259475-05	-6.51	14.58	22.56
77000.	75972.8	1.8275000+02	1.8275000+02	2.0245552-04	3.8509607-05	-7.38	12.65	21.63
78000.	76947.5	1.7850000+02	1.7850000+02	1.6777992-04	3.2638311-05	-8.27	10.53	20.50
79000.	77921.9	1.7425000+02	1.7425000+02	1.3800621-04	2.7534485-05	-9.19	8.21	19.16
80000.	78896.0	1.7000000+02	1.7000000+02	1.1290073-04	2.3151398-05	-10.13	5.67	17.58
81000.	79869.7	1.7000000+02	1.7000000+02	9.2306137-05	1.8935204-05	-8.79	3.19	13.13
82000.	80843.2	1.7000000+02	1.7000000+02	7.5511932-05	1.5504837-05	-7.39	.99	9.05
83000.	81816.4	1.7000000+02	1.7000000+02	6.1855316-05	1.2674332-05	-5.90	-.92	5.30
84000.	82789.2	1.7000000+02	1.7000000+02	5.0659180-05	1.0385513-05	-5.90	-2.59	3.51
85000.	83761.9	1.7000000+02	1.7000000+02	4.1408538-05	8.5029602-06	-5.90	-4.24	1.76
86000.	84734.0	1.7000000+02	1.7000000+02	3.3922195-05	6.9713593-06	-5.90	-5.87	.03
87000.	85706.0	1.7000000+02	1.7000000+02	2.7647018-05	5.7010650-06	-5.90	-7.47	-1.67
88000.	86677.6	1.7000000+02	1.7000000+02	2.2735596-05	4.6710968-06	-5.90	-9.05	-3.35
89000.	87649.0	1.7000000+02	1.7000000+02	1.8634796-05	3.8394928-06	-5.90	-10.61	-5.01
90000.	88620.0	1.7000000+02	1.7000000+02	1.5134811-05	3.1070709-06	-5.90	-12.15	-6.64

TABLE 10.13B KENNEDY SPACE CENTER WINTER (COLD) ATMOSPHERE (KCA-71)

Geometric Altitude	Geopotential Altitude	Virtual Temperature	Kinetic Temperature	Pressure	Density	Rel. Dev. (T*) with respect to PRA-63	Rel. Dev. (P) with respect to PRA-63	Rel. Dev. (D) with respect to PRA-63
Z(m)	H(m)	T* (°K)	T (°K)	P (N/cm²)	D (kg/m³)	RD(T*)%	RD(P)%	RD(D)%
0.	.0	2.7500000+02	2.7450000+02	1.0270000+01	1.3009948+00	-8.14	.98	9.32
1000.	998.5	2.7000000+02	2.6960000+02	9.0598171+00	1.1689434+00	-7.67	-.01	8.30
2000.	1996.6	2.6500000+02	2.6470000+02	7.9735277+00	1.0481959+00	-7.51	-.98	7.06
3000.	2994.5	2.6000000+02	2.5980000+02	7.0004350+00	9.3797119-01	-7.46	-1.95	5.95
4000.	3992.0	2.5500000+02	2.5490000+02	6.1305847+00	8.3752835-01	-7.38	-2.92	4.80
5000.	4989.2	2.5000000+02	2.5000000+02	5.3547301+00	7.4616589-01	-7.16	-3.89	3.51
6000.	5986.1	2.4523591+02	2.4523591+02	4.6646548+00	6.6278387-01	-6.65	-4.92	1.96
7000.	6982.7	2.4044706+02	2.4044706+02	4.0522889+00	5.8710627-01	-6.03	-5.69	.36
8000.	7979.0	2.3586761+02	2.3586761+02	3.5107186+00	5.1842328-01	-4.97	-6.46	-1.37
9000.	8975.0	2.3160561+02	2.3160561+02	3.0333981+00	4.5620410-01	-3.77	-7.09	-3.49
10000.	9970.6	2.2767153+02	2.2767153+02	2.6141402+00	4.0002236-01	-2.42	-7.55	-5.27
11000.	10965.9	2.2401892+02	2.2401892+02	2.2471262+00	3.4951847-01	-.74	-7.81	-7.15
12000.	11961.0	2.2058508+02	2.2058508+02	1.9269158+00	3.0436223-01	.77	-7.85	-8.59
13000.	12955.7	2.1733175+02	2.1733175+02	1.6484578+00	2.6421523-01	2.16	-7.70	-9.68
14000.	13950.1	2.1428577+02	2.1428577+02	1.4071002+00	2.2869338-01	2.95	-7.41	-10.05
15000.	14944.2	2.1157970+02	2.1157970+02	1.1985998+00	1.9732939-01	3.26	-7.03	-9.94
16000.	15937.9	2.0949258+02	2.0949258+02	1.0191326+00	1.6953508-01	3.19	-6.61	-9.47
17000.	16931.4	2.0849504+02	2.0849504+02	8.6531102-01	1.4460154-01	2.78	-6.20	-8.75
18000.	17924.5	2.0828323+02	2.0828323+02	7.3453635-01	1.2283195-01	1.44	-5.95	-7.19
19000.	18917.4	2.0846620+02	2.0846620+02	6.2346069-01	1.0417007-01	.34	-5.91	-6.13
20000.	19909.9	2.0899749+02	2.0899749+02	5.2929926-01	8.8229208-02	-.64	-6.01	-5.33
21000.	20902.1	2.0982848+02	2.0982848+02	4.4959301-01	7.4658779-02	-1.41	-6.23	-4.87
22000.	21894.0	2.1090961+02	2.1090961+02	3.8218424-01	6.3142604-02	-2.12	-6.54	-4.57
23000.	22885.6	2.1219170+02	2.1219170+02	3.2519529-01	5.3396919-02	-2.52	-6.95	-4.65
24000.	23876.9	2.1362711+02	2.1362711+02	2.7700539-01	4.5168960-02	-2.83	-7.42	-4.85
25000.	24867.8	2.1517109+02	2.1517109+02	2.3622634-01	3.8234467-02	-2.94	-7.94	-5.26
26000.	25858.5	2.1678299+02	2.1678299+02	2.0168165-01	3.2396351-02	-2.97	-8.50	-5.76
27000.	26848.8	2.1842757+02	2.1842757+02	1.7237698-01	2.7482916-02	-2.88	-9.09	-6.38
28000.	27838.9	2.2007615+02	2.2007615+02	1.4748703-01	2.3345394-02	-2.84	-9.67	-7.03
29000.	28828.6	2.2170800+02	2.2170800+02	1.2632431-01	1.9857147-02	-3.04	-10.22	-7.40
30000.	29818.0	2.2331153+02	2.2331153+02	1.0832073-01	1.6910702-02	-3.16	-10.79	-7.87
31000.	30807.1	2.2488554+02	2.2488554+02	9.2998886-02	1.4416779-02	-3.55	-11.39	-8.13
32000.	31795.9	2.2644049+02	2.2644049+02	7.9957733-02	1.2301918-02	-3.79	-12.03	-8.57
33000.	32784.4	2.2799975+02	2.2799975+02	6.8840331-02	1.0507172-02	-4.07	-12.71	-9.01
34000.	33772.6	2.2960097+02	2.2960097+02	5.9314604-02	8.9853973-03	-4.32	-13.40	-9.49
35000.	34760.4	2.3125000+02	2.3125000+02	5.1093979-02	7.6969605-03	-4.65	-14.12	-9.94
36000.	35748.0	2.3383928+02	2.3383928+02	4.4116459-02	6.5724525-03	-4.57	-14.85	-10.77
37000.	36735.2	2.3642857+02	2.3642857+02	3.8148088-02	5.6209221-03	-4.51	-15.56	-11.57
38000.	37722.1	2.3901786+02	2.3901786+02	3.3039589-02	4.8153172-03	-4.45	-16.24	-12.34
39000.	38708.8	2.4160714+02	2.4160714+02	2.8661022-02	4.1323890-03	-4.41	-16.91	-13.08
40000.	39695.1	2.4419643+02	2.4419643+02	2.4901237-02	3.5523605-03	-4.35	-17.57	-13.32
41000.	40681.1	2.4678571+02	2.4678571+02	2.1667652-02	3.0585937-03	-4.28	-18.21	-14.55
42000.	41666.8	2.4937500+02	2.4937500+02	1.8880863-02	2.6376419-03	-4.19	-18.84	-15.29
43000.	42652.2	2.5196428+02	2.5196428+02	1.6474552-02	2.2778053-03	-4.06	-19.46	-16.65
44000.	43637.3	2.5455357+02	2.5455357+02	1.4394226-02	1.9698486-03	-3.88	-20.05	-15.83
45000.	44622.0	2.5714286+02	2.5714286+02	1.2593651-02	1.7059479-03	-3.63	-20.62	-17.63
46000.	45606.5	2.5973214+02	2.5973214+02	1.1034660-02	1.4797821-03	-3.30	-21.15	-18.46
47000.	46590.7	2.6232143+02	2.6232143+02	9.6825027-03	1.2858047-03	-2.87	-21.63	-19.32
48000.	47574.5	2.6491071+02	2.6491071+02	8.5065841-03	1.1187134-03	-2.31	-22.05	-20.20
49000.	48558.0	2.6750000+02	2.6750000+02	7.4803328-03	9.7417116-04	-1.61	-22.37	-21.10
50000.	49541.3	2.6750000+02	2.6750000+02	6.5834379-03	8.5736990-04	-1.15	-22.71	-21.81
51000.	50524.2	2.6750000+02	2.6750000+02	5.7941055-03	7.5457335-04	-.59	-22.99	-22.53
52000.	51506.3	2.6750000+02	2.6750000+02	5.0981116-03	6.6395879-04	.07	-23.19	-23.25
53000.	52489.1	2.6607143+02	2.6607143+02	4.4871795-03	5.8748722-04	.28	-23.35	-23.57
54000.	53471.1	2.6464286+02	2.6464286+02	3.9456653-03	5.1935887-04	.58	-23.49	-23.92
55000.	54452.8	2.6321429+02	2.6321429+02	3.4663939-03	4.5875263-04	.94	-23.59	-24.30
56000.	55434.2	2.6178572+02	2.6178572+02	3.0428338-03	4.0491104-04	1.37	-23.65	-24.68
57000.	56415.3	2.6035714+02	2.6035714+02	2.6690495-03	3.5713458-04	1.85	-23.67	-25.06
58000.	57395.1	2.5892857+02	2.5892857+02	2.3394966-03	3.1478500-04	2.40	-23.65	-25.44
59000.	58376.6	2.5750000+02	2.5750000+02	2.0493507-03	2.7727747-04	2.99	-23.57	-25.79
60000.	59356.7	2.5607143+02	2.5607143+02	1.7940330-03	2.4408293-04	3.63	-23.44	-26.13
61000.	60336.6	2.5464286+02	2.5464286+02	1.5695310-03	2.1473479-04	4.31	-23.24	-26.41
62000.	61316.1	2.5321429+02	2.5321429+02	1.3722539-03	1.8879223-04	5.02	-22.98	-26.66
63000.	62295.4	2.5178572+02	2.5178572+02	1.1990118-03	1.6587544-04	5.76	-22.65	-26.86
64000.	63274.3	2.5035714+02	2.5035714+02	1.0467529-03	1.4563131-04	6.53	-22.24	-27.01
65000.	64253.0	2.4892857+02	2.4892857+02	9.1317415-04	1.2776279-04	7.32	-21.75	-27.09
66000.	65231.3	2.4750000+02	2.4750000+02	7.9591989-04	1.1199284-04	8.13	-21.19	-27.11
67000.	66209.3	2.4607143+02	2.4607143+02	6.9297552-04	9.8073482-05	8.95	-20.51	-27.05
68000.	67187.0	2.4464286+02	2.4464286+02	6.0273170-04	8.5805893-05	9.73	-19.76	-26.91
69000.	68164.5	2.4321429+02	2.4321429+02	5.2362918-04	7.4997425-05	10.62	-18.90	-26.69
70000.	69141.5	2.4178572+02	2.4178572+02	4.5454579-04	6.5495014-05	11.47	-17.93	-26.37
71000.	70118.4	2.4035714+02	2.4035714+02	3.9408684-04	5.7145119-05	12.31	-16.85	-25.97
72000.	71094.9	2.3892857+02	2.3892857+02	3.4146309-04	4.9815655-05	13.16	-15.65	-25.46
73000.	72071.1	2.3750000+02	2.3750000+02	2.9575348-04	4.3401718-05	14.01	-14.33	-24.86
74000.	73047.0	2.3607143+02	2.3607143+02	2.5612631-04	3.7804127-05	14.87	-12.97	-24.15
75000.	74022.6	2.3464286+02	2.3464286+02	2.2185302-04	3.2925129-05	15.77	-11.27	-23.33
76000.	74997.9	2.3321429+02	2.3321429+02	1.9212246-04	2.8688431-05	16.59	-9.51	-22.39
77000.	75972.9	2.3178572+02	2.3178572+02	1.6645908-04	2.4969101-05	17.48	-7.60	-21.35
78000.	76947.5	2.3035714+02	2.3035714+02	1.4385223-04	2.1701813-05	18.38	-5.52	-20.19
79000.	77921.9	2.2892857+02	2.2892857+02	1.2365341-04	1.8788338-05	19.30	-3.26	-18.91
80000.	78896.0	2.2750000+02	2.2750000+02	1.0559136-04	1.6231239-05	20.27	-.80	-17.52
81000.	79869.7	2.2425000+02	2.2425000+02	9.1113408-05	1.4154732-05	20.31	1.80	-15.39
82000.	80843.2	2.2100000+02	2.2100000+02	7.8145265-05	1.2319863-05	20.39	4.49	-13.21
83000.	81816.4	2.1775000+02	2.1775000+02	6.6890716-05	1.0700285-05	20.53	7.25	-11.01
84000.	82789.2	2.1450000+02	2.1450000+02	5.7106018-05	9.2763901-06	18.74	10.06	-7.30
85000.	83761.8	2.1125000+02	2.1125000+02	4.8654079-05	8.0223083-06	16.94	12.67	-3.65
86000.	84734.0	2.0800000+02	2.0800000+02	4.1339397-05	6.9222450-06	15.14	15.65	-.08
87000.	85706.0	2.0475000+02	2.0475000+02	3.5033226-05	5.9589148-06	13.34	17.16	3.37
88000.	86677.5	2.0150000+02	2.0150000+02	2.9604435-05	5.1189661-06	11.54	19.00	6.69
89000.	87649.0	1.9825000+02	1.9825000+02	2.4955273-05	4.3857098-06	9.74	20.52	9.83
90000.	88620.0	1.9500000+02	1.9500000+02	2.0947456-05	3.7453175-06	7.94	21.72	12.76

ORIGINAL PAGE IS OF POOR QUALITY

ORIGINAL PAGE IS
OF POOR QUALITY

TABLE 10.14A VANDENBERG SUMMER (HOT) ATMOSPHERE (VHA-73) (Ref. 10.7)

GEO-METRIC ALTITUDE	GEO-POTENTIAL ALTITUDE	VIRTUAL TEMPERATURE	KINETIC TEMPERATURE	PRESSURE	DENSITY	REL. DEV. (T*) WITH RESPECT TO VRA-71	REL. DEV. (P) WITH RESPECT TO VRA-71	REL. DEV. (D) WITH RESPECT TO VRA-71
Z(m)	H(m)	T* (°K)	T (°K)	P (N/cm²)	D(kg/m³)	RD(T*)%	RD(P)%	RD(D)%
0.	.0	3.1270000+02	3.1040000+02	1.0100000+01	1.1252041+00	8.90	-.88	-8.98
1000.	999.5	3.0564445+02	3.0360000+02	9.0433741+00	1.0307463+00	6.50	-.05	-6.15
2000.	1998.8	2.9858889+02	2.9680000+02	8.0764169+00	9.4228634-01	5.29	.65	-4.41
3000.	2997.7	2.9153334+02	2.9000000+02	7.1933711+00	8.5957158-01	4.71	1.25	-3.30
4000.	3996.3	2.8447778+02	2.8320000+02	6.3887244+00	7.8235457-01	4.45	1.79	-2.54
5000.	4994.6	2.7742223+02	2.7640001+02	5.6572052+00	7.1039269-01	4.39	2.32	-1.97
6000.	5992.5	2.7036667+02	2.6960000+02	4.9937766+00	6.4344846-01	4.47	2.88	-1.53
7000.	6990.2	2.6331112+02	2.6280000+02	4.3936325+00	5.8128933-01	4.73	3.49	-1.19
8000.	7987.5	2.5625556+02	2.5600000+02	3.8521923+00	5.2368783-01	5.15	4.18	-.93
9000.	8984.5	2.4920000+02	2.4920000+02	3.3650957+00	4.7042153-01	5.64	4.92	-.67
10000.	9981.3	2.4053334+02	2.4053334+02	2.9268444+00	4.2389880-01	5.27	5.64	.35
11000.	10977.7	2.3186667+02	2.3186667+02	2.5326658+00	3.8051989-01	4.47	6.43	1.87
12000.	11973.7	2.2320000+02	2.2320000+02	2.1795295+00	3.4017810-01	2.48	6.95	4.37
13000.	12969.5	2.1453334+02	2.1453334+02	1.8645094+00	3.0276635-01	-.23	7.11	7.36
14000.	13965.0	2.0586667+02	2.0586667+02	1.5847846+00	2.6817733-01	-3.30	6.80	10.43
15000.	14960.1	1.9720000+02	1.9720000+02	1.3376402+00	2.3630346-01	-6.55	5.90	13.31
16000.	15954.9	1.9570000+02	1.9570000+02	1.1241228+00	2.0010632-01	-6.57	4.66	12.02
17000.	16949.5	1.9720000+02	1.9720000+02	9.4465147-01	1.6687632-01	-5.57	3.48	9.61
18000.	17943.7	2.0073846+02	2.0073846+02	7.9573023-01	1.3810093-01	-4.59	2.53	7.44
19000.	18937.6	2.0427692+02	2.0427692+02	6.7212328-01	1.1462151-01	-3.49	1.60	5.33
20000.	19931.2	2.0781538+02	2.0781538+02	5.6937122-01	9.5439698-02	-2.61	.97	3.73
21000.	20924.4	2.1135385+02	2.1135385+02	4.8373771-01	7.9729042-02	-1.86	.61	2.53
22000.	21917.4	2.1489231+02	2.1489231+02	4.1213909-01	6.6814438-02	-1.13	.41	1.52
23000.	22910.0	2.1843077+02	2.1843077+02	3.5205753-01	5.6153625-02	-.32	.29	.56
24000.	23902.4	2.2196923+02	2.2196923+02	3.0146263-01	4.7317459-02	.58	.21	-.41
25000.	24894.4	2.2550769+02	2.2550769+02	2.5873474-01	3.9969986-02	1.60	.19	-1.39
26000.	25886.1	2.2904615+02	2.2904615+02	2.2257759-01	3.3848221-02	2.66	.25	-2.30
27000.	26877.5	2.3258462+02	2.3258462+02	1.9194649-01	2.8744659-02	3.66	.52	-2.98
28000.	27868.6	2.3612308+02	2.3612308+02	1.6595856-01	2.4485870-02	4.44	1.15	-3.16
29000.	28859.4	2.3966154+02	2.3966154+02	1.4382187-01	2.0913849-02	5.05	1.64	-3.24
30000.	29849.9	2.4320000+02	2.4320000+02	1.2477411-01	1.7872536-02	5.54	2.23	-3.14
31000.	30840.0	2.4631765+02	2.4631765+02	1.0854021-01	1.5351728-02	5.90	2.90	-2.84
32000.	31829.9	2.4943529+02	2.4943529+02	9.4560565-02	1.3207052-02	6.30	3.64	-2.50
33000.	32819.4	2.5255294+02	2.5255294+02	8.2517347-02	1.1382030-02	6.68	4.43	-2.11
34000.	33808.7	2.5567059+02	2.5567059+02	7.2130870-02	9.8276710-03	7.05	5.26	-1.66
35000.	34797.6	2.5878823+02	2.5878823+02	6.3160133-02	8.5018768-03	7.36	6.13	-1.15
36000.	35786.2	2.6190588+02	2.6190588+02	5.5398216-02	7.3685989-03	7.62	7.01	-.57
37000.	36774.5	2.6502353+02	2.6502353+02	4.8666973-02	6.3975410-03	7.82	7.91	.08
38000.	37762.5	2.6814117+02	2.6814117+02	4.2817249-02	5.5634384-03	7.96	8.81	.79
39000.	38750.2	2.7125882+02	2.7125882+02	3.7723102-02	4.8452492-03	8.04	9.71	1.55
40000.	39737.5	2.7437647+02	2.7437647+02	3.3279228-02	4.2256546-03	8.07	10.62	2.36
41000.	40724.6	2.7749411+02	2.7749411+02	2.9397774-02	3.6904526-03	8.08	11.52	3.18
42000.	41711.4	2.8061176+02	2.8061176+02	2.6005630-02	3.2279282-03	8.09	12.42	4.01
43000.	42697.8	2.8372941+02	2.8372941+02	2.3039207-02	2.8282852-03	8.13	13.33	4.81
44000.	43683.9	2.8684706+02	2.8684706+02	2.0444488-02	2.4828949-03	8.24	14.25	5.55
45000.	44669.6	2.8996470+02	2.8996470+02	1.8168831-02	2.1834793-03	8.47	15.20	6.20
46000.	45655.3	2.9308235+02	2.9308235+02	1.6164093-02	1.9223480-03	8.88	16.18	6.71
47000.	46640.5	2.9620000+02	2.9620000+02	1.4385190-02	1.6918819-03	9.51	17.22	7.04
48000.	47625.4	2.9620000+02	2.9620000+02	1.2818198-02	1.5075772-03	9.31	18.27	8.19
49000.	48610.0	2.9620000+02	2.9620000+02	1.1421840-02	1.3433490-03	9.51	19.27	8.92
50000.	49594.3	2.9620000+02	2.9620000+02	1.0177627-02	1.1970084-03	9.24	20.37	10.20
51000.	50578.3	2.9620000+02	2.9620000+02	9.0689635-03	1.0666158-03	9.19	21.31	11.10
52000.	51561.9	2.9620000+02	2.9620000+02	8.0805098-03	9.5040369-04	9.39	22.32	11.82
53000.	52545.3	2.9205714+02	2.9205714+02	7.1950161-03	8.5820842-04	8.27	23.32	13.91
54000.	53528.4	2.8791429+02	2.8791429+02	6.3955581-03	7.7381164-04	7.33	24.23	15.75
55000.	54511.1	2.8377143+02	2.8377143+02	5.6750142-03	6.9666314-04	6.54	25.04	17.37
56000.	55493.6	2.7962857+02	2.7962857+02	5.0267339-03	6.2623221-04	5.88	25.77	18.78
57000.	56475.7	2.7548571+02	2.7548571+02	4.4443536-03	5.6202674-04	5.33	26.41	20.01
58000.	57457.5	2.7134286+02	2.7134286+02	3.9221644-03	5.0357592-04	4.87	26.97	21.07
59000.	58439.1	2.6720000+02	2.6720000+02	3.4547555-03	4.5044625-04	4.48	27.45	21.99
60000.	59420.3	2.6305714+02	2.6305714+02	3.0370307-03	4.0222382-04	4.13	27.86	22.79
61000.	60401.2	2.5891429+02	2.5891429+02	2.6644552-03	3.5852188-04	3.83	28.21	23.48
62000.	61381.8	2.5477143+02	2.5477143+02	2.3327088-03	3.1897581-04	3.54	28.48	24.09
63000.	62362.1	2.5062857+02	2.5062857+02	2.0378721-03	2.8325033-04	3.26	28.69	24.63
64000.	63342.1	2.4648571+02	2.4648571+02	1.7762542-03	2.5102877-04	2.97	28.83	25.12
65000.	64321.6	2.4234286+02	2.4234286+02	1.5446758-03	2.2201657-04	2.66	28.91	25.57
66000.	65301.2	2.3620000+02	2.3820000+02	1.3400006-03	1.9594312-04	2.33	28.93	26.00
67000.	66280.3	2.3405714+02	2.3405714+02	1.1594701-03	1.7254829-04	1.96	28.87	26.40
68000.	67259.0	2.2991429+02	2.2991429+02	1.0006714-03	1.5160394-04	1.55	28.75	26.78
69000.	68237.5	2.2577143+02	2.2577143+02	8.6121321-04	1.3288224-04	1.10	28.55	27.15
70000.	69215.7	2.2162857+02	2.2162857+02	7.3911667-04	1.1619067-04	.61	28.28	27.50
71000.	70193.5	2.1748571+02	2.1748571+02	6.3246489-04	1.0133731-04	.08	27.92	27.82
72000.	71171.1	2.1334286+02	2.1334286+02	5.3967237-04	8.8149071-05	-.49	27.47	28.09
73000.	72146.3	2.0920000+02	2.0920000+02	4.5900583-04	7.6471567-05	-1.08	26.92	28.30
74000.	73125.3	2.0505714+02	2.0505714+02	3.8919926-04	6.6153764-05	-1.69	26.26	28.43
75000.	74101.9	2.0091429+02	2.0091429+02	3.2905102-04	5.7063579-05	-2.29	25.48	28.42
76000.	75078.3	1.9677143+02	1.9677143+02	2.7727127-04	4.9075842-05	-2.88	24.56	28.26
77000.	76054.3	1.9262857+02	1.9262857+02	2.3281574-04	4.2071342-05	-3.42	23.51	27.88
78000.	77030.0	1.8848571+02	1.8848571+02	1.9471169-04	3.5943508-05	-3.89	22.29	27.24
79000.	78005.4	1.8434286+02	1.8434286+02	1.6204834-04	3.0591488-05	-4.24	20.91	26.26
80000.	78980.6	1.8020000+02	1.8020000+02	1.3420582-04	2.5944710-05	-4.45	19.33	24.90
81000.	79955.4	1.8020000+02	1.8020000+02	1.1[illegible]2200-04	2.1450996-05	-2.22	17.82	20.49
82000.	80929.9	1.8020000+02	1.8020000+02	9.1891288-05	1.7744064-05	-.25	16.73	17.02
83000.	81904.1	1.8020000+02	1.8020000+02	7.5950622-05	1.4689445-05	-.25	16.10	16.39
84000.	82878.0	1.8020000+02	1.8020000+02	6.2980652-05	1.2176514-05	-.25	15.48	15.77
85000.	83851.6	1.8020000+02	1.8020000+02	5.2146911-05	1.0068893-05	-.25	14.85	15.13
86000.	84824.9	1.8020000+02	1.8020000+02	4.3191910-05	8.3389282-06	-.25	14.22	14.50
87000.	85798.0	1.8020000+02	1.8020000+02	3.5724639-05	6.8874359-06	-.25	13.58	13.86
88000.	86770.7	1.8020000+02	1.8020000+02	2.9678345-05	5.7106018-06	-.25	12.94	13.22
89000.	87743.1	1.8020000+02	1.8020000+02	2.4518966-05	4.7130584-06	-.25	12.30	12.58
90000.	88715.1	1.8020000+02	1.8020000+02	2.0151138-05	3.9081573-06	-.25	11.65	11.93

TABLE 10. 14B VANDENBERG WINTER (COLD) ATMOSPHERE (VCA-73) (Ref. 10.7)

GEO-METRIC ALTITUDE Z(m)	GEO-POTENTIAL ALTITUDE H(m)	VIRTUAL TEMPERATURE T* (°K)	KINETIC TEMPERATURE T (°K)	PRESSURE P (N/cm²)	DENSITY D(kg/m³)	REL. DEV. (T*) WITH RESPECT TO VRA-71 RD(T*)%	REL. DEV. (P) WITH RESPECT TO VRA-71 RD(P)%	REL. DEV. (D) WITH RESPECT TO VRA-71 RD(D)%
0.	.0	2.7270000+02	2.7210000+02	1.0180000+01	1.3004703+00	-5.03	-.10	5.20
1000.	999.5	2.6696000+02	2.6648000+02	8.9693283+00	1.1704464+00	-6.98	-.87	6.57
2000.	1998.8	2.6122000+02	2.6086000+02	7.8809177+00	1.0510132+00	-7.89	-1.79	6.62
3000.	2997.7	2.5548000+02	2.5524000+02	6.9047076+00	9.4151269-01	-8.24	-2.81	5.92
4000.	3996.3	2.4974000+02	2.4962000+02	6.0312689+00	8.4131451-01	-8.30	-3.90	4.80
5000.	4994.6	2.4400000+02	2.4400000+02	5.2517769+00	7.4981523-01	-8.19	-5.01	3.47
6000.	5992.5	2.3830000+02	2.3830000+02	4.5580398+00	6.6633385-01	-7.92	-6.09	1.98
7000.	6990.2	2.3260000+02	2.3260000+02	3.9423968+00	5.9045721-01	-7.49	-7.14	.37
8000.	7987.5	2.2690000+02	2.2690000+02	3.3976520+00	5.2165361-01	-6.90	-8.12	-1.31
9000.	8984.5	2.2120000+02	2.2120000+02	2.9171181+00	4.5941659-01	-6.23	-9.04	-2.99
10000.	9981.3	2.2086667+02	2.2086667+02	2.4993697+00	3.9421944-01	-3.34	-9.79	-6.68
11000.	10977.7	2.2053333+02	2.2053333+02	2.1409279+00	3.3819378-01	-.63	-10.03	-9.46
12000.	11973.7	2.2020000+02	2.2020000+02	1.8334731+00	2.9006479-01	1.11	-10.03	-11.01
13000.	12969.5	2.1986667+02	2.1986667+02	1.5698082+00	2.4872811-01	2.25	-9.82	-11.80
14000.	13965.0	2.1953333+02	2.1953333+02	1.3437376+00	2.1323162-01	3.12	-9.45	-12.19
15000.	14960.1	2.1920000+02	2.1920000+02	1.1499446+00	1.8275709-01	3.88	-8.96	-12.37
16000.	15954.9	2.1886667+02	2.1886667+02	9.8387086-01	1.5660159-01	4.49	-8.39	-12.33
17000.	16949.5	2.1853333+02	2.1853333+02	8.4159365-01	1.3415970-01	4.64	-7.81	-11.89
18000.	17943.7	2.1820000+02	2.1820000+02	7.1969167-01	1.1490234-01	3.71	-7.26	-10.59
19000.	18937.6	2.1870000+02	2.1870000+02	6.1554150-01	9.8050058-02	3.32	-6.96	-9.91
20000.	19931.2	2.1920000+02	2.1920000+02	5.2659444-01	8.3690010-02	2.72	-6.63	-9.05
21000.	20924.4	2.1970000+02	2.1970000+02	4.5065654-01	7.1458278-02	2.01	-6.28	-8.11
22000.	21917.4	2.2020000+02	2.2020000+02	3.8582201-01	6.1038803-02	1.32	-6.00	-7.25
23000.	22910.0	2.2070000+02	2.2070000+02	3.3044670-01	5.2159878-02	.71	-5.85	-6.57
24000.	23902.4	2.2120000+02	2.2120000+02	2.8312334-01	4.4589290-02	.24	-5.87	-6.13
25000.	24894.4	2.2170000+02	2.2170000+02	2.4265535-01	3.8130028-02	-.12	-6.05	-5.94
26000.	25886.1	2.2220000+02	2.2220000+02	2.0803276-01	3.2615742-02	-.41	-6.32	-5.90
27000.	26877.5	2.2270000+02	2.2270000+02	1.7840172-01	2.7907043-02	-.74	-6.59	-5.85
28000.	27868.6	2.2320000+02	2.2320000+02	1.5304207-01	2.3886475-02	-1.28	-6.70	-5.53
29000.	28859.4	2.2370000+02	2.2370000+02	1.3134525-01	2.0454262-02	-1.95	-7.12	-5.28
30000.	29849.9	2.2420000+02	2.2420000+02	1.1278137-01	1.7524437-02	-2.71	-7.61	-5.04
31000.	30840.0	2.2470000+02	2.2470000+02	9.6878738-02	1.5020203-02	-3.39	-8.17	-4.95
32000.	31829.9	2.2520000+02	2.2520000+02	8.3202466-02	1.2870590-02	-4.03	-8.80	-4.97
33000.	32819.4	2.2740000+02	2.2740000+02	7.1553249-02	1.0961954-02	-3.94	-9.46	-5.74
34000.	33808.7	2.2960000+02	2.2960000+02	6.1612920-02	9.3484401-03	-3.87	-10.10	-6.48
35000.	34797.6	2.3180000+02	2.3180000+02	5.3127079-02	7.9842872-03	-3.83	-10.74	-7.18
36000.	35786.2	2.3400000+02	2.3400000+02	4.5877666-02	6.8298111-03	-3.84	-11.37	-7.83
37000.	36774.5	2.3620000+02	2.3620000+02	3.9674339-02	5.8514099-03	-3.90	-12.02	-8.45
38000.	37762.5	2.3840000+02	2.3840000+02	3.4357967-02	5.0206642-03	-4.02	-12.68	-9.02
39000.	38750.2	2.4060000+02	2.4060000+02	2.9792671-02	4.3138504-03	-4.17	-13.35	-9.57
40000.	39737.5	2.4280000+02	2.4280000+02	2.5866051-02	3.7113266-03	-4.37	-14.03	-10.10
41000.	40724.6	2.4500000+02	2.4500000+02	2.2482605-02	3.1968689-03	-4.58	-14.73	-10.64
42000.	41711.4	2.4720000+02	2.4720000+02	1.9566269-02	2.7571029-03	-4.78	-15.43	-11.19
43000.	42697.8	2.4940000+02	2.4940000+02	1.7048912-02	2.3811340-03	-4.95	-16.15	-11.78
44000.	43683.9	2.5160000+02	2.5160000+02	1.4876175-02	2.0595932-03	-5.06	-16.86	-12.43
45000.	44669.8	2.5380000+02	2.5380000+02	1.2999268-02	1.7843018-03	-5.06	-17.56	-13.17
46000.	45655.3	2.5600000+02	2.5600000+02	1.1371536-02	1.5476761-03	-4.90	-18.25	-14.03
47000.	46640.5	2.5820000+02	2.5820000+02	9.9526405-03	1.3428264-03	-4.54	-18.90	-15.05
48000.	47625.4	2.5820000+02	2.5820000+02	8.7191319-03	1.1764016-03	-4.71	-19.55	-15.57
49000.	48610.0	2.5820000+02	2.5820000+02	7.6385498-03	1.0306020-03	-4.54	-20.23	-16.44
50000.	49594.3	2.5820000+02	2.5820000+02	6.6919231-03	9.0289450-04	-4.78	-20.85	-16.88
51000.	50578.3	2.5820000+02	2.5820000+02	5.8625937-03	7.9098797-04	-4.82	-21.58	-17.61
52000.	51561.9	2.5820000+02	2.5820000+02	5.1332330-03	6.9265652-04	-4.65	-22.26	-18.47
53000.	52545.3	2.5681290+02	2.5681290+02	4.4989681-03	6.1026216-04	-4.80	-22.90	-19.02
54000.	53528.4	2.5542581+02	2.5542581+02	3.9384305-03	5.3709328-04	-4.78	-23.54	-19.70
55000.	54511.1	2.5403871+02	2.5403871+02	3.4440768-03	4.7223997-04	-4.62	-24.15	-20.48
56000.	55493.6	2.5265162+02	2.5265162+02	3.0088639-03	4.1485059-04	-4.33	-24.74	-21.33
57000.	56475.7	2.5126452+02	2.5126452+02	2.6263249-03	3.6413980-04	-3.93	-25.30	-22.24
58000.	57457.5	2.4987742+02	2.4987742+02	2.2906935-03	3.1939316-04	-3.42	-25.82	-23.19
59000.	58439.1	2.4849033+02	2.4849033+02	1.9965887-03	2.7995395-04	-2.84	-26.29	-24.14
60000.	59420.3	2.4710323+02	2.4710323+02	1.7391419-03	2.4523735-04	-2.18	-26.72	-25.06
61000.	60401.2	2.4571613+02	2.4571613+02	1.5140176-03	2.1469426-04	-1.47	-27.09	-26.00
62000.	61381.8	2.4432904+02	2.4432904+02	1.3173056-03	1.8785143-04	-.71	-27.40	-26.88
63000.	62362.1	2.4294194+02	2.4294194+02	1.1454892-03	1.6426373-04	.09	-27.64	-27.71
64000.	63342.1	2.4155484+02	2.4155484+02	9.9539518-04	1.4354014-04	.91	-27.82	-28.47
65000.	64321.8	2.4016774+02	2.4016774+02	8.6441278-04	1.2535453-04	1.74	-27.93	-29.16
66000.	65301.2	2.3878065+02	2.3878065+02	7.5002193-04	1.0937738-04	2.58	-27.95	-29.76
67000.	66280.3	2.3739355+02	2.3739355+02	6.5010309-04	9.5343113-05	3.41	-27.90	-30.27
68000.	67259.0	2.3600645+02	2.3600645+02	5.6287288-04	8.3035469-05	4.24	-27.75	-30.69
69000.	68237.5	2.3461936+02	2.3461936+02	4.8666954-04	7.2222710-05	5.06	-27.52	-31.01
70000.	69215.7	2.3323226+02	2.3323226+02	4.2019844-04	6.2745095-05	5.88	-27.19	-31.23
71000.	70193.5	2.3184517+02	2.3184517+02	3.6225796-04	5.4427624-05	6.69	-26.76	-31.35
72000.	71171.1	2.3045807+02	2.3045807+02	3.1198025-04	4.7175884-05	7.49	-26.23	-31.37
73000.	72148.3	2.2907097+02	2.2907097+02	2.6816368-04	4.0837288-05	8.31	-25.58	-31.29
74000.	73125.3	2.2768387+02	2.2768387+02	2.3046970-04	3.5318852-05	9.16	-24.82	-31.13
75000.	74101.9	2.2629678+02	2.2629678+02	1.9808292-04	3.0550003-05	10.05	-23.95	-30.89
76000.	75078.3	2.2490968+02	2.2490968+02	1.7026424-04	2.6429176-05	11.01	-22.94	-30.59
77000.	76054.3	2.2352258+02	2.2352258+02	1.4659405-04	2.2873878-05	12.07	-21.81	-30.23
78000.	77030.0	2.2213549+02	2.2213549+02	1.2646675-04	1.9824028-05	13.27	-20.54	-29.85
79000.	78005.4	2.2074839+02	2.2074839+02	1.0934830-04	1.7206192-05	14.67	-19.13	-29.48
80000.	78980.6	2.1936129+02	2.1936129+02	9.4366073-05	1.4900207-05	16.31	-17.58	-29.13
81000.	79955.4	2.1797420+02	2.1797420+02	8.1052780-05	1.2870789-05	18.28	-15.86	-28.87
82000.	80929.9	2.1658710+02	2.1658710+02	6.8445205-05	1.0972977-05	19.89	-13.90	-28.19
83000.	81904.1	2.1520000+02	2.1520000+02	5.7823956-05	9.3609094-06	19.13	-11.63	-25.82
84000.	82878.0	2.1520000+02	2.1520000+02	4.9337446-05	7.9868436-06	19.13	-9.36	-23.91
85000.	83851.6	2.1520000+02	2.1520000+02	4.2093396-05	6.8143606-06	19.13	-7.03	-21.95
86000.	84824.9	2.1520000+02	2.1520000+02	3.5912990-05	5.8139562-06	19.13	-4.64	-19.95
87000.	85798.0	2.1520000+02	2.1520000+02	3.0642449-05	4.9605370-06	19.13	-2.21	-17.91
88000.	86770.7	2.1520000+02	2.1520000+02	2.6143789-05	4.2325258-06	19.13	.29	-15.81
89000.	87743.1	2.1520000+02	2.1520000+02	2.2305846-05	3.6112070-06	19.13	2.84	-13.67
90000.	88715.1	2.1520000+02	2.1520000+02	1.9032955-05	3.0813813-06	19.13	5.45	-11.48

ORIGINAL PAGE IS
OF POOR QUALITY

TABLE 10. 15A EDWARDS SUMMER (HOT) ATMOSPHERE (EHA-75) (Ref. 10.8)

GEO-METRIC ALTITUDE	GEO-POTENTIAL ALTITUDE	VIRTUAL TEMPERATURE	KINETIC TEMPERATURE	PRESSURE	DENSITY	REL. DEV. (T*) WITH RESPECT TO ERA-74	REL. DEV. (P) WITH RESPECT TO ERA-74	REL. DEV. (D) WITH RESPECT TO ERA-74
Z(m)	H(m)	T* (°K)	T (°K)	P (N/cm²)	D(kg/m³)	RD(T*)%	RD(P)%	RD(D)%
706.	705.2	3.1805000+02	3.1695000+02	9.2900006+00	1.0175555+00	9.23	-2.16	-10.44
1000.	998.9	3.1209859+02	3.1091518+02	8.9927101+00	1.0037756+00	7.61	-1.95	-8.89
2000.	1997.5	3.0146334+02	3.0067381+02	8.0421432+00	9.2934106-01	5.82	-1.23	-6.66
3000.	2995.7	2.9323000+02	2.9257657+02	7.1692100+00	8.5172758-01	5.22	-.61	-5.54
4000.	3993.7	2.8499667+02	2.8448333+02	6.3701480+00	7.7865946-01	4.79	-.02	-4.59
5000.	4991.3	2.7676334+02	2.7638810+02	5.6405716+00	7.0999023-01	4.42	.53	-3.72
6000.	5988.6	2.6915546+02	2.6892273+02	4.9766757+00	6.4413065-01	4.36	1.08	-3.14
7000.	6985.6	2.6196455+02	2.6187727+02	4.3758858+00	5.8191729-01	4.59	1.67	-2.80
8000.	7982.3	2.5492273+02	2.5492273+02	3.8339298+00	5.2393019-01	5.03	2.32	-2.58
9000.	8978.6	2.4810455+02	2.4810455+02	3.3469597+00	4.6995209-01	5.64	3.05	-2.44
10000.	9974.7	2.4123065+02	2.4123065+02	2.9107930+00	4.2035543-01	6.07	3.91	-2.04
11000.	10970.5	2.3413387+02	2.3413387+02	2.5210631+00	3.7510884-01	5.86	4.81	-.99
12000.	11965.9	2.2703710+02	2.2703710+02	2.1738746+00	3.3356114-01	4.69	5.64	.92
13000.	12961.0	2.1994032+02	2.1994032+02	1.8656988+00	2.9551155-01	2.67	6.24	3.47
14000.	13955.8	2.1284355+02	2.1284355+02	1.5932018+00	2.6076429-01	.34	6.50	6.14
15000.	14950.3	2.0574678+02	2.0574678+02	1.3532391+00	2.2912859-01	-2.03	6.35	8.56
16000.	15944.5	1.9865000+02	1.9865000+02	1.1428509+00	2.0041875-01	-4.83	5.74	11.11
17000.	16938.4	2.0315000+02	2.0315000+02	9.6412891-01	1.6533133-01	-2.87	5.05	8.16
18000.	17931.9	2.0765000+02	2.0765000+02	8.1639213-01	1.3696300-01	-1.17	4.70	5.94
19000.	18925.2	2.1215000+02	2.1215000+02	6.9376273-01	1.1392114-01	.28	4.63	4.33
20000.	19918.1	2.1422692+02	2.1422692+02	5.9106988-01	9.6119186-02	.42	4.69	4.25
21000.	20910.7	2.1630384+02	2.1630384+02	5.0430077-01	8.1219940-02	.46	4.76	4.29
22000.	21903.0	2.1838077+02	2.1838077+02	4.3092430-01	6.8741142-02	.49	4.84	4.33
23000.	22895.0	2.2045769+02	2.2045769+02	3.6879513-01	5.8276230-02	.59	4.92	4.31
24000.	23886.7	2.2253461+02	2.2253461+02	3.1610081-01	4.9484573-02	.84	5.04	4.16
25000.	24878.1	2.2461154+02	2.2461154+02	2.7132461-01	4.2083160-02	1.19	5.05	3.82
26000.	25869.1	2.2668846+02	2.2668846+02	2.3320557-01	3.5839356-02	1.60	5.01	3.40
27000.	26859.9	2.2876538+02	2.2876538+02	2.0070293-01	3.0563484-02	1.96	5.08	3.11
28000.	27850.3	2.3084231+02	2.3084231+02	1.7295921-01	2.6100494-02	2.10	5.44	3.22
29000.	28840.5	2.3291923+02	2.3291923+02	1.4926132-01	2.2323105-02	2.09	5.55	3.39
30000.	29830.3	2.3499615+02	2.3499615+02	1.2900001-01	1.9123856-02	1.98	5.68	3.63
31000.	30819.8	2.3707308+02	2.3707308+02	1.1164329-01	1.6407257-02	1.93	5.83	3.83
32000.	31809.0	2.3915000+02	2.3915000+02	9.6693582-02	1.4084936-02	1.91	5.99	4.00
33000.	32797.9	2.4295333+02	2.4295333+02	8.3927593-02	1.2034792-02	2.63	6.20	3.48
34000.	33786.5	2.4675666+02	2.4675666+02	7.2992877-02	1.0305168-02	3.31	6.51	3.09
35000.	34774.8	2.5056000+02	2.5056000+02	6.3616809-02	8.8447494-03	3.95	6.89	2.83
36000.	35762.7	2.5436333+02	2.5436333+02	5.5563488-02	7.6092987-03	4.53	7.34	2.69
37000.	36750.4	2.5816666+02	2.5816666+02	4.8630504-02	6.5619659-03	5.03	7.84	2.67
38000.	37737.7	2.6197000+02	2.6197000+02	4.2648144-02	5.6715698-03	5.47	8.39	2.77
39000.	38724.7	2.6577333+02	2.6577333+02	3.7471504-02	4.9119873-03	5.85	8.99	2.97
40000.	39711.5	2.6957666+02	2.6957666+02	3.2981186-02	4.2625046-03	6.18	9.62	3.24
41000.	40697.9	2.7338000+02	2.7338000+02	2.9078445-02	3.7055740-03	6.48	10.29	3.58
42000.	41684.0	2.7718333+02	2.7718333+02	2.5681953-02	3.2275543-03	6.77	11.00	3.96
43000.	42669.8	2.8098666+02	2.8098666+02	2.2720108-02	2.8166123-03	7.08	11.75	4.35
44000.	43655.3	2.8479000+02	2.8479000+02	2.0137253-02	2.4629745-03	7.47	12.54	4.72
45000.	44640.5	2.8859333+02	2.8859333+02	1.7879410-02	2.1583862-03	7.96	13.39	5.03
46000.	45625.3	2.9239666+02	2.9239666+02	1.5899658-02	1.8949432-03	8.62	14.31	5.24
47000.	46609.9	2.9620000+02	2.9620000+02	1.4151964-02	1.6644580-03	9.51	15.32	5.30
48000.	47594.2	2.9620000+02	2.9620000+02	1.2610335-02	1.4831369-03	9.31	16.35	6.44
49000.	48578.1	2.9620000+02	2.9620000+02	1.1236606-02	1.3215718-03	9.51	17.34	7.15
50000.	49561.8	2.9620000+02	2.9620000+02	1.0012529-02	1.1776111-03	9.24	18.42	8.41
51000.	50545.1	2.9620000+02	2.9620000+02	8.9216640-03	1.0493240-03	9.19	19.34	9.30
52000.	51528.1	2.9620000+02	2.9620000+02	7.9498910-03	9.3500948-04	9.39	20.33	10.01
53000.	52510.9	2.9205714+02	2.9205714+02	7.0783657-03	8.4429538-04	8.27	21.32	12.06
54000.	53493.3	2.8791429+02	2.8791429+02	6.2918555-03	7.6126856-04	7.33	22.22	13.87
55000.	54475.4	2.8377143+02	2.8377143+02	5.5830145-03	6.8536967-04	6.54	23.02	15.46
56000.	55457.2	2.7962857+02	2.7962857+02	4.9452281-03	6.1607957-04	5.88	23.73	16.85
57000.	56438.7	2.7548571+02	2.7548571+02	4.3723237-03	5.5291355-04	5.33	24.36	18.06
58000.	57419.9	2.7134286+02	2.7134286+02	3.8586056-03	4.9541217-04	4.87	24.91	19.11
59000.	58400.7	2.6720000+02	2.6720000+02	3.3987260-03	4.4314373-04	4.48	25.39	20.01
60000.	59381.3	2.6305714+02	2.6305714+02	2.9877829-03	3.9570284-04	4.13	25.79	20.80
61000.	60361.6	2.5891429+02	2.5891429+02	2.6212478-03	3.5270774-04	3.83	26.13	21.48
62000.	61341.6	2.5477143+02	2.5477143+02	2.2948933-03	3.1380439-04	3.54	26.40	22.08
63000.	62321.2	2.5062857+02	2.5062857+02	2.0048475-03	2.7866054-04	3.26	26.60	22.61
64000.	63300.6	2.4648571+02	2.4648571+02	1.7474222-03	2.4696028-04	2.97	26.75	23.09
65000.	64279.6	2.4234286+02	2.4234286+02	1.5195846-03	2.1841669-04	2.66	26.82	23.54
66000.	65258.4	2.3820000+02	2.3820000+02	1.3182855-03	1.9276726-04	2.33	26.84	23.95
67000.	66236.8	2.3405714+02	2.3405714+02	1.1406493-03	1.6975212-04	1.96	26.79	24.35
68000.	67214.9	2.2991429+02	2.2991429+02	9.8444938-04	1.4914501-04	1.55	26.66	24.73
69000.	68192.8	2.2577143+02	2.2577143+02	8.4723949-04	1.3072944-04	1.10	26.47	25.09
70000.	69170.3	2.2162857+02	2.2162857+02	7.2718143-04	1.1430716-04	.61	26.20	25.43
71000.	70147.5	2.1748571+02	2.1748571+02	6.2217712-04	9.9694729-05	.08	25.85	25.75
72000.	71124.4	2.1334286+02	2.1334286+02	5.3091288-04	8.6722613-05	-.49	25.40	26.02
73000.	72101.0	2.0920000+02	2.0920000+02	4.5154095-04	7.5232028-05	-1.08	24.86	26.22
74000.	73077.3	2.0505714+02	2.0505714+02	3.8289547-04	6.5082788-05	-1.69	24.21	26.34
75000.	74053.3	2.0091429+02	2.0091429+02	3.2369137-04	5.6139469-05	-2.29	23.44	26.34
76000.	75029.0	1.9677143+02	1.9677143+02	2.7274609-04	4.8282385-05	-2.88	22.54	26.18
77000.	76004.4	1.9262857+02	1.9262857+02	2.2906303-04	4.1390419-05	-3.42	21.50	25.81
78000.	76979.5	1.8848571+02	1.8848571+02	1.9156933-04	3.5361767-05	-3.89	20.31	25.17
79000.	77954.3	1.8434286+02	1.8434286+02	1.5939712-04	3.0099630-05	-4.24	18.95	24.22
80000.	78928.8	1.8020000+02	1.8020000+02	1.3204098-04	2.5506019-05	-4.45	17.40	22.87
81000.	79903.0	1.8020000+02	1.8020000+02	1.0919571-04	2.1103859-05	-2.22	15.91	18.54
82000.	80876.8	1.8020000+02	1.8020000+02	9.0289115-05	1.7478943-05	-.25	14.83	15.12
83000.	81850.4	1.8020000+02	1.8020000+02	7.4744225-05	1.4459610-05	-.25	14.22	14.51
84000.	82823.7	1.8020000+02	1.8020000+02	6.1969757-05	1.1974335-05	-.25	13.60	13.89
85000.	83796.7	1.8020000+02	1.8020000+02	5.1279068-05	9.9201202-06	-.25	12.99	13.27
86000.	84769.3	1.8020000+02	1.8020000+02	4.2343139-05	8.2015991-06	-.25	12.36	12.64
87000.	85741.7	1.8020000+02	1.8020000+02	3.5085678-05	6.7825317-06	-.25	11.74	12.02
88000.	86713.8	1.8020000+02	1.8020000+02	2.9077530-05	5.6247711-06	-.25	11.11	11.39
89000.	87685.5	1.8020000+02	1.8020000+02	2.4003982-05	4.6634674-06	-.25	10.48	10.76
90000.	88657.0	1.8020000+02	1.8020000+02	1.9807816-05	3.8452148-06	-.25	9.84	10.11

ORIGINAL PAGE IS
OF POOR QUALITY

TABLE 10.15B EDWARDS WINTER (COLD) ATMOSPHERE (ECA-75) (Ref. 10.8)

GEO-METRIC ALTITUDE	GEO-POTENTIAL ALTITUDE	VIRTUAL TEMPERATURE	KINETIC TEMPERATURE	PRESSURE	DENSITY	REL. DEV. (T*) WITH RESPECT TO ERA-74	REL. DEV. (P) WITH RESPECT TO ERA-74	REL. DEV. (D) WITH RESPECT TO ERA-74
Z(m)	H(m)	T* (°K)	T (°K)	P (N/cm²)	D(kg/m³)	RD(T*)%	RD(P)%	RD(D)%
706.	705.2	2.7365000+02	2.7315000+02	9.3900000+00	1.1953854+00	-6.01	-1.11	5.22
1000.	998.9	2.7169868+02	2.7123291+02	9.0436318+00	1.1595598+00	-6.32	-1.40	5.25
2000.	1997.5	2.6506151+02	2.6471218+02	7.9626412+00	1.0465218+00	-6.96	-2.21	5.11
3000.	2995.7	2.5842434+02	2.5819145+02	6.9882666+00	9.4204977-01	-7.27	-3.11	4.48
4000.	3993.7	2.5178717+02	2.5167073+02	6.1123285+00	8.4568942-01	-7.43	-4.07	3.62
5000.	4991.3	2.4515001+02	2.4515000+02	5.3270900+00	7.5700013-01	-7.51	-5.05	2.66
6000.	5988.6	2.3965000+02	2.3965000+02	4.6267853+00	6.7257345-01	-7.08	-6.02	1.14
7000.	6985.6	2.3415000+02	2.3415000+02	4.0054143+00	5.9592430-01	-6.51	-6.94	-.46
8000.	7982.3	2.2865000+02	2.2865000+02	3.4556265+00	5.2649399-01	-5.80	-7.78	-2.11
9000.	8978.6	2.2315000+02	2.2315000+02	2.9706049+00	4.6375200-01	-4.99	-8.53	-3.73
10000.	9974.7	2.2248333+02	2.2248333+02	2.5483443+00	3.9902337-01	-2.17	-9.03	-7.01
11000.	10970.5	2.2181667+02	2.2181667+02	2.1850870+00	3.4317250-01	.29	-9.16	-9.42
12000.	11965.9	2.2115000+02	2.2115000+02	1.8727532+00	2.9500646-01	1.97	-8.99	-10.75
13000.	12961.0	2.2048333+02	2.2048333+02	1.6043217+00	2.5348568-01	2.93	-8.64	-11.24
14000.	13955.8	2.1981667+02	2.1981667+02	1.3737173+00	2.1770802-01	3.62	-8.18	-11.39
15000.	14950.3	2.1915000+02	2.1915000+02	1.1756991+00	1.8689287-01	4.35	-7.60	-11.45
16000.	15944.5	2.1848333+02	2.1848333+02	1.0057510+00	1.6036523-01	4.67	-6.95	-11.10
17000.	16938.4	2.1781667+02	2.1781667+02	8.5996912-01	1.3754010-01	4.14	-6.30	-10.02
18000.	17931.9	2.1715000+02	2.1715000+02	7.3495366-01	1.1790656-01	3.35	-5.74	-8.80
19000.	18925.2	2.1731667+02	2.1731667+02	6.2800190-01	1.0067124-01	2.73	-5.29	-7.80
20000.	19918.1	2.1748333+02	2.1748333+02	5.3667863-01	8.5965850-02	1.94	-4.94	-6.75
21000.	20910.7	2.1765000+02	2.1765000+02	4.5869091-01	7.3417381-02	1.08	-4.71	-5.73
22000.	21903.0	2.1781667+02	2.1781667+02	3.9208290-01	6.2708206-02	.23	-4.62	-4.83
23000.	22895.0	2.1798333+02	2.1798333+02	3.3518764-01	5.3567505-02	-.54	-4.64	-4.13
24000.	23886.7	2.1815000+02	2.1815000+02	2.8658279-01	4.5764786-02	-1.15	-4.77	-3.66
25000.	24878.1	2.1903125+02	2.1903125+02	2.4511787-01	3.8985798-02	-1.32	-5.09	-3.82
26000.	25869.1	2.1991250+02	2.1991250+02	2.0978271-01	3.3232181-02	-1.43	-5.53	-4.11
27000.	26859.9	2.2079375+02	2.2079375+02	1.7965517-01	2.8345894-02	-1.59	-5.94	-4.37
28000.	27850.3	2.2167500+02	2.2167500+02	1.5394886-01	2.4193466-02	-1.95	-6.16	-4.33
29000.	28840.5	2.2255625+02	2.2255625+02	1.3200119-01	2.0662117-02	-2.45	-6.67	-4.32
30000.	29830.3	2.2343750+02	2.2343750+02	1.1325157-01	1.7657204-02	-3.04	-7.22	-4.32
31000.	30819.8	2.2431875+02	2.2431875+02	9.7223701-02	1.5098938-02	-3.55	-7.82	-4.42
32000.	31809.0	2.2520000+02	2.2520000+02	8.3514365-02	1.2918991-02	-4.03	-8.46	-4.62
33000.	32797.9	2.2740000+02	2.2740000+02	7.1818008-02	1.1002544-02	-3.94	-9.12	-5.39
34000.	33786.5	2.2960000+02	2.2960000+02	6.1841039-02	9.3830738-03	-3.87	-9.77	-6.13
35000.	34774.8	2.3180000+02	2.3180000+02	5.3324127-02	8.0138092-03	-3.83	-10.41	-6.84
36000.	35762.7	2.3400000+02	2.3400000+02	4.6047458-02	6.8551330-03	-3.84	-11.05	-7.49
37000.	36750.4	2.3620000+02	2.3620000+02	3.9820938-02	5.8730812-03	-3.90	-11.69	-8.11
38000.	37737.7	2.3840000+02	2.3840000+02	3.4485111-02	5.0392494-03	-4.02	-12.35	-8.69
39000.	38724.7	2.4060000+02	2.4060000+02	2.9902954-02	4.3298111-03	-4.17	-13.03	-9.24
40000.	39711.5	2.4280000+02	2.4280000+02	2.5961265-02	3.7250938-03	-4.37	-13.71	-9.77
41000.	40697.9	2.4500000+02	2.4500000+02	2.2566185-02	3.2086792-03	-4.58	-14.41	-10.30
42000.	41684.0	2.4720000+02	2.4720000+02	1.9638176-02	2.7674408-03	-4.78	-15.12	-10.86
43000.	42669.8	2.4940000+02	2.4940000+02	1.7112656-02	2.3899994-03	-4.95	-15.84	-11.45
44000.	43655.3	2.5160000+02	2.5160000+02	1.4932060-02	2.0672607-03	-5.06	-16.55	-12.11
45000.	44640.5	2.5380000+02	2.5380000+02	1.3047066-02	1.7909775-03	-5.06	-17.26	-12.85
46000.	45625.3	2.5600000+02	2.5600000+02	1.1413879-02	1.5535202-03	-4.90	-17.94	-13.72
47000.	46609.9	2.5820000+02	2.5820000+02	9.9894762-03	1.3477931-03	-4.54	-18.60	-14.73
48000.	47594.2	2.5820000+02	2.5820000+02	8.7515234-03	1.1807566-03	-4.71	-19.26	-15.26
49000.	48578.1	2.5820000+02	2.5820000+02	7.6668501-03	1.0344262-03	-4.54	-19.94	-16.13
50000.	49561.8	2.5820000+02	2.5820000+02	6.7167425-03	9.0621996-04	-4.78	-20.56	-16.57
51000.	50545.1	2.5820000+02	2.5820000+02	5.8843326-03	7.9390049-04	-4.82	-21.29	-17.31
52000.	51528.1	2.5820000+02	2.5820000+02	5.1550770-03	6.9551897-04	-4.65	-21.97	-18.17
53000.	52510.9	2.5681290+02	2.5681290+02	4.5156181-03	6.1251270-04	-4.80	-22.62	-18.72
54000.	53493.3	2.5542581+02	2.5542581+02	3.9530086-03	5.3908073-04	-4.78	-23.25	-19.40
55000.	54475.4	2.5403871+02	2.5403871+02	3.4568083-03	4.7398329-04	-4.62	-23.87	-20.18
56000.	55457.2	2.5265162+02	2.5265162+02	3.0199671-03	4.1638064-04	-4.33	-24.46	-21.04
57000.	56438.7	2.5126452+02	2.5126452+02	2.6360655-03	3.6548161-04	-3.93	-25.02	-21.96
58000.	57419.9	2.4987742+02	2.4987742+02	2.2991598-03	3.2056808-04	-3.42	-25.54	-22.90
59000.	58400.7	2.4849033+02	2.4849033+02	2.0039630-03	2.8098631-04	-2.84	-26.02	-23.86
60000.	59381.3	2.4710323+02	2.4710323+02	1.7455506-03	2.4613547-04	-2.18	-26.44	-24.80
61000.	60361.6	2.4571613+02	2.4571613+02	1.5196228-03	2.1548581-04	-1.47	-26.82	-25.73
62000.	61341.6	2.4432904+02	2.4432904+02	1.3221478-03	1.8854141-04	-.71	-27.13	-26.61
63000.	62321.2	2.4294194+02	2.4294194+02	1.1497116-03	1.6486597-04	.09	-27.38	-27.44
64000.	63300.6	2.4155484+02	2.4155484+02	9.9906682-04	1.4407182-04	.91	-27.55	-28.21
65000.	64279.6	2.4016774+02	2.4016774+02	8.6760521-04	1.2580705-04	1.74	-27.66	-28.89
66000.	65258.4	2.3878065+02	2.3878065+02	7.5278520-04	1.0977697-04	2.58	-27.68	-29.50
67000.	66236.8	2.3739355+02	2.3739355+02	6.5249681-04	9.5687866-05	3.41	-27.63	-30.02
68000.	67214.9	2.3600645+02	2.3600645+02	5.6492328-04	8.3339691-05	4.24	-27.48	-30.44
69000.	68192.8	2.3461936+02	2.3461936+02	4.8845291-04	7.2479725-05	5.06	-27.25	-30.76
70000.	69170.3	2.3323226+02	2.3323226+02	4.2174339-04	6.2973022-05	5.88	-26.92	-30.98
71000.	70147.5	2.3184517+02	2.3184517+02	3.6359310-04	5.4621220-05	6.69	-26.49	-31.10
72000.	71124.4	2.3045807+02	2.3045807+02	3.1306743-04	4.7340393-05	7.49	-25.95	-31.11
73000.	72101.0	2.2907097+02	2.2907097+02	2.6913643-04	4.0983200-05	8.31	-25.31	-31.04
74000.	73077.3	2.2768387+02	2.2768387+02	2.3127556-04	3.5448551-05	9.16	-24.55	-30.88
75000.	74053.3	2.2629678+02	2.2629678+02	1.9875049-04	3.0649185-05	10.05	-23.67	-30.64
76000.	75029.0	2.2490968+02	2.2490968+02	1.7086029-04	2.6510239-05	11.01	-22.66	-30.33
77000.	76004.4	2.2352258+02	2.2352258+02	1.4707565-04	2.2944450-05	12.07	-21.52	-29.98
78000.	76979.5	2.2213549+02	2.2213549+02	1.2694359-04	1.9889831-05	13.27	-20.25	-29.60
79000.	77954.3	2.2074839+02	2.2074839+02	1.0971069-04	1.7252922-05	14.67	-18.83	-29.22
80000.	78928.8	2.1936129+02	2.1936129+02	9.4690323-05	1.4957428-05	16.31	-17.27	-28.87
81000.	79903.0	2.1797420+02	2.1797420+02	8.1262589-05	1.2902260-05	18.28	-15.55	-28.60
82000.	80876.8	2.1658710+02	2.1658710+02	6.8721771-05	1.1002541-05	19.89	-13.58	-27.92
83000.	81850.4	2.1520000+02	2.1520000+02	5.8037340-05	9.3953013-06	19.13	-11.31	-25.55
84000.	82823.7	2.1520000+02	2.1520000+02	4.9518347-05	8.0164671-06	19.13	-9.02	-23.63
85000.	83796.7	2.1520000+02	2.1520000+02	4.2247176-05	6.8390966-06	19.13	-6.68	-21.67
86000.	84769.3	2.1520000+02	2.1520000+02	3.6045611-05	5.8352351-06	19.13	-4.29	-19.66
87000.	85741.7	2.1520000+02	2.1520000+02	3.0755102-05	4.9785376-06	19.13	-1.84	-17.60
88000.	86713.8	2.1520000+02	2.1520000+02	2.6241243-05	4.2478442-06	19.13	.66	-15.50
89000.	87685.5	2.1520000+02	2.1520000+02	2.2386909-05	3.6240816-06	19.13	3.22	-13.35
90000.	88657.0	2.1520000+02	2.1520000+02	1.9102097-05	3.0027062-06	19.13	5.84	-11.15

ORIGINAL PAGE IS
OF POOR QUALITY

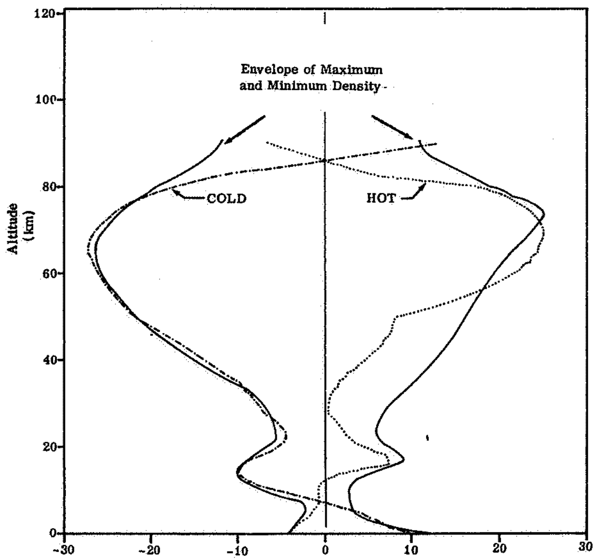

FIGURE 10.1 RELATIVE DEVIATIONS (%) OF EXTREME KENNEDY SPACE CENTER DENSITY PROFILES WITH RESPECT TO PRA-63

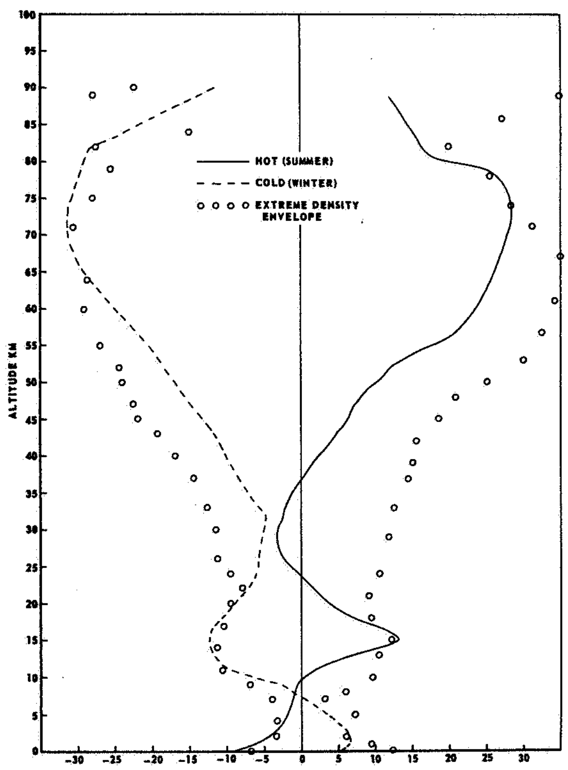

FIGURE 10.2 RELATIVE DEVIATIONS (%) OF EXTREME VANDENBERG DENSITY PROFILES WITH RESPECT TO VRA-71

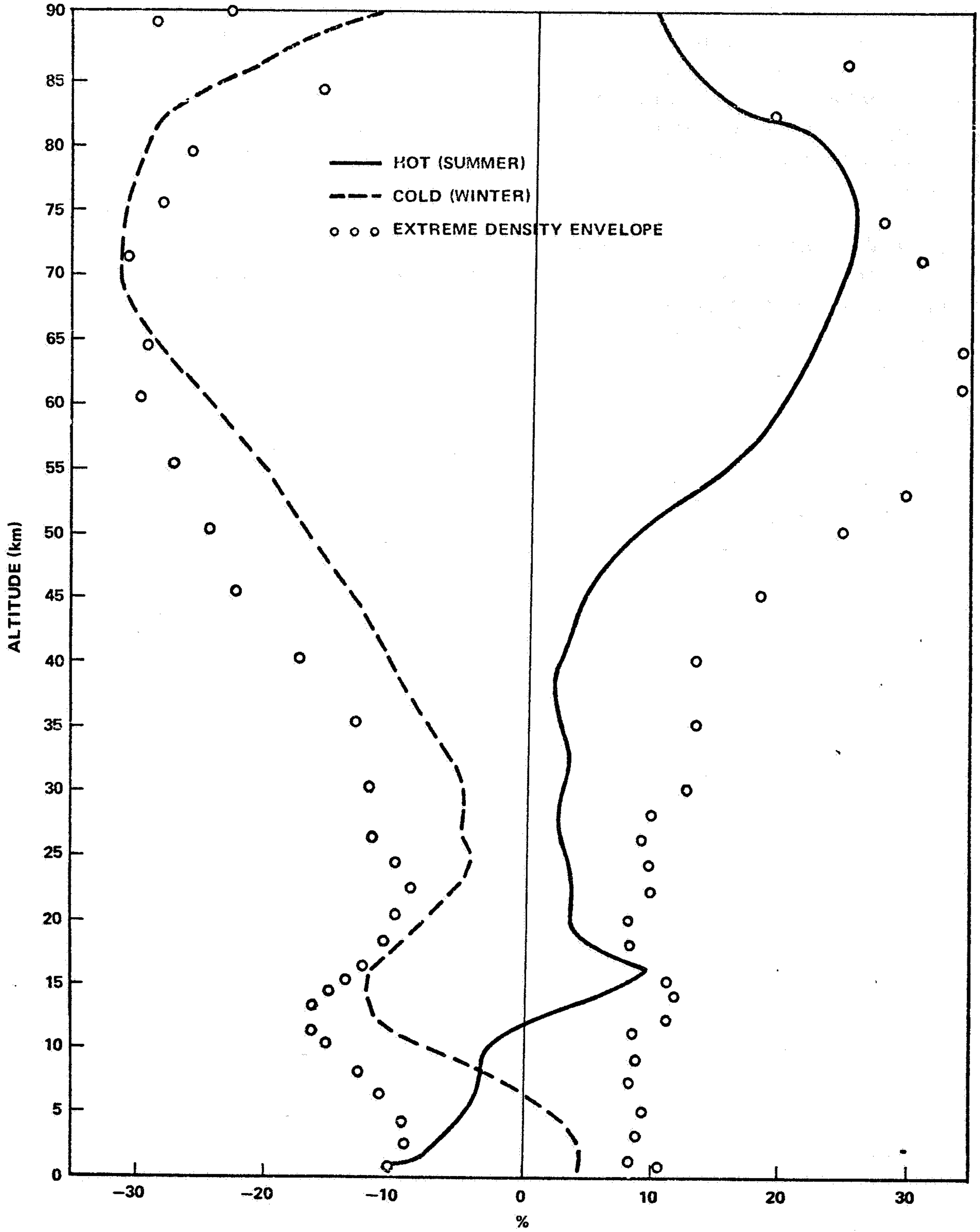

FIGURE 10.3 RELATIVE DEVIATIONS (%) OF EXTREME EDWARDS DENSITY PROFILES WITH RESPECT TO ERA-75

observed in the atmosphere. The results shown above 30 km are somewhat speculative because of the limited data from this region of the atmosphere. Isopycnic levels (levels of minimum density variation) are noted at approximately 8 and 86 km. Another level of minimum density variability is seen at 24 km, and levels of maximum variability occur at 0, 15, and 68 km altitude. The associated extreme temperature* profiles for Kennedy Space Center are given in Figure 10.4.

The two Vandenberg extreme density profiles are shown in Figure 10.2 as percent deviations from the Vandenberg Reference Atmosphere, 1971. Levels of minimum density variation are located at ~ 8, 30 and 90 km altitude. Levels of maximum variability occur at 0, 15 and 73 km. The Hot and Cold Vandenberg temperature* profiles are shown in Figure 10.5.

The two Edwards AFB extreme density profiles are shown in Figure 10.3 as percent deviations from the Edwards Reference Atmosphere, 1975. The Hot and Cold Edwards temperature profiles are shown in Figure 10.6. These extreme density and temperature profiles again have structures similar to the Kennedy and Vandenberg models. Temperatures below 10 km altitude are virtual temperatures. Virtual temperature includes moisture to avoid computation of specific gas constant for moist air.

$$T_v = T(1 + 0.61\,w) \;,$$

where

T_v = virtual temperature (°K)

T = kinetic temperature (°K)

w = mixing ratio, grams of water vapor/kilograms of dry air (g/kg).

Tables 10.13 A and B, 10.14 A and B, and 10.15 A and B give the numerical data used to prepare Figures 10.1 through 10.6. These three sets of extreme atmospheres are available as computerized subroutines upon request from the NASA-MSFC Space Sciences Laboratory, Atmospheric Sciences Division.

10.7 Reference Atmospheres

In design and preflight analysis of space vehicles, special nominal atmospheres are used to represent the mean or median thermodynamic conditions with respect to altitude. For general worldwide design, the U. S. Standard

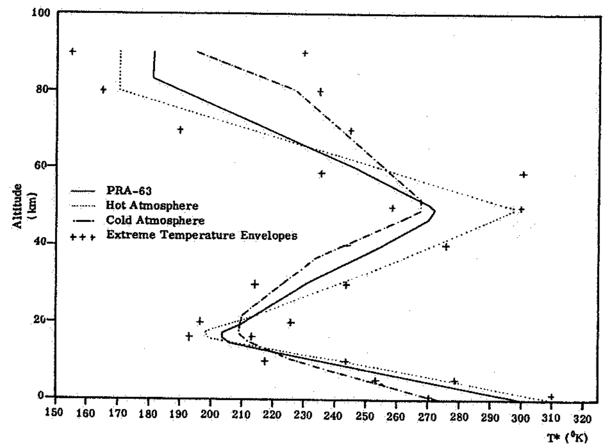

FIGURE 10.4 VIRTUAL TEMPERATURE PROFILES OF THE KENNEDY SPACE CENTER HOT, COLD, AND PRA-63

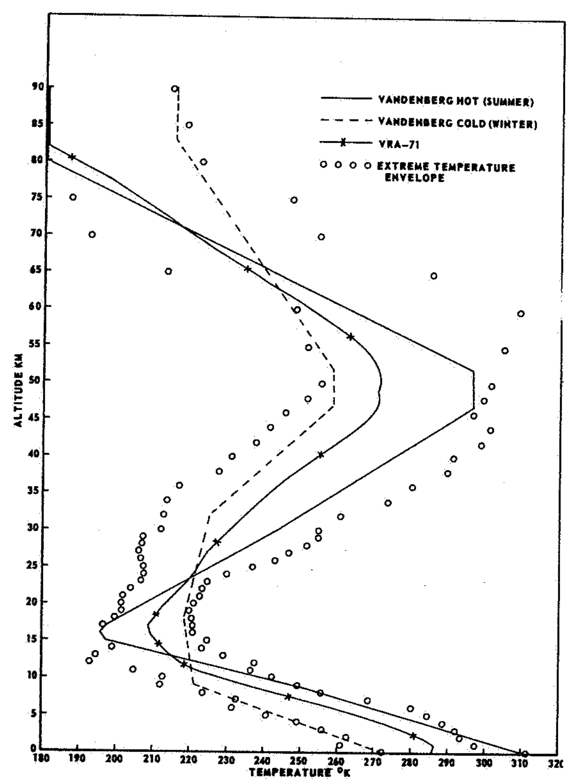

FIGURE 10.5 VIRTUAL TEMPERATURE PROFILES OF THE VANDENBERG HOT, COLD, AND VRA-71 (Ref. 10.7)

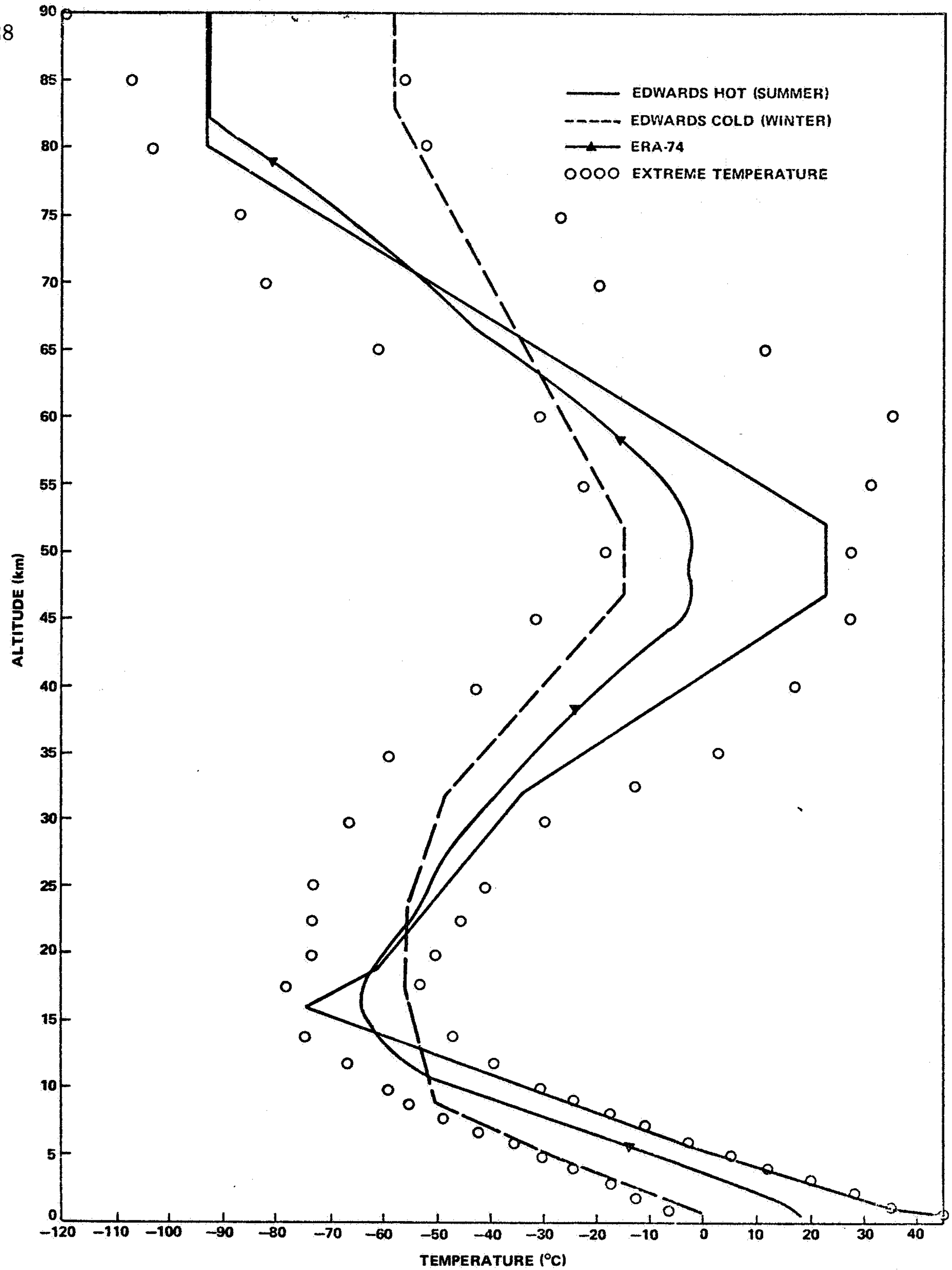

FIGURE 10.6 VIRTUAL TEMPERATURE PROFILES OF THE EDWARDS HOT, COLD, AND ERA -75

Atmosphere, 1976 (US 76) (Ref. 10.1), is used, but more specific atmospheres are needed at each launch area. A group of Range Reference Atmospheres (Ref. 10.3) have been prepared to represent the thermodynamic medians in the first 30 km at various launch areas. References 10.11 and 10.12 which describe Global Reference Atmospheres (GRA-74) are also used.

The Patrick Reference Atmosphere (PRA-63) is a more extensive reference atmosphere presenting data to 700 km for the Eastern Test Range. Because of the utility of this atmosphere, a simplified version is given as Table 10.8 from Reference 10.2. The computer subroutine used to prepare these values is available from the Atmospheric Sciences Division, Space Sciences Laboratory, MSFC, NASA, as Computer Subroutine PRA-63. Criteria for orbital studies are in Reference 10.9.

Reference atmospheres are also available for SAMTEC (Vandenberg AFB) (Ref. 10.5 and Table 10.9) and Edwards AFB (Ref. 10.8 and Table 10.10). These provide an annual atmospheric model to 700 km and have been designated as Computer Subroutines VRA-71 and ERA-75, respectively.

In Tables 10.8, 10.9 and 10.10 the values are given in standard computer printout, where the two-digit numbers that are at the end of the tabular value (number preceded by E) indicate the power of 10 by which the respective principal value must be multiplied. For example, a tabular value indicated as 2.9937265E 02 is 299.37265 or .15464054E-04 is 0.000015464054.

10.8 Reentry – Global Reference Atmosphere Model

10.8.1 Reentry Atmospheric Model

The atmospheric model to be used for all reentry analyses except lower altitudes specified in subsection 10.6 is the GRA-74 (Ref. 10.11 and 10.12). This model generates realistic profiles of atmospheric variables – wind, pressure, temperature, and density – along any vehicle trajectory from orbital altitudes to sea level on a worldwide basis.

A computer technique described in Refs. 10.11 and 10.12 is available to give these variables and their structure as a function of the three spatial coordinates – latitude, longitude, and altitude – and of the time domain (seasonal). Called the GRA-74, it is a composite of other atmospheric models along with new techniques to join models and simulate perturbations. This computer program is available upon request to the Atmospheric Sciences Division, Space Sciences Laboratory, Marshall Space Flight Center, Alabama 35812.

REFERENCES

10.1 "U. S. Standard Atmosphere, 1976," United States Government Printing Office, Washington, D. C., October 1976.

10.2 Smith, Orvel E.; and Weidner, Don K., "A Reference Atmosphere for Patrick AFB, Florida, Annual (1963 Revision)." NASA TM X-53139, Sept. 23, 1964.

10.3 IRIG Document No. 104-63, Range Reference Atmosphere Documents published by Secretariat, Range Commander's Council, White Sands Missile Range, New Mexico. The following reference atmospheres have been published under this title:

(1) Atlantic Missile Range Reference Atmosphere for Cape Kennedy, Florida (Part I), Sept. 1963.

(2) White Sands Missile Range Reference Atmosphere (Part I), Aug. 1964.

(3) Fort Churchill Missile Range Reference Atmosphere for Fort Churchill, Canada (Part I), Dec. 1964.

(4) Pacific Missile Range Reference Atmosphere for Eniwetok, Marshall Islands (Part I), Dec. 1964.

(5) Fort Greely Missile Range Reference Atmosphere (Part I), Nov. 1964.

(6) Pacific Missile Range Reference Atmosphere for Point Arguello, California (Part I), Aug. 1965.

(7) Eglin Gulf Test Range Reference Atmophere, Eglin AFB, Florida (Part I), Aug. 1965.

(8) Wallops Island Test Range Reference Atmosphere (Part I), Sept. 1965.

(9) Eastern Test Range Reference Atmosphere for Ascension Island, South Atlantic (Part I), July 1966.

REFERENCES (Continued)

(10) Lihu, Kauai, Hawaii Reference Atmosphere (Part I), January 1970.

(11) Johnston Island Test Site Reference Atmosphere (Part I), January 1970.

(12) Edwards Air Force Base Reference Atmosphere (Part I), Sept. 1972.

(13) Cape Kennedy, Florida Reference Atmosphere (Part II), July 1971.

(14) White Sands Missile Range Reference Atmosphere (Part II), July 1971.

(15) Wallops Island Test Range Reference Atmosphere (Part II), July 1971.

(16) Fort Greely Missile Range Reference Atmosphere (Part II), July 1971.

(17) Kwajalein Missile Range, Kwajalein, Marshall Islands Reference Atmosphere (Part I), October 1974.

(18) Pacific Missile Test Center Reference Atmosphere for Point Arguello, California (Part II), November 1975.

10.4 Smith, J. W., "Density Variations and Isopycnic Layer." Journal of Applied Meteorology, vol. 3, no. 3, June 1964, pp. 290-298.

10.5 Carter, E. A.; and Brown, S. C., "A Reference Atmosphere for Vandenberg AFB, California, Annual (1971 Version)." NASA TM X-64590, NASA-Marshall Space Flight Center, Alabama, May 10, 1971.

10.6 Buell, C. E., "Some Relations Among Atmospheric Statistics." Journal of Meteorology, vol. 11, June 1954, pp. 238-244.

10.7 Johnson, D. L.; "Hot and Cold Atmospheres for Vandenberg AFB, California (1973 Version)", NASA TM X-64756, NASA-Marshall Space Flight Center, Alabama, June 26, 1973.

REFERENCES (Concluded)

10.8 Johnson, D. L., "Hot, Cold, and Annual Reference Atmospheres for Edwards Air Force Base, California (1975 Version)." NASA TM X-64970, November 1975.

10.9 "Space and Planetary Environment Criteria Guidelines for Use in Space Vehicle Development, 1971 Revision." NASA TM X-64627, November 15, 1971. (Revision in process for publication; contact the Atmospheric Sciences Division, Space Sciences Laboratory, Marshall Space Flight Center, Alabama 35812, for copy when available.)

10.10 "U. S. Standard Atmosphere Supplements 1966." United States Government Printing Office, Washington, D. C. 20402, 1966.

10.11 Justus, C. G., et al., "Four-D Global Reference Atmosphere Technical Description, Part I." NASA TM X-64871, NASA/Marshall Space Flight Center, Huntsville, Ala., September 1974.

10.12 Justus, C. G., et al., "Four-D Global Reference Atmosphere Users Manual and Programmers Manual, Part II." NASA TM X-64872, NASA/Marshall Space Flight Center, Huntsville, Ala., September 1974.

SECTION XI. ATMOSPHERIC ATTENUATION

11.1 Introduction

Earth-viewing space missions offer exciting new possibilities in several earth resources disciplines – geography, hydrology, agriculture, geology, and oceanography, to name a few. A most useful tool in planning experiments and applying space technology to earth observation is a statistical description of atmospheric parameters. For example, cloud cover statistics might be used to predict mission feasibility or the probability of observing a given target area in a given number of satellite passes.

To meet the need for atmospheric statistics, NASA-MSFC has sponsored the development of the four-dimensional atmospheric models (subsection 11.4) and the world-wide cloud model (subsection 11.3). The goal of this work was to produce atmospheric attenuation models to predict degradation effects for all classes of sensors for application to earth-sensing experiments from space-borne platforms. To insure maximum utility and application of these products NASA-MSFC also sponsored the development of an "Interaction Model of Microwave Energy and Atmospheric Variables," a complete description of the effects of atmospheric moisture upon microwaves.

11.2 Interaction Model of Microwave Energy and Atmospheric Variables

While the visible and infrared wavelengths find clouds opaque, the microwave part of the electromagnetic spectrum is unique in that cloud and rain particles vary from very weak absorbers and scatterers to very significant contributors to the electromagnetic environment. This is illustrated in Figures 11.1, 11.2, and 11.3, which are extracted from the final report on the interaction model (Ref. 11.1).

11.2.1 Scattering and Extinction Properties of Water Clouds Over the Range 10 cm to 10 μm

Figures 11.1 and 11.2 show the unit-volume scattering and extinction properties of two modeled cloud drop distributions computed using the Mie theory. Figure 11.1 gives the extinction coefficient as a function

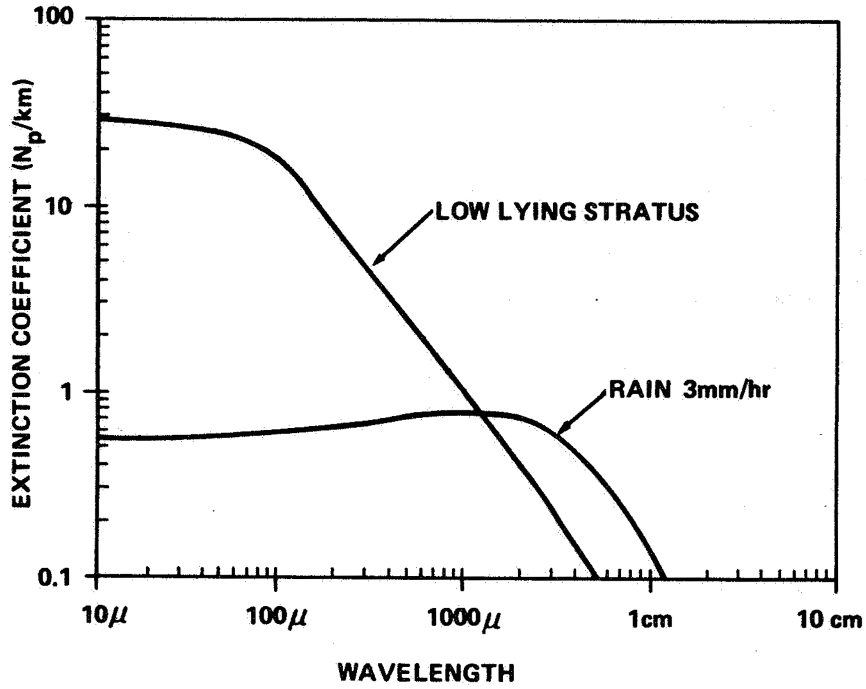

FIGURE 11.1 EXTINCTION COEFFICIENT AS A FUNCTION OF WAVELENGTH

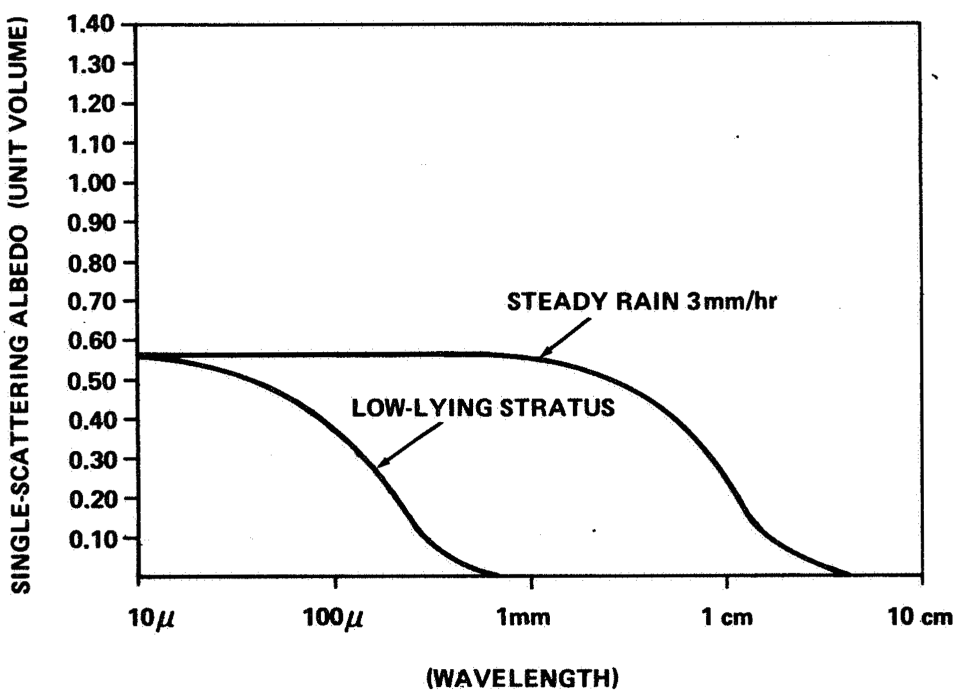

FIGURE 11.2 SINGLE SCATTERING ALBEDO FOR TWO CLOUD MODELS

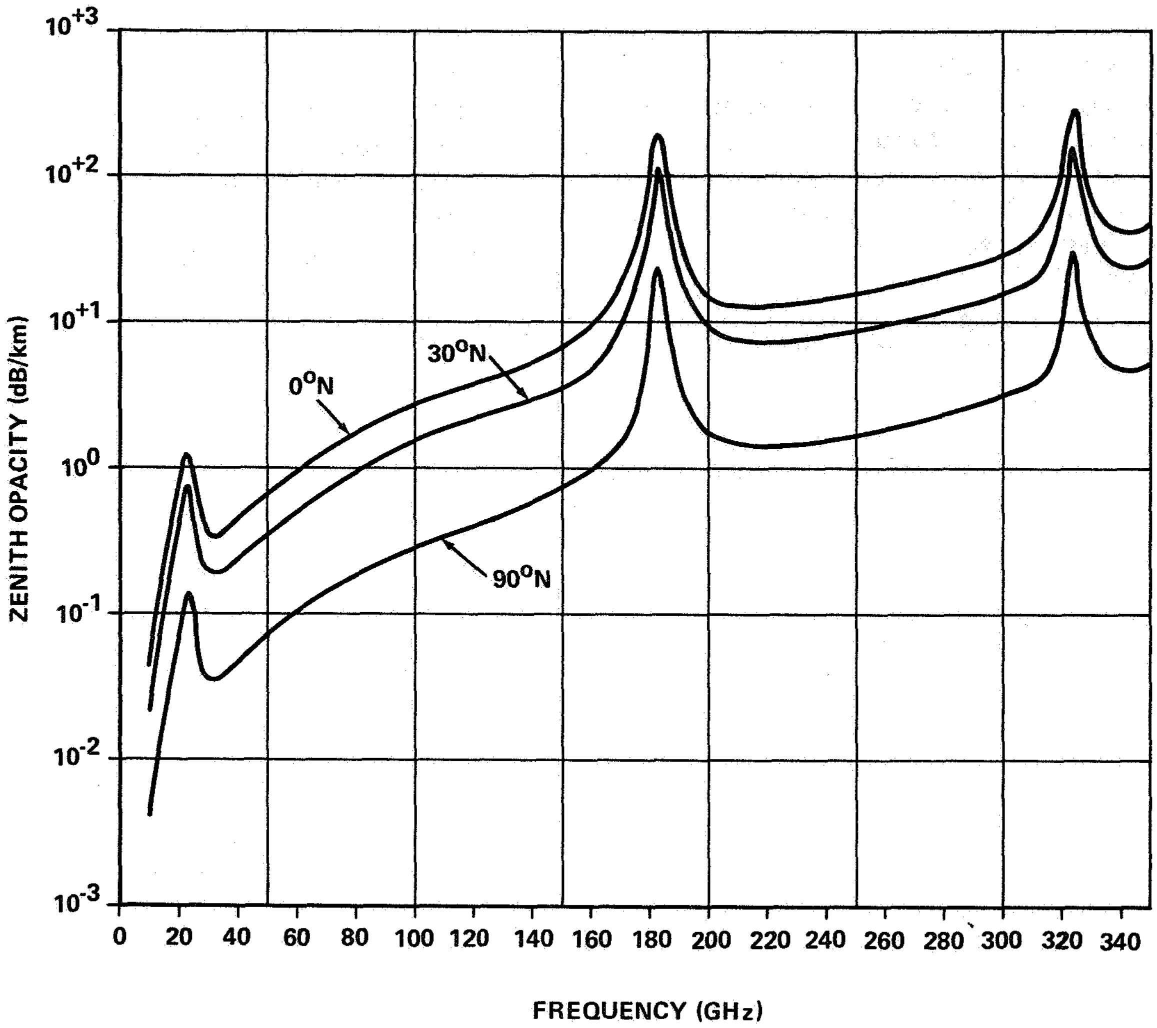

FIGURE 11.3 ZENITH OPACITY

of wavelength while Figure 11.2 presents the single scattering albedo for two cloud models representing low clouds and rainy conditions. The curves show the wavelength regimes appropriate to the two cloud types in which scattering effects are relatively unimportant, and in which the extinction coefficient follows the simple Rayleigh ($1/\lambda^2$) dependence.

11.2.2 Zenith Opacity due to Atmospheric Water Vapor as a Function of Latitude

In the preparation of Figure 11.3 five years of climatological data from the MIT Planetary Circulations Project were used to obtain mean water vapor distributions applicable to the latitudes 0° N, 30° N, and 90° N, corresponding to tropical, mid-latitude, and arctic conditions. The total water vapor content for the three cases are 4.5, 2.5, and 0.5 g/cm^2, respectively. The curves demonstrate the effect of climatological extremes in simulating and predicting the influence of atmospheric water vapor upon surface observations from a space observer, over the range from 10 to 350 gigahertz. A detailed report on the interaction model (Ref. 11.1) is available upon request to the Atmospheric Sciences Division, Space Sciences Laboratory, MSFC/NASA.

11.3 Cloud Cover (World-Wide Cloud Cover Model)

11.3.1 Introduction

One of the main obstructions to observing the earth's surface from satellite altitudes is cloud cover. Although some sensors show less cloud effect than others, of the three main classes of sensors (cameras — visual, thermal infrared, and radar) cameras are the most advanced, but are also the most sensitive to cloud cover.

The expense and complexity of space missions demand that the consequence of cloud cover be evaluated in advance. First, mission feasibility must be determined. Then, the mission must be planned to provide sufficient time and expendables to insure a high probability of success. Previously, in computer simulations of earth-oriented space missions, clouds were either disregarded completely or were assumed to be present about 50 percent of the time. Now, by using the world-wide cloud cover statistics (Refs. 11.2 through 11.5) and the simulation procedure described here, it is possible to provide a realistic evaluation of the consequence of cloud cover on earth-viewing space missions.

Results of the simulations, which can be made for target areas of various size on a global basis, are generally given in two forms. First, the satellite pass number and probability of success are considered as variables with the required percent photographic coverage of the target area fixed. For example, if 95 percent photographic coverage of the target area is required for success, the results would be given as the probability of success versus the pass number. A plot of these results (Figure 11.4) might show that there is a 60 percent chance of photographing 95 percent of the target area in six satellite passes. Second, the pass number is fixed while the percentage of area photographed and the chance of success are treated as variables. Results in this case are given as the percent chance of achieving some percent of photographic coverage of the target area by some limiting pass number. These results (Figure 11.5) might show that after eight satellite passes, there is a 60 percent chance of photographing 90 percent of the target area.

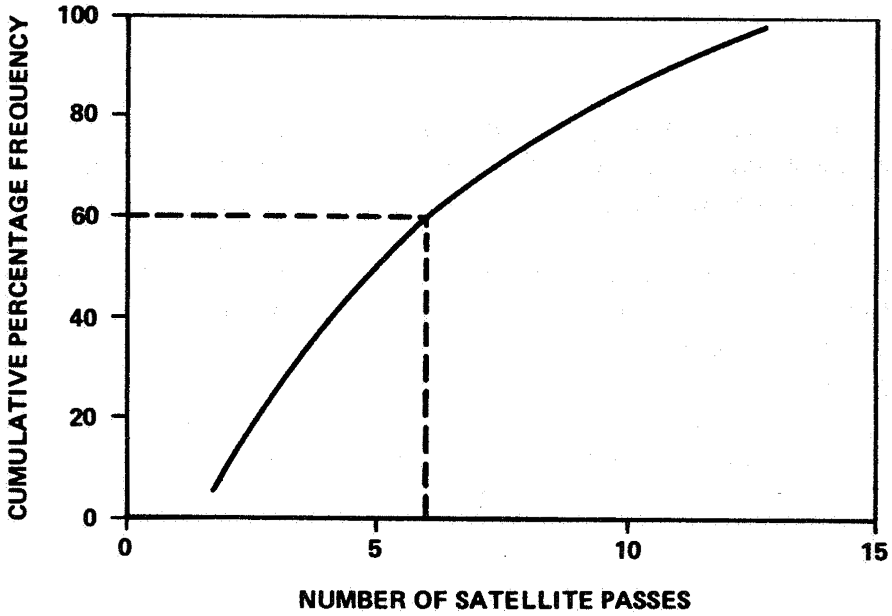

FIGURE 11.4 PROBABILITY OF 95-PERCENT PHOTOGRAPHIC COVERAGE OF TARGET AREA

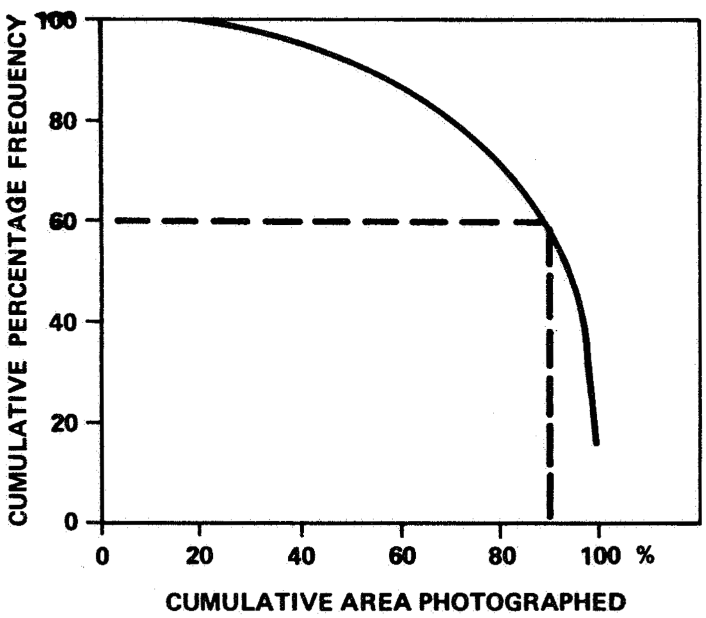

FIGURE 11.5 PHOTOGRAPHIC COVERAGE OF TARGET AREA AFTER EIGHT SATELLITE PASSES

11.3.2 Background

Before the simulation procedure is outlined, it may be helpful to briefly describe the world-wide cloud cover statistics and some simulation applications. These cloud statistics, representing a first effort toward providing cloud data designed expressly for computer simulation exercises, were developed during the period January 1967–January 1968 and March 1970–January 1971. After dividing the earth into 30 homogeneous cloud regions, probability distributions for cloud categories by region and monthly reference periods were prepared for each 3-hour interval (Tables 11.1 and 11.2). For application to computer simulation programs, the cloud region boundaries were adjusted to the nearest even numbered lines of latitude and longitude (Figure 11.6).

TABLE 11.1 CLOUD COVER DEFINITION

Category	Tenths	Eighths (Octas)
1	0	0
2	1,2,3	1,2
3	4,5	3,4
4	6,7,8,9	5,6,7
5	10	8

TABLE 11.2 BASIC CLOUD STATISTICS — CLOUD REGION: 19; MONTH: JANUARY

Cloud Category	Time (LST)							
	01	04	07	10	13	16	19	22
1	0.31	0.30	0.18	0.16	0.15	0.16	0.24	0.30
2	0.08	0.06	0.09	0.08	0.12	0.10	0.10	0.08
3	0.04	0.04	0.04	0.04	0.04	0.06	0.05	0.05
4	0.11	0.10	0.15	0.16	0.17	0.21	0.16	0.14
5	0.46	0.50	0.54	0.56	0.52	0.47	0.45	0.43

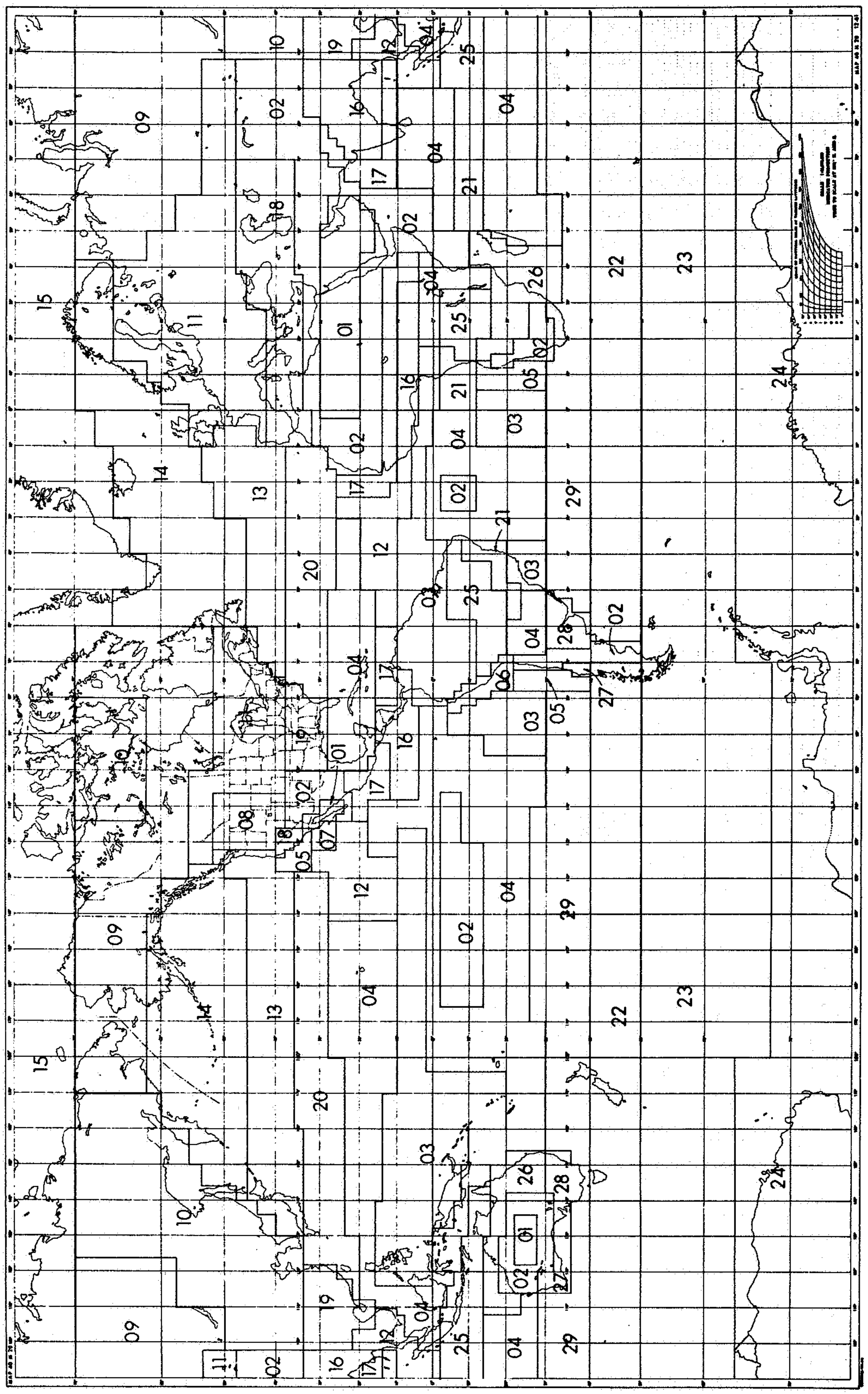

FIGURE 11.6 CLOUD REGION LOCATION MAP

Since clouds generally display some degree of persistence, time and space conditional statistics were developed for each homogeneous cloud region (Table 11.3). The basic statistics (Table 11.2) apply to an area approximately 55.6 kilometers (30 n. mi.) in diameter (Ref. 11.2), while the conditional data are based on a time separation of 24 hours and space separation of 371 kilometers (200 n. mi.). In these same studies, techniques were developed to adjust the conditional statistics for times and distances other than 24 hours and 371 kilometers (200 n. mi.), and to scale both the basic and conditional statistics for application to enlarged target areas.

TABLE 11.3 CONDITIONAL CLOUD STATISTICS, CLOUD REGION 19, JANUARY

Given Cloud Category	Space Conditionals					Given Cloud Category	Time Conditionals				
	Cloud Category						Cloud Category				
	1	2	3	4	5		1	2	3	4	5
1	0.68	0.11	0.05	0.09	0.07	1	0.41	0.12	0.09	0.25	0.13
2	0.13	0.32	0.07	0.13	0.35	2	0.23	0.29	0.10	0.23	0.15
3	0.09	0.20	0.12	0.42	0.17	3	0.14	0.26	0.13	0.35	0.12
4	0.09	0.14	0.10	0.58	0.09	4	0.16	0.15	0.06	0.43	0.20
5	0.11	0.12	0.11	0.27	0.39	5	0.18	0.07	0.10	0.28	0.37

11.3.3 The Simulation Procedure

A typical space mission for earth resources might require that an area 185 × 185 kilometers (100 × 100 n. mi.) be photographed in color. Perhaps the orbital parameters are such that the spacecraft will pass over the target area at 24-hour intervals and the photographic requirements will be satisfied with a montage pieced together from increments obtained on each pass. The mission planner might ask, "How many passes will be required to be 95 percent confident of photographing 80 percent of the area?" If the mission were also limited to a specific number of passes by the amount of film or other expendables, the planner would also need an analysis of that limiting pass number. For example, "With what degree of confidence can one expect to photograph 80 percent of the area by pass number 12?" To answer these and other questions, a computer program using a Monte Carlo mission simulation procedure was developed. In this procedure, the target area is divided into 100 equal parts so that each part represents one percent of the area. Before starting the process, the unconditional and conditional statistics, after being scaled for the area size, are arranged in cumulative form by summing across each row. The fraction of target areas that can be photographed under each cloud category is decided upon at some earlier time, primarily on the basis of the sensors being used. In any case, as part of the input, it can be changed as the experimenter desires. Table 11.4 shows a basic set of cloud statistics plus the cumulative arrangement and the maximum part of the area photographable under each cloud category. In this case, it was decided that the photographable part of the area would be 1 minus the mean cloud cover for each category.

To start the procedure, a random number is generated and used to extract from the unconditional summation the cloud category for the first satellite pass. For example, if the first random number gave cloud category 3, to which a 55 percent cloud cover had been assigned, 45 percent of the target area would be photographed on the first pass. Of course, the photographic coverage obtained from each satellite pass over the target could be incremented without specifying which 45 parts were photographed. However, specifying by number those parts of the target area photographed on each pass permits a more realistic accumulation after 80 to 90 percent of the area has been photographed and a finite probability of acquiring 100 percent of the area. The next step then is to determine which 45 parts of the area were photographed on the first pass. This is done according to the season. If frontal clouds predominate, the 45 parts are arranged in an organized contiguous pattern. On the other hand, if air mass cumulus clouds are expected (tropical regions or midlatitude summer months), the 45 parts are scattered randomly throughout the area. For the first pass, then, after the cloud cover was determined by a random number process, the locations of the cloud-free parts of the target area were specified by a prearranged design. Finally, the percentage of the target area photographed was tallied.

The cloud cover encountered on the second pass is selected from the conditional row (summed across) designated by the first pass, or the given category, by means of a new random number. If the random number selects cloud category 4, then 75 percent of the area is cloud covered and 25 percent (or 25 numbered parts) is cloud-free and can be photographed. However, all or part of the 25 percent might have been acquired on the first pass. To account for this possibility, 25 discrete random numbers are drawn to identify the numbered parts of the target area to be photographed on this pass. Of course, only the newly acquired parts of the target area are incremented; those photographed for the second time do not contribute to the total photographic coverage.

TABLE 11.4 ARRANGEMENT OF CLOUD STATISTICS FOR COMPUTER SIMULATION

	Maximum Area Photographable per Pass				
	CC-1	CC-2	CC-3	CC-4	CC-5
	1.000000	0.750000	0.450000	0.250000	0.000000
	Unconditional Probability Statistics				
	CC-1	CC-2	CC-3	CC-4	CC-5
	0.000000	0.030000	0.050000	0.550000	0.370000
Given Cloud Category	Conditional Probability Statistics				
	CC-1	CC-2	CC-3	CC-4	CC-5
1	0.000000	0.110000	0.000000	0.000000	0.890000
2	0.000000	0.130000	0.100000	0.360000	0.410000
3	0.010000	0.100000	0.100000	0.470000	0.320000
4	0.000000	0.070000	0.060000	0.460000	0.410000
5	0.010000	0.090000	0.080000	0.410000	0.410000
	Cumulative Unconditional Probability Statistics				
	CC-1	CC-2	CC-3	CC-4	CC-5
	0.000000	0.030000	0.080000	0.630000	1.000000
Given Cloud Category	Cumulative Conditional Probability Statistics				
	CC-1	CC-2	CC-3	CC-4	CC-5
1	0.000000	0.110000	0.110000	0.110000	1.000000
2	0.000000	0.130000	0.230000	0.590000	1.000000
3	0.010000	0.110000	0.210000	0.680000	1.000000
4	0.000000	0.070000	0.130000	0.590000	1.000000
5	0.010000	0.100000	0.180000	0.590000	1.000000

All subsequent passes are handled in the same way. The cloud cover encountered on the previous pass becomes the given condition and identifies the conditional statistics to be used on the current pass. After selecting the cloud cover, several additional random numbers are generated to identify the parts of the target area that are cloud-free. The parts acquired on each pass are accumulated until the entire area has been photographed or until the maximum number of passes has been made. This procedure is illustrated in Table 11.5. The top sections represent the target area divided into 100 parts; the "1's" depict clouds while the "0's" show the clear parts. The summary at the bottom shows the cumulative percentage of area photographed, the random number used to select each cloud cover, the cloud cover selected for each pass, and the pass number. In this example, the first random number, 0.072, specifies cloud category 3: 55 cloud-covered parts and 45 clear parts. The arrangement of the cloudy area as shown at the top left is an arbitrary design chosen because frontal clouds were considered more likely at this time and location.

To account for cloud persistence, the cloud-cover category selected for pass 2 is taken from row 3 of the cumulative conditional probability statistics (Table 11.4). Entering that row with the new random number, 0.531, give cloud category 4, or 25 clear parts, for pass 2. The locations of the 25 clear parts ("0's") as given by additional random numbers is shown in the top center section of Table 11.5. The top right section showing the cumulative area photographed after pass 2 contains 60 "0's" rather than 70(45 + 25) because 10 of the 25 clear sections of pass 2 were already photographed on pass 1.

A summary of the subsequent passes, comprising one iteration, is shown at the bottom of Table 11.5. Generally, 300 iterations are made to simulate a photographic mission.

This Monte Carlo procedure is most useful when the satellite passes over the target area at intervals of 24 hours or less, where cloud persistence must be considered. If there are long time intervals between satellite passes (perhaps 3 days or more), the cloud events may be considered independent and the probability of success computed from the basic combinatorial equation:

$$P_{100\%} = 1 - [1 - P(1)]^N \tag{11.1}$$

or

$$N = \frac{\ell n \left(1 - P_{100\%}\right)}{\ell n \; [1 - P(1)]} \tag{11.2}$$

TABLE 11.5 PHOTOGRAPHIC PARTS OF THE TARGET AREA

CAP = 45.0 PASS = 1	AP = 25 PASS = 2	CAP = 60.0 PASS = 2
1 1 1 1 1 1 1 1 1 1	1 1 0 1 1 1 1 1 0 1	1 1 0 1 1 1 1 1 0 1
1 1 1 1 1 1 1 1 1 1	0 0 0 1 0 1 0 0 1 1	0 0 0 1 0 1 0 0 1 1
1 1 1 1 1 1 1 1 1 1	1 1 1 1 0 1 1 1 1 1	1 1 1 1 0 1 1 1 1 1
1 1 1 1 1 1 1 1 1 1	1 1 0 0 1 1 0 1 1 1	1 1 0 0 1 1 0 1 1 1
1 1 1 1 1 1 1 1 1 1	1 1 1 1 1 0 1 1 1 1	1 1 1 1 1 0 1 1 1 1
1 1 1 1 1 0 0 0 0 0	0 1 1 0 1 1 0 1 1 1	0 1 1 0 1 0 0 0 0 0
0 0 0 0 0 0 0 0 0 0	1 0 0 1 0 1 0 1 1 1	0 0 0 0 0 0 0 0 0 0
0 0 0 0 0 0 0 0 0 0	1 1 1 1 1 1 1 0 1 1	0 0 0 0 0 0 0 0 0 0
0 0 0 0 0 0 0 0 0 0	0 1 0 1 1 1 1 1 1 1	0 0 0 0 0 0 0 0 0 0
0 0 0 0 0 0 0 0 0 0	0 1 0 1 1 1 1 1 1 1	0 0 0 0 0 0 0 0 0 0

B(N)	RAN	C(N)	N
45.000	0.072	3	1
60.000	0.531	4	2
79.000	0.110	3	3
84.000	0.609	4	4
84.000	0.629	5	5
84.000	0.659	5	6
84.000	0.877	5	7
89.000	0.410	4	8
92.000	0.166	4	9
93.000	0.392	4	10
93.000	0.690	5	11
93.000	0.733	5	12
93.000	0.727	5	13
93.000	0.913	5	14
93.000	0.821	5	15
93.000	0.875	5	16
98.000	0.176	3	17
98.000	0.359	4	18
100.000	0.232	4	19

CAP – Cumulative Area Photographed (%)

AP – Area Photographed (%)

B(N) – Total Area Photographed

RAN – Random Number Used to Select the Cloud Cover

C(N) – Cloud Category Encountered on Each Pass

N – Satellite Pass Number

where

$P_{100\%}$ = required probability level of photographing 100 percent of the area

$P(1)$ = relative frequency of cloud category 1

N = number of independent satellite passes.

11.3.4 Results

11.3.4.1 Individual Target Areas

Statistics from three homogeneous cloud regions (2, 13, and 19, Figure 11.6) were used to illustrate the type of information available from the simulation procedure and to compare the simulation results with those obtained from the combinatorial equation.

One convenient way of comparing the two procedures was to address the question, "How many independent satellite passes are required to be 95 percent confident of encountering at least one pass with 3/10 or less (cloud categories 1 or 2) cloud cover over the target area?" The number of passes obtained from each procedure, as shown in Table 11.6, apply to a target area 185 kilometers (100 n. mi.) in diameter. This mission is flown in January, and the satellite passes over the target area at 1300 hours LST.

TABLE 11.6 COMPARISON OF COMPUTER SIMULATION AND COMBINATORIAL RESULTS

Cloud Region	Combinatorial	Computer Simulation
2	8	8
13	116	119
19	12	12

For this comparison, the computer simulation program was adjusted to consider only the unconditional cloud statistics.

Since the number of passes required to satisfy the conditions stated above may be excessive for some cloudy areas of the earth (for example, region 13), the mission planner may be willing to accept incremental photographic coverage. Also, the satellite may pass over the target area at such frequent intervals that the passes cannot be considered independent. When conditions such as these are imposed, a computer simulation is required to evaluate the consequence of cloud cover on the proposed mission.

Results from the simulation program giving analyses of at least 95 percent coverage of the target area and the photographic coverage after 10 satellite passes are shown in Figures 11.7 and 11.8. In both cases, the

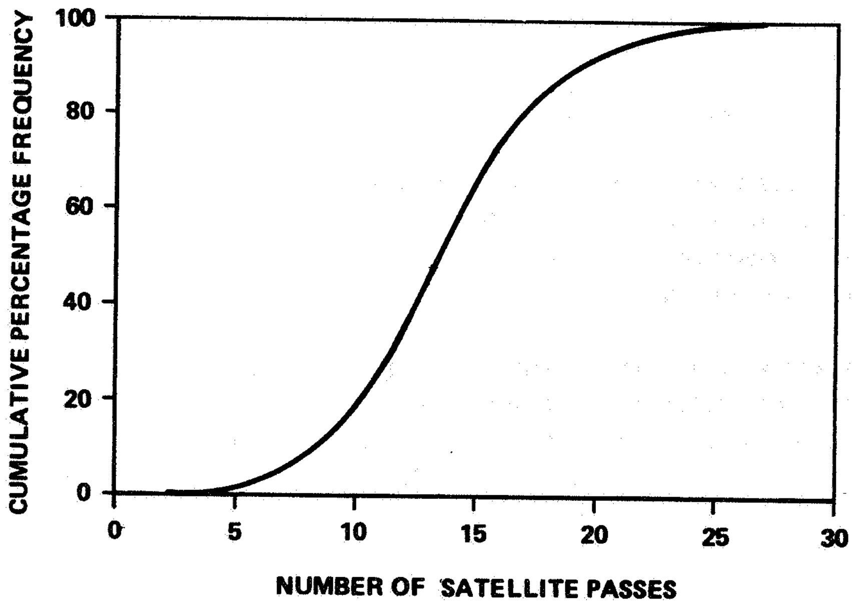

FIGURE 11.7 ANALYSIS OF AT LEAST 95 PERCENT PHOTOGRAPHIC COVERAGE

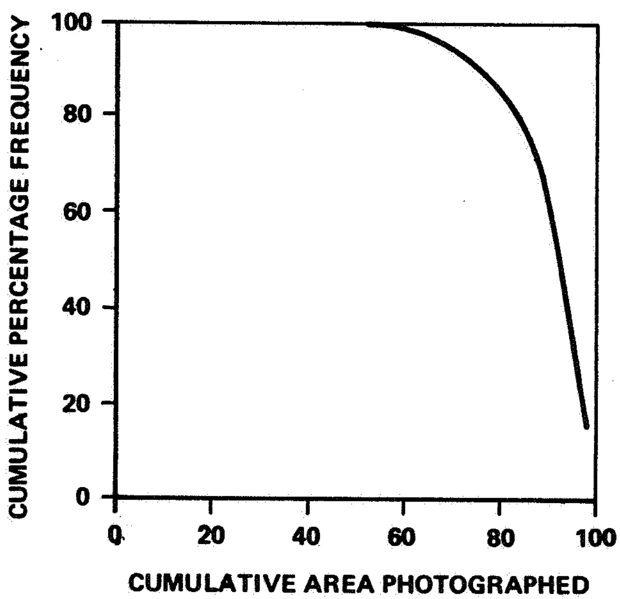

FIGURE 11.8 ANALYSIS OF PHOTOGRAPHIC COVERAGE AFTER TEN PASSES

target is a 185-kilometer (100-n. mi.) diameter area in cloud region 13. The mission is planned for January, and the spacecraft passes over the target area every day at 1300 LST.

Figure 11.7 shows a 50-percent chance of photographing 95 percent of the area in 13 passes, while 19 passes are required to be 90 percent confident.

After 10 passes (Figure 11.8), there is a 50-percent chance of photographing 92 percent of the area and a 90-percent chance of acquiring 76 percent of the target area. These results comprise a summary of 300 iterations of the simulation procedure.

11.3.4.2 Contiguous Target Areas – A Swath

The simulation can also be applied to a series of contiguous target areas, for example, a swath from the Texas Gulf Coast to the Canadian Border (Figure 11.9). To evaluate this type target the swath is divided into several equal-sized areas based upon the width of the swath. If the swath is 185-kilometers (100-n. mi.) with the dimensions of each target area or "box" become 185 × 185 kilometers (100 × 100 n. mi.). In the case illustrated there are approximately six boxes in cloud region 19 and five boxes in cloud region 11. As before, random numbers dictate the cloud cover applicable to each box. The unconditional cloud distribution is used for pass number 1 over the first box but space conditionals are used for all subsequent boxes. That is, the clouds in box 2 depend upon those in box 1, box 3 depends upon box 2, etc. Box 1 of cloud region 11 depends upon box 6 of cloud region 19, but the cloud draw is made from the statistics applicable to cloud region 11.

Subsequent satellite passes over the swath may use either unconditional or time conditional statistics for box 1 of region 19 depending upon the time interval between passes. All other boxes, however, depend only upon the preceding box and always use the space conditional statistics.

Simulation results evaluating the swath are presented in the same manner as the individual target results.

A question that presents some difficulty is that of identifying and fitting into the mosaic small disjointed fractional parts of the target area. For example, can all of the "0's" of Figure 11.7 acquired on pass 2 really be considered useful? Those isolated parts may be difficult, if not impossible, to identify. Perhaps meaningful photographic results can be obtained only

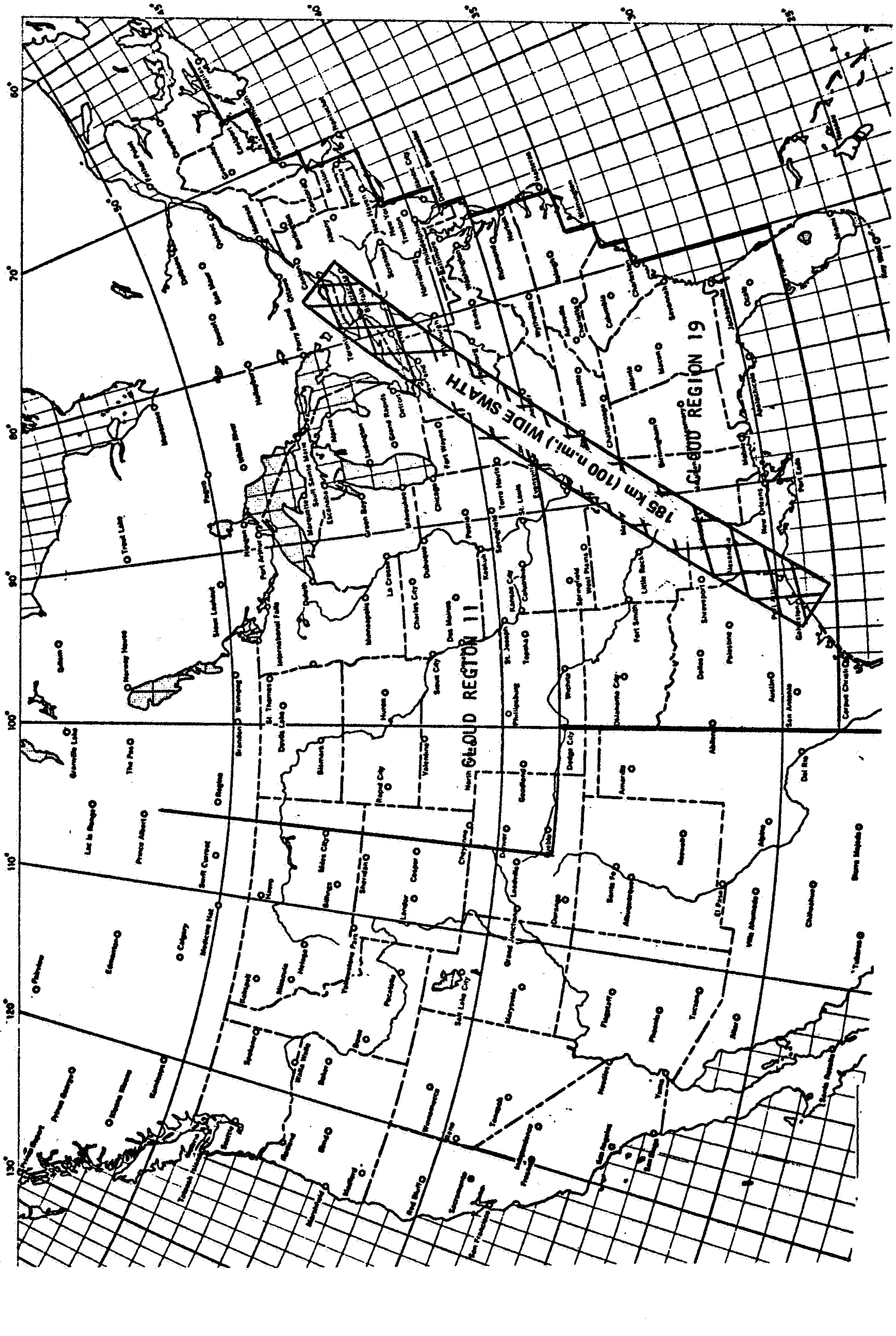

FIGURE 11.9 EXAMPLE OF 100-n.mi. WIDE SWATH

when small cloud amounts are present. Although this may be a serious problem for the experiment designer, the mission planner, and the atmospheric scientists, it does not affect the simulation program directly. If it is decided that a cloud-cover category will not provide useable photographic results, that category can be assigned 100 percent cloud cover, and nothing will be added to the cumulative coverage when it occurs. It might also be stipulated that isolated parts of the target may not contribute to the total photographic coverage. Many contingencies can be handled as input changes; some may require minor program changes.

11.4 Four-Dimensional Atmospheric Models

In this part of the attenuation model project the emphasis was placed on water vapor rather than clouds. Also, since attenuation calculations are usually made from reference atmosphere inputs the other atmospheric parameters found in reference atmospheres were included in the 4-D work. The basic data are comprised of monthly statistics (mean and standard deviations) of pressure, temperature, density, and moisture content from 0 to 25 kilometers altitude on a global grid network. These data provide information on latitudinal, longitudinal, altitudinal, and temporal variation of the parameters; hence the name "four-dimensional atmospheric models." Of course, a profile of temperature, pressure, density, and moisture content for any global location may be retrieved from these data. Still, to reduce the data to a more manageable amount it was decided to outline homogeneous moisture content regions for which a single set of profile statistics would apply. This procedure would permit the use of one set of profiles for all locations within a homogeneous region. While parts of this procedure are still under development, the basic statistics have been computed and the retrieval plans formulated. For each region analytical functions have been fitted to the statistical data. For moisture, exponential functions were most appropriate, while for temperature, a series expansion technique was used. The result of fitting analytic functions to the statistical climatological profile data is a library of coefficients for the temperature and moisture profiles. These coefficients are then used to develop computer subroutines to regenerate the model profiles of temperature and moisture which are a function of the homogeneous region and month of the year.

In the compilation of the global statistics, pressure and density were determined from the hypsometric equation and the equation of state, rather than linear or logarithmic interpolation. The purpose of this was to insure hydrostatic consistency, thus, it is likely that the pressure and density profiles can be generated from the temperature profile and the hydrostatic assumption.

The final result of this data analysis is a series of computer programs that provide mean, maximum, and minimum profiles of moisture, temperature, pressure, and density from the surface to 25 kilometers altitude for any location on the globe and month of the year. The computer programs contain the equations. data, and library of coefficients necessary to produce the desired results.

The 4-D atmospheric model is described in References 11.6 through 11.9.

REFERENCES

11.1 Gaut, N. E., and Reifenstein, E. C. III, "Interaction Model of Microwave Energy and Atmospheric Variables," Environmental Research and Technology, Inc., Final Report of Contract NAS8-26275, Feb. 1971.

11.2 Sherr, P. E., et. al., "World Wide Cloud Cover Distribution for Use in Computer Simulations," Allied Research Associates, NASA CR-61226, Jun. 14, 1968.

11.3 Greaves, J. R., et. al., "Development of a Global Cloud Model for Simulating Earth-Viewing Space Missions," Allied Research Associates, Final Report Contract NAS8-25812, Jan. 1971.

11.4 Brown, S. C., "Simulating the Consequence of Cloud Cover on Earth-Viewing Space Missions," Bulletin of the American Meteorological Society, vol. 51, no. 2, Feb. 1970.

11.5 Chang, D. T., and Willand, J. H., "Further Developments In Cloud Statistics For Computer Simulations," Allied Research Associates, Inc., NASA CR 61389, July, 1972.

11.6 Spiegler, D. B. and Greaves, J. R., "Development of Four-Dimensional Atmospheric Models (Worldwide), Allied Research Associates, Inc., NASA CR-61362, August 1971.

11.7 Spiegler, D. B. and Fowler, M. G., "Four Dimensional World-wide Atmospheric Models (Surface to 25 km Altitudes), Allied Research Associates, Inc., NASA CR-2082, July 1972.

11.8 Chang, David T. and Fowler, Mary Grace, "Use of 4-D Atmospheric Models in the Simulation of Radiometric Measurements," NASA CR-129007, July 1973.

11.9 Fowler, Mary Grace; Lisa, Anthony S.; and Tung, Shu Lin, "Extension of Four-Dimensional Atmospheric Models," NASA CR-143964, October 1975.

SECTION XII. CLOUD PHENOMENA

12.1 Introduction

This section contains general information on cloud characteristics. (See Section XI for the discussion on 4-D Worldwide Cloud Cover Models.) Standard cloud types are stated (Ref. 12.1) as are currently recognized by the National Weather Service. Information is also provided on maximum water content of clouds in Subsection 12.7. Herein, generalizations are stated in broad terms and do not include explicit information on the statistical data on clouds for any particular location. A great amount of specific information about clouds may have to be requested from atmospheric cloud physicists should detailed cloud criteria be needed for a given station or region.

A wealth of information is being accumulated and utilized from satellite photographs of clouds by the National Weather Service, the World Meteorological Organization, NASA, and others.

With the reality of the Space Shuttle and other large aerospace vehicles, an understanding of cloud dynamics is imperative. Of special concern is the extremely complex wind velocity environment associated with certain cloud forms. Water content in clouds needs to be considered, especially its physical and chemical states. Reference should be made to specific details on atmospheric electricity, which is discussed in Section XIII.

12.2 Cloud Terminology

Cloud bases are given in the height in which they are above the local terrain. The vertical dimension of clouds is the actual vertical thickness or cloud depth. Clouds are commonly categorized into height groups as low, middle, or high clouds. Low clouds are cumulus, cumulonimbus, stratocumulus, stratus, and nimbostratus types. The middle clouds are altocumulus, altostratus, and nimbostratus, and certain forms of cumulus clouds are middle-altitude clouds. High clouds are the cirrus types. Of course, cumulonimbus clouds reach well into the upper altitudes as well.

Luke Howard (Ref. 12.1) divided clouds into five major groups as follows:

1. Genera — The main characteristic forms of clouds.

2. Species — The pecularities in shape and difference in the internal structure of clouds.

3. Varieties — Special characteristics of the arrangement of clouds, their transparency, etc.

4. Supplementary Features (accessory, outgrowth clouds) — Appended and associated minor cloud forms.

5. Mother Cloud — The original clouds if formed from other clouds.

The 10 cloud genera are cirrus, cirrocumulus, cirrostratus, altocumulus, altostratus, nimbostratus, stratocumulus, stratus, cumulus, and cumulonimbus. The 14 cloud species are fibratus, uncinus, spissatus, castellanus, floccus, stratiformis, nebulous, lenticularis, fractus, humilis, mediocris, congestus, clavus, and capillatus. The 9 cloud varieties are intortus, vertebratus, undulatus, radiatus, lacunosis, duplicatus, translucidus, perlucidus, and opacus. Nine supplementary features are incus, mamma, virga, praecipitatio, arcus, tuba, pileus, velum and pannus.

Additional comments on particular clouds are included in the following paragraphs.

12.3 Cloud Description (Ref. 12.1)

Altocumulus — A principal cloud type, white and/or gray in color, which occurs as a layer or patch with a waved aspect, the elements of which appear as laminae, rounded masses, rolls, etc. These elements usually are sharply outlined, but they may become partly fibrous or diffused; they may or may not be merged; they generally have shadowed parts, and, by convention, when observed at an angle of more than 30 deg above the horizon, an altocumulus element subtends an angle between 1 and 5 deg. Small liquid water droplets invariably comprise the major part of the composition of altocumulus.

Altocumulus often forms directly in clear air. Virga may appear with most species of altocumulus, which is trailing ice particles falling from the bases of altocumulus clouds. The numerous varieties of altocumulus clouds include altocumulus castellanus, altocumulus floccus, altocumulus lenticularis, altocumulus opacus, altocumulus translucidus, altocumulus undulatus, etc.

Altostratus — A principal cloud type in the form of a gray or bluish sheet or layer of straited, fibrous, or uniform appearance. Altostratus very often totally covers the sky and may, in fact, cover an area of several thousand square miles. The layer has parts thin enough to reveal the position of the sun. Altostratus may extend vertically several hundreds of feet. The upper portion of such clouds is usually ice crystals, the middle portion is ice crystals and snow flakes or supercooled water, and the lower portion may be supercooled water or ordinary water droplets. Altostratus clouds are precipitating clouds. Other named altostratus clouds are altostratus duplicatus, altostratus opacus, altostratus radiatus, altostratus translucidus, and altostratus undulatus (Ref. 12.1).

Billow Cloud (undulatus) — Broad, nearly parallel, lines of clouds oriented normal to the wind direction, with cloud bases near an inversion temperature surface. The distance between billows is usually approximately 1000 m to 2000 m (about 3300 to 6600 ft). Billow clouds are formed by positive vertical motion in free gravity waves on the inversion surface.

Black Squall Cloud — A squall accompanied by dark clouds and generally by heavy rain.

Cirrocumulus — A principal cloud type, appearing as a thin, white patch of cloud without shadows, composed of very small elements in the form of grains, ripples, etc. Holes or rifts often occur in a sheet of cirrocumulus. Cirrocumulus may be composed of highly supercooled water droplets, as well as small ice crystals, or a mixture of both.

Cirrostratus — A principal cloud type, appearing as a whitish veil, usually fibrous but sometimes smooth, which may totally cover the sky and which often produces halo phenomena, either partial or complete. Cirrostratus clouds are composed of ice crystals, some of which attain sizes large enough to fall. Cirrostratus clouds are classified as duplicatus, fibratus, filosus, nebulosus, etc.

Cirrus — A principal cloud type, composed of detached cirriform elements in the form of white, delicate filaments, of white patches, or of narrow bands. These clouds have a fibrous aspect and/or a silky sheen. Cirrus are composed of ice crystals, some of which become large enough to fall out of the cloud. Other classes of cirrus are cirrus castellanus, densus, duplicatus, fibratus, filosus, floccus, etc.

Cumulonimbus — A principal cloud type, exceptionally dense and vertically developed, occurring either as isolated clouds or as a line or wall of clouds with separated upper portions. These clouds appear as mountains or huge towers, at least a part of the upper portions of which are usually smooth, fibrous, and sometimes flattened. Precipitation from cumulonimbus is often heavy, with associated lightning and thunder. The upper air associated with a cumulonimbus is unstable and cloud growth is encouraged by the convection of warm, moist air from the surface layers. Moisture within the cumulonimbus clouds exists in about every physical state. The pronounced dynamic behavior of the air within and about cumulonimbus clouds is hazardous to aircraft and aerospace vehicle operations. The upper portions of the mature cumulonimbus cloud that has flattened out is commonly referred to as having an anvil (incus) shape.

Cumulus — A cloud in the form of individual, detached elements which are generally dense and possess sharp, nonfibrous outlines. Large mounds of clouds often having domes and vertically developed shapes resembling the shape of a cauliflower. Although cumulus clouds are composed of a great amount of water, they are often referred to as fair weather clouds. Cumulus clouds are subdivided into many classes.

Fractus — A cloud species in which the cloud elements are irregular but generally small in size and which presents a ragged, shredded appearance, as if torn (fragmented). Fractocumulus and fractostratus are two classes of fractus-type clouds.

Mammatus (mamma) — Hanging protuberances, like pouches, on the under surface of a cloud. They indicate a very unstable state with broad-scale mixing of the air. Any vehicle flying through such cloud forms would experience a great amount of roughness to the point where structural fatigue could result to the airframe.

Nimbostratus — A principal cloud type, gray colored and often dark, where precipitation is characterized by more or less continuously falling rain, snow, sleet, etc., of the ordinary varieties but not accompanied by lightning, thunder, or hail. In most cases the precipitation reaches the ground, but not necessarily. Nimbostratus clouds have well-defined bases but are vertically quite thick and moist, which attenuates the sunlight quite effectively.

Stratocumulus — A principal type of cloud predominantly stratiform or in the form of a gray and/or whitish layer or patch, which nearly always has dark parts and is nonfibrous. Its elements are tesselated (patched together like a mosaic), rounded, roll shaped, etc. The elements of the stratocumulus clouds are arranged in orderly groups and have a definite pattern. Stratocumulus clouds are generally thin and composed of small water droplets and/or soft ice particles. Stratocumulus clouds form in fair weather and are further classified as stratocumulus castellanus, floccus, lenticularis, mamma, opacus, etc.

Stratus — These are gray, layered clouds with a rather uniform base. Stratus usually does not produce precipitation but when it does occur, it is in the form of small particles such as drizzle, ice crystals, or snow granules. Several subclasses of stratus clouds have been identified.

Virga — Wisps or streaks of water or ice particles falling out of a cloud but evaporating before reaching the ground. Virga is frequently seen trailing from altocumulus and altostratus clouds. It frequently appears to have a hooked shape, where the lower portion of the streak may even appear to be horizontally inclined. The hooked appearance is caused by horizontal wind shear conditions.

White Squall — A sudden squall in tropical or subtropical waters; it is so called because the usual squall cloud is absent; thus, the only warning of its approach is the whiteness of a line of broken water or whitecaps.

12.4 Cloud Observations (Ref. 12.2)

Cloud observations are taken regularly by ground observers at weather stations throughout the world. The four observations which are made are (1) record observation, (2) special observation, (3) record special observation, and (4) local observation. The record observations are made every hour, on the hour. The special and local observations are made whenever necessary, but the local observation is not transmitted to a weather communications center unless requested. Special observations are recorded to show any significant change in the weather conditions.

12.4.1 Cloud Cover Amount

Cloud cover amount is determined by visual observations. The amount of coverage is recorded in tenths. Less than one-tenth is designated as clear sky; one-tenth through five-tenths, where half or more is thin, is designated as thin scattered; one-tenth through five-tenths where more than half is opaque is scattered; six-tenths through nine-tenths where half or more is thin coverage is designated as thin broken; six-tenths through nine-tenths where more than half is opaque is designated as broken; ten-tenths of which half or more is thin is thin overcast, and ten-tenths where more than half the sky is opaque is overcast.

12.4.2 Cloud Height Values

Cloud heights are reported as follows:

a. If the cloud bases are 1500 m (5000 ft) or less they are reported to the nearest 30 m (100 ft).

b. If the cloud bases are between 1500 m (5000 ft) and 3000 m (10 000 ft) they are reported to the nearest 150 m (500 ft).

c. If the clouds are above 3000 m (10 000 ft) they are reported to the nearest 300 m (1000 ft).

(NOTE: Reference 12.2 reflects other essential facts about properly recording cloud heights.)

12.4.3 Cloud Cover Ceiling Height Classification Designators

Numerous methods are used to determine the height of clouds. Measured heights are made by ceilometer, ceiling light, buildings, etc. Other methods to obtain cloud heights are by radar, aircraft reports, balloon ascents (ceiling, pilot, and raob), by estimating the height, and by vertical visibility into obscuration.

Pilot and radar reports of cloud bases and tops are recorded at many weather stations. Available heights of cloud bases, not visible at the station, and tops of sky cover layers within 37 km (20 n. mi.) of the airport for non-cirriform layers and within 92 km (50 n. mi) of the airport for cirriform layers are reported. Cloud data older than 15 minutes are disregarded unless considered operationally significant. In the event of multiple reports, the one used is that which is most complete and in best agreement with other observed data. The pilot and radar data entered in standard logs are as follows:

a. Time in hours and minutes preceding data more than 15 minutes old.

b. Distance and direction from station if reported.

c. Height of bases in hundreds of feet above mean sea level (MSL) if reported.

d. Sky cover symbol for amount reported by pilot or amount of individual layer if reported by radar (i.e., do not use the summation principle). "U" is entered in the log if amount or symbol is not reported or is unknown.

e. Height of tops in hundreds of feet (MSL), if reported.

12.5 Clouds in General

Clouds are visible atmospheric moisture formed by the physical decrease in temperature of humid air to a point that water vapor condenses. Condensation forms by water adhering to hygroscopic nuclei which are minute solid particles of sand, salt, silt, etc. Cooling of the air by adiabatic expansion is a method by which many clouds are formed.

Water will not condense as quickly when clean, moist air is cooled as it will when the air has ample condensation nuclei. The clean, moist air must be supercooled to actually attain droplet formation. Many research programs, both laboratory and field, have been performed to determine the microphysical characteristics of clouds, fogs, haze, etc. Some of the microphysical characteristics investigated are (1) the nuclei size and distribution, (2) the liquid water content in the cloud, (3) the chemical composition of the nuclei producing the cloud, fog or haze, and (4) the nucleating characteristics of various chemicals to produce artificial rain, snow, and fog as well as to dissipate fogs in general. Rainmaking, fog dissipating, severe flood control, etc., fall into this type research (Ref. 12.3).

Such properties as the temperature lapse rate of air, moisture of air, convective behavior of air, etc., are all important in forming clouds. Low stratocumulus-type clouds contain a great amount of moisture. From these clouds cumulus congestus and cumulonimbus clouds can form to introduce pronounced storm conditions. Thunderstorms, which are an example of such storms, are costly to the aerospace industry in that excessive amounts of material are lost and schedule time delays are introduced. Such storms (Ref. 12.4) develop locally where ample heat and unstable moist air are available; can be associated with squall-line activity, fronts, or hurricanes; and can be formed by orographic processes, etc. During vehicle operations and launch, considerable attention is placed on the occurrence of lightning associated with these storms.

Reference 12.5 includes extensive information resulting from research of thunderstorm activity with emphasis on storm development and life cycle. Tornadoes and other severe weather phenomena are discussed, including damage resulting from extreme winds, flying debris, and heavy rainfall.

Cumulonimbus (thunderstorm clouds) have been measured to attain altitudes in the neighborhood of 20 km (60 000 ft). Such storms actually penetrate the tropopause. Because of such vastness and of the many other disturbing dynamic properties associated with thunderstorms, much study and attention is given to storms, especially those that affect the space research effort.

Altocumulus and cumulus clouds are higher in altitude than the stratocumulus and cumulonimbus types. Altocumulus and cumulus clouds are not generally precipitation-type clouds although light rain or snow can be observed to fall from them. Puffy cumulus clouds are associated with fair weather conditions as is common with high atmospheric pressure. Aircraft flight through such clouds is not severely hampered except for limited visibility and possible moderate turbulence.

Cirrus clouds form at high altitudes and cause little concern to aviation or space vehicle operations and launch. These clouds are indicators of possible changing weather. The study of cirrus and the many forms of cirrus clouds provide an excellent weather forecast tool to determine imminent weather changes.

To space vehicle and aircraft flight in general, stratocumulus, cumulonimbus, fractocumulus, nimbostratus, fractocumulus, and similar types of clouds are of concern. Extensive cloud systems, as associated with frontal conditions, result from the interaction of air masses at fronts. The type of front, its slope, motion, etc., are necessary data to have available in determining the clouds and weather that will be associated with such large weather systems.

Clouds formed over mountain terrain are often caused by orographic lifting of the air. As warm, moist air moves up mountain slopes, it reaches heights at which condensation takes place. Initially, cumulus-type clouds form but will change to cumulonimbus formations as conditions continue to favor such cloud development to cause rainshowers, hail, violent winds, lightning, etc. These clouds and storm conditions, as weather frontal activity, can be predicted quite well.

The ocean-land interface plays a special role in creating cloudy conditions. As the warm, moist air flows in over heated land, significant convective activity will take place, which results in the generation of massive cloud formations. Multiple thunderstorms can develop under this atmospheric situation. A favorable factor is the availability of oceanic salt particles to serve as hygroscopic nuclei upon which water droplets will form.

12.6 Cloud Ceiling and Visibility Reporting for Aircraft Flight

Routine cloud ceiling data are provided as routine aircraft flight information. Visibility as well as frontal position and atmospheric pressure centers are also shown on nephanalysis maps. Obscurations that limit visibility such as fog, haze, smoke, blowing sand, etc., are provided. These maps show areas where cloud ceilings and visibility are restrictive to aircraft flight in regard to the following:

a. Instrument Flight Regulations (IFR)

b. Marginal Visual Flight Regulation (MVFR)

c. Visual Flight Regulation (VFR).

Such Federal Aviation Administration (FAA) regulations will apply to Space Shuttle Orbiter operations; therefore, awareness of available information on cloud ceiling and visibility is required. Such regulations as stated above may be more applicable to Carrier Aircraft/Shuttle Orbiter Flights than to the actual reentry and landing of the Shuttle Orbiter.

12.7 Maximum Water Content of Clouds (Ref. 12.6)

Water in clouds is found in gaseous (vapor), liquid, and solid (ice crystals) states. Water vapor exists at all temperatures and is always present in the atmosphere, even in clear air. Liquid water is found in clouds from about 25°C down to a -35° or -40°C. Ice crystals are found at all sub-zero temperatures and frequently at a few degrees above zero but generally will not form in the free atmosphere at temperatures warmer than -12°C.

Water vapor in the atmosphere is indicated by the humidity. For practical purposes, the relative humidity in clouds is 100%. The amount of water vapor depends on the cloud temperature, doubling to tripling for each 10°C increase in temperature. For example, clouds at 25°C will have 23 g m^{-3} of water vapor whereas those at 0°C will have only 5 g m^{-3} of vapor.

Because measurements of the amount of water in the liquid and solid states in clouds are not extensive, it is impossible to provide a frequency distribution of the amounts contained in various types of clouds. Information given here is limited to estimates of the maximum amounts of water (gaseous, liquid, and solid) likely to be encountered in cloud form.

Because the amount of water vapor approximately doubles for each 10°C rise in temperature, more water will be available during the summer, and heavier clouds are to be expected below 25 000 ft. Investigations of warm convective clouds (types found to have the highest water content) indicate an average liquid water content 4 to 5 times that observed in the winter, and 5 to 10 times that observed in stratus clouds irrespective of season (Ref. 12.7). Data from these investigations are shown in Table 12.1 and Figures 12.1 and 12.2. The droplet size, water content, visibility, and droplet concentration data in Figure 12.2 represent average values regardless of the altitude at which they were collected, whereas Figure 12.1 depicts these parameters as functions of thickness in convective type clouds.

TABLE 12.1 OBSERVED LIQUID WATER CONTENT OF CUMULUS TYPE CLOUDS OVER NEW JERSEY AND FLORIDA DURING THE SUMMER

Clouds		Water Content (g m^{-3})	
Type	Temperature (°C)	Average	Maximum
Cumulus Humilis	10 to 24	1.0	3.0
Cumulus Congestus	3 to 11	2.0*	6.6
Cumulonimbus	10 to -8	2.5	10.0

*Estimated

The water content curve in Figure 12.1 indicates that cumulonimbus clouds contain the greatest amount of liquid water. The maximum content observed, 10 g m^{-3}, was found in a cumulonimbus cloud near 4000 m (13 000 ft) above the cloud base. The cumulonimbus data have been questioned, however, because there was evidence that a number of raindrops was included in each cloud sample. Figure 12.1 also indicates that the liquid water content of cumulus congestus clouds, from which there is apparently no precipitation, can exceed 6 g m^{-3}. The formation of precipitation inside a cumulus cloud is a complex function of physical, chemical, and meteorological variables that are poorly understood. Therefore, when precipitation is not actually falling from a cloud, it is difficult to determine what part of the total liquid water content should be classified as cloud particles and what part as suspended precipitable water. Apparently the maximum liquid water content that can exist in a nonprecipitating cloud is between 6 and 10 g m^{-3}. A study by the University of Chicago indicates cloud water densities of at least 1.7 g m^{-3} are required before rain is produced.

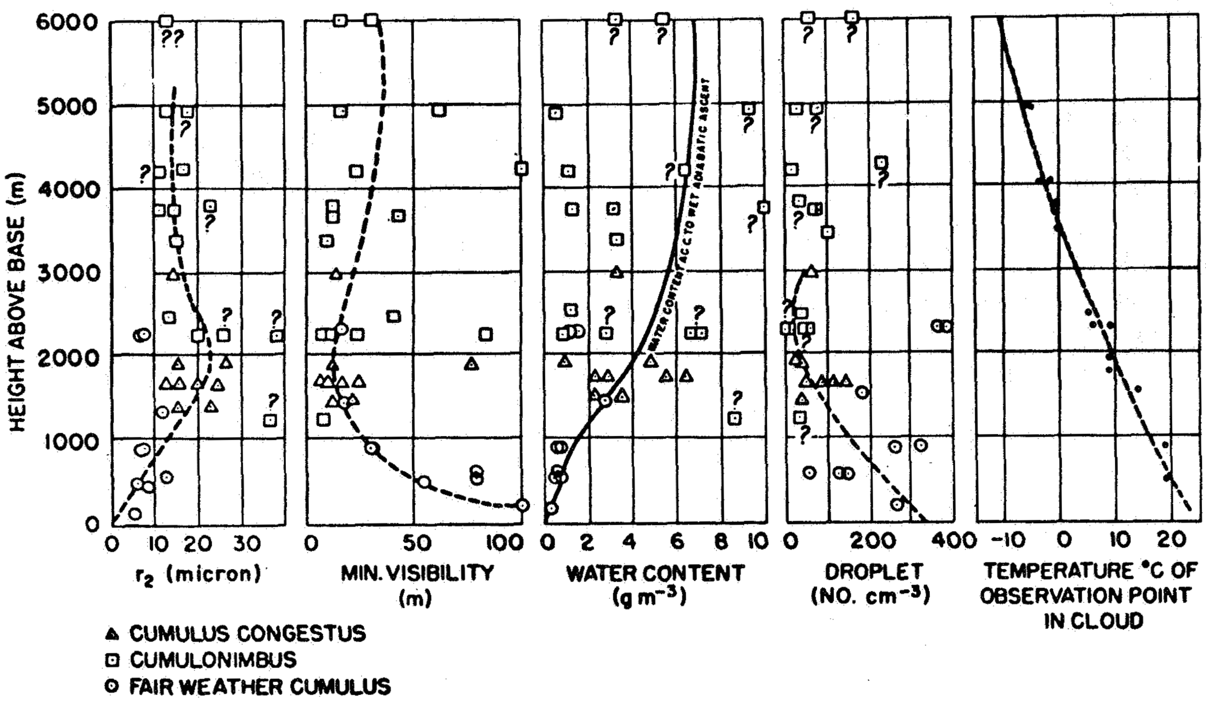

Figure 12.1. Physical properties in cumuliform clouds versus heights above base of cloud (Ref. 12.6).

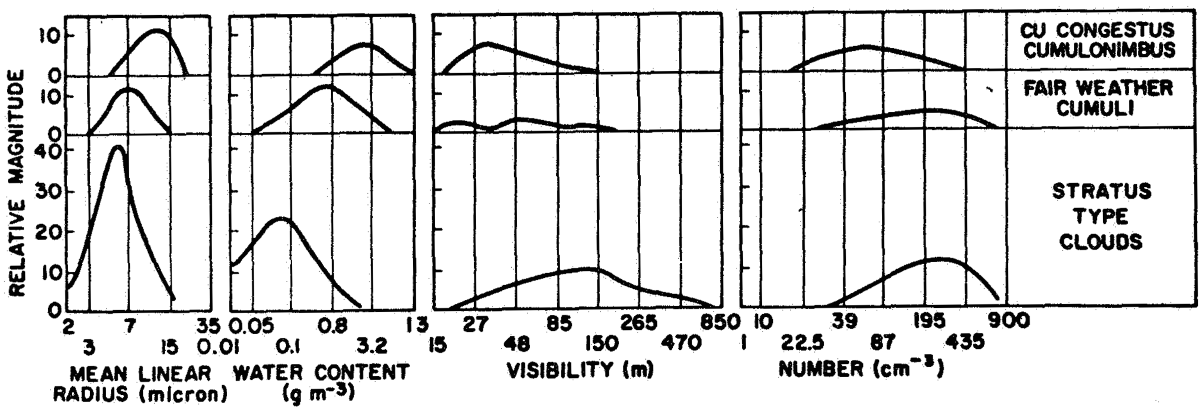

Figure 12.2. Physical properties of different types of clouds (Ref. 12.7).

From Table 12.1 the water content appears to be increasing with decreasing temperature. This can be attributed to the higher flight altitudes at which observations were made in the more developed convective clouds. Theoretically, more moisture is available for condensation at the lower level because of higher temperatures and, therefore, a heavier cloud density would be expected. Strong vertical currents in convective clouds of this type, however, are such that condensed cloud particles originating in the lower levels will be carried aloft. In well-developed convective clouds, with no precipitation, the maximum liquid water content occurs near the top. As the cloud builds to high altitudes and the drop size goes up, down drafts occur. Thus, the maximum liquid concentration will be observed at an altitude corresponding to 1/2 to 7/8 of the cloud height. After precipitation begins there will be little variation in the amount of liquid (or frozen) water with height, from the base of the cloud to the level of maximum concentration, because falling raindrops and downward currents redistribute the liquid. Examples of the vertical distribution of precipitating water in a thunderstorm are shown in Figures 12.3 and 12.4.

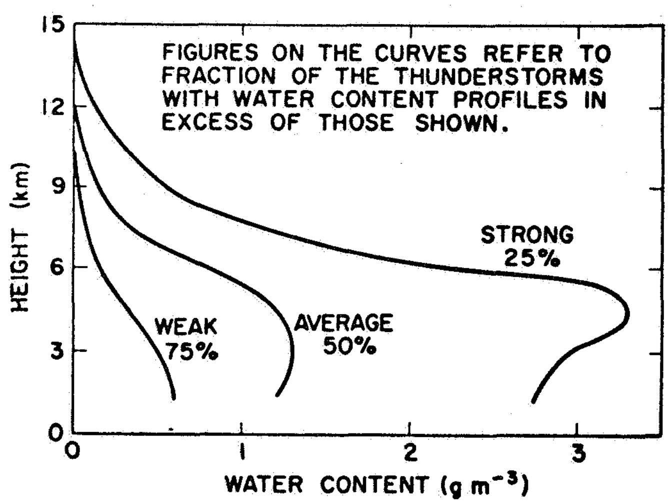

Figure 12.3. Profiles of concentration of water in the centers of mildly, average, and strongly reflective New England thunderstorms.

A temperature of about 20° C appears reasonable for the lower part of cumulonimbus clouds (not indicated in Table 12.1 because observations were made only at the higher levels), yielding a water vapor content of 17 g m^{-3}. A rough estimate of the maximum water content in cloud form of a cumulonimbus cloud at this level, using the 8 g m^{-3} of liquid water, a mean value between the maximum amounts observed in precipitating and nonprecipitating clouds in Figure 12.1, and the above vapor content, would be 25 g m^{-3}. This value probably would include some precipitable water held in suspension and would be encountered near the base of cumulonimbus clouds, about 2000 ft above the ground. The liquid water content would remain fairly constant to altitudes of

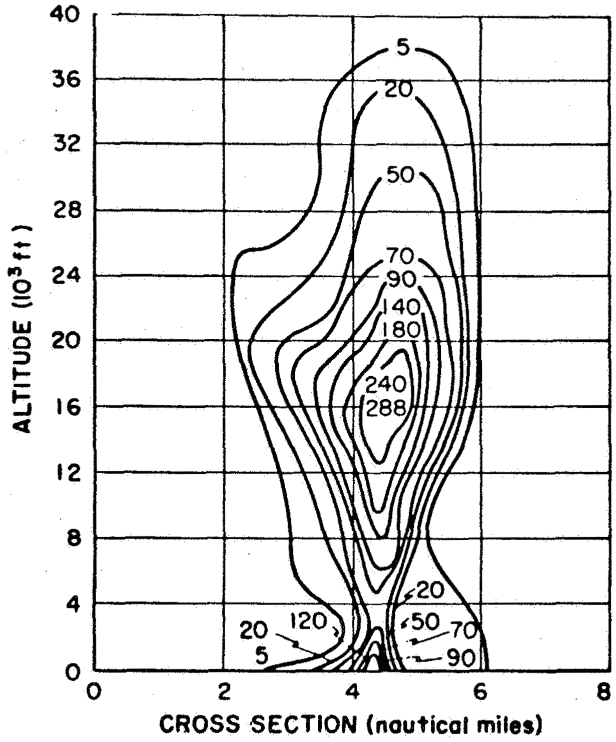

Figure 12.4. West-east cross section through an Ohio thunderstorm showing the distribution of rainfall rate in mm h^{-1}.

15 000 to 20 000 ft but the vapor will decrease rapidly with height commensurate with decreasing temperature. If total precipitable water is considered, this value could be considerably higher. For example, calculations based upon extreme tropical rains indicate a liquid water content (both cloud and precipitable water) of 30 g m^{-3}, mostly as raindrops. This value added to the 17 g m^{-3} of water vapor would give a maximum value of 47 g m^{-3}.

Few direct observations have been made of the water content of clouds above 25 000 ft. The estimates of the maximum amount of moisture likely to be encountered in clouds above 25 000 ft are based on the few observations available, theoretical studies, and extrapolation upward from lower levels; the information is semiquantitative. It may be used, however, as a first approximation in determining, for example, the effect of the water content in clouds above 25 000 ft on a particular jet engine or aircraft design.

Usually, cloud formation above 25 000 ft will be composed entirely of ice crystals and the total solid water content will not exceed 0.1 g m^{-3}. Temperature within the clouds will range from -20° to -52°C, depending on altitude. Excluding cumulonimbus clouds, which frequently extend above 25 000 ft, the water content when both liquid and ice are present in clouds at or above 25 000 ft will be between 0.1 and 1.0 g m^{-3}. Temperatures at 25 000 ft when this extreme water content is experienced will be near -20°C. Temperature and water content will decrease with increasing altitude.

In cumulonimbus clouds the water content, liquid and ice, may occasionally attain a density of 10 g m^{-3} at 25 000 ft. This value will decrease rapidly at altitudes above 35 000 to 40 000 ft. Temperatures in the clouds above 25 000 ft will range from -15° to -50°C, depending on altitude and latitude.

12.8 Concluding Remarks

Clouds of the earth's atmosphere greatly influence aerospace vehicle operations. Although sometimes very disturbing, clouds can be a very useful tool in categorizing current weather and in predicting future weather conditions. Subsequently, plans can be more adequately executed by using criteria on cloud phenomena in accomplishing space vehicle missions. The use of cloud models is becoming an effective means to schedule aerospace vehicle events to cloud/weather conditions. An example is where a Worldwide Cloud Cover Model was used in the Skylab Earth Resources Mission. Before the mission it was used to predict the probability of viewing successive earth surface targets; after the mission the statistics of actual successes of viewing the targets were compared with predicted data. Several contractual groups, other NASA centers, and military agencies have used the model in a variety of ways. Reference should be made to Section XI, where the Worldwide Cloud Cover Model and the 4-D Atmospheric Model are discussed. Although a great deal of information and research is needed to determine more about the dynamics of clouds, much available information on cloud statistics is being used within the space industry program, serving as part of the necessary environmental criteria for the design of space vehicle systems.

REFERENCES

12.1 "Glossary of Meteorology." American Meteorological Society, Boston, Mass., 1959.

12.2 "Federal Meteorological Handbook: Surface Observations." U.S. Department of Commerce, Defense, and Transportation, Washington, D.C., Jan. 1, 1970 (most recent subsection change Jan. 1, 1976).

12.3 Mason, B.J.: "The Physics of Clouds," Second Edition, Clarendon Press, Oxford, Ely House, London, 1971.

12.4 Hess, Wilmont N. (Editor): "Weather and Climate Modification," John Wiley and Sons, New York, New York, 1974.

12.5 Eagleman, Joe R., Vincent U. Muirhead, and Willems Nicholas: "Thunderstorms, Tornadoes, and Building Damage," D.C. Heath and Company, Lexington, Massachusetts, 1975.

12.6 Valley, Shea L.: "Handbook of Geophysics and Space Environments," Air Force Cambridge Research Laboratories, Office of Aerospace Research, United States Air Force, 1965.

12.7 Aufm Kampe, H. J., and H. K. Weickmann: "Physics of Clouds," Meteorological Monographs, vol. 3, pp. 182, 1957.

SECTION XIII. ATMOSPHERIC ELECTRICITY

13.1 Introduction

At present there are no design handbooks, military specifications, or standards for atmospheric electricity hazards protection (Ref. 13.1). This is especially true where aerospace vehicles/systems ground launch and atmospheric flight operations are concerned. The Air Force Systems Command (AFSC) Design Handbook 1-4, "Electromagnetic Compatibility," is the most complete design handbook currently available (Ref. 13.2) which discusses lightning strike phenomena, design to prevent lightning, etc., but the information included on protection from lightning hazards is very limited. During the past year, the Society of Automotive Engineers (SAE) Committee AE-4 on Electromagnetic Compatibility published a report defining lightning test waveforms and techniques for aerospace vehicles and hardware (Ref. 13.3). The committee is presently working on standards for transient test levels for aerospace electronics equipment.

Reference 13.4 contains the Space Shuttle Program lightning protection criteria available to date. Also, some information regarding atmospheric electricity hazards associated with lightning and static electricity is documented in military standards entitled, "Electrical Bonding and Lightning Protection for Aircraft Systems" (Ref. 13.5), "General Specifications for Lightning Arresters" (Ref. 13.6), "Systems Electromagnetic Compatibility Requirements" (Ref. 13.7), and "Electromagnetic Interference Characteristics Requirements for Equipment" (Ref. 13.8). Portions of the material found in these documents are included in the technical statements of this section.

The Aerospace Safety Research and Data Institute of NASA's Lewis Research Center has sponsored the documentation by the General Electric Company of a handbook on lightning protection of aircraft that is scheduled tentatively for publication in 1977. Such information, together with the findings from lightning research tasks being conducted by Air Force, Navy, NASA, and private industry (General Electric, the Rand Corporation, Brunswick Company, McDonnell Aircraft Company, Stanford Research Institute, etc.), should provide excellent material for the preparation of a handbook on lightning and static electricity protection for aerospace vehicles and systems.

A document entitled, "Review of Lightning Protection Technology for Tall Structures," (Ref. 13.9) discusses the ability of corona-point arrays to absorb, suppress, eliminate, or in some way protect against direct strike of lightning to surface structures. Some statistics are included relative to four tall structural facilities at Kennedy Space Center which have lightning dissipation arrays. These facilities are: (1) NASA's 150-meter Ground Wind Tower, (2) Unified S-Band Station, (3) Mobile Service Structure, LC-39, and (4) Mobile Service Tower, LC-41 (Cape Canaveral Air Force Station).

Atmospheric electricity must be considered in the design, transportation, and operation of aerospace vehicles. The effect of the atmosphere as an insulator and conductor of high-voltage electricity, at various atmospheric pressures, must also be considered. Aerospace vehicles that are not adequately protected can be damaged by the following:

1. A direct lightning stroke to the vehicle or the launch support equipment while on the ground or after launch.

2. Current induced in the vehicle from the transport of a charge from nearby lightning.

3. A large buildup of the atmospheric potential gradient near the ground as a result of charged clouds nearby.

4. High-voltage systems aboard the vehicle which are not properly designed can arc or break down at low-atmospheric pressures.

The vehicle can be protected as follows:

1. By insuring that all metallic sections are connected by electrical bonding so that the current flow from a lightning stroke is conducted over the skin without any gaps where sparking would occur or current would be carried inside. Reference 13.5 gives the requirements for electrical bonding.

2. By protecting buildings and other structures on the ground with a system of lightning rods and wires over the outside to carry the lightning stroke into the ground.

3. By providing a zone of protection (as shown in Ref. 13.10 for the lightning protection plan for Shuttle Launch Complex 39).

4. By providing protection devices in critical circuits (Ref. 13.11).

5. By using systems which have no single failure mode. [The Saturn V launch vehicle used triple redundant circuitry on the auto-abort system, which requires two out of the three signals to be correct before abort is initiated (Ref. 13.12)].

6. By appropriate shielding of units sensitive to electromagnetic radiation.

7. For horizontally flying vehicles, by avoiding potentially hazardous thunderstorm areas with proper flight planning and flight operations. Reference 13.13 has an excellent discussion on geographic areas where thunderstorms and thus potentially dangerous lightning discharges occur frequently.

If lightning should strike a vehicle or the test stand or launch umbilical tower (LUT), sufficient system checks should be made to insure that all electrical components and subsystems of the vehicle are functional.

13.2 Thunderstorm Electricity

On a cloudless day, the potential electrical gradient in the atmosphere near the surface of the earth is relatively low (<300 V/m); but when clouds develop, the potential gradient near the surface of the earth will increase. If the clouds become large enough to have water droplets of sufficient size to produce rain, the atmospheric potential gradient may be sufficient to result in a lightning discharge which would require measured gradients greater than 10,000 volts per meter at the surface. Gradients may be considerably higher at altitude above the surface.

13.2.1 Potential Gradient

The earth-ionospheric system can be considered a large capacitor, with the earth's surface as one plate, the ionosphere the other plate, and the atmosphere the dielectric. The earth is negatively charged.

13.2.2 Fair-Weather[1] Potential Gradients

The fair-weather electrical field intensity (the negative of the electrical gradient) measured near the ground is approximately 100 to 300 volts per meter and negative; i.e., the earth is negatively charged and the atmosphere above the earth is positively charged. The fair-weather value of 100 to 300 volts per meter will vary with time at any specific location and will also be different at various locations. These variations in fair weather are caused by the amount of particulate matter in the atmosphere (dust, salt particles, etc.), atmospheric humidity, and location and exposure of the measuring devices (Ref. 13. 14). The fair-weather potential gradient decreases with altitude and has a value near zero at 10 kilometers. Fair-weather potential gradient over a 100-meter-high vehicle could result in a 10,000-volt, or greater, potential difference between the air near the ground and the air around the vehicle top, causing the vehicle to assume the charge if not grounded.

13.2.3 Potential Gradients with Clouds

When clouds develop, the potential gradient at the ground increases. Because of the increased potential gradient on days when scattered cumulus clouds occur, severe shock may result from charges carried down metal cables connected to captive balloons. Similarly induced charges on home television antennas have been great enough to explode fine wire coils in antenna circuits in television sets. Damage to equipment connected to wires and antennas can be reduced or prevented by the use of lightning arresters with air gaps close enough to discharge the current before the voltage reaches values high enough to damage the equipment.

13.2.4 Potential Gradients During Thunderstorms

When the cloud develops into the cumulo-nimbus state, lightning discharges result. For a discharge to occur, the potential gradient at a location reaches a value equal to the critical breakdown value of air at that location. Laboratory data indicate this value to be as much as 10^6 volts per meter at standard sea-level atmospheric pressure. Electrical fields measured at the

1. The term fair weather is used to mean without clouds. The term fine weather is sometimes used.

surface of the earth are much less than 10^6 volts per meter during lightning discharges for several reasons:

1. Most clouds have centers of both polarities which tend to neutralize values measured at the surface.

2. Each charge in the atmosphere and its image within the earth resembles an electrical dipole, and the intensity of the electrical field decreases with the cube of the distance to the dipole.

3. The atmospheric electric field measured over land at the surface is limited by discharge currents arising from grounded points, such as grass, trees, and other structures, which ionize the air around the points, thus producing screen space charges.

For these reasons, the measured electrical field at the surface is never more than about 15×10^3 volts per meter. The potential gradient values indicated by measuring equipment at the surface will show high values when the charged cloud is directly overhead. As the horizontal distance between the projection of the charged center of the cloud to the ground and the measuring equipment becomes greater, the readings become lower, reaching zero at some distance, and then change to the opposite sign at greater distances (References 13.5 and 13.14).

13.2.5 Corona Discharge

As the atmospheric potential gradient increases, the air surrounding exposed sharp points becomes ionized by corona discharge. The charge induced by a nearby lightning stroke may aid such a discharge. The corona discharge may be quite severe when lightning storms or large cumulus clouds are within about 16 kilometers (10 mi) of the launch pad.

13.3 Characteristics of Lightning Discharges

The following definitions define a lightning discharge and its parts:

Lightning flash or discharge, the total series of electrical and luminous effects comprising a single lightning phenomena with a typical duration of several tenths of a second.

Lightning stroke, any one of the major electrical and luminous effects, the entire series which combined, make up the lightning flash. Many authors restrict the term "stroke" to the "return stroke" of the cloud ground flash.

Continuing currents, the current which flows at the end of a high current stroke for hundreds of milliseconds.

The characteristics of various types of lightning discharges are summarized in Table 13.1 and References 13.8 and 13.15.

13.3.1 Lightning Currents[2]

The current flows[3] in a lightning flash (cloud to ground) are conveniently separated into categories as follows:

a. Return stroke surges

Peak current from under 20,000 amperes to over 200,000 amperes, with durations of tens of microseconds.

b. Intermediate currents

Peak current from under 2,000 amperes to over 20,000 amperes, with duration of milliseconds.

c. Continuing currents

Peak current from under 200 amperes to over 2,000 amperes with durations of hundreds of milliseconds.

Currents of category (a) mainly produce explosive effects and undesirable coupling transients, while categories (b) and (c) mainly cause hole burning type damage.

The time structure of the ligntning currents is usually less variable between individual flashes, than the amplitudes. Furthermore, there is little connection within an individual discharge between the severity of the three categories, i.e., an initial severe return stroke has minimal influence on the severity of a following continuing current.

---

2. The information in this section was prepared in cooperation with Dr. E. T. Pierce of Stanford Research Institute, Menlo Park, California. See Appendix A, Reference 13.4.

3. Note that a broad range of current values is given for each category.

TABLE 13.1 CHARACTERISTICS OF LIGHTNING DISCHARGES

Type of Lightning	Average Peak Current per Stroke (A)	Maximum Rate of Rise of Current (A/μsec)	Average Amount of Charge Transferred		Average Total Duration of Stroke (msec)	Average Number of Strokes (unitless)	Average Time Between Strokes (msec)	Remarks
			Per Stroke (C)	Total (C)				
Intercloud lightning	100–2000	100–500	1–5	1–5	300	1		
Discrete lightning strokes to ground								
Leader	100		1–5	5	20	1		
Return stroke	20 000	200 000	5	4–20	0.3	3 to 4	40	Peak current exceeding 100 000 A have been measured about 2 percent of the time.
Long continuing current lightning strokes to ground								
Leader	100		1–5	5	20	1		
Return stroke	20 000	10 000	12–40	12–40	200	1		Average current value of 185 A for long periods (175 msec).

13.3.2 Lightning Characteristics for Design on the Launch Pad or During Ground Transportation

Three models of lightning flashes are presented in this section for use in design studies as follows:

Model 1. A very severe discharge model.

This model involves two high current peak strokes (return strokes), the model is as follows:

a. The first return stroke surge with a current peak of 200,000 amperes and a maximum current rise at a rate of 100,000 amperes per microsecond (100 kA/μs) then falling off at a rate of about 2,000 amperes per microsecond for 98 microseconds to 7,000 amperes.

b. An intermediate current, following the first return stroke surge, of an average of 4,000 amperes (7 kA to 1 kA) for 5 milliseconds (5,000 μs).

c. A first continuing current, following the intermediate current, of an average of 700 amperes (1,000 A to 400 A) for 50 milliseconds.

d. A second continuing current, following the first intermediate of an average of 400 amperes, for 300 milliseconds at constant current.

e. A second return stroke surge, following the second continuing current, with a peak current of 100,000 amperes and a maximum current rise at a rate of 50,000 amperes per microsecond then falling off at a rate of about 1,000 amperes per microsecond for 98 microseconds to 3,500 amperes.

f. An intermediate current, following the second return stroke surge, of an average of 2,000 amperes (3.5 kA to 500 A) for 5 milliseconds.

The current time history for this model is shown in Figure 13.1 and Table 13.2. This model is the basis of the Space Shuttle Lightning Protection Design and was developed from measurements of Florida lightning by Dr. Uman (Ref. 13.16) and work by Dr. Pierce and Dr. Cianos (Ref. 13.17).

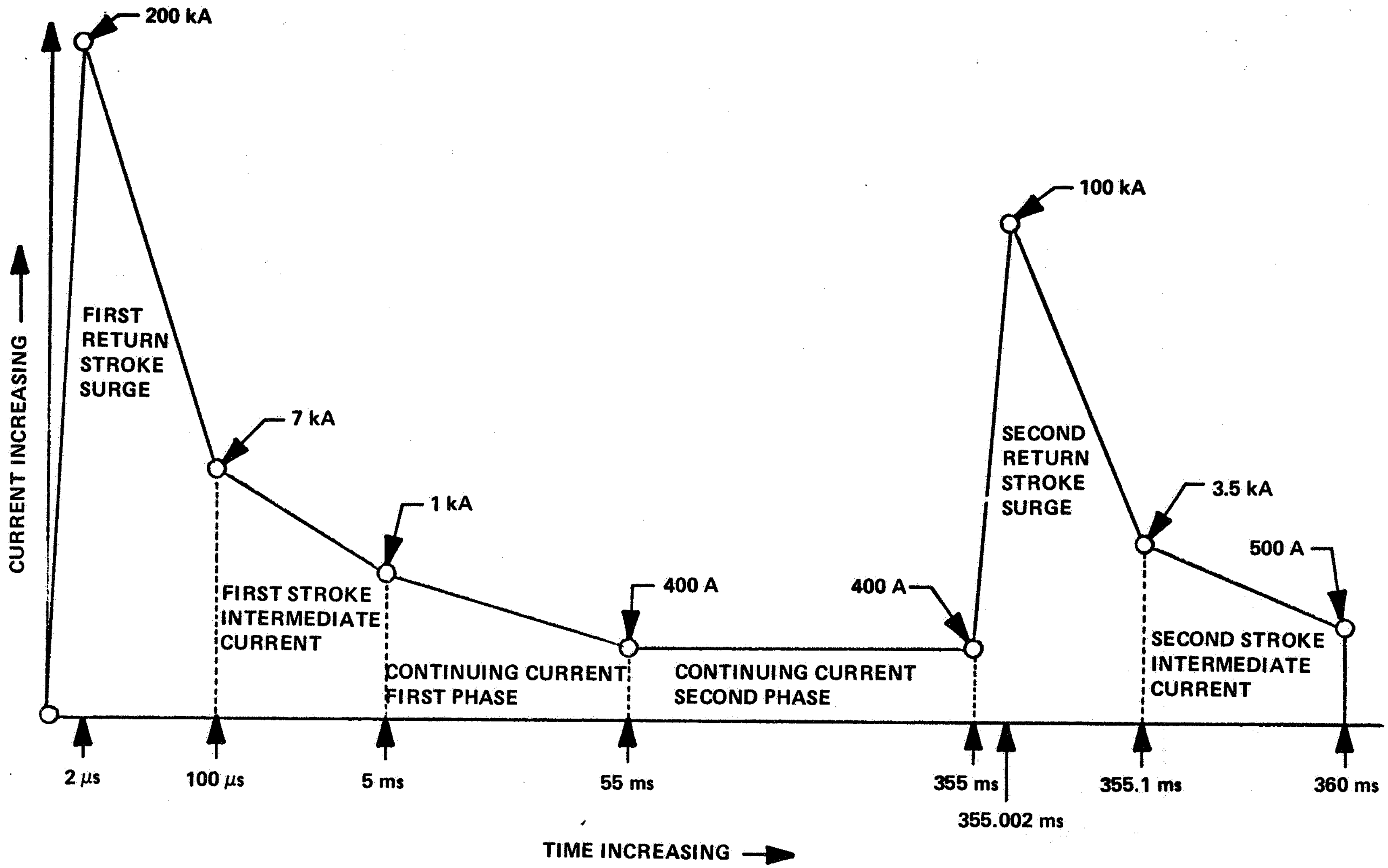

FIGURE 13.1 DIAGRAMMATIC REPRESENTATION OF A VERY SEVERE LIGHTNING MODEL (MODEL 1) (Note that the diagram is not to scale)

TABLE 13.2 DETAILS OF A VERY SEVERE LIGHTNING MODEL (MODEL 1)

Stage	Key Points	Rate of Current Change	Charge Passing
1. First Return Stroke Surge	t = 0, i = 0 t = 2 μs, i = 200 kA t = 100 μs, i = 7 kA	Linear Rise - 100 kA/μs Linear Fall - 193 kA in 98 μs	0.2 C* ~ 10.2 C
2. First Stroke Intermediate Current	t = 100 μs, i = 7 kA t = 5 ms, i = 1 kA	Linear Fall - 6 kA in 4.9 ms	19.6 C
3. Continuing Current--First Phase	t = 5 ms, i = 1 kA t = 55 ms, i = 400 A	Linear Fall - 600 A in 50 ms	35.0 C
4. Continuing Current--Second Phase	t = 55 ms, i = 400 A t = 355 ms, i = 400 A	Steady Current	120.0 C
5. Second Return Stroke Surge	t = 355 ms, i = 400 A t = 355.002 ms, i = 100 kA t = 355.1 ms, i = 3.5 kA	Linear Rise ~ 50 kA/μs Linear Fall - 96.5 kA in 98 μs	~ 0.1 C ~ 5.1 C
6. Second Stroke Intermediate Current	t = 355.1 ms, i = 3.5 kA t = 360 ms, i = 500 A	Linear Fall - 3 kA in 4.9 ms	9.8 C

* Coulomb (C) is the quantity of electricity transported in one second by a current of one ampere.

Model 2. A 98 percentile peak current model.[4]

This model involves one high current peak stroke (return stroke). The model is as follows:

a. The first return stroke surge with a current peak of 100,000 amperes and a maximum current rise at a rate of 20,000 amperes per microsecond (20 kA/μs) then falling off at a rate of about 1,000 amperes per microsecond for 95 microseconds to 3,500 amperes.

b. An intermediate current, following the first return stroke surge, of an average of 2,000 amperes (3,500 A to 500 A) for 5 milliseconds (5,000 μs).

c. A first continuing current, following the intermediate current, of an average of 350 amperes (500 A to 200 A) for 50 milliseconds.

d. A second continuing current, following the first intermediate current, of an average of 200 amperes, for 300 milliseconds at constant current.

This model current time history is shown in Figure 13.2 and Table 13.3.

Model 3. An average peak current model.

This model involves one high current peak stroke (return stroke). The model is as follows:

a. The first return stroke surge with a current peak of 20,000 amperes and a maximum current rise at a rate of 4,000 amperes per microsecond (4 kA/μs) then falling off at a rate of about 190 amperes per microsecond for 95 microseconds to 2,000 amperes.

b. An intermediate current, following the first return stroke surge, of an average of 1,150 amperes (1,700 A to 850 A) for 5 milliseconds (5,000 μs).

4. The intermediate and continuing currents are not necessarily the 98 percentile values, but are added to represent a more severe burning phase.

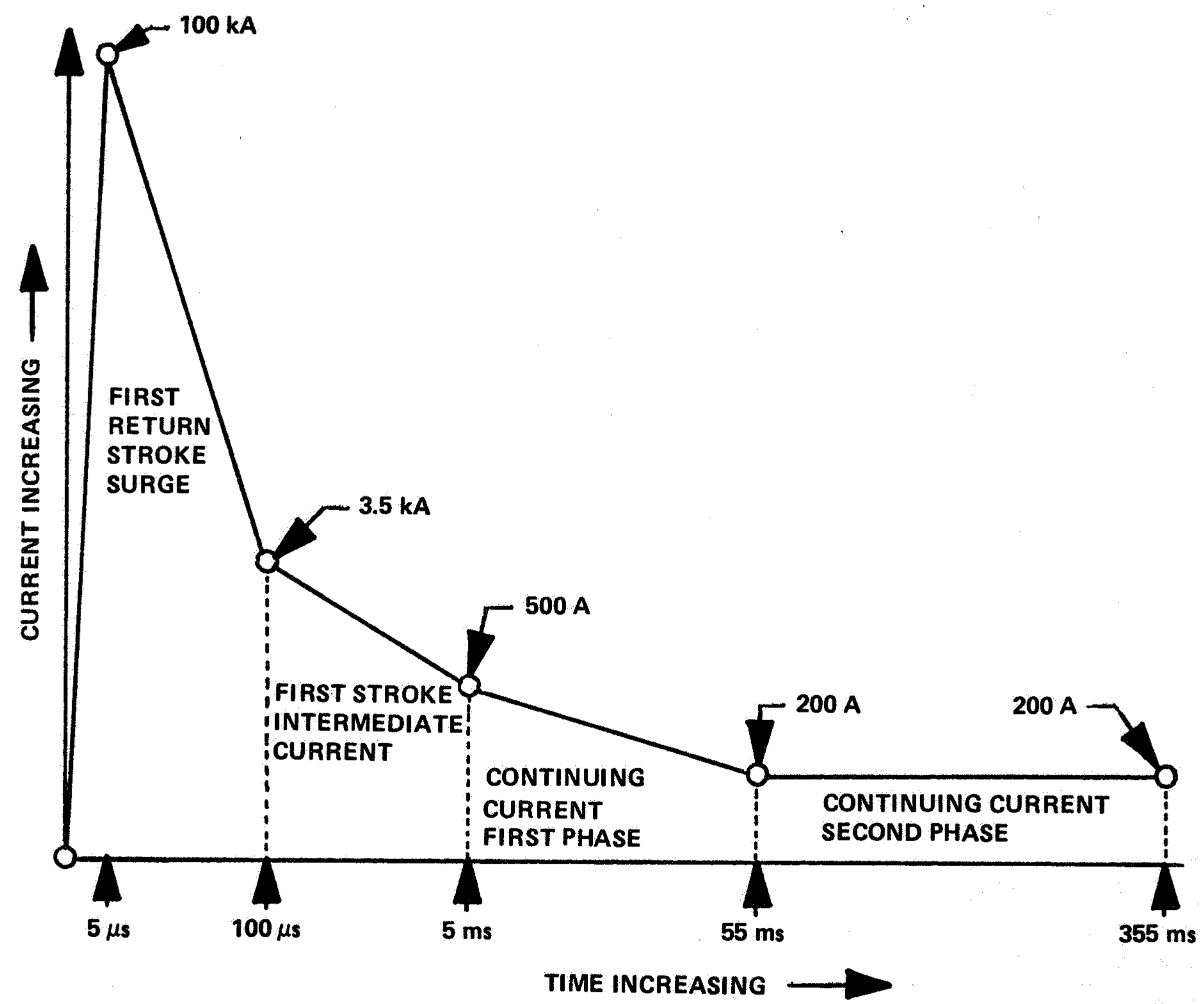

FIGURE 13.2 DIAGRAMMATIC REPRESENTATION OF A 98 PERCENTILE PEAK CURRENT LIGHTNING MODEL (MODEL 2) (Note that the diagram is not to scale.)

TABLE 13.3 DETAILS OF A 98 PERCENTILE PEAK CURRENT LIGHTNING MODEL (MODEL 2)

Stage	Key Points	Rate of Current Change	Charge Passing
1. First Return Stroke Surge	$t = 0$ $i = 0$ $t = 5\ \mu s$ i 100 kA $t = 100\ \mu s$ i 3.5 kA	Linear Rise - 20 kA/μs Linear Fall - 96.5 kA in 95 μs	0.3 C ~ 4.9 C
2. First Stroke Intermediate Current	$t = 100\ \mu s$ i 3.5 kA $t = 5$ ms i 500 A	Linear Fall - 3 kA in 4.9 ms	9.8 C
3. Continuing Current-- First Phase	$t = 5$ ms i 500 A $t = 55$ ms i 200 A	Linear Fall - 300 A in 50 ms	17.5 C
4. Continuing Current-- Second Phase	$t = 55$ ms i 200 A $t = 355$ ms i 200 A	Steady Current	60 C

c. A first continuing current, following the intermediate current, of an average of 100 amperes, for 300 milliseconds at constant current.

d. A second continuing current, following the first intermediate current, of an average of 100 amperes, for 300 milliseconds at constant current.

The current-time history for this model is shown in Figure 13.3 and Table 13.4.

13.3.3 Lightning Characteristics for Design During Flight (Triggered Lightning).

The space vehicle while in flight should be capable of withstanding an electrical discharge from triggered lightning equal to Model 3, given in Section 13.3.2 for an average cloud to ground discharge. Designs of most solid and liquid rocket engines are such that more extreme lightning currents may result in serious damage when the engines are burning. Therefore, launch mission rules are needed to prevent a launch when any severe lightning discharges are possible (Ref. 13. 18).

13.3.4 Current Flow Distribution from a Lightning Discharge

When lightning strikes an object, the current will flow through a path to the true earth ground. The voltage drop along this path may be great enough over short distances to be dangerous to personnel and equipment. Cattle and humans have been electrocuted from the current flow through the ground and the voltage potential between their feet while standing under a tree struck by lightning.

The flow of dc and low frequency current in objects struck by lightning will divide into each possible path of resistance, with the lowest resistance paths carrying the greater current inversely proportional to the resistance if we assume no inductance coupling. Figure 13.4 illustrates this principle for the Saturn V vehicle on the launch pad.

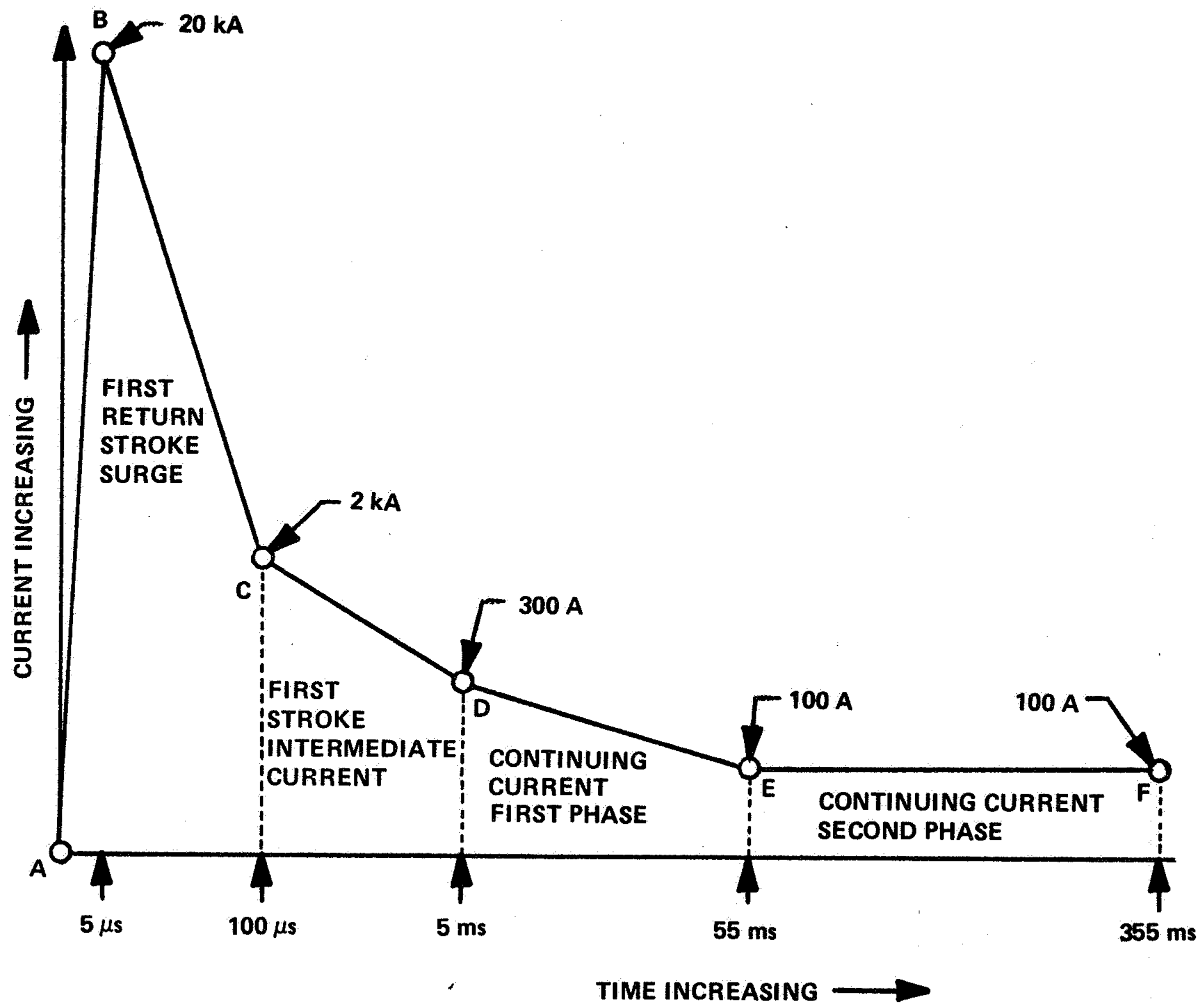

FIGURE 13.3 DIAGRAMMATIC REPRESENTATION OF AN AVERAGE LIGHTNING MODEL (MODEL 3) (Note that the diagram is not to scale.)

TABLE 13.4 DETAILS OF AN AVERAGE LIGHTNING MODEL (MODEL 3)

Stage	Key Points	Rate of Current Change	Charge Passing
1. First Return Stroke Surge	$t = 0$ $i = 0$ $t = 5\ \mu s$ $i = 20$ kA $t = 100\ \mu s$ $i = 2$ kA	Linear Rise - 4 kA/μs Linear Fall - 18 kA in 95 μs	0.1 C ~ 1.0 C
2. First Stroke Intermediate Current	$t = 100\ \mu s$ $i = 2$ kA $t = 5$ ms $i = 300$ A	Linear Fall - 1.7 kA in 4.9 ms	5.6 C
3. Continuing Current -- First Phase	$t = 5$ ms $i = 300$ A $t = 55$ ms $i = 100$ A	Linear Fall - 200 A in 50 ms	10.0 C
4. Continuing Current -- Second Phase	$t = 55$ ms $i = 100$ A $t = 355$ ms $i = 100$ A	Steady Current	30.0 C

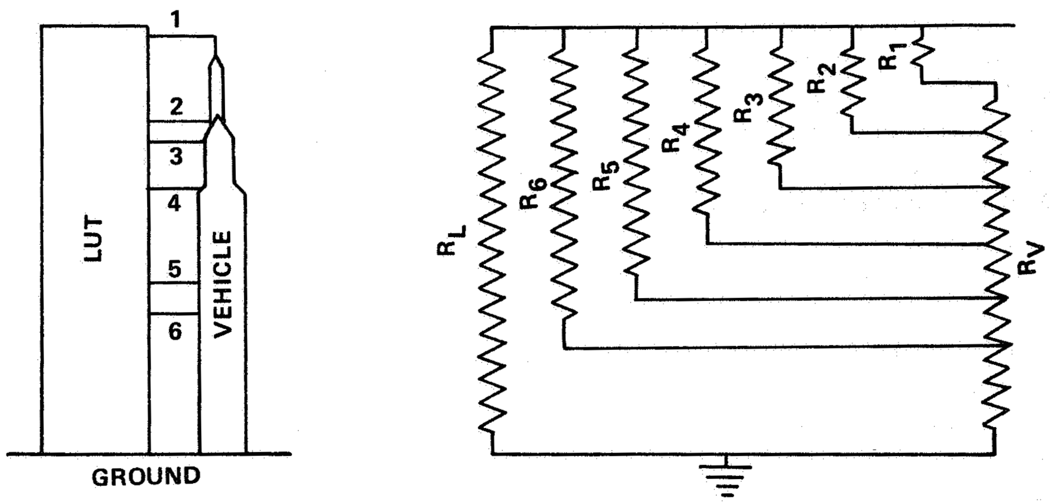

FIGURE 13.4 EXAMPLE OF dc AND LOW FREQUENCY CURRENT FLOW IN AEROSPACE VEHICLE ON LAUNCH PAD AND COMPARABLE RESISTANCE ANALOGY, ASSUMING NO INDUCTANCE COUPLING

Therefore,

$$I_L = \frac{R_L}{R_T} I_T \quad ,$$

where

I_L = current through LUT,

I_T = total current of lightning stroke,

R_L = resistance of LUT,

R_T = total resistance of system,

R_1, R_2, etc = resistance of each connecting arm to vehicle,

R_V = resistance of vehicle.

In the case of the Saturn V vehicle, a sizable percentage ~ 30 percent flows through the Saturn V vehicle.

Since lightning usually strikes the highest exposed point, the only ways to be certain that damaging currents will not flow through a space vehicle on the launch pad are to either: (1) prevent the lightning discharge to the launch complex (2) to conduct the lightning discharge around the launch complex using sufficient mass to carry the current through conductors well insulated (high-resistance supports) from the launch complex equipment, or (3) to design the space vehicle to carry the currents without damage.

13.3.5 Radio Interference

When an electrical charge produces a spark between two points, electromagnetic radiation is emitted. This discharge is not limited to a narrow band of frequencies but covers most of the electromagnetic radiation spectrum with various intensities. Most static heard in radio reception is related to electrical discharges, with lightning strokes contributing much of the interference. This interference from lightning strokes is propagated through the atmosphere in accordance with laws valid for ordinary radio transmission and may travel great distances. With the transmission of interference from lightning strokes over great distances, certain frequencies remain prominent, with those near 30 kilohertz being the major frequencies. Interference with telemetering and guidance needs to be considered only when thunderstorms are occurring within 100 kilometers (60 mi) of the space vehicle launch site (Refs. 13.8 and 13.19).

13.4 Frequency of Occurrence of Thunderstorms

According to standard United States weather observing and recording practice, a thunderstorm is reported whenever thunder is heard at the station. It is recorded along with other atmospheric phenomena on the standard weather observer's form, indicating when the thunder is heard. The report ends 15 minutes after thunder is last heard. This type of reporting of thunderstorms may contain a report as one, or one or more thunderstorms during a period. For this reason, these types of observations will be referred to as thunderstorm events, i.e., a period during which one or more thunderstorms are reported. Because of the method of reporting thunderstorms, most analyses of thunderstorm data are based on the number of days per year in which thunder is heard one or more times on a day; i.e., thunderstorm days. Reference 13.20 is a detailed study on frequencies of thunderstorms occurring in the KSC area.

13.4.1 Thunderstorm Days per Year (Isoceraunic[5] Level)

The frequency of occurrence of thunderstorm days is an approximate guide to the probability of lightning strokes to earth in a given area. The number of thunderstorm days per year is called the isoceraunic level. A direct lightning stroke is possible at all locations of interest, but the frequency of such an occurrence varies among the locations (Table 13.5).

13.4.2 Thunderstorm Occurrence per Day

In a study using weather observation data, which reports a thunderstorm when thunder is heard, the frequencies were computed on the number of days which had 0, 1, 2, . . . , thunderstorms reported; i.e., none or more thunderstorm events. Tables 13.6 and 13.7 and Reference 13.20 give this information.

13.4.3 Thunderstorm Hits

There were sufficient data for the summer months (June-August) at Kennedy Space Center to make an analysis of the frequency of occurrence of thunderstorm hits as:

1. A thunderstorm actually reported overhead.

2. A thunderstorm first reported in a sector and last reported in the opposite sector, if it is assumed that thunderstorms move in straight lines over small areas. This information is listed in Tables 13.8 and 13.9 and Reference 13.20.

13.4.4 Hourly Distribution of Thunderstorms

Figure 13.5 presents the empirical probability that a thunderstorm will occur in the Kennedy Space Center area at each hour of the day during each month. The highest frequency of thunderstorms (24 percent) is around 1600 EST in July. A thunderstorm is reported by standard observational practice if thunder is heard, which it can be over a radius of approximately 25 kilometers. Thus, the statistics presented in Figure 13.5 are not necessarily the probability that a thunderstorm will "hit," for example, a vehicle on the launch pad, or occur at a given location at Kennedy Space Center.

5. This word is also spelled isokeraunic.

TABLE 13.5 FREQUENCY-OF-OCCURRENCE OF "THUNDERSTORM DAYS" (ISOCERAUNIC LEVEL)

Location	Mean Number of Days Per Year of Thunderstorms	Monthly Distribution (% of Annual No. Days)											
		Jan.	Feb.	Mar.	Apr.	May	Jun.	Jul.	Aug.	Sep.	Oct.	Nov.	Dec.
Huntsville	70	1 0.70	3 2.10	6 4.20	8 5.60	11 7.70	19 13.30	22 15.40	18 12.60	9 6.30	1 0.70	1 0.70	1 0.70
River Transportation and New Orleans	75	3 2.25	3 2.25	5 3.75	5 3.75	8 6.0	16 12.0	21 15.75	20 15.0	10 7.5	3 2.25	3 2.25	3 2.25
Gulf Transportation	90	1 0.90	1 0.90	4 3.60	2 1.80	9 8.10	18 16.20	24 21.60	23 20.70	12 10.80	4 3.60	1 0.90	1 0.90
Eastern Test Range	70.09	0.77 0.54	1.94 1.36	4.28 3.00	4.02 2.82	9.73 6.82	18.55 13.00	21.27 14.91	20.23 14.18	13.22 9.27	3.89 2.73	1.18 0.82	0.92 0.64
Panama Canal Transportation	100	1 1.0	1 1.0	4 4.0	2 2.0	9 9.0	18 18.0	24 24.0	23 23.0	12 12.0	4 4.0	1 1.0	1 1.0
West Coast Transportation	6	9 0.54	11 0.66	19 1.14	13 0.78	7 0.42	4 0.24	3 0.18	7 0.42	8 0.48	8 0.48	3 0.24	8 0.48
Vandenberg AFB, California	2	5 0.1	15 0.3	15 0.3	5 0.1	2 0.04	1.5 0.03	10 0.2	10 0.2	25 0.5	1.5 0.03	5 0.1	5 0.1
Sacramento	4	6 0.24	16 0.64	12 0.48	15 0.60	9 0.54	6 0.24	3 0.12	3 0.12	10 0.40	12 0.48	5 0.20	3 0.12
Wallops Test Range[a]	40.6	0.5 0.2	1.2 0.5	5.2 2.1	8.4 3.4	12.6 5.1	17.2 7.0	21.7 8.8	20.4 8.3	7.9 3.2	3.2 1.3	1.0 0.4	0.7 0.3
White Sands Missile Range[b]	38.1	0.8 0.3	0.1 0.05	1.8 0.7	4.7 1.8	7.6 2.9	15.2 5.8	30.5 11.6	23.9 9.1	8.7 3.3	5.2 2.0	0.5 0.2	1.0 0.4
Edwards AFB, California	4.3	2.3 0.1	2.3 0.1	2.3 0.1	7.0 0.3	4.7 0.2	2.3 0.1	23.3 1.0	25.6 1.1	20.9 0.9	7.0 0.3	2.3 0.1	0 0

a. Data from Norfolk, Virginia

b. Data from Holloman AFB, New Mexico

TABLE 13.6 FREQUENCIES OF THE OBSERVED NUMBER OF DAYS THAT EXPERIENCED x THUNDERSTORM EVENTS AT KSC FOR THE 11-YEAR PERIOD OF RECORD JANUARY 1957 THROUGH DECEMBER 1967

x	Jan	Feb	Mar	Apr	May	Jun	Jul	Aug	Sep	Oct	Nov	Dec	Spring	Summer	Fall
0	335	295	308	299	266	187	177	185	228	311	321	334	873	549	860
1	4	9	20	18	43	77	80	89	54	17	6	3	81	246	77
2	2	4	9	10	25	40	47	30	33	9	3	2	44	117	45
3		2	3	3	3	17	26	24	12	4		2	9	67	16
4			1		3	6	9	10	3				4	25	3
5					0	2	2	3					0	7	
6					1	1							1	1	
n	341	310	341	330	341	330	341	341	330	341	330	341	1012	1012	1001

TABLE 13.7 RELATIVE FREQUENCY OF DAYS THAT EXPERIENCED AT LEAST ONE THUNDERSTORM EVENT AT KSC

Jan	Feb	Mar	Apr	May	Jun	Jul	Aug	Sep	Oct	Nov	Dec	Spring	Summer	Fall
0.018	0.048	0.097	0.094	0.220	0.433	0.481	0.457	0.309	0.088	0.027	0.021	0.137	0.458	0.141

TABLE 13.8 FREQUENCIES OF THE OBSERVED NUMBER OF DAYS THAT EXPERIENCED x THUNDERSTORM HITS AT KSC FOR THE 11-YEAR PERIOD OF RECORD JANUARY 1957 THROUGH DECEMBER 1967

x	Jun	Jul	Aug	Summer
0	293	305	300	898
1	27	24	30	81
2	5	6	7	18
3	3	3	2	8
4 or more	2	3	2	7
Total	330	341	341	1012

TABLE 13.9 RELATIVE FREQUENCY OF DAYS THAT EXPERIENCED AT LEAST ONE THUNDERSTORM HIT AT KSC

Jun	Jul	Aug	Summer
0.112	0.106	0.121	0.113

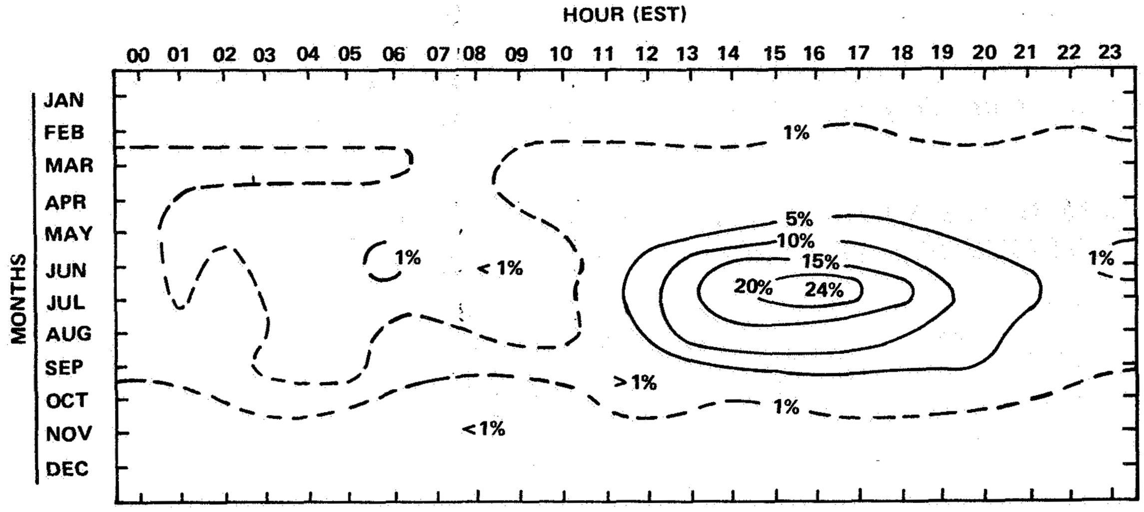

FIGURE 13.5 PROBABILITY (%) OF OCCURRENCE OF THUNDERSTORMS BY MONTHS VERSUS TIME OF DAY IN THE KSC AREA

13.5 Frequency of Lightning Strokes to Earth

Only limited data have been obtained on the number of lightning strokes to ground. These data are difficult ot obtain because lightning stroke measuring equipment does not usually differentiate between cloud-to-ground and cloud-to-cloud strokes. In addition, the equipment may record a strong stroke at a great distance and not record a weak stroke much closer. Therefore, the most reliable data of cloud-to-ground lightning strokes have been obtained visually. Such observations are limited in both number and length of time of observations.

Comparison of data published on cloud-to-ground lightning strokes from measuring equipment, visual observations, actual strikes to objects from insurance claims and magnetic links, and electrical outages confirms that the average number of lightning strokes per year to objects of different heights given in Table 13.10 is realistic of the KSC area.

Table 13.10 should not be interpreted to mean that 4.4 lightning strokes will be observed on a 152-meter (500-ft) object at KSC each year (Ref. 13.9). There may be no strokes or very few during a year, then in another year, a considerable number of strokes. Also one can assume that all strokes that occur will not be observed or known to have occurred within the launch area. Although numerous aerospace vehicles have been launched from KSC during the last 15 years, only a few lightning strokes are known to have struck the launch complexes until Apollo 15, when 11 separate strokes were known to have struck the launch complex during 5 different days between June 14 and July 21, 1971 (a period of 37 days) (Ref. 13.21).

TABLE 13.10 ESTIMATE OF THE AVERAGE NUMBER OF LIGHTNING STROKES PER YEAR FOR VARIOUS HEIGHTS FOR KSC

Height		Average Number of Lightning Strokes per Year
(m)	(ft)	
30.5	100	0.4
61.0	200	1.1
91.4	300	2.3
121.9	400	3.5
152.4	500	4.4
182.9	600	5.3
213.4	700	5.8

13.6 Static Electricity

A static electrical charge may accumulate on an object from its motion through an atmosphere containing raindrops, ice particles, or dust. A stationary object, if not grounded, can also accumulate a charge from windborne particles (often as nuclei too small to be visible) or rain or snow particles striking the object. This charge can build up until the local electric field at the point of sharpest curvature exceeds the breakdown field. The quantity of maximum charge will depend on the size and shape of the object (especially if sharp points are on the object). Methods of calculating this charge are given in Reference 13.15.

If a charge builds up on a vehicle on the launch pad which is not grounded, any discharges which occur could ignite explosive gases or fuels, interfere with radio communications or telemetry data, or cause severe shocks to personnel. Static electrical charges occur more frequently during periods of low humidity and can be expected at all geographical areas.

13.7 Electrical Breakdown of the Atmosphere

The atmosphere of the earth at normal sea-level pressure (101 325 N/m^2) is an excellent insulator, having a resistance greater than 10^{16} ohms for a column 1 square centimeter in cross section and 1 meter long. When there is a charge in the atmosphere, ionization takes place, thus increasing the conductivity of the air. This charge can be from either cloud buildups or electrical equipment. If the voltage is increased sufficiently, the ionization will be high enough for a spark to discharge.

The breakdown voltage (voltage required for a spark to jump a gap) for direct current is a function of atmospheric pressure. The breakdown voltage decreases with altitude until a minimum is reached of 327 volts per millimeter at an atmosphere pressure of 760 newtons per square meter (7.6 mb), representing an altitude of 33.3 kilometers. Above and below this altitude, the breakdown voltage increases rapidly (Ref. 13.22), being several thousands volts per millimeter at normal atmospheric pressure (Fig. 13.6).

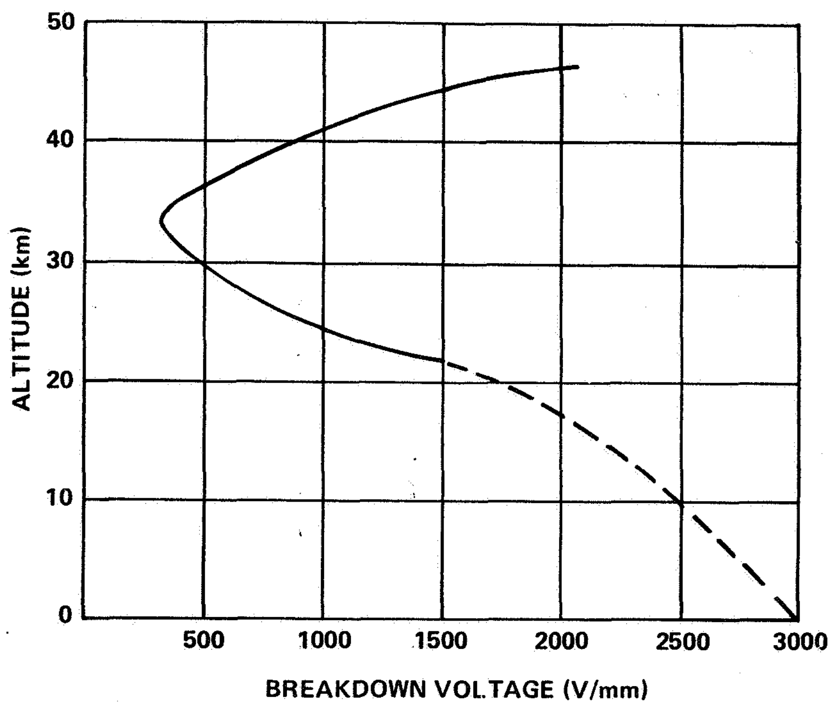

FIGURE 13.6 BREAKDOWN VOLTAGE VERSUS ALTITUDE

The breakdown voltage is also a function of frequency of an alternating current. With an increase of frequency the breakdown voltage decreases. A more complete discussion can be found in Reference 13.23.

The following safety measures can be taken to prevent arcing of high voltage in equipment:

1. Have equipment voltages off at the time the space vehicle is going through the critical atmospheric pressures. Any high-voltage capacitors should have bleeding resistors to prevent high-voltage charges remaining in the capacitors.

2. Eliminate all sharp points and allow sufficient space between high-voltage circuits.

3. Seal high-voltage circuits in containers at normal sea-level pressures.

4. Have materials available to protect, with proper use, against high-voltage arcing by potting circuits.

C-5

REFERENCES

13.1 Corbin, John C., Jr.: Protection of Systems Avionics Against Atmospheric Electricity Hazards — Lightning and Static Electricity. IEEE 1977 National Aerospace and Electronics Conference Proceedings, May 1977.

13.2 Electromagnetic Compatibility. Air Force Systems Command Design Handbook, AFSC DH1-4, Third Edition, January 5, 1975.

13.3 Lightning Test Waveforms and Techniques for Aerospace Vehicles and Hardware. Report of SAE Committee AE-4, Special Task F, May 5, 1976.

13.4 Space Shuttle Program Lightning Protection Criteria Document. Document No. JSC-07636, Johnson Space Center, National Aeronautics and Space Administration, November 4, 1975.

13.5 Military Specification, Bonding, Electrical (for Aircraft). MIL-B-5087B(ASG), 1964, and Amendment 1, February 6, 1968.

13.6 Military Specification, Arrester, Lightning, General Specification For. MIL-A-9094D (ASG), March 17, 1969.

13.7 Military Specification, Electromagnetic Compatibility Requirements, Systems. MIL-E-6051D, September 7, 1967.

13.8 Military Standard, Electromagnetic Interference Characteristics, Requirements for Equipment. MIL-STD-461A, August 1, 1968.

13.9 Review of Lightning Protection Technology for Tall Structures. Sponsored by Office of Naval Research, National Aeronautics and Space Administration, Federal Aviation Administration, and U. S. Air Force. Johnson Space Flight Center, November 6, 1975.

13.10 Statement on Space Shuttle Lightning Protection Shield (80-Foot Fiberglass Cylinder on Top of LC39 Launch Pad Structure) as Employed During ASTP-Apollo Mission on Launch Complex 39 at KSC. Official contacts: William B. Durrett and Clyde Whittaker, DD-EDD, Kennedy Space Center, Florida.

REFERENCES (Continued)

13.11 Lightning Protection Guidelines for STADAN Ground Equipment. NASA CR-94682, N68-24516, High Voltage Laboratory, General Electric Company, Pittsfield, Massachusetts, Goddard Space Flight Center, Greenbelt, Maryland, November 1967.

13.12 Analysis of Apollo 12 Lightning Incident. Document No. MSC-01540, prepared jointly by Marshall Space Flight Center, Kennedy Space Center, and Manned Spacecraft Center, National Aeronautics and Space Administration, February 1970.

13.13 Appleman, Herbert S.: Lightning Hazard to Aircraft. Technical Report 179 (Rev.), Headquarters Air Weather Service (MAC), United States Air Force, Scott AFB, Illinois, April 1971.

13.14 Chalmers, J. Alan: Atmospheric Electricity. Pergamon Press, New York, 1957.

13.15 Brook, M.; Holmes, C. R.; and Moore, C. B.: Lightning and Rockets — Some Implications of the Apollo 12 Lightning Event. Naval Research Reviews, Vol. 23, No. 4, April 1970, pp. 1-17.

13.16 Uman, Martin A., and McLain, D. Kenneth: Lightning Currents Relative to Space Shuttles: Currents and Electric Field Intensity in Florida Lightning. NASA CR-2161, Marshall Space Flight Center, Alabama, November 1972.

13.17 Cianos, N., and Pierce, E. T.: A Ground-Lightning Environment for Engineering Usage. Stanford Research Institute, 1972.

13.18 Prentice, S. A., and Mackerras, D.: Recording Range of Lightning-Flash Counter. Proceedings IEEE, Vol. 116, No. 2, February 1969, pp. 294-302.

13.19 Electromagnetic Interference Characteristics, Measurement of. MIL-STD-462, July 31, 1967.

13.20 Falls, Lee W.; Williford, W. O.; and Carter, M. C.: Probability Distributions for Thunderstorm Activity at Cape Kennedy, Florida. NASA TM X-53867, NASA/Marshall Space Flight Center, Alabama, 1970.

REFERENCES (Concluded)

13.21 Apollo 15 Mission Report. MSC 05161, NASA, Manned Spacecraft Center (Johnson Space Center), Houston, Texas, December 9, 1971.

13.22 Spink, Bradley R.: A Practical Solution to the Arcing Problem at High Altitudes. Planetary and Space Science, Vol. 7, July 1961, pp. 11-18.

13.23 Paul, Fred W., and Burrowbridge, Donald: The Prevention of Electrical Breakdown in Spacecraft. NASA SP-208, National Aeronautics and Space Administration, Washington, D. C., 1969.

SECTION XIV. ATMOSPHERIC CORROSION AND ABRASION

14.1 Introduction

Salt-laden oceanic air causes corrosion to many materials. Wind moving over roughened sea surfaces enhances small droplets of salt water to become suspended in the air. Many droplets are small enough to remain suspended for long periods of time and may be transported significant distances. When these salt droplets and tiny salt particles accumulate on the surface of objects, a film of highly concentrated salt results. When the atmospheric moisture condition becomes saturated, or when light rain or drizzle occurs, these salt films become highly concentrated solutions, causing corrosion to many materials. Salt film on optical surfaces causes equipment dependent on such components to become totally inoperative. Salt solutions also provide a conductive path between voltage potentials in electrical circuits which alter or completely short out the flow of electricity. Also, corrosion by electrolytic action can result when two dissimilar metals are involved. Numerous other objects, organic or inorganic, are affected by ocean salt as well as other impurities dispersed by the atmosphere.

Solid particles (sand, dust, silt, etc.) carried by the wind can remove protective coatings of objects upon impact. Painted surfaces can become seriously scratched, abraded, and even pitted by the large variety of airborne particles. Under low wind speed conditions, damage results when the hardness of particulates is equal to or greater than exposed surfaces. Particles moved by high wind speeds, even particles with lesser hardness than the surfaces on which they impact, can cause abrasion. An aerospace vehicle and associated equipment must be designed to withstand or be protected from airborne abrasives.

14.2 Corrosion Tests of Salt Spray (Salt Fog)

14.2.1 Purpose

A salt spray test (salt fog) is conducted to determine the resistance of equipment to the effects of a salt atmosphere. Damage is primarily corrosion of metals; however, salt deposits may cause clogging or binding of moving parts. A salt spray test (Ref. 14.1) is outlined below. This accelerated test does not duplicate conditions of the natural salt air environment in that specified concentrations of moisture and salt are greater than are found in nature.

14.2.1.1 Application

This test is valuable for determining the durability of coatings and finishes exposed to a corrosive salt atmosphere. For other applications, this test should be applied only after full recognition of its deficiencies and limitations which are as follows:

14.2.1.1.1 Deficiencies

a. The successful withstanding of this test does not guarantee that the test item will prove satisfactory under all corrosive conditions.

b. The salt fog used in this test does not truly duplicate the effects of a marine atmosphere.

c. It has not been demonstrated that a direct relationship exists between salt fog corrosion and corrosion due to other media.

d. This test is generally unreliable for comparing the corrosion resistance of different materials or coating conditions, or for predicting their comparative service life. (Some idea of the service life of different samples of the same, or closely related metals, or of protective coating-base metal combinations exposed to marine or seacoast locations can be gained by this test provided the correlation of field service test data with laboratory tests that such a relationship does exist, as in the case of aluminum alloys, such correlation tests are also necessary to show the degree of acceleration, if any, produced by the laboratory test.)

14.2.1.1.2 Limitations

a. The salt fog test is acceptable for evaluating the uniformity (i.e., thickness and degree of porosity) of protective coatings, metallic and nonmetallic, of different lots of the same product, once some standard level of performance has been established. (When used to check the porosity of metallic coatings, the test is more dependable when applied to coatings which are cathodic rather than anodic toward the basic metal.)

b. This test can also be used to detect the presence of free iron contaminating the surface of another metal by inspection of the corrosion products.

14.2.1.2 Apparatus

The apparatus used in the salt fog test shall include the following:

a. Exposure chamber with racks for supporting test items.

b. Salt solution reservoir with means for maintaining an adequate level of solution.

c. Means for atomizing salt solution, including suitable nozzles and compressed air supply.

d. Chamber heating means and control.

e. Means for humidifying the air at a temperature above the chamber temperature.

14.2.1.2.1 Chamber

The chamber and all accessories shall be made of material that will not affect the corrosiveness of the fog, e.g., glass, hard rubber, plastic, or kiln dried wood other than plywood. In addition, all parts which come in contact with test items shall be of materials that will not cause electrolytic corrosion. The chamber and accessories shall be constructed and arranged so that there is no direct impingement of the fog or dripping of the condensate on the test items, that the fog circulates freely about all test items to the same degree, and that no liquid which has come in contact with the test items returns to the salt-solution reservoir. The chamber shall be properly vented to prevent pressure buildup and allow uniform distribution of salt fog. The discharge end of the vent shall be protected from strong drafts which can create strong air currents in the test chamber.

14.2.1.2.2 Atomizers

The atomizers used shall be of such design and construction as to produce a finely divided, wet, dense fog. Atomizing nozzles shall be made of material that is nonreactive to the salt solution.

14.2.1.2.3 Air Supply

The compressed air entering the atomizer shall be essentially free from all impurities, such as oil and dirt. Means shall be provided to humidify and warm the compressed air as required to meet the operating conditions. The air pressure shall be suitable to produce a finely divided dense fog with the atomizer or atomizers used. To insure against clogging the atomizers by salt deposition, the air should have a relative humidity of at least 85 percent at the point of release from the nozzle. A satisfactory method is to pass the air in very fine bubbles through a tower containing heated water which should be automatically maintained at a constant level. The temperature of the water should be at least 35°C (95°F). The permissible water temperature increases with increasing volume of air and with decreasing insulation of the chamber and the chamber's surroundings. However, the temperature should not exceed a value above which an excess of moisture is introduced into the chamber [for example 43°C (109°F) at an air pressure of 12 psi] or a value which makes it impossible to meet the requirements for operating temperature.

14.2.1.3 Preparation of Salt Solution

The salt used shall be sodium chloride containing on the dry basis not more than 0.1 percent sodium iodide and not more than 0.5 percent of total impurities. Unless otherwise specified, a 5 ± 1 percent solution shall be prepared by dissolving five parts by weight of salt in 95 parts by weight of distilled or demineralized water. The solution shall be adjusted to and maintained at a specific gravity between the limits shown in Figure 14.1 by utilizing the measured temperature and density of the salt solution. Sodium tetraborate (common borax) may be added to the salt solution in a ratio not to exceed 0.7 grams (1/4 level teaspoon) sodium tetraborate to 20 gallons of salt solution as a pH stabilization agent.

Adjustment of pH of the salt solution shall be so maintained that the solution atomized at 35°C (95°F) and collected by the method specified in 14.2.1.5.2 will be in the pH range of 6.5 to 7.2. Only diluted C.P. hydrochloric acid or C. P. sodium hydroxide shall be used to adjust the pH. The addition of sodium tetraborate as recommended in 2.4 will aid in maintaining a stable pH value. The pH measurement shall be made electrometrically, using a glass electrode with a saturated potassium chloride bridge, or by a colorimetric method, such as bromothymol blue, provided the results are equivalent to those obtained with the electrometric method. The pH shall be measured when preparing each new batch of solution and as specified in 14.2.1.6.

14.2.1.4 Filter

A filter fabricated of noncorrosive materials similar to that shown in Figure 14.2 shall be provided in the supply line and immersed in the salt solution reservoir in a manner such as that illustrated in Figure 14.3.

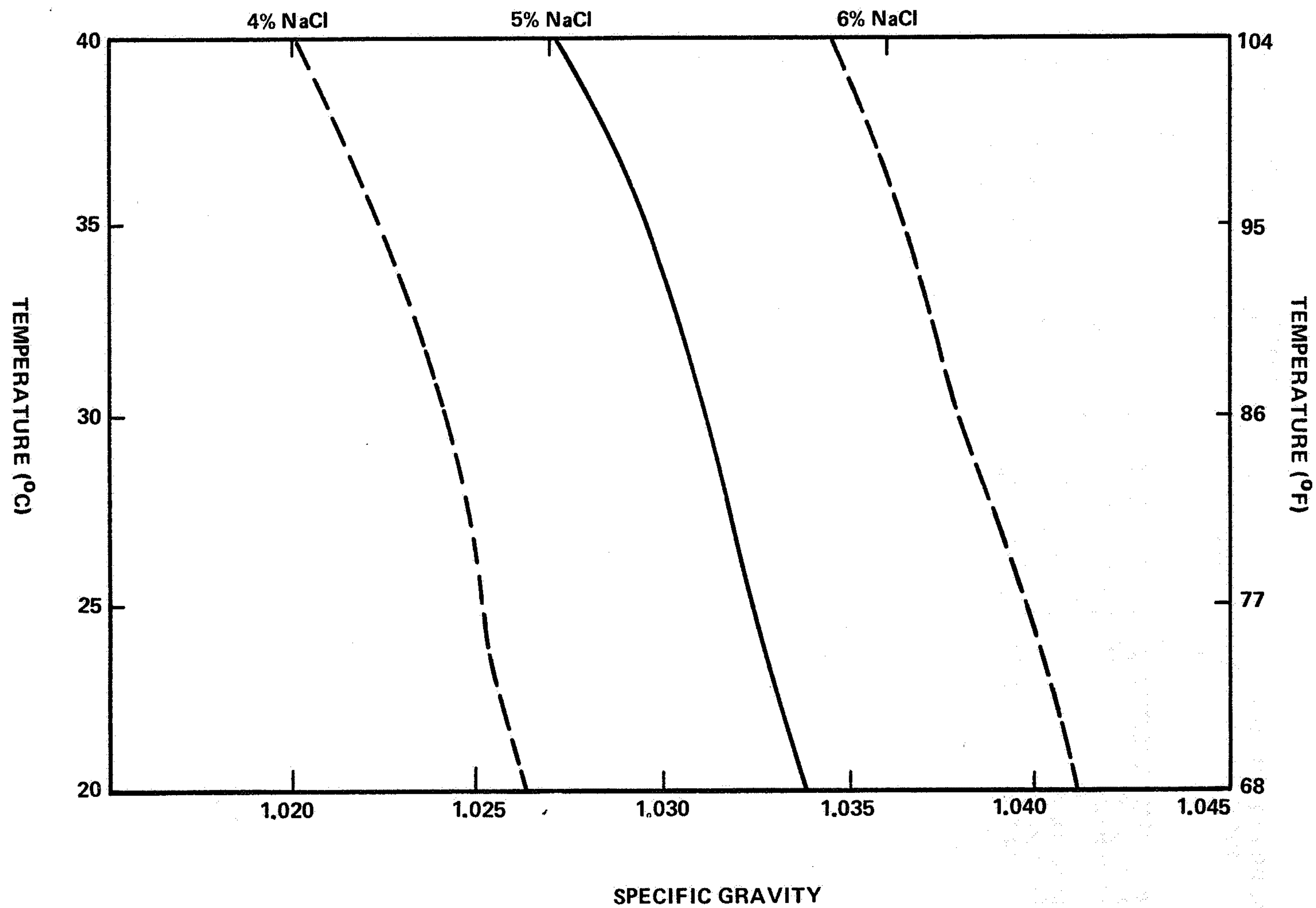

Figure 14.1 Variations of specific gravity of salt (NaCl) solution with temperature.

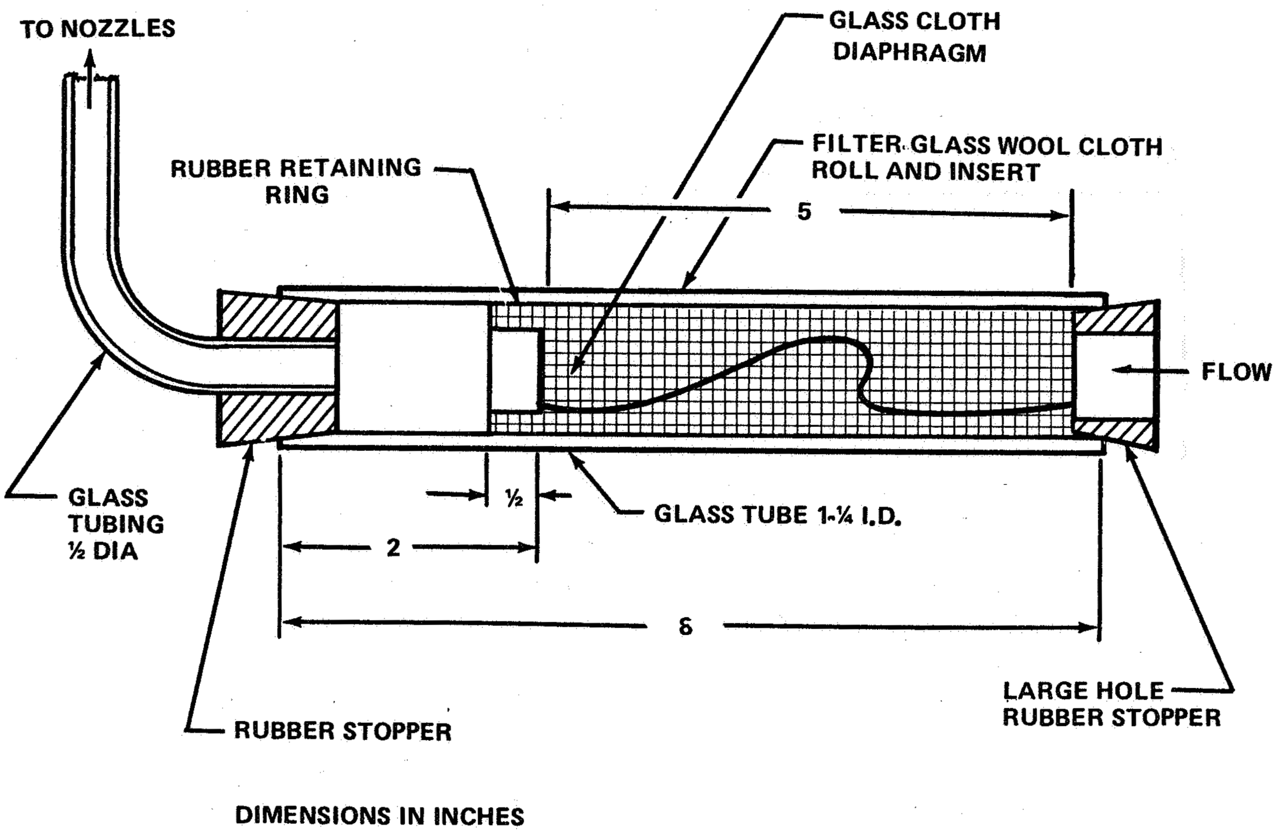

Figure 14.2 Salt solution filter.

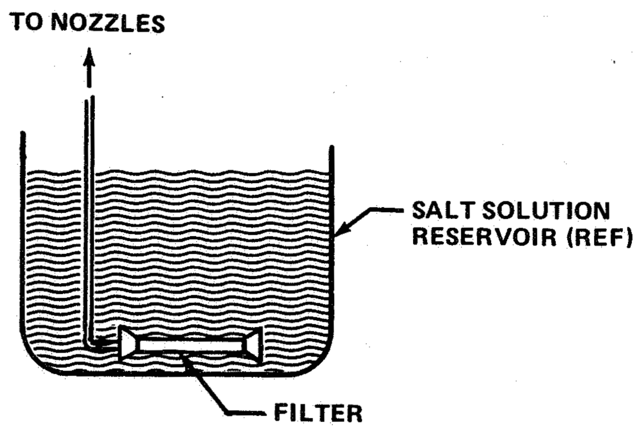

Figure 14.3 Location of salt solution filter.

14.2.1.5 Procedure

14.2.1.5.1 Temperature

The test shall be conducted with a temperature in the exposure zone maintained at 35°C (95°F). Satisfactory methods for controlling the temperature accurately are by housing the apparatus in a properly controlled constant temperature room, by thoroughly insulating the apparatus and preheating the air to the proper temperature prior to atomization, or by jacketing the apparatus and controlling the temperature of the water or of the air used in the jacket. The use of immersion heaters within the chamber for the purpose of maintaining the temperature within the exposure zone is prohibited.

14.2.1.5.2 Atomization

Suitable atomization has been obtained in chambers having a volume of less than 12 ft^3 under the following conditions:

a. Nozzle pressure shall be as low as practicable to produce fog at the required rate.

b. Orifices between 0.02 and 0.03 in. in diameter.

c. Atomization of approximately 3 quarts of salt solution per 10 ft^3 of chamber volume per 24 hr.

When using large size chambers having a volume considerably in excess of 12 ft^3, the conditions specified may require modification to meet the requirements for operating conditions.

14.2.1.5.3 Placement of Salt Fog Collection Receptacles

The salt fog conditions maintained in all parts of the exposure zone shall be such that a clean fog collecting receptacle placed at any point in the exposure zone will collect from 0.5 to 3 ml of solution per hour for each 80 cm^2 of horizontal collecting area (10 cm diameter) based on an average test of at least 16 hr. A minimum of two receptacles shall be used, one placed nearest to any nozzle and one farthest from all nozzles. Receptacles shall be placed so that they are not shielded by test items and so no drops of solution from test items or other sources will be collected.

14.2.1.6 Measurement of Salt Solution

The solution, collected in a manner specified in 14.2.1.5.2, shall have the sodium chloride content and pH specified in 2.4 when measured at a temperature of 35°C (95°F). The salt solution from all collection receptacles used can be combined to provide that quantity required for the measurements specified.

14.2.1.6.1 Measurement of Sodium Chloride Content

The solution, maintained at the specified temperature, can be measured in a graduate of approximately 2.5 cm inside diameter. A small laboratory type hydrometer will be required for measurement within this volume.

14.2.1.6.2 Measurement of pH

The pH shall be measured as specified in 14.2.1.3.

14.2.1.6.3 Time of Measurements

The measurement of both sodium chloride content and pH shall be made at the following specified times:

a. For salt fog chambers in continuous use, the measurements shall be made following each test.

b. For salt fog chambers that are used infrequently, a 24 hr test run shall be accomplished followed by the measurements. The test item shall not be exposed to this test run.

14.2.1.7 Preparation of Test Item

The test item shall be given a minimum of handling, particularly on the significant surfaces, and shall be prepared for test immediately before exposure. Unless otherwise specified, uncoated metallic or metallic coated devices shall be thoroughly cleaned of oil, dirt, and grease as necessary until the surface is free from water break. The cleaning methods shall not include the use of corrosive solvents nor solvents which deposit either corrosive or protective films, nor the use of abrasives other than a paste of pure magnesium oxide. Test items having an organic coating shall not be solvent cleaned. Those portions of test items which come in contact with the support and, unless otherwise specified in the case of coated devices or samples, cut edges and surfaces not required to be coated, shall be protected with a suitable coating of wax or similar substance impervious to moisture.

14.2.1.7.1 Performance of Test

The test item shall be placed in the test chamber in accordance with General Requirements, 14.2.1.8.3, and exposed to the salt fog for a period of 48 hr or as specified in the equipment specification. At the end of the exposure period, unless otherwise specified, the test item shall be operated and the results compared with the data obtained in accordance with General Requirements, 14.2.1.8.2. The test item shall be inspected for corrosion in accordance with General Requirements 14.2.1.8.4. If necessary to aid in examination, a gentle wash in running water not warmer than 38°C (100°F) may be used. The test item shall then be stored in an ambient atmosphere for 48 hr or as specified in the equipment specification for drying. At the end of the drying period, when specified, the test item shall be again operated and the results compared with the data obtained in accordance with General Requirements, 14.2.1.8.1. The test item shall then be inspected in accordance with General Requirements, 14.2.1.8.2.

14.2.1.8 General Requirements

14.2.1.8.1 Test Conditions

Unless otherwise specified herein or in the equipment specification, measurements and tests shall be made at standard ambient conditions. Standard ambient conditions are:

a.	Temperature	23° ± 10°C (73° ± 18°F)
	Relative humidity	50 percent ± 30 percent
	Atmospheric pressure	725^{+50}_{-75} mm Hg. ($28.5^{+2.0}_{-3.0}$ in. Hg.)

When these conditions must be closely controlled, the following shall be maintained:

b.	Temperature	23° ± 1.4°C (73° ± 2.5°F)
	Relative humidity	50 percent ± 5 percent
	Atmospheric pressure	725^{+50}_{-75} mm Hg. ($28.5^{+2.0}_{-3.0}$ in. Hg.)

(For additional details see Reference 14.1.)

14.2.1.8.2 Pretest Performance Record

Prior to proceeding with any of the environmental tests, the test item shall be operated under standard ambient conditions (see 14.2.1.8.1) to obtain data for determining satisfactory operation of the item as specified in the equipment specification, before, during and after the environmental test, as applicable. A record of specific pretest data shall be made to determine that the test item performs within prime item specification requirements. The pretest record shall also include the following, as applicable:

a. The functional parameters to be monitored during and after the test, if not specified in the equipment specification. This shall include acceptable functional limits (with permissible degradation) when operation of the test item is required.

14.2.1.8.3 Installation of Test Item in Test Facility

Unless otherwise specified, the test item shall be installed in the test facility in a manner that will simulate service usage, making connections and attaching instrumentation as necessary. Plugs, covers, and inspection plates not used in operation, but used in servicing shall remain in place. When mechanical or electrical connections are not used, the connections normally protected in service shall be adequately covered. For tests where temperature values are controlled, the test chamber shall be at standard ambient conditions when the test item is installed. The test item shall then be operated to determine that no malfunction or damage was caused due to faulty installation or handling.

14.2.1.8.4 Post-Test Data

At the completion of each environmental test, the test item shall be inspected in accordance with the equipment specification and the results shall be compared with the pretest data obtained in accordance with 14.2.1.8.2.

14.2.2 Summary

The following details shall be specified in the equipment specification:

a. Pretest data required

b. Failure criteria

c. Applicable salt solution, if other than 5 percent

d. Salt fog exposure period if other than 48 hr (see 3.1.6)

e. Drying period if other than 48 hr (see 3.1.6)

f. Inspection and operation after 24 hr of salt fog exposure where buildup of salt deposits are critical to the proper operation of the test item.

g. Specify if operation of electrical system is required (see 3.1.6).

A "Handbook on Corrosion Testing and Evaluation" (Ref. 14.9) contains additional information on the subject of corrosion and corrosion testing.

14.3 Corrosion in General

The amount of corrosion is a function of several factors. Among the most important factors are (Ref. 14.2):

a. The distance of the exposed test site from the ocean.

b. Air temperature.

c. Corrosion rates vary with elevation above sea level.

d. The length of time the humidity is high.

e. Corrosion depends on exposure direction, shelter around or near the material, and the direction and magnitude of the prevailing winds.

14.4 On-the-Spot Corrosion Tests

In any area where corrosion by the atmosphere can be an important factor, on-the-spot tests are needed. A test such as Sample's Wire-on-Bolt Test (Ref. 14.3) should be conducted on the site, with tests made at various heights above the ground.

14.5 Potential Corrosion Areas Regarding Aerospace Vehicle Operations

a. New Orleans (Michoud, Mississippi)

b. Gulf Transportation

c. Eastern Test Range

d. Panama Canal Transportation

e. Space and Missile Test Center

f. West Coast Transportation

g. Sacramento

h. Wallops Flight Center

14.6 Deposition of Salt Particles

The accumulation of salt on exposed surfaces is greatest during on-shore winds when many waves are breaking and forming white caps. Extremes expected are as follows (Ref. 14.4):

a. Particle size: Range from 0.1 to 20 μm, with 98 percent of the total mass greater than 0.8 μm.

b. Distribution is uniform above 3048 m (10 000 ft), but below cloud level.

c. Fallout of salt particles at Eastern Test Range:

(1) Maximum: 5.0×10^{-7} g cm^{-2} day^{-1}, to produce a coating on an exposed surface of 100 μm day^{-1}. This extreme occurs during precipitation.

(2) Minimum: 2.5×10^{-8} g cm^{-2} day^{-1}, to produce a coating on an exposed surface averaging 5 μm day^{-1}. This fallout occurs continuously during periods of no precipitation and is independent of wind direction. This coating will not usually be of uniform thickness but will be spots of salt particles unevenly distributed over the open surfaces.

14.7 Atmospheric Abrasion

When a stream of air flows around an object, the particles in the stream flow will also tend to flow around the object. However, the particles may collide with the object if they are too large. Small particles (sand, dust, silt, etc.) will impact with the object if their speed is too high and they resist the necessary change in motion. Also, if the particle inertia is sufficiently high and the flow direction change is great enough, particles will not swerve sufficiently to miss the object and will impact upon it. Particles impacting on, and colliding with, objects will abrade surfaces, depending upon their hardness and speed of motion (see subsection 14.1 above).

14.7.1 Mineral Hardness

Particle hardness is expressed according to Mohs' hardness scale. It is based on the relative hardness of 10 minerals as shown in Table 14.1 (Ref. 14.5).

TABLE 14.1 MOHS' SCALE-OF-HARDNESS FOR MINERALS

Mohs' Relative Hardness	Mineral	Mohs' Relative Hardness	Mineral
1	Talc	6	Orthoclase
2	Gypsum	7	Quartz
3	Calcite	8	Topaz
4	Fluorite	9	Corundum
5	Apatite	10	Diamond

14.8 Sand and Dust at Surface*

The presence of sand and dust can be expected in all geographical areas of interest but will occur more frequently in the areas with lower water vapor concentration. The extreme values expected are as follows.

14.8.1 Size of Particles

a. Sand particles will be between 0.080 mm (0.0031 in.) and 1.0 mm (0.039 in.) in diameter. At least 90 percent of the particles will be between 0.080 mm (0.0031 in.) and 0.30 mm (0.012 in.) in diameter.

b. Dust particles will be between 0.0001 mm (0.0000039 in.) and 0.080 mm (0.0031 in.) in diameter. At least 90 percent of these particles will be between 0.0001 mm (0.0000039 in.) and 0.002 mm (0.000079 in.) in diameter.

*Also see Reference 14.10 for additional information on atmospheric dust over selected geographical areas.

14.8.2 Hardness and Shape

More than 50 percent of the sand and dust particles will be composed of angular quartz or harder material, with a hardness of seven to eight.

14.8.3 Number and Distribution of Particles

a. Sand. For a wind speed of 10 m sec^{-1} (19.4 knots) at 3 m (9.8 ft) above a surface and relative humidity of 30 percent or less, 0.02 g cm^{-3} (1.2 lb ft^{-3}) of sand will be suspended in the atmosphere during a sand storm. Under these conditions, 10 percent of the sand grains will be between 0.02 m (0.079 ft) and 1.0 m (3.3 ft) above the ground surface, with the remaining 90 percent below 0.02 m (0.079 ft), unless disturbed by an object moving through the storm. When the wind speed decreases below 10 m sec^{-1} (19.4 knots), the sand grains will be distributed over a smaller distance above the ground surface, while a steady-state wind speed below 5 m sec^{-1} (9.7 knots) will not be sufficient to set the grains of sand in motion. As the wind speed increases above 10 m sec^{-1} (19.4 knots), the sand grains will be distributed over higher and higher distances above the ground surface.

b. Dust. For a wind speed of 10 m sec^{-1} (19.4 knots) at 3 m (9.8 ft) above surface, and relative humidity of 30 percent or less, 6×10^{-9} g cm^{-3} (3.7×10^{-7} lb ft^{-3}) of dust will be suspended in the atmosphere. Distribution will be uniform to about 200 m (656 ft) above the ground.

14.8.3.1 Dust (Fine Sand) Test (Ref. 14.1)

14.8.3.1.1 Purpose

The dust test is used to ascertain the ability of equipment to resist the effects of a dry dust (fine sand) laden atmosphere. This test simulates the effect of sharp edged dust (fine sand) particles, up to 150 μ in size, which may penetrate into cracks, crevices, bearings, and joints. This test is applicable to all mechanical, electrical, electronic, electrochemical, and electromechanical devices for which exposure to the effects of a dry dust (fine sand) laden atmosphere is anticipated. However, this method is not applicable to Southeast Asian dust conditions.

14.8.3.1.1.1 General Effects

General effects resulting from the penetration of dust can cause a variety of damage such as fouling moving parts, making relays inoperative, forming electrically conductive bridges with resulting shorts and acting as a nucleus for the collection of water vapor, and hence a source of possible corrosion and malfunction of equipment.

Many items, such as rifles, vehicles, and helicopters, will encounter sand particles up to 1000 μ, as opposed to the 149 μ maximum for 14-mesh silica flour sand tests, that would require a much coarser formulation than that covered by this method.

14.8.3.1.2 Apparatus

The test facility shall consist of a chamber and accessories to control dust concentration, velocity, temperature, and humidity of dust laden air. In order to provide adequate circulation of the dust laden air, no more than 50 percent of the cross-sectional area (normal to air flow) and 30 percent of the volume of the chamber shall be occupied by the test item(s). The chamber shall be provided with a suitable means of maintaining and verifying the dust concentration in circulation. A minimum acceptable means for doing this is by use of a properly calibrated smoke meter and standard light source. The dust laden air shall be introduced into the test space in such a manner as to allow it to become approximately laminar in flow before it strikes the test item.

14.8.3.1.2.1 Dust Requirements

The dust used in this test shall be a fine sand (97-99 percent by weight SiO_2) of angular structure, and shall have the following size distribution as determined by weight, using the U.S. Standard Sieve Series:

a. 100 percent of this dust shall pass through a 100-mesh screen

b. 98 ± 2 percent of the dust shall pass through a 140-mesh screen

c. 90 ± 2 percent of the dust shall pass through a 200-mesh screen

d. 75 ± 2 percent of the dust shall pass through a 325-mesh screen.

NOTE: 140-mesh silica flour as produced by the Ottawa Silica Company, Ottawa, Illinois, or equal, is satisfactory for use in the performance of these tests.

14.8.3.1.3 Procedure

14.8.3.1.3.1 Procedure I

Prepare the test item in accordance with General Requirements 14.2.1.8.3, positioning the test item as near the center of the chamber as practicable. If more than one item is being tested, there shall be a minimum clearance of 4 in. between surfaces of test items or any other material or object capable of furnishing protection. Also, no surface of the test item shall be closer than 4 in. from any wall of the test chamber. Orient the item so as to expose the most critical or vulnerable parts to the dust stream. The test item orientation may be changed during the test if so required by the equipment specification.

Step 1 — Set the chamber controls to maintain an internal chamber temperature of 23°C (73°F) and a relative humidity of less than 22 percent. Adjust the air velocity to 1750 ± 250 ft/min. Adjust the dust feeder to control the dust concentration at 0.3 ± 0.2 grams/ft^3. With the test item nonoperating, maintain these conditions for 6 hr.

Step 2 — Stop the dust feed and reduce the air velocity to 300 ± 200 ft/min. Raise the internal chamber air temperature to 63°C (145°F). Hold these conditions for 16 hr.

Step 3 — While holding chamber temperature at 63°C (145°F) adjust the air velocity to 1750 • 250 fpm. Adjust the dust feeder to control the dust concentration at 0.3 ± 0.2 grams/ft^3. Unless otherwise specified, with the test item nonoperating, maintain these conditions for 6 hr.

Step 4 — Turn off all chamber controls and allow the test item to return to standard ambient conditions. Remove accumulated dust from the test item by brushing, wiping, or shaking, care being taken to avoid introduction of additional dust into the test item. Dust shall not be removed by either air blast or vacuum cleaning.

Step 5 — Operate and inspect the test item in accordance with General Requirements 14.2.1.8.3.

Step 6 — Inspect the test item and obtain results as specified in General Requirements (Ref. 14.1). In the performance of this inspection, test items containing bearings, grease seals, lubricants, etc., shall be carefully examined for the presence of dust deposits.

14.8.3.1.4 Summary

The following details shall be as specified in the equipment specification:

a. Pretest data required

b. Failure criteria

c. Change in orientation during test if required

d. Whether equipment is to operate during test and length of time required for operation and measurements (see steps 1 and 3)

e. Whether the second 6 hr test at 63°C (145°F) shall be performed immediately after reaching stabilization (see step 2)

f. Temperatures for steps 2 and 3, if different from 63°C (145°F).

14.9 Sand and Dust at Altitude

Only small particles [less than 0.002 mm (0.000079 in.)] will be in the atmosphere above 400 m (1312 ft) in the areas of interest. During actual flight, the vehicle should pass through the region of maximum dust in such a short time that little or no abrasion can be expected.

14.10 Snow and Hail at Surface

Snow and hail can cause abrasion at the Huntsville, River Transportation, New Orleans, Wallops Flight Center, and White Sands Missile Range areas. Extreme values expected with reference to abrasion are as follows.

14.10.1 Snow Particles

Snow particles will have a hardness of two to four (Ref. 14.6) and a diameter of 1.0 mm (0.039 in.) to 5.0 mm (0.20 in.). A wind speed of 10 m sec^{-1} (19.4 knots) at a minimum air temperature of -17.8°C (0°F) should be considered for design calculations. At new Orleans a minimum air temperature of -9.4°C (15°F) should be used.

14.10.2 Hail Particles

Hail particles will have a hardness of two to four and a diameter of 5.0 mm (0.20 in.) or greater. A wind speed of 10 m sec^{-1} (19.4 knots) at an air temperature of 10.0°C (50°F) should be considered for design calculations.

14.11 Snow and Hail at Altitude

Snow and hail particles will have higher hardness values at higher altitudes. The approximate hardness of snow and hail particles in reference to temperature is given in Table 14.2.

TABLE 14.2 HARDNESS OF HAIL AND SNOW FOR ALL LOCATIONS

Temperature		Relative Hardness
(°C)	(°F)	(Mohs' Scale)
0	32.0	2
-20	- 4.0	3
-40	-40.0	4
-60	-76.0	5
-80	-112.0	6

Although the flight time of a vehicle through a cloud layer will be extremely short, if the cloud layer contains a large concentration of moderate-sized hailstones [25 mm (1 in.) or larger] at temperatures below -20.0°C (-4°F), considerable damage may be expected (especially to antennas and other protrusions) because of the kinetic energy of the hailstones at impact. Tests have shown a definite relationship between the damage to aluminum aircraft wing sections and the velocity of various-sized hailstones. Equal dents (sufficient to require repair) of 1 mm (0.039 in.) in 75 S-T aluminum resulted from the following impacts (Ref. 14.7):

a. A 19-mm (0.75 in.) ice sphere at 190 m sec^{-1} (369 knots).

b. A 32-mm (1.25 in.) ice sphere at 130 m sec^{-1} (253 knots).

c. A 48-mm (1.88 in.) ice sphere at 90 m sec^{-1} (175 knots).

14.12 Raindrops

With the advent of high-speed aircraft, a new phenomenon has been encountered in the erosion of paint coatings, of structural plastic components, and even of metallic parts by the impingement of raindrops on surfaces. The Space Shuttle Orbiter will be a high-speed vehicle that must be considered. Tests conducted by the British Ministry of Aviation (Ref. 14.8) have resulted in a table of rates on erosion for various materials and coatings. These materials and coatings were tested at speeds of 220 m sec^{-1} (428 knots). Sufficient data are not available to present any specific extreme values for use in design but results of the tests indicate that the material used should be carefully considered and weather conditions evaluated prior to launch.

REFERENCES

14.1 "Military Standards, Environmental Test Methods." MIL-STD-810C, March 10, 1975.

14.2 May, T. P.; and Taylor, V. G.: "Corrosion Testing in Marine Atmospheres." The Journal of Environmental Sciences, Vol. 7, No. 7, December 1964, pp. 23-27.

14.3 Doyle, D. P.; and Godard, Hugh P.: "A Rapid Method for Determining the Corrosivity of the Atmosphere at Any Location." Nature, Vol. 200, No. 4912, Dec. 21, 1963, pp. 1167-1168.

14.4 Brierly, William B.: "Atmosphere Sea-Salts Design Criteria Areas." The Journal of Environmental Sciences, Vol. 8, No. 5, October 1965, pp. 15-23.

14.5 Hurlbut, C. S., Jr.: "Dana's Manual on Mineralogy." Sixteenth Ed., John Wiley and Sons, Inc., New York, 1953.

14.6 Blackwelder, Eliot: "The Hardness of Ice." American Journal of Science, Vol. 238, 1940, pp. 61-63.

14.7 Sonter, Robert K.; and Emerson, Joseph B.: "Summary of Available Hail Literature and the Effect of Hail on Aircraft in Flight." NASA TN D-2734, Langley Aeronautical Laboratory, Langley Field, Va., 1952.

14.8 Fyall, A. A.; King, R. B.; and Strain, R. N.: "Rain Erosion Aspects of Aircraft and Guided Missiles." Journal of the Royal Aeronautical Society, Vol. 66, July 1962, pp. 447-453.

14.9 "Handbook on Corrosion Testing and Evaluation," edited by W. H. Ailor, John Wiley and Sons, Inc., New York, 1971.

14.10 Hinds, B. D., and Hoidale, G. B.: "Boundary Layer Dust Occurrence IV Atmospheric Dust over Selected Geographical Areas." ECOM-DR-77-3 (OSD-1366), Atmospheric Sciences Laboratory, U.S. Army Electronics Command, White Sands Missile Range, New Mexico, June 1977.

SECTION XV. ATMOSPHERIC OXIDANTS

15.1 Introduction

Oxides of metals and nonmetals substantiate the vast growth of technology directly involved in space research, nuclear technology, electronic and mechanical engineering, chemical technology, and many other scientific areas. Atmospheric chemistry, which includes numerous oxidation processes, plays a prime role in aerospace physics. The "nuts and bolts" that make up complex space create a special phenomenon of concern. Some factors influence the lower atmosphere; however, vehicle exhausts and other oxidant byproducts generated and released into the higher altitudes are also of concern.

This treatment of atmospheric oxidants is a very brief commentary on the subject. The main purpose is to recognize the importance of studying oxidants and how their physiochemical processes apply to missile and space vehicle research.

15.2 Oxidants and Their Source

Webster defines an oxidant as an oxidizer. Other words used are combustant, fermenter, respirator, etc. The term oxidase is the process in which various enzymes are used to catalyze oxidation, which is the main role in biological oxidation-reduction processes. A collection of articles on oxides is contained in Reference 15.1. Therein emphasis is placed on the electrical, mechanical, and magnetic properties of oxidants, which are discussed in great detail.

The present-day extraordinary expansions in the exploration of the ocean, atmosphere, and interplanetary space have made the "solid earth" science of geology somewhat bounded. As for the atmosphere, the study of oxygen involves the most important oxidant of concern. Photosynthesis is the principal process that produces oxygen (Ref. 15.2), which, in its abundance, associates with nearly all elements, making it the primary atmospheric oxidant. At extreme altitudes water is photodissociated and the hydrogen excapes into space, leaving oxygen behind in the upper atmosphere. This oxygen is then available to combine with molecular oxygen to produce ozone. Although another oxidant, ozone plays a significant part in absorbing a sizeable amount of the sun's ultraviolet radiation within the wavelengths of from 200 nm (2000 Å) to 300 nm (3000 Å), which is lethal to terrestrial organisms. Reference 15.3 goes into detail on the need for the earth's ozone.

The natural atmospheric substances play an extensive part in oxidizing materials; however, with the ever-increasing amount of pollutants the problem is becoming very harsh. Under certain atmospheric conditions such as high humidity, intense radiation, high temperature, and intermittent condensation with additional pollution, the life expectancy of many substances such as paint has been drastically reduced. Atmospheric oxidation and corrosion processes cause an endless retirement roster of ships, planes, space vehicle components and facilities, buildings, weapons, automobiles, etc. This leads to a loss of millions of dollars annually.

Research conducted by the British Corrosion Committee of the Iron and Steel Institute (Ref. 15.4) shows that industrial areas such as Pittsburgh, Pennsylvania, and Sheffield, Great Britain, have atmospheric conditions that are extreme oxidant aggressors whereas dry, unpolluted regions reveal minimum corrosion rates. With the extensive climatic variations of the United States where aerospace systems are fabricated and tested, special concern must be placed on the atmospheric oxidant problem.

Oxidation rates are commonly studied by the analyses of atmospheric water droplets, the determination of the amount of oxidation of test films, the study of the mineral content of atmospheric mist, and by various controlled experiments (see Section XIV on Atmospheric Corrosion and Abrasion).

In addition to oxygen and ozone, water vapor, carbon dioxide, sulfur dioxide, fluorine, etc., are active oxidants (Ref. 15.5). Such elements and compounds either serve as an oxidizer or aid in the oxidation processes.

The term "antioxidant" pertains to the protection against oxidation and inhibits attack by oxygen or ozone. Antioxidants are widely used not only to protect materials from atmospheric oxidation but also in consummables to prevent foods from spoiling. Such practices are expanding, with intense studies being carried out within the aerospace industry to improve food preservation methods. Reference 15.6 gives the extensive results of research on atmospheric oxidants and antioxidants. A treatment on the degradation of rubber and rubber products by ozone is also included.

Work began as early as 1922 (Ref. 15.7) to theoretically define the principles of oxidation and the tarnishing of metals. An electrochemical interpretation of ionic theory helped provide the basis for the equations which express the rate of oxidation and tarnishing of metals under normal atmospheric conditions. The three equations are as follows:

a. The linear equation is expressed by

$$y = K_1 t + A_1 \quad ;$$

b. The parabolic equation by

$$y^2 = K_2 t + A_2 \quad ,$$

c. And the logarithmic equation by

$$y = K_3 t \log(A_3 + B) \ ,$$

where y = film thickness, t = time, and K, A, and B are constants (Ref. 15.8). The values for K, for example, depend upon the temperature of the test item in question.

Reference 15.9 includes several scientific reports dealing with atmospheric influences on introduced and natural atmospheric constituents, electronic and mechanical systems, atmospheric diffusion, turbulence, etc.

15.3 Ozone and Oxides

Ozone, in high concentrations, is explosive and poisonous. One hundred parts per hundred million (phm) of ozone is toxic to man. The use of the air at high altitudes for breathing by pressurizing requires removal of the ozone. Ozone may be formed in high concentrations by short wavelength ultraviolet light [below 253.7 nm (2537 Å)] or by the arcing or discharge of electrical currents. A motor or generator with arcing brushes is an excellent source of ozone. The natural ozone concentration at the earth's surface is normally less than 3 phm except during periods of intense smog, where it may exceed 5 phm. Ozone concentration increases with altitude, with the maximum concentrations of 1100 phm being at 30 km (98 000 ft).

Maximum expected values of natural atmospheric ozone, for the purpose of design studies, are as follows: (1) surface, at all areas, a maximum concentration of 3 phm except during smog, where a maximum of 6 phm should be used, and (2) maximum concentration, with altitude, is given in Table 5.1 (Ref. 15.10).

At the surface, a maximum of 60 phm of oxidants composed of nitrogen oxides, hydrocarbons, sulfur dioxide, sulfur trioxides, peroxides, and ozone can be expected for 72 hours when smog occurs. The effect of these oxidants on rubber cracking and in some chemical reactions will be equivalent to 22 phm of ozone, but not necessarily equivalent to this concentration of ozone in other reactions (Ref. 15.11).

TABLE 15.1 DISTRIBUTION OF MAXIMUM DESIGN VALUES OF OZONE CONCENTRATION WITH ALTITUDE FOR ALL LOCATIONS

Geometric Altitude		Ozone (phm)	Ozone Concentration (cm/km)
(km)	(ft)		
SFC*	SFC*	6	0.006
9.1	30 000	30	0.010
15.2	50 000	200	0.030
21.3	70 000	700	0.040
27.4	90 000	1100	0.024
33.5	110 000	1100	0.009
39.6	130 000	600	0.002
45.7	150 000	400	0.0005

* Surface

The Handbook of Geophysics and Space Environments (Ref. 15.12) contains information on atmospheric ozone in regard to regions of formation, average distribution of ozone over the Northern Hemisphere in the spring and fall, and the vertical distribution of ozone.

Oxidants, including oxidation methods and examination and testing of oxidation products, are discussed in the Handbook on Corrosion Testing and Evaluation (Ref. 15.13).

REFERENCES

15.1 Samsonov, S. V.: "The Oxide Handbook." Institute of Problems in Materials Science, Academy of Sciences of the Ukrainian SSR, Kiev, USSR1 IFI/Plenum, New York-Washington-London, 1973.

15.2 Goody, Richard M.; and Walker, James C. G.: "Atmospheres." Prentice-Hall Inc., Englewood Cliffs, N.J., 1972.

15.3 Gibson, Edward G.: "The Quiet Sun." NASA SP-303, Manned Spacecraft Center, Houston, Tex., 1973.

15.4 "Official Investigation of the Corrosion Committee of the Iron and Steel Institute." Paper No. 10, British Corrosion Committee of the Iron and Steel Institute, 1943. (See also C. P. Larrabee, Translations of the Electrochemical Society, Vol. 87, No. 161, 1945.)

15.5 Bargmann, C. W., et al.: "Corrosion of Metals — A Series of Lectures." American Society of Metals, Cleveland, Ohio, 1946.

15.6 Scott, Gerald: "Atmospheric Oxidation and Antioxidations." Elsevier Publishing Co., Amsterdam-London-New York, 1965.

15.7 Miley, H. A.: "Theory of Oxidation and Tarnishing of Metals." Transactions of the Electrochemical Society, Vol. 81, 00 391-411, 1942.

15.8 Miley, H. A.: "Copper Oxide Films." Journal of American Chemistry Society, Vol. 59, 1937, pp. 2626-2629.

15.9 Simpson, C. L.: "Annual Report for 1971 to the USAEC Division of Biology and Medicine." Vol. II: Physical Sciences, Part 1; Atmospheric Sciences. Battelle, Pacific Northwest Laboratories, Richland, Wash., December 1972.

15.10 Ditaranto, R. A.; and Lamb, J. J.: "Preliminary Investigation of Hyger-Environments and Methods of Simulation, Part 1, Natural and Induced Environments Above 75,000 ft." WADC Technical Report 57-456, Part 1, ASTIA Doc. No. AD-142002, 1957.

15.11 Haagen-Smit, A. J.: "Chemistry and Physiology of Los Angeles Smog." Industrial and Engineering Chemistry, Vol. 44, No. 6, June 1952.

REFERENCES (Concluded)

15.12 "Handbook of Geophysics and Space Environments." Air Force Cambridge Research Laboratories, United States Air Force, 1965.

15.13 "Handbook on Corrosion Testing and Evaluation." W. H. Ailor, ed., John Wiley and Sons, Inc., New York, 1971.

SECTION XVI. FUNGI, BACTERIA, AND OTHER MICROORGANISMS

16.1 Introduction

Throughout the space research and technology industry, systematic sterilization principles are emphasized. The vast variety of microorganisms that thrive on earth enjoy environments conducive to their existence and reproduction. Essential sanitary measures are continuously employed to assure that fungi, bacteria, algae, etc., are not permitted to thrive where not desired. Subsequently, the success of any aerospace vehicle mission greatly depends on proper sanitation and sterilization practices.

Molds, mildew, and mushrooms are types of fungi. Fungi are parasitic organisms that lack chlorophyll production mechanism and therefore lack pigment for color. There are few, if any, organic substances that some form of fungus cannot disintegrate, given the proper environmental conditions. Plants and animals are constantly attacked by fungi; subsequently, fungicides and medicines must be used to control illnesses and infections resulting from their presence.

One of the most important issues in space travel is to control fungi and bacteria in space systems so as to eliminate possible infections and especially to warrant against the contamination of other planetary environments. It is well known that many microorganisms can remain in a dormant state for long periods of time, even under extreme climatic conditions, only to thrive once exposed to a favorable atmosphere.

16.2 Fungi

With regard to reproduction, most fungi are classified into the three following groups (Ref. 16.1):

1. Hermophroditic, in which each thallus (an individual fungus) bears both male and female organs.

2. Dioecious, in which some thalli have only male organs, whereas others have only female organs.

3. Sexually Indifferent, in which production occurs without distinction of sex.

16.2

Griseofulvin is an unusual antimicrobial substance that has unique value in treating some fungal infections. Although low in toxicity, excessive doses can be lethal, as are many other therapeutic agents. Administration of the drug must be conducted only through close direction of a physician who specializes in the treatment of fungal diseases. Early experiments with antifungal agents showed that they were ineffective because of their inability to penetrate the keratin of skin, fingernails and toenails, and hair (Ref. 16.2).

16.2.1 The Fungus Test (Ref. 16.3)

16.2.1.1 Purpose

The fungus test is used to determine the resistance of equipment to fungi and to determine if such equipment is adversely affected by fungi under conditions favorable for their development, namely high humidity, warm atmosphere, and presence of inorganic salts.

Typical materials which will support and are damaged by fungi are:

Cotton

Wood

Linen

Cellulose nitrate

Regenerated cellulose

Leather

Paper and cardboard

Cork

Hair and felts

Natural rubber

Plastic materials containing linen, cotton or wood flour as a filler

Vinyl films containing fungus susceptible plasticizers

Formulations of elastomers containing fungus susceptible catalysts, plasticizers or fillers.

16.2.1.2 Apparatus

The apparatus required to conduct this test consists of chambers or cabinets together with auxiliary instrumentation capable of maintaining the specified condition of temperature and humidity. Provisions shall be made to prevent condensation from dripping on the test item. There shall be free circulation of air around the test item and the surface area of fixtures supporting the test item shall be kept to a minimum.

16.2.1.3 Procedures

16.2.1.3.1 Preparation of Mineral-Salts Solution

The solution shall contain the following:

Potassium dihydrogen orthophosphate (KH_2PO_4)	0.7 g
Potassium monohydrogen orthophosphate (K_2HPO_4)	0.7 g
Magnesium sulfate ($MgSO_4 \cdot 7H_2O$)	0.7 g
Ammonium nitrate (NH_4NO_3)	1.0 g
Sodium chloride (NaCl)	0.005 g
Ferrous sulfate ($FeSO_4 \cdot 7H_2O$)	0.002 g
Zinc sulfate ($ZnSO_4 \cdot 7H_2O$)	0.002 g
Manganous sulfate ($MnSO_4 \cdot 7H_2O$)	0.001 g
Distilled water	1000 ml

Sterilize the mineral salts solution by autoclaving at 121°C (250°F) for 20 min. Adjust the pH of the solution by the addition of 0.01 normal solution of NaOH so that after sterilization the pH is between 6.0 and 6.5. Prepare sufficient salts solution for the required tests.

16.2.1.3.2 Purity of Reagents

Reagent grade chemicals shall be used in all tests. Unless otherwise specified, it is intended that all reagents shall conform to the specifications of the Committee on Analytical Reagents of the American Chemical Society, where such specifications are available.

16.2.1.3.3 Purity of Water

Unless otherwise specified, references to water shall be understood to mean distilled water or water of equal purity.

16.2.1.4 Preparation of Mixed Spore Suspension

The following test fungi shall be used:

Fungi	ATCC No.[1]	NLABS No.[2]
Aspergillus niger	9 642	386
Aspergillus flavus	9 643	380
Aspergillus versicolor	11 730	432
Penicillium funiculosum	9 644	391
Chaetomium globosum	6 205	459

1. American Type Culture Collection, 12301 Parklawn Drive, Rockville, Maryland 20852
2. Pioneering Research Division, U.S. Army Natick Laboratories, Natick, Massachusetts 01760

Maintain cultures of these fungi separately on an appropriate medium such as potato dextrose agar. However, the culture of Chaetomium globosum shall be cultured on strips of filter paper on the surface of mineral — salts agar. (Mineral salts agar is identical to mineral salts solution described in 16.2.1.3.1, but contains in addition 15.0 g of agar per liter.) The stock cultures may be kept for not more than 4 months at 6 ± 4°C (43°F). Use subcultures incubated at 29°C (84°F) for 7 to 20 days in preparing the spore suspension.

Prepare a spore suspension of each of the five fungi by pouring into one subculture of each fungus a sterile 10-ml portion of water or of a sterile solution containing 0.05 g per liter of a nontoxic wetting agent such as sodium dioctyl sulfosuccinate. Use a sterile platinum or nichrome inoculating wire to scrape gently the surface growth from the culture of the test organism. Pour the spore charge into a sterile 125-ml glass-stoppered Erlenmeyer flask containing 45 ml of sterile water and 10 to 15 solid glass beads, 5 mm in diameter. Shake the flask vigorously to liberate the spores from the fruiting bodies and to break the spore clumps.

Filter the shaken suspension through a thin layer of sterile glass wool in a glass funnel into a sterile flask in order to remove mycelial fragments.

Centrifuge the filtered spore suspension aseptically, and discard the supernatant liquid. Resuspend the residue in 50 ml of sterile water and centrifuge.

Wash the spores obtained from each of the fungi in this manner three times. Dilute the final washed residue with sterile mineral-salts solution in such a manner that the resultant spore suspension shall contain 1 000 000 ± 200 000 spores per ml as determined with a counting chamber.

Repeat this operation for each organism used in the test and blend equal volumes of the resultant spore suspension to obtain the final mixed spore suspension.

The spore suspension may be prepared fresh each day or may be held at 6° ± 4°C (43°F) for not more than 4 days.

16.2.1.4.1 Viability of Inoculum Control

With each daily group of tests place each of three pieces of sterilized filter paper, 1 in. square, on hardened mineral-salts agar in separate Petri dishes. Inoculate these with the spore suspension by spraying the suspension from a sterilized atomizer so that the entire surface is moistened with the spore suspension. Incubate these at 29°C (84°F) at a relative humidity not less than 85 percent and examine them after 14 days' incubation. There shall be copious growth on all three of the filter paper control specimens. Absence of such growth requires repetition of the test.

16.2.1.4.2 Control Items

In addition to the viability of inoculum control, a number of known susceptible substrates shall be inoculated along with the test item to insure that proper conditions are present in the incubation chamber to promote fungus growth. The control items shall include three pieces each of preservative free vegetable tanned leather and protein-glue bonded cork.

16.2.1.4.3 Inoculation of Test and Control Items

a. Mount the test and control items on suitable fixtures or suspended from hangers.

b. Precondition the chamber and its contents at 29°C (84°F) and 95 percent R.H. for at least 4 hr.

c. Inoculate the test and control items with the mixed fungus spore suspension (16.2.1.4) by spraying it on the test and control items in the form of a fine mist from a previously sterilized atomizer or nebulizer until they are thoroughly wet with the spray. Incubation is to be started immediately following the inoculation.

16.2.1.5 Incubation

a. Maintain the test chamber at 29°C (84°F) and 95 percent R.H. (minimum) during the life of the test. Keep the test chamber closed during the incubation period except during inspection or for addition of other test items.

b. After 14 days, inspect the control items. They should show an abundant growth of fungus. If the control items do not show an abundant growth, the entire test shall be repeated.

c. If the control items show satisfactory fungus growth, continue the test for a period of 28 days from the time of inoculation or as specified in the equipment specification.

16.2.1.6 Criteria for Passing Test

At the end of the incubation period, the test item shall be removed from the test chamber and inspected in accordance with subsection 16.2.1.6.1 below. If so specified in the equipment specification, the test item shall be operated and the results compared with those obtained in accordance with subsection 16.2.1.6.2 below.

16.2.1.6.1 Visual Inspection and Failure Criteria

When specified herein, the test item shall be visually inspected and a record made of any damage or deterioration resulting from the test. If a test chamber is used for the test, perform a visual inspection of the test item within the chamber at test conditions, when possible. Upon completion of the test, visually inspect the test item again after the test item has been returned to standard ambient conditions. Deterioration, corrosion, or change in tolerance limits of any internal or external parts which could in any manner prevent the test item from meeting operational service or maintenance requirements shall provide reason to consider the test item as having failed to withstand the conditions of the test.

16.2.1.6.2 Pretest Performance Record

Prior to proceeding with any of the test methods, the test item shall be operated under standard ambient conditions (see 16.2.1.6.2.1) and a record made of all data necessary to determine compliance with required performance. These data shall provide the criteria for checking satisfactory performance of the test item either during, or at the conclusion of the test, or both, as required. Certification by signature and date block is required as specified in subsection 16.2.1.6.2.2 below.

16.2.1.6.2.1 Test Conditions

Unless otherwise specified herein, or in the equipment specification, all measurements and tests shall be made at standard ambient conditions. Standard ambient conditions are:

Temperature	23° ± 10°C (73° ± 18°F)
Relative humidity	50 percent ± 30 percent
Atmospheric pressure	725^{+50}_{-115} mm of mercury ($28.5^{+2.0}_{-4.5}$ in. of mercury)

When these conditions must be closely controlled, the following shall be maintained:

Temperature	23° ± 1.4°C (73° ± 2.5°F)
Relative humidity	50 percent ± 5 percent
Atmospheric pressure	725^{+50}_{-75} mm of mercury ($28.5^{+2.0}_{-3.0}$ in. of mercury)

16.2.1.6.2.2 Test Data

Test data shall include complete identification of all test equipment and accessories. The data shall include the actual test sequence used and ambient test conditions recorded periodically during the test period. The test record shall contain a signature and date block for certification of the test data by the test engineer.

16.2.1.7 Summary

The following details shall be designated in the equipment specification:

a. Pretest data required (see Paragraph 16.2.1.6.2)

b. Test period if other than 28 days (see Paragraph 16.2.1.5.c)

c. Whether test items shall be operated (see Paragraph 16.2.1.6).

16.3 Bacteria and Other Microorganisms

Bacteria, as well as other microorganisms, require nutrients. Bacteria differ from fungi in that they can produce useable energy by the oxidation of inorganic chemicals in order to develop and reproduce. Most bacteria use organic compounds and light energy for growth. To regulate or restrict the life of the fungi or bacteria, definite life-supporting needs must be realized. They are categorized as follows:

1. Organisms that need light energy to survive are known as PHOTOTROPHS.

2. Organisms existing on chemical energy for survival are CHEMOTROPHS.

3. Parasites are the PARATROPHS which live on other organic cells. Fungi and some bacteria are found in this category.

4. AUTOTROPHS exist on carbon dioxide only.

5. HETEROTROPHS exist on organic sources of carbon.

6. HYPOTROPHS are organisms that exist on the enzymic substances of host cells.

Subsequently, it can be seen that definite means to control fungi and bacteria would necessitate the exhaustion of the life-sustaining substance or substances (Ref. 16.4).

The growth rate characteristics for fungi and bacteria under optimum conditions are exponential. This means that these organisms can multiply from a few hundred to literally billions in a very few hours. This is why needed attention is placed on sterilization processes of all planetary and interplanetary space systems.

Some common bacteria that infect man and animals are as follows (Ref. 16.5):

1. Staphylococci cause infection of varying severity.

2. Streptococci are highly infectious to man and spread readily.

3. Pneumococci settle in the respiratory tract and can cause pneumonia.

4. Neisseriae infect the upper respiratory tract.

5. Mycobacteria are somewhat of a pathogenetic to man but are not too severe.

6. Carditis is associated with rheumatic fever.

7. Bacilli or any bacillus anthracis is infectious to man.

8. Clostridia are a type in which some are common in the intestinal tract of both man and animals.

9. Enteric bacteria normally are found in the intestinal tract, where they infect man and animals.

10. Pseudomonas pyocyanea are commensal in the intestinal tract; also found in wounds, burns, and in the urinary tract.

These are only a few bacteria with related pathological conditions. Expertise in fungal and bacterial research should be consulted to determine proper identification, causes, cure (if infected), control, etc., of infection due to these microorganisms.

The most important characteristics of air which relate to the survival of microorganisms such as fungi and bacteria appear to be temperature, moisture, and ultraviolet radiation (Ref. 16.6). These organisms are particularly sensitive to radiation. Low temperature conditions are more favorable for survival of most microorganisms than high temperature because of the reduced metabolic rate allowing for longer viability. Low humidity is the least attractive condition for the existence of almost all such organisms.

Algae are individual to multicellular plants found to grow in most regions of the earth. Certain varieties are even found in the icy regions of the earth where other living organisms are not found. Although algae are disturbing in many situations, they are quite essential to many other forms of life. Many types of fish use algae as their main food supply. Man, of course, uses algae in many ways, of which several advances are recognized in medical research. Two basic groups of algae are distinguished — the nonmotile algae (Rhizochrysis) and the mobile algae (Flagellate).

Algae are abundant everywhere except in very arid and hot regions which lack moisture. Also, algae are not found in extreme frigid environments as on permanent ice and snow fields. A favorable feature of algae is that they add chemicals to the soil upon death if mixed well with the soil. The flora can, however, be very disturbing when it completely infects water systems and other moist environments. To control algae the main nutrient, carbon, can be controlled (i.e., carbon, carbon dioxide, carbonate, organic compounds, etc.). Herbicides have been developed to control algae and not disturb other living organisms in areas where algae need to be reduced or eliminated.

16.4 Basic Criteria

Fungi and bacteria have their highest rate of growth at temperatures between 20°C and 38°C (68° and 100°F). The most ideal relative humidity is about 70 percent and above.

Proper fungus- and bacteria-proofing protection is required at all locations where aerospace vehicles are being developed, tested, and launched. Emphasis is placed on cleanliness of space capsules and space laboratories where interspatial transport of such microorganisms is possible.

Additional comments on fungi and bacteria contamination control in regard to packaging, handling, and transporting aerospace components are stated in Reference 16.7. References 16.8 through 16.12 contain detailed information on fungi and bacteria, including microbiology of the atmosphere and oceans.

16.5 Principal Sterilization Methods — (Methods Employed at MSFC/NASA)

Processes of purification and sterilization of certain materials and systems are of prime concern. Some recognized methods of sterilization are:

1. Pressurization Sterilization.
2. Dry Heat Sterilization.
3. Steam Sterilization.
4. Chemical Sterilization.

5. Hot Air Sterilization.

6. Electronic (radiation) Sterilization.

Item 6 refers to a large number of methods. This could pertain to sterilization methods such as high-frequency, ultra-high oscillatory techniques, optical penetration as by laser, etc.

Some methods employed to sterilization systems and components at the Marshall Space Flight Center are by the steam/autoclave method, the use of ultraviolet radiation, and by compounds such as ethylene oxide. Numerous other sterilization processes are available.

REFERENCES

16.1 Alexopoulos, C. J.: "Introduction Mycology." John Wiley and Sons, Inc., New York, 1952.

16.2 Ciegler, Alex, et al.: "Microbial Toxins." Vol. 6, Academy Press, New York and London, 1971.

16.3 "Military Standard, Environmental Test Methods." MIL-STD-810C, March 10, 1975.

16.4 Sokatch, J. R.: "Bacterial Physiology and Metabolism." Academy Press, London and New York, 1969.

16.5 Gillies, R. R.; and Dodds, T. C.: "Bacteriology Illustrated." The Williams and Wilkins Company, Baltimore, 1965.

16.6 Tromp, S. W.; and Wieke, W. H.: "Biometeorology." Vol. 2, Pergamon Press, New York, 1967.

16.7 Space Shuttle Flight and Ground System Specifications, JSC 07700, vol. X, Revision B, August 18, 1975.

16.8 Johnson, T. W.; and Sparrow, F. K.: "Fungi in Oceans and Estuaries." Stechert Publishing Co., 1970.

16.9 Funder, Sigurd: "Practical Mycology: Manual for Identification of Fungi." Hafner Publishing Co., Third revision, 1968.

16.10 Gregarg, P.: "Microbiology of the Atmosphere." Halsted Press, Second Edition, 1973.

16.11 Doetsch, R.: "Introduction to Bacteria and Their Ecobiology." University Park Press, 1973.

16.12 Hayes, W.: "The Genetics of Bacteria and Their Viruses." Halsted Press, Second Edition, 1976.

SECTION XVII. DISTRIBUTION OF SURFACE EXTREMES IN THE UNITED STATES

17.1 Introduction

Most NASA programs involving the launch and re-entry of space vehicles originate in the continental United States. This section provides the extremes of those meteorological variables not included elsewhere in this document that are critical to such programs. Statistical data discussed in this section include air temperature, snowfall, hail, and atmospheric pressure. Section XVIII, Worldwide Surface Extremes, provides a more general discussion of atmospheric extremes on a global scale.

17.2 Environments Included

(a) Air temperature, extreme maximum and minimum,

(b) Snow fall — snow loads, 24-hour maximum and storm maximum,

(c) Hail, maximum size,

(d) Atmosphere pressure, extreme maximum and minimum.

Information is available for other extreme atmospheric parameters by consulting the appropriate section in this document.

17.3 Source of Data

The extremes presented have been prepared using data from National Weather Service stations and published articles. These extremes represent the highest or lowest extreme value measured at each station. The length of record varies from station to station, but most values represent more than 15 years of record. Where the local surroundings have a geographical area with a special influence on an extreme value (such as the minimum temperature on a high mountain peak or other local condition), it will not in general be shown on the maps presented unless a Weather Service station is located there. If there is a facility at such a locality and an item of equipment is especially sensitive to an environment, a study is needed of the local environment where fabrication is to be made.

The extremes noted reflect measurements during the available period of record for essentially all meteorological parameters. Because this period of record covers only a few decades for most locations, it is obvious that there is a finite risk that extreme values used will be exceeded in future years. However, the values shown are considered appropriate as criteria guidelines to establish critical engineering design problems requiring more in-depth assessment relative to probable meteorological extremes during expected operational lifetime.

17.4 Extreme Design Environments[1]

17.4.1 Air Temperature

The distribution, by state and location, of extreme maximum air temperatures in the United States is shown in Figure 17.1A, while Figure 17.1B shows the extreme minimum temperature distribution. Given in Table 17.1 are the extreme U. S. Temperatures (° F) along with their locations and dates of occurrence (Ref. 17.1). To convert to ° C, use the formula: ° C = 5/9(F-32). The maps (Figs. 17.2A and 17.2B) from Reference 17.2 show the mean temperature and standard deviations of the temperatures for January and July.

To estimate the temperature $\hat{T}$ that is less than or equal to a probability p (corresponding to the normal distribution), from Figures 17.2A and 17.2B, find from the appropriate figure, by interpolation as needed, the mean temperature $\bar{T}$ and standard deviation S_T and substitute these in the equation

$$\hat{T} = \bar{T} + S_T \cdot y_s \ [°F].$$

Values of y_s for various normal probability levels are:

Cold Temperatures (Figure 17.2A) p	y_s	Hot Temperatures (Figure 17.2B) p	y_s
0.20	- 0.84	0.80	+ 0.84
0.10	- 1.28	0.90	+ 1.28
0.05	- 1.65	0.95	+ 1.65 (See footnote 2.)
0.025	- 1.96	0.975	+ 1.96
0.01	- 2.33	0.99	+ 2.33

1. All values of extreme maxima and minima in this section are for design guidelines and may or may not exactly reflect extrapolations (theoretical or otherwise) of actual measured values over the available period of record.

2. The 95th percentile value is recommended for hot-day design ambient temperatures over runways for landing-takeoff performance calculation using Figure 17.2B; the 5th percentile is for cold-day design.

ORIGINAL PAGE IS
OF POOR QUALITY

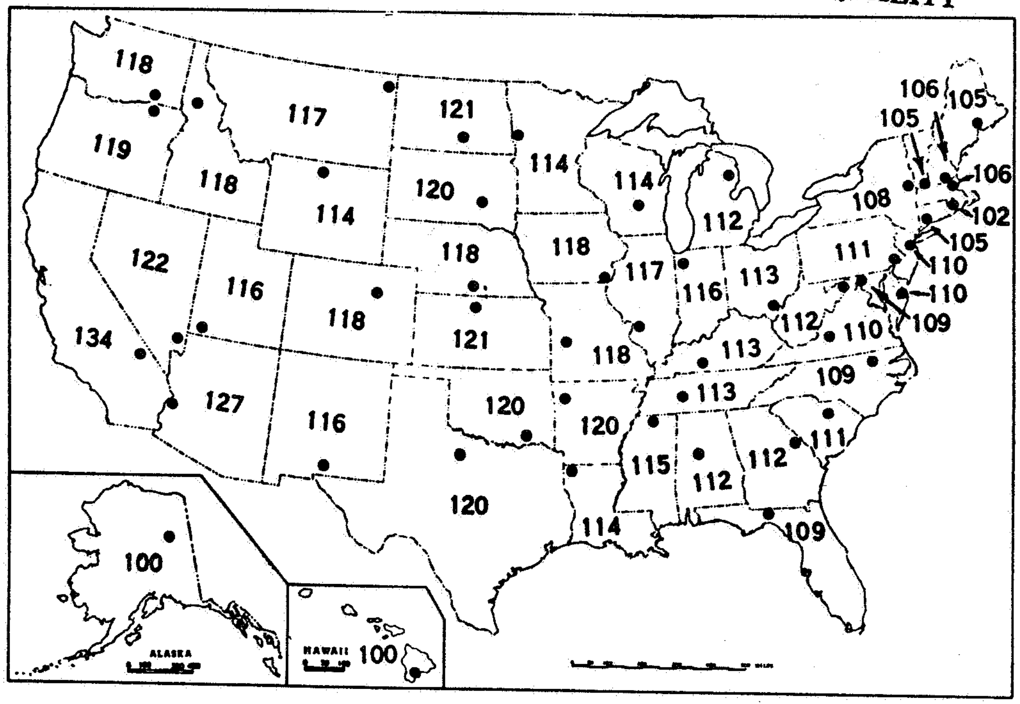

FIGURE 17.1A HIGHEST TEMPERATURES (°F) OF RECORD AND LOCATIONS, BY STATES

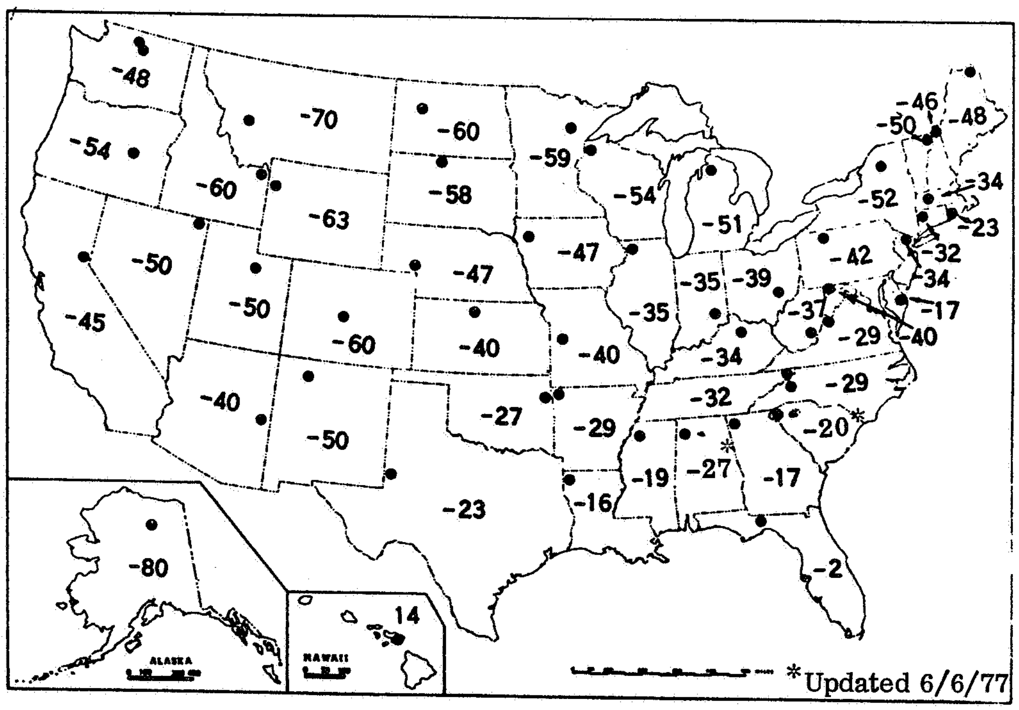

FIGURE 17.1B LOWEST TEMPERATURES (°F) OF RECORD AND LOCATIONS, BY STATES

TABLE 17.1 EXTREMES OF TEMPERATURE AND SEA-LEVEL PRESSURE FOR THE UNITED STATES

Temperature [°C (°F)]		Location	Date	Sea-Level Pressure [N/m^2 (mb)(in.)]	Location	Date
High				High		
Contiguous United States	57 (134)	Greenland Ranch, Ca.	July 10, 1913	106 330 (1063.3)(31.40)	Helena, Mont.	Jan. 9, 1962
Hawaii	38 (100)	Pahala	April 27, 1931	102 670 (1026.7)(30.32)	Honolulu	Feb. 10, 1919
Alaska	38 (100)	Fort Yukon	June 27, 1915	106 220 (1062.2)(31.36)	Bethel	Dec. 21, 1937
Low				Low		
Contiguous United States	-57 (-70)	Rogers Pass, Mont.	Jan. 20, 1954	95 490 (954.9)(28.20)	Canton, N.Y. Block Island, R. I.	Jan. 3, 1913 Mar. 7, 1932
U.S. (Hurricane)				89 230 (892.3)(26.35)	Matecumbe Key, Fla.	Sept. 2, 1935
Hawaii	10 (14)	Haleakala	Jan. 2, 1961	99 350 (993.5)(29.34)	Honolulu	Feb. 3, 1936
Alaska	-62 (-80)	Prospect Creek	Jan. 23, 1971	95 290 (952.9)(28.14)	Anchorage	Jan. 1, 1948

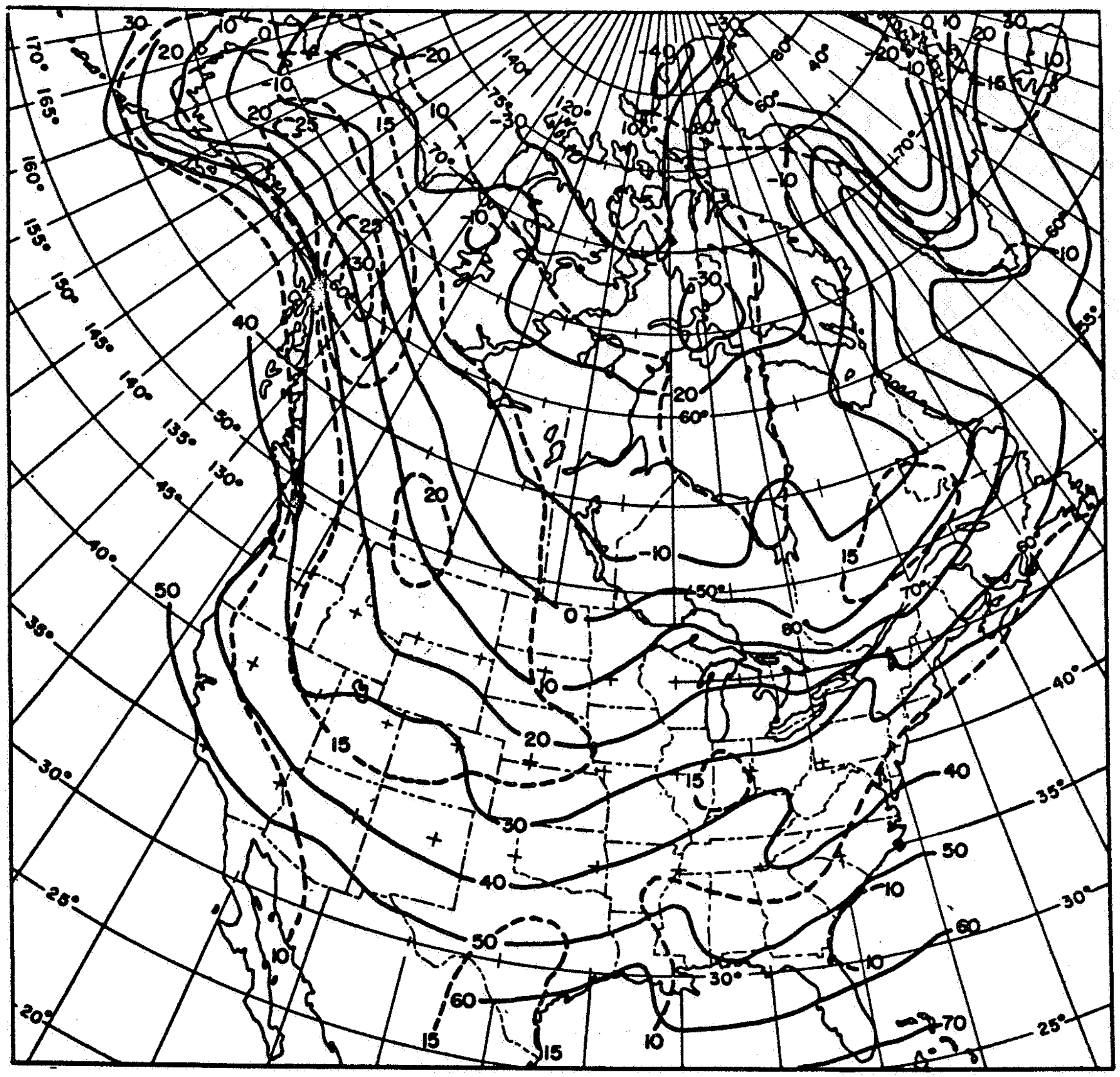

FIGURE 17.2A ISOTHERMS OF JANUARY HOURLY SURFACE TEMPERATURES (Approximate mean values (° F) are shown by solid lines, standard deviations (° F) by broken lines. The approximations were made to give best estimates of lower 1- to 20-percentile values of temperature by normal distribution.)[3]

---

3. Valley, Shea L., "Handbook of Geophysics and Space Environments," McGraw-Hill Book Company, Inc., New York, 1965.

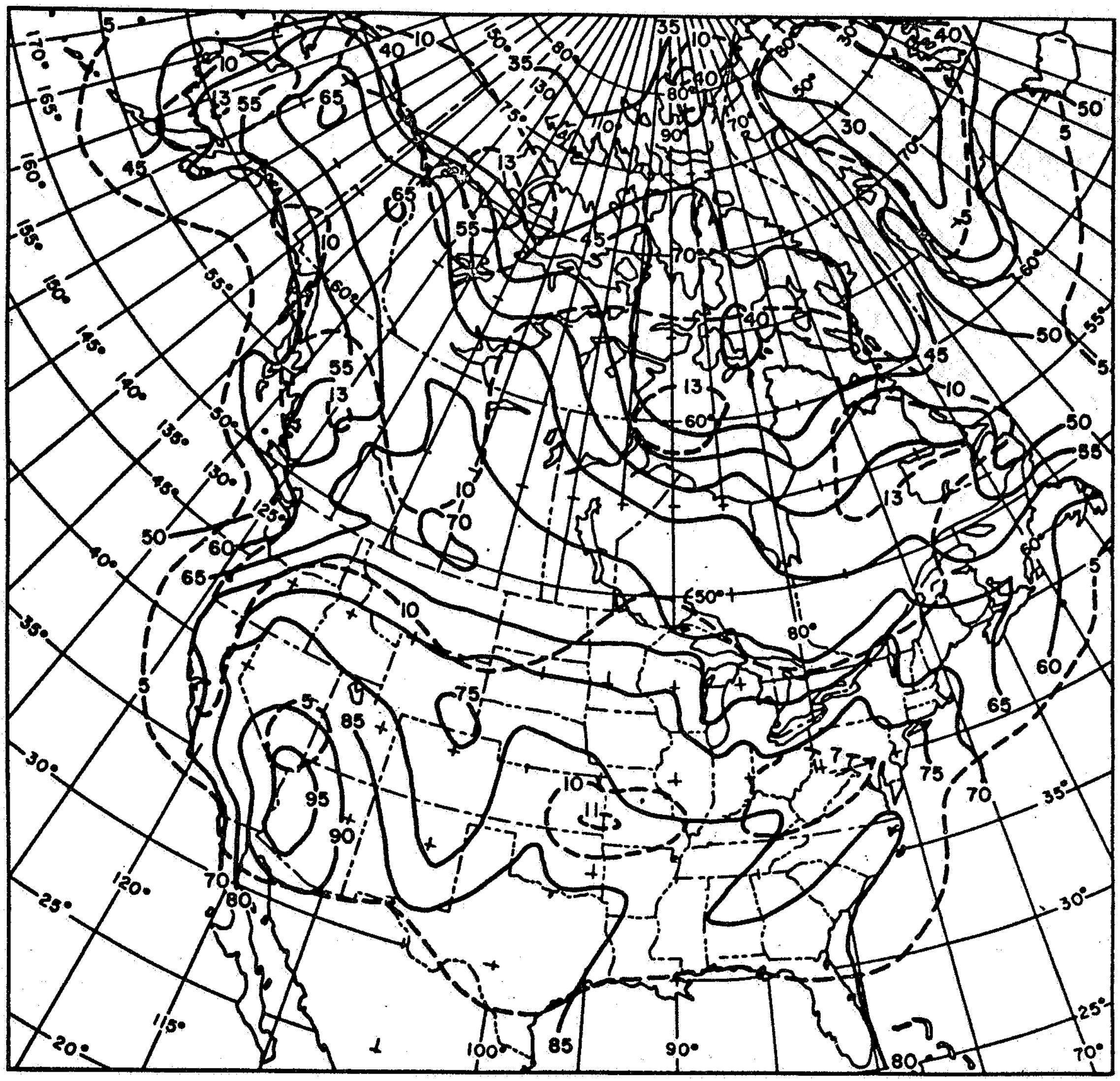

FIGURE 17.2B ISOTHERMS OF JULY HOURLY SURFACE TEMPERATURES (Approximate mean values (° F) are shown by solid lines, standard deviations (° F) by broken lines. The approximation were made to yield the best estimates of upper 80- to 99-percentile values by normal distribution)[3]

---

3. Ibid.

17.4.2 Snow Fall — Snow Load

The maps in Figures 17.3 and 17.4 show the maximum depth of snow and the corresponding snow loads. Figure 17.3 shows the maximum depth for a 24-hour period; Figure 17.4 shows the maximum depth and the corresponding snow loads for a storm period. The storm total map shows the same snow depth as in the 24-hour map in the southern low elevation areas of the United States since snow storms seldom exceed 24 hours in these areas. The greatest 24-hour snowfall was 1930 mm (76 in.) at Silver Lake, Colorado, on April 14-15, 1921. One storm gave 4800 mm (189 in.) at Mt. Shasta Ski Bowl, California, from February 13 to 19, 1959 (Ref. 17.3).

The terrain combined with the general movement of weather patterns has a great effect on the amount of fall, accumulation, and melting of the snow. Also, the length of a single storm varies for various areas. In some areas in mountain regions much greater amounts of snowfall have been recorded than shown on the maps. Also, the snow in these areas may remain for the entire winter. For example, in a small valley near Soda Springs, California, a seasonal snow accumulation of 7.9 m (26 ft) with a density of about 0.35 gm/cm^3 was recorded. This gives a snow load of 2772 kg/m^2 (567.7 lb/ft^2). Such a snow pack can do considerable damage to improperly protected equipment buried deep in the snow. This snow pack at Soda Springs is the greatest on record in the United States and was nearly double the previous records in the same area. A study of the maximum snow loads in the Wasatch Mountains of Utah (Ref. 17.4) showed that for a 100-year return period at 2740 m (9000 ft) altitude, a snow load of 1220 kg/m^2 (250 lb/ft^2) could be expected.

17.4.3 Hail

The distribution of maximum-sized hailstones in the United States is shown in Figure 17.5. The sizes are for single hailstones and not conglomerates of several hailstones frozen together. The largest officially recorded hailstone in the United States weighed 757 gm (1.67 lb). It fell Sept. 3, 1970, at Coffeyville, Kansas (Ref. 17.5).

17.4.4 Atmospheric Pressure

Atmospheric pressure extremes normally given in the literature are given as the pressure which would have occurred if the station were at sea level. The surface weather map published by the United States National Weather Service uses sea-level pressures for the pressure values to assist in map analysis and forecasting. These sea-level pressure values are obtained from the station pressures by use of the hydrostatic equation:

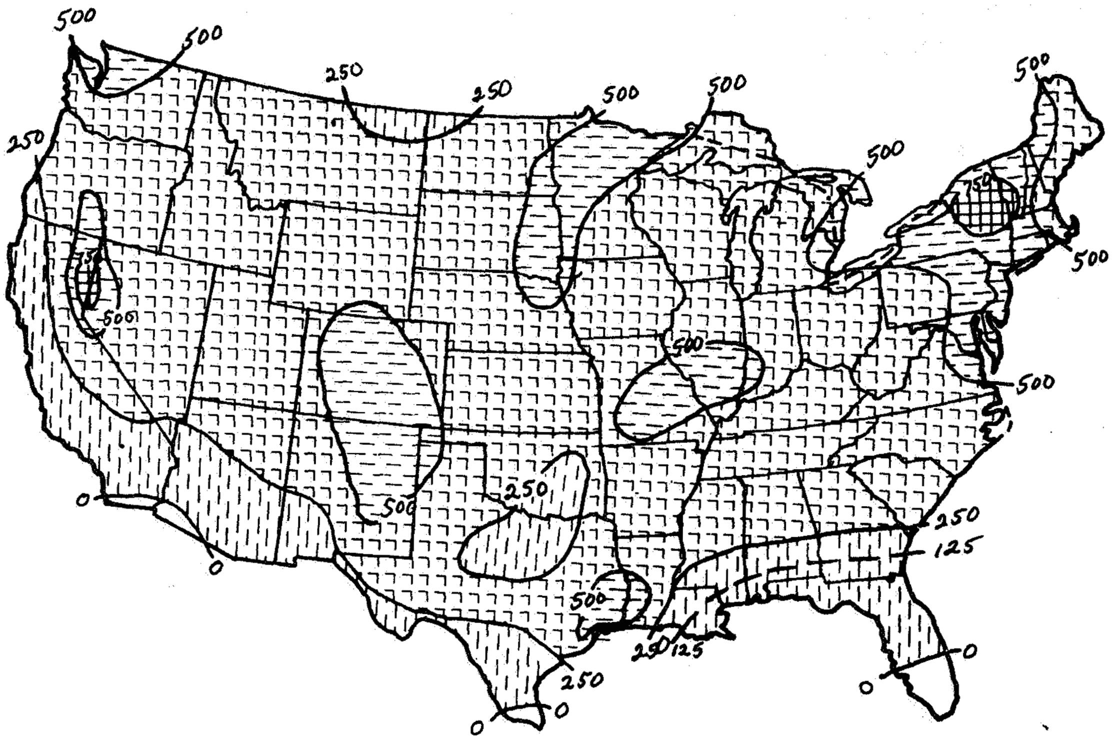

MAXIMUM SNOW LOAD

mm		kg/m^2
0-250		25
250-500		50
500-750		75
over 750		100

FIGURE 17.3 EXTREME 24-HOUR MAXIMUM SNOW FALL (mm)

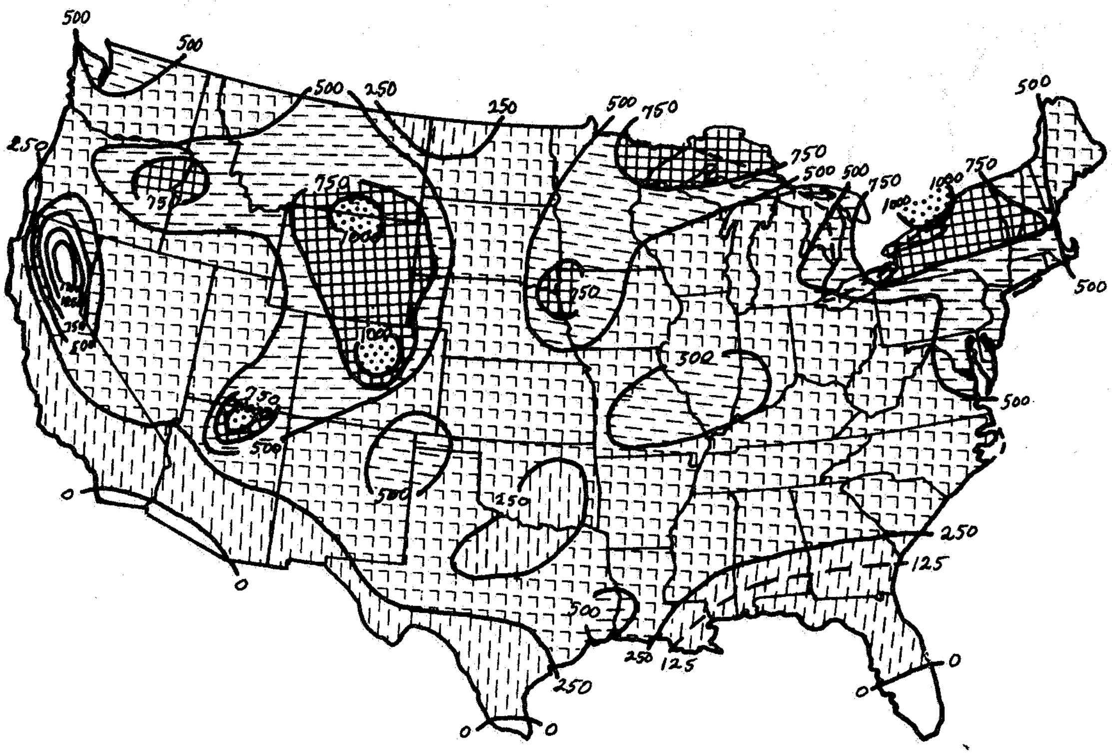

MAXIMUM SNOW LOAD

mm	kg/m²
0-250	25
250-500	50
500-750	75
750-1000	100
1000-1250	125

FIGURE 17.4 EXTREME STORM MAXIMUM SNOW FALL (mm)

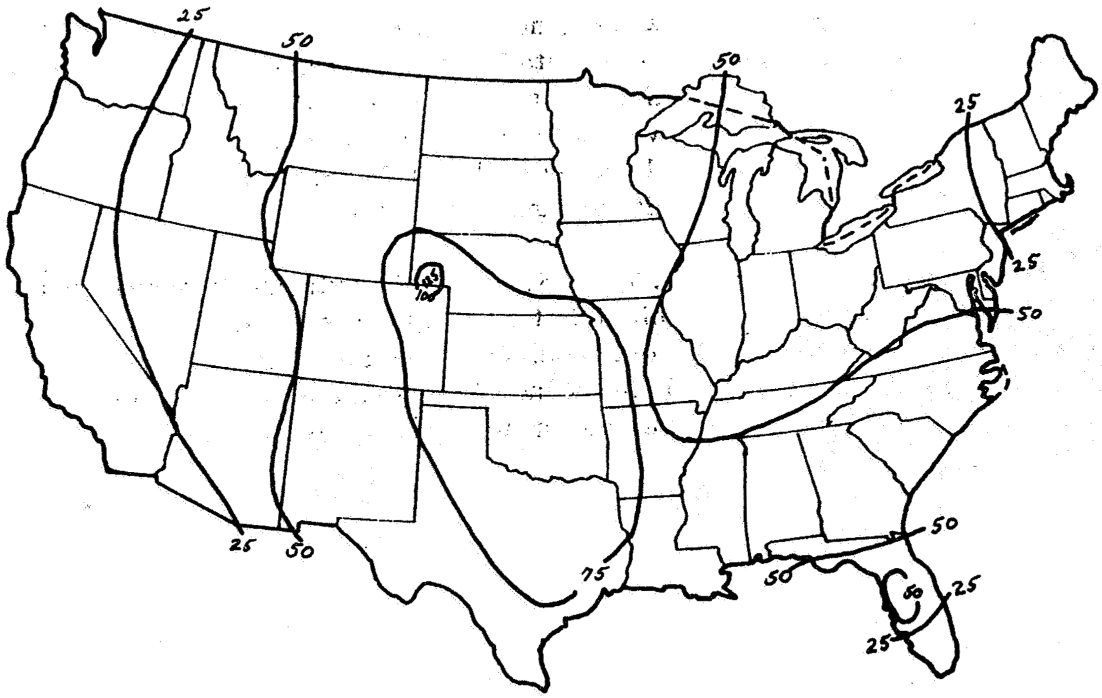

FIGURE 17.5 EXTREME MAXIMUM HAILSTONE DIAMETERS (mm)

$$dP = \rho g dZ$$

where

dP = pressure difference

ρ = density

g = gravity

dZ = altitude difference.

These sea level data are valid only for design purposes at locations with elevation near sea level. As an example, when the highest officially reported sea level pressure observed in the United States of 106 330 N/m^2 (1063.3 mb) occurred at Helena, Montana (Ref. 17.6), the actual station pressure was about 92 100 N/m^2 (921 mb) because the station is 1187 m (3893 ft) above mean sea level.

Figures 17.6 and 17.7 show the general distribution of extreme maximum and minimum station pressures in the United States. Because of the direct relationship between pressure and station elevation, Figures 17.8 through 17.11 should be used with the station elevation to obtain the extreme maximum and minimum pressure values for any location in the United States. Similar maps and graphs in U. S. Customary Units are given in Reference 17.7.

Using References 17.1, 17.6, 17.8, and 17.9, extreme temperatures and sea-level pressures for the United States are given in Table 17.1. (See Section III containing temperature extremes for selected sites. Section V contains station pressure extremes.) Reference 17.9 also contains surface atmosphere extreme criteria for vehicle launch and transporation areas.

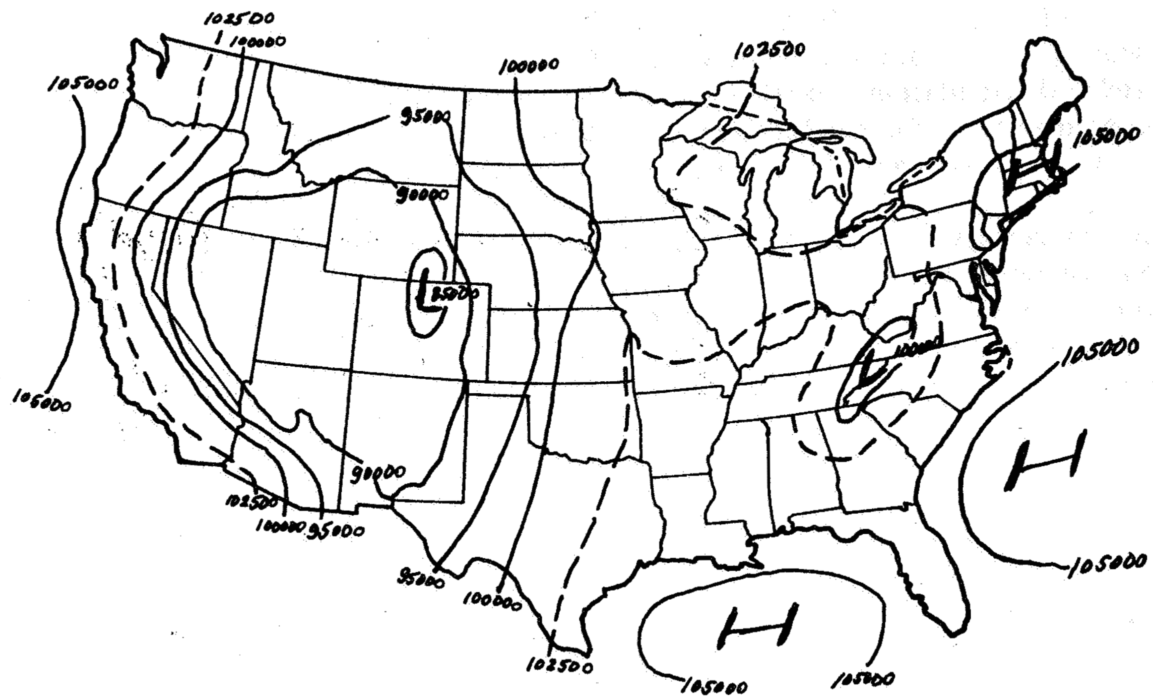

FIGURE 17.6 MAXIMUM ABSOLUTE STATION PRESSURE (N/m^2)

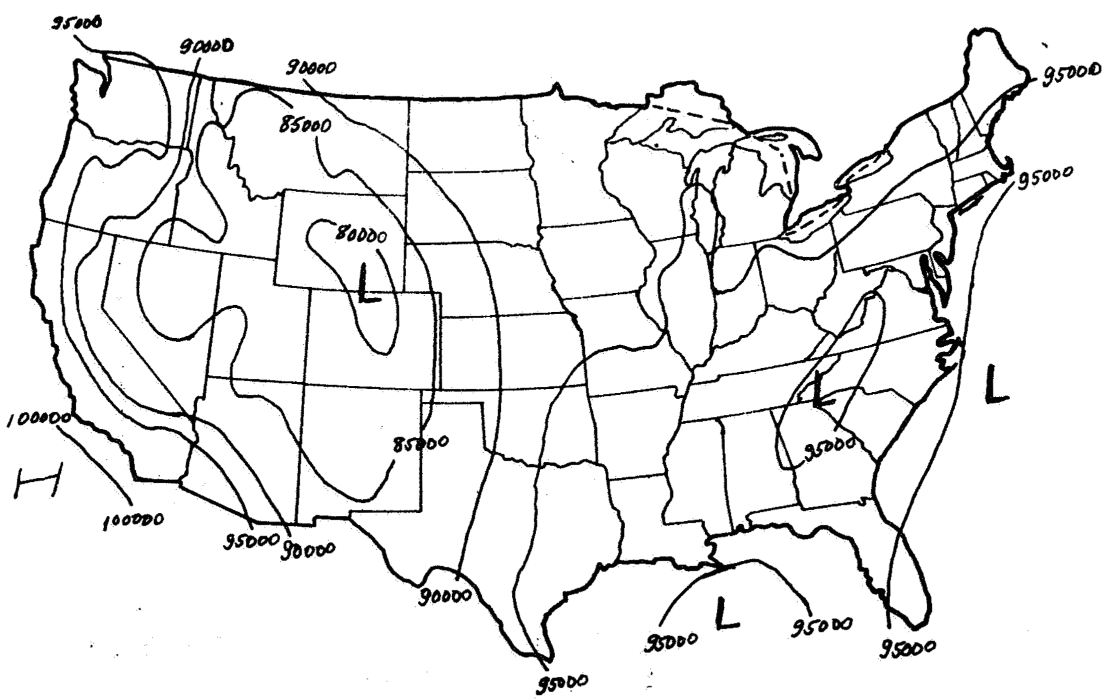

FIGURE 17.7 MINIMUM ABSOLUTE STATION PRESSURE (N/m^2)

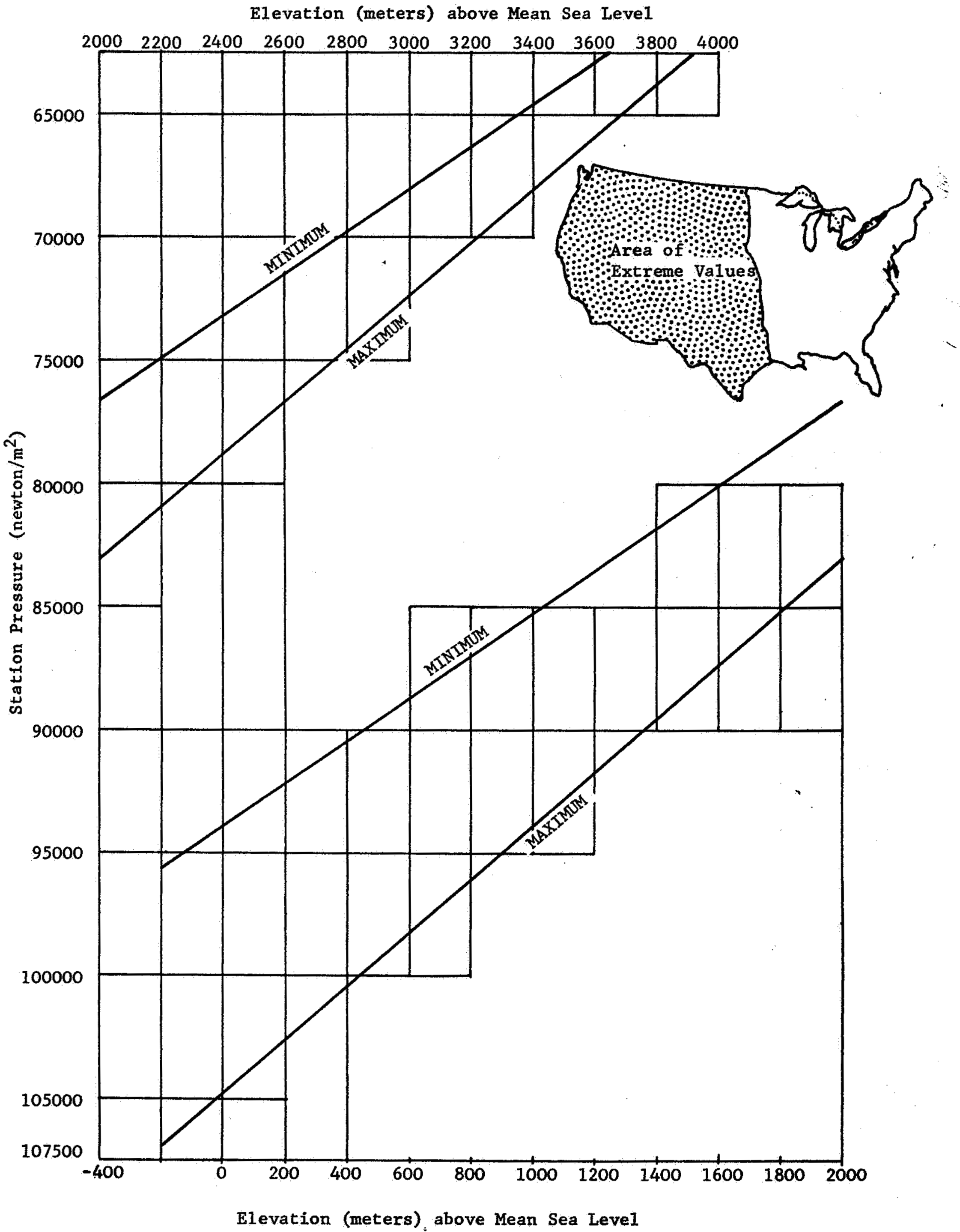

FIGURE 17.8 EXTREME PRESSURE VALUES VERSUS ELEVATION FOR WESTERN UNITED STATES

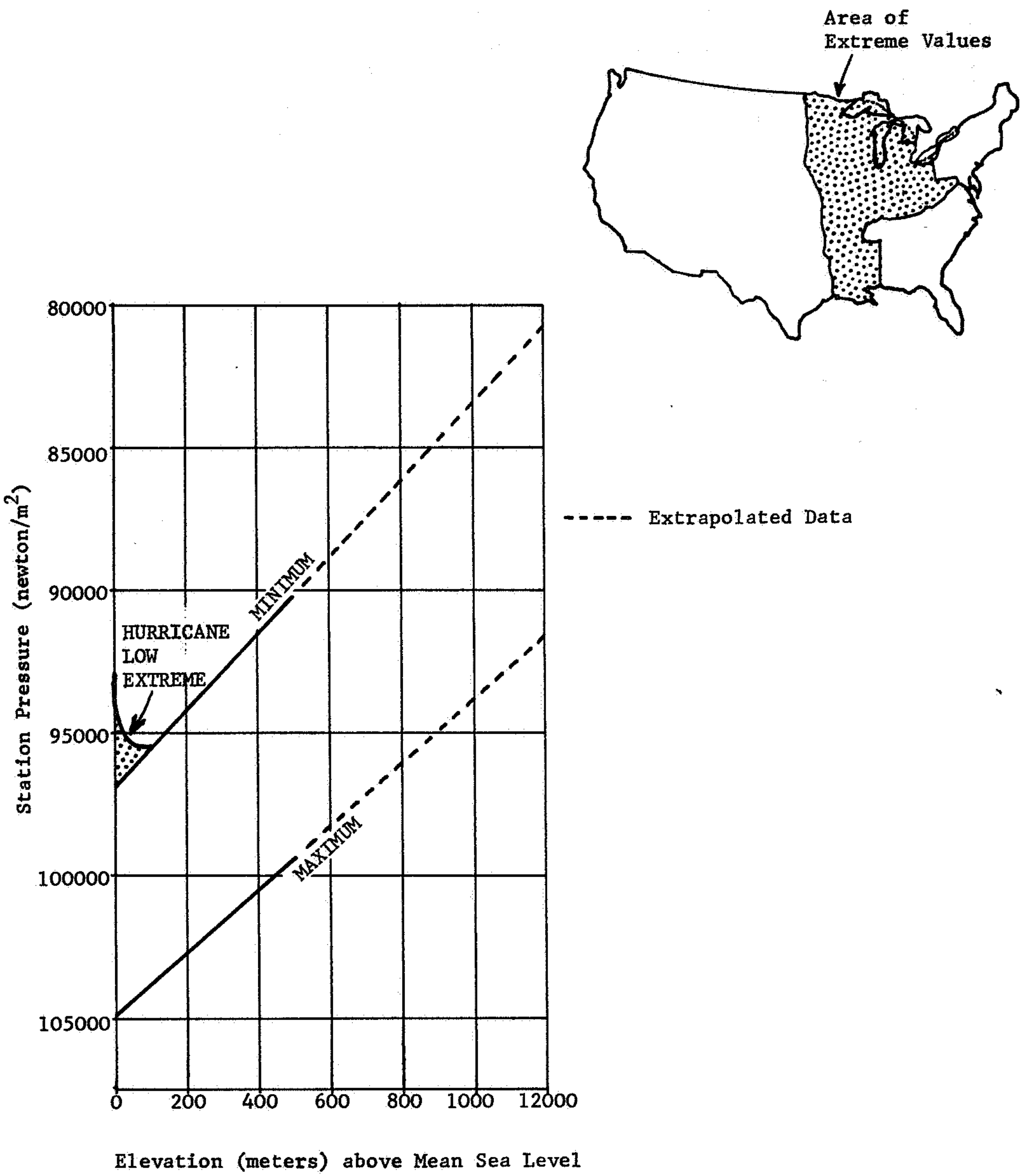

FIGURE 17.9 EXTREME PRESSURE VALUES VERSUS ELEVATION FOR CENTRAL UNITED STATES

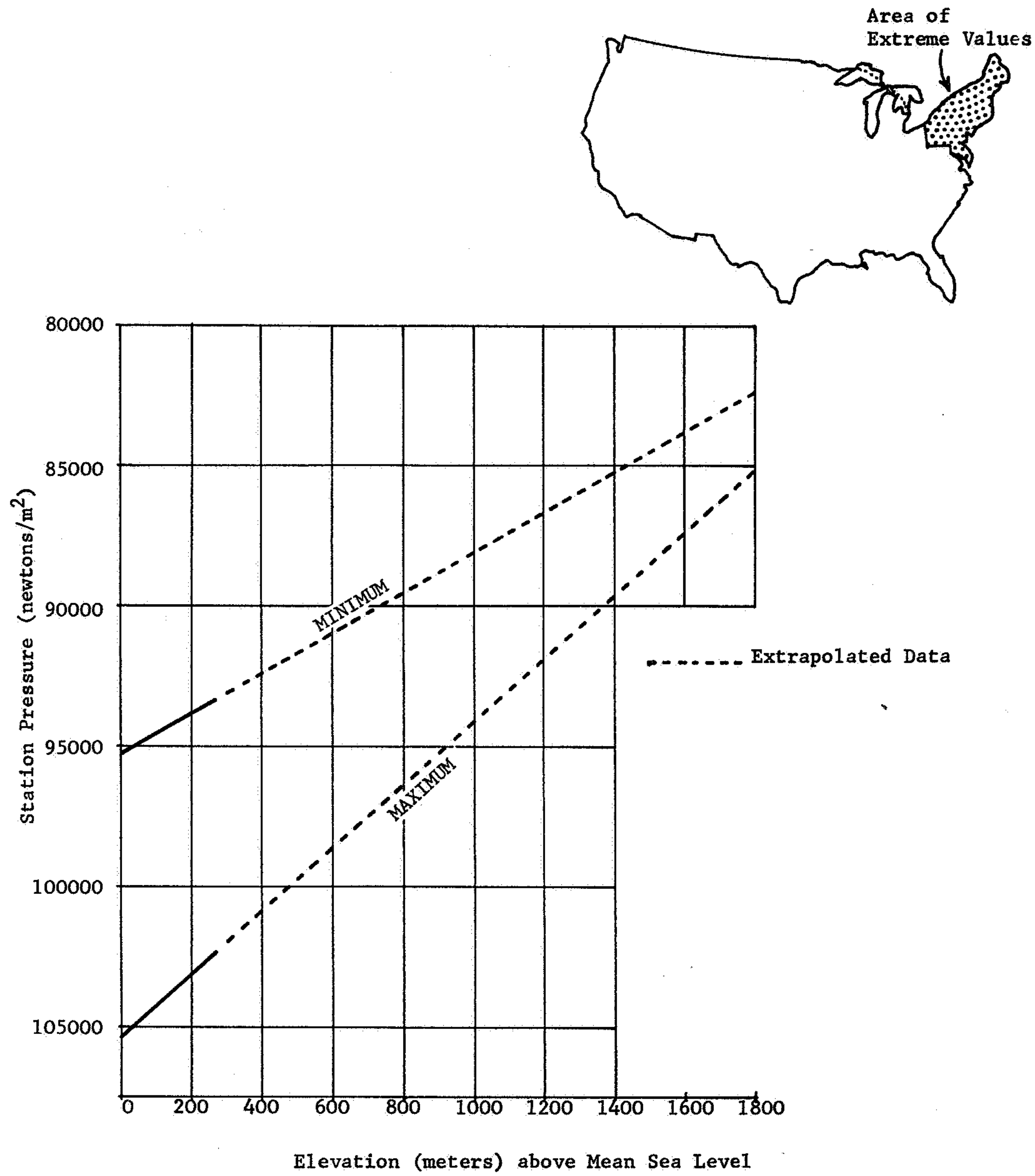

FIGURE 17.10 EXTREME PRESSURE VALUES VERSUS ELEVATION FOR NORTHEASTERN UNITED STATES

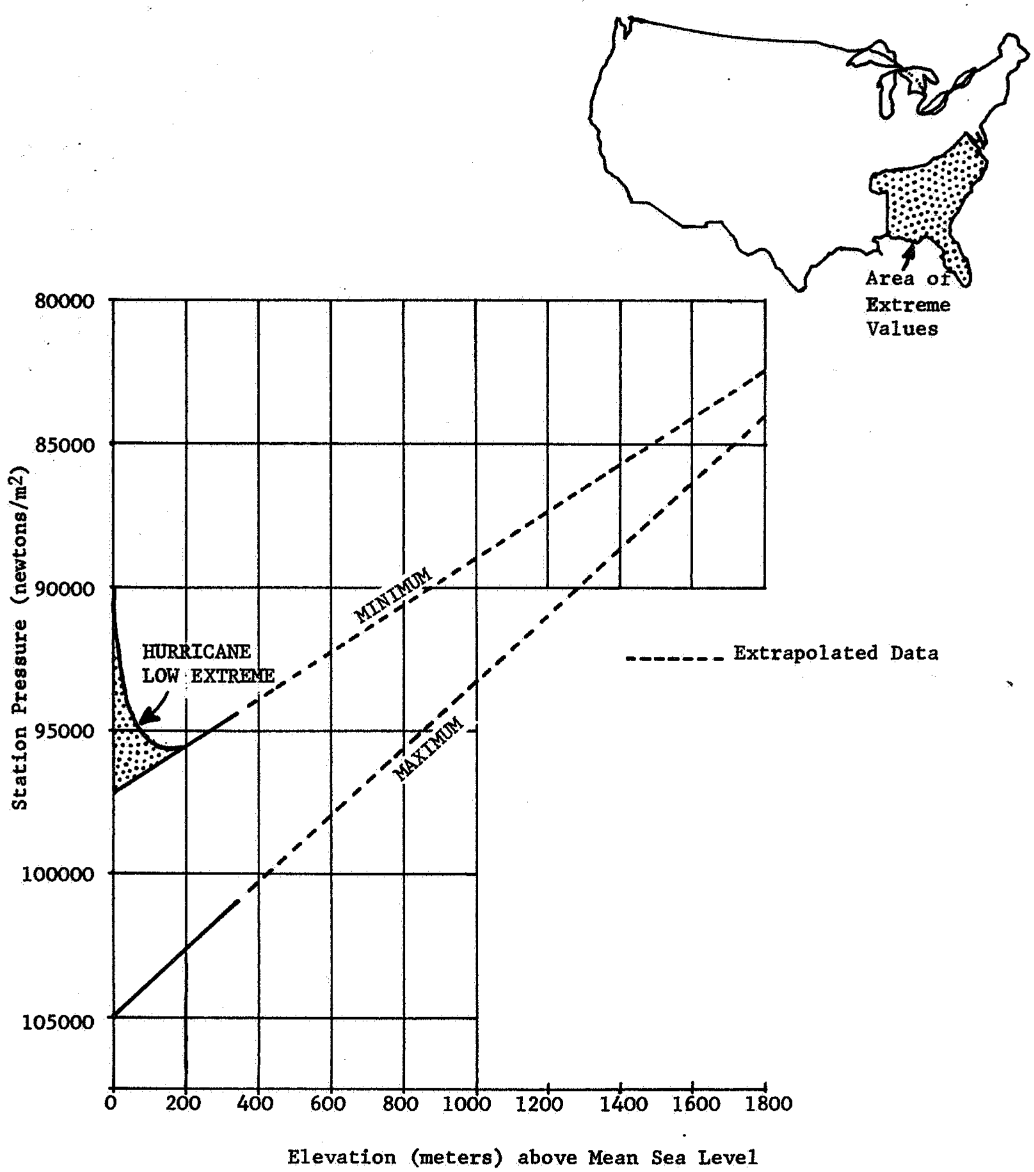

FIGURE 17.11 EXTREME PRESSURE VALUES VERSUS ELEVATION FOR SOUTHEASTERN UNITED STATES

REFERENCES

17.1 "Temperature Extremes in the United States." Environmental Information Summaries, C-5, NOAA Environmental Data Service, Asheville, N.C., July 1971.

17.2 Valley, Shea L.: "Handbook of Geophysics and Space Environments." McGraw-Hill Book Company, Inc., New York, 1965.

17.3 Riordan, Pauline: "Weather Extremes Around the World." Tech. Rpt. 70-45-ES, U. S. Army Natick Laboratories, Natick, Mass., January 1970.

17.4 Brown, Merly J.; and Williams, Philip Jr.: "Maximum Snow Loads Along the Western Slopes of the Wasatch Mountains of Utah." Journal of Applied Meteorology, Vol. 15, No. 3, 1962, pp. 123-126.

17.5 Ludlum, David M.: "The 'New Champ' Hailstone." Weatherwise, Vol. 24, No. 4, August 1971, p. 151.

17.6 Ludlum, David M.: "Extremes of Atmospheric Pressure in the United States." Weatherwise, Vol. 15, No. 3, 1962, pp. 106-115.

17.7 Daniels, Glenn E.: "Values of Extreme Surface Pressure for Design Criteria." Institute of Environmental Sciences, 1965 Proceedings, Institute of Environmental Sciences, Mt. Prospect, Ill., pp. 283-288.

17.8 Ludlum, David M.: "Extremes of Atmospheric Pressure." Weatherwise, Vol. 24, No. 3, 1971, pp. 130-131.

17.9 Surface Atmospheric Extremes (Launch and Transportation Areas) NASA Space Vehicle Design Criteria (Environment), NASA SP-8084, May 1972.

SECTION XVIII. WORLDWIDE SURFACE EXTREMES

18.1 Introduction

This section provides worldwide extreme values for temperature, dew point, precipitation, pressure, wind speed, etc. Section XVII, Distribution of Surface Extremes in the United States, provides more detailed statistics on atmospheric extremes for the United States.

18.2 Sources of Data

A great amount of meteorological data have been collected throughout the world. Various agencies have collected data in a form that may be used for statistical studies. Kendrew's "Climates of the Continents" (Ref. 18.1) is a summary of mean values of the meteorological parameters, temperature, pressure, and precipitation, and it is also the source of many interesting discussions of local meteorological conditions around the world. "World Weather Records" (Ref. 18.2), compiled by the Weather Bureau (now part of the National Oceanic and Atmospheric Administration), provides another summary of mean values of meteorological data. Climatological data have also been prepared for numerous worldwide airfield locations by the U. S. Air Force ETAC in support of the Naval Weather Service (18.3). Eleven volumes have been published to date which contain monthly mean (some extreme) climatic information for all areas around the globe.

Recently, in revising AR 705-15 (now AR 70-38, Ref. 18.4), the Earth Sciences Laboratory NLABS, U. S. Army Natick Laboratories at Natick, Massachusetts, has collected worldwide data on meteorological extremes. For the revised AR 70-38, the Earth Sciences Laboratory NLABS prepared world maps that show worldwide absolute maximum and absolute minimum temperatures.[1] These maps are reproduced in this section as Figures 18.1 and 18.2, and due credit is given to the Earth Sciences Laboratory NLABS, U. S. Army Natick Laboratories. In addition, MIL-STD-210B, "Climatic Extremes for Military Equipment," (Ref. 18.5) issued on December 15, 1973, is a standard guidebook used by the U. S. military branches which contains worldwide extreme values. Reference 18.6, prepared by Air Force Cambridge Research Laboratories, gives more background information on the preparation of MIL-STD-210B.

The several climatic atlases for various areas of the world provide other sources of data; those of interest will be referred to in the following sections. For essentially all meteorological parameters, the extremes noted reflect measurements during the available period of record. Since this period of record

1. Absolute is defined as the highest and lowest values of data of record.

covers only a few decades for most locations, it is obvious that there exists a finite risk that extreme values used will be exceeded in future years. However, the values shown are considered appropriate as criteria guidelines to establish critical engineering design problems requiring more in-depth assessment relative to probable meteorological extremes during expected operational lifetime.

18.3 Worldwide Extremes Over Continents

To present all the geographic extremes properly, many large maps similar to Figures 18.1 and 18.2 would be required; therefore, only worldwide extremes of each parameter will be discussed, and available references on each parameter will be given. Individual geographic extremes will be mentioned when pertinent.

18.3.1 Temperature

Absolute maximum and absolute minimum world temperature extremes are shown in Figures 18.1 and 18.2. Some geographical extreme air temperatures of record are given in Table 18.1.

TABLE 18.1 EXTREME AIR TEMPERATURES OF RECORD

Location	Air Temperature of Record [° C(° F)]
Salah, Africa	48 (118), mean daily max. for 45 days 53 (127), absolute max.
El Azizia, Africa*	58 (136), absolute max.
Tirat Tsvi, Israel	54 (129), absolute max.
Death Valley, Calif.*	57 (134), absolute max. for U. S.
Cloncurry Queensland, Australia	53 (128), absolute max.
Vostok, Antarctica	-87 (-124), absolute min.
Oimekon, U.S.S.R.	-68 (-90), absolute min.
Northice, Greenland	-66 (-87), absolute min.
Rogers Pass, Mont.	-57 (-70), absolute min. for U. S.
Snag, Yukon Territory, Canada	-63 (-81), absolute min. for North America

* The validity of these temperatures has been questioned; see Ref. 18.7.

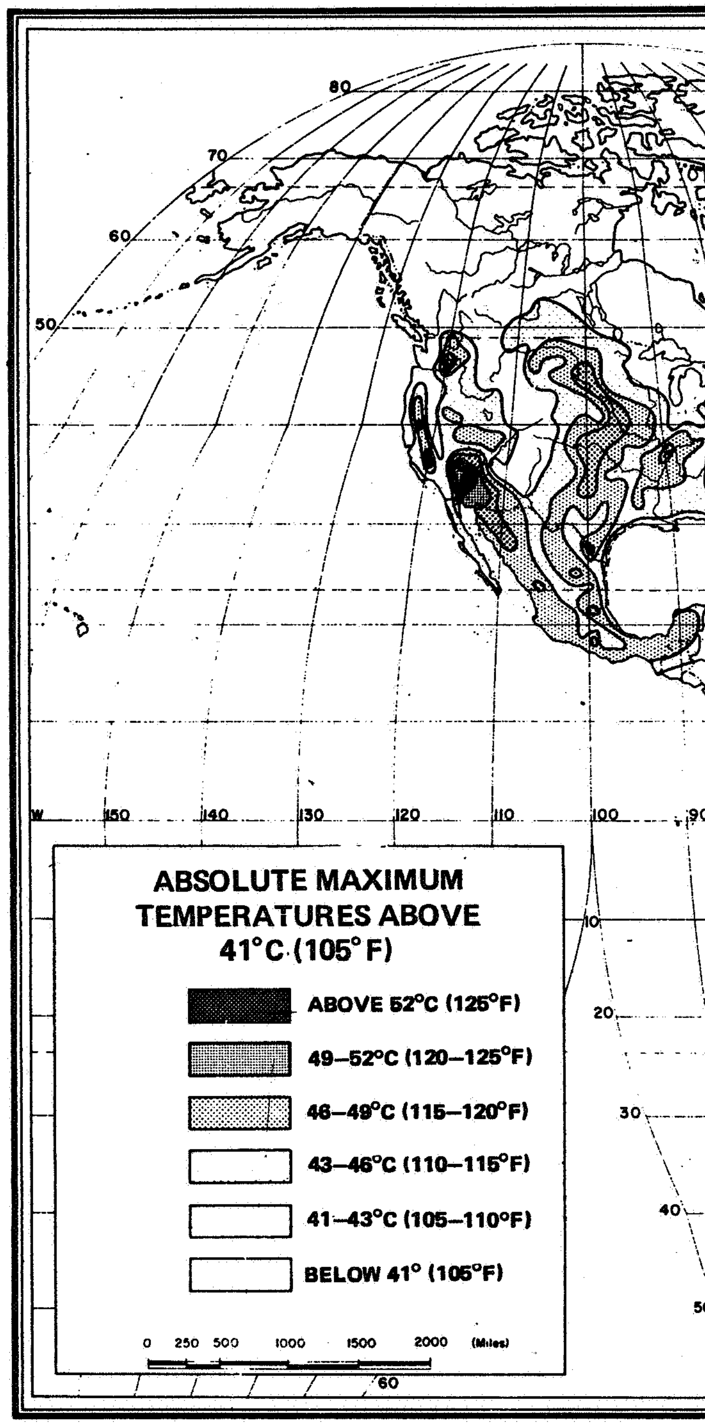

FIGURE 18.1 WORLDWIDE GEOGRA
TEMPERATURES ABOV

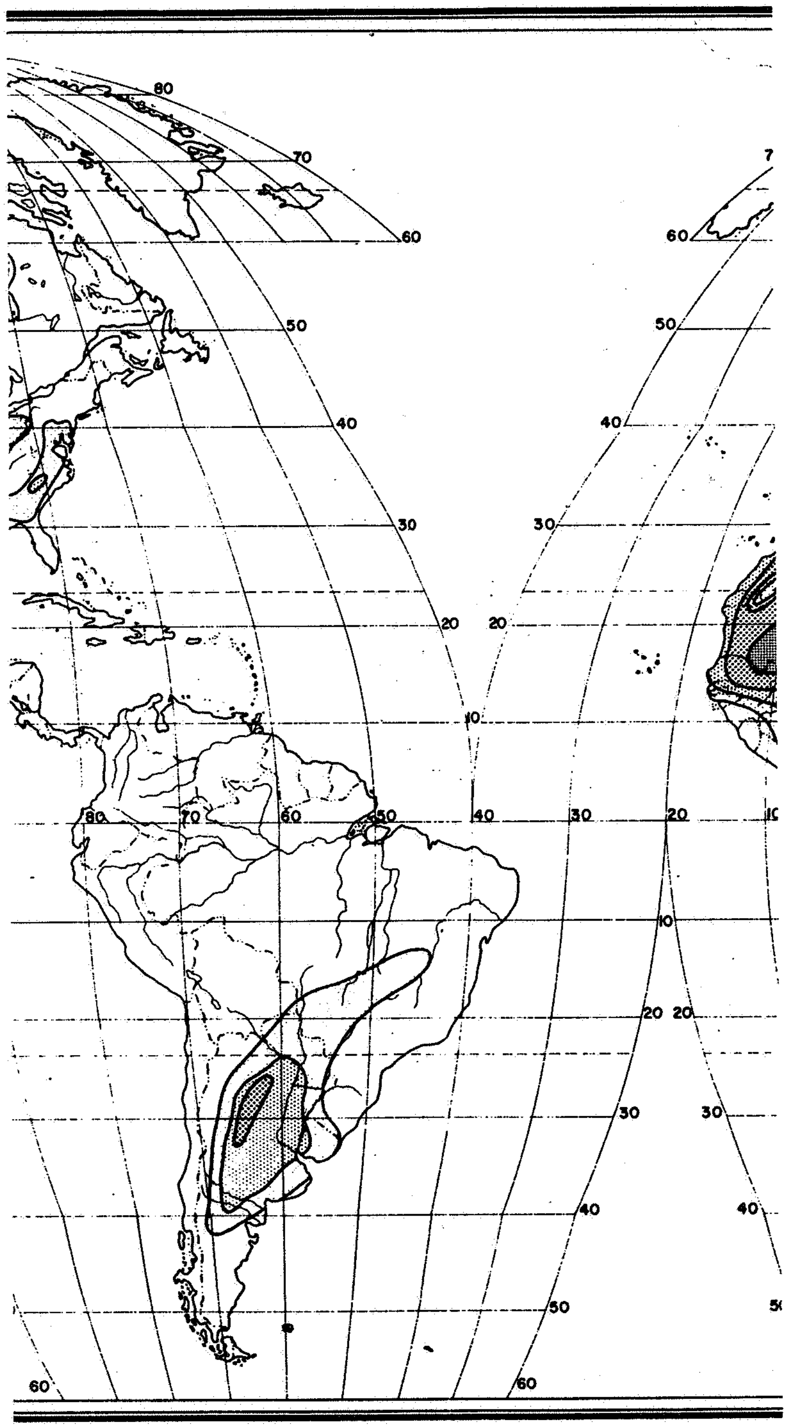

ıPHIC ABSOLUTE MAXIMUM
'E 41°C (105°F)

FOLDOUT FRAME 2

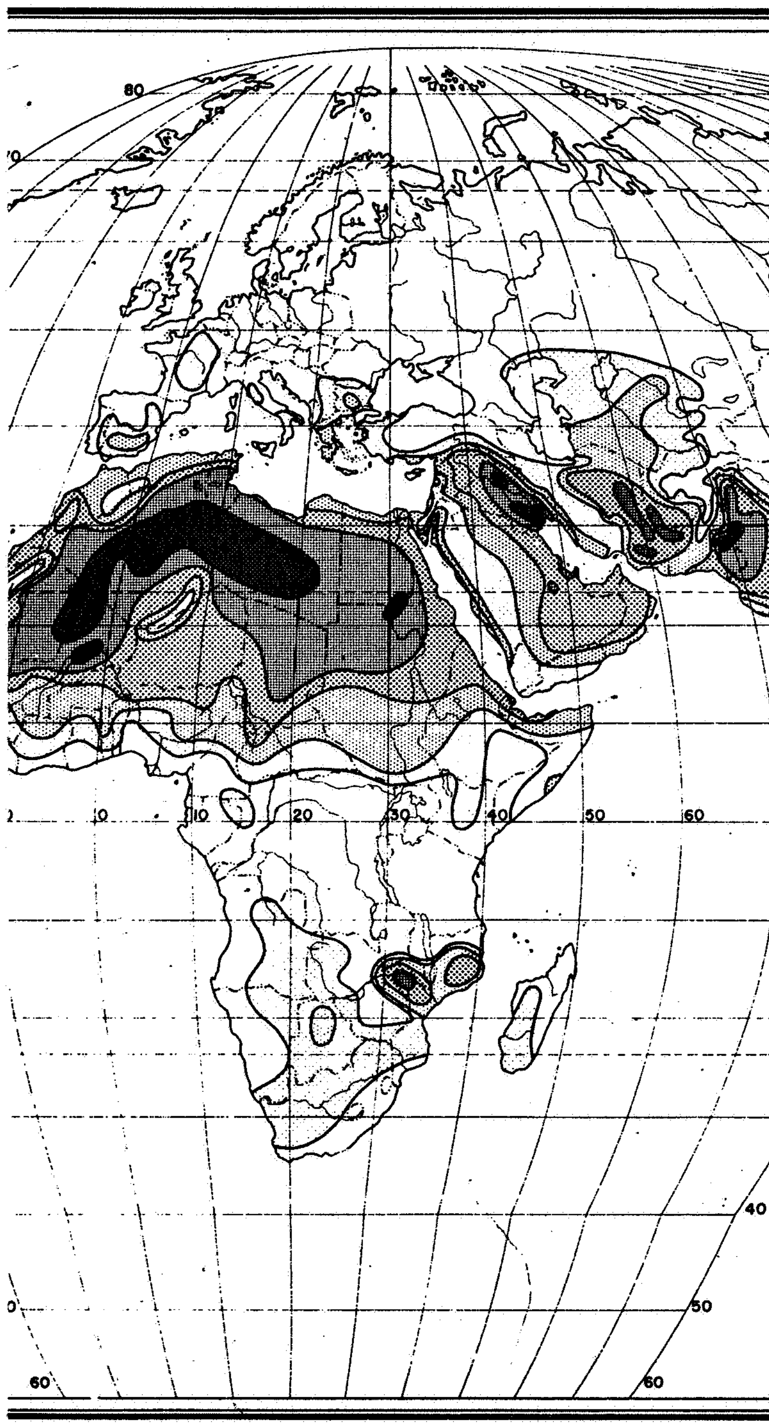

FOLDOUT FRAME 3

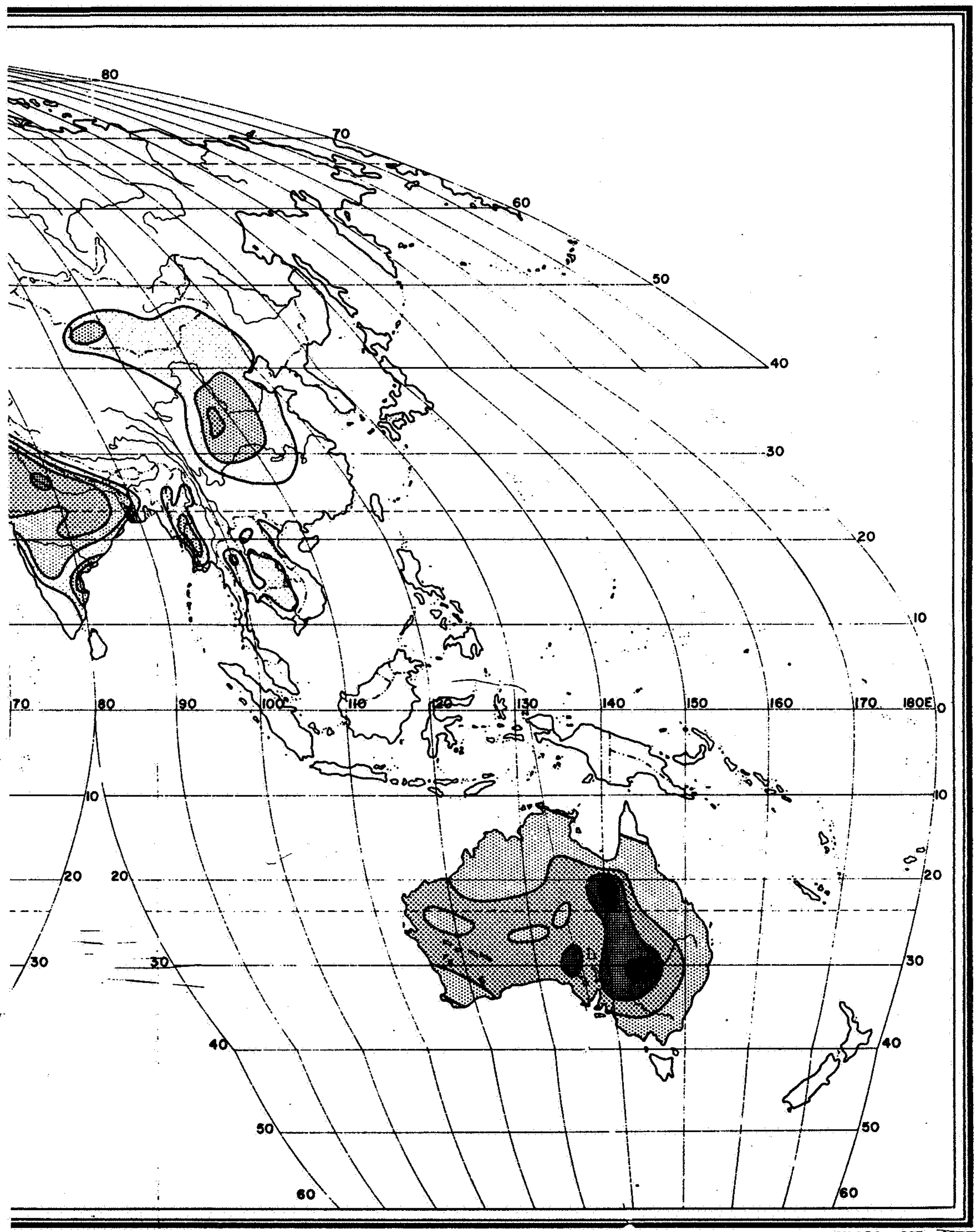

NLABS - ESD - 1966

[redacted]

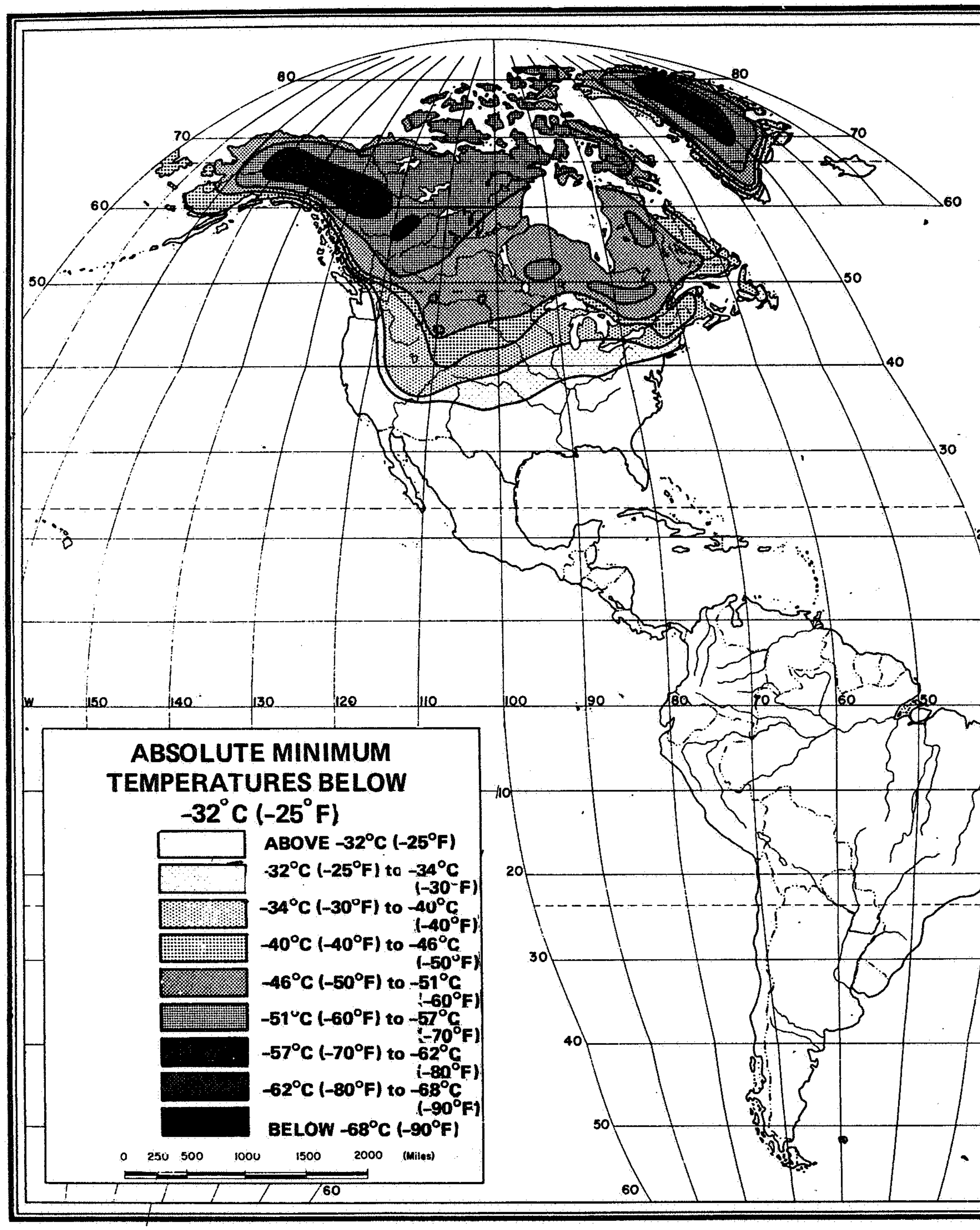

FIGURE 18.2 WORLDWIDE GEOGRAPHIC ABSOLUTE MINIMUM TEMPERATURES BELOW -32°C (-25°F)

FO

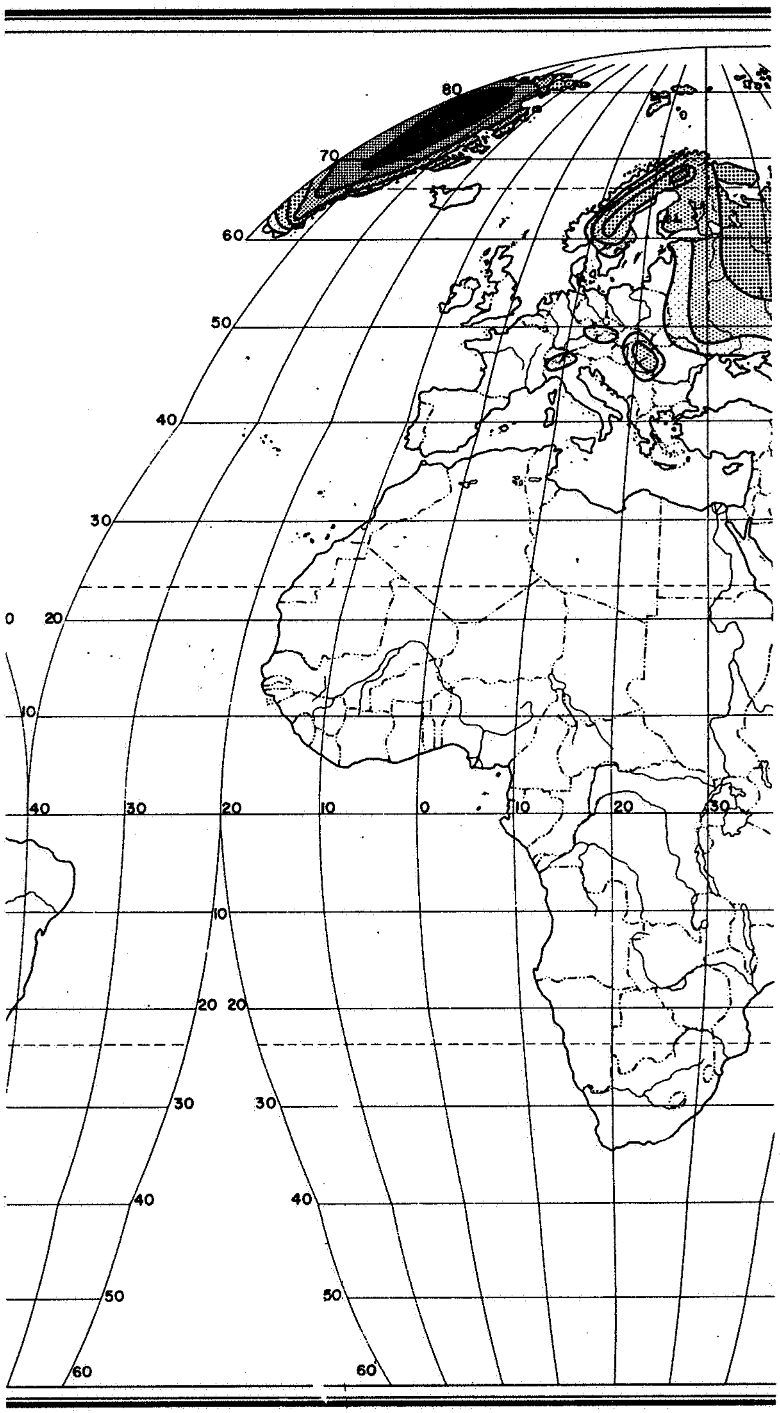
80
70
60
50
40
30
20
10
40 30 20 10 0 10 20 30
10
20 20
30 30
40 40
50 50
60 60

ILDOUT FRAME 2

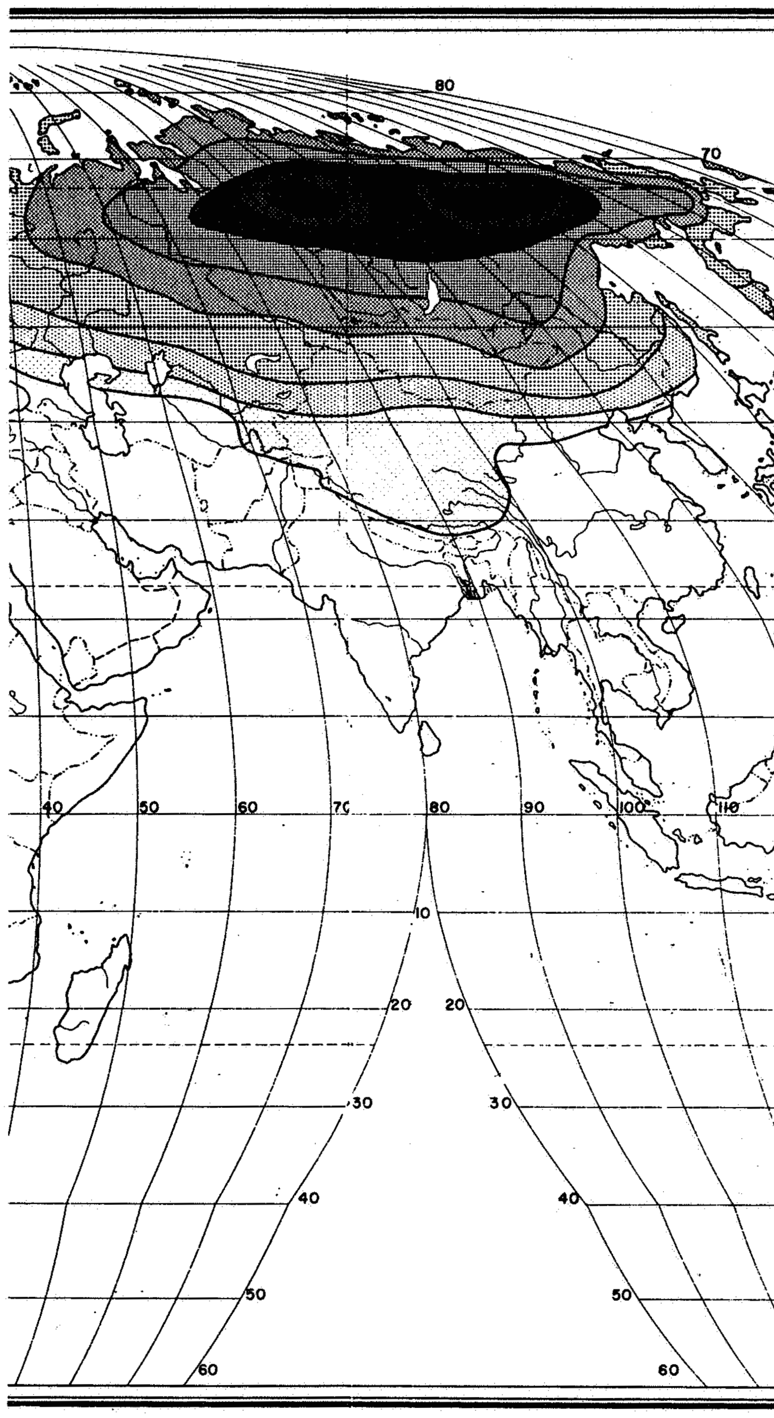

FOLDOUT FRAME 3

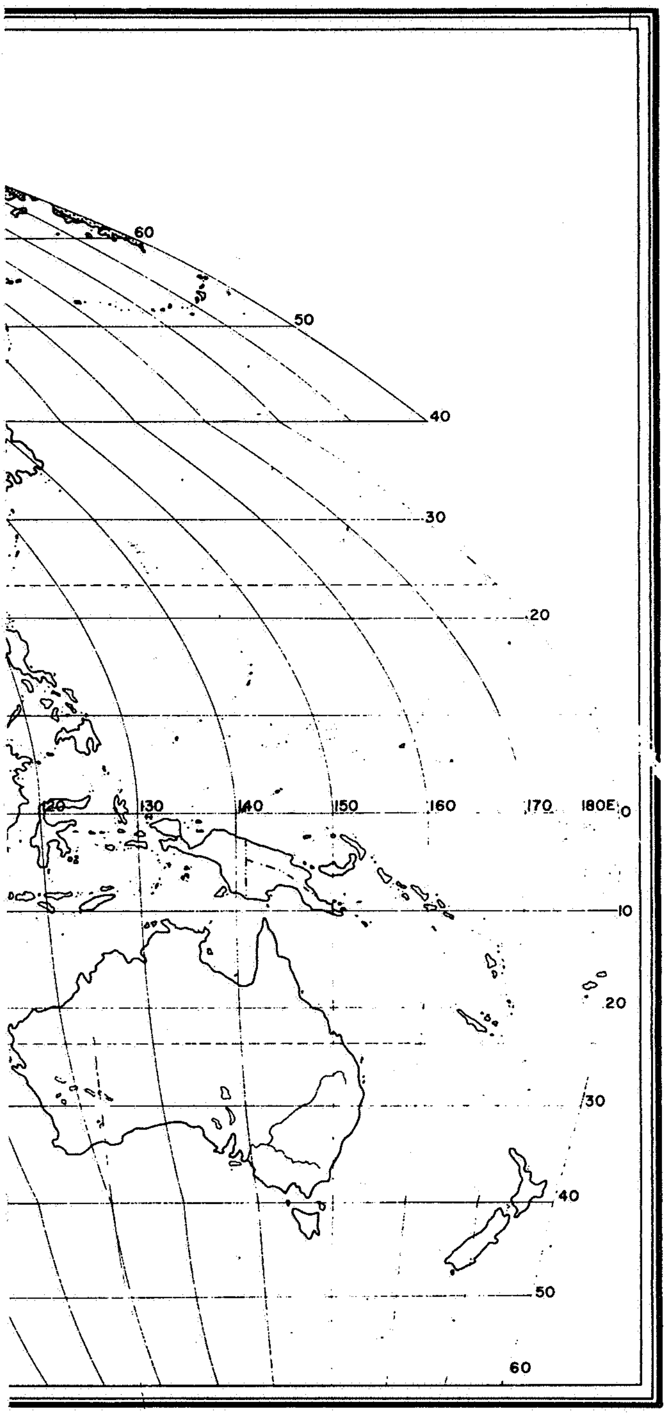

NLABS - ESD - 1966

Temperatures of the ground are normally hotter than the air temperatures during the daytime. In the Sahara Desert of Africa, temperatures of sand as high as 78°C (172°F) have been measured. At Stuart, Australia, the sand has reached temperatures so hot that matches dropped into it burst into flame.

In the design of equipment for worldwide ground environment operations, MIL-STD-210B now uses extreme temperature values of 58°C (136°F) for a hot temperature and -68°C (-90°F) for a cold temperature.

The above recommendation for hot temperature was based upon risk tables, shown in Table 18.2, of extreme high temperatures developed by extreme value theory using 57 extreme annual temperatures at Death Valley, California (Ref. 18.6). Such temperatures persist for 1 or 2 hours during a day.

TABLE 18.2 EXTREME HIGH TEMPERATURES WITH RELATION TO RISK AND DESIRED LIFETIME

Risk (%)	Temperatures [°C(°F)] Planned Lifetime (years)				
	1	2	5	10	25
1	55 (131)	56 (133)	57 (134)	57 (135)	58 (137)
10	53 (127)	53 (128)	54 (130)	55 (13[illegible])	56 (133)
25	52 (125)	53 (127)	53 (128)	54 (129)	55 (131)
50	51 (124)	52 (125)	53 (127)	53 (128)	54 (130)

The recommendation for cold temperature was based upon the risk table, shown in Table 18.3, of extreme low temperatures, developed by extreme value

TABLE 18.3 EXTREME LOW TEMPERATURES WITH RELATION TO RISK AND DESIRED LIFETIME*

Risk (%)	Temperature [°C (°F)] Planned Lifetime (years)			
	2	5	10	25
10	-66 (-86)	-67 (-89)	-69 (-92)	-71 (-95)

* Temperatures in Antarctica were not considered in the study.

theory using 18 annual extreme low temperatures at two Siberian locations (Ref. 18.6). The extreme low temperatures will persist for longer periods since they occur during polar darkness. (Also see References 18.12 and 18.13 regarding probabilities of surface temperature extremes.)

18.3.2 Dew Point

High dew points are associated with high temperatures near large bodies of water. Besides being detrimental to equipment, high dew points make living conditions very uncomfortable. Extremely high dew points occur in the following areas, in the vicinity of the water bodies specified:

a. The northern portion of the Arabian Sea in April and May, to 29°C (85°F) dew point.

b. The Red Sea in July, to 32°C (89°F) dew point.

c. The Caribbean Sea (includes the western end of Cuba and the Yucatan Penninsula, Mexico) in July, to 27°C (81°F) dew point.

d. The northern portion of the Gulf of California, to 30°C (86°F) dew point (data from Puerto Penasco, Mexico, Ref. 18.8).

The Air Force has published the "Atmospheric Humidity Atlas for the Northern Hemisphere" (Ref. 18.9), which shows maps for various percentile levels of dew point for midseason months (January, April, July, and October).

18.3.3 Precipitation

The worldwide distribution of precipitation is extremely variable; some areas do not receive rain for years, while others receive torrential rain many months of the year.[3] Precipitation is also seasonal; for example, Cherrapunji, India, with its world record total of 2647 cm (1042 in.) of precipitation in a year, has a mean monthly precipitation of less than 2.54 cm (1 in.) in December and January. The heaviest precipitation for long periods (greater than 12 hours) usually occurs in the monsoon type of weather. High rates of rainfall for short periods (less than 12 hours) usually occur in the thunderstorm type of rain and over much smaller areas than the monsoon rain. Some world records for various periods of rainfall are given in Table 18.4 (Refs. 18.1, 18.10, and 18.11).

---

3. Iquique, Chile had no rain for 14 consecutive years. The longest dry period for a United States location was 767 days for Bagdad, Calif. (Oct. 3, 1912, to Nov. 8, 1914).

TABLE 18.4 WORLD RAINFALL RECORDS

Station	Time Period	Amount (in.)
Unionville, Ind.	1 min.	1.23
Plum Point, Jamaica	15 min.	8.0
Holt, Mo.	42 min.	12.0
D'Hanis, Tex.	3 hours	20.0
Belouve, LaReunion Is.	12 hours	53.0
Cilaos, LaReunion Is.	1 day	74.0
Cherrapunji, India	30 days	366.0
Cherrapunji, India	1 year	1042.0
Highest average annual precipitation: World — 460 in. — Mt. Waialeale, Kanai, Hawaii Contiguous U.S. — 144 in. — Wynoochee, Wash. Lowest average annual precipitation: World — 0.03 in. — Arica, Chile U.S. — 1.63 in. — Death Valley, Calif.		

Even though the values given in Table 18.4 are considerably higher than the values given in Table 7.2 of Section VII, values in Table 7.2 are considered adequate for most space vehicle design problems within currently expected operational areas.

18.3.4 Pressure

Surface atmospheric pressure extremes for use in design must be derived from the measured station pressures, not from the computed sea level pressures that are usually published.

Station pressures between stations have great variability because of the difference in altitude of the stations. The lowest station pressures occur at the highest altitudes. The highest station pressures occur at either the lowest elevation stations (below sea level), or in the arctic regions in cold air masses at or near sea level.

Court (Ref. 18.10) has an interesting discussion on worldwide pressure extremes. Some typical high and low pressure values are given in Table 18.5 (Refs. 18.1 and 18.10).

TABLE 18.5 TYPICAL PRESSURE VALUES OF SELECTED AREAS

Station	Elevation Above Sea Level [m (ft)]	Pressure (mb)	
		Lowest	Highest
Lhasa, Tibet	3685 (12 090)	645[a]	652[a]
Sedom, Israel	-389 (-1 275)	—	1081.8
Portland, Maine	19 (61)	—	1056
Qutdligssat, Greenland	3 (10)	—	1063.4
In typhoon Ida, 14°N, 135°E, Sept. 24, 1958	~0	877[b]	—

a. Monthly means.
b. Lowest sea level pressure of record.

18.3.5 Ground Wind

Worldwide extreme surface winds have occurred in several types of meteorological conditions: tornadoes, hurricanes or typhoons, mistral winds, and Santa Ana winds. In design, each type of wind needs special consideration. For example, the probability of tornado winds is very low compared with the probability of mistral winds, which may persist for days (see Section 8.2.10).

18.3.5.1 Tornadoes

Tornadoes are rapidly revolving circulations normally associated with a cold front squall line or with warm, humid, unsettled weather; they usually occur in conjunction with a severe thunderstorm. Although a tornado is extremely destructive, the average tornado path is only about 400 m (1/4 mi) wide and seldom more than 26 km (16 mi) long, but there have been a few instances in which tornadoes have caused heavy destruction along paths more than 1.6 km (1 mi) wide and 483 km (300 mi) long. The probability of any one point being in a tornado path is very small; therefore, design of structures to withstand tornadoes is usually not considered except for special situations where tornado shelters are built underground. Velocities have been estimated to exceed 134 m s^{-1} (260 knots) in tornadoes. See Section XIX for further information regarding tornadoes.

18.3.5.2 Hurricanes (Typhoons)

Hurricanes (also called typhoons, Willy-willies, tropical cyclones, and many other local names) are large tropical cyclones of considerable intensity. They originate in tropical regions between the equator and 25 deg latitude. A hurricane may be 1600 km (1000 mi) in diameter with winds in excess of 67 m s^{-1} (130 knots). A hurricane is defined as a storm of tropical origin when winds are equal to or greater than 33 m s^{-1} (64 knots). Hurricanes are always accompanied by heavy rain. Since the hurricanes of the West Indies are as intense as others throughout the world, design winds based upon these hurricanes would be representative for any geographical area. Section 8.2.10 gives hurricane design winds for the area of Kennedy Space Center, Florida. Although the highest winds recorded in a hurricane in the area of KSC, Florida, were lower than winds from thunderstorms in the same area, the probability still exists that much higher winds could result from hurricanes in the vicinity of Kennedy Space Center.

For extremes applicable to equipment, Table 18.6 from a study of 19 years of wind data for Naha, Okinawa (in the Pacific typhoon belt) (Ref. 18.6), is representative of all hurricane areas of the world. See Section XIX for further information regarding hurricanes.

TABLE 18.6 EXTREME WINDS IN HURRICANE (typhoon) AREAS WITH RELATION TO RISK AND DESIRED LIFETIME (3.1-m reference height)

Risk (%)	Extreme Wind Speeds (m s^{-1}) * †			
	Planned Lifetime (years)			
	2	5	10	25
10	* 69	79	86	97
	† 61	72	80	91

* Based on 2-sec gusts (annual extreme)

† Based on 1-min steady wind associated with the 2-sec gust

18.3.5.3 Mistral Winds (Ref. 18.1)

The mistral wind is a strong polar current between a large anticyclone and a low pressure center. These winds frequently have temperatures below freezing. The mistral of the Gulf of Lions and the Rhone Valley, France, is the best known of these winds. Although winds of 37 m s^{-1} (83 mph) have been recorded in the area of Marseilles, France, much higher winds have occurred to the west of Marseilles in the more open terrain, where even railway trains have been blown over. Mistrals blow in the Rhone Valley for about 100 days a year.

18.3.5.4 Santa Ana Winds

In contrast to the mistrals, the Santa Ana Winds, which occur in Southern California west of the coast range of mountains, are hot and dry and have speeds up to 21 m s^{-1} (41 knots). Similar winds, called Fohn winds, occur in the Swiss Alps and in the Andes, but, because of the local topography, they have lower speeds. The destructiveness of these winds is not from their speeds, but from their high temperatures and dryness, which can do considerable damage to blooming trees, crops, exposed equipment and instruments that may be sensitive to prolonged heat and dryness.

REFERENCES

18.1 Kendrew, W. G., "The Climates of the Continents," Oxford University Press, Amen House (London), 1961.

18.2 "World Weather Records," U. S. Department of Commerce, Weather Bureau, Superintendent of Documents, U. S. Government Printing Office, Washington, D. C., 1968.

18.3 "Worldwide Airfield Climatic Data," Environmental Technical Applications Center, Air Weather Service, U. S. Air Force, Vol. XI, April 1973.

18.4 "Research, Development, Test, and Employment of Material for Extreme Climatic Conditions," AR-70-38 (Supersedes AR-705-15), July 1, 1969.

18.5 Military Standard Climatic Extremes for Military Equipment, Department of Defense, MIL-STD-210B, December 15, 1973.

18.6 Sissenwine, Norman, and Cormier, René V., "Synopsis of Background Material for MIL-STD-210B, Climatic Extremes for Military Equipment," AFCRL-TR-74-0052, Air Force Cambridge Research Laboratories, January 24, 1974.

18.7 Billions, Novella S., "Frequencies and Durations of Surface Temperatures in Hot-Dry Climatic Category Areas. (Cat. 4, AR 70-38)," Technical Report RR-72-13, Dec. 1972, U. S. Army Missile Command, Redstone Arsenal, Alabama.

18.8 Dodd, Arthur V., "Aerial and Temporal Occurrence of High Dew Points and Associated Temperatures," Technical Report 70-4-ES, Department of the Army, U. S. Army Natick Laboratories, Earth Sciences Laboratory, Natick, Mass., August 1969.

18.9 Gringorten, I. I., et al., "Atmospheric Humidity Atlas — Northern Hemisphere," AFCRL-66-621, Air Force Cambridge Research Laboratories, L. G. Hanscom Field, Bedford, Mass., Aug. 1966.

18.10 Court, Arnold, "Improbable Pressure Extreme: 1070 mb," Bulletin of the American Meteorological Society, vol. 50, no. 4, Apr. 1969, pp. 248-250.

18.11 Riordan, Pauline, "Weather Extremes Around the World." TR 70-45-ES, U. S. Army Natick Laboratories, Natick, Mass., January 1970.

REFERENCES (Concluded)

18.12 Tattelman, P., and Kantor, A. J., "Atlas of Probabilities of Surface Temperature Extremes: Part I - Northern Hemisphere," AFGL-TR-76-0084, 1976.

18.13 Tattelman, P., and Kantor, A. J., "Atlas of Probabilities of Surface Temperature Extremes: Part II - Southern Hemisphere," AFGL-TR-77-0001, December 27, 1976.

SECTION XIX. INFORMATION ON OCCURRENCES OF TORNADOES AND HURRICANES PLUS SELECTED CLIMATOLOGICAL DATA SOURCE

19.1 Introduction

Severe weather may adversely affect the design, transportation, and operation of aerospace vehicles. This section contains a discussion of such atmospheric phenomena. (The reader is referred to Section XIII for a discussion of thunderstorm activity and to Section XVIII for information regarding severe worldwide weather conditions.) Also included is climatological information pertinent to vehicle operations for 32 selected foreign and United States sites.

19.2 Tornadoes

Tornadoes are recognized as the most destructive force winds; because of differential pressures created by tornadoes, buildings have been known to literally explode. Fortunately, the aerial extent of tornadoes is small compared with hurricanes. Tornadoes are observed at times in association with hurricanes in Florida and along the coastal states. Based on Thom's analysis of the number of tornado occurrences (Ref. 19.1), Table 19.1 has been prepared giving tornado statistics for stations of interest. The statistics included in Table 19.1 are based upon an area (A_2) of a 1-deg square of latitude and longitude on the earth's surface. The period of record is 1955-1973 except as noted in the table.

The probability of one or more tornadoes in N years in an area (A_1) is given by[1]

$$P(A_1;N) = 1 - \exp\left(-\bar{x}\,\frac{A_1}{A_2}\,N\right) \quad ; \quad (A_1 \subset A_2) \quad . \tag{19.1}$$

where $\bar{x}$ is the mean number of tornadoes per year in a 1-degree square.

We choose the area size for A_1 as 7.3 km^2 (2.8 mi^2) because Thom (Ref. 19.1) reports that 7.2572 km^2 (2.8209 mi^2) is the average ground area covered by tornadoes in Iowa, and the vital industrial complexes for most locations are of this general size. Thus, taking $A_1 = 7.3$ km^2 (2.8 mi^2) and $A_1 = 2.59$ km^2 (1 mi^2) and evaluating equation (19.1) for the values of $\bar{x}$ and A_2 for the stations given in Table 19.1 yields the data in Table 19.2. Table 19.2 gives

1. Credit is due Prof. J. Goldman, Institute Storm Research, St. Thomas University, Houston, Texas, for this form of the probability expression.

TABLE 19.1 TORNADO STATISTICS FOR STATIONS SPECIFIED, 1955-1973

Station	Number of Tornadoes in 1 deg Square	Mean ($\bar{x}$) No. of Tornadoes Per Year in 1 deg Square	Area (A_2) of 1 deg Square (km^2)	(mi^2)	Mean Probability of a Tornado Striking a Point in Any Year in a 1 deg Square	Mean Recurrence Interval (yr) for a Tornado Striking a Point in a 1 deg Square
Huntsville	55	2.89	10 179	3 930	0.002074	482
Kennedy Space Center	33	1.74	10 839	4 185	0.001173	853
Vandenberg AFB	0	0	10 179	3 930	0.00000	∞
Edwards AFB	2	0.11	10 179	3 930	0.000079	12 665
Honolulu	5*	0.23	11 474	4 430	0.000146	6 828
Guam	0**	0	11 979	4 625	0.00000	∞
Santa Susana	4	0.21	10 179	3 930	0.000151	6 634
Brigham City	6	0.32	9 259	3 575	0.000253	3 960
New Orleans	35	1.84	10 645	4 110	0.001263	792
NSTL–Bay St. Louis	47	2.47	10 645	4 110	0.001695	590
Houston	89	4.68	10 736	4 145	0.003185	314
Wallops Is.	4	0.21	9 803	3 785	0.000149	6 709
White Sands	5	0.26	10 412	4 020	0.000182	5 481

* Period of record (10/48 – 12/73).

** Waterspouts have been sighted off the island of Guam.

TABLE 19.2 PROBABILITY OF ONE OR MORE TORNADOES IN A 7.3-km^2 AREA AND A 2.59-km^2 AREA IN 1, 10, AND 100 YEARS

Station	Mean ($\bar{x}$) No. of Tornadoes Per Year in 1 deg Square	$P(A_1;N)$ for A_1 = 7.3 km^2 (2.8 mi^2)			$P(A_1;N)$ for A_1 = 2.59 km^2 (1.00 mi^2)		
		N=1 Year	N=10 Years	N=100 Years	N=1 Year	N=10 Years	N=100 Years
Huntsville	2.89	0.002057	0.020380	0.086088	0.000735	0.007327	0.070898
Kennedy Space Center	1.74	0.001163	0.011574	0.109895	0.000416	0.004149	0.040725
Vandenberg AFB	0	0.00000	0.00000	0.00000	0.00000	0.00000	0.00000
Edwards AFB	0.11	0.000078	0.000783	0.007807	0.000028	0.000280	0.002795
Honolulu	0.23	0.000145	0.001453	0.014432	0.000052	0.000519	0.005178
Guam	0	0.00000	0.00000	0.00000	0.00000	0.00000	0.00000
Santa Susana	0.21	0.000150	0.001495	0.014850	0.000053	0.000534	0.005329
Brigham City	0.32	0.000251	0.002503	0.024751	0.000090	0.000895	0.008911
New Orleans	1.84	0.001253	0.012457	0.117814	0.000448	0.004467	0.043782
NSTL–Bay St. Louis	2.47	0.001681	0.016686	0.154876	0.000601	0.005992	0.058327
Houston	4.68	0.003156	0.031119	0.271043	0.001128	0.011227	0.106766
Wallops Is.	0.21	0.000148	0.001478	0.014686	0.000053	0.000528	0.005270
White Sands	0.26	0.000181	0.001809	0.017946	0.000065	0.000647	0.006447

$$P(A_1;N) = 1 - e^{-\bar{x}\frac{A_1}{A_2}N}$$

the probability of one or more tornadoes in a 7.3-km^2 (2.8-mi^2) area and a 2.59-km^2 (1-mi^2) area in 1 year, 10 years, and 100 years for the indicated 13 locations. It is noted that for $A_1 << A_2$ and $N < 100$, equation (19.1) can be approximated by

$$P(A_1; N) \doteq \bar{x} \frac{A_1}{A_2} N \tag{19.2}$$

An interpretation of the statistics in Table 19.2 is given using Kennedy Space Center as an example. There is an 11.0-percent chance that at least one tornado will "hit" within a 7.3-km^2 (2.8-mi^2) area at KSC in 100 years. For a 2.59-km^2 (1-mi^2) area at KSC, the chance of at least one tornado hit in 100 years is 4.1 percent. If several structures within a 7.3-km^2 (2.8-mi^2) area at KSC are vital to a space mission and these structures are not designed to withstand the wind and internal pressure forces of a tornado, then there is an 11.0-percent chance that one or more of these vital structures will be destroyed by a tornado in 100 years. If the desired lifetime of these structures [or 7.3-km^2 (2.8-mi^2) industrial complex] is 100 years and the risk of destruction by tornadoes is accepted in the design, then the design risk or calculated risk of failure of at least one structure due to tornado occurrences is 11.0 percent. This example serves to point out that the probability of occurrence of an event which is rare in one year becomes rather large when taken over many years and that estimates for the desired lifetime versus design risk for structures discussed in subsection 8.2.10 of Section VIII should be made with prudence.

Figures 19.1 and 19.2 show tornado incidence statistics by state and area and also by month for the United States.

19.3 Hurricanes and Tropical Storms

The occurrence of hurricanes at Kennedy Space Center and other locations for the Eastern Test Range is of concern to the space program because of high winds and because range support for space operations is closed during passage or near approach of a hurricane. This discussion will be restricted to the frequency of tropical storms, hurricanes, and tropical storms and hurricanes combined (tropical cyclones) for annual reference periods and certain monthly groupings, as a function of radial distances from KSC only.

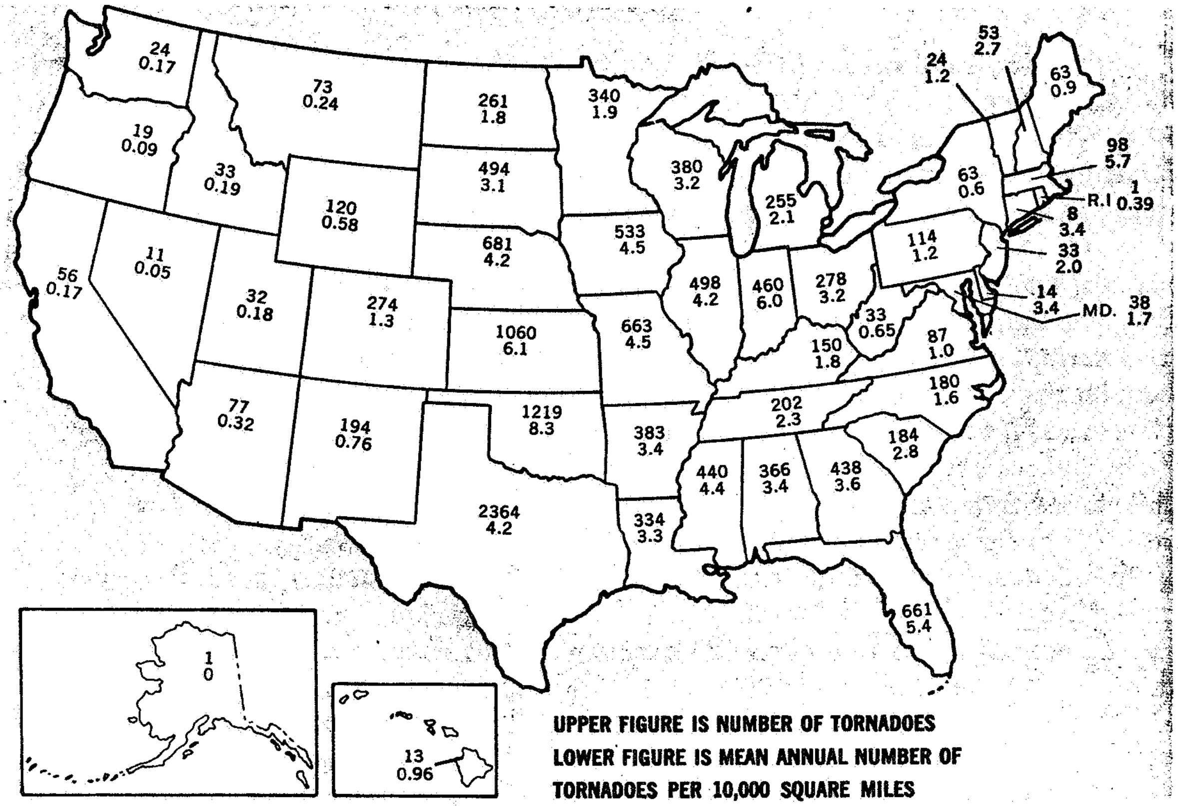

FIGURE 19.1 TORNADO INCIDENCE BY STATE AND AREA, 1953-1973 (from NOAA)

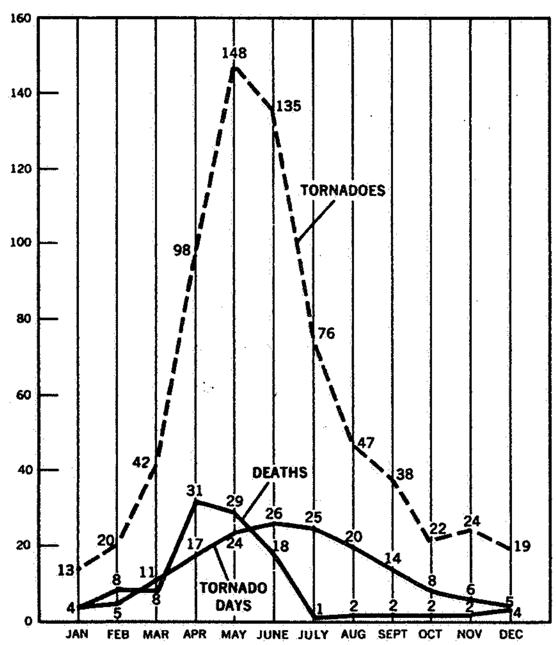

FIGURE 19.2 TORNADO INCIDENCE BY MONTH FOR THE U.S., 1953-1973 (from NOAA)

By definition, a hurricane is a storm of tropical origin with winds greater than 33 m/sec (64 knots), and a tropical storm is a cyclone whose origin is in the tropics with winds less than 33 m/sec (64 knots). There is no known upper limit for wind speeds in hurricanes, but estimates are as high as 82 m/sec (160 knots). Also, tornadoes have been observed in association with hurricanes.

Tables 19.3 and 19.4 give a general indication of the frequency of tropical storms and hurricanes by months within 161- and 644-km (100- and 400-n. mi.) radii of Kennedy Space Center. From Table 19.3 it is noted that hurricanes within 161 and 644 km (100 and 400 n. mi.) of KSC have been observed as early as May and as late as December, with the highest frequency during September. In the 77-year period (1899 to 1975), there were 126 hurricanes whose path (eye) came within a 644-km (400-n.mi.) radius of KSC; there were 20 hurricanes that came within a 161-km (100-n.mi) radius of KSC during this period. From all available wind records along the coast from Melbourne, Florida, to Titusville, Florida, the highest wind gusts during the passage of 16 of the 20 hurricanes that came within a 161-km (100-n. mi.) radius of KSC were obtained. For the three hurricanes for the years 1899, 1906, and 1925, the peak gusts were not available. Of the 16 hurricanes that came within a 161-km (100-n. mi.) radius of KSC for which the wind records are available, 5 produced wind gusts greater than 33.5 m/sec (65 knots),[2] 10 produced wind gusts to 26 m/sec (50 knots), and 12 had wind gusts less than 18.5 m/sec (36 knots). Thus, from these records, even if a defined hurricane path comes within a 161-km (100-n. mi.) radius of KSC, hurricane force winds [speeds > 33 m/sec (64 knots)] are not always observed at KSC. Hurricanes at greater distances than 161 km (100 n. mi.) could possibly produce hurricane force winds at KSC. It is recognized that hurricanes approaching KSC from the east (from the sea) will, in general, produce higher winds than those approaching KSC after crossing the peninsula of Florida (from land).

19.3.1 Distribution of Hurricane and Tropical Storm Frequencies

Knowing the mean number of tropical storms or hurricanes (events) per year that come within a given radius of KSC, without knowing other information, is of little use. If the distribution of the number of tropical storms or hurricanes is known to be a Poisson distribution, then the mean number of events per year (or any reference period) can be used to completely define the Poisson distribution function.

2. Highest recorded KSC hurricane-associated wind speed was about 39 m/sec (76 knots).

TABLE 19.3 NUMBER OF HURRICANES IN A 77-yr PERIOD (1899-1975) WITHIN A 161- AND 644-km (100- and 400-n. mi.) RADIUS OF KENNEDY SPACE CENTER

Month	Number of Hurricanes Within	
	161-km (100-n. mi.) radius	644-km (400-n. mi.) radius
Jan.	0	0
Feb.	0	0
Mar.	0	0
Apr.	0	0
May	1	1
Jun.	2	4
Jul.	2	12
Aug.	3	24
Sep.	5	46
Oct.	6	33
Nov.	0	5
Dec.	1	1
Total	20	126

TABLE 19.4 NUMBER OF TROPICAL STORMS IN A 105-yr PERIOD (1871-1975) WITHIN A 161- AND 644-km (100- and 400-n. mi.) RADIUS OF KENNEDY SPACE CENTER

Month	Number of Tropical Storms Within	
	161-km (100-n. mi.) radius	644-km (400-n. mi.) radius
Jan.	0	0
Feb.	1	1
Mar.	0	0
Apr.	0	0
May	2	4
Jun.	7	30
Jul.	6	29
Aug.	22	68
Sep.	23	109
Oct.	32	101
Nov.	1	17
Dec.	1	1
Total	95	360

From Figure 19.3, the probability of no event, $P(E_0, r)$ where $r =$ radius, for the following can be read: (1) tropical cyclones, tropical storms, and hurricanes for annual reference periods; and (2) tropical storms and hurricanes for July-August-September; and (3) tropical storms and hurricanes for July-August-September-October, versus radius, in kilometers, from KSC. To obtain the probability for one or more events, $P(E_1, r)$, from Figure 19.3, the reader is required to subtract the $P(E_0, r)$, read from the abscissa, from unity; that is, $[1 - P(E_0, r)] = P(E_1, r)$. For example, the probability that no hurricane path (eye) will come within 556 km (300 n. mi.) of KSC in a year is 0.31 $[P(E_0, r = 300) = 0.31]$, and the probability that there will be one or more hurricanes within 556 km (300 n.mi.) of KSC in a year is 0.69 (1 - 0.31 = 0.69).

In addition to the Eastern Test Range, the Island of Guam is quite susceptible to hurricane (typhoon) passages. Chances are one in three in a given year that a typhoon will pass close enough to affect operations on Guam. This is an average of 1.07 typhoons per year. There is a one in eight chance that a typhoon will pass directly over Guam in a given year (0.42 typhoon per year). These statistics were taken from a 43-year data record of Guam typhoons (1911 through 1930, 1946 through 1968).

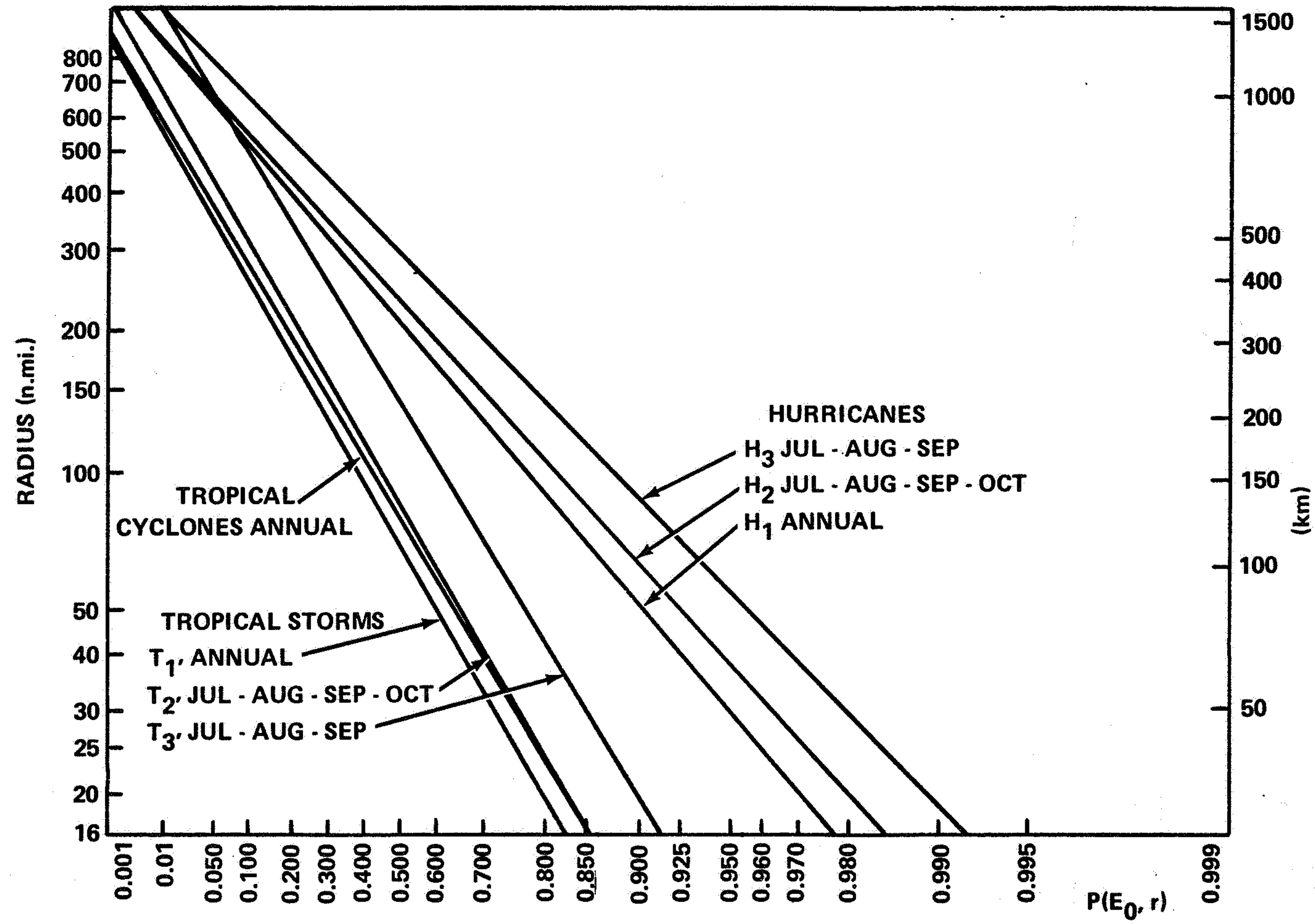

FIGURE 19.3 PROBABILITY OF NO TROPICAL CYCLONES, TROPICAL STORMS, OR HURRICANES FOR VARIOUS REFERENCE PERIODS VERSUS VARIOUS RADII FROM KENNEDY SPACE CENTER

19.4 Climatological Information for Selected Geographic Locations

Climatological information pertinent to aerospace vehicle operations is given in two NASA contractor reports (Refs. 19.2 and 19.3). Both documents follow the same format and contain for each site: (1) a short narrative description of the climate, (2) monthly and annual temperature and precipitation summaries, (3) percentage frequency of occurrence of specified weather conditions for monthly and annual reference periods (the weather conditions, ceiling and visibility, thunderstorms, precipitation, fog, and other obstructions to vision are given for 3-hour periods to show the diurnal changes and for all hours combined), and (4) ground winds for monthly and annual reference periods. These data give the percentage frequency of occurrence of wind speed versus wind direction.

NASA CR-61319 contains data for nine foreign and three United States sites, while NASA CR-61342 contains 20 United States (2 in Alaska) locations, as follows:

NASA CR-61319

Edwards AFB, California
Langley AFB, Virginia
Patrick AFB, Florida
Moron, Argentina
Moron De LaFrontera, Spain
Ambala, India
Dhahran, Saudi Arabia
Bloemfontein, South Africa
Reggan, Algeria
Alice Springs, Australia
Honolulu, Hawaii
Perth, Australia

NASA CR-61342

Eielson AFB, Fairbanks, Alaska
Elmendorf AFB, Anchorage, Alaska
Castle AFB, Merced, California
Vandenberg AFB, Santa Maria, California
McCoy AFB, Orlando, Florida
Columbus AFB, Columbus, Mississippi
Whiteman AFB, Knob Noster, Missouri

Cherry Point MCAS, Havelock, North Carolina
Seymour-Johnson AFB, Goldsboro, North Carolina
Holloman AFB, Alamogordo, New Mexico
McGuire AFB, Wrightstown, New Jersey
Shaw AFB, Sumter, South Carolina
Ellsworth AFB, Rapid City, South Dakota
Bergstrom AFB, Austin, Texas
Biggs AFB, El Paso, Texas
Carswell AFB, Ft. Worth, Texas
Dyess AFB, Abilene, Texas
Ellington AFB, Houston, Texas
Kelly AFB, San Antonio, Texas
Sheppard AFB, Wichita Falls, Texas

REFERENCES

19.1 Thom, H. C. S.: "Tornado Probabilities." Monthly Weather Review, Vol. 91, Nos. 10-12, Oct.-Dec. 1963, pp. 730-736.

19.2 Lee, Russel F.; Goodge, Grant W.; and Crutcher, H. L.: "Surface Climatological Information for Twelve Selected Stations for Reentry Vehicles." NASA CR-61319, Marshall Space Flight Center, Ala., 1970.

19.3 Goodge, G. W.; Bilton, T. H.; and Quinlin, F. T.: "Surface Climatological Information for Twenty Selected Stations for Reentry Vehicles." NASA CR-61342, Marshall Space Flight Center, Ala., 1971.

SECTION XX. GEOLOGIC HAZARDS

20.1 Introduction

The construction of large launching and support facilities for aerospace vehicles at the Kennedy Space Center (KSC) has been under way for a number of years. Planning for such structures has involved little more than routine assessment of geologic conditions because major geologic hazards are few in the KSC area. With the decision to construct a Space Shuttle Launch Complex at Vandenberg Air Force Base (VAFB) or Edwards Air Force Base (EAFB), California, certain geologic hazards should be carefully considered in the initial planning phase. These geologic hazards are as follows:

a. Earthquake Shaking

b. Fault Displacement

c. Tsunami and Seiche

d. Landsliding

e. Flooding

Several other geologic hazards of lesser importance at the potential sites should also be considered.

20.2 Earthquake Shaking

20.2.1 General

The greatest losses in terms of life and property in California due to geologic hazards have been caused by ground shaking during earthquake activity (Ref. 20.1). Earthquake shaking is largely the result of seismic energy release during sudden displacement along a fault. The amount of ground shaking and seismic-induced damage to a structure at a particular point depends on the following:

a. Magnitude of earthquake at its source

b. Areal surface of the causative fault

c. Distance from epicenter

d. Amplitude of the earthquake waves at the site of observation

e. Duration of strong motion or shaking at the site of observation

f. The rock acceleration at the site of observation (Greensfelder, Ref. 20.2, has discussed maximum credible rock acceleration from earthquakes in California, and Page and others, Ref. 20.3, have discussed ground motion values used in the seismic design of structures).

g. Characteristics of the substrat at the site of observation (observations upon thick deposits of saturated unconsolidated sediments cause the intensity of ground shaking to be several times greater than observations on bedrock, Ref. 20.4).

h. The fundamental period of the structure to the ground on which it rests (taller buildings or structures have larger fundamental periods and are subject to greater damage when standing on ground with long fudamental period (Refs. 20.4 and 20.5, Figure 20.1).

i. The structural integrity of the structure subjected to earthquake shaking.

Although at present it is not possible to prevent or control earthquakes and accurate prediction is only in its infancy, several mainly qualitative approaches can be used in developing predictive models for ground shaking and guidelines for earthquake-resistant design (Ref. 20.6). Correlations of general firmness of soil or rock with shaking damage from historical seismic events can provide information on the effects of shaking on various local substrat types. Geologic maps and engineering field and test data for various substrats can aid in projecting characteristics into areas with little or no historical seismic damage data. In addition, intensity maps based on the Modified Mercalli or a similar intensity scale have been made in many areas from damage studies of historical seismic events. The generalized distribution of maximum expectable earthquake intensity in California is shown in Figure 20.2 and the effects in each zone described in Table 20.1. In addition, maximum credible rock acceleration values have been derived for California along with maximum expected earthquake magnitude for various faults (Ref. 20.2; Figure 20.3), the predominent period of bedrock acceleration (based on data Seed and others, Ref. 20.7) and the duration of strong shaking (based on data from Housner, Ref. 20.8; Table 20.2). Such data is useful in developing guidelines for earthquake-resistant design.

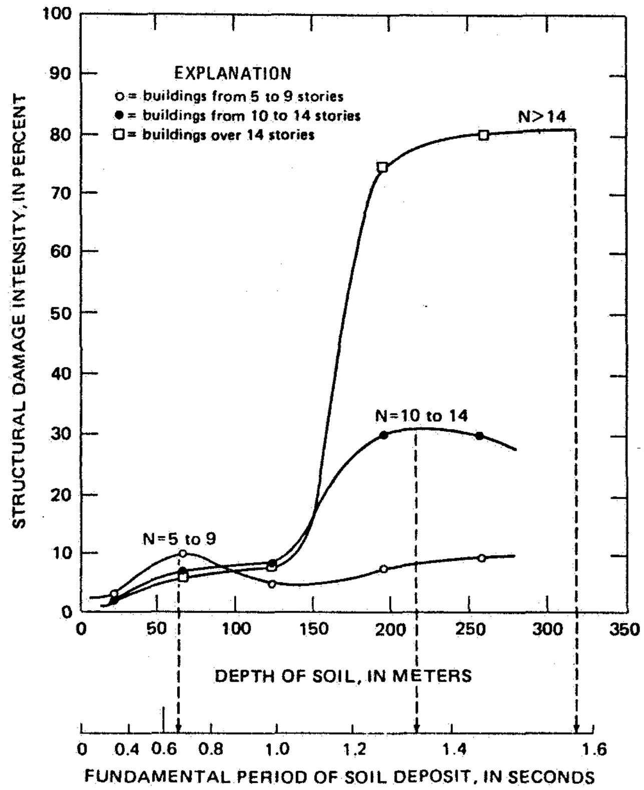

FIGURE 20.1 STRUCTURAL DAMAGE INTENSITY FOR BUILDINGS OF VARIOUS HEIGHTS RELATED TO DEPTH OF SOIL AND COMPUTED FUNDAMENTAL PERIOD OF SOIL DEPOSIT N = NUMBER OF STORIES. WHERE THE FUNDAMENTAL PERIOD OF A SOIL DEPOSIT IS SHORT (BETWEEN 0.6 AND 0.8 s), THE GREATEST DAMAGE WILL OCCUR TO BUILDINGS FROM 5 TO 9 STORIES TALL. WITH LONGER SOIL PERIODS, DAMAGE INTENSITY TO HIGHER STRUCTURES INCREASE. (From Seed and others, 1972, Fig. 12, Ref. 20.5).

The serious concern for damage and loss of life due to earthquake shaking is reflected in recent legislation in California, both at the state and local levels. The Uniform Building Code of 1970 categorizes the United States into four zones of relative seismic risk based on the known distribution of damaging earthquakes and the Modified Mercalli intensities associated with these earthquakes; on evidence of strain release; and on considerations of major geologic structures

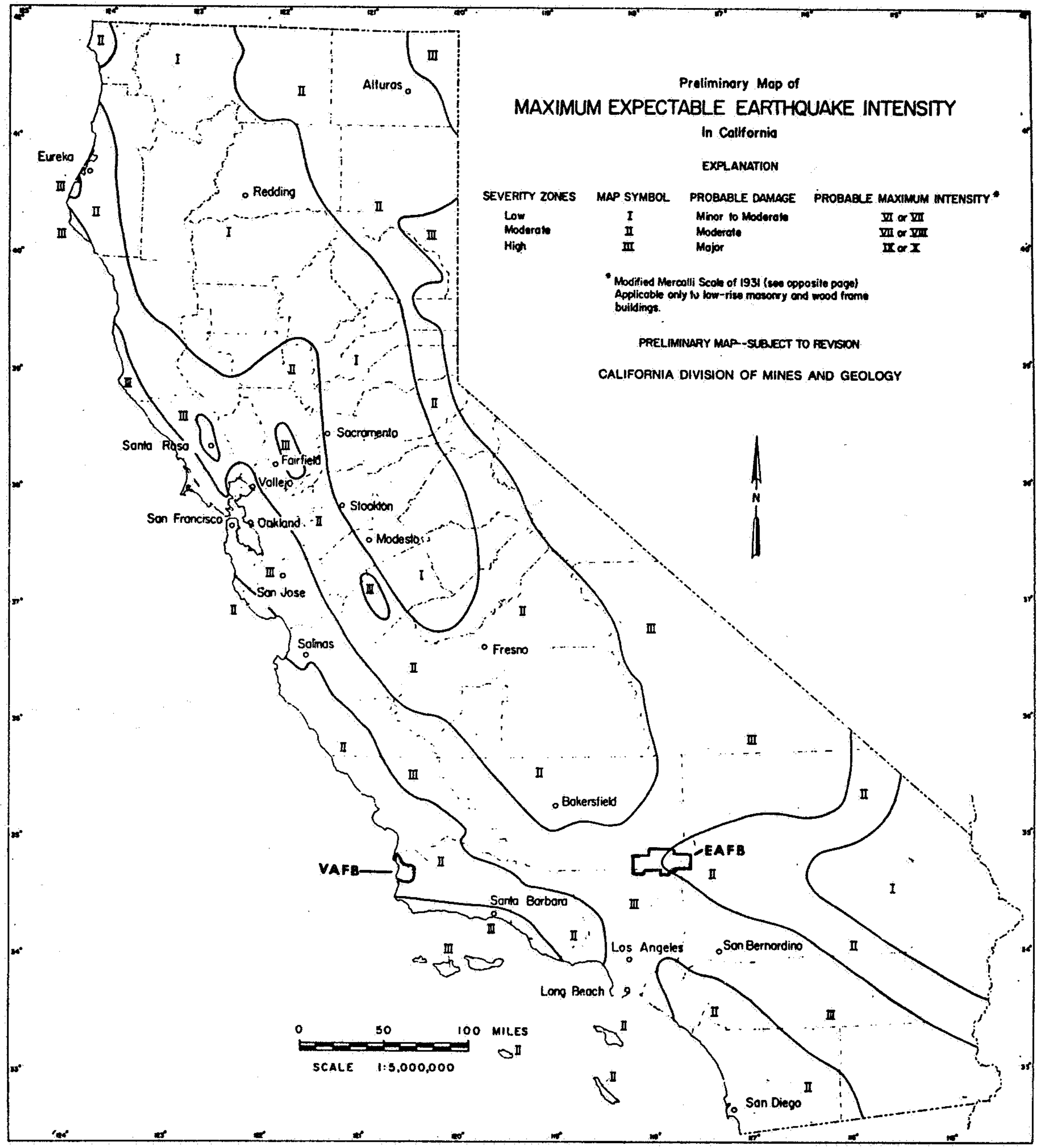

FIGURE 20.2

FIGURE 20.2 PRELIMINARY MAP OF MAXIMUM EXPECTABLE EARTHQUAKE INTENSITY IN CALIFORNIA. (From Alfors and others, 1973, Fig. 3, Ref. 20.1).

TABLE 20.1 MODIFIED MERCALLI SCALE OF EARTHQUAKE INTENSITIES. (From Alfors and others, 1973, Table 3, Ref. 20.1).

THE MERCALLI INTENSITY SCALE
(As modified by Charles F. Richter in 1956 and rearranged)

If most of these effects are observed	*then the intensity is:*
Earthquake shaking not felt. But people may observe marginal effects of large distance earthquakes without identifying these effects as earthquake-caused. Among them: trees, structures, liquids, bodies of water sway slowly, or doors swing slowly.	*I*
Effect on people: Shaking felt by those at rest, especially if they are indoors, and by those on upper floors.	*II*
Effect on people: Felt by most people indoors. Some can estimate duration of shaking. But many may not recognize shaking of building as caused by an earthquake; the shaking is like that caused by the passing of light trucks.	*III*
Other effects: Hanging objects swing. *Structural effects:* Windows or doors rattle. Wooden walls and frames creak.	*IV*
Effect on people: Felt by everyone indoors. Many estimate duration of shaking. But they still may not recognize it as caused by an earthquake. The shaking is like that caused by the passing of heavy trucks, though sometimes, instead, people may feel the sensation of a jolt, as if a heavy ball had struck the walls. *Other effects:* Hanging objects swing. Standing autos rock. Crockery clashes, dishes rattle or glasses clink. *Structural effects:* Doors close, open or swing. Windows rattle.	*V*
Effect on people: Felt by everyone indoors and by most people outdoors. Many now estimate not only the duration of shaking but also its direction and have no doubt as to its cause. Sleepers wakened. *Other effects:* Hanging objects swing. Shutters or pictures move. Pendulum clocks stop, start or change rate. Standing autos rock. Crockery clashes, dishes rattle or glasses clink. Liquids disturbed, some spilled. Small unstable objects displaced or upset. *Structural effects:* Weak plaster and Masonry D* crack. Windows break. Doors close, open or swing.	*VI*
Effect on people: Felt by everyone. Many are frightened and run outdoors. People walk unsteadily. *Other effects:* Small church or school bells ring. Pictures thrown off walls, knicknacks and books off shelves. Dishes or glasses broken. Furniture moved or overturned. Trees, bushes shaken visibly, or heard to rustle. *Structural effects:* Masonry D* damaged; some cracks in Masonry C*. Weak chimneys break at roof line. Plaster, loose bricks, stones, tiles, cornices, unbraced parapets and architectural ornaments fall. Concrete irrigation ditches damaged.	*VII*
Effect on people: Difficult to stand. Shaking noticed by auto drivers. *Other effects:* Waves on ponds; water turbid with mud. Small slides and caving in along sand or gravel banks. Large bells ring. Furniture broken. Hanging objects quiver. *Structural effects:* Masonry D* heavily damaged; Masonry C* damaged, partially collapses in some cases; some damage to Masonry B*; none to Masonry A*. Stucco and some masonry walls fall. Chimneys, factory stacks, monuments, towers, elevated tanks twist or fall. Frame houses moved on foundations if not bolted down; loose panel walls thrown out. Decayed piling broken off.	*VIII*
Effect on people: General fright. People thrown to ground. *Other effects:* Changes in flow or temperature of springs and wells. Cracks in wet ground and on steep slopes. Steering of autos affected. Branches broken from trees. *Structural effects:* Masonry D* destroyed; Masonry C* heavily damaged, sometimes with complete collapse; Masonry B* is seriously damaged. General damage to foundations. Frame structures, if not bolted, shifted off foundations. Frames racked. Reservoirs seriously damaged. Underground pipes broken.	*IX*
Effect on people: General Panic. *Other effects:* Conspicuous cracks in ground. In areas of soft ground, sand is ejected through holes and piles up into a small crater, and, in muddy areas, water fountains are formed. *Structural effects:* Most masonry and frame structures destroyed along with their foundations. Some well-built wooden structures and bridges destroyed. Serious damage to dams, dikes and embankments. Railroads bent slightly.	*X*
Effect on people: General panic. *Other effects:* Large landslides. Water thrown on banks of canals, rivers, lakes, etc. Sand and mud shifted horizontally on beaches and flat land. *Structural effects:* General destruction of buildings. Underground pipelines completely out of service. Railroads bent greatly.	*XI*
Effect on people: General panic. *Other effects:* Same as for Intensity X. *Structural effects:* Damage nearly total, the ultimate catastrophe. *Other effects:* Large rock masses displaced. Lines of sight and level distorted. Objects thrown into air.	*XII*

*Masonry A: Good workmanship and mortar, reinforced, designed to resist lateral forces.
Masonry B: Good workmanship and mortar, reinforced.
Masonry C: Good workmanship and mortar, unreinforced.
Masonry D: Poor workmanship and mortar and weak materials, like adobe.

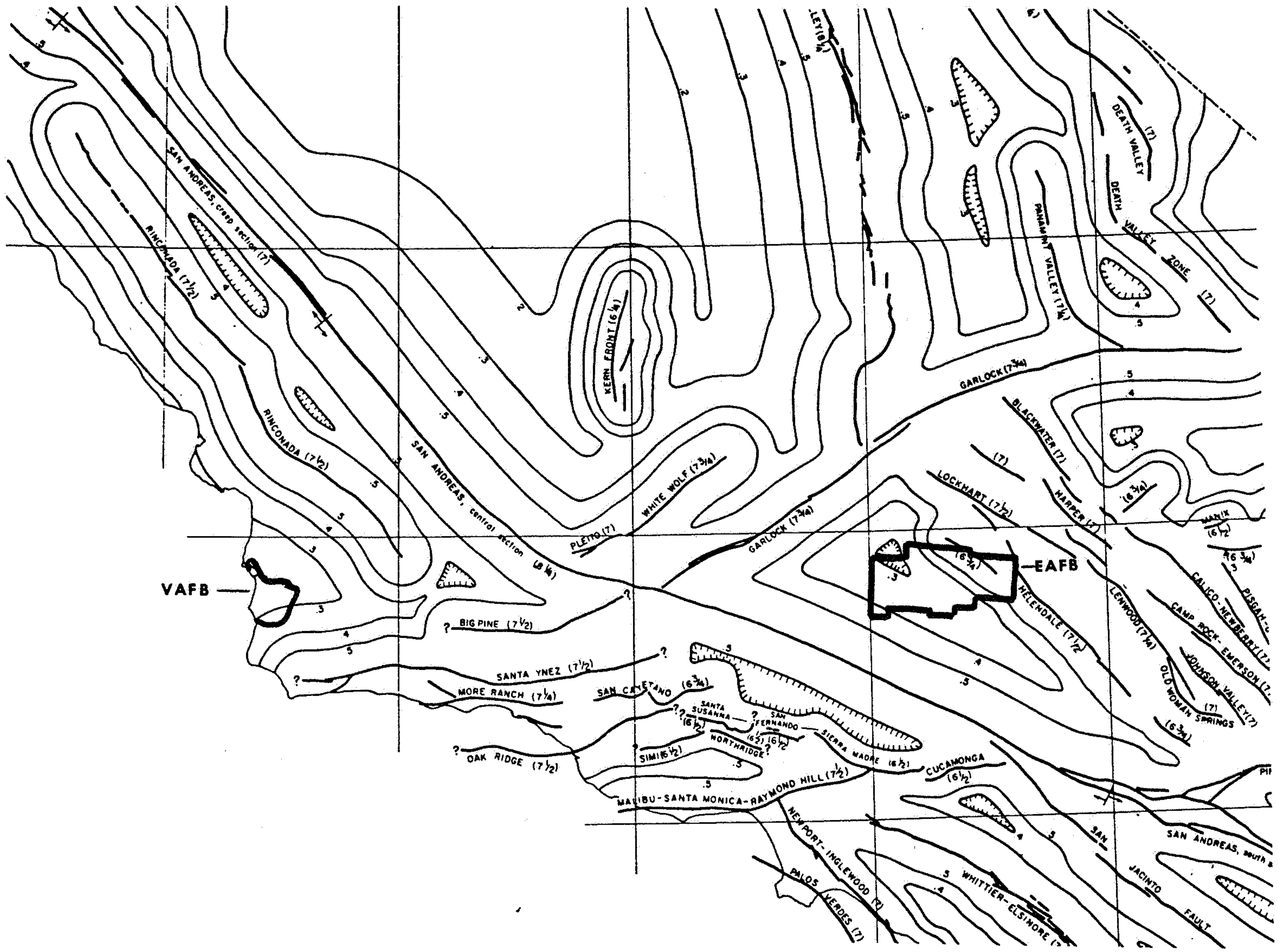

FIGURE 20.3 MAXIMUM CREDIBLE ROCK ACCELERATION FROM EARTHQUAKES IN CENTRAL CALIFORNIA. BED ROCK ACCELERATION CONTOURS IN DECIMAL FRACTIONS OF THE ACCELERATION DUE TO GRAVITY, FROM 0.2 g TO 0.5 g. NUMBERS IN PARENTHESES ARE THE MAXIMUM EXPECTED EARTHQUAKE MAGNITUDE FOR THE FAULTS. (From Greensfelder, 1974, p. 1, Ref. 20.2).

TABLE 20.2 DURATION OF STRONG SHAKING (data from Housner, 1970, p. 79, Ref. 20.8).

Magnitude	Duration (seconds)
6.5	18
7.0	24
7.5	30
8.0	34
8.5	37

and provinces believed associated with earthquake activity (Ref. 20.6; Figure 20.4). California lies entirely within zones 2 and 3 of the seismic risk map (Fig. 20.4). The Code also describes strength and lateral force requirements for buildings in the various zones (Section 2314). In 1971, the state enacted legislation (Government Code Section 65302) requiring cities and counties to include a seismic safety element in their general plans, consisting of "...identification and appraisal of seismic hazards..." The Governor's Earthquake Council was developed in 1972 to act in recommending methods of reducing losses in future earthquakes (Refs. 20.9 and 20.10). In addition, the Structural Engineers Association of California (Ref. 20.11) and the Department of the Army (Ref. 20.12) have recommendations for seismic design of structures.

20.2.2 Areas of Interest

The relative seismic risk in the areas of both potential sites (VAFB and EAFB) fall within the highest category — zone 3 (Figure 20.4). The maximum expectable earthquake intensity in the vicinity of VAFB is VII or VIII and that of EAFB ranges from VII or VIII to IX or X (Figure 20.2; Table 20.1). Maximum credible rock acceleration from earthquakes in the area of VAFB range from about 0.2 to 0.3 acceleration due to gravity (g), while those in the EAFB area range from about 0.3 - 0.5 g. (Figure 20.3).

20.3 Fault Displacement

20.3.1 General

Fault displacements of only a few centimeters (inches) at the surface can have catastrophic effects on structures built across them. The earth is

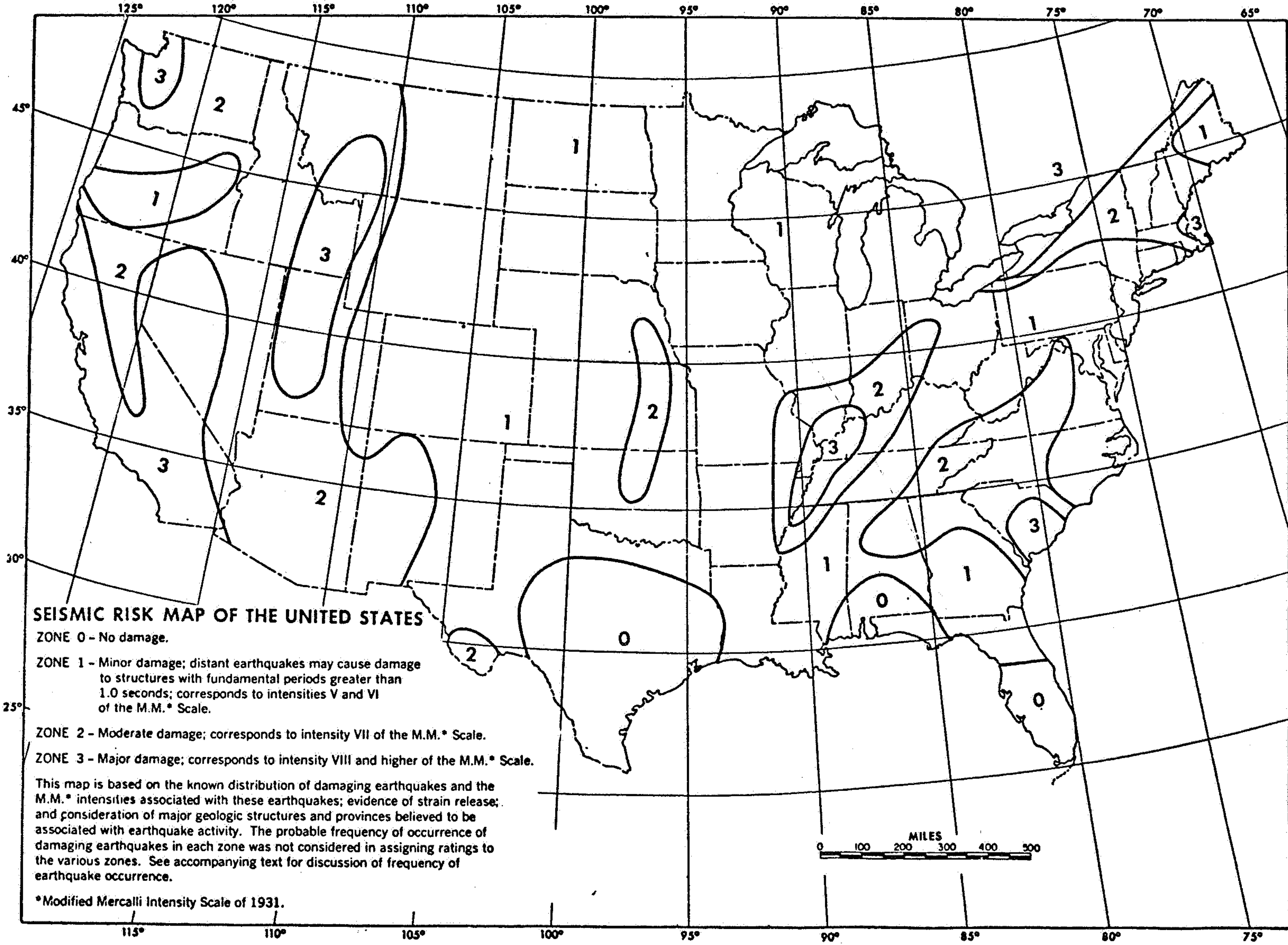

FIGURE 20.4 SEISMIC RISK MAP OF THE UNITED STATES. (From Algermissen, 1960, Fig. 8).

characterized by faults, but most of them may be considered inactive. The definition of an active fault depends on the importance attached to the use of the area or the structure built upon it (Ref. 20.6). In the case of nuclear reactors, the U. S. Nuclear Regulatory Commission considers an active or "capable" fault as one that has experienced movement at or near the surface at least once in the last 35,000 years or recurrent movement within the past 500,000 years (Ref. 20.13). In response to the Alquist-Priolo Geologic Hazard Zones Act of 1972, (Chapter 7.5, Division 2 of the California Public Resources Code), and for purposes of delineating special studies zones, the California State Geologist considers any fault that has been active during Quaternary time (last 2-3 million years) to be potentially active. An exception is Quaternary faulting that can be shown to have become inactive before Holocene (last 11,000 years) (Ref. 20.14, Figure 20.5). Generally the forces resulting from fault movement are so great that critical structures should avoid construction across or near active fault zones. The distribution of potentially active faults in California is shown in Figure 20.6.

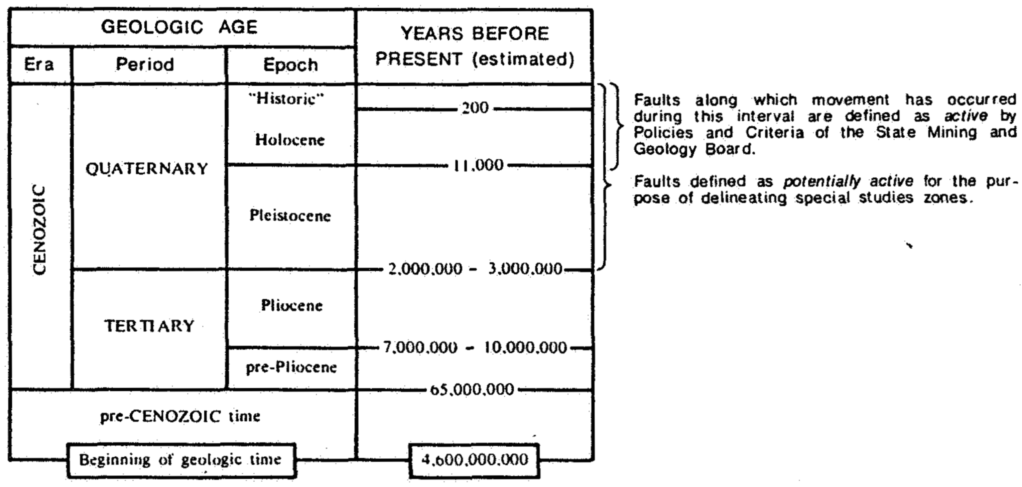

FIGURE 20.5 GEOLOGIC TIME SCALE FOR CENOZOIC TIME INDICATING RELATIONSHIPS TO ACTIVE — AND POTENTIALLY ACTIVE — FAULT DEFINITIONS (from Hart, 1975, Fig. 2, Ref. 20.14).

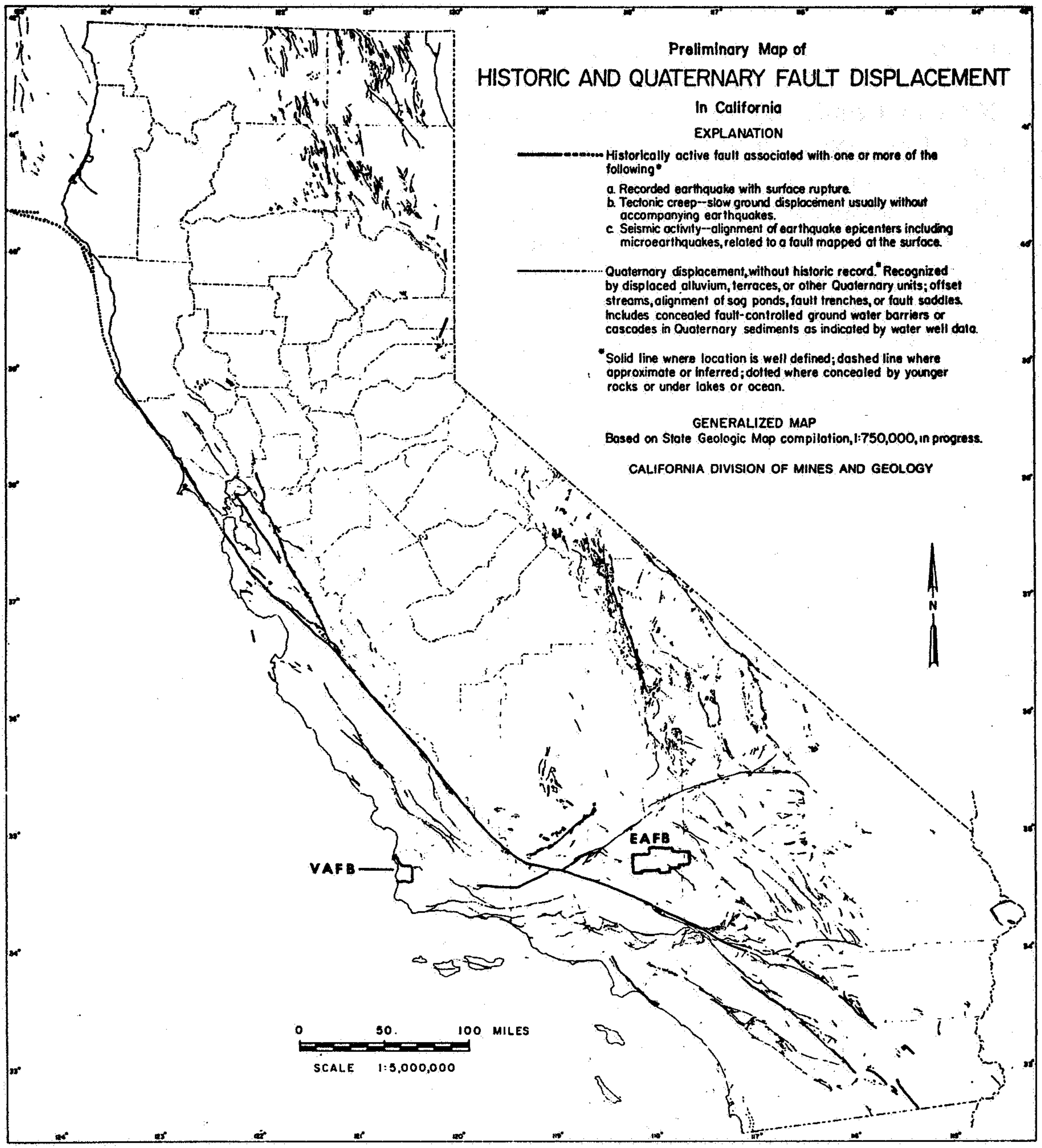

FIGURE 20.6 PRELIMINARY MAP OF HISTORIC AND QUATERNARY FAULT DISPLACEMENT IN CALIFORNIA. (From Alfors and others, 1973, Fig. 9, Ref. 20.1)

Several generalizations can be made about active faulting as follow:

1. Movement is most likely to occur along fault zones that ruptured most recently, especially if there is evidence of recurrent movement (Refs. 20.15 and 20.16; Figure 20.7).

2. The longer the fault, the greater the potential for a significantly large earthquake, and the greater the amount of displacement likely (Refs. 20.16, 20.17 and 20.18).

3. Strike-slip movement along a fault is less potentially damaging than normal or thrust faulting (Ref. 20.6).

Existing state and local legislation pertaining to various structures and building sites either require special studies and board approval or prohibit construction on active fault zones (Section 65302, Government Code; Section 15002.1, State Education Code; Chapter 7.5, Division 2, Public Resources Code; Earthquake Fault Ordinance No. 10,362, Los Angeles County). In Los Angeles County, any site for a structure designed for human occupancy that is within "50 feet" (15.24 m) of a known active fault must be trenched to determine whether an active fault is present. Setback limits from active faults should depend on the degree of critical importance of the structures or buildings.

20.3.2 Areas of Interest

The distribution of potentially active surface faulting for VAFB and EAFB are shown in Figures 20.8 and 20.9 respectively (Ref. 20.19). No potentially active surface faults occur within the limits of VAFB, however, several occur in the surrounding areas (Figure 20.8). Several potentially active surface faults are present within the boundaries of EAFB, especially in the eastern part (Figure 20.9). In addition, EAFB is located between the Garlock and San Andreas fault zones both of which are of considerable length and therefore of great potential danger. Interestingly, both this central segment of the San Andreas fault and the Garlock fault have been seismically inactive in recent years, but by no means should be considered inactive. Any evaluation of either site should include detailed geologic mapping, closely investigating the area for unrecorded active faults. Placement of any critical structures should avoid active or potentially active fault zones and should adhere to all state and local codes and ordinances, as well as to Federal recommendations.

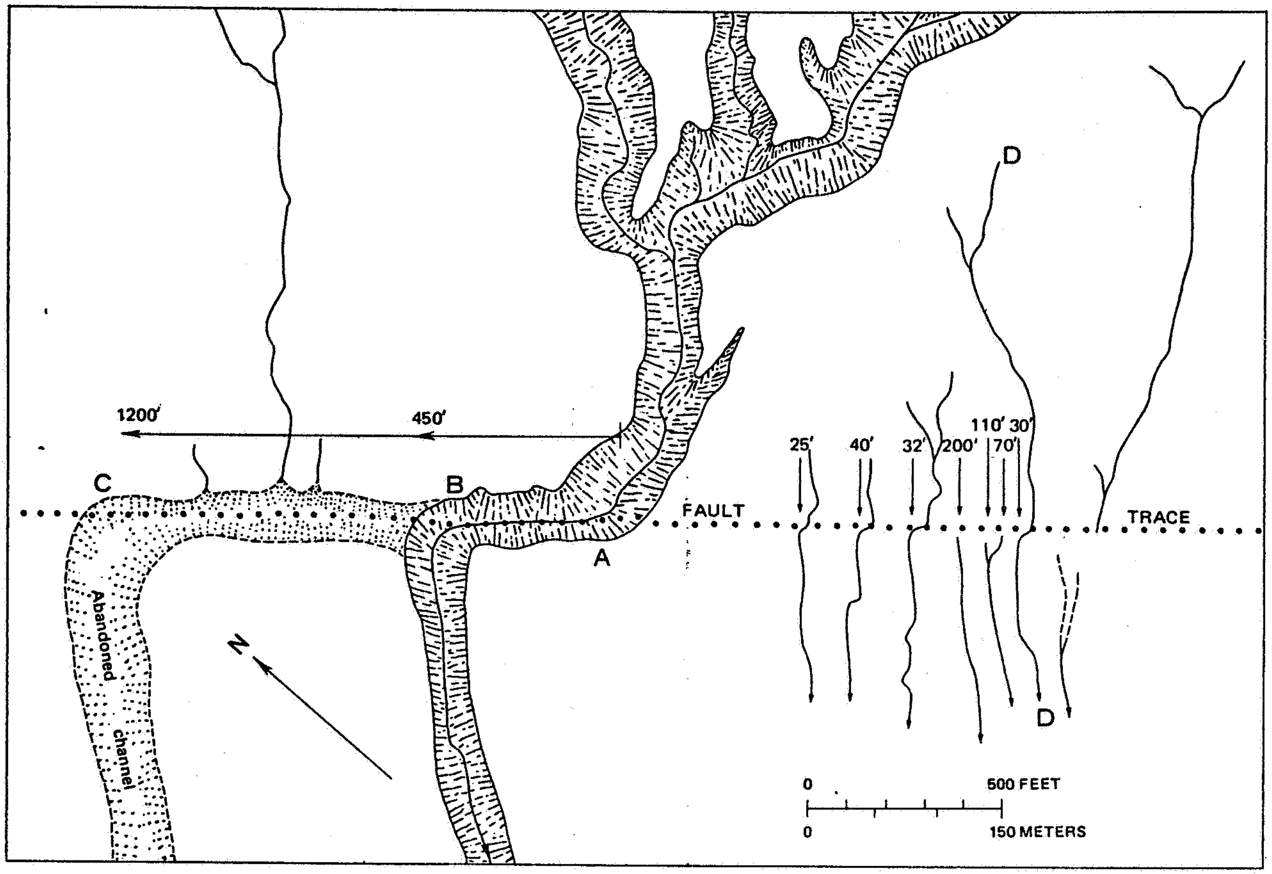

FIGURE 20.7 PROGRESSIVE LATERAL SHIFTING IN STREAM ALIGNMENT DUE TO REPEATED DISPLACEMENT ALONG A SINGLE TRACE OF THE SAN ANDREAS FAULT. THE MAJOR STREAM CHANNEL HAS BEEN DEFLECTED 450 FEET FROM A TO B. EAVILEV DISPLACEMENTS ARE SUGGESTED BY THE BEHEADED STREAM SEGMENT AT C, 1,200 FEET FROM A. THE SMALL STREAM CHANNEL AT D DISPLAYS A SERIES OF OFF-SETS REPRESENTED BY ONE DEFLECTION AND THREE ABANDONED DOWNSTREAM SEGMENTS (measuring 30, 70, 110 and 200 feet). (From Wallace 1968, Fig. 8, Ref. 20.15)

20.4 Tsunami and Seiche

20.4.1 General

Tsunamis or seismic sea waves are great ocean waves generated by earthquakes, submarine volcanic eruptions, large submarine slides or any rapid change in elevation of large masses of earth and ocean. The waves can move thousands of kilometers (miles) across deep ocean areas where their wave

C-6

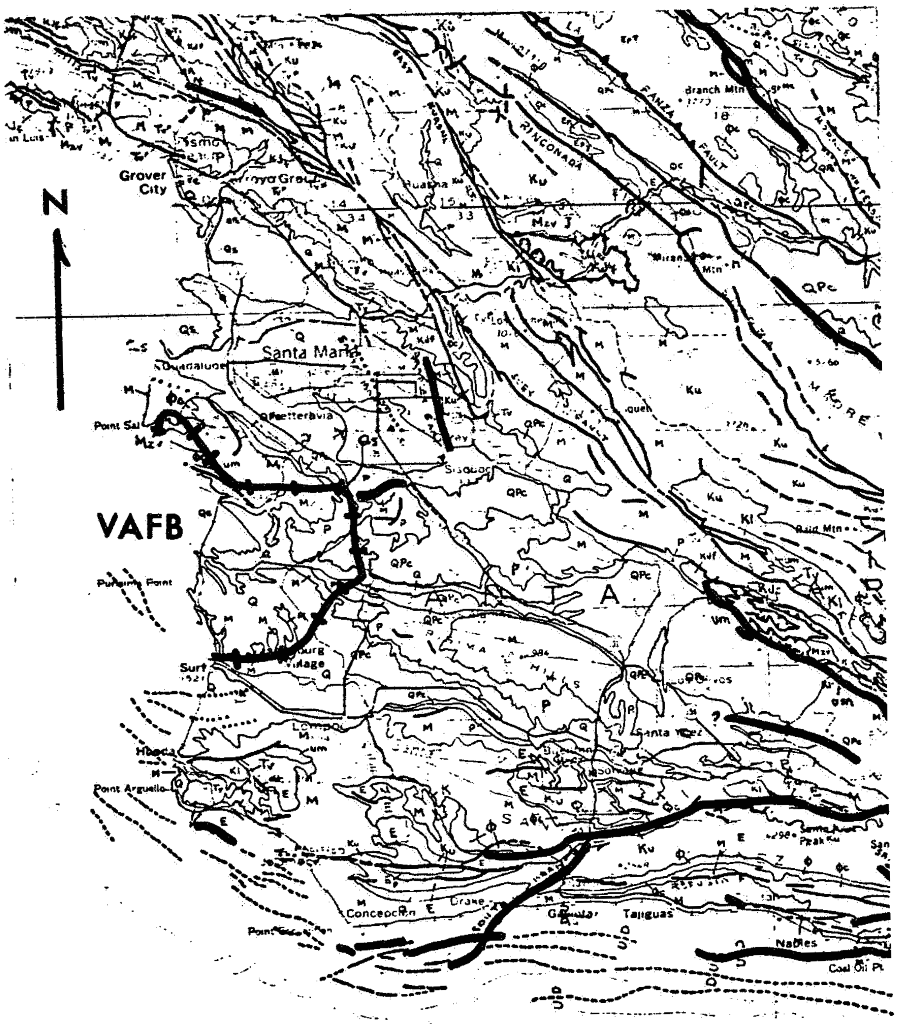

FIGURE 20.8 POTENTIALLY ACTIVE SURFACE FAULTS (those with Quaternary movement — heavy black lines) AND OLDER FAULTS IN THE VICINITY OF VAFB (boundary delineated by crossed line). SEE FIGURE 20.5 FOR DEFINITION OF QUATERNARY. (From Jennings, 1973, Ref. 20.19).

lengths may be 200 km (125 mi.) and amplitudes only a few decimeters (feet) (Ref. 20.1). In shallower waters along coastlines, wave amplitides increase and can crest at heights of more than 30 m (100 ft.), exerting devastating forces (Ref. 20.20). The effects of the tsunamis can be greatly amplified by the configuration of local shorelines and sea bottoms. The distribution of tsunami hazard areas in California are shown in Figure 20.10. The forces involved in

ORIGINAL PAGE IS
OF POOR QUALITY

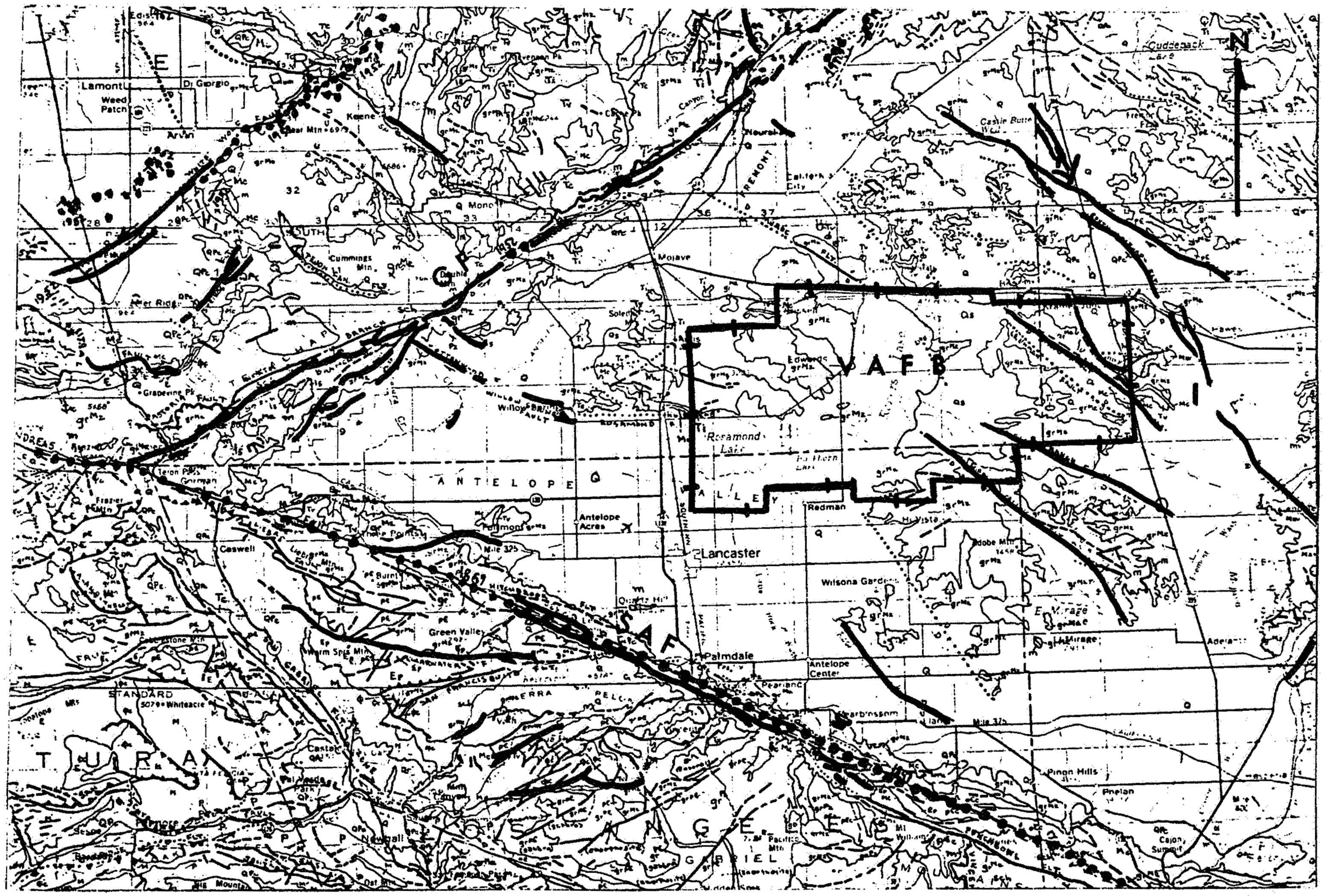

FIGURE 20.9 POTENTIALLY ACTIVE SURFACE FAULTS (those with historic movement-dots and those with Quaternary movement — heavy black lines) AND OLDER FAULTS IN THE VICINITY OF EAFB (boundary delineated by crossed line): SAF = SAN ANDREAS FAULT, GF = GARLOCK FAULT. SEE FIGURE 20.5 FOR DEFINITION OF QUATERNARY. (From Jennings, 1973, Ref. 20.19)

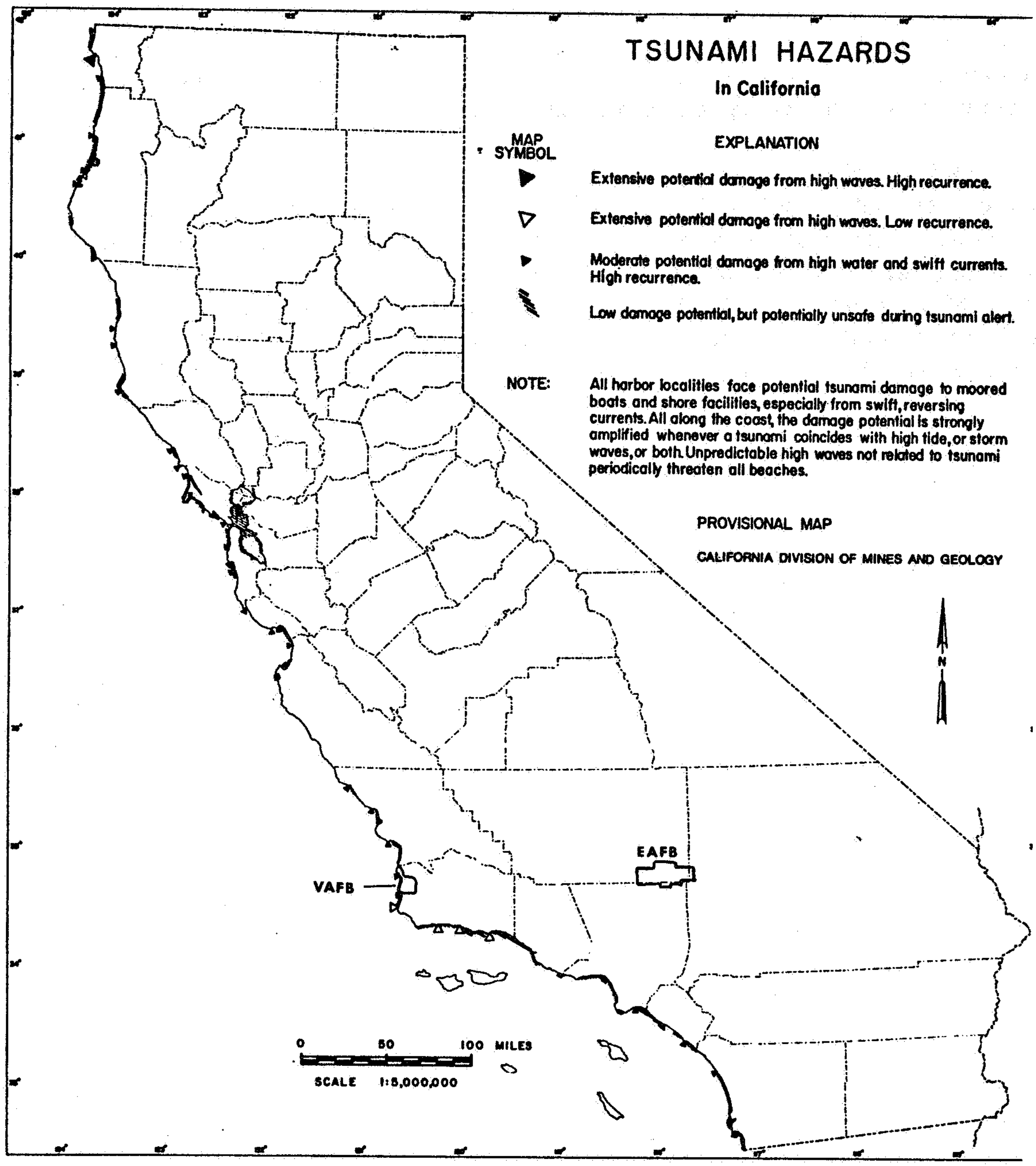

FIGURE 20.10 TSUNAMI HAZARDS IN CALIFORNIA. (From Alfors and others, 1973, Fig. 11, Ref. 20.1).

tsunamis are so great that areas of potential damage should be avoided in construction of critical structures. The national Oceanic and Atmospheric Administration administers a seismic sea-wave warning system to provide early warnings of the approach of potentially damaging tsunamis.

Seismic seiches or earthquake-generated standing waves occur within enclosed or restricted bodies of water such as lakes, reservoirs, bays and rivers. Seiches generally have amplitudes of less than 3 decimeters (a foot) and low energies, but where water is constricted wave runup can approach 6 to 9 m (20 to 30 ft) (Ref. 30.21). Such runup can have disasterous effects especially in areas downstream from dams and reservoirs. California legislation now requires dam owners to prepare maps showing areas of potential inundation.

20.4.2 Areas of Interest

The coastline at VAFB faces moderate potential damage from high water and swift currents related to tsunamis (Fig. 20.10). Seiche hazards may exist along some of the small streams and lakes on the base. No related hazards affect EAFB.

20.5 Landsliding

20.5.1 General

Landsliding is the downhill movement of masses of earth material under the influence of gravity. Movement rates range from instantaneous to so slow that change in position can be measured only over a period of months or years. Areas of landsliding can range upward to several square kilometers (miles) and can involve zones a hundred meters (several hundred feet) thick.

In California, landsliding is common and one of the costliest of the geologic hazards. Figure 20.11 shows the distribution of relative amounts of landsliding in California.

The recognition of old landslide areas is critical because future sliding can generally be anticipated in these zones. Through the use of detailed geologic and topographic mapping and interpretation, trenching, drilling and air photo interpretation, many old landslide areas can be delineated. Slope zones covered with thick soils, or heavily saturated with ground water; areas characterized by rock bedding, fracturing or jointing that parallel hill slopes; and fault zones all constitute potentially dangerous landslide areas.

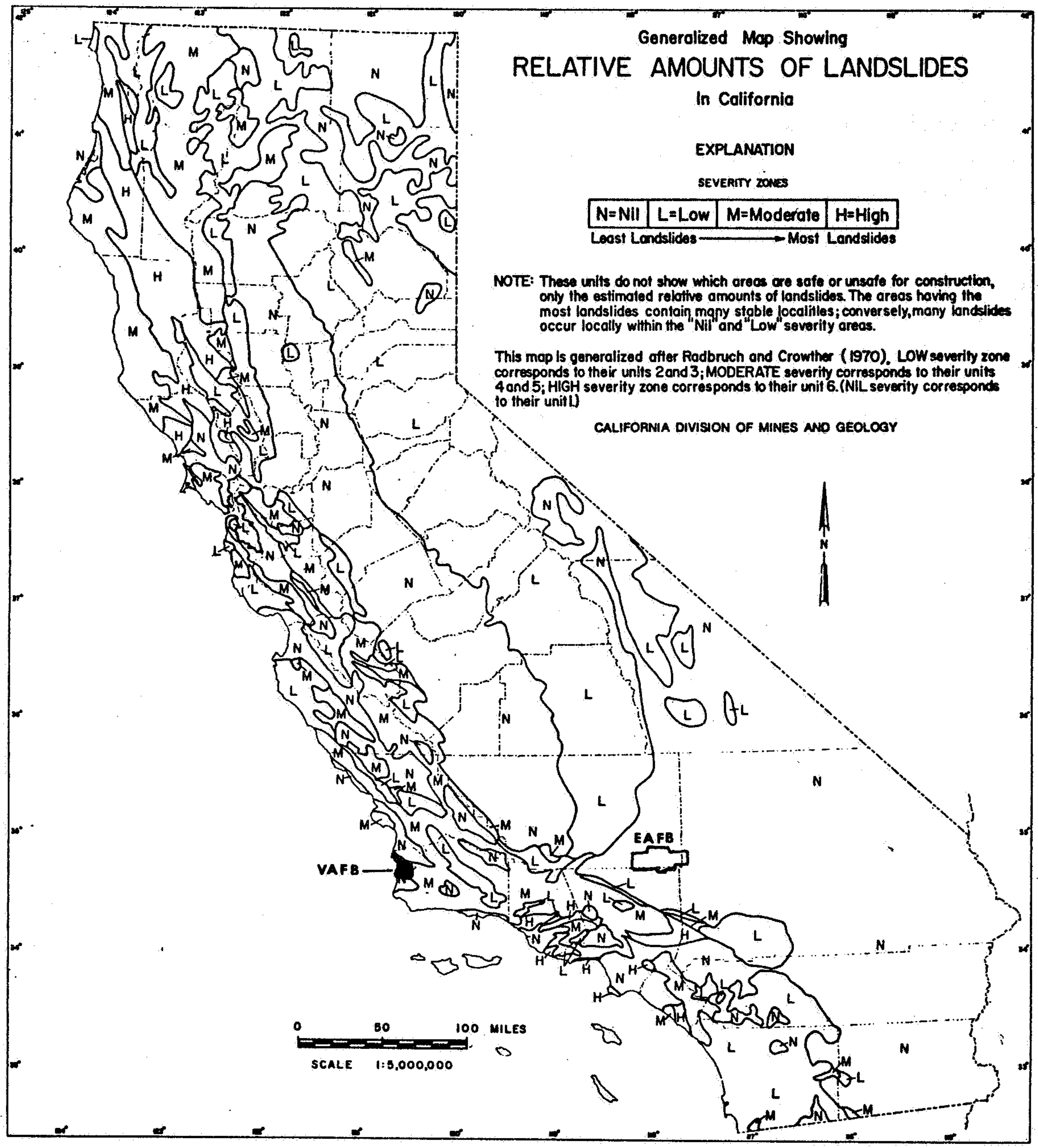

FIGURE 20.11 GENERALIZED MAP SHOWING RELATIVE AMOUNTS OF LANDSLIDES IN CALIFORNIA. (From Alfors and others, 1973, Fig. 5, Ref. 20.1).

A number of techniques including dewatering, loading or buttressing the toe of slopes and removing landslide debris at their heads may stabilize landslide zones.

California legislation requires studies to detect geologic hazards including the dangers posed by landsliding (Section 15002.1 of the Education Code and Section 65302.1 of the Government Code).

20.5.2 Areas of Interest

Very low to moderate amounts of landsliding can be expected in the VAFB area, but generally the chances of landsliding in the EAFB area are quite low (Figure 20.11). In both cases, however, detailed studies would be required for complete evaluation.

20.6 Flooding

20.6.1 General

In spite of flood-control measures, flooding remains one of the costliest natural hazards in California. The distribution of flood-prone areas in the state is shown in Figure 20.12. Flooding is of two main types as follow:

1. Off-site flooding, caused by rain or snow-melt water from up-stream areas.

2. On-site flooding, caused by local runoff of water (Ref. 20.1).

A large number of laws relating to flooding are in effect in California.

20.6.2 Areas of Interest

Both VAFB and EAFB contain flood-prone areas within their boundaries. This factor should be seriously considered in the evaluation of the potential sites.

20.7 Other Geologic Considerations

Several other geologic considerations, that from a general point of view do not appear to merit detailed discussion because of their relatively small effect on either of the proposed California sites, should at least be mentioned. Erosion problems involving both the wear and removal of material from one site and its deposition in another can in some instances be destructive to major structures and buildings. Expansive soils that greatly increase in volume when they absorb water and shrink when they dry out can likewise cause foundation problems in major structures. In addition similar problems may be caused by subsidence due to various mechanisms including the withdrawal of groundwater, oil or gas, hydrocompaction, or peat oxidation. All of these factors should be considered in any detailed evaluation of the potential sites.

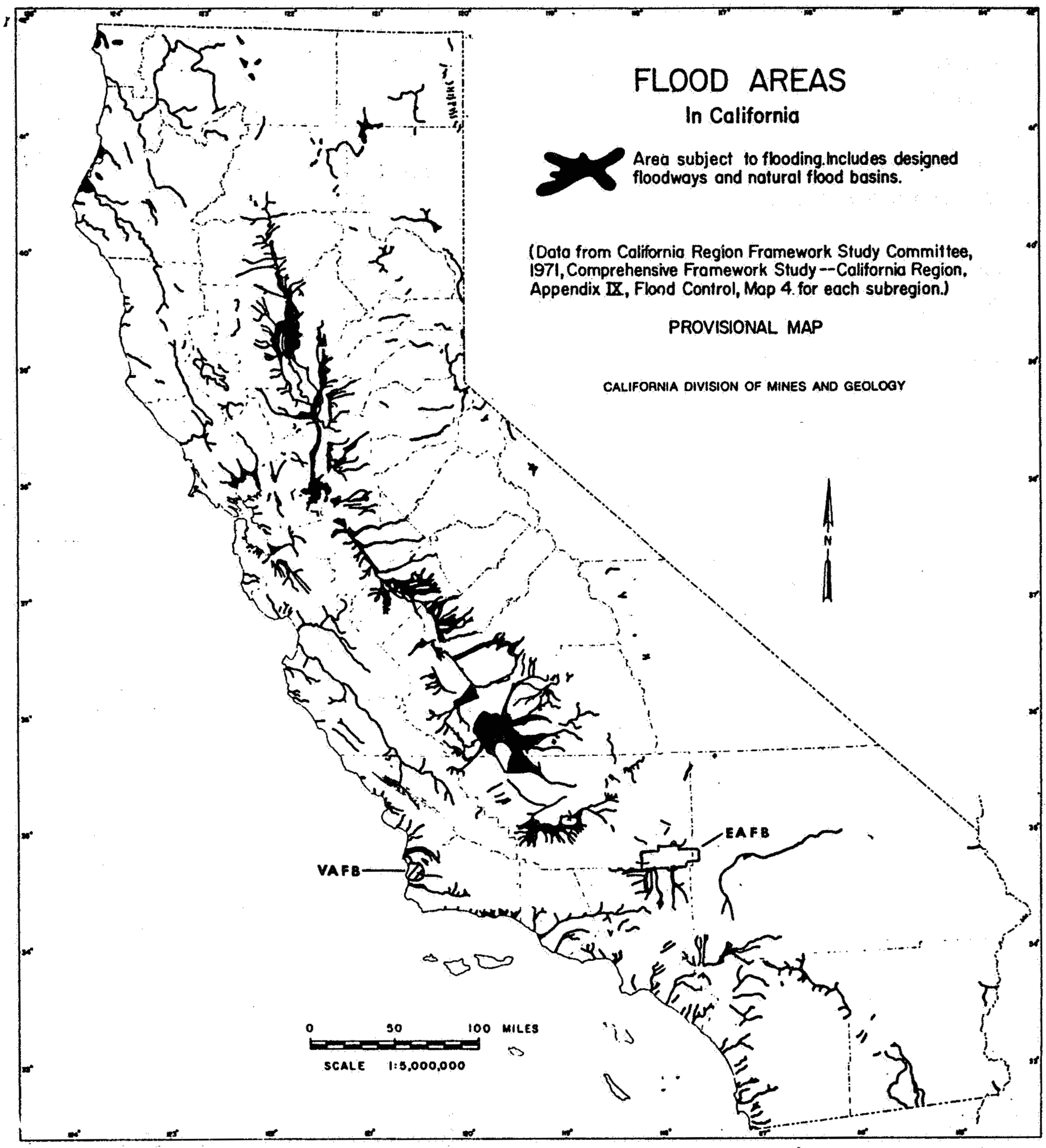

FIGURE 20.12 FLOOD-PRONE AREAS OF CALIFORNIA. (From Alfors and others, 1973, Fig. 6, Ref. 20.1)

20.8 Appendix — Definitions

All definitions are from the Glossary of Geology (Ref. 20.22) unless otherwise stated.

Fault — A surface or zone of rock fracture along which there has been displacement from a few centimeters to a few kilometers in scale.

Focus — That point within the earth which is the center of an earthquake and the origin of elastic waves.

Epicenter — That point on the Earth's surface which is directly above the focus of an earthquake.

Magnitude — A measure of the strength of an earthquake or the strain energy released by it, as determined by seismographic observations. The concept was introduced by seismologist C. F. Richter, who first applied it to southern California earthquakes. For that region, he defined local magnitude to the logarithm, to the base 10, of the amplitude in microns of the largest trace deflection that would be observed on a standard torsion seismograph (static magnification = 2800, period = 0.8 sec., damping constant = 0.8) at a distance of 100 km from the epicenter. Arabic numerals are applied and are referred to as Richters on a scale ranging from negative values for microearthquakes to an upper limit of slightly less than 9.

Intensity — A measure of the effects of an earthquake at a particular place on humans and/or structures. The intensity at a point depends not only upon the strength of the earthquake, or the earthquake magnitude, but also upon the distance from the earthquake to the epicenter and the local geology at the point. The scale in common use is the Modified Mercalli Intensity Scale of 1931 which is shown in modified form in Table 20.1.

Tsunami — A gravitational sea wave produced by any large-scale, short-duration disturbance of the ocean floor, principally by a shallow submarine earthquake, but also by submarine earth movement, subsidence, or volcanic eruption, characterized by great speed of propagation (up to 950 km/hr, long wavelength (up to 200 km), long period (varying from 5 min. to a few hours, generally 10 to 60 min), and low observable amplitude on the open sea although it may pile up to great heights (30 m or more) and cause considerable damage on entering shallow water along an exposed coast, of ten thousands of kilometers from the source.

Seiche — A free or standing-wave oscillation of the surface of water in an enclosed or semi-enclosed basin (as a lake, landlocked sea, bay, or harbor) that varies in period (depending on the physical dimensions of the basin) from a few minutes to several hours and in height from several centimeters to a few meters, that is initiated chiefly by local changes in atmospheric pressure aided by winds, tidal currents, and small earthquakes, and that continues pendulum fashion for a time after the cessation of the originating force. The term has also been applied to an oscillation superimposed upon the tidal waves of the open ocean.

Fundamental period — The longest period (duration in time of one full cycle of oscillatory motion) for which a structure or soil column shows a response peak — commonly the period of maximum response (Ref. 20.6).

Normal fault — A fault in which the hanging wall appears to have moved downward relative to the footwall.

Reverse fault — A fault in which the hanging wall appears to have moved upward relative to the footwall.

Footwall — The underlying side of a fault.

Hanging Wall — The overlying side of a fault.

Strike-Slip Fault — A fault, the actual movement of which is parallel to the strike of the fault.

REFERENCES

20.1 Alfors, J. T., Burnett, J. L. and Gay, T. E., Jr., "Urban Geology." California Division of Mines and Geology, Bull 198, 1973.

20.2 Greensfelder, R. W., "Maximum Credible Rock Acceleration from Earthquakes in California." California Division of Mines and Geology, Map Sheet 23, Aug. 1974.

20.3 Page, R. A., Boone, D. M., Joyner, W. B., and Coulter, H. W., "Ground Motion Valves for Use in the Seismic Design of the Trans-Alaska Pipeline System." U. S. Geol. Survey Circ. 672, 1972.

20.4 Wallace, R. E., "Minimizing Earthquake Hazards." Am. Inst. of Architects Jour., v. 19, no. 1, 1968, pp. 65-69.

20.5 Seed, H. B., Whitman, R. V., Dezfulian Houshang, Dobry, Ricardo, and Idriss, I. M., "Soil Conditions and Building Damage in 1967 Caracas Earthquake," Am. Soc. Civil Engineers Proc., Jour. Soil Mechanics and Found. Div., v. 98, no. 8, 1972, pp. 787-806.

20.6 Nichols, D. R. and Buchanan-Banks, J. M., "Seismic Hazards and Land-Use Planning." U. S. Geol. Survey Circ. 690, 1974.

20.7 Seed, H. B., Idris, I. M., Kiefer, F. W., "Characteristics of Rock Motions During Earthquakes." Earthquake Eng. Research Center, University of California, Berkeley, Rpt. No. EERC 68-5, 1968.

20.8 Housner, G. W. "Strong Ground Motion," in "Earthquake Engineering," Wiegel, Robert (ed.) Prentice-Hall, Inc., New York, 1970. pp. 75-92.

20.9 Governor's Earthquake Council, "First Report of the Governor's Earthquake Council," Nov. 21, 1972.

20.10 Governor's Earthquake Council, "Second Report of the Governor's Earthquake Council." California Div. of Mines and Geology Spec. Pub. 46, Sept. 1974.

20.11 Structural Engineers Association of California, "Recommended Lateral Force Requirements and Commentary." Seismology Committee, Third Edition with Commentary, 1973.

REFERENCES (Concluded)

20.12 Department of the Army, the Navy and the Air Force, "Seismic Design for Buildings." Army TM 5-809-10, Navy NAV FAC P-2255, and Air Force AFM 88-3, Chapter 13, April, 1973.

20.13 U. S. Nuclear Regulatory Commission, "Reactor Site Criteria, Rules and Regulations." Title 10, Chap. 1, Code of Federal Regulations-Energy, Part 100, Appendix A, 1975, pp. 3-6.

20.14 Hart, E. W., "Fault Hazard Zones in California." California Div. of Mines and Geology, Spec. Pub. 42, Revised Ed. March 7, 1975.

20.15 Wallace, R. E., "Notes on Stream Channels Offset by San Andreas Fault, Southern Coast Ranges, California." in Dickinson, W. R. and Grantz, Arthur (eds.); "Proc. of Converence on Geologic Problems of San Andreas Fault System." Stanford Univ. Pubs. Geol. Sci. v. 11, 1968, pp. 6-21.

20.16 Allen, C. R., "Geologic Criteria for Evaluating Seismicity." Geol. Soc. of America Bull, v. 86, 1975, pp. 1041-1057.

20.17 Albee, A. L. and Smith, J. L., "Geologic Criteria for Nuclear Power Plant Location." Soc. Mining Engineers Trans., v. 238, no. 4, 1967, pp. 430-434.

20.18 Bonilla, M. G., "Surface Faulting and Related Effects." Chap. 3 in Wiegel, R. L. (ed.), "Earthquake Engineering." Prentice-Hall, Inc., Englewood Cliffs, N.J., pp. 47-74.

20.19 Jennings, C. W." State of California Preliminary Fault and Geologic Map." California Div. of Mines and Geology Prelim. Rpt. 13, 1973.

20.20 U. S. Coast and Geodetic Survey, "The Story of the Seismic Sea-Wave Warning System," 1965.

20.21 McCulloch, D. S., "Slide-Induced Waves, Seiching and Ground Fracturing Caused by the Earthquake of March 27, 1964, at Kenai Lake, Alaska." U. S. Geol. Survey Prof. Paper 543-A, 1966.

20.22 Gary, Margaret, McAfee, Robert, Jr., Wolf, C. L., (eds.) "Glossary of Geology." American Institute of Geology, Washington, D.C., 1972.

BIBLIOGRAPHY

Algermissen, S. T., "Seismic Risk Studies in the United States." U. S. Dept. of Commerce, Environmental Sci. Services Administration, Coast and Geodetic Survey, preprint, 1969.

Crowell, J. C. (ed), "San Andreas Fault in Southern California — A Guide to San Andreas Fault from Mexico to Carrizo Plain." California Div. of Mines and Geology, Spec. Rept. 118, 1975,

Dobrin, Milton B.: "Geophysical Prospecting." McGraw-Hill Book Company, Inc., 1960.

"Earthquake Engineering." Proceedings of the Third European Symposium on Earthquake Engineering, Sofia, Bulgaria, Sept. 11-17, 1970.

Lomnitz, Cinna, "Global Tectonics and Earthquake Risk." Elsevier Scientific Publishing Company, Amsterdam, 1974.

Richter, C. F., "Elementary Seismology." W. H. Freeman and Company, San Francisco, Calif., 1958.

"State of the Art for Assessing Earthquake Hazards in the United States." Design Earthquakes for the Central United States by Otto W. Nuttil. Prepared for the Army Engineer Waterways Experiment Station, January, 1973. [Distributed by the National Technical Information Service (NTIS); U. S. Department of Commerce.]

Sverdrup, Johnson, and Fleming: "The Oceans." Prentice-Hall, Inc., New York, February 1954, pp. 542-544.

Wallace, R. E., "Goals, Strategy, and Tasks of the Earthquake Hazard Reduction Program." U. S. Geol. Survey Circ. 701, 1974.

Wiegel, R. L., (ed.), "Earthquake Engineering." Prentice-Hall, Inc., Englewood Cliffs, N.J., 1970.

SECTION XXI. AEROSPACE VEHICLE EFFLUENT DIFFUSION MODELING FOR TROPOSPHERIC AIR QUALITY AND ENVIRONMENTAL ASSESSMENTS

21.1 Introduction

Modeling of rocket exhaust effluent transport for air quality and environmental assessments is in progress to minimize the possibility of environmental launch constraints for aerospace operations and yet afford maximum public safety (Ref. 21.1). Without an effective operational transport model, significant additional launch constraints would be necessary to insure safe launch operations. An effective transport model requires an integration of atmospheric kinematic and thermodynamic processes within the surface mixing layer with the rocket exhaust chemical kinetics and the turbulent diffusion. To insure public safety (Refs. 21.2 and 21.3), NASA has conducted (Ref. 21.4) and is conducting environmental assessments of the effects of aerospace operations (Refs. 21.5-21.10). The tropospheric environmental effects program has advanced to the research operational stage; however, prior to vehicle operations, there must be a fully operational rocket exhaust transport predictive and monitoring capability within NASA.

Monitoring of large-scale rocket launches provides a data base for transport model refinements as well as empirical support for the transport model predictions. Launch monitoring also provides verification of results obtained in laboratory and chamber studies. Finally, the joint NASA Centers rocket launch prediction monitoring program provides a safeguard for the agency against possible erroneous or adverse public opinion that might result from misinformation concerning the use of solid-rocket boosters.

In this section, the terms "air quality" and "environmental effects" are used with slightly different meanings. Air quality is utilized to refer to only the quantitative transport of effluents and is normally evaluated in terms of a toxicity standard. Environmental effects refers subjectively to the effects that the transport of the effluents has on the bioecology where standards do not generally exist. For this reason, the general thrust of this discussion will be toward air quality; however, the NASA/MSFC Rocket Exhaust Effluent Diffusion (REED) description does afford the potential for the assessment of environmental effects. Because most of the NASA environmental assessments are for aerospace propellants, we normally refer to this subject area as rocket exhaust effluents in spite of the fact that the REED description is utilized to assess the effects of conflagration involving these propellants.

The details of the NASA/MSFC REED description will be considered in terms of the three models — the meteorological model, the cloud rise model, and the Multilayer Diffusion Model — which comprise this description. In addition, the toxicity criteria relevant to solid rocket motors are included.

21.2 The NASA/MSFC Rocket Exhaust Effluent Diffusion (REED) Description

21.2.1 Definitions

Concentration — The amount of the effluent present at a specific time. The average concentration is the average amount present during the event.

Dosage — The measure of the total amount of effluent (time-integrated concentration) due to the launch vehicle at a specific location.

Plume Cloud — The cloud of rocket effluents emitted from the vehicle in flight. This cloud has a cylindrical shape whose height is defined by the vertical thickness of the layer.

Ground Cloud — That cloud of rocket effluents emitted during the initial phase of vehicle launch. This cloud is assumed to have an ellipsoidal shape.

COORDINATE SYSTEM

Centerline — The locus of points traced by the model cloud centroid which extends from the point of cloud stabilization in the mean wind direction. This is defined as the X-direction.

Quasi-Homogeneous Layer — This layer is defined as an atmospheric layer whose parameters can be represented by average values which permit the layer to be modeled as homogeneous.

21.2.2 REED Description Structure

The terminology structure for the REED description is designed both to reduce ambiguities that have existed and to provide a degree of physical association (Fig. 21.1). The description utilizes three basic models, i.e., a meteorological model, a cloud-rise model, and a diffusion model. Each model is subdivided into first- and second-order techniques to distinguish the degree of complexity of the analysis. There is a set of options which are appropriate to both orders of techniques. (This division into orders is not meant to imply the precise mathematical meanings normally associated with these terms. Rather the intent is to provide a subjective indication of complexity.)

In accord with this structure, each model with its associated techniques and options will be considered in each of the following parts.

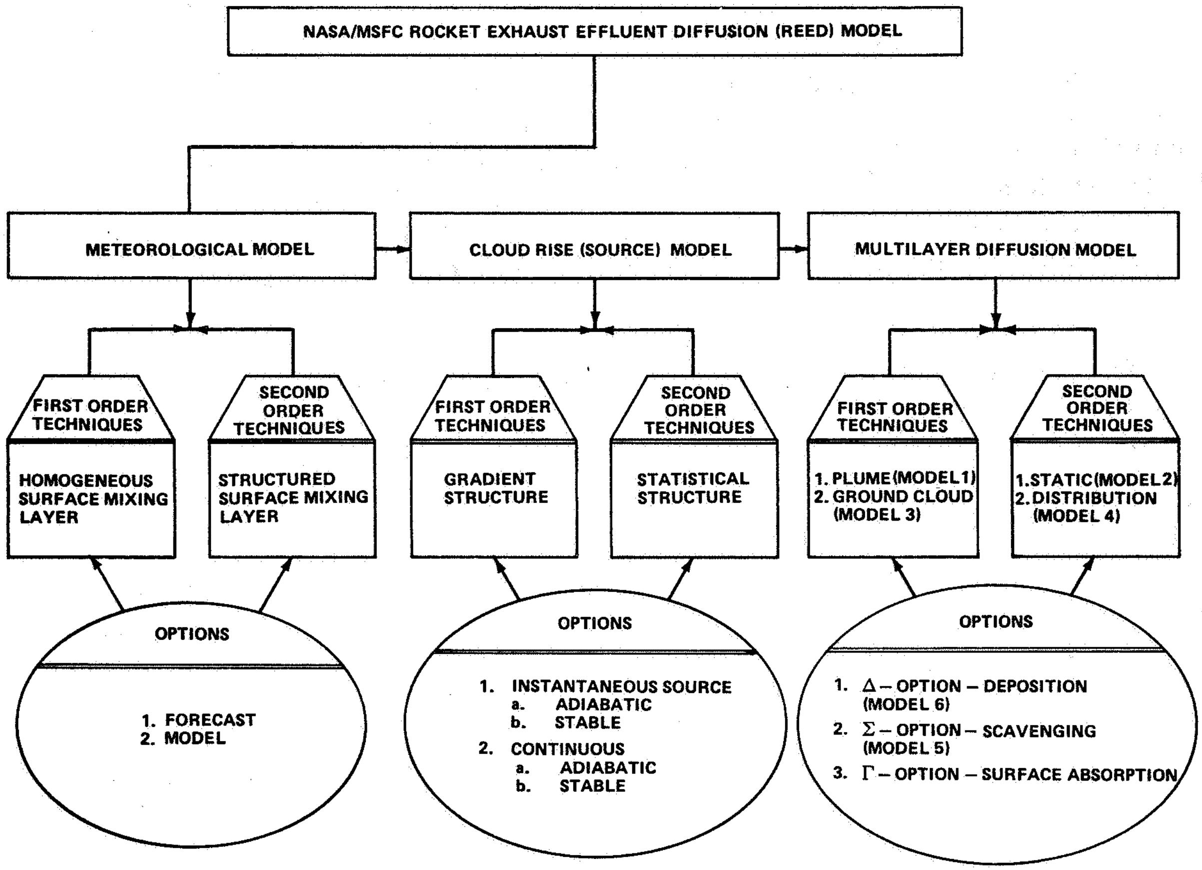

FIGURE 21.1 NASA/MSFC REED MODEL

21.2.3 NASA/MSFC Meteorological Model

The NASA/MSFC meteorological model is designed to support the NASA/MSFC cloud-rise model and the NASA/MSFC Multilayer Diffusion Model with the necessary atmospheric parameters for the effects analysis of the transport of the exhaust effluents from aerospace vehicles. The constraints on the meteorological model are the nonstationary stochastic nature of the atmosphere and the limitation on the information retrieval for the atmospheric kinematic and thermodynamic profiles.

A deterministic solution for the mesoscale structure currently is not only unfeasible, it is impossible by the stochastic nature of a turbulent transport process (Refs. 21.11–21.15). To circumvent this problem, statistical techniques are used to obtain average values for the atmospheric diffusion parameters. These parameters should be structured so that their measurement is feasible.

Within the confines of Kennedy Space Center and Vandenberg Air Force Base, a network of meteorological towers provides a continuous temporal history of the horizontal wind kinematics, the humidity profiles, and the temperature profile for approximately the first 100 m of the atmosphere (see Ref. 21.26). The surface barometric pressure is also available at the weather stations. Other variables, such as the surface density and virtual temperature, are calculated using the standard thermodynamic models (Ref. 21.16).

To obtain data concerning the atmospheric kinematics and thermodynamics at altitudes between 100 m to 3000 m (Fig. 21.2), a radiosonde must be used (aircraft have been used but are not cost-effective). The radiosonde measures only the temperature and humidity as it ascends through the atmosphere (Ref. 21.16). The rawinsonde telemetry system is utilized to determine

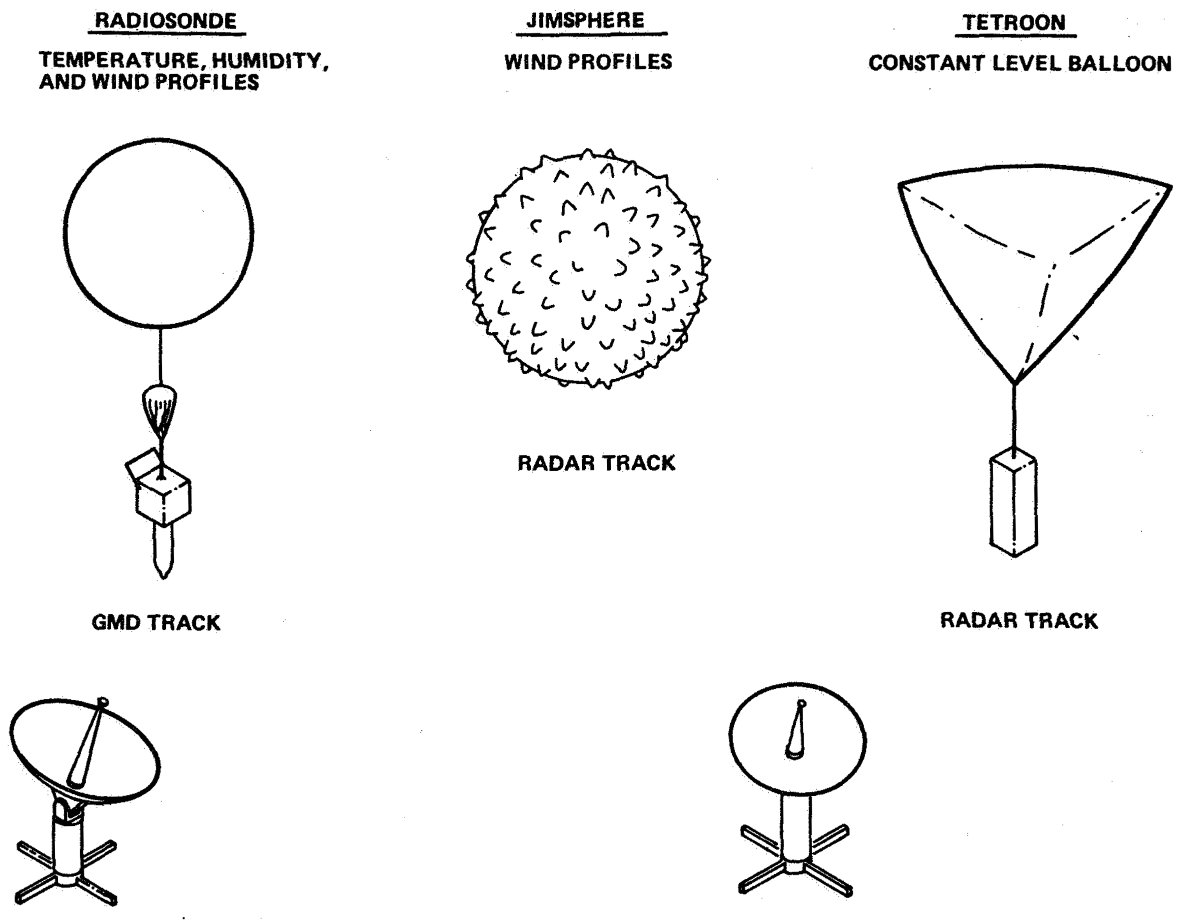

FIGURE 21.2 DEVICES FOR ATMOSPHERIC SOUNDINGS

the wind velocity as a function of altitude. Under normal operations, only two radiosonde soundings are made per day; however, it is feasible during launch operations to obtain a sounding every 2 hours. More accurate wind velocity information can be obtained using a Jimsphere because of its improved aerodynamics. During launch operations, a Jimsphere and a rawinsonde sounding are alternately released each hour. The time duration over which these measurements are made in an atmospheric layer is relatively short (a matter of minutes). The pressures and densities aloft are obtained using standard thermodynamic relations with rawinsonde measurements; that is, neither pressure nor density is measured directly but rather is calculated from the temperature, humidity, altitude, and surface pressure.

The primary point of this rather basic review of the information retrieved from normal meteorological soundings of the atmosphere is to emphasize how limited our data base is for the surface mixing layer in the atmosphere. Because of the stochastic nature of the atmosphere, modeling of local atmospheric conditions aloft based on surface measurements of the kinematics and thermodynamics is very crude and is not, in general, reliable enough for a highly sophisticated transport model.

The assumption that a sounding is representative of the local conditions states that the local meteorological parameters are horizontally homogeneous and ergodic (statistically stationary) and therefore the local terrain effects and land-sea interfaces can be neglected. For synoptic meteorological work where the interest is in large-scale (thousands of kilometers) and mesoscale (tens to a few hundred kilometers) frontal systems, these soundings, along with the associated first-order assumptions, are serviceable. However, in the transport modeling of the diffusion process, the scales of interest are small — similar to those associated with thunderstorms and tornadoes. Thus, the precision in the predictions for the transit path and concentration field associated with the rocket exhaust effluents is subject to constraints similar to those in the prediction for thunderstorms and tornadoes. The measurements aloft are being made over intervals that are less than the coherency time for the atmospheric stochastic process. This means that the thermodynamic and kinematic parameters do not necessarily represent an ensemble average. The ability of the sounding to represent an ensemble average is directly proportional to the length scale of the process being modeled. The local variation of these atmospheric parameters in small-scale processes is large compared with the local variation in mesoscale processes (or large-scale processes). In mesoscale or synoptic processes the statistical error of these parameters tends to be relatively small because of spatial averaging. Hence, normally the meteorological model is designed to interface with medium or large-scale models (that is, a bulk model), which tend to suppress local variations in the thermodynamic and kinematic parameters.

The temporal and spatial variability of the atmosphere caused in part by the effects of terrain and the land-sea interface complicates any attempt at diffusion modeling. Information on the real temporally and spacially varying atmosphere can be incorporated into the NASA/MSFC REED description if supporting data are available. The tetroon (constant density balloon) has the potential to provide some of this information. It may well be that the tetroon could be the most important single tool for obtaining a spatial description of the horizontal kinematics. However, a model is needed to determine the most representative altitude at which to fly tetroons to obtain a representative transport description for the surface mixing layer.

There are still other measurement techniques for determining atmospheric parameters and thermodynamics for the surface mixing layer, but consideration will be omitted here because they are either research techniques that have not been adequately validated or they are not cost-effective. In general then, detailed information is not available to establish small-scale operational models for the atmosphere at the present time.

21.2.4 NASA/MSFC Rocket Exhaust Cloud Rise Model

During the initial 5 to 10 minutes of exhaust effluent transport, thermodynamic processes which result in cloud rise are important. Methods of handling this initial transport phase are discussed here.

The atmospheric thermodynamic parameters (pressure, temperature, density) along with the exhaust cloud characteristics govern the magnitude of the buoyant force on the exhaust cloud and hence determine the cloud-rise height. These atmospheric parameters are obtained from a standard balloon sounding or from a forecast.

The cloud-rise height is an important factor in determining surface concentrations. The cloud-rise equations that are discussed on the following pages are based on procedures similar to those given by Briggs (Ref. 21.17). There are two sets of cloud rise equations, one each for an instantaneous and for a continuous source. The difference between instantaneous and continuous sources is related to the manner in which the rising exhaust cloud entrains air. If entrainment is independent of direction, spherical or instantaneous entrainment results. Cylindrical entrainment is synonomous with continuous entrainment. For vehicles with long residence times (e.g., Saturn), entrainment can be considered continuous. For fast-rise, solid-propellant vehicles such as the Titan III, instantaneous entrainment can be assumed. For vehicles such as the Delta-Thor with both solid-propellant and liquid-propellant boosters, the mean of the continuous cloud-rise heights is used.

21.2.4.1 Instantaneous Source (Ref. 21.5).

The exhaust cloud-rise algorithms for the instantaneous source are designed to be utilized with solid-rocket motor launches such as the Titan III or Scout-Algol III. Spherical entrainment is assumed. The solutions take two different forms — the adiabatic and the stable.

The cloud rise z as a function of time (t) downwind from an instantaneous source in an adiabatic atmosphere is given by

$$z_I = \left[\frac{2F_I t_{sI}^2}{\gamma_I^3 \bar{u}^2} + \left(\frac{r_R}{\gamma_I}\right)\right]^{1/4} - \frac{r_R}{\gamma_I} \simeq \left[\frac{2F_I t_{sI}^2}{\gamma_I^3 \bar{u}^2}\right]^{1/4} \tag{21.1}$$

whereas the cloud rise z_I as a function of time downwind from an instantaneous source in a stable atmosphere is given by

$$\begin{aligned} z_I &= \left[\frac{4F_I}{\gamma_I^3 s}\left[1 - \cos\left(s^{1/2} t\right)\right] + \left(\frac{r_R}{\gamma_I}\right)^4\right]^{1/4} - \frac{r_R}{\gamma_I} \\ &\simeq \left[\frac{4F_I}{\gamma_I^3 s}\left[1 - \cos\left(s^{1/2} t\right)\right]\right]^{1/4} , \end{aligned} \tag{21.2}$$

where the subscript I refers to instantaneous quantities and

t_{SI} = time in seconds for the cloud to achieve stabilization in an adiabatic atmosphere

t = time elapsed from launch ,

$F_I = [(3gQ_I)/(4\pi\rho c_p T)]$,

Q_I = effective heat released ,

ρ = density of the ambient air ,

$\bar{u}$ = mean wind velocity ,

g = acceleration of gravity ,

C_p = specific heat of air at constant pressure ,

T = atmospheric temperature ,

γ_I = instantaneous entrainment coefficient (0.64) ,

r_R = initial cloud radius at the surface ,

$$s = \frac{g}{T_s} \frac{\Delta \Phi}{\Delta z} ,$$

T_s = surface atmospheric temperature

$$\Phi = T\left(\frac{1000}{P}\right)^{0.288} = \text{potential temperature} ,$$

A maximum cloud-rise height does not exist for an adiabatic atmosphere, since buoyant equilibrium cannot be obtained. In the case of a stable atmosphere, the maximum instantaneous exhaust cloud-rise height (z_{mI}) is

$$\begin{aligned} z_{mI} &= \left[\frac{8F_I}{\gamma_I^{3} s} + \left(\frac{r_R}{\gamma_I}\right)^4\right]^{1/4} - \frac{r_R}{\gamma_I} \\ &\simeq \left(\frac{8F_I}{\gamma_I^{3} s}\right)^{1/4} . \end{aligned} \tag{21.3}$$

In the above equations $\Delta\Phi/\Delta z$ enters through the stability parameter, s .

$$\frac{\Delta \Phi}{\Delta z} = \frac{\Phi_H - \Phi_s}{z_H - z_s} , \tag{21.4}$$

where

Φ_H = potential temperature at the cloud stabilization height

Φ_s = surface potential temperature

Z_H = cloud stabilization altitude

Z_s = surface reference altitude

The disadvantage of the above method is that a linear potential temperature profile is assumed between the surface and cloud stabilization. If linear regression is utilized to obtain an approximation for $\Phi(z)$, the data points between the surface and cloud stabilization have some influence on the value of $\Delta\Phi/\Delta z$. The equation for this $\Delta\Phi/\Delta z$ is

$$\frac{\Delta\Phi}{\Delta z} = \frac{N \sum_{i=1}^{N} z_i \Phi_i - \sum_{i=1}^{N} z_i \sum_{i=1}^{N} \Phi_i}{N \sum_{i=1}^{N} z_i^2 - \left(\sum_{i=1}^{N} z_i\right)^2} \quad . \tag{21.5}$$

Note that the right-hand side of equation (21.3) is a function of altitude z. To determine the cloud stabilization height, an iterative technique must be used to obtain a value z to satisfy that equation. This value of z is the cloud stabilization height. In equation $\Delta\Phi/\Delta z$ would be calculated using either equations (21.4) or (21.5).

21.2.4.2 Continuous Source (Refs. 21.5 and 21.18)

The cloud rise z_c as a function of time [equation (21.5)] downwind from a continuous source in an adiabatic atmosphere is given by

$$z_c = \left[\frac{3F_c t^2}{2\gamma_c^3 \bar{u}} + \left(\frac{r_R}{\gamma_c}\right)^3\right]^{1/3} - \frac{r_R}{\gamma_c} \simeq \left(\frac{3F_c t^2}{2\gamma_c^2 \bar{u}}\right)^{1/3} \quad . \tag{21.6}$$

The exhaust cloud altitude, z_c as a function of time downwind from a continuous source in a stable atmosphere is given by

$$z = \left[\frac{3F_c}{\bar{u}\gamma_c^2 s} [1 - \cos(s^{1/2} t)] + \left(\frac{r_R}{\gamma_c}\right)^3 \right]^{1/3} - \frac{r_R}{\gamma_c} \simeq \left[\frac{3F_c}{\bar{u}\gamma_c^2 s} [1 - \cos(s^{1/2} t)] \right]^{1/3} . \tag{21.7}$$

The subscript c refers to continuous values and

$F_c = (gQ_c)/(\pi\rho C_p T_s)$,

Q_c = rate of heat released ,

and

γ_c = continuous extrainment coefficient = 0.5 .

Similar to the instantaneous cloud-rise algorithms, the adiabatic condition does not afford a maximum height. The maximum height of cloud rise in the stable atmosphere is

$$z_{mc} = \left[\frac{6F_c}{\bar{u}\gamma_c^2 s} + \left(\frac{r_R}{\gamma_c}\right)^3 \right]^{1/3} - \frac{r_R}{\gamma_c} \tag{21.8}$$

As before, an iterative scheme must be used to obtain the cloud stabilization height.

21.2.4.3 Summary Remarks

It is recognized that the cloud-rise relations could be improved; however, they are presently affording reasonable results. Two primary parameters are subject to question — the entrainment coefficient and the heat released.

The entrainment coefficient (γ) is defined to be the ratio of the cloud radius to the cloud centroid height. This empirical coefficient is very difficult to evaluate because of the complex exhaust-cloud geometry and because it is a function of altitude. We believe that the current entrainment coefficients are about as good as can be reasonably obtained using cloud photographs.

The amount of heat released is currently undergoing reevaluation for solid-rocket motors. Earlier values were calculated based on single-phase flow and afterburning. Recent calculations (Ref. 21.19) show that this must be treated as a two-phase flow — gas and particles. In addition to the afterburning heat losses due to radiation (Ref. 21.20) and to the evaporation of pad cooling water (Ref. 21.5) must be considered. These refinements should improve the reliability of the estimates of the heat released and thereby allow a more precise estimate of the stabilization height. (This height can be underestimated to prevent underestimating the maximum concentrations.)

21.2.5 NASA/MSFC Multilayer Diffusion Model (Refs. 21.5 and 21.27)

The discussion of modeling techniques can now be focused on the transport of aerospace vehicle exhaust effluents in terms of the available information concerning boundary conditions and the chemical kinetics. The primary concern here will be to define the general diffusion model that will be used in the kinematic phase of the transport description. The general logic will be given for model selection, along with the behavioral features of the model and the reasons for the selection of a two-mode description. The reasons for not applying the diffusion model to the thermodynamic mode should become more apparent. If we assume that the basic chemical constituents of the source are known at cloud stabilization — which is basically what we do know — we can move directly to the central issue, the diffusion process.

Diffusive transport in the troposphere is characterized by turbulent diffusion. Because of the complexity of description of turbulent diffusion, simplified models are used. The model described as follows will be based on linear solutions of the diffusion equation which, in general form, is given by

$$\frac{\partial \chi(\vec{r},t)}{\partial t} + \vec{v} \cdot \nabla \chi(\vec{r},t) = \nabla \cdot [\widetilde{K}(\vec{r},t,p,T) \cdot \nabla \chi(\vec{r},t)] \quad , \tag{21.9}$$

where $\chi(\vec{r},t)$ is the scalar concentration of the diffusing gas, $\vec{v}$ is the wind velocity, and $\widetilde{K}(r,t,p,T)$ is the diffusion tensor which is diagonalized if the principal axes are selected. The determination of K in a nonisotropic medium such as the atmosphere is extremely complex. In practice K values are usually determined by reference to observed diffusion data; hence, this theory (K-theory) is a semiempirical diffusion theory (Ref. 21.12).

The starting point for the NASA/MSFC Multilayer Diffusion Model is analytical solutions of a linearized form of equation (21.9). These solutions can be obtained from equation (21.9) if a number of restrictions are imposed on the equation, rendering it linear. The forms of the analytical solutions can be structured so that parameters in the solutions can be obtained empirically from observations of turbulent diffusion in the atmosphere. The approach employed in the NASA/MSFC REED description is to restrict our model to a homogeneous kinematic description by assuming that the average kinematic parameters and the eddy-diffusion coefficient (K) are time and spatial average values which are thermodynamically independent. This implies that the initial conditions for the diffusion model occur when the rocket-exhaust cloud achieves thermodynamic equilibrium with the atmosphere at cloud stabilization. Consequently, it becomes apparent that the effluent transport problem must be decomposed into a two-mode description: the thermodynamic mode during cloud rise and the kinematic mode of diffusion.

In an infinite, homogeneous, isotropic medium, the solution of equation (21.9) for an instantaneous point source is

$$\overline{\chi}(r,t) = \frac{\psi}{(4\Pi Kt)^{3/2}} \left[\exp\left(- \frac{r^2}{4Kt} \right) \right] , \tag{21.10}$$

where r refers to radial distance, t is time, ψ is source strength and K, the diffusion tensor, has collapsed to the scalar K. The assumption of Gaussianly distributed material is based on time-averaged values. Even though an instantaneous smoke plume in general is not Gaussian in nature, time exposures of the plume indicate that the average concentration over a 10-minute period is normally distributed. Aerospace vehicle exhaust effluents from one launch will not in general exhibit Gaussian characteristics, but if several launches under similar meteorological conditions are made, the ensemble average concentration would closely approximate a Gaussian distribution.

The eddy-diffusivity coefficient (K) is assumed to be the variance of the distribution (σ^2). That is, the ith dimension of the exhaust cloud is then assumed to be 4.3 σ_i. There are two procedures for determining σ_i: the Pasquill diffusion curves (Ref. 21.12) and the Cramer diffusion coefficients (Ref. 21.5). Because the numerical techniques are better suited to operational use, we have selected the Cramer diffusion coefficients. Another feature we find of value in the Cramer diffusion coefficients is the fact that they more fully reflect the totality of the available local atmospheric data. The Cramer coefficients also have the flexibility to incorporate new diffusion information as the information is verified.

Chemistry is incorporated into the model in two ways. First, the assumption is made that most chemical reactive processes occur during the thermodynamic phase so that source terms reflect the chemistry. Additionally, a number of damping factors have been developed to reflect surface absorption, gravitational settling, and precipitation scavenging.

In summary, then, the model used for the kinematic phase of the transport process is based on the gradient transport theory. The semi-empirical solution is based on the Gaussian distribution assumption and utilizes the Cramer diffusion coefficients to model the atmospheric turbulence parameters. The model accounts for some chemical processes through source terms and damping coefficients. The results of this diffusion description are ensemble averages and may not always reflect the instantaneous (less than the atmospheric coherency time) local values commonly measured in the near field (Ref. 21.21).

The NASA/MSFC multilayer diffusion model is designed to provide a description of the kinematic turbulent transport of effluents released by aerospace vehicles for use in air quality and environmental assessments. The various techniques available in this model, along with the associated assumptions, will be reviewed here. Since the detailed algorithms are beyond the interest of many readers, a general summary of the model and how it functions is presented as a preface to the algorithms.

The general diffusion equations can be linearized by assuming that the meteorological profile represents the homogeneous average atmospheric conditions over the layer of interest and solved by the separation of variables for the spatial distribution of the concentration and dosage resulting from the launch of an aerospace vehicle. A general formulation for the diffusion equation was provided previously.

The generalized concentration model for a nearly instantaneous source is expressed as the product of seven modular terms,

$$\begin{aligned} \text{Concentration} = & \{\text{Peak Concentration Term}\} \times \{\text{Alongwind Term}\} \\ & \times \{\text{Lateral Term}\} \times \{\text{Vertical Term}\} \\ & \times \{\text{Depletion Term}\} \times \{\text{Scavenging Term}\} \\ & \times \{\text{Surface Absorption Term}\} \quad ; \end{aligned}$$

whereas the generalized dosage model for a nearly instantaneous source is defined by the product of six modular terms,

$$\text{Dosage} = \{\text{Peak Dosage Terms}\} \times \{\text{Lateral Term}\}$$
$$\times \{\text{Vertical Term}\} \times \{\text{Depletion Term}\}$$
$$\times \{\text{Scavenging Term}\} \times \{\text{Surface Absorption Term}\} \quad .$$

Thus, the mathematical description for the concentration and dosage models permits flexibility in its application to various sources and in the ability to change atmospheric parameters while always maintaining a rigorous mass balance.

Two obvious differences between the dosage and concentration models exist. First, the peak concentration term refers to the concentration at the point $x, y = 0$, $z = H$ (where x is the wind direction and H is any height) and is defined by the expression

$$\text{Peak Concentration} = \frac{\psi}{(2\pi)^{3/2}\,\sigma_x\,\sigma_y\,\sigma_z} \quad , \tag{21.11}$$

where ψ is the mass source strength and σ_i is the Cramer coefficient for the standard deviation of the concentration distribution in the ith direction. The peak dosage term is given by

$$\text{Peak Dosage} = \frac{\psi}{2\pi\,\bar{u}\,\sigma_y\,\sigma_z} \quad , \tag{21.12}$$

where $\bar{u}$ is the mean wind speed over the layer. The second difference between these models is that the concentration contains a modular alongwind term (x-direction) to account for downstream temporal effects not considered in the dosage model. The alongwind term affords an exponential decay in concentration as a function of cloud transit time, concentration distribution, and the mean wind speed.

The lateral term (y-direction) is another exponential decay term and is a function of the Gaussian spreading rate and the distance laterally from the mean wind azimuth. The vertical term (z-direction) is a rather complex decay function since it contains a multiple reflection term for the point source which stops the vertical cloud development at the top of the mixing layer and eventually changes the form of the vertical concentration distribution from Gaussian to rectangular. The remaining three terms represent the options associated with the techniques. The deposition term accounts for gravitational settling. The scavenging term accounts for the precipitation scavenging of effluents by rain falling through the exhaust cloud. The surface absorption term accounts for the fraction of material absorbed at a surface.

This, then, is the form of the diffusion model. Two primary problems now exist: how to distribute the effluents and how to maintain quasi-homogeneous layers. The first-order diffusion techniques can be viewed as addressing just the source geometry, while the second-order diffusion techniques address source geometry and establish quasi-homogeneous layers within the surface mixing layer (Fig. 21.3).

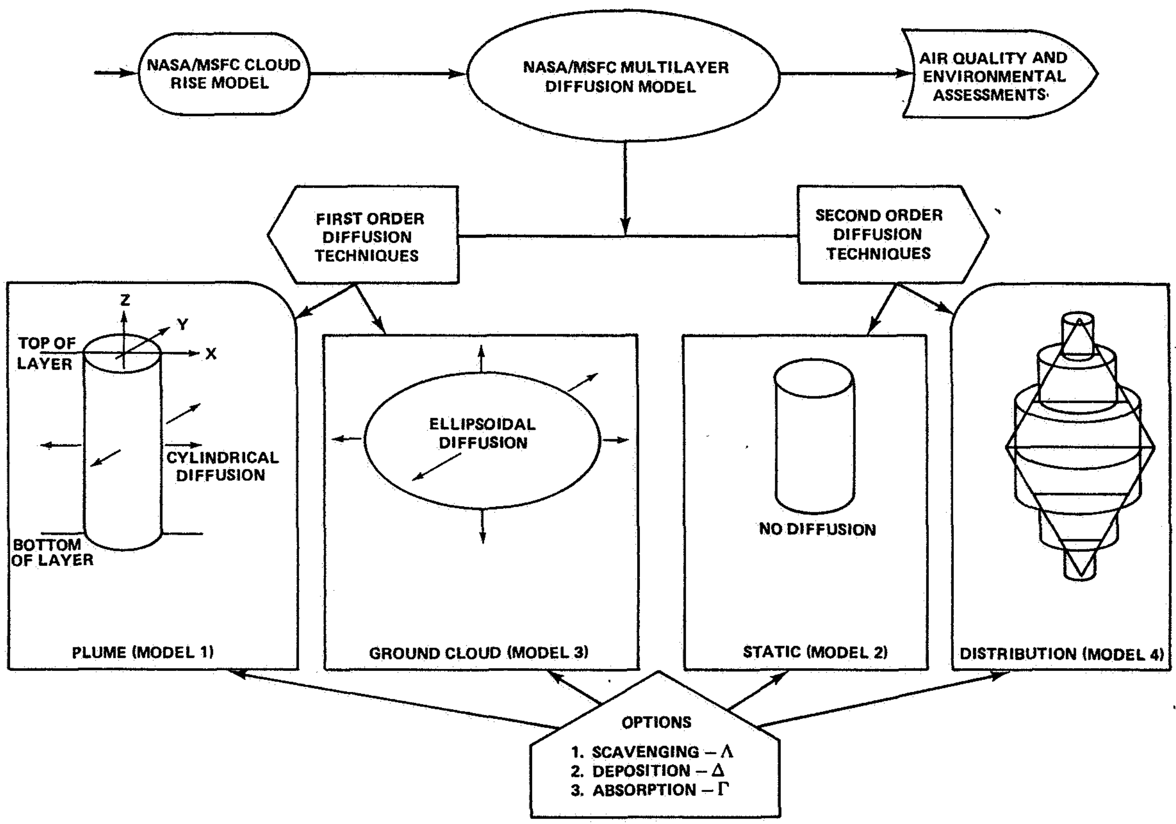

FIGURE 21.3 NASA/MSFC MULTILAYER DIFFUSION MODEL

21.2.5 First-Order Diffusion Techniques

The plume source and the ground cloud source will be considered here. Within our computer program, the plume source is known as model 1 and the ground cloud source as model 3. Names have been introduced to permit visualization.

21.2.5.1.1 First-Order Plume Technique

The first-order plume technique is a cylindrical distribution of material constrained within a layer. The x- and y-distributions are assumed to be Gaussian, while the vertical distribution is maintained uniform. This technique is employed when modeling the exhaust plume aloft.

The dosage equation for the plume technique in the Kth layer is

$$D_K(x_K, y_K, z_K) = \frac{\psi_K}{\sqrt{2\pi}\, \bar{u}_K\, \sigma_{yK}\, (z_{TK} - z_{BK})} \exp\left[\left(\frac{-y_K^{\,2}}{2\sigma_{yK}^{\,2}}\right)\right] \tag{21.13}$$

where

ψ_K = the source strength in mass units ,

z_{TK} = height of the top of the kth layer ,

z_{BK} = height of the base of the kth layer ,

σ_{yK} = crosswind standard deviation of the dosage distribution

$\bar{u}_K$ = mean wind speed in the kth layer ,

x_K = downwind distance from source ,

y_K = cross wind distance from cloud axis ,

z_K = vertical dimension in kth layer .

The Cramer coefficients used here are rather complex in formulation and will not be given here (see Ref. 21.27). The maximum concentration for the plume technique is

$$\chi_K\,(x_K, y_K, z_K) = \frac{D_K\,\bar{u}_K}{\sqrt{2\pi}\,\sigma_{xK}} \quad , \tag{21.14}$$

where D_K is given in equation (21.13).

21.2.5.1.2 First-Order Ground Cloud Technique

The first-order ground cloud technique is an ellipsoidal distribution of material that can be either totally or partially distributed within the surface mixing layer. (This model could be utilized above the surface mixing layer; however, in general it is not. Therefore, in the interest of clarity, we will neglect the additional notation for this application.) Here we assume that the surface mixing layer is quasi-homogeneous. The material is assumed to be Gaussianly distributed in all three directions.

The dosage for the ground cloud technique is given by

$$\begin{aligned} D(x,y,z_B < z < z_T) = {} & \frac{\psi}{2\pi\,\sigma_y\,\sigma_z\,\bar{u}} \left\{ \exp\left[-\frac{1}{2}\left(\frac{y}{\sigma_y}\right)^2 \right] \right\} \\ & \times \left\{ \sum_{i=0}^{\infty} \left[\Gamma^i \left[\exp\left(-\frac{1}{2}\left(\frac{2i(z_T - z_B) + (H - z)}{\sigma_z} \right)^2 \right) \right] \right. \right. \\ & \left. + \Gamma^{i+1} \left[\exp\left(-\frac{1}{2}\left(\frac{2i(z_T - z_B) + (H - 2z_B + z)}{\sigma_z} \right)^2 \right) \right] \right] \\ & + \sum_{i=1}^{\infty} \left[\Gamma^i \left[\exp\left(-\frac{1}{2}\left(\frac{2i(z_T - z_B) - (H - z)}{\sigma_z} \right)^2 \right) \right] \right. \end{aligned}$$

$$+ \Gamma^{i-1}\left[\exp\left(-\frac{1}{2}\left(\frac{2i(z_T - z_B) - (H - 2z_B + z)}{\sigma_z}\right)^2\right)\right]\Bigg\}.$$

where

ψ = total mass of material in surface mixing layer

H = effective height of the centroid of the stabilized cloud

$\sigma_x, \sigma_y, \sigma_z$ = standard deviations of dosage distribution in the alongwind, crosswind and vertical directions respectively.

Γ = fraction of the material reflected at the surface. 0° is defined as unity.

$\bar{u}$ = mean wind speed in the surface mixing layer.

Normally, we assume that the ground surface (z_B) and the top of the surface mixing layer (z_T) totally reflect the effluents. However, the surface absorption option (Γ-option) has been introduced to account for surface effects: Γ equal to one is for complete reflection and Γ equal to zero is for no reflection. For convenience, the definition that $0^0 = 1$ has been used in developing the vertical term. The maximum concentration for the ground cloud technique is

$$\chi(x,y,z) = \frac{D\,\bar{u}}{\sqrt{2\pi}\,\sigma_x} \quad . \tag{21.16}$$

Again, it should be noted that the concentration follows from the dosage and therefore can be considered as the ensemble average for the maximum concentration.

21.2.5.2 Second-Order Diffusion Techniques

The static source and the distributed source techniques will be described here. The static source in the computer program is model 2, and the distributed source is model 4.

21.2.5.2.1 Second-Order Static Technique

The second-order static technique is the first-order plume technique without turbulent mixing. The primary (admittedly weak) reason for considering this a second-order technique is that an extremely accurate knowledge of the wind structure aloft is required to justify using this model.

The dosage equation for the static technique in the Kth layer is

$$D_K(x_K, y_K, z_K) = \frac{\psi_K}{\sqrt{2\pi}\,\bar{u}_K\,\sigma_{yo}\,(z_{TK} - z_{BK})}\left[\exp\left(\frac{-y_K^{\;2}}{2\sigma_{yo}^2}\right)\right] \cdot \quad (21.17)$$

The maximum concentration for the static technique is

$$\chi_K(x_K, y_K, z_K) = \frac{D_K\,\bar{u}_K}{\sqrt{2\pi}\,\sigma_{xo}} \quad , \qquad (21.18)$$

where σ_{xo} and σ_{yo} are the source dimensions. Thus, the static technique says that the exhaust cloud is transported downstream without spreading from its initial dimensions at cloud stabilization. This condition has been actually observed in layers at altitudes between 3000 and 8000 m; therefore, such a technique was required.

21.2.5.2.2 Second-Order Distribution Technique

The second-order distribution technique permits the layering of the source into quasi-homogeneous layers and permits a more flexible distribution of the exhaust effluents which better reflects the actual exhaust-cloud distribution. In each layer before layer breakdown at t = 1 sec, the source is given a plume source distribution – cylindrical distribution with two-dimensional diffusion. After layer breakdown, the plume sources in each new layer are permitted three-dimensional diffusion. The distribution technique does require a better knowledge of both the atmospheric structure and the effluent distribution within the layer than do the first-order techniques. This distribution technique is really the best technique to describe complex meteorology such as that encountered in the Helios-A launch on December 10, 1974. This technique is currently being refined to increase its potential flexibility, based on experience during the Helios launch.

The following expression for the dosage (for the second-order distribution technique) gives the dosage contribution from the exhaust cloud in the Kth layer before layer breakdown to the receiving position in layer L after breakdown:

$$D_{LK} = \frac{\psi_K}{2\sqrt{2\pi}\,\bar{u}_L\,\sigma_{yLK}\,x\,(z_{TK} - z_{BK})} \left\{ \exp\left[-\frac{1}{2}\left(\frac{y_L}{\sigma_{yLK}}\right)^2 \right] \right\}$$

$$\times \left\{ \sum_{i=0}^{\infty} \left[\Gamma^i \left[\operatorname{erf}\left(\frac{2i(z_{TL} - z_{BL}) + z_{TK} - z_L}{\sqrt{2}\,\sigma_{zLK}} \right) \right.\right.\right.$$

$$\left. + \operatorname{erf}\left(\frac{-2i(z_{TL} - z_{BL}) - z_{BK} + z_L}{\sqrt{2}\,\sigma_{zLK}} \right) \right]$$

$$+ \Gamma^{i+1} \left[\operatorname{erf}\left(\frac{2i(z_{TL} - z_{BL}) - 2z_{BL} + z_{TK} + z_L}{\sqrt{2}\,\sigma_{zLK}} \right) \right.$$

$$\left.\left. + \operatorname{erf}\left(\frac{-2i(z_{TL} - z_{BL}) + 2z_{BL} - z_{BK} - z_L}{\sqrt{2}\,\sigma_{zLK}} \right) \right] \right]$$

$$+ \sum_{i=1}^{\infty} \left[\Gamma^i \left[\operatorname{erf}\left(\frac{2i(z_{TL} - z_{BL}) - z_{BK} + z_L}{\sqrt{2}\,\sigma_{zLK}} \right) \right.\right.$$

$$\left. + \operatorname{erf}\left(\frac{-2i(z_{TL} - z_{BL}) + z_{TK} - z_L}{\sqrt{2}\,\sigma_{zLK}} \right) \right]$$

$$+ \Gamma^{i-1} \left[\operatorname{erf}\left(\frac{2i(z_{TL} - z_{BL}) + 2z_{BL} - z_{BK} - z_L}{\sqrt{2}\,\sigma_{zLK}} \right) \right.$$

$$+ \operatorname{erf}\left(\frac{-2i(z_{TL} - z_{BL}) - 2z_{BL} + z_{TK} + z_L}{\sqrt{2}\,\sigma_{zLK}}\right)\Bigg]\Bigg]\Bigg\} \quad , \quad (21.19)$$

where

Γ = surface reflection coefficient

σ_{yLK} = the standard deviation of the crosswind dosage distribution in the Lth layer

σ_{zLK} = the standard deviation of the vertical dosage distribution in the Lth layer.

The total dosage for the Lth layer is

$$D_L = \sum_{K=1}^{N} D_{LK} \quad , \qquad (21.20)$$

where N is the number of old layers in the new Lth layer.

The form of the dosage algorithm in the distribution technique is similar to the form of the dosage algorithm in the ground cloud technique except that the error function is used instead of the exponential function in the vertical diffusion term.

The maximum concentration algorithm for the distribution technique is

$$\chi_L(x_L, y_L, z_L) = \sum_{K=1}^{N} \frac{D_{LK}\,\bar{u}_L}{\sqrt{2\pi}\,\sigma_{xLK}} \quad , \qquad (21.21)$$

where σ_{xLK} is along the standard deviation of the dosage distribution.

It should be recognized that the source strength, ψ_K, for each layer is normally obtained by assuming that the effluents are distributed in a diamond distribution, but the effluents could be assumed to be distributed in any manner — even the observed manner. This is one primary advantage of this technique.

21.2.5.3 Diffusion Options

Three diffusion options exist — the deposition (Δ) option, the scavenging (Σ) option, and the absorption (Γ) option — which can be used with any of the techniques. These options represent the state of development in our ability to account for some of the exhaust-cloud chemistry.

21.2.5.3.1 Σ-Option

The Σ-option is the option to account for precipitation scavenging (model 5). The ground level-deposition (WD_K) resulting from precipitation scavenging is given basically by

$$WD_K(x_K, y_K, z = 0) = \frac{\Lambda \psi_K}{\sqrt{2\pi}\, \sigma_{yK}\, \bar{u}_K} \left\{ \exp\left[-\frac{1}{2} \left(\frac{y_K}{\sigma_{yK}} \right)^2 \right] \right\}$$

$$\times \left\{ \exp\left[-\Lambda \left(\frac{x_K}{\bar{u}_K} - t_1 \right) \right] \right\} , \qquad (21.22)$$

where t_1 is the time the rain begins. The scavenging coefficient Λ for gaseous HCl obtained in laboratory tests is (Ref. 21.22):

$$\Lambda \text{ (HCl gas)} = 1.11 \times 10^{-4}\, R^{0.625} \quad , \qquad (21.23)$$

where R (mm/hour) is the rainfall intensity. Results obtained in preliminary chamber tests are approximately the same magnitude (Ref. 21.23); that is,

$$\Lambda \text{ (HCl gas)} = 8.3 \times 10^{-5}\, R^{0.567} \quad . \qquad (21.24)$$

Since the scavenging coefficients obtained in the chamber tests were measured with all exhaust constituents present, they may be slightly better; however, data are needed from an actual rocket launch to obtain the best answer.

The dosage or concentration at a point in space, assuming precipitation scavenging occurs, is obtained by multiplying the appropriate dosage or concentration equation by the exponential term in equation (21.22) containing the coefficient Λ.

21.2.5.3.2 Δ -Option

The Δ-option (model 6) is the deposition option for gravitational settling of particles such as Al_2O_3. The deposition at the surface (DEP) assuming partial reflection is given by

$$
\begin{aligned}
\mathrm{DEP} = \frac{\psi}{2\pi\,\sigma_y} \Bigg\{ & \sum_{i=1}^{\infty} \left[\Gamma^{i} + \Gamma^{i+1} \right] \\
& \times \left[\left[\frac{\beta(2iH_m + H) + \left(1 - \left(\frac{\beta x}{x + x_z - x_{rz}(1-\beta)}\right)\right) V_s [x + x_z - x_{rz}(1-\beta)]/\bar{u}}{\sigma_z [x + x_z - x_{rz}(1-\beta)]} \right] \right. \\
& \times \left. \left[\exp\left(-\frac{1}{2} \left(\frac{2iH_m + H - V_s x/\bar{u}}{\sigma_z} \right)^2 \right) \right] \right] + \sum_{i=1}^{\infty} \left[\Gamma^{i} + \Gamma^{i-1} \right] \\
& \times \left[\left[\frac{\beta(2iH_m - H) - \left(1 - \left(\frac{\beta x}{x + x_z - x_{rz}(1-\beta)}\right)\right) V_s [x + x_z - x_{rz}(1-\beta)]/\bar{u}}{\sigma_z (x + x_z - x_{rz}(1-\beta)} \right] \right. \\
& \times \left. \left[\exp\left(-\frac{1}{2} \left(\frac{2iH_m - H + V_s x/\bar{u}}{\sigma_z} \right)^2 \right) \right] \right] \Bigg\} . \qquad (21.25)
\end{aligned}
$$

where

V_s = settling velocity

β = vertical diffusion coefficient of order unity.

TABLE 21.1 AIR QUALITY TOXICITY STANDARDS

Toxic Solid Rocket Exhaust Product	Time Interval (min)	Concentration: Public**	Concentration: Emergency	Concentration: Occupational
Alumina (Al_2O_3)* (Aluminum Oxide)	10	5.0 mg/m^3	—	50 mg/m^3
	30	2.5 mg/m^3	—	25 mg/m^3
	60	1.5 mg/m^3	—	15 mg/m^3
	480	1.0 mg/m^3	—	10 mg/m^3
	Ceiling	8 ppm	14 ppm	30 ppm
Hydrogen Chloride (HCl) (Ref. 21.29)	10	4 ppm***	7 ppm	30 ppm Threshold
	30	2 ppm	3 ppm	20 ppm
	60	2 ppm	3 ppm	10 ppm
Carbon Monoxide* (CO)	10	90 ppm	275 ppm	1000 (1500****) ppm
	30	35 ppm	100 ppm	500 (800****) ppm
	60	25 ppm	66 ppm	200 (400****) ppm
Dosage:		200 ppm/ time interval		
Carbon Dioxide (CO_2)	480	—	—	Average - 5000 ppm
		—	—	Peak - 6250 ppm
Nitrogen Dioxide (NO_2) (Ref. 21.30)	10	1 ppm	5 ppm	
	30	1 ppm	3 ppm	
	60	1 ppm	2 ppm	

*These values were reviewed by letter and telephone communication by Ralph C. Wands, director, Advisory Center on Toxicology, National Academy of Sciences, Washington, D.C., April 1975.

**EPA suggests a safety factor of 10 be applied to occupational exposure limits.

***Parts of vapor or gas per million parts of contaminated air by volume at 25°C and 760 mm Hg.

****At these concentrations, headaches will occur, along with a loss in work efficiency.

This interfaces with the diffusion technique in a similar manner to the Σ-option.

In practice, the Δ-option is usually not used because of a general lack of supporting empirical data. However, with the particle data being obtained at Titan launches, we hope soon to be in a position to operationally employ this model.

21.2.5.3.3 Γ-Option

The Γ-option for surface absorption is the latest option that has been introduced into the NASA/MSFC Multilayer Diffusion Model. Data obtained in chamber tests (Ref. 21.23) showed that most HCl contacting a water surface is absorbed. The Γ-option, which is an integral part of the various diffusion equations and has been given in the preceding discussions, was introduced to account for this process.

21.3 Toxicity Criteria

A realistic evaluation of the potential hazard arising from high near-field concentrations of toxic effluents from solid-rocket exhausts requires a knowledge of both the surface deposition of these effluents — which can be obtained with the MSFC/NASA Multilayer Diffusion Model — and a toxicity criterion to evaluate the hazard from this surface deposition of effluent, which is the motivation for this discussion. The Federal Air Quality Criteria do not presently include any of the solid-rocket exhaust effluents; however, the National Academy of Sciences does afford definite guidelines for exposure to the toxic effluents associated with these exhausts. The Environmental Protection Agency (EPA) suggests that a safety factor of 10 be applied to the occupational exposure limits. These guidelines are based on the current limited knowledge of the effects of these effluents and are the basis of the toxicity criteria given in Table 21.1 (Ref. 21.24).

In table 21.1 ceiling values are values that should not be exceeded for any period of time. The basis for the values in the table is reviewed in Ref. 21.28.

The primary effluents from any solid-rocket exhaust are aluminum oxide, (Al_2O_3), hydrogen chloride (HCl), carbon monoxide (CO), carbon dioxide (CO_2), hydrogen (H_2), nitrogen (N_2) and water vapor (H_2O). While only the first four compounds are toxic in significant concentrations, there is always a potential hazard of suffocation from any gas which results in the reduction of the partial pressure of oxygen to a level below 135 mm Hg (18 percent by volume at standard temperature and pressure). Oxygen level reduction does not appear to be a hazard from solid-rocket exhaust due to the large volume of air which is entrained into these exhaust clouds; therefore, this potential hazard can be neglected in this discussion and attention directed only to the initial four toxic compounds.

The exposure levels for toxic effluents are divided into three categories: (1) public exposure level, (2) emergency public exposure level, and (3) occupational exposure level. The public exposure levels are designed to prevent any detrimental health effects both to all classes of human beings (children, men, women, the elderly, those of poor health, etc.) and to all forms of biological life. The emergency level is designed as a limit in which some detrimental effects may occur. The occupational level gives the maximum allowable concentration which a man in good health can tolerate – this level could be harmful to some aspects of the ecology.

The toxicity criteria for the toxic effluents in solid rocket exhausts are given in Table 21.1. Public health levels for aluminum oxide are not given because the experience with these particulates is so limited that, at best, the industrial limits are just good estimates.

Hydrogen chloride is an irritant; therefore, the concentration criterion for an interval should not be exceeded (Ref. 21.25). Since hydrogen chloride is detrimental to plant and animal life, and because most launch sites are encompassed by wild-life refuges, the emergency and industrial criteria for hydrogen chloride are not appropriate to the ecological constraints. Because of the large volume of air entrained in the exhaust cloud, the potential hazard from carbon monoxide and carbon dioxide can be neglected.

Any detrimental health effects due to combined toxicological action of these ingredients has been omitted because of a lack of knowledge in this area. However, investigations are currently underway to study this problem and to learn more about the biological effects of hydrogen chloride.

21.4 Applications

There are three primary applications for the rocket-exhaust effluent transport predictions obtained with the NASA/MSFC REED description. The REED description is used in air quality and environmental assessments for:

1. Mission planning activities and environmental assessments.

2. Prelaunch forecasts of the environmental effects of launch operations.

3. Postlaunch environmental analysis.

Each of the above applications imposes different modeling requirements that will be considered as a prologue to a discussion of the REED description.

Presently the primary aerospace requirement for the REED description is in preparing the environmental assessments and defining the environmental launch constraints. Both of these functions require a climatological assessment for atmospheric conditions as the meteorological model in the REED description. This means that large numbers of rawinsonde soundings must be used in the diffusion model to obtain the statistical base in these climatological environment assessments. Hence, we want a simple reliable model requiring a minimum of detailed structure that will address on the central question. The reason is that details in the diffusion prediction will be averaged out in the volume of data being employed. Also, these details only add more confusion to complex problems. The data reduction procedures must be automated to the greatest possible degree and the computation time must be reduced to a minimum to keep the assessments cost-effective.

In forecasting the transport of rocket-exhaust effluents in advance of a launch, we are limited primarily by the variability of the atmospheric conditions. The accuracy of the forecasted atmospheric parameters does not in general warrant a sophisticated diffusion prediction. However, the speed and reliability of the diffusion calculation are extremely important. For this reason a real-time diffusion analysis system such as the NASA/MSFC REED system is important; that is, it is very desirable to have a small computer at the launch site to make real-time diffusion predictions for both the use of launch operation personnel and for the deployment of an exhaust monitoring network. This means that the diffusion calculations must be simple enough to be placed on a small portable computer (32K words) and run in less than 10 minutes. Ideally, the on-line real-time diffusion system should be interactive so that the forecaster and the users can quickly test the results of a small perturbation in atmospheric parameters or call for specific information that they may desire.

Postlaunch analysis of the transport of the rocket-exhaust effluents requires detailed computations of the diffusion process. Because normally there will be at least a rawinsonde sounding of the atmosphere at launch time, this detailed analysis is justified. In general, then, a more exact diffusion model is required for postlaunch analysis than for either climatological investigations or for forecasting environmental effects. This diffusion model must, however, be of the same form as the other diffusion models to maintain continuity.

A great deal of experience has been obtained at Titan launches and is reflected in the evolution of the REED description in this section. It should be recognized that while the central core of the diffusion model is well defined, the peripheral aspects of this model are still flexible. These peripheral aspects still depend somewhat on the future applications that may evolve and on the state of the art of atmospheric soundings and models.

REFERENCES

21.1 Stephens, J. Briscoe, and Stewart, Roger B.: "Rocket Exhaust Effluent Modeling for Tropospheric Air Quality and Environmental Assessments." NASA TR R-473, 1977.

21.2 National Environmental Policy Act, Public Law 91-190. 42nd U. S. Congress, 4321, 1969.

21.3 U. S. Clean Air Act. 42nd U. S. Congress, 1857-18571, as amended by Public Law 91-604, 1971.

21.4 "Environmental Statement for the Space Shuttle." National Aeronautics and Space Administration, Washington, D.C., July 1972.

21.5 Dumbauld, R. K., et al.: "NASA/MSFC Multilayer Diffusion Models and Computer Program for Operational Prediction of Toxic Fuel Hazards." TR 73-301-02, H. E. Cramer Co., NASA Contract NAS8-29033, 1973.

21.6 Stewart, Roger B.; and Grose, William L.: "Parametric Studies with an Atmospheric Diffusion Model that Assesses Toxic Fuel Hazards Due to the Ground Clouds Generated by Rocket Launches." NASA TN D-7852, December 1974.

21.7 Gregory, Gerald L.; Hulten, William C.; and Wornom, Dewey E.: "Apollo Saturn 511 Effluent Measurements from the Apollo 16 Launch Operations — An Experiment." NASA TM X-2910, March 1974.

21.8 Hulten, William C. et al.: "Effluent Sampling of Scout "D" and Delta Launch Vehicle Exhausts." NASA TM X-2987, July 1974.

21.9 Gregory, Gerald L.; Hudgins, Charles H.; and Emerson, Burt R., Jr.: "Evaluation of Chemiluminescent Hydrogen Chloride and a NDIR Carbon Monoxide Detector for Environmental Monitoring." 1974 JANNAF Propulsion Meeting, San Diego, Calif., Oct. 22-24, 1974.

21.10 Stephens, J. Briscoe, ed.: "Atmospheric Diffusion Predictions for the Exhaust Effluents from the Launch of a Titan IIIC, December 13, 1973." NASA TM X-64925, Sept. 27, 1974.

21.11 Slade, D. H., ed.: "Meteorology and Atomic Energy 1968." U. S. Atomic Energy Commission, 1968.

REFERENCES (Continued)

21.12 Pasquill, F.: "Atmospheric Diffusion." Halsted Press, 2nd edition, 1975.

21.13 Barad, M. L., ed.: "Project Prairie Grass, A Field Program in Diffusion." Geophysical Research Papers No. 59, Vols. I and II, AD-152572 and 152573, Air Force Cambridge Research Center, 1958.

21.14 "Winds Aloft Summary and Parameters." Card Deck 600, Station 12868, Cape Kennedy, Fla.; U. S. Department of Commerce, Environmental Science Services Administration, Environmental Data Service (Book 1 of 2), June 2, 1969.

21.15 Kaufman, J. W.; and Keene, L. E.: "NASA's 150 Meter Meteorological Tower Located at the Kennedy Space Center, Florida." NASA TM X-53699, 1968.

21.16 Nunge, Richard J.: "Application of an Analytical Solution for Unsteady, Advective — Diffusion to Dispersion in the Atmosphere I-II." Atmospheric Environment, Vol. 8, No. 10, October 1974, pp. 969-1001.

21.17 Briggs, G. A.: "Some Recent Analyses of Plume Rise Observations." Paper presented at the 1970 International Union of Air Pollution Prevention Associations, Atmospheric Turbulence and Diffusion Laboratory, National Oceanic and Atmospheric Administration, Oak Ridge, Tenn., ATDL, No. 38, 1970.

21.18 Stephens, J. Briscoe; Susko, Michael; Kaufman, John W.; and Hill, C. Kelly: "An Analytical Analysis of the Dispersion Predictions for Effluents from the Saturn V and Scout-Algol III Rocket Exhausts." NASA TM X-2935, Oct. 1973.

21.19 Goldford, A. I.: "Rocket Exhaust Chemistry Studies Relating to the Space Shuttle and Titan III Vehicles." Northrop Services, TN-230-1430, 1975.

21.20 Hart, W. S.: "Dynamics of Large Buoyant Clouds Generated by Rocket Launches." J. of Basic Engineering, March 1973.

21.21 Chung, T. J.: Finite Element Analysis in Fluid Dynamics. University of Alabama in Huntsville Press, July 1974.

REFERENCES (Concluded)

21.22 Pellett, G. L.: "Washout of HCl and Application to Solid Rocket Exhaust Clouds." Paper presented at Precipitation Scavenging Symposium 1974, Champaign, Ill., October 14-18, 1974.

21.23 Knutson, E. O.; and Fenton, D. L.: "Atmospheric Scavenging of Hydrochloric Acid." IITRI Report No. C6312-5, December 1974.

21.24 "National Primary and Secondary Ambient Air Quality Standards." Environmental Protection Agency, Part II Of Federal Register, Vol. 36, No. 84, April 1971 (updated November 1971).

21.25 "Guides for Short Term Exposures of the Public to Air Pollutants, Vol. II Guide for Hydrogen Chloride." Committee on Toxicilogy of the National Academy of Sciences — National Research Council, Washington, D. C., August 1971.

21.26 Susko, Michael, and Stephens, J. Briscoe: "Baseline Meteorological Soundings for Parametric Environmental Investigations at Kennedy Space Center and Vandenberg Air Force Base." NASA TM X-64986, Feb. 1976.

21.27 Dumbauld, R. K.; Bjorklund, J. R.: "NASA/MSFC Multilayer Diffusion Models and Computer Programs — Version 5." NASA CR-2631, 1973, H. E. Cramer Co., NASA Contract NAS8-29033, 1975.

21.28 "Basis for Establishing Guides for Short-Term Exposures of the Public to Air Pollutants." Committee on Toxicology, National Academy of Sciences, National Research Council Report PB 199 904, May, 1971.

21.29 "Guides for Short-Term Exposures of the Public to Air Pollutants. II Guide for Hydrogen Chloride." Committee on Toxicology, National Academy of Sciences — National Research Council Report PB 203 464, August 1971.

21.30 "Guides for Short-Term Exposures of the Public to Air Pollutants, I. Guide for Oxides of Nitrogen." Committee on Toxicology, National Academy of Sciences, National Research Council Report PB 199 903, April, 1971.

SECTION XXII. CONVERSION UNITS

22.1 Physical Constants and Conversion Factors

Numerical values in this document are given in the International System of Units (SI, Système International d'Unités) (Ref. 22.1). The values in parentheses are equivalent U. S. Customary Units, which are English units adapted for use by the United States of America (Ref. 22.2). The SI and U. S. Customary Units provided in Table 22.1 are those normally used for measuring and reporting atmospheric data. Reference 22.3 provides and discusses select conversion factors used as the National Bureau of Standards guidelines for utilization of the metric system.

By definition, the following fundamental conversion factors are exact:

Type	U. S. Customary Units	Metric
Length	1 U. S. yard (yd)	0.9144 meter (m)
Mass	1 avoirdupois pound (lb)	453.59237 gram (g)
Time	1 second (s)	1 second (s)
Temperature	1 degree Rankine (°R)	9/5 degree Kelvin (°K)
Electric current	1 ampere (A)	1 ampere (A)
Light intensity	1 candela (cd)	1 candela (cd)

To aid in the conversion of units given in this document, conversion factors based on the above fundamental conversion factors are given in Table 22.1. Geometric altitude as employed herein is with reference to mean sea level (MSL) unless otherwise stated.

TABLE 22.1. CONVERSION UNITS

	TYPE OF DATA	METRIC		U.S. CUSTOMARY		CONVERSION		
		UNIT	ABBREVIATION	UNIT	ABBREVIATION	MULTIPLY	BY	TO GET
SOLAR RADIATION	Solar Intensity	langley (per minute)	ly (min^{-1})	watt per square foot	watt ft^{-2}	ly (min^{-1})	0.69733	kJ m^{-2} (s^{-1})
		gram-calorie per square centimeter (per minute)	g-cal cm^{-2} (min^{-1})	British Thermal Unit per square foot (per minute)	Btu ft^{-2} (min^{-1})	kJ m^{-2} (s^{-1})	1.4340	ly (min^{-1})
						ly (min^{-1})	1.000*	g-cal cm^{-2} (min^{-1})
		watt per square meter	watt m^{-2}			g-cal cm^{-2} (min^{-1})	1.000*	ly (min^{-1})
						watt m^{-2}	0.09290304*	watt ft^{-2}
		kilojoule per square meter (per second)	kJ m^{-2} (s^{-1})			watt ft^{-2}	10.7639	watt m^{-2}
						g-cal cm^{-2} (min^{-1})	64.784	watt ft^{-2}
						g-cal cm^{-2} (min^{-1})	697.33	watt m^{-2}
						watt ft^{-2}	0.015436	g-cal cm^{-2} (min^{-1})
						watt m^{-2}	0.0014340	g-cal cm^{-2} (min^{-1})
						g-cal cm^{-2} (min^{-1})	3.6867	Btu ft^{-2} (min^{-1})
						Btu ft^{-2} (min^{-1})	0.27125	g-cal cm^{-2} (min^{-1})
	Insolation	gram-calorie per square centimeter per minute	g-cal cm^{-2} min^{-1}	British Thermal Unit per square foot per hour	Btu ft^{-2} hr^{-1}	g-cal cm^{-2} min^{-1}	221.20	Btu ft^{-2} hr^{-1}
						Btu ft^{-2} hr^{-1}	0.0045208	g-cal cm^{-2} min^{-1}
TEMPERATURE	Ambient Temperature	degree Celsius	$^{\circ}$C	degree Fahrenheit	$^{\circ}$F	$^{\circ}$F -32	0.5556	$^{\circ}$C
		degree Kelvin	$^{\circ}$K	degree Rankine	$^{\circ}$R	$^{\circ}$C	1.8*	$^{\circ}$F - 32
						$^{\circ}$R	1.00*	$^{\circ}$F + 459.67
						$^{\circ}$R - 459.67	1.00*	$^{\circ}$F
						$^{\circ}$K	1.00*	$^{\circ}$C + 273.15
						$^{\circ}$K - 273.15	1.00*	$^{\circ}$C
	Temperature Change	degree Celsius	$^{\circ}$C	degree Fahrenheit	$^{\circ}$F	$^{\circ}$C or $^{\circ}$K	1.8*	temp. change $^{\circ}$F or $^{\circ}$R
		degree Kelvin	$^{\circ}$K	degree Rankine	$^{\circ}$R	$^{\circ}$F or $^{\circ}$R	0.5556	temp. change $^{\circ}$C or $^{\circ}$K

* Defined exact conversion factor

TABLE 22. 1 (Continued)

	TYPE OF DATA	METRIC		U.S. CUSTOMARY		CONVERSION		
		UNIT	ABBREVIATION	UNIT	ABBREVIATION	MULTIPLY	BY	TO GET
DENSITY	Water Vapor Vapor Concentration (Absolute Humidity)	gram per cubic meter	$g\ m^{-3}$	grain per cubic foot	$gr\ ft^{-3}$	$g\ m^{-3}$	0.43700	$gr\ ft^{-3}$
		gram per cubic centimeter	$g\ cm^{-3}$			$gr\ ft^{-3}$	2.2883	$g\ m^{-3}$
						$g\ m^{-3}$	10^{-6}*	$g\ cm^{-3}$
						$g\ cm^{-3}$	4.370×10^{5}	$gr\ ft^{-3}$
						$gr\ ft^{-3}$	2.288×10^{-6}	$g\ cm^{-3}$
	Air, Dust, and Hail	gram per cubic centimeter	$g\ cm^{-3}$	pound per cubic foot	$lb\ ft^{-3}$	$g\ cm^{-3}$	62.43	$lb\ ft^{-3}$
						$lb\ ft^{-3}$	1.6018×10^{-2}	$g\ cm^{-3}$
PRECIPITATION	Snow Unit Depth Mass	kilogram per square meter per centimeter (of depth)	$kg\ m^{-2}\ cm^{-1}$	pound per square foot per inch (of depth)	$lb\ ft^{-2}\ in.^{-1}$	$kg\ m^{-2}\ cm^{-1}$	0.5202	$lb\ ft^{-2}\ in.^{-1}$
						$lb\ ft^{-2}\ in.^{-1}$	1.922	$kg\ m^{-2}\ cm^{-1}$
	Snow Storm Total Mass	kilogram per square meter	$kg\ m^{-2}$	pound per square foot	$lb\ ft^{-2}$	$kg\ m^{-2}$	0.2048	$lb\ ft^{-2}$
						$lb\ ft^{-2}$	4.882	$kg\ m^{-2}$
	Depth	centimeter	cm	inch	in.	cm	0.3937	in.
						in.	2.54*	cm
WIND	Wind Speed	meter per second	$m\ s^{-1}$	mile per hour	mph	$m\ s^{-1}$	2.2369	mph
				knots	knots	mph	0.44704*	$m\ s^{-1}$
				feet per second	$ft\ s^{-1}$	$m\ s^{-1}$	1.9438	knots
						knots	0.51444	$m\ s^{-1}$
						mph	0.868976	knots
						knots	1.15078	mph
						$m\ s^{-1}$	3.2808	$ft\ s^{-1}$
						$ft\ s^{-1}$	0.3048*	$m\ s^{-1}$

*Defined exact conversion factor

ORIGINAL PAGE IS OF POOR QUALITY

TABLE 22.1 (Continued)

TYPE OF DATA		METRIC		U.S. CUSTOMARY		CONVERSION		
		UNIT	ABBREVIATION	UNIT	ABBREVIATION	MULTIPLY	BY	TO GET
DISTANCE	Length	meter	m	feet	ft	m	3.2808	ft
		micron	μ	inch	in.	ft	0.3048*	m
		Ångstrom unit	Å			in.	$2.54 \times 10^{+4}$*	μ
						in.	$2.54 \times 10^{+8}$*	Å
						m	10^{+6}*	μ
						m	10^{+10}*	Å
						μ	10^{-6}*	m
						μ	3.937×10^{-5}	in.
						Å	10^{-10}*	m
						Å	3.937×10^{-9}	in.
MASS	Weight	gram	g	grain	gr	lb	0.45359237*	kg
		kilogram	kg	pound	lb	lb	453.59237*	g
						kg	2.20462	lb
						g	15.4324	gr
						gr	0.06480	g

* Defined exact conversion factor

TABLE 22.1 (Concluded)

TYPE OF DATA		METRIC		U.S. CUSTOMARY		CONVERSION		
		UNIT	ABBREVIATION	UNIT	ABBREVIATION	MULTIPLY	BY	TO GET
PRESSURE	Atmospheric	newton per square meter	newton m^{-2}	pound force per square inch	lb $in.^{-2}$	mb	10^{-3}*	bar
						bar	10^{3}*	mb
		millimeter of Mercury	mmHg	inch of Mercury	in.Hg	newton m^{-2}	10^{-2}*	mb
						newton m^{-2}	$1.4504X10^{-4}$	lb $in.^{-2}$
						lb $in.^{-2}$	$6.8948X10^{3}$	newton m^{-2}
		bar	bar			mb	$1.4504X10^{-2}$	lb $in.^{-2}$
		millibar	mb			lb $in.^{-2}$	68.948	mb
		dyne per square centimeter (microbar)	dyne cm^{-2}			mb	10^{3}*	dyne cm^{-2}
						dyne cm^{-2}	10^{-3}*	mb
		kilogram force per square meter	kg m^{-2}			lb $in.^{-2}$	$6.8948X10^{4}$	dyne cm^{-2}
						dyne cm^{-2}	$1.4504X10^{-5}$	lb $in.^{-2}$
						mb	10.1972	kg m^{-2}
						kg m^{-2}	0.0980665	mb
						lb $in.^{-2}$	703.0696	kg m^{-2}
						kg m^{-2}	0.0014223	lb $in.^{-2}$
						mb	$2.9530X10^{-2}$	in.Hg (32^{o} F)
						mb	0.75006	mmHg (0^{o} C)
						in.Hg(32^{o} F)	25.40*	mmHg (0^{o} C)
						mmHg(0^{o} C)	1.33322	mb
						in.Hg(32^{o} F)	33.8639	mb
		pascal	Pa			Pa	1.00*	newton m^{-2}

* Defined exact conversion factor

REFERENCES

22.1 Mechtly, E. A.: "The International System of Units: Physical Constants and Conversion Factors." NASA SP-7012, Second Revision, National Aeronautics and Space Administration, Washington, D. C., 1973.

22.2 "Units of Weight and Measure (United States Customary and Metric) Definitions and Tables of Equivalents." United States Department of Commerce, National Bureau of Standards, Miscellaneous Publication 233, 1960.

22.3 "NBS Guidelines for Use of the Metric System." U. S. Department of Commerce, National Bureau of Standards, LC 1056, November 1974.

INDEX

1. Report No. NASA TM-78118	2. Government Accession No.	3. Recipient's Catalog No.
4. Title and Subtitle Terrestrial Environment (Climatic) Criteria Guidelines for Use in Aerospace Vehicle Development, 1977 Revision		5. Report Date November 1977
		6. Performing Organization Code
7. Author(s) John W. Kaufman, Editor		8. Performing Organization Report No. M-234
9. Performing Organization Name and Address George C. Marshall Space Flight Center Marshall Space Flight Center, Alabama 35812		10. Work Unit No.
		11. Contract or Grant No.
12. Sponsoring Agency Name and Address National Aeronautics and Space Administration Washington, D. C. 20546		13. Type of Report and Period Covered Technical Memorandum
		14. Sponsoring Agency Code

15. Supplementary Notes This document was prepared based on the engineering problems which developed or are anticipated for future programs by design and operational personnel of the NASA field centers. Various staff members of the Atmospheric Sciences Division, Space Sciences Laboratory, MSFC/NASA, contributed to the contents of this document.

16. Abstract

This document provides guidelines on terrestrial environment data specifically applicable for NASA aerospace vehicles and associated equipment development. The primary geographic areas encompassed are the Kennedy Space Center, Florida; Huntsville, Alabama; Vandenberg AFB, California; Edwards AFB, California; Honolulu, Hawaii; Guam; Santa Susana, California; Brigham, Utah; New Orleans, Louisiana; Bay St. Louis, Mississippi; Houston, Texas; Wallops Flight Center, Wallops Island, Virginia; and the White Sands Missile Range, New Mexico. In addition, a section has been included to provide information on the general distribution of natural environmental extremes in the conterminous United States that may be needed to specify design criteria in the transportation of space vehicle subsystems and components. Although not considered as a specific vehicle design criterion, a section on atmospheric attenuation has been added since certain earth orbital experiment missions are influenced by the earth's atmosphere. A summary of climatic extremes for worldwide operational needs is also included. This document presents the latest available information on probable climatic extremes and succeeds information presented in TM X-64589 and TM X-64757. Information is included on atmospheric chemistry, seismic criteria, and on a mathematical model to predict atmospheric dispersion of aerospace engine exhaust cloud rise and growth. There is also a new section on cloud phenomena. The information in this report is recommended for use in the development of aerospace vehicle and associated equipment design and operational criteria, unless otherwise stated in contract work specifications.

The environmental data in this report are primarily limited to information below 90 km. Environmental criteria for 90 km and above are documented in NASA Technical Memorandum TM-78119, Space and Planetary Environment Criteria Guidelines for Use in Space Vehicle Development (1977 Revision).

17. Key Words (Suggested by Author(s)) Environment Criteria, Terrestrial Environment, Surface Extremes, Wind, Temperature, Solar Radiation, Humidity, Precipitation, Density, Pressure, Atmospheric Electricity, Cloud Cover	18. Distribution Statement Cat. 15

19. Security Classif. (of this report)	20. Security Classif. (of this page)	21. No. of Pages	22. Price
Unclassified	Unclassified	526	A23

* For sale by the National Technical Information Service, Springfield, Virginia

*U.S. GOVERNMENT PRINTING OFFICE: 1977 - 735-078/46